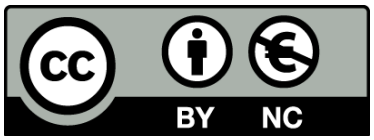


UNIVERSITAT DE BARCELONA

Causes, effects, and management of river salinization in Spain with special attention to wastewater treatment

Alvaro Javier Moyano Salcedo



Aquesta tesi doctoral està subjecta a la llicència ***Reconeixement- NoComercial 4.0. Espanya de Creative Commons***.

Esta tesis doctoral está sujeta a la licencia ***Reconocimiento - NoComercial 4.0. España de Creative* Commons**.

This doctoral thesis is licensed under the ***Creative Commons Attribution-NonCommercial 4.0. Spain License***.



UNIVERSITAT DE BARCELONA

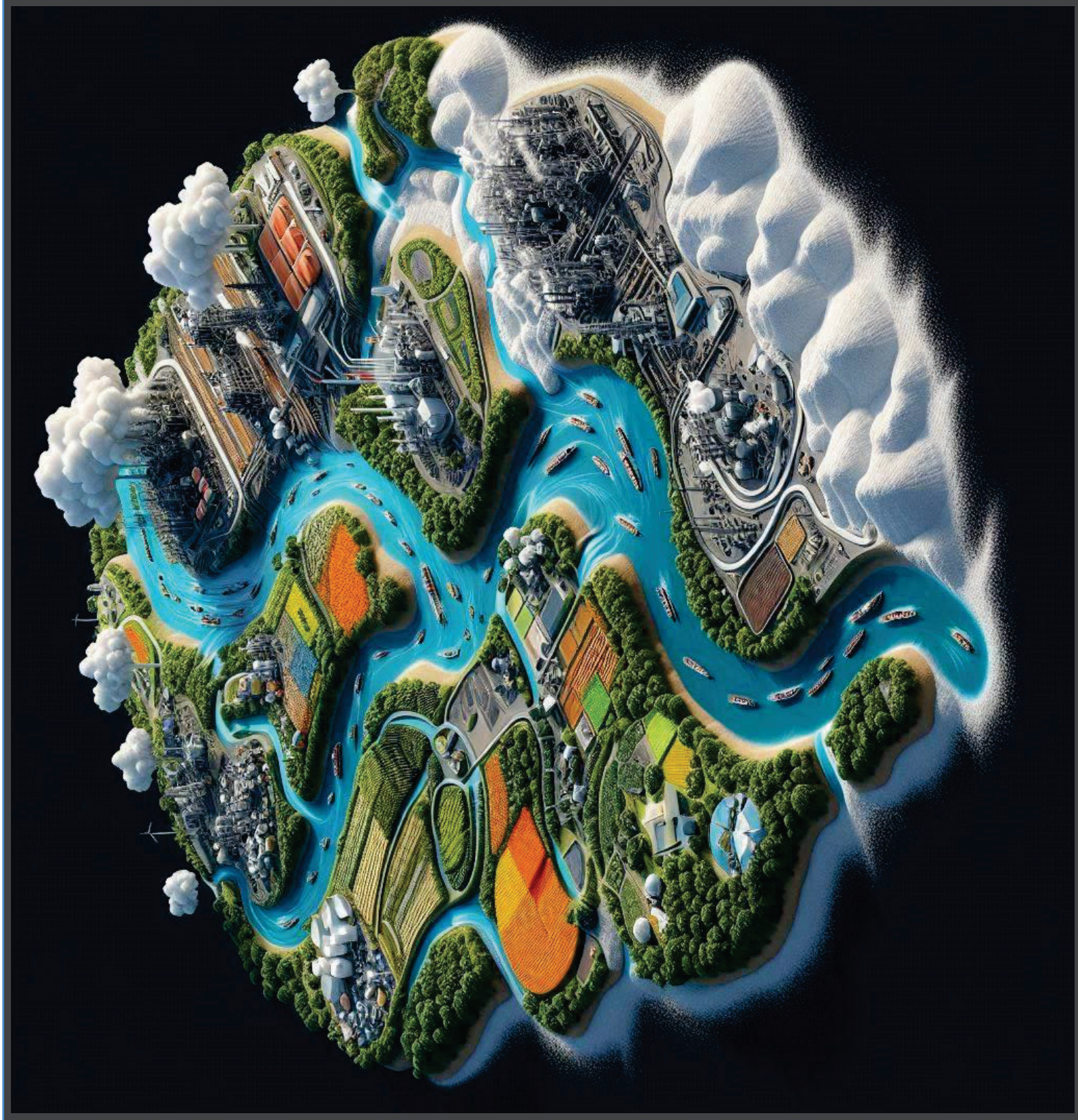
Doctoral Program in Ecology, Environmental Sciences and Plant Physiology

Department of Evolutionary Biology, Ecology and Environmental Science

Causes, effects, and management of river salinization in Spain with special attention to wastewater treatment

Alvaro Javier Moyano Salcedo

Barcelona, September 2024



Faculty of Biology

Doctoral Program in Ecology, Environmental Sciences and Plant Physiology
Department of Evolutionary Biology, Ecology and Environmental Science

Causes, effects, and management of river salinization in Spain with special attention to wastewater treatment

Thesis submitted by

Alvaro Javier Moyano Salcedo

to qualify for the

Doctorate degree by the Universitat de Barcelona

Doctorate candidate

Alvaro Moyano S.

Alvaro Javier Moyano Salcedo

Barcelona, September 2024

Supervisor

Dr. Miguel Cañedo-Argüelles Iglesias
Senior Scientist
IDAEA-CSIC

Supervisor and Tutor

Dr. Humbert Salvadó Cabré
Professor Agregat
Universitat de Barcelona

A Margoth y Alfonso, mis padres

A mi familia

A los ríos y a la vida

Acknowledgements

Vull expressar el meu profund agraïment a la meva família per tot el suport que m'ha brindat. Moltes gràcies als que estan presents i als que ja no hi són; el seu amor m'ha ajudat a arribar fins aquest punt.

Als meus directors, Humbert Salvadó i Miguel Cañedo-Argüelles, pel seu suport, acompanyament i l'enorme aportació en la meva formació com a científic. Moltes gràcies per donar-me l'oportunitat de venir a la Universitat de Barcelona.

A la Universitat de Barcelona i a la coordinació del doctorat per tot el suport administratiu i acadèmic. A la comissió de seguiment per la seva dedicació i tot el suport i les recomanacions.

Al Ministeri de Ciència, Tecnologia i Innovació de Colòmbia i a Colfuturo per l'ajut econòmic proporcionat.

Al grup FEMH i al laboratori de Protistologia de la Universitat de Barcelona, per ser la meva família i la meva casa durant aquest procés.

A l'IDAEA-CSIC, per ser part de la meva família i la meva segona casa, així com per les oportunitats i els reptes brindats.

Agraeixo a Miguel, Pau Fortuño, Raúl Acosta i José María Fernández-Calero per la seva ajuda ensenyant-me sobre macroinvertebrats. A Martí Piñero Fernández per la seva ajuda en l'experiment sobre la interacció de la salinització i els nutrients. A Narcís Prat i Humbert, per tot el temps d'ensenyament personalitzat sobre quironòmids i protozous, respectivament.

Al grup Beta, especialment a Lorenzo Proia i Lluís Bertrans-Tubau, per tot el suport en l'experiment sobre la interacció de la salinització i els nutrients.

A Ben Kefford, Elisabeth Berger, Ralf Schäfer i Sujay Kaushal, així com als seus equips de treball de les universitats de Canberra, Koblenz-Landau i Maryland, per acollir-me, per la seva hospitalitat i per tot allò que he après.

Si fóssim fills de rius, jo hauria nascut del riu Fortalecillas en aquest punt (2.9454969, -75.0389365, WGS84). Riu que neix a la cordillera oriental dels Andes a Colòmbia i desemboca al riu Magdalena molt abans d'arribar a Bocas de Cenizas i al mar Carib. Gràcies als rius i als sistemes ambientals per ser la font vital que ens sustenta.

Abstract

Freshwater salinization (FS) represents a pressing global environmental challenge, significantly impacting aquatic ecosystems. Despite extensive research, critical gaps remain in understanding the full extent and implications of FS. This thesis aims to address and contribute to filling some of these gaps by providing global information necessary to explore FS patterns, temporal variability, and the interaction of FS with other pollutants, particularly nutrients. One of the key focuses of this thesis is the evaluation of the salinity effects on urban wastewater treatment plants (WWTPs), as well as WWTP contributions to FS.

The objectives of this thesis are fourfold. First, it aims to compile a global database integrating river salinity parameters and both natural and anthropogenic drivers of freshwater salinization to explore patterns and temporal variability across various regions. Second, it seeks to examine the seasonal dynamics of primary salinization sources such as mining, transportation, agriculture, and urban wastewater discharges, and their effects on the temporal variability of river salinity in Spanish rivers. Third, the thesis investigates the interactive effects of nutrient and salt pollution on river ecosystems through controlled experiments in artificial channels. Fourth, it assesses how increasing salinity impacts microbial communities and pollutant removal efficiency in WWTPs.

Chapter 1 presents a global dataset, GlobSalt, which includes 13 parameters related to river salinity and associated ions, with approximately 15 million records. This dataset reveals substantial spatial variability in salinity and serves as a crucial resource for understanding FS dynamics and identifying high-risk regions. Chapter 2 analyzes temporal variations in electrical conductivity (EC) across 91 Spanish rivers, demonstrating how human activities disrupt EC patterns and influence aquatic biodiversity. Chapter 3 explores the combined effects of nutrient and salt pollution on stream microcosms, highlighting significant declines in macroinvertebrate diversity and the complex interactions between pollutants. Chapter 4 assesses the impact of salinity on WWTP performance, revealing how high EC levels affect microbial communities and pollutant removal efficiency. Moreover, each chapter presents an application of the GlobSalt data: (i) the temporal variation of river EC influenced by WWTP discharges and seasonal patterns, (ii) the concentration of phytoplankton in rivers in relation to EC levels for pristine and impacted sites, and (iii) the increase in river EC associated with wastewater discharges in different seasons.

In summary, this thesis not only advances scientific understanding of freshwater salinization and its drivers but also offers practical insights for managing and mitigating FS impacts. By integrating global and local data, addressing seasonal and interactive effects, and evaluating WWTP performance and contributions, this research provides valuable information for developing effective management strategies and guiding future studies in the field of freshwater ecology.

Table of contents

1. GENERAL INTRODUCTION 1
1.1. Natural and human driver of river salinity 3
Geological processes 3
Atmospheric contributions 4
Fluvial, soil and biological processes 4
Saltwater Intrusion 5
Climate-Related Factors 6
Human activities perturbing natural salt cycle 7
Agricultural food systems 8
Road de-icing 10
Natural resource extraction 11
Wastewater discharge 12
1.2. Freshwater salinization: state of the art and main knowledge gaps 16
1.3. Introduction to Chapter I: GLOBal river SALiniTy and associated ions (GlobSalt) 19
1.4. Introduction to Chapter II: Human activities as drivers of temporal changes in salinity 22
1.5. Introduction to Chapter III: Freshwater salinization and eutrophication: interactive effects on aquatic biofilm and macroinvertebrates 26
1.6. Introduction to Chapter IV: Salinization in WWTPs: effects on microbial communities and pollutant removal efficiency 30
2. OBJECTIVES 39
3. RESULTS 43
3.1. Report from the thesis supervisors 45
3.2. Chapter I: GLOBal river SALiniTy and associated ions (GlobSalt) 47
3.3. Chapter II: Human activities disrupt the temporal dynamics of salinity in Spanish rivers 73
3.4. Chapter III: What happens when salinization meets eutrophication? A test using stream microcosms 91
3.5. Chapter IV: Assessing the effects of salinity on microbial communities and pollutant removal in urban wastewater treatment plants 107

4. OVERALL DISCUSSION 121
4.1. GlobSalt: A comprehensive global river salinity dataset and its implications for freshwater salinization studies 123
Geographic and temporal coverage 124
Geographic distribution and data density 124
Temporal Coverage 126
Data Quality and Validity: Identification and Handling of Erroneous Data 127
Correlation between EC and major ions 128
Key drivers of FS: Insights from GlobSalt and HydroAtlas 129
4.2. Impact of human activity and environmental variables on temporal variability of conductivity in river ecosystems 135
Assessing temporal variations in FS influenced by WWTPs using GlobSalt and HydroWaste data 137
4.3. Responses of aquatic communities to the interactive effects of salinization and nutrient enrichment: Additive and antagonistic effects 146
Salinity influence on river phytoplankton using WQP and GlobSalt Data 147
4.4. Disruption of the microbial community and reduced efficiency of pollutant removal due to high conductivity in WWTPs 150
Assessment wastewater discharges effect on freshwater salinization: A global approach with HydroWaste and GlobSalt 154
5. GENERAL RECOMMENDATIONS 161
5.1. Recommendations for Spain 165
For policy makers and technical bodies 165
For businesses and the private sector 166
For society 169
5.2. Open questions 170
5.3. Future scenarios 171
6. CONCLUSIONS 175
7. REFERENCES 183
8. APPENDICES 211
Supplementary material: Chapter I 213
Supplementary material: Chapter II 269
Supplementary material: Chapter III 309
Supplementary material: Chapter IV 353

List of tables and figures

Table 1. 1. Salinity Effects on Wastewater Treatment Processes: A comprehensive review and summary of studies on the impact of salinity in wastewater treatment. 33

Table 4. 1. Attributes, structure and parameter statistics of the GlobSalt and HydroWaste integration. Variable names and descriptions, including reported units, of both databases. ……...139

Table 4. 2. Mean, Maximum, and Minimum conductivity values upstream and downstream of WWTPs by Season according to the GlobSalt and HydroWaste integration. 155

Figure 1. 1. Natural salt cycle: main sources, causes, transport, dynamics, and storage. Source: Created by the author based on Kaushal et al. (2023). 7

Figure 1. 2. Anthropic salt cycle: main sources, causes, transport, dynamics, and storage. Source: Created by the author based on Kaushal et al. (2023). 9

Figure 1. 3. A global overview of studies on salinization from 2017 to 2021, focusing on the causes of salinity changes within the examined systems (as indicated by bar plot colors), which include factors such as mining, road de-icing, saltwater intrusion, and oil extraction (e.g., fracking). Source: Cunillera-Montcusí et al. (2022). 14

Figure 4. 1. Plot representing the main natural and anthropogenic variables from the HydroAtlas, according to the random forest analysis, that explain the conductivity of rivers included in GlobSalt. 131

Figure 4. 2. Generalized Additive Model (GAM) plot with smooth terms presenting the relationship of soil water content, precipitation, and road density with conductivity.. 131

Figure 4. 3. Plot representing the mean value and variability in conductivity of river stations from GlobSalt, both upstream and downstream of WWTPs from HydroWaste. The point represents the mean value, and the irregular line represents the standard

deviation. Panel A: river stations upstream of WWTPs; Panel B: river stations downstream of WWTPs. 141

Figure 4. 4. Plot showing the mean value and variability in conductivity at river stations from GlobSalt across different seasons, both upstream and downstream of WWTPs from HydroWaste. Panels A-D display data for upstream stations in Winter (SD: 714 µS cm-1) , Spring (SD: 474 µS cm-1), Summer (SD: 506 µS cm-1), and Fall (SD: 552 µS cm-1), respectively. Panels E-H display data for downstream stations in Winter (SD: 1724 µS cm-1), Spring (SD: 1710 µS cm-1), Summer (SD: 1859 µS cm-1), and Fall (SD: 1754 µS cm-1) respectively. 145

Figure 4. 5. Scatter plot showing the LMER model between phytoplankton and conductivity levels in U.S. rivers. Points and linear regression lines in orange and blue represent impacted and pristine areas, respectively..... 148

Figure 4. 6. Linear Mixed-Effects Regression (LMER) between conductivity and river station associated with upstream and downstream WWTPs by season. A: Winter, B: Spring, C: Summer, D: Fall. 155

List of Abbreviations

FS: Freshwater Salinization

EC: Electrical Conductivity

WWTPs: Wastewater Treatment Plants

WFD: Water Framework Directive

RD: Real Decreto

WGS84: World Geodetic System 1984

GIS: Geographic Information System

GLORICH: Global River Chemistry Database GlobSalt: Global River Salinity and Associated Ions Database

GPS: Global Positioning System

WQP: Water Quality Portal

COD: Chemical Oxygen Demand

BOD: Biochemical Oxygen Demand

TOC: Total Organic Carbon

SBR: Sequencing Batch Reactor

AnMBR: Anaerobic Membrane Bioreactor

BF-MBR: Biofilm Membrane Bioreactor

AGS: Aerobic Granular Sludge

FAS: Flocculent Activated Sludge

PAO: Polyphosphate Accumulating Organism

RO: Reverse Osmosis

NF: Nanofiltration

W/V: weight/volume

MN_AGR: Mean Agriculture

P_DIR: Distance to Nearest Icy Road

P_DMN: Distance to Nearest Mining Site

MN_SSH: Mean Area Occupied by Moors, Heathland, Scrub, and Shrubs

MN_PAS: Mean Pasture

MN_UHD: Mean Urban Areas

MN_CNF: Mean Area Occupied by Coniferous Forest

CVA: Coefficient of Variation (Annual)

CVM: Coefficient of Variation (Monthly)

JMax: Julian Day of Annual Maximum EC

JMin: Julian Day of Annual Minimum EC

AFDM: Ash-Free Dry Mass

Yeff: Photosynthetic Efficiency

HSD: Honest Significant Difference

VIF: Variance Inflation Factor

CIs: Confidence Intervals

SD: Standard deviation

PCA: Principal Component Analysis

RF: Random Forest

ANOVA: Analysis of Variance

GAMs: Generalized Additive Models

IndVal: Indicator Species Analysis

NMDS: Non-metric Multidimensional Scaling

SEM: Structural Equation Model

BAIN: Biotic-Abiotic Interaction Networks

LASSO: Least Absolute Shrinkage and Selection Operator

LMER: Linear Mixed-Effects Model

1. GENERAL INTRODUCTION

1.1. Natural and human driver of river salinity

Salts are a natural component of freshwater ecosystems. For instance, precipitation dissolves carbonate-rich rocks, transporting their minerals into rivers and streams (Cañedo-Argüelles et al., 2013; Herbert et al., 2015). Also, sodium chloride (NaCl) enters inland water from the sea via atmospheric deposition (Gorham et al., 1958; Kaushal et al., 2023). Overall, the natural concentration and composition of salts in freshwater ecosystems results from a complex interplay of geological processes, atmospheric contributions, soil and fluvial processes, biological influences, saltwater intrusion and climate-related factors (Figure 1) (Kaushal et al., 2018; Cañedo-Argüelles, 2021; Cunillera-Montcusí et al., 2022).

Geological processes

Geological processes are crucial as they serve as the primary source of salts in freshwater systems (Roveri et al., 2003; Jordán et al., 2004; Kaushal et al., 2023). Tectonic movements, such as those that occur along geological faults, result in the release of salts stored in rocks into the environment (Roveri et al., 2003; Weinberger et al., 2006; Hudec and Jackson, 2007). As tectonic plates shift and collide, rocks are fractured and crushed, exposing mineral surfaces to weathering processes (Daliakopoulos et al., 2016; Kirkham et al., 2020). Over time, these processes result in the release of significant quantities of salts, which are then transported by water into rivers and streams (Rahman et al., 2018; Kaushal et al., 2023). Another significant geological process contributing to natural salinity is chemical weathering (Moreira-Nordemann, 1984; Meybeck 1987; Singh et al., 2008). This process involves the breakdown of rocks and minerals through chemical reactions with water and atmospheric gasses. For example, the dissolution of carbonates and sulfates releases calcium (Ca^{2+}), magnesium (Mg^{2+}), and sulfate (SO_4^{2-})

ions into the water (Meybeck 1987; Kaushal et al., 2023). This process not only increases the salinity of freshwater but also alters its ionic composition.

Given the different types of geologic compositions and the varying magnitude of tectonic and chemical processes releasing salts, significant differences are expected in both the amounts of salts entering rivers and the types of ions (e.g. sodium, chloride, calcium, silicates, or sulfates) contributing to their salinity (Meybeck 1987; Singh et al., 2008; Kaushal et al., 2023).

Atmospheric contributions

Atmospheric deposition is another important source of salts. Salts are transported through the atmosphere in aerosols and dust particles, primarily originating from sea spray and arid regions (Blackburn and Mcleod, 1983; Guerzoni et al., 1999; Kaushal et al., 2018, 2023). These salts settle on land and water surfaces through wet deposition (e.g., rainfall) and dry deposition (e.g., gravitational settling) (Guerzoni et al., 1999; Kaushal et al., 2023). For instance, sodium chloride from sea spray can be carried inland by wind and deposited far from coastal areas. Thus, atmospheric salt transport includes the movement of salts in aerosols and dust over long distances (Blackburn and Mcleod, 1983; Kaushal et al., 2023). Wind can carry sea salt particles and dust containing various salts, contributing to the salinity of surface waters (Blackburn and Mcleod, 1983). This process is particularly significant in regions downwind of large deserts or dry lake beds, where dust storms can transport substantial quantities of salts (Kaushal et al., 2023).

Fluvial, soil and biological processes

The dynamics of natural salinity are also strongly influenced by rivers, which play a crucial role in the movement of sediments and, due to their flow, in the transport and

distribution of salts (Prosser et al., 2001; Canavan et al., 2006; Kaushal et al., 2018, 2023). Sediment movement, or fluvial salt transport, involves the erosion and deposition of mineral particles containing salts (Hatch et al., 2010; Kaushal et al., 2023, 2018). As rivers flow, they erode rocks and soils, carrying these materials downstream (Prosser et al., 2001). During periods of high flow, such as spring snowmelt or heavy rains, the capacity of rivers to transport sediments and associated salts increases, spreading these salts over wider areas (Prosser et al., 2001; Hatch et al., 2010).

Furthermore, natural salinity is significantly influenced by soil erosion processes, which are driven by both water and wind, and are closely linked to fluvial dynamics (Neave and Rayburg, 2006; Ondrasek and Rengel, 2021; Li and Guo, 2022). Erosion can occur through water runoff, wind, and gravitational forces, dislodging soil particles that contain salts (Neave and Rayburg, 2006; Kaushal et al., 2018, 2023). These particles are then carried into rivers and streams, where the salts dissolve and increase the salinity of the water (Neave and Rayburg, 2006; Ondrasek and Rengel, 2021). Moreover, the biological decomposition of organic matter releases salts back into the environment, adding to the contributions of soil erosion (Entrekin et al., 2019; Kaushal et al., 2023). When plants and animals die, their bodies break down, and the salts that they contain are returned to the soil and water. Also, some organisms can concentrate salts in their tissues, which are then released upon decomposition (Kaushal et al., 2023).

Saltwater Intrusion

Saltwater intrusion is a natural process that affects continental freshwater systems near coastal areas (Alfarrah and Walraevens, 2018; Kaushal et al., 2018, 2023). It is primarily driven by an imbalance between freshwater and saltwater pressures. When freshwater flow decreases, often due to reduced rainfall or increased evaporation

(Alfarrah and Walraevens, 2018), the pressure that typically keeps seawater at bay diminishes, allowing seawater to infiltrate freshwater aquifers and rivers (Kaushal et al., 2023). Also, changes in sea level, especially during high tides or storm surges, can further facilitate the intrusion of seawater into continental areas. This process can significantly increase the salinity of coastal freshwater ecosystems (Venâncio et al., 2022).

Climate-Related Factors

Climatic events, such as extreme rainfall or storms, play a critical role in modulating FS (Kaushal et al., 2018b; Des et al., 2021; Perri et al., 2022). For instance, heavy rainfall can increase the weathering of rocks, increasing the release of salts into the environment (Des et al., 2021). These intense rainfall events can also lead to increased runoff that transports these dissolved salts into rivers (Des et al., 2021; Kaushal et al., 2023). At the same time, the increase in river flow enhances the dilution capacity of the water, thereby reducing the concentration of salts (Kaushal et al., 2023). Similarly, storm surges exacerbate saltwater intrusion, introducing higher concentrations of salts into coastal freshwater aquifers and rivers (Des et al., 2021; Yang and Zhang, 2024). Conversely, droughts can concentrate salts in surface waters by reducing the amount of water available for dilution in rivers, while potentially increasing atmospheric transport of salts from the oceans (i.e., increased coastal evaporation) (Perri et al., 2020, 2022; Kaushal et al., 2023).

These natural processes of river salinity are interconnected and often occur simultaneously, creating a complex and dynamic system (Figure 1) (Kaushal et al., 2018, 2023). Geological weathering, climate variations, atmospheric deposition, fluvial transport, biological activity, and saltwater intrusion all contribute to the natural salinity. Understanding these baseline processes is essential for distinguishing natural salinity

from human-induced freshwater salinization (FS) and for developing effective management strategies to protect freshwater resources.

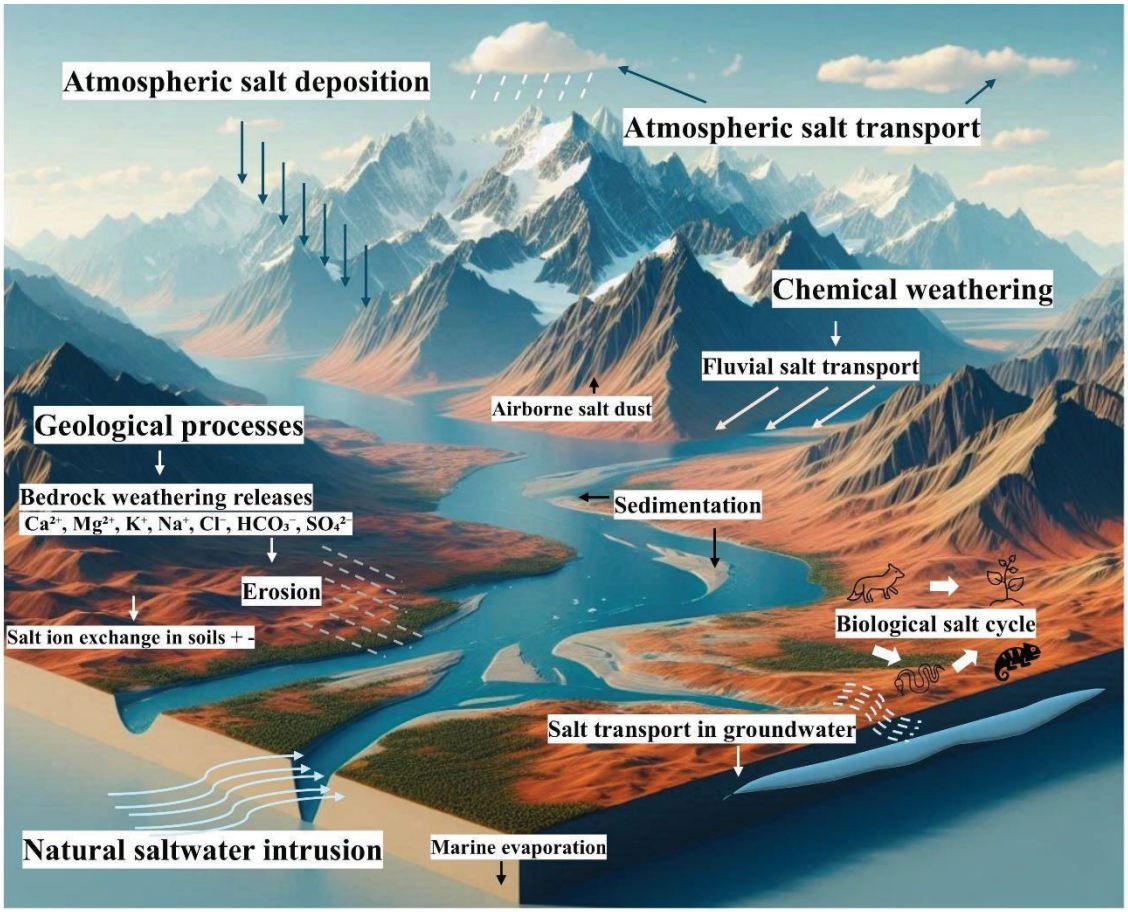


Figure 1. 1. Natural salt cycle: main sources, causes, transport, dynamics, and storage. Source: Created by the author based on Kaushal et al. (2023).

Human activities perturbing natural salt cycle

Humans have significantly increased salt concentrations in freshwaters and altered the balance of ions (Cañedo-Argüelles et al., 2016). FS is a complex process characterized by concurrent changes in specific conductance, pH, alkalinity, and base cations, reflecting a disrupted ionic balance (Kaushal et al., 2018). FS is caused by different human activities such as transportation, agriculture or resource extraction (Figure 2) (Cañedo-Argüelles et al., 2013; Kaushal et al., 2018; Kefford et al., 2016). Over time, FS has caused significant shifts in water chemistry, impacting the health and stability of aquatic ecosystems,

infrastructure, and water quality (Kaushal et al., 2018; Cañedo-argüelles, 2021; Cunillera-Montcusí et al., 2022). This directly affects aquatic life, as organisms need to maintain an internal osmotic balance to survive, and consequently the structure and functioning of aquatic ecosystems (Kefford, 1998, 2019; Kefford et al., 2003; Hassell et al., 2006; Szöcs et al., 2012; Cañedo-Argüelles et al., 2012). Moreover, FS-induced changes in water quality can also have strong impacts on socioeconomic structures (Rahman et al., 2018; Kaushal et al., 2021; Cunillera-Montcusí et al., 2022), thereby limiting the use and conservation of water resources (Kausal et al., 2005; Cañedo-Argüelles et al., 2013; Herbert et al., 2015; Estévez et al., 2019). These impacts are exacerbated in vulnerable populations (e.g., pregnant women, the elderly, children), especially in the context of climate change (e.g., extreme droughts) (Vineis et al., 2011; Cañedo-Argüelles et al., 2013; Radwanur et al., 2015).

Agricultural food systems

The increasing demand for food to meet the needs of current and future populations has put pressure on agricultural food systems (Vineis et al., 2011; Serraj and Pingali, 2019). Although there are several regions (e.g., the U.S., Europe) where efforts have been made to make these systems more sustainable and strict environmental regulations are in place, in many areas there is still a lack of control over the use and application of salts from products used to maintain these systems (Kaushal et al., 2018; Cunillera-Montcusí et al., 2022; Yang et al., 2024). Thus, intensive agriculture is a major driver of FS in many anthropized regions (Estevéz et al., 2019; Thorslund et al., 2021).

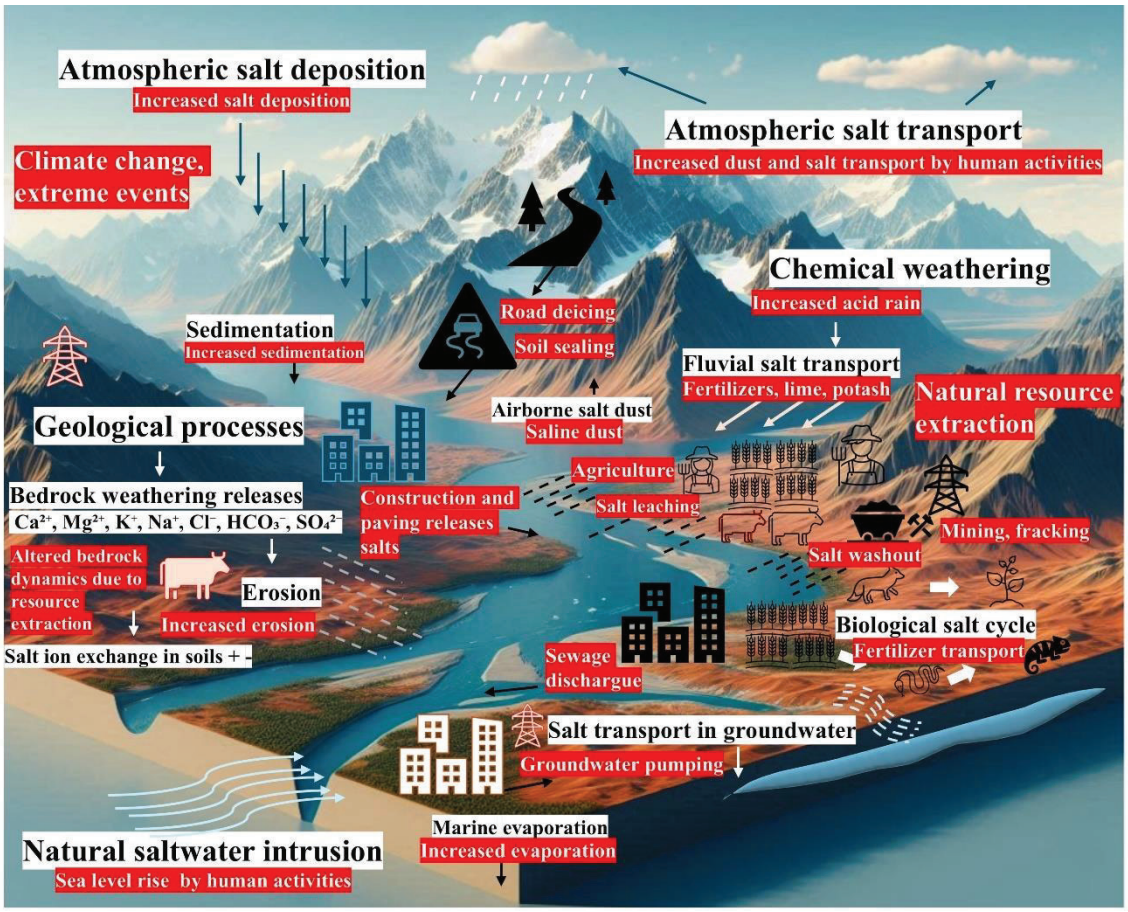


Figure 1. 2. Anthropic salt cycle: main sources, causes, transport, dynamics, and storage. Source: Created by the author based on Kaushal et al. (2023).

The use and application of agrochemicals, pesticides and fertilizers, as well as irrigation practices, accelerate the anthropogenic salt cycle by increasing the leaching and dispersion of salts into aquatic systems (Kaushal et al., 2018, 2021, 2023; Cañedo-Argüelles et al., 2013, 2016). Fertilizers, especially those high in potassium and chloride, contribute significantly to the salt load in streams and rivers (Kaushal et al., 2018, 2021, 2023). For example, it is estimated that approximately 50 kg of chloride per hectare per year is applied in agricultural fertilizers, though this can vary depending on agrifood system (e.g., crop type or livestock) and production techniques (David et al., 2016; Kaushal et al., 2023). Also, the use of irrigation exacerbates soil erosion by mobilizing salts previously stored in the soil. When irrigation water is saline, the evaporation process

further concentrates these salts in the soil, which could eventually be washed into rivers (Estevéz et al., 2019; Thorslund et al., 2021; Kaushal et al., 2024). This increased salt flux results from human-induced land use changes that not only accelerate natural processes of salt release and transport but also add additional salt, contributing to elevated salinity levels in surrounding freshwater resources (Figure 2).

Road de-icing

Road de-icing practices, particularly during winter and in the coldest regions of the world or high-altitude areas, contribute to the anthropogenic salt cycle by introducing large quantities of sodium chloride into the environment (Crowther and Hynes, 1977; Hintz and Relyea, 2017; Jackson and Funk, 2019; Niedrist et al., 2021; Kaushal et al., 2023). This runoff carries salts into freshwater systems, raising salinity levels (Roe and Patterson, 2014; Stoler et al., 2017; Szklarek et al., 2022; Tauber et al., 2021). Road salts can be transported to streams through conduits, subsurface piping, and preferential flow paths; diffusely through aquifers; and vertically as salt plumes through unsaturated zones and aquitards (Asensio et al., 2017; Brown and Yan, 2015; Kaushal et al., 2023). The extent of this transport depends on several factors, including the distance from the road to the river, the slope of the terrain, and seasonal variations such as snowmelt in spring or heavy rainfall, which can enhance salt runoff (Jackson and Jobbágy, 2005; Kelly et al., 2008; Laceby et al., 2019). For example, lateral salt transport in roadside soils occurs at a rate of 25-50 cm per day, while vertical salt transport occurs at a rate of 1.3-2.3 cm per day. The chloride mass input to aquifers averages 30 g per square meter per year (Jackson and Jobbágy, 2005; Kaushal et al., 2023). Moreover, during winter months or in cold regions, road salts can undergo aerosolization (i.e., salts becoming airborne as fine particles or droplets due to wind or traffic) (Kolesar et al., 2018; Kaushal et al., 2023).

This occurs due to the interaction between the fine nature of the applied salt particles, dry and cold winter conditions, vehicular traffic, and melting processes. These combined factors facilitate the suspension of salt particles in the air, contributing to atmospheric pollution and affecting air quality (Kolesar et al., 2018; Kaushal et al., 2024). The aerosolization of road salts into particulate matter impacts atmospheric salt fluxes, which can lead to the deposition of salt particles into water bodies and their dispersion over large areas. This disruption of the natural salt cycle is compounded by increased atmospheric deposition of salts from urban and industrial sources (Kaushal et al., 2023).

Natural resource extraction

Resource extraction (e.g. coal and potash mining, oil and gas production) also affects the salt cycle by altering groundwater dynamics and increasing FS (Cañedo-argüelles et al., 2016; Cañedo-argüelles, 2021, Kaushal et al., 2018, 2023). For instance, mining operations significantly contribute to FS through the extraction and weathering of mineral deposits (Cañedo-Argüelles et al., 2017; Rico-Sánchez et al., 2022; Vendrell-Puigmitja et al., 2022). Mining exposes geologically locked-up salts, accelerating their release into the environment (Kaushal et al., 2023). Additionally, mining waste, including tailings and runoff, can introduce high concentrations of salts into rivers and streams (Cañedo-argüelles et al., 2016). For example, the extraction of salt-rich materials such as limestone and dolomite for construction purposes results in approximately 22 billion tons of material being mined globally each year (Almeida et al., 2020; Kaushal et al., 2023). Also, mountaintop mining releases a range of salt ions from the bedrock, including Ca^{2+}, Mg^{2+}, K^{+}, Na^{+}, Cl^{-}, HCO_3^{-}, and SO_4^{2-}, exporting dissolved solids downstream at a rate of about 7600 kg ha^{-1} $year^{-1}$ (Kaushal et al., 2023, 2024). Hydraulic fracturing (fracking) can also introduce saline groundwater into surface water bodies, raising salinity levels

(Vengosh et al., 2014; Kaushal et al., 2019, 2023). Besides, the extraction processes and the disposal of brines and waste products contribute to increased salt concentrations in both surface and groundwater (which ultimately affects rivers) (Cañedo-Argüelles et al., 2017; Vendrell-Puigmitja et al., 2022; Kaushal et al., 2024). Overall, these alterations of the salt cycle occur at a much faster rate than natural weathering and erosion processes, leading to an accumulation of salts in aquatic systems.

Wastewater discharge

The discharge of saline wastewater from wastewater treatment plants (WWTPs) also contributes to the anthropogenic salt cycle (Kaushal et al., 2018, 2023, 2024; Cañedo-Argüelles et al., 2013, 2016). This is particularly relevant in regions where WWTPs lack the capacity to remove salts from wastewater, which can then be discharged into aquatic environments (Shon et al., 2006; Li et al., 2022). Municipal and industrial treated wastewater often contains elevated levels of chloride, sodium, and other ions (Duan et al., 2024; Zimmer et al., 2014). Salts present in consumer products and cleaning agents, such as Ca^{2+}, Mg^{2+}, K^{+}, Na^{+}, Cl^{-}, and SO_4^{2-}, are rapidly transported into freshwater systems, altering the natural salt flux. For example, the average release rates of these ions in domestic wastewater are: Ca^{2+}: 11,236 mg L^{-1}; Cl^{-}: 38,768 mg L^{-1}; K^{+}: 18,713.8 mg L^{-1}; Mg^{2+}: 3,528 mg L^{-1}; and Na^{+}: 90,629 mg L^{-1} (Albert, 2005; Moglia, 2008; Kaushal et al., 2023). When these salts reach WWTPs, they are usually not efficiently removed, especially in mid-sized and small cities that lack advanced technologies (Salcedo Moyano et al., 2022; Singh et al., 2022; Srivastava et al., 2021). Moreover, adopting treatment upgrades such as reverse osmosis systems to remove salts may not be feasible for all cities due to high costs, increased energy consumption, and the generation of problematic byproducts like brine (Malaeb and Ayoub, 2011; Pérez-González et al., 2012; Venkatesan

and Wankat, 2011). Consequently, salts from populated areas continuously enter the biosphere when humans consume food and beverages and excrete these salts through domestic wastewater. For instance, in the USA, the average daily intake of Na^+ is 3,400-4,000 mg per person, and the average daily excretion of Na^+ is 3,414-3,803 mg, plus additional contributions from cleaning products, pharmaceuticals, and personal care items. In the industrial sector, salt discharges into water bodies can be significant; for example, a microfabrication facility can discharge approximately 1,000 kg of Na^+ per day (Wallace et al., 2019; Kaushal et al., 2023). Also, while industries have their own treatment systems and strive to meet quality standards for contaminant removal, many of these systems do not include specific processes or strict regulations for salt removal (Moyano-Salcedo et al., 2021).

Although significant progress has been made in understanding various aspects of the anthropogenic salt cycle, the role of wastewater discharges remains a critical and understudied driver of salt pollution. Overall, most studies have focused on agriculture, mining, and road deicing, while the contribution of wastewater has received less attention (Cañedo-argüelles et al., 2016; Kaushal et al., 2018). For example, there is limited knowledge of salinity gradients associated with WWTPs, the effectiveness of salt removal based on treatment type, how salts affect treatment processes, and the seasonal dynamics of salinization driven by WWTPs.

Different drivers FS have received varying levels of attention depending on the region. For instance, road de-icing has been extensively studied in North America (Kaushal et al., 2005, 2018, 2021, Hintz et al., 2017, 2022, Hintz and Relyea, 2019), though it also occurs in Europe (Niedrist et al., 2021; Cañedo-Argüelles et al., 2021). In contrast, other regions like South America, Africa, and Asia remain largely underexplored

in terms of FS drivers, where information is still scarce. Also, while agriculture is often cited as a primary contributor to salt fluxes in rivers, its impact may differ across catchments, highlighting the need for a more comprehensive understanding of both natural and anthropogenic sources. It is crucial to expand our monitoring efforts to include less-studied areas and account for diverse factors such as geology, precipitation patterns, mining activities, and wastewater discharges (Figure 3) (Estevéz et al., 2019; Cunillera-Montcusí et al., 2022).

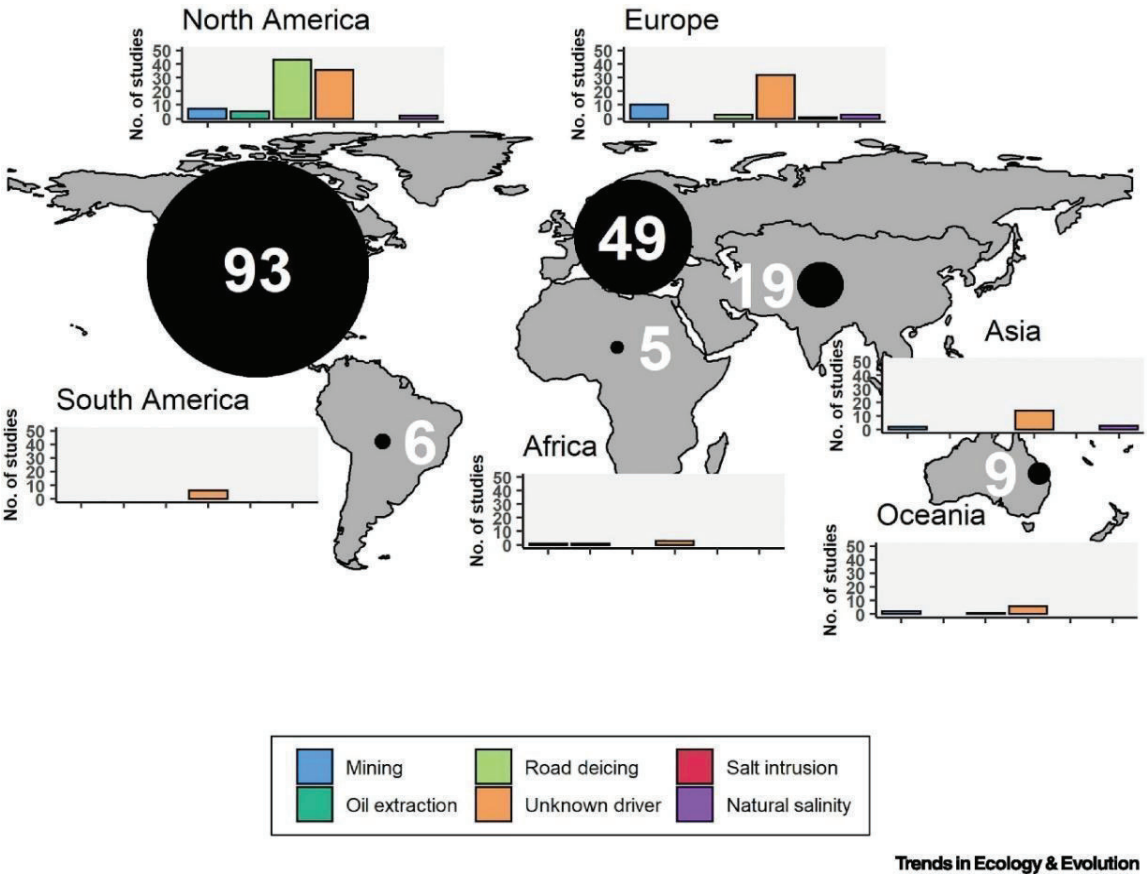


Figure 1. 3. A global overview of studies on salinization from 2017 to 2021, focusing on the causes of salinity changes within the examined systems (as indicated by bar plot colors), which include factors such as mining, road de-icing, saltwater intrusion, and oil extraction (e.g., fracking). Source: Cunillera-Montcusí et al. (2022).

To the complex dynamics of FS in different watersheds, it is vital to include both natural and anthropogenic drivers of salinity. These drivers (e.g. precipitation, salt

application in roads, irrigation of crops) experience strong temporal fluctuations that can modulate salt concentrations. However, most studies on FS are focused on short-duration experiments or snapshot field studies, thereby neglecting temporal dynamics (Tortajada et al., 2011; En Guo et al., 2019; Benjankar et al., 2021). It is important to assess the time of year when salts are introduced into freshwater ecosystems (e.g., seasonal variations) as well as sudden ion variations due to specific events (Benjankar et al., 2021). For instance, during intense rainfall, runoff can rapidly transport de-icing salts from roads into nearby rivers, leading to a sharp increase in chloride concentrations (Kaushal et al., 2021, Benjankar et al., 2021). Similarly, an uncontrolled industrial discharge of wastewater containing high levels of sodium and chloride can lead to a sudden spike in these ions in the receiving water body (Moyano-Salcedo et al., 2021). These factors can significantly impact the concentration and distribution of salts in freshwater ecosystems (Tortajada et al., 2011; En Guo et al., 2019). The extent to which ion concentrations fluctuate in time depending on anthropogenic factors such as the application of road salts during winter, fertilizer use, industrial discharges, mining activities, and wastewater discharge is far from being understood, especially when these factors are exacerbated by extreme climatic events like heavy rainfall and droughts (Estevéz et al., 2019; Thorslund et al., 2021; Benjankar et al., 2021). Conversely, droughts can concentrate salts due to reduced water volumes and increase the impact of anthropogenic activities by decreasing the dilution capacity of freshwater systems (Kaushal et al., 2021). Understanding these temporal variations is fundamental for predicting FS under future scenarios, including climate change scenarios. Also, integrating it is essential for developing effective management strategies that not only respond to average salinity conditions, but also adapt to salinity fluctuations (Cañedo-argüelles, 2021; Cunillera-Montcusí et al., 2022).

Furthermore, assessing temporal dynamics could improve our understanding of how aquatic species and entire ecosystems adapt to FS (e.g. phenological shifts), which is essential for the conservation of biodiversity in salinized aquatic ecosystems (Kefford, 1998; Kefford et al., 2003).

1.2. Freshwater salinization: state of the art and main knowledge gaps

In recent years, river salinization has gained increasing attention as an environmental issue, and several studies have evaluated its causes and impacts (Kefford et al., 2003; Cañedo-argüelles et al., 2016, 2017; Hintz and Relyea et al., 2019; Kaushal et al., 2018, 2021; Cunillera-Montcusí et al., 2022). These studies have not only assessed its effects on aquatic communities but have also adopted an integrated perspective, recognizing that the decline in water quality affects entire ecosystems and societies (Cañedo-argüelles, 2021; Kaushal et al., 2023, 2024). Thus, to better understand the dynamics of FS, it is essential to consider not only the drivers but also the myriad interactions across all trophic levels (e.g., algal and macroinvertebrate dynamics), with other pollutants and environmental and temporal variations (Cochero et al., 2017; Greco et al., 2023; Wang et al., 2023). For example, river salinization often co-occurs with nutrients from several activities such as agriculture, aquaculture, wastewater discharge (both municipal and industrial), the food industry (including wineries and breweries), energy systems (such as ethanol production), and construction (involving the use of cement and landscaping fertilizers) (Greco et al., 2023; Wang et al., 2023). However, accurate quantification of salinity parameters (e.g. electrical conductivity, ion concentrations) in the many rivers and streams affected by concurrent activities and pollutants at different temporal scales remains a challenge (Cochero et al., 2017; Cunillera-Montcusí et al., 2022).

Furthermore, the potential effects of such interactions, not only on ecosystems but also on operational processes and infrastructure, are poorly understood. For example, high salinity has been linked to adverse effects on materials such as asphalt and certain metals (i.e., corrosion), as well as on processes such as effective flocculation, sedimentation, or biological treatment in wastewater treatment plants (WWTPs) (Hamoda and Al-attar, 1995; Salvadó et al., 2001; Lee and Oleszkiewicz, 2003). This knowledge is critical not only in natural environments such as rivers, but also in contexts where water is used as a raw material and subsequent treatment is aimed at mitigating its impact on the environment and promoting reuse (Becerra-Castro et al., 2015; Bhide et al., 2021; Cunillera-Montcusí et al., 2022).

Comprehensive monitoring of water chemistry (e.g., in rivers, WWTPs), especially major ions (Na^+, K^+, Mg^{2+}, Ca^{2+}, Cl^-, SO_4^{2-}, SiO_3^{2-}), is crucial to monitor FS (Serra et al., 2017; Paul et al., 2018; Boutron et al., 2021; Lagarias and Stratigea, 2021). These ions serve to trace both natural and human drivers of river salinity and the potential interactions between them (Le Bonté et al., 2008; Cañedo-Argüelles et al., 2016; Kaushal et al., 2017). Also, electrical conductivity (EC), an indirect measure of total salts in water, has become a widely used parameter for estimating FS due to its practicality in monitoring, control, and cost-effectiveness (Cañedo-Argüelles et al., 2016; Kaushal et al., 2017). However, it is important to recognize that EC may oversimplify the complex dynamics of FS. Therefore, effective measurement and regulation of both EC and major ions is critical to assessing the impact of FS on aquatic ecosystems and other processes (e.g., industry, WWTPs) and ensuring water quality for various uses (Serra et al., 2017; Cañedo-Argüelles et al., 2016; Paul et al., 2018).

Despite the growing importance of FS and efforts to understand its dynamics and impacts, it remains an understudied and underrepresented topic in water quality monitoring programs in some countries (Cañedo-Argüelles et al., 2016; Lagarias and Stratigea, 2021). As a result, obtaining comprehensive data on both major ions and EC can be challenging and varies from region to region (Meybeck, 2003; Hartmann et al., 2014; Thorslund and Vliet, 2020; Cunillera-Montcusí et al., 2022). Moreover, when salinity data is available, it is often difficult to match this information at a spatiotemporal scale with environmental and meteorological data, which is crucial for addressing salinity dynamics (Hartmann et al., 2014; Thorslund and Vliet, 2020). Therefore, it is critical to collect and standardize existing data that integrate salinity and environmental variables across diverse regions and temporal scales to ensure the consistency and reliability of water quality monitoring programmes (Meybeck, 2003; Hartmann et al., 2014; Thorslund and Vliet, 2020). Enhanced data collection and harmonization would facilitate the evaluation of FS dynamics and improve our understanding of its impacts on ecosystems and infrastructure, leading to more effective management and mitigation strategies (Thorslund and Vliet, 2020).

Overall, FS is a global environmental issue that is still poorly understood and, therefore, not properly managed. Within this context, the present doctoral thesis aims to address some of the most critical knowledge gaps related to FS, providing data, scientific evidence and recommendations that can serve to inform management and policy decisions. The following sections include a description and the objectives of each chapter.

1.3. Introduction to Chapter I: GLOBal river SALiniTy and associated ions (GlobSalt)

Currently, there are diverse and varied sources of information on salinization (e.g. electrical conductivity, concentrations of major ions) and associated environmental and geoclimatic variables, such as monitoring programs or geographic information systems (Pettorelli et al., 2018; Thorslund and Vliet, 2020; Benjankar et al., 2021). In countries where periodic water quality measurements are conducted in rivers, these monitoring programs often make this information easily accessible and publicly available (Meybeck, 2003; Hartmann et al., 2014; Thorslund and Vliet, 2020). However, this is not the case in all countries, nor for all watersheds within the same country, leading to significant variability in the availability of spatial and temporal data worldwide (i.e., there are watersheds and countries with very good information and areas for which no data is available) (Thorslund and Vliet, 2020). Also, not all countries measure the same parameters, with some only measuring EC, others only measuring salinity, and some also having information on certain ions such as chloride (Meybeck, 2003; Hartmann et al., 2014; Thorslund and Vliet, 2020). An even more concerning issue is that, in places where information is available, much of it is not integrated or utilized in FS assessments (Cunillera-Montcusí et al., 2022). Therefore, compiling and harmonizing a global database that includes salinization parameters, water quality data, and additional environmental and meteorological variables is crucial. This effort would address the challenges posed by inconsistent data coverage and help create a more comprehensive understanding of salinization trends and impacts worldwide (Le Bonté et al., 2008; Hartmann et al., 2014). It is also important to highlight the significant variation in how data is presented (e.g., variations in reported parameters, units, and spatiotemporal

resolution), the measurement methods used, and the detection limits for each parameter, which hinders their use (Ros Sum, 1946; McCleskey et al., 2012; Le Bonté et al., 2008).

Although there have been considerable efforts to compile and harmonize water quality information, including salinity parameters, at a global scale, a significant portion of this information remains scattered (Meybeck, 2003; Hartmann et al., 2014; Thorslund and Vliet, 2020). There are few globally available databases that can effectively identify spatial patterns (e.g., hotspots of freshwater salinization) and temporal variations (e.g., how salinization changes over time) in FS (Meybeck, 2003). Moreover, some of these databases with global information on FS are fragmented by specific regions and time periods, resulting in an unharmonized distribution across sites. For instance, databases such as the Global Occurrence of Major Elements (excluding EC measurements) and the GLORICH database provide data on major ions and other physicochemical parameters of water, but they require updates due to persistent spatial and temporal gaps (Meybeck, 2003; Hartmann et al., 2014). Similarly, the Thorslund and Vliet (2020) database primarily focuses on EC and lacks data on specific ions and other water quality parameters essential for understanding and managing the effects of freshwater salinization syndrome (Kaushal et al., 2019; 2021).

It is important to emphasize efforts to not only implement monitoring programs and measure water quality parameters (e.g., salinity, nutrients), but also to establish global databases of these quality parameters, especially those related to river salinization and across sectors (e.g., industry, WWTPs, agricultural catchments) (Cañedo-Argüelles et al., 2016). Global data sets are an essential first step in developing predictive models of water salinity and formulating effective management strategies at local, regional, and global scales (Cañero et al., 2002; Melesse et al., 2020). Furthermore, along with these

comprehensive compilations of global water quality data, it is imperative to identify the primary drivers of salinity increase, distinguishing the contributions of both natural phenomena and human activities (Kaushal et al., 2023). Analyzing the natural and anthropogenic salinity cycles in rivers on a global scale with the available data represents a significant challenge, but also opens avenues for future research using advanced computational technologies (Irrgang et al., 2021.; Tiyasha et al., 2020). This will allow the development of salinity prediction models under current and future scenarios (Le et al., 2019; Zhao et al., 2020). Understanding these spatio-temporal salinity dynamics, including how natural and anthropogenic salt cycles interact with environmental and climatic variables, communities (both biological and social), and other pollutants, may be one of the most promising approaches to manage and mitigate salinity problems, particularly in areas where it is increasingly critical to prevent river salinization (Cañedo-Argüelles et al., 2016; Kaushal et al., 2023)

Global river salinity dynamics highlight the intricate interplay between natural processes and human activities, underscoring the complexity of FS. This recognition has led to a growing interest not only in understanding how human activities drive spatial and temporal variations in river salinity, but also in elucidating how FS interact with other environmental factors and pollutants (Estevéz et al., 2019; Thorslund et al., 2021; Wang et al., 2023). However, addressing FS requires an understanding of the enormous complexity associated with hydrological systems at the scale of each watershed context, highlighting the need for increased efforts to fill gaps in river dynamics at the local scale. This complexity extends not only across regions (e.g., rivers in Australia compared to those in Europe or USA), but also within countries. For example, rivers in the Mediterranean climate may have different dynamics than those in northern Spain (Munoz

and Prat, 1994; Machado et al., 2011; Belmonte and Beltrán, 2001; Casquin et al., 2020). Thus, the lack of availability of information on basin characteristics, especially with respect to FS, further complicates the task and underscores the importance of targeted efforts to address this local knowledge gap. Only by focusing on these efforts can we generate reliable data and insights that can serve as robust input to global-scale models.

In this chapter, publicly available information from environmental agencies, research centers, universities, and more than 60 global information sources are evaluated for the collection, standardization, harmonization, and integration of salinization parameters, water quality data, and environmental variables into a global dataset called GlobSalt. Moreover, potential salinization hotspots are evaluated based on global average EC levels, their temporal variations, data distribution, including the balance of information obtained by country (e.g., amount of data per km^2), identification of potential outliers, and correlation of EC with major ions. This database, covering the period from 1980 to 2024, aims to provide organized and up-to-date spatial and temporal data for researchers and managers, especially in regions with limited information (e.g., Africa and South America). The chapter describes the steps and methods used to create and interpret this comprehensive dataset and discusses its potential applications for advancing research and policy in salinized watersheds.

1.4. Introduction to Chapter II: Human activities as drivers of temporal changes in salinity

So far, research on FS dynamics has primarily focused on understanding the critical salinity and ion concentrations that affect freshwater biodiversity and ecosystem functioning, largely neglecting the temporal dynamics of FS **(**Kefford et al. 2003; Horrigan et al. 2007, Birk et al., 2020). Most research has centered on short-term

laboratory experiments or snapshot field studies, overlooking the long-term temporal variability of FS (Timpano et al., 2018; Niedrist et al., 2021). Moreover, there has been limited investigation into the interaction between FS and specific natural variables that vary seasonally, such as temperature, flow rate, and precipitation (Timpano et al., 2018; Perri et al., 2022). Also, the temporal dynamics of FS can be impacted by climate change and extremes, resulting in increased or decreased impact of salinity peaks on ecosystems (e.g., greater when there are fires and droughts, compared to floods) (Machado et al., 2011; Kaushal et al., 2018; Des et al., 2021).

Although there is little information about the analysis of how human activities disrupt the temporal dynamics of FS, emerging evidence suggests that different human activities have distinct 'temporal signatures' that influence the temporal patterns of salinity in freshwater systems (Crosa et al. 2006; Cañedo-Argüelles et al. 2012; Kulmatov et al. 2020). For instance, in agricultural regions, the temporal dynamics of salinity are closely linked to cropping practices and seasonal variations (Timpano et al., 2018; Estévez et al., 2019). Thus, salinity is strongly driven by irrigation during low-flow periods in agricultural catchments, with conductivity peaks likely to occur during planting or fertilizer application periods (Crosa et al., 2006; Kulmatov et al., 2020). Similarly, in mining regions, heavy rainfall events can leach salts (e.g., from stockpiled residues) into surrounding surface waters, leading to sharp, unexpected, and repeated increases in salinity (Cañedo-Argüelles et al. 2012; Sauer et al., 2016). In cold regions, salt applied to roads for deicing purposes contributes to increased salinity in nearby rivers and streams, especially during periods of snowmelt and snow removal (e.g., spring) (Ruth, 2003; Niedrist et al., 2021). Urban areas also contribute significantly to temporal changes in FS through wastewater discharge, especially during the summer when most streams are low-

flow (e.g., in arid or flat regions where snowmelt does not affect stream flow) (Levlin, 2007; van Vliet and Zwolsman, 2008). However, the effect of wastewater discharges on temporal FS may be influenced by several factors, including the use of consumer products and the limited ion removal capacity typically installed in wastewater treatment plants (Moyano-Salcedo et al., 2021).

Understanding the temporal dynamics of salinity is critical because it can strongly influence the structure and functioning of aquatic communities. For example, the sensitivity of macroinvertebrate communities to increases in salinity depends largely on the timing of these changes, as each developmental stage of the species has a different tolerance to salinity (Bailey et al., 2004; Hassell et al., 2006; Kefford et al., 2007). Salinity tolerance can vary considerably between these stages, with eggs and larvae often more sensitive to salinity changes than later stages (Kefford et al., 2007). Therefore, macroinvertebrates may be more sensitive to temporal changes in salinity during their early developmental stages when they are more vulnerable and exposed to repeated salinity fluctuations (Hassell et al., 2006; Kefford et al., 2007). These changes often occur at specific times, such as spring, when egg deposition is more common and salinity sensitivity is higher compared to later stages (Crosa et al., 2006; Kefford et al., 2003, 2007). Also, many invertebrates that feed on leaf litter are particularly sensitive to salinization, which can affect their survival and consequently the dynamics of the aquatic community (Bailey et al., 2004; Kefford et al., 2011). This may also have implications for ecosystem functioning, as aquatic invertebrates contribute to the carbon cycle by decomposing leaf litter (Canhoto et al. 2021). Therefore, these temporal effects of FS dynamics could be extended not only to other aquatic communities, but also to entire ecosystems and humans (Kaushal, 2016; Cañedo-Argüelles, 2021).

Given the potential distinct 'temporal signatures' of salinity variations driven by different human activities, it is essential to tailor monitoring systems to capture these specific patterns effectively (Schuler et al., 2019; Hintz et al., 2022; Kelly et al., 2024). Monitoring efforts should be strategically designed to align with the timing and intensity of the salinity fluctuations unique to each activity (Schuler et al., 2019; Kelly et al., 2024). For instance, in areas affected by road salts, continuous EC monitoring during snowmelt periods may be necessary, while in agricultural regions, intensified monitoring during planting and fertilizer application periods will help to capture the associated salinity spikes (Kelly et al., 2008; Estévez et al., 2019; Hintz and Relyea, 2019, 2017). In mining areas, the focus should be on the rainy season, when the risk of sharp increases in salinity due to runoff is highest (Cañedo-Argüelles et al., 2017, 2012; Rico-Sánchez et al., 2022). Urban areas might require more frequent monitoring during low-flow periods, especially where wastewater discharges are significant (Moyano-Salcedo et al., 2021; Singh et al., 2022). By adapting the frequency and placement of monitoring stations according to these specific temporal patterns, decision-makers can better manage and mitigate the impacts of temporary freshwater salinization (Cunillera-Montcusí et al., 2022; Kelly et al., 2024). Moreover, further research into the responses of aquatic communities to both average EC levels and short-term peaks is crucial for developing more effective biological indicators and improving the resilience of freshwater ecosystems (Kefford et al., 2007; Cañedo-Argüelles, 2021).

In this chapter, the temporal fluctuations of salinity driven by several human activities (e.g., agriculture, mining, road de-icing, and wastewater discharge) are evaluated at an interannual scale using high temporal resolution data from 91 Spanish river monitoring stations. Moreover, the relationship between these activities, EC peaks,

and environmental variables is assessed to examine how these drivers contribute to salinity variations in the selected watersheds. The chapter describes the steps taken to collect salinity parameter data, as well as the load (expressed in parts per million or percentage) of the different drivers within the area of influence of the monitoring stations, and environmental variables such as precipitation and geology. Also, the methods used to analyze and interpret these temporal EC variations are presented, along with a discussion of their potential implications for aquatic communities. The chapter also highlights the need for improved monitoring programs that incorporate finer temporal resolution, as well as research and policy developments aimed at managing and controlling FS fluctuations.

1.5. Introduction to Chapter III: Freshwater salinization and eutrophication: interactive effects on aquatic biofilm and macroinvertebrates

The responses of aquatic communities to the effects of FS extend beyond the toxic effects of salinity because they are modulated by its interaction with other stressors (Velasco et al., 2019; Tockner et al., 2010; Markert et al., 2022). As noted above, FS often coincides with multiple stressors, including climate change, eutrophication, and pesticide contamination, but despite efforts, little is known about how salinity interacts with these stressors (Velasco et al., 2019; Birk et al., 2020).

This task requires accurate knowledge of the magnitude, and potential interactive effects of the stressors and pollutants involved, as well as an understanding of the environmental characteristics of the receiving river or stream (Aristi et al., 2016; Romero et al., 2019; Pereda et al., 2021). In practice, achieving a clear separation of each stressor

is a significant challenge (Aristi et al., 2016; Velasco et al., 2019). This is due to the multitude of natural and anthropogenic drivers and contaminants (some of which are not fully known) and their temporal variability interacting in surface waters (Romero et al., 2019; Pereda et al., 2021). Therefore, analyzing the interactive effects of contaminants on aquatic communities in controlled environments (e.g., artificial channels or mesocosms recreating natural environments) is a strategy that can provide an initial basis for understanding these dynamics (Martin, 2001; Cañedo-Argüelles et al., 2014; Cotta et al., 2023). However, mesocosms also present disadvantages because they fail to adequately represent the complexity of natural ecosystems (e.g., habitat heterogeneity, community adaptation) (Martin, 2001). Moreover, in the case of human activities, it is imperative to understand what type of contaminant is being released, its levels, characteristics (e.g., mobility, reactions), and interactions (e.g., synergistic, cumulative) to anticipate how it might interact with salinization (Cañedo-Argüelles et al., 2012; Jackson and Funk, 2019; Silver and Donini, 2021).

Agriculture, and wastewater discharges (from cities, industries, agro-industries, etc.) are the main drivers for the co-occurrence of nutrient and salt pollution (Larson and Belovsky, 2013; Cochero et al., 2017; Estevéz et al., 2019; Bhide et al., 2021). In agriculture, the application of fertilizers and agrochemicals results in diffuse discharge of nutrients and salts (e.g., through irrigation return flows) (Pereda et al., 2021; Li et al., 2021; Luna Juncal et al., 2023). This dispersion is influenced by various factors (e.g., rainfall, soil water content, topographic slope), making it challenging to control and predict their effects effectively when reaching rivers (e.g., from diffused agricultural wastewater discharge) (Kaushal et al., 2018; Bolan et al., 2024). Urban wastewater discharges typically occur at specific points, resulting in a concentrated presence of salts

and nutrients in the immediate vicinity (Moyano-Salcedo et al., 2021). This localized concentration can lead to increased salt and nutrient levels and their interactions, potentially causing greater impacts on the surrounding area (Bernhardt et al., 2008; Moyano-Salcedo et al., 2021; Shelton et al., 2024). This, in turn, can make control measures (e.g., through the use of WWTPs) and prediction more effective (Bernhardt et al., 2008; Moyano-Salcedo et al., 2021). However, it is important to note that in areas where WWTPs have been implemented, they are primarily designed to effectively remove organic matter and nutrients, although some small and medium-sized cities lack nutrient removal processes (Di Giacomo and Romano, 2022; Salcedo Moyano et al., 2022). Moreover, although WWTPs are not installed to remove salinity, their physicochemical and biological processes can indirectly remove certain concentrations of ions (Salcedo Moyano et al., 2022)

Therefore, the impact of salt and nutrient load on freshwater ecosystems varies depending on agricultural and industrial practices, climate factors, and the efficiency of wastewater treatment plants (Lind et al., 2018; Velasco et al., 2019; Birk et al., 2020). Most studies on FS have focused on its interaction with temperature, pesticides, and metals, while the interaction between salt and nutrient enrichment has received less attention, particularly in rivers and across different trophic levels (Velasco et al., 2019; Birk et al., 2020). However, available research suggests that both synergistic and antagonistic relationships between nutrients and salts are possible, depending on community tolerance and cascading effects (Lind et al., 2018; Osburn et al., 2022).

For example, increased salt pollution may promote algal growth by reducing the abundance of certain organisms (e.g., reduction in copepod abundance), while nutrient pollution enhances algal growth independently (Hintz et al. 2017; Lind et al. 2018; Greco

et al., 2021, Silver and Donini, 2021). Yet, some algal species may be negatively impacted by salt pollution, leading to complex effects on primary production and trophic structure (Lind et al., 2018; Osburn et al., 2022; Zadereev et al., 2023). These changes can influence aquatic invertebrates, with some studies suggesting that nutrient enrichment may mitigate the toxic effects of salt on certain species (e.g., predators, or salinity tolerant species that can become dominants (Brown and Yan, 2015; Isanta-Navarro, et al., 2021; Greco et al., 202). However, research on the interactive effects of salt and nutrient pollution on stream invertebrates has yielded conflicting results. Some studies have documented declines in benthic macroinvertebrates due to synergistic effects, while others suggest antagonistic effects (Braukmann and Böhme et al., 2001; Schröder et al., 2015; Encina-Montoya et al., 2020). For example, nutrients may counteract the effects of salt to some extent by providing energy and potentially greater resistance, especially in dominant species (Braukmann and Böhme et al., 2001; Schröder et al., 2015).

In this chapter, the response of algal and macroinvertebrate communities to the interactive effects of nutrient and salt pollution is evaluated using microcosms (i.e., small artificial channel systems). Therefore, the diversity and abundance of the communities exposed to different treatments, where various levels of salt and nutrients were combined, are assessed. The chapter describes the steps taken to collect communities from the Llobregat River, their adaptation to the microcosms, and the effects of treatment exposure over time under controlled environmental conditions. It also outlines the methods used to analyze and interpret community responses and interactions and discusses the potential implications for aquatic ecosystems. The chapter emphasizes the importance of understanding the complex interactions between salt and nutrient pollution across

different trophic levels, which is crucial for the effective management and conservation of freshwater ecosystems.

1.6. Introduction to Chapter IV: Salinization in WWTPs: effects on microbial communities and pollutant removal efficiency

Wastewater treatment is a critical global challenge that is constantly evolving through ongoing research and implementation. However, the dynamics of salinity within full-scale WWTPs, particularly its effects on microeukaryotic communities (e.g., protozoa) and their impact on pollutant removal, are not yet fully understood. Salinity in the influent can significantly impact WWTP functioning by disrupting microbial communities (acting as a toxic agent on taxa), affecting treatment processes such as sedimentation, and damaging WWTP infrastructure (Salvadó et al., 2001; Cui et al., 2015; Wang et al., 2020). These disruptions can lead to reduced overall pollutant removal efficiency, thereby increasing not only the amount of salt reaching rivers but also the levels of other contaminants, such as nutrients.

WWTPs are increasingly burdened with saline wastewater from a variety of sources, including domestic, industrial, and agricultural activities (Thorslund et al., 2021; Moyano Salcedo et al., 2023). Thus, urban wastewater can collect liquid (i.e., from unit-type sewers) not only from domestic activities but also from raw materials used in construction (e.g., highway paving and building expansion wastes), transportation maintenance (e.g., road de-icers, salts from asphalt wear), and a large number of industrial facilities (e.g., food additive, cosmetic, and cleaning product industries) (Moyano-Salcedo et al., 2021; Singh et al., 2022; Kaushal et al., 2023). For example, annually, approximately 360 km^3 of wastewater with variable salinity levels is produced, but only 11% of this is treated and reused, 41% is treated and discharged, and a significant 48% is

released untreated into the environment (Jones et al., 2021). However, despite the presence of conventional and advanced WWTPs in large, medium, and small cities, there is limited information on the ion and EC load in the influent, salinity dynamics within urban WWTPs, and the rates of ion removal. Thus, the amount of salt entering and leaving WWTPs and flowing into rivers, as well as its interaction with treatment processes, is not well understood. In areas lacking sewage systems and WWTPs, which account for approximately 48% of the global population (WHO and UNICEF, 2024), uncontrolled discharges release pollutants, including salts.

Furthermore, it is important to consider not only the typical average concentrations of salinity entering WWTPs, but also how these levels can vary between regions and seasons. For instance, the concentration of salt ions in wastewater can increase due to the use of water softeners in regions with hard water (Kelly et al., 2008; Venkatesan et al., 2011), or from salt used for frost prevention in municipalities with combined sewer systems, leading to seasonal salinity peaks during winter months (Niedrist et al., 2021; Moyano Salcedo et al., 2023). In coastal areas, salinity variations can also occur due to seawater intrusion during high tide seasons (Berde and Jolis, 2021; Egea-Corbacho et al., 2021). These salinity variations could have different temporal impacts on WWTPs communities, influenced by several factors (Salvadó et al., 2001). For instance, temperature changes can lead to shifts in microbial community composition, with greater diversity expected during warmer months compared to cooler ones (Sun et al., 2021; Peces et al., 2022). This, in turn, could influence the resilience and response of certain communities.

Given the challenges posed by increasing salinity, WWTPs are essential for preserving water quality on a global scale. To effectively address these challenges, it is

critical not only to expand the coverage of sanitation systems, but also to find economically and environmentally viable technologies for upgrading existing conventional treatment plants, including those in small and medium-sized cities, as well as for future facilities (Honey-Rosés et al., 2014; Srivastava et al., 2021). For example, high loads of salt may force the upgrade of WWTPs with advanced treatment such as reverse osmosis and membrane treatments to meet water quality standards (Honey-Rosés and Schneider, 2014). However, these treatment systems are expensive, energy-intensive, have a short lifespan (e.g., membrane system), and produce brines with very high salinity, which poses an environmental challenge associated with its safe disposal into the environment (Malaeb and Ayoub, 2011; Pérez-González et al., 2012). Alternatives have been proposed to integrate regenerated wastewater from WWTPs with seawater reverse osmosis (SWRO) desalination, recovering energy while eliminating salts through these systems in regions subjected to water scarcity (Gómez-Coma et al., 2020; Sampedro et al., 2023). However, this upgrade of urban WWTPs still needs greater attention and investment on a global scale, and the challenges are still enormous even for places with water scarcity and the economic capacity to do so (Salcedo Moyano et al., 2022; Sheikh et al., 2023). Consequently, most urban WWTPs use indirect approaches to manage salt, such as standard physicochemical and biological processes, and often neglect to track variations in salinity and their effects on microbial communities.

Understanding how microbial communities are modulated by salinity is crucial, as it can significantly impact pollutant removal. However, existing studies offer conflicting information about the extent of this influence. For example, it has been reported effects on community composition, abundance, diversity, and function of microorganisms due to increased salinity (e.g., loss of taxa during high salinity levels) in

laboratory experiments (Uygur and Kargi, 2004; Wang et al., 2005; Hosseiniyan Khatibi et al., 2019) (Table 1.1). Conversely, some studies have not observed significant effects of saline wastewater on pollutant removal, provided that there is no impact on the colonization of microeukaryotic species associated with efficient contaminant removal (Table 1.1).

Moreover, it has been reported that the efficiency of wastewater treatment when there is high conductivity depends on many factors such as the type of treatment (Begmatov et al., 2022), the bacterial community acting or inoculated (Sivaprakasam, et al., 2008), operating conditions and acclimatization and tolerance of individuals responsible for the pollutant removal (Zhao et al., 2016; Hou et al. 2019). For instance, in systems where biofilm formation is favored, such as BF-MBR, biofilms have been discovered to provide protection to microorganisms in hostile environments (i.e. exposure to antimicrobial agents, UV light) (Simões et al., 2010). Furthermore, it has been reported that the variation in operating conditions of dissolved oxygen concentration in activated sludge is the main factor influencing changes in diversity (i.e. Shannon, Chao1) and richness of communities (Jin et al., 2023; Moyano-Salcedo et al., 2021).

Table 1. 1. Salinity Effects on Wastewater Treatment Processes: A comprehensive review and summary of studies on the impact of salinity in wastewater treatment.

Salinity level in wastewater	Observed effect on WWTP process	WWTP system	Reference
10 g L^{-1} and 30 g L^{-1} NaCl	Increased salinity did not affect pollutant removal efficiency, did not inhibit biomass growth, and favored salt-tolerant species.	Bench-scale, completely mixed reactors	Hamoda and Al-attar, 1995
0.4, 3, 5, 10, 20, and 40 g L^{-1} NaCl	Salinity affected microeukaryotic communities, with ciliates reduced	Sequencing-scale batch reactors (SBRs)	Salvadó et al., 2001

Salinity level in wastewater	Observed effect on WWTP process	WWTP system	Reference
	at 20 g L^{-1} and absent at 40 g L^{-1} NaCl.		
0- 6% (w/v) salt in reactor	Decreased COD, NH_4-N, and PO_4-P removal efficiency with increased salinity.	SBRs	Uygur and Kargi, 2004
0.1, 0.5, 2, 5, 10 and 20 g L^{-1} NaCl	TOC removal efficiency drops with higher NaCl concentrations.	Completely mixed batch reactors	Wang et al., 2005
5 and 40 g L^{-1} NaCl	Ammonia oxidizers inhibited at 40 g L^{-1} NaCl. Lower microbial diversity under high salt.	SBRs	Moussa et al., 2006
10, 20, and 40 g L^{-1} NaCl	Microbial diversity decreased with higher salinity and community structure significantly altered.	SBRs	Wu et al., 2008
0, 3.7, 24.1, and 44.1 g L^{-1} NaCl	Decreased enzymatic activities and COD/BOD_5 removal with increasing salinity.	Submerged fixed-bed bioreactor	Cortés-Lorenzo et al., 2012
40 g L^{-1} NaCl	NH_4-N removal improved at low NaCl load but inhibited at higher salinities.	Submerged Biofilter Reactor	Aslan and Simsek, 2012
1.93, 3.58, and 4.83 psu	Increased diversity and abundance of ammonia-oxidizing bacteria with reduced salinity.	Conventional activated sludge plant	Wu et al., 2013
0.02 to 3.02% (W/V) NaCl	Elevated salinity inhibited aerobic PAO metabolism and energy efficiency.	SBRs	Wells et al., 2014
0.2 to 6.6 g L^{-1} NaCl	Increased NaCl disrupted floc structure, reducing size and stability.	SBRs	Cui et al., 2015
0 to 20 g L^{-1} NaCl	Reduced microbial richness and COD/NH_4-N/PO_4-P removal efficiency by 45% at 20 g L^{-1} NaCl	SBRs	Chen et al., 2018

Salinity level in wastewater	Observed effect on WWTP process	WWTP system	Reference
30 and 70 g L^{-1} NaCl	Reduced BOD_5 removal efficiency, nitrification and denitrification recovered after 5 days of salinity acclimatation.	Aerobic granular sludge (AGS) and flocculent activated sludge (FAS)	Corsino et al., 2018
0.6, 14, and 20 g L^{-1} NaCl	Decreased biofilm coverage at high salinity, with taxa such as *Pseudomonas* and *Planococcus* showing sensitivity and tolerance to NaCl, respectively.	Moving Bed Biofilm Reactor (MBBR)	Wang et al., 2020
Intermittent salinity peaks (road salt) 1 and 3 g L^{-1} NaCl	Increased microbial activity below 1 g L-1 NaCl. 30% inhibition at 1-3 g L^{-1} NaCl	Conventional activated sludge plant	Tauber et al., 2021
0 to 60 g L^{-1} NaCl	High concentrations of NaCl regulated cell motility, transcription and membrane transport functions.	Anoxic–oxic (A/O) biofilm reactor	Ji et al., 2021
20-60 g L^{-1} NaCl	High salinity reduced microbial diversity; oxic microorganisms more tolerant than anoxic.	Anoxic–oxic (A/O) reactor	Chen et al., 2023
0, 5, 10, and 20 g L^{-1} NaCl	Elevated salinity reduced COD removal efficiency; microbial shift to salt-tolerant species.	Anaerobic membrane bioreactor (AnMBR)	Wang et al., 2023
0%, 1%, 2%, and 3% NaCl	High salinity reduced microbial diversity and led to less efficient treatment performance.	SBRs	Ya et al., 2023
91.3 g L^{-1} NaCl	Salinity altered microbial groups but bioaugmentation offset these effects, improving efficiency.	Activated sludge industrial wastewater plant	Wen et al., 2022

However, it is worth noting that the vast majority of studies addressing the impact of salinity on the biological community have primarily simulated industrial effluents characterized by exceedingly high salinity levels (e.g. from 30 to 60 g L^{-1}), employing advanced treatment processes (e.g., reverse osmosis, RO or nanofiltration, NF) (Wang et al., 2020; Zhao et al., 2022; Chen et al., 2023). These experiments have neglected EC ranges and their effects in conventional municipal wastewater treatment plants that generally do not have such extreme salinities (> 20 g/L) (Wang et al., 2005). Salinity levels in urban WWTPs can vary depending on the size and hydro-sanitary design of cities, consumption patterns, season of the year, percentage of contribution from sectors other than domestic, climate and other environmental factors (Hughes et al., 2021; Obaideen et al., 2022).

Salinity tolerance of taxa in activated sludge can vary among different groups involved, as well as among different families, genus, and species within the same group (Salvadó et al., 2001; Correa-Galeote et al., 2021). For example, salinity effects were found to be a lethal agent primarily affecting protozoa and metazoa, with relatively little effects on bacterial activity (Moussa et al., 2005). Thus, some studies have reported that most of the microeukaryotic population (e.g. rotifers, nematodes) is strongly reduced or even disappears when the salinity exceeds a certain concentration (Wang et al., 2005; Salvadó et al., 2001). For example, studies have shown that ciliates have the ability to self-regulate their internal ionic composition, and their tolerance limits to salt in activated sludge vary widely (from 3 to 10 g/L NaCl) depending on the duration of exposure (Salvadó et al., 2001; Moussa et al., 2005; Lefebvre and Moletta, 2006). Moreover, among these ciliates, *Vorticella spp*. and *Opercularia articulata* have shown greater resistance to higher NaCl concentrations compared to other ciliates (Salvadó et al., 2001).

Also, ciliates and flagellates have shown greater resistance to other inhibitors, such as metronidazole, than rotifers and nematodes (Lee et al., 1985; Lee and Oleszkiewicz, 2003).

In the fourth chapter, the dynamics of EC (used as a proxy for salinity) are evaluated within seven urban WWTPs and their effects on protozoa communities are assessed, with a particular emphasis placed on salinity peaks, and salinity implications for pollutant removal efficiency. Additionally, the protozoa community is used as a biomonitoring method to understand the impacts of salinization on WWTPs, due to its role as a filtering community responsible for the elimination of suspended solids, as well as its use as a bioindicator for monitoring effluent quality. Finally, the salinity load reaching WWTPs is presented and discussed (i.e., the concentration and variation of salinity), and the efficiency of salt removal is examined based on the type of conventional treatment applied (e.g., sequential batch reactor, activated sludge reactor). The effects on protozoa composition, structure, and interactions are also analyzed, along with how the processes and reactions required for organic matter and nutrient removal influence salinity dynamics in WWTPs, and how salinity conditions, in turn, affect pollutant removal.

2. OBJECTIVES

Salinization of rivers is a global environmental issue caused by a wide range of human activities. Despite extensive efforts to understand the effects of salinization on aquatic ecosystems in various regions, there are important knowledge gaps that need to be addressed. For example, most research has focused on North America, Europe and Australia, with Asia, Africa, and South America being far less explored. Also, most studies have neglected the temporal variability of FS and while some drivers of salinization (agriculture, resource extraction and road de-icing) have received considerable attention, others (e.g. WWTPs) have rarely been studied. Within this context, this thesis addresses notable information gaps regarding: i) river salinization patterns and their temporal variability across different regions of the world; ii) seasonal variations in salinization and their relationship with human and natural drivers; iii) the interactions between salinization and other prevalent river contaminants, such as nutrients; and iv) the impact of salinization on WWTPs functioning and their role as a driver of river salinization.

The **main objective** of this thesis is to evaluate the main causes and consequences of river salinization, with a special focus on urban wastewater treatment. Based on the findings, this research aims to propose management strategies that address the prevention and control of salinization in aquatic ecosystems and inform future studies and research directions. The **specific objectives** of this research are to:

I. Provide a global database that integrates river salinity parameters and both primary natural and anthropogenic drivers of freshwater salinization and examine the patterns and temporal variability of river salinization across different regions of the world.

II. Describe the seasonal dynamics of the main sources of salinization (mining, transportation, agriculture, urban wastewater discharges) and their impact on the temporal variability of salinity in Spanish rivers.

III. Determine the effect of the interaction between nutrient and salt enrichment on the river ecosystem, through experiments in artificial channels.

IV. Assess the impact of increasing salinity on microbial communities and pollutant removal in urban wastewater treatment

The objectives achieved are presented in the following chapters: “GLOBal river SALiniTy and associated ions (GlobSalt)” (Chapter I), “Human activities disrupt the temporal dynamics of salinity in Spanish rivers” (Chapter II), “What happens when salinization meets eutrophication? A test using stream microcosms” (Chapter III), and “Assessing the effects of salinity on microbial communities and pollutant removal in urban wastewater treatment plants” (Chapter IV).

3. RESULTS

3.1. Report from the thesis supervisors

As supervisors of the doctoral thesis titled “Causes, Effects, and Management of River Salinization in Spain, with Special Attention to Wastewater Treatment,” we present the following report regarding the impact factor of the published articles according to the Journal Citation Reports of the Web of Science of each corresponding year.

The first published article, Human Activities Disrupt the Temporal Dynamics of Salinity in Spanish Rivers, was published in Hydrobiologia on November 22, 2022. This journal has an impact factor of 2.7, is ranked in Quartile Q1, and covers fields such as Water Sciences and Aquatic Biology. **The second published article**: What Happens When Salinization Meets Eutrophication? A Test Using Stream Microcosms, appeared in Science of The Total Environment on February 20, 2024. The journal has an impact factor of 8.2, is in Quartile Q1, and focuses on Environmental Sciences and Ecology. **The third published article**: Assessing the Effects of Salinity on Microbial Communities and Pollutant Removal in Urban Wastewater Treatment Plants, was published in the Journal of Water Process Engineering on August 16, 2024. With an impact factor of 6.3 and a Quartile Q1 ranking, this journal is relevant to Environmental Engineering and Water Treatment Processes. The PhD candidate made significant contributions as the first author for all three articles, leading the writing and data analysis processes.

All articles presented in the thesis were authored with the PhD candidate as the first author. The contributions of co-authors have been appropriately recognized in each publication. No additional work from co-authors was used implicitly or explicitly in the preparation of this doctoral thesis beyond what is detailed in this report.

Supervisor

CAÑEDO-ARGUELLES IGLESIAS MIGUEL - DNI 53547569G

Firmado digitalmente por CAÑEDO-ARGUELLES IGLESIAS MIGUEL - DNI 53547569G
Fecha: 2024.10.25 17:07:07 +02'00'

Dr. Miguel Cañedo-Argüelles Iglesias

Senior Scientist

IDAEA-CSIC

Supervisor and Tutor

HUMBERT SALVADÓ CABRÉ - DNI 77106213R

Digitally signed by HUMBERT SALVADÓ CABRÉ - DNI 77106213R
Date: 2024.10.25 09:16:50 +02'00'

Dr. Humbert Salvadó Cabré

Professor Agregat

Universitat de Barcelona

3.2. Chapter I: GLOBal river SALiniTy and associated ions (GlobSalt)

Article submitted to Scientific Reports on April 12, 2024.

GLOBal river SALiniTy and associated ions (GlobSalt)

Alvaro Javier Moyano Salcedo*[1,2,9], Theresa Piana[4], Julie Crabot[9], Ben J. Kefford[3], Elisabeth Berger[4], Shelley E. Arnott[5], Josefin Thorslund[6], Michel Meybeck[7], Sujay S. Kaushal[8], Ralf B. Schäfer[4], Miguel Cañedo-Argüelles Iglesias*[9]

1 FEHM-Lab (Freshwater Ecology, Hydrology and Management), Departament de Biologia Evolutiva, Ecologia i Ciències Ambientals, Facultat de Biologia, Universitat de Barcelona, Barcelona, Spain.

2 Geohazards and Civil Engineering Research Group, Department of Civil Engineering, Saint Thomas Villavicencio University, C/22 No 1a, 500003, Villavicencio, Colombia.

3 Centre for Applied Water Science, Institute for Applied Ecology, University of Canberra, ACT, Australia

4 RPTU Kaiserslautern-Landau, iES - Institute for Environmental Sciences, Landau, Germany

5 Department of Biology, Queen's University, Kingston, Ontario, Canada K7L 3N6

6 Department of Physical Geography and the Bolin Centre for Climate Research, Stockholm University, Stockholm, Sweden. Department of Physical Geography, Utrecht University, Utrecht, The Netherlands.

7 UMR 7619 METIS, Sorbonne Université-CNRS-EPHE, Paris, France

8 Department of Geology & Earth System Science Interdisciplinary Center, University of Maryland, College Park, MD, USA

9 FEHM-Lab (Freshwater Ecology, Hydrology and Management), SHE-2, Institute of Environmental Assessment and Water Research (IDAEA), CSIC, Carrer de Jordi Girona, 18-26, 08034, Barcelona, Spain.

*Corresponding authors: Alvaro Javier Moyano Salcedo, alvaromoyano@ub.edu

Miguel Cañedo-Argüelles Iglesias, mcahse@cid.csic.es

Abstract: Freshwater salinization (FS) is a threat to freshwater ecosystems, but its impact remains relatively poorly understood compared to other stressors (e.g. nutrient pollution), with some regions (e.g. Asia, Africa) remaining poorly explored. To assess how pervasive this issue is globally and identify salinization hotspots, we compiled global data on river salinity and associated ions. We retrieved information from different sources, harmonized it and merged it with HydroATLAS watersheds. Our global data set (GlobSalt) features 13 parameters, including electrical conductivity (EC), major ions, and nutrients. GlobSalt contains approximately fifteen million records on a monthly scale for

river stations from 1980 to 2023 from all continents except Antarctica. The global median EC was 509 ± 205 µS cm^{-1}, with 60% of rivers falling in the range of 50 to 500 µS cm^{-1}, which is within the salinity niche of most freshwater organisms. We found a large spatial variability in EC, with some regions such as the Mediterranean, the Midwest of the US, arid regions of Argentina and Chile and Southwestern Australia having high mean salinity values. Temporally, EC was fairly stable. GlobSalt represents a critical resource for improving our understanding of FS dynamics, identifying regions at high risk and informing management strategies.

Key words: Freshwater salinization, Global salinity data, Salinization hotspots, Electrical Conductivity, Major Ions

Background & Summary

Freshwater salinization (FS) is a growing water quality challenge that poses a risk to the health of aquatic ecosystems. FS has the potential not only to degrade water use across sectors[1,2] (e.g., agricultural irrigation, drinking water supply), but also to cause strong negative changes in both the structure (e.g., by shifting community composition) and functioning (e.g., e.g., biomass production) of river ecosystems [3–8]. FS can result from a combination of natural processes such as chemical weathering (e.g., dissolution of ions), fluvial salt transport (e.g., sediment transport), soil erosion (e.g., runoff carrying saline minerals from the soil into rivers), atmospheric deposition (e.g., salt deposition by rainfall or gravitational settling), and atmospheric transport of salts (e.g., wind transport of sea salt particles in aerosols or dusts)[9]. Other natural sources are saltwater intrusion, biological (e.g., natural release of salts through decomposition and the salt transportation of biological vectors such as migratory animals), geological (e.g., salt release due to tectonic movements such as geologic faults) and climate-related processes (e.g., El Niño and La Niña events)[9]. Furthermore, human activities have strongly increased FS on a global scale, modifying and intensifying natural salt fluxes. For instance, chemical weathering can be induced by factors such as fertilizers, acid rain, or mining[10–12]. This is concurrent with other activities that increase fluvial salt transport like road de-icing, as well as domestic and industrial discharges [13–17]. Moreover, the intensification of agricultural irrigation can lead to soil erosion, which, in turn, may result in the dissolution of chemicals (e.g., sodium, chloride)[18–20] that can alter the biological cycle of salt [9,21,22]. Also, the anthropogenic water cycle can directly affect atmospheric conditions (resulting in increased salt deposition), surface water (e.g., causing fluctuations in river flow due to

water extraction), and groundwater dynamics (e.g., influenced by groundwater pumping), thereby altering salinity concentrations[9,23,24]. These effects extend to geologic uplift and resource extraction activities such as fracking[9,25,26]. Finally, FS may be driven by climatic conditions, exacerbating its impact in arid and semi-arid areas, and affecting rivers globally [27–31].

Water quality monitoring programs should consider FS not only based on electrical conductivity (EC) as a salinity indicator but also on the concentrations of individual ions (Na^+, K^+, Mg^{2+}, Ca^{2+}, Cl^-, SO_4^{2-}, SiO_3^{2-}) and their interactions with other chemicals. For example, river salinization often co-occurs with nutrients and pesticides from agriculture, the food industry, and energy systems[22,32,33]. Agriculture is the primary source of increased levels of NaCl, as well as NO_3^-, PO_4^{3-} , K^+, Ca^{2+}, and Mg^{2+} [34]. However, the concentration of these ions in many rivers and streams remains unknown[16,20]. Similar challenges arise from other activities, such as wastewater discharge in urban areas and industrial production (e.g., ethanol and agro-food industries), which generate by-products that release high concentrations of both nutrients and salts, significantly amplifying FS[33,35–37]. In the ethanol industry, sugarcane vinasse emerges as a substantial and continuous by-product with elevated nutrient levels (e.g., pure vinasse has a total N: 639 mg L−1, total P: 150 mg L^{-1}) and salinity (e.g., sodium: 60 mg L^{-1}, conductivity: 8420 µS cm^{-1})[32,33]. Moreover, many river basins may experience the combined effects of agricultural and wastewater discharges[38–40]. The resulting "chemical cocktails" can have profound effects on aquatic communities[18] by disrupting ecological dynamics and potentially favoring the dominance of certain species while threatening the survival of other[22]. Therefore, monitoring chemical mixtures associated with FS is important for the conservation and sustainable management of aquatic ecosystems.

So far, although EC is routinely measured as a proxy to anthropogenic FS activities, FS has been often neglected in water quality monitoring programs[41,42]. and there are no legally enforced FS standards to protect aquatic life[2] . While there have been considerable efforts to compile and harmonize water quality information, including salinity parameters, at the global scale[34,43–46] a significant part of this information remains scattered. For example, the global occurrence of major elements (excluding EC measurements) in rivers has been compiled[34]. Also, the GLORICH[43] database updates and provides data on major ions and other physicochemical parameters of water. However, spatial and temporal gaps persist in both datasets. Similarly, the global dataset of surface water and groundwater salinity measurements from 1980 to 2019[46] provides a

valuable contribution to understanding the distribution and evolution of salinity over time, but includes only EC data, providing only a narrow understanding of FS dynamics. Within this context, our database presents two significant improvements: 1) We provide new data for some regions of the world that were poorly represented, mainly in Asia and Africa. 2) We provide data on specific ions and on other water quality parameters that are important to understand and manage the effects of FS[18,47]. Data related to FS (e.g., EC, water ion composition) and other pollutants (e.g., nutrients) often vary in reported parameters, units, and spatiotemporal resolution. This hampers the comparison of information across scales. Thus, the compilation, harmonization, and access to these data are crucial for the development of models and analyses that can elucidate the dynamics of FS and propose management measures at local, regional, and global scales.

We provide a global, standardized database with a set of key water quality parameters related to salinity, including nutrients, covering the period from 1980 to 2023. We collected and compiled observational data with a primary focus on EC, as it is the most widely monitored parameter for salinity worldwide. However, whenever more detailed information on other major ions parameters was available, this was considered. Data were collected from a variety of sources, including local, regional, and global water quality databases, governmental organizations, river basin management commissions, water development boards, and individual research projects. This is the most comprehensive dataset on FS to date, with the potential to be used by researchers, policymakers, conservation organizations and other stakeholders to anticipate, mitigate and restore the impacts of FS on aquatic ecosystems around the world.

Methods

A total of 62 data sources were used to compile the GLOBal river SALiniTy and associated ions database (GlobSalt). The GlobSalt database features 13 parameters, including major ions, EC, ammonium, nitrate, and phosphate (Table 1). All datasets were publicly available online, and some have been explored and used in previous studies [43,44,46]. The number of available parameters differed strongly between countries and the parameters with the highest global coverage and temporal representativeness were selected.

Data compilation was divided into three parts: (1) raw data was downloaded and converted into a common format and the corresponding metadata was harmonized; (2); subsequently, the data were merged based on parameters, ensuring a unified structure for

all information, including aspects like identifiers and temporal scales; (3) finally, we cleaned and organized the final dataset.

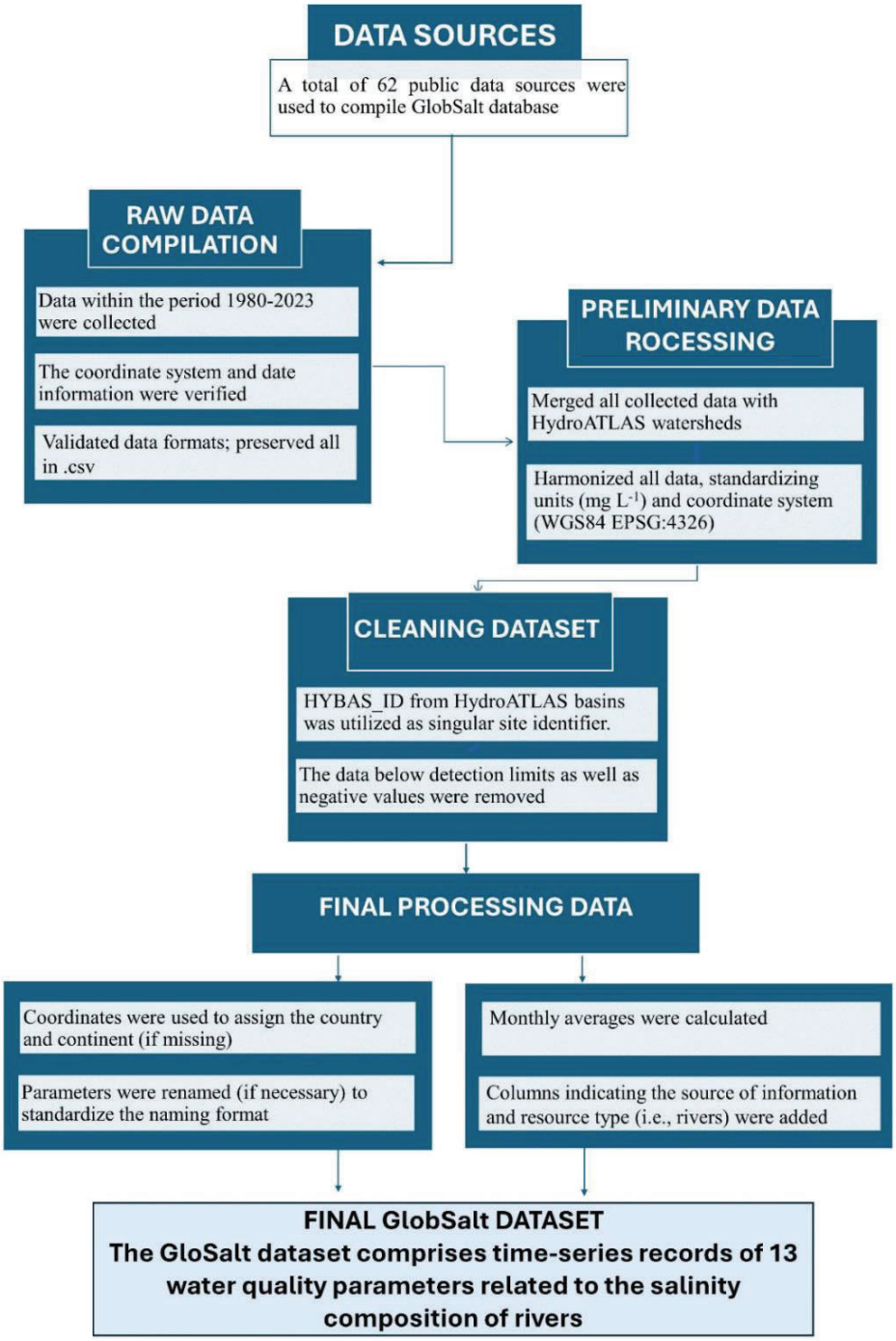


Figure 1. Methodology overview flowchart. The figure illustrates the data compilation, processing, and harmonizing steps of the GlobSalt dataset.

Compilation and source data preparation

All raw data compilation was downloaded or queried from a total of 62 online sources listed in Table 1 including existing global datasets. Also, in some cases (e.g. India) direct requests were made to the environmental authorities who authorized the use of the data. Preliminary processing data from each source revealed ambiguities in parameter names, codes, units, or chemical forms, as well as in the complementary information for each watershed, including the geographic coordinate systems used. This was expected when dealing with water quality data from multiple sources [48,49].

Parameter selection and harmonization

The selection of parameters followed those of previous studies and datasets that address the global salinization of rivers, such as Global Occurrence of Major Elements in Rivers[34], GLORICH[43], and more recently a global dataset of surface water and groundwater salinity measurements from 1980–2019[46]. All these studies stand out as global datasets that strive to compile salinity variables with the least number of discrepancies in source data (e.g., parameters with a single matching code and consistent units).

The nomenclature for the included parameters varied across the data sources, with various abbreviations, names, and chemical forms. To address this issue, we undertook a comprehensive renaming of all variables (Table 1).

Unit conversion

The units for each parameter were harmonized to ensure consistency. Conversions were made where necessary, and all units except pH and EC (measured in µS cm^{-1} 25°C) were standardized to milligrams per liter (mg L^{-1}), which was the most prevalent unit in source data. A consistent review approach was also adopted for all parameters across continents (e.g., distinguishing between dissolved and total concentration). For GLORICH, which reported major ion parameters in micromoles per liter (µmol L^{-1}), conversions to mg L^{-1} were performed. However, no conversion was required for most of the sources (e.g., WQP), as its units matched those intended for the GlobSalt dataset (i.e., mg L^{-1}). A detailed list of all unit conversion procedures can be found in Table S2, where the conversion was determined using the equation (1):

$$x_2 = \frac{x_1 * Mx_2}{n * Mx_1}$$

Here, $\mathbf{x_1}$ represents the observation value before conversion; $\mathbf{x_2}$ represents the observation value after conversion; $\mathbf{Mx_1}$ is the molar mass corresponding to the compound (e.g. NO3 = 62.005 g mol^{-1}), and $\mathbf{Mx_2}$ is the molar mass corresponding to the elemental parameter (e.g. N = 14.007 g mol^{-1}); n is the magnitude difference between the source and converted units (e.g. µmol L^{-1} to mg L^{-1}, 1000).

Site ID duplication and watershed characteristics

The information was intersected with the basins from HydroAtlas[50], and subsequently, a single basin identifier (i.e., HYBAS_ID) was used to link all information. We selected HydroATLAS for its global coverage and standardized watershed and river categorization. Additionally, it provides a comprehensive dataset with a wide range of hydro-environmental attributes at high spatial resolution, derived from publicly available data and categorized into six groups: hydrology, physiography, climate, land cover and land use, geology and soils, and anthropogenic impacts. The integration of these data not only unifies all EC and major ion information from GlobSalt into a single, organized structure, but also summarizes it at the sub-catchment scale and enhances its utility for future analyses. Also, to distinguish each basin from each country, the original identifiers from each source and database were retained. Duplicate identifiers were then systematically identified and eliminated. The number of watershed characteristics for a site varied strongly, where some provided details such as state, watershed, city, and river name that were lacking for other sites. This complicated the use of a common watershed characteristic (e.g., watershed name) across sites. We created a general summary for each watershed in our final dataset, including an identifier (station_ID), country, continent, water type, and data source. However, all details regarding watershed descriptions were preserved in a separate file linked to the station_ID.

Coordinate conversion

Verification of the coordinate systems used by each data source revealed some variability between them. For example, information from countries such as the US, Germany, and France sometimes used specific datums such as the North American Datum of 1983 (NAD83), Gauss-Krueger, and Lambert 93 (EPSG:2154). In these cases, the spTransform() function in R, a component of the sp (spatial) package, was used to convert geographic coordinates to the World Geodetic System 1984 (WGS84). All information was then

standardized to the chosen coordinate system (WGS84 EPSG:4326) and integrated into the final dataset (Table 1).

Information filtering

Preliminary data cleaning included removing observations with negative or missing values, or those from unreliable sources. In addition, observations marked as below (<) or above (>) the detection limit in the source data were excluded from the GlobSalt when the information sources included data on the detection limits. Four source datasets (WQP, GEMStat, GLORICH, and Waterbase) had this type of quality assessment included in the metadata. In all cases, a review was performed to identify the column representing the final validated measurement parameter result for each source, and this value was used in GlobSalt.

Time and date processing

The source datasets used different date formats, all of which were converted to a common format (%Y-%m-%d) using the "as.Date()" function in R. Observations with incorrectly formatted or implausible dates were removed. In addition, the hour was omitted because it was a rare parameter across sources. Some sources provided daily measurements, and some provided monthly and annual averages. For date manipulation, including extraction of month and day, the "lubridate" package in R was used with functions such as "year()", "month()" and "day()". The final time unit for presenting data was the monthly average of all available data per month. This was done to harmonize the data into a common global unit, to reduce the volume of data, and to include as much data as possible (e.g. from areas where daily data were lacking).

Outlier processing, time series availability, and continuity

The total number of observations varies considerably between sources. The North American WQP stands out with a large data set of 9.649.775 records, much higher than other sources. This variability in data volume is also accompanied by differences in the temporal coverage of the measurements (Table S1). For example, the European Waterbase covers several decades, while others, such as RCHB-T (Bogotá Water Quality Network, Colombia), are limited to specific years (Table S1). The specific number of observations per country and continent vary for each parameter but, as expected, EC and pH show greater continuity and number of records.

Data distribution checking involved a visual examination and a plausibility check. First, the bean plot was used to examine the distribution of the log-transformed data of each parameter (Figures S1 to S26). The log transformation was used to normalize the data distribution by effectively mitigating the effects of extreme values or outliers, which are common in environmental data sets. Subsequently, adherence to a distribution within the lognormal distribution family was evaluated using histograms. For example, the bean plot of EC (Figure S1) showed that, although most of the data ranged around the median, values that could be potential outliers were visible and should be considered cautiously when using our data in analyses. The histogram of EC (Figure S2) showed a strong deviation from a theoretical log normal distribution. However, all measurements from the GlobSalt database were retained, as both EC concentration data and major ions can vary widely between geographic locations due to natural and anthropogenic processes, seasonality, and different measurement methodologies[44].

GlobSalt dataset records

The GlobSalt dataset consists of time series observations of water quality parameters that reflect the salinity composition of rivers. These parameters (Table 1) are consolidated into a single CSV file ("GlobSalt_dataset.csv") along with location data and simplified identifiers. Additional information, such as catchment characteristics, is stored in a separate file 'GlobSalt_catchment_characteristics.csv' (files available for download in the Data Availability section). Each dataset is accompanied by metadata files (tables and images) that provide comprehensive details on the spatial and temporal characteristics of the respective time series. Figures S1 to S26 illustrate the distribution of records for each parameter. Also, a data catalogue ('GlobSalt data catalogue' section in the supplementary information) contains maps showing the spatio-temporal coverage and violin plots describing the concentration by continent, the temporal dispersion of the data, as well as correlations of all salinity parameters (Figures C1 to C41).

The spatial distribution and ranges of EC by continent, compiled on a global scale in the GlobSalt dataset (as a proxy for salinity), are shown in Figures 2 and 3. Across all continents, the median EC did not exceed 800 µS cm^{-1} (Figure 4). The global median EC was 509 ± 205 µS cm^{-1} (Table 1), with 60% of samples ranging from 50 to 500 µS cm^{-1}, which is within the salinity niche of most freshwater organisms[51–53]. However, the computed median EC did not consider factors such as country size and spatiotemporal data availability by region and

thus does not directly reflect FS. Note that the spatial and temporal distribution of samples within GlobSalt, and thereby the median, was strongly biased to North America and somewhat by Europe, where the largest data sets originated (Figure 4). To capture this, a detailed breakdown of EC by country is provided in Table 2, along with its relation to the geographic area (km^2) and the number of available monitoring data and sites in each case. Table 2 shows strong variability in the median EC by country and its relationship with area, available data, and monitoring sites. The USA stands out as the country with fewer discrepancies in the relationship between data availability and factors such as country size (Nº data/ km^2 = 0.86), followed by Germany (Nº data/ km^2 = 0.78).

Despite the bias in available information on FS, a large spatial variability in mean EC was found when plotted by river station. Regions such as the Mediterranean[54], the Midwest USA[55], arid regions of Argentina and Chile, and southwestern Australia[52] had high mean salinity values (Figure 2) as well as greater relative variation (Figure 3). Temporally, EC remained relatively stable, with no evidence of strong increasing or decreasing trends from 1980 to 2023 (Figure 5). Across continents and over time, we found an upper EC limit ranging between 25000 and 30000 µS cm^{-1} (Figure 5). We subset the data by filtering for "ceiling values" (i.e., EC data in the range of 25,000 to 30,000 µS cm^{-1}) as well as extreme values (i.e., EC above 30,000 µS cm^{-1}) to visually explore whether this could be due to measurement error or artifact (Figures C37-C40). Since the location of these sites corresponded to saline or coastal regions and the correlation between EC and salt ions was strong in the high salinity subset data (Figures C38-C39), we suggest that these values are correct and should not be removed from the dataset.

The correlations between EC and the major ions using the data from GlobSalt are shown in Figure C41. This correlation shows that sodium and chloride were the elements most strongly correlated with EC ($r^2 > 0.5$), but also reveals some discrepancies mainly related to the association of very low EC values with very high ion levels (e.g., sodium). To validate the EC measurements in relation to the sodium, potassium, and calcium concentrations (as a proxy for the relationship between EC and ions), the ratio (e.g., sodium/EC) between them was used. First, the theoretical EC was calculated based on the chemical composition of the measured ion concentrations (i.e., sodium, potassium, calcium) using the equation and methodology described in a previous study[56]. Then, the theoretical ratio (e.g., sodium/theoretical EC) was computed, yielding a mean and median of 0.43 and 0.44 for sodium, 0.35 and 0.36 for

potassium, and 0.29 and 0.30 for calcium. These results are higher than with previously reported ion and EC ratio values (e.g., ratio of 0.3 for Sodium/EC)[57]. Also, it is important to note that this method has limitations related to the theoretical predictability of extreme values (both low and high), as highlighted in previous studies[58–60]. However, despite these limitations, the methodology remains useful for EC and ion data falling outside of these extreme intervals (e.g., where EC ranges from 100 to 1000 $\mu S\ cm^{-1}$)[58,59], albeit with a cautionary note on interpretation. After computing the theoretical ratio, we calculated the empirical ratio between each ion and EC measured. In our study, the mean of these theoretical ratios (e.g., sodium/theoretical EC) was used as a reference point to establish a baseline for the empirical ratio (e.g., sodium/measured EC). Thus, when the empirical ratio exceeded the mean of these theoretical ratios (sodium: 0.43, potassium: 0.35, and calcium: 0.29), the corresponding data points were flagged in GlobSalt as potentially erroneous (0 represents accurate data, and 1, potentially erroneous data). Figure 6 shows the pairwise correlations between EC and the major ions present in GlobSalt after filtering out potentially erroneous data. The final distribution of the filtered GlobSalt data resulted in approximately 65% of the data set falling within the used ratios (i.e., considered as accurate information), while the remaining 35% were flagged as 'errors'. Also, with this approach, it was possible to obtain a stronger correlation of EC with sodium and chloride ($r^2 > 0.8$), which remained the ions most correlated with EC.

Table 1. GlobSalt attributes, structure, and parameters statics. Variable names and descriptions, including reported units, of the GlobSalt database.

Attribute	Description	Unit	Number of total records by attribute	Number of sites	Median value per water parameter
HYBAS_ID	Sampling point basin ID HydroAtlas	#	14235780	-	-
x	Longitudinal coordinate of sample location	Decimal Degrees	14235780	-	-
y	Latitudinal coordinate of sample location	Decimal Degrees	14235780	-	-
year	Year of the sample in record	yyy	14235780	-	-
month	Month of the sample in record	mm	14235780	-	-
Station_ID	Sampling river point ID associated with each basin	#	14235780	-	-
Country	Geographic location	Name	14235780	-	-
Continent	Geographic location	Name	14235780	-	-
Source	Data source information of the dataset (See Table A1 for source names)	Name	14235780	-	-
Water_type	Water resource type sampled	River	14235780	-	-
Quality_data_flag	Flagged records. 0 for accurate, 1 for potentially erroneous data	#	14235780	-	-
Conductivity	Measurement of electrical EC in the surface water	$\mu S\ cm^{-1}$ @25C	10708168	40765	509
pH	Measurement of acidity or alkalinity in the surface water	-	11050350	39897	7.7
Sodium, dissolved	Concentration of dissolved Sodium ions in the surface water	$mg\ L^{-1}$	5493436	18676	30
Potassium, dissolved	Concentration of dissolved Potassium ions in the surface water	$mg\ L^{-1}$	5206061	17613	4
Magnesium, dissolved	Concentration of dissolved Magnesium ions in the surface water	$mg\ L^{-1}$	5953892	21308	16
Calcium, dissolved	Concentration of dissolved Calcium ions in the surface water	$mg\ L^{-1}$	6086082	22505	46
Chloride, dissolved	Concentration of dissolved Chloride ions in the surface water	$mg\ L^{-1}$	5818505	17460	33
Sulphate, dissolved	Concentration of dissolved Sulphate ions in the surface water	$mg\ L^{-1}$	5457049	26495	57
Silicate, dissolved	Concentration of dissolved Silicate ions in the surface water	$mg\ L^{-1}$	427933	11080	9
Nitrate	Concentration of Nitrate ions in the surface water	$mg\ L^{-1}$	1795382	56389	0.37
Ammonium	Concentration of Ammonium ions in the surface water	$mg\ L^{-1}$	1358805	26315	0.40
Phosphate	Concentration of Phosphate ions in the surface water	$mg\ L^{-1}$	956913	9466	0.16
Total organic carbon (TOC)	Measurement of the total amount of organic carbon in the surface water	$mg\ L^{-1}$	821194	25883	4.2

Table 2. Distribution of mean conductivity (EC) data relative to area by country in GlobSalt.

Country	Number of sites	Number of data	Area (km^2)	Nº data/ km^2	Median Conductivity (EC)
Argentina	203	5529	2780400	0.0020	190
Australia	2160	284661	7741220	0.0368	380
Austria	16	1474	83871	0.0176	370
Bangladesh	5	311	148460	0.0021	150
Belarus	1	60	207600	0.0003	424
Belgium	63	5361	30689	0.1747	822
Bolivia	11	118	1098581	0.0001	100
Bosnia and Herzegovina	14	1002	51197	0.0196	400
Brazil	1961	37754	8515770	0.0044	55
Bulgaria	74	3849	110879	0.0347	414
Burundi	5	5	27830	0.0002	37
Cambodia	12	960	181035	0.0053	12
Cameroon	7	904	475440	0.0019	18
Canada	2774	158603	9984670	0.0159	223
Central African Republic	1	12	622984	0.0000	40
Chile	557	19014	756102	0.0251	387
China	10	890	9596960	0.0001	258
Colombia	175	8917	1138910	0.0078	141
Croatia	51	4057	56594	0.0717	388
Cyprus	37	1480	9251	0.1600	737
Czech Republic	2	489	78867	0.0062	522
Democratic Republic of the Congo	1	12	342000	0.0000	42
Denmark	11	18	42930	0.0004	425
Ecuador	11	408	283561	0.0014	52
Egypt	7	102	1001450	0.0001	285
Estonia	263	4659	45227	0.1030	445
Finland	106	5400	338145	0.0160	13
France	6642	370873	643801	0.5761	326
Germany	4048	281889	357022	0.7895	565
Ghana	4	15	238533	0.0001	119
Greece	360	2008	131957	0.0152	346
Greenland	14	14	2166086	0.0000	16
Guatemala	83	2566	108889	0.0236	205
Hungary	16	2844	93028	0.0306	386
India	961	79421	3287263	0.0242	240
Indonesia	11	478	1904569	0.0003	158
Ireland	190	25535	70273	0.3634	240
Italy	2654	29074	301340	0.0965	488
Japan	17	5258	377915	0.0139	118
Kenya	43	259	580367	0.0004	160
Laos	14	1622	236800	0.0068	118
Latvia	15	648	64589	0.0100	493

Country	Number of sites	Number of data	Area (km^2)	Nº data/ km^2	Median Conductivity (EC)
Lesotho	1	95	30355	0.0031	521
Lithuania	463	9150	65300	0.1401	521
Luxembourg	2	58	2586	0.0224	797
Malaysia	7	476	329847	0.0014	55
Mali	13	159	1240192	0.0001	44
Mexico	2125	71386	1964375	0.0363	589
Moldova	6	597	33846	0.0176	540
Morocco	8	560	446550	0.0013	1445
Netherlands	5	261	41543	0.0063	489
New Zealand	113	40396	268838	0.1503	90
Nigeria	1	5	1267000	0.0000	110
South Korea	32	2070	120538	0.0172	151
Norway	182	15584	323802	0.0481	30
Pakistan	4	801	796095	0.0010	300
Panama	57	4399	75420	0.0583	112
Papua New Guinea	1	1	462840	0.0000	150
Peru	14	174	1285216	0.0001	588
Philippines	1	1	300000	0.0000	227
Poland	3293	43144	312685	0.1380	479
Portugal	87	3886	92090	0.0422	479
Romania	27	4699	238391	0.0197	391
Russia	3	180	17098242	0.0000	312
Rwanda	20	20	26338	0.0008	211
Senegal	10	40	196722	0.0002	151
Serbia	83	7288	77474	0.0941	411
Slovakia	9	1287	49037	0.0262	423
Slovenia	3	556	20273	0.0274	314
South Africa	3404	470581	1219090	0.3860	156
Spain	1440	82162	505370	0.1626	558
Sri Lanka	34	2086	65610	0.0318	70
Sudan	2	188	1861484	0.0001	250
Sweden	948	26583	450295	0.0590	10
Switzerland	126	11118	41290	0.2693	425
Tanzania	6	120	947300	0.0001	142
Thailand	22	2400	513120	0.0047	182
Tunisia	1	12	163610	0.0001	706
Uganda	2	5	241038	0.0000	112
UK	898	23020	243610	0.0945	198
Ukraine	3	130	603550	0.0002	289
Uruguay	8	365	176215	0.0021	65
USA	4437	8529874	9833517	0.8674	553
Venezuela	4	65	912050	0.0001	33
Viet Nam	54	3633	331212	0.0110	192

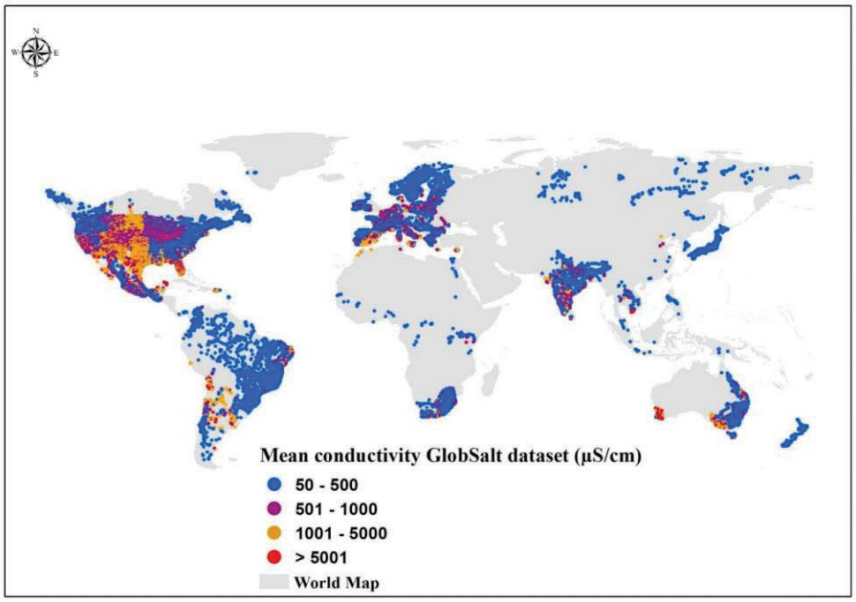


Figure 2. Global distribution of measured mean electrical conductivity (EC) and station density. The global map in the panel shows the measured mean EC values per river in each country, based on observations included in the GlobSalt database, over the entire data period (1980-2023). Blue, purple, orange, and red dots represent low, moderate, moderately high, and high EC, respectively.

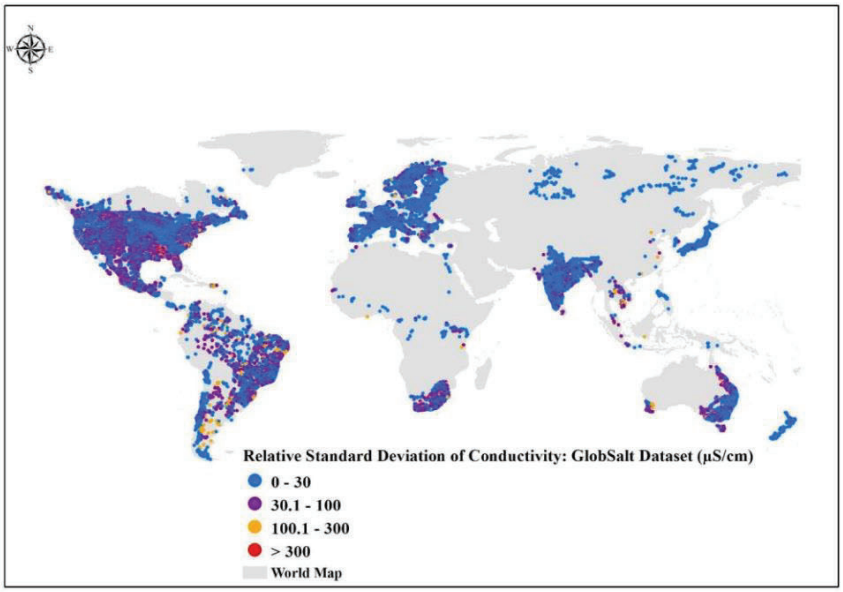


Figure 3. Global Distribution of Relative Standard Deviation (RSD) of Electrical Conductivity (EC) and Station Density. The global map illustrates the RSD of EC values per river in each country, calculated as (SD/Mean) × 100%, from observations in the GlobSalt database (1980-2023). Blue, purple, orange, and red dots represent low, moderate, moderately high, and high RSD of EC, indicating variability around the mean conductivity.

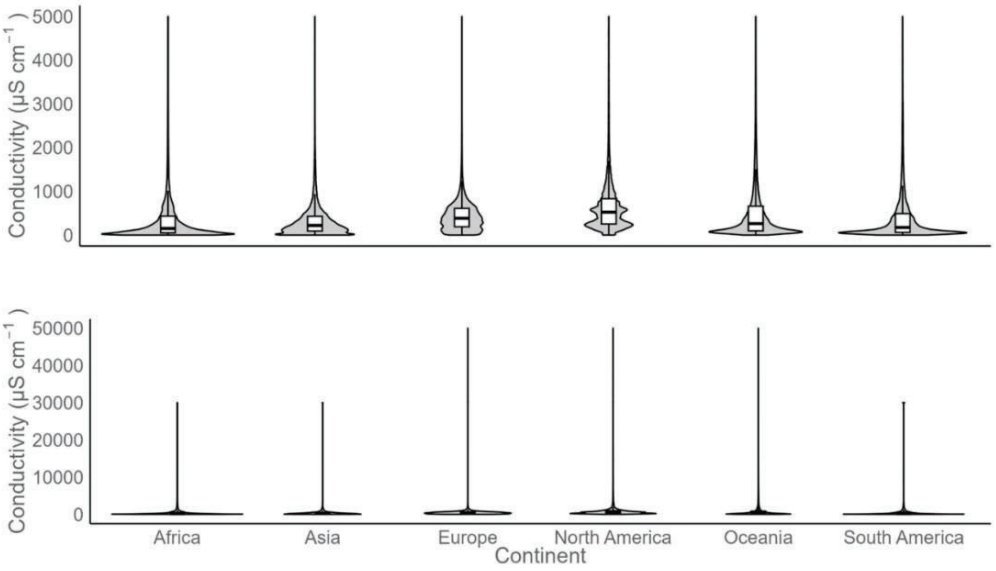


Figure 4. Violin plot of electrical conductivity (EC) by continent. Top: Global Violin Plot of Electrical Conductivity (EC) by Continent with Zoom to 5000 µS cm^{-1}. Bottom: Violin Plot of Electrical Conductivity (EC) across the entire scale by Continent. EC observations are included in the GlobSalt database, over the entire data period (1980-2023). Each gray violin plot represents the available data set according to the number (n) of observations per continent (Africa n = 473083, Asia n = 112049, Europe n = 958793, North America n = 8728636, Oceania n = 325057, South America n = 110550).

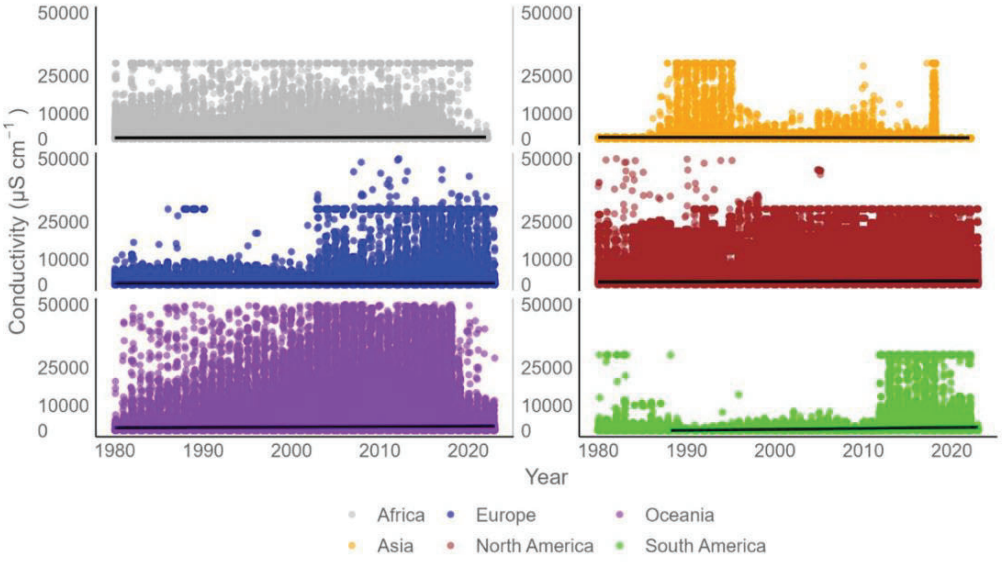


Figure 5. Global temporal dispersion plot of electrical conductivity (EC) by continent. EC observations are included in the GlobSalt database over the entire data period (1980-2023). Each color (gray, yellow, blue, brown, purple, and green) represents the number (n) of observations per continent (Africa n = 473083, Asia n= 112049, Europe n = 958793, North America n =8728636, Oceania n = 325057, South America n = 110550).

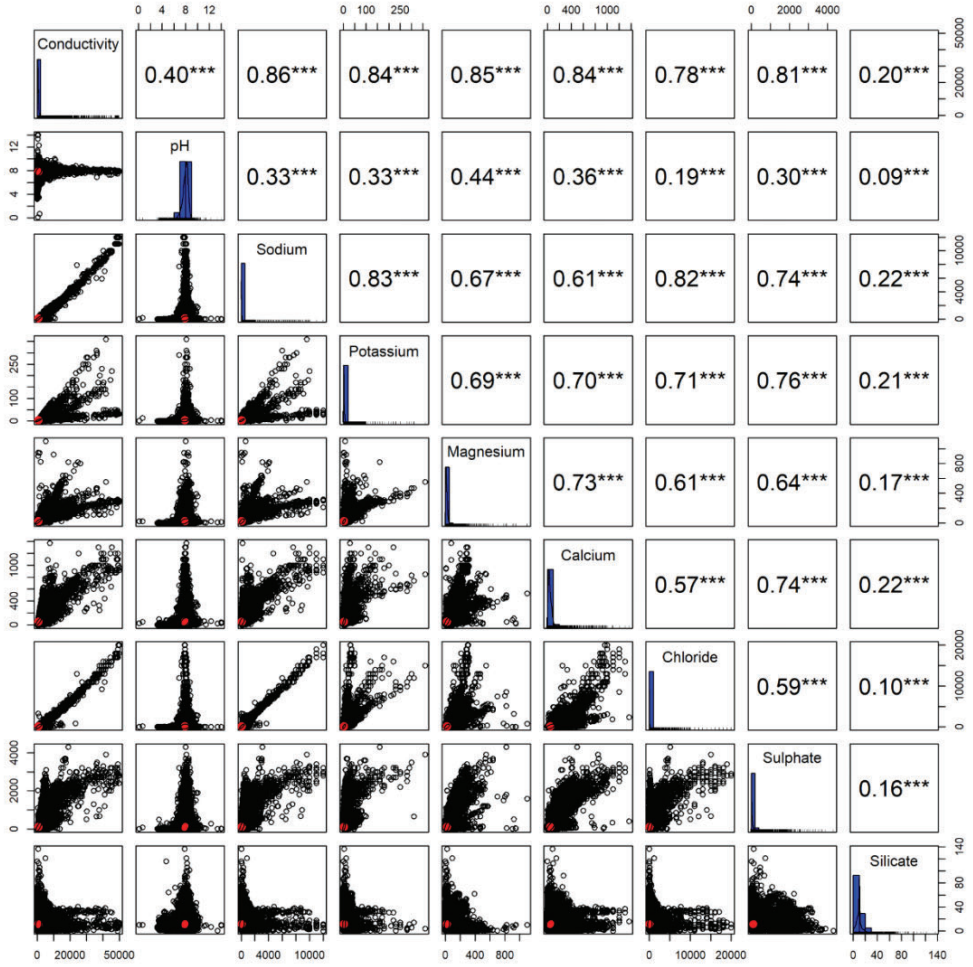


Figure 6. Correlation plot of electrical conductivity (EC) and ion concentrations in the GlobSalt dataset, including inter-ion correlations (ions unit, mg L^{-1}). Red dots indicate the strength of the correlation between variables.

Code availability

The data for this study was mainly processed in R (version 3.6.0), but with cross-checking and corrections of spatial coordinates conducted using ArcGIS.

Acknowledgments

We gratefully acknowledge all people who assisted in the data collection process, either with direct data, processing advice or data ideas. Particularly, we appreciate the collaboration provided by each university, research center, and governmental agency in the various countries we visited and/or through telecommunications communications in terms of providing data, experiences, and channels to collect the information contained in GlobSalt. This research was supported by the IDAEA-CSIC ILink associated with the

GlobSalt project. Also, this work was supported by a doctoral grant from the Ministerio de Ciencia, Tecnología e innovación y Colfuturo (Colombia) and IDAEA-CSIC contract associated to Ramón y Cajal (RYC2020-029829-I) and IDAEA-CSIC ILink project for Alvaro Moyano.

Author contributions

A.M. Conceptualization, mainly responsible for collecting and processing the data, Methodology, Formal analysis, Investigation as well as writing – original draft & editing, Visualization, project administration. **M.M.** Conceptualization, Methodology, Investigation, Writing – review, data collection for France. **J.C.** Conceptualization, Methodology, Investigation, Writing – review, data collection for France. **S.K.** Conceptualization, Methodology, Investigation, Writing – review, data collection for USA. **S.A.** Conceptualization, Methodology, Investigation, Writing – review, data collection for Canada. **B.K.** Conceptualization, Methodology, Investigation, Writing – review, data collection for Australia. **R.S.** Conceptualization, Methodology, Investigation, Writing – review, data collection for Germany. **E.B.** Conceptualization, Methodology, Investigation, Writing – review, data collection for Germany. **T.P.** Conceptualization, Methodology, Investigation, Writing – review, data collection for Germany. **J.T.** Conceptualization, Methodology, Investigation, Writing – review, data collection globally. **M.C.** Conceived the idea of the database and associated information and Conceptualization, Methodology, Formal analysis, Investigation, Writing – final draft & editing, Visualization, Supervision, Project administration.

Data Availability and Supplementary information

The data supporting the results of this study are available in the Zenodo repository (https://zenodo.org/records/10965865). Files available include:

1. GlobSalt_data.CSV: This file contains processed observation data for 13 water quality parameters, along with associated metadata (observation site information, etc.) for 13 different water quality parameters.
2. GloSalt_catchment_characteristics file: This file contains processed observation data along with the catchment characteristics metadata included in GlobSalt_data.CSV.

Readers can access these data by visiting the link provided and downloading the appropriate files. These data are available for non-commercial use and are intended to facilitate interpretation, replication, and further development of the results reported in this article.

Supplementary data to this article can be found online.

Competing interests

The authors declare no competing interests.

References

1. Kaushal, S. S. Increased Salinization Decreases Safe Drinking Water. *Environmental Science and Technology* vol. 50 2765–2766 Preprint at https://doi.org/10.1021/acs.est.6b00679 (2016).
2. Cañedo -Argüelles M, Kefford B, S. R. Salt in freshwaters: causes, effects, and prospects - introduction to the theme issue. (2018).
3. Kefford, B. J., Palmer, C. G. & Nugegoda, D. *Relative Salinity Tolerance of Freshwater Macroinvertebrates from the South-East Eastern Cape, South Africa Compared with the Barwon Catchment, Victoria, Australia*. *Marine and Freshwater Research* vol. 56 (2005).
4. Kefford, B. J. *et al.* Global scale variation in the salinity sensitivity of riverine macroinvertebrates: Eastern Australia, France, Israel, and South Africa. *PLoS One* **7**, (2012).
5. Cañedo-Argüelles, M. *et al.* Response of stream invertebrates to short-term salinization: A mesocosm approach. *Environmental Pollution* **166**, 144–151 (2012).
6. Cañedo-Argüelles, M. *et al.* Can salinity trigger cascade effects on streams? A mesocosm approach. *Science of the Total Environment* **540**, 3–10 (2016).
7. Cañedo-Argüelles, M. *et al.* Saving freshwater from salts: Ion-specific standards are needed to protect biodiversity. *Science (1979)* **351**, 914–916 (2016).
8. Cunillera-Montcusí, D. *et al.* Freshwater salinisation: a research agenda for a saltier world. *Trends in Ecology and Evolution* vol. 37 440–453 Preprint at https://doi.org/10.1016/j.tree.2021.12.005 (2022).
9. Kaushal, S. S. *et al. The Anthropogenic Salt Cycle*.
10. Kaushal, S. S. *et al.* Increased river alkalinization in the eastern U.S. *Environ Sci Technol* **47**, 10302–10311 (2013).
11. Drake, T. W. *et al.* Increasing Alkalinity Export from Large Russian Arctic Rivers. *Environ Sci Technol* **52**, 8302–8308 (2018).
12. Kaushal, S. S. *et al.* Human-accelerated weathering increases salinization, major ions, and alkalinization in fresh water across land use. *Applied Geochemistry* **83**, 121–135 (2017).
13. Cañedo-argüelles, M. A review of recent advances and future challenges in freshwater salinization. **39**, 185–211 (2021).

14. Niedrist, G. H., Cañedo-Argüelles, M. & Cauvy-Fraunié, S. Salinization of Alpine rivers during winter months. *Environmental Science and Pollution Research* **28**, 7295–7306 (2021).

15. Ersoy, Z. *et al.* Experimental assessment of salinization effects on freshwater zooplankton communities and their trophic interactions under eutrophic conditions. *Environmental Pollution* **313**, (2022).

16. Estévez, E., Rodríguez-Castillo, T., González-Ferreras, A. M., Cañedo-Argüelles, M. & Barquín, J. Drivers of spatio-temporal patterns of salinity in Spanish rivers: A nationwide assessment. *Philosophical Transactions of the Royal Society B: Biological Sciences* **374**, (2019).

17. Laceby, J. P. *et al.* Chloride inputs to the North Saskatchewan River watershed: the role of road salts as a potential driver of salinization downstream of North America's northern most major city (Edmonton, Canada). *Science of the Total Environment* **688**, 1056–1068 (2019).

18. Kaushal, S. S. *et al.* Novel 'chemical cocktails' in inland waters are a consequence of the freshwater salinization syndrome. *Philosophical Transactions of the Royal Society B: Biological Sciences* **374**, (2019).

19. Kaushal, S. S. *et al.* Freshwater salinization syndrome alters retention and release of chemical cocktails along flowpaths: From stormwater management to urban streams. *Freshwater Science* **41**, 420–441 (2022).

20. Thorslund, J., Bierkens, M. F. P., Oude Essink, G. H. P., Sutanudjaja, E. H. & van Vliet, M. T. H. Common irrigation drivers of freshwater salinisation in river basins worldwide. *Nat Commun* **12**, (2021).

21. Cochero, J., Licursi, M. & Gómez, N. Effects of pulse and press additions of salt on biofilms of nutrient-rich streams. *Science of the Total Environment* **579**, 1496–1503 (2017).

22. Moyano Salcedo, A. J. *et al.* What happens when salinization meets eutrophication? A test using stream microcosms. *Science of the Total Environment* **912**, (2024).

23. Gholampour, A. *et al.* Characterization of saline dust emission resulted from Urmia Lake drying. *J Environ Health Sci Eng* **13**, (2015).

24. Neff, J. C. *et al.* Increasing eolian dust deposition in the western United States linked to human activity. *Nat Geosci* **1**, 189–195 (2008).

25. Ellison, R. A., Thomas, R. J., Jacobs, J. & Pharaoh, T. C. Anatomy and uplift history of the emergent salt domes of the United Arab Emirates. *Arabian Journal of Geosciences* **15**, (2022).

26. Yager, R. M., McCoy, K. J., Voss, C. I., Sanford, W. E. & Winston, R. B. The role of uplift and erosion in the persistence of saline groundwater in the shallow subsurface. *Geophys Res Lett* **44**, 3672–3681 (2017).

27. Le, T. D. H. *et al.* Predicting current and future background ion concentrations in German surface water under climate change. *Philosophical Transactions of the Royal Society B: Biological Sciences* **374**, (2019).

28. Kulmatov, R., Mirzaev, J., Abuduwaili, J. & Karimov, B. Challenges for the sustainable use of water and land resources under a changing climate and increasing salinization in the Jizzakh irrigation zone of Uzbekistan. *J Arid Land* **12**, 90–103 (2020).

29. Paul, W. L. *et al.* Long-Term Monitoring of Macroinvertebrate Communities Over 2,300 km of the Murray River Reveals Ecological Signs of Salinity Mitigation Against a Backdrop of Climate Variability. *Water Resour Res* **54**, 7004–7028 (2018).

30. Vandersande, M. W., Glenn, E. P. & Walworth, J. L. Tolerance of five riparian plants from the lower Colorado River to salinity drought and inundation. *J Arid Environ* **49**, 147–159 (2001).

31. Machado, M. J., Benito, G., Barriendos, M. & Rodrigo, F. S. 500 Years of rainfall variability and extreme hydrological events in southeastern Spain drylands. *J Arid Environ* **75**, 1244–1253 (2011).

32. Dreux Fraga, P. Sugarcane vinasse provokes acute and chronic responses and bioaccumulation of metals in benthic macroinvertebrates. (2023) doi:10.21203/rs.3.rs-2140305/v1.

33. Cotta, C. P. *et al.* Exposure to fipronil, 2,4-D and vinasse influences macroinvertebrate assemblage structure: An experimental mesocosm approach. *Science of the Total Environment* **888**, (2023).

34. Meybeck, M. *Global Occurrence of Major Elements in Rivers*. (2003).

35. Christofoletti, C. A., Escher, J. P., Correia, J. E., Marinho, J. F. U. & Fontanetti, C. S. Sugarcane vinasse: Environmental implications of its use. *Waste Management* **33**, 2752–2761 (2013).

36. Marinho, J. F. U., Correia, J. E., Marcato, A. C. de C., Pedro-Escher, J. & Fontanetti, C. S. Sugar cane vinasse in water bodies: Impact assessed by liver histopathology in tilapia. *Ecotoxicol Environ Saf* **110**, 239–245 (2014).

37. Lefebvre, O. & Moletta, R. Treatment of organic pollution in industrial saline wastewater: A literature review. *Water Research* vol. 40 3671–3682 Preprint at https://doi.org/10.1016/j.watres.2006.08.027 (2006).

38. Meybeck, M. Global analysis of river systems: From Earth system controls to Anthropocene syndromes. *Philosophical Transactions of the Royal Society B: Biological Sciences* vol. 358 1935–1955 Preprint at https://doi.org/10.1098/rstb.2003.1379 (2003).

39. Blaas, H. & Kroeze, C. Excessive nitrogen and phosphorus in European rivers: 2000-2050. *Ecol Indic* **67**, 328–337 (2016).

40. Bhide, S. V. *et al.* Addressing the contribution of indirect potable reuse to inland freshwater salinization. *Nat Sustain* **4**, 699–707 (2021).

41. Cañedo-Argüelles, M. *et al.* Salinisation of rivers: An urgent ecological issue. *Environmental Pollution* **173**, 157–167 (2013).

42. Moyano Salcedo, A. J., Estévez, E., Salvadó, H., Barquín, J. & Cañedo-Argüelles, M. Human activities disrupt the temporal dynamics of salinity in Spanish rivers. *Hydrobiologia* **850**, 4531–4546 (2023).

43. Hartmann, J., Lauerwald, R. & Moosdorf, N. A Brief Overview of the GLObal RIver Chemistry Database, GLORICH. *Procedia Earth and Planetary Science* **10**, 23–27 (2014).

44. Virro, H., Amatulli, G., Kmoch, A., Shen, L. & Uuemaa, E. GRQA: Global River Water Quality Archive. *Earth Syst Sci Data* **13**, 5483–5507 (2021).

45. Feio, M. J. *et al.* Fish and macroinvertebrate assemblages reveal extensive degradation of the world's rivers. *Glob Chang Biol* **29**, 355–374 (2023).

46. Thorslund, J. & van Vliet, M. T. H. A global dataset of surface water and groundwater salinity measurements from 1980–2019. *Sci Data* **7**, (2020).

47. Kaushal, S. S. *et al. Freshwater Salinization Syndrome: From Emerging Global Problem to Managing Risks*. *Biogeochemistry* vol. 154 (Springer International Publishing, 2021).

48. Mcmillan, H., Krueger, T. & Freer, J. Benchmarking observational uncertainties for hydrology: Rainfall, river discharge and water quality. *Hydrol Process* **26**, 4078–4111 (2012).

49. Sprague, L. A., Oelsner, G. P. & Argue, D. M. Challenges with secondary use of multi-source water-quality data in the United States. *Water Res* **110**, 252–261 (2017).

50. Linke, S. *et al.* Global hydro-environmental sub-basin and river reach characteristics at high spatial resolution. *Sci Data* **6**, (2019).

51. Kaczmarek, N. *et al.* Macroinvertebrate community responses to salinity around non-saline–saline confluences in the Draa River basin, Morocco. *Hydrobiologia* (2024) doi:10.1007/s10750-023-05445-7.

52. Kefford, B. J. *The Relationship between Electrical Conductivity and Selected Macroinvertebrate Communities in Four River Systems of South-West Victoria, Australia*. *International Journal of Salt Lake Research* vol. 7 (1998).

53. Kefford, B. J. *et al.* Understanding salt-tolerance and biota-stressor interactions in freshwater invertebrate communities. *Mar Freshw Res* **73**, 140–146 (2021).

54. Sabater, F., Sabater, S. & Armengol, J. *CHEMICAL CHARACTERISTICS OF A MEDITERRANEAN RIVER AS INFLUENCED BY LAND USES IN THE WATERSHED*. *War. Res* vol. 24 (1990).

55. Kaushal, S. S. *et al.* Freshwater salinization syndrome on a continental scale. **115**, E574–E583 (2018).

56. McCleskey, R. B., Nordstrom, D. K., Ryan, J. N. & Ball, J. W. A new method of calculating electrical conductivity with applications to natural waters. *Geochim Cosmochim Acta* **77**, 369–382 (2012).

57. Hem, J. D. *Study and Interpretation of the Chemical Characteristics of Natural Water Third Edition*. (1985).

58. Lxxe'n, D. P. H. *A Specific Conductance Method for Quality Control in Water Analysis*. vol. 11 (1977).

59. Miles, L. J. & Yost, K. J. *Quality Analysis of USGS Precipitation Chemistry Data for New York*. (1982).

60. Ros Sum, J. R. *Conductance Method for Checking of Water Analyses*. *Public Health Assoc* vol. 11 https://pubs.acs.org/sharingguidelines (1946).

3.3. Chapter II: Human activities disrupt the temporal dynamics of salinity in Spanish rivers

Article published in Hydrobiologia on November 22, 2022.

Hydrobiologia (2023) 850:4531–4546
https://doi.org/10.1007/s10750-022-05063-9

EFFECTS OF CHANGES IN SALINITY

Human activities disrupt the temporal dynamics of salinity in Spanish rivers

Alvaro Javier Moyano Salcedo · Edurne Estévez · Humbert Salvadó · José Barquín · Miguel Cañedo-Argüelles

Received: 12 July 2022 / Revised: 7 October 2022 / Accepted: 12 October 2022 / Published online: 18 November 2022
© The Author(s) 2022

Abstract Human activities are not only increasing salinization of rivers, they might also be altering the temporal dynamics of salinity. Here, we assess the effect of human activities on the temporal dynamics of electrical conductivity (EC) in 91 Spanish rivers using daily measures of EC from 2007 to 2011. We expected rivers weakly affected by human activities to have low and constant ECs, whereas rivers strongly affected by human activities should have high and variable ECs throughout the year. We collected information on land use, climate, and geology that could explain the spatiotemporal variation in EC. We identified four groups of rivers with differences in EC trends that covered a gradient of anthropogenic pressure. According to Random Forest analysis, temporal EC patterns were mainly driven by agriculture, but de-icing roads, mining, and wastewater discharges were also important to some extent. Linear regressions showed a moderate relationship between EC variability and precipitation, and a weak relationship to geology. Overall, our results show strong evidence that human activities disrupt the temporal dynamics of EC. This could have strong effects on aquatic

Handling editor: Sidinei M. Thomaz

Guest editors: Erik Jeppesen, Miguel Cañedo-Argüelles, Sally Entrekin, Judit Padisák &S.S.S. Sarma / Effects of induced changes in salinity on inland andcoastal water ecosystems

Supplementary Information The online version contains supplementary material available at https://doi.org/10.1007/s10750-022-05063-9.

A. J. Moyano Salcedo (✉)
FEHM-Lab (Freshwater Ecology, Hydrology and Management), Departament de Biologia Evolutiva, Ecologia i Ciències Ambientals, Facultat de Biologia, Universitat de Barcelona, Barcelona, Spain
e-mail: alvaromoyano@ub.edu

A. J. Moyano Salcedo
Geohazards and Civil Engineering Research Group, Department of Civil Engineering, Saint Thomas Villavicencio University, C/22 No 1a, Villavicencio 500003, Colombia

E. Estévez
Department of Ecology, University of Innsbruck, Technikerstrasse 25, 6020 Innsbruck, Austria
e-mail: Edurne.Estevez-Cano@uibk.ac.at

H. Salvadó
Department of Evolutive Biology, Ecology and Environmental Sciences, University of Barcelona, 08028 Barcelona, Spain
e-mail: hsalvado@ub.edu

J. Barquín
Environmental Hydraulics Institute 'IH Cantabria', University of Cantabria, PCTCAN. C/ Isabel Torres 15, 39011 Santander, Spain
e-mail: jose.barquin@unican.es

M. Cañedo-Argüelles
Institute of Environmental Assessment and Water Research (IDAEA-CSIC), Carrer de Jordi Girona, 18-26, 08034 Barcelona, Spain
e-mail: miguel.canedo@idaea.csic.es

biodiversity (e.g., aquatic organisms might not adapt to frequent and unpredictable salinity peaks) and should be incorporated into monitoring and management plans.

Keywords Freshwater salinization · Temporal dynamics · Variability · Agriculture · Precipitation · Water quality

Introduction

Freshwater ecosystems are becoming saltier worldwide due to human activities (i.e., freshwater salinization, FS). Agriculture is the main driver of FS (Thorshlund et al., 2021), but there are others such as mining or the use of salts as de-icing agents in roads (Estevéz et al. 2019; Cañedo-Argüelles, 2020). Overall, FS is a global water quality problem that not only harms biodiversity and ecosystems (Cañedo-Argüelles et al. 2013; Berger et al., 2018; Hintz & Reylea, 2019), but also poses risks to human health (Kaushal, 2016; Cañedo-Argüelles, 2020) and can limit our use of hydric resources (Van Vliet et al., 2017; Thorshlund et al., 2021). The vast majority of studies on FS have focused on short-term laboratory or mesocosm experiments, or on snapshot field studies (Kefford et al., 2003; Horrigan et al., 2007; Birk et al., 2020). Thus, the temporal dynamics of FS have been largely overlooked. The few available studies addressing temporal variability in FS show that human activities can disrupt the natural temporal dynamics of salinity in freshwater ecosystems (Timpano et al., 2018; Niedrist, 2020). We argue that each type of human activity might have a different "temporal signature" (i.e., a characteristic temporal behavior) due to its intrinsic properties.

In agricultural landscapes the temporal dynamics of salinity might depend on the cultivation period and practices (e.g., rainfed vs. irrigated crops). For example, Gardner & Young (1988) showed that salt accumulation in the Colorado River Basin was primarily driven by excess irrigation water from croplands, and that irrigation explained more than a third of the basin salt load. Also, Heimhuber et al. (2019) found that extended dry periods increased salinity due to reduced river discharge and salt accumulation in agricultural regions of the Murray-Darling Basin (Australia). Finally, Leng et al. (2021) found a strong correlation between nutrients and salinity with the discharge of agricultural irrigation water into the Amu Darya and Syr Darya Rivers, in Central Asia. Overall, salinity is strongly driven by irrigation during low-flow periods in agricultural catchments (Crosa et al., 2006; Kulmatov et al., 2020). Therefore, peaks in conductivity are most likely to occur during planting periods, when fertilizer addition and irrigation are maximum. During these periods, the salts that have not been used by the plants are washed into surrounding rivers and streams (Williams, 2001; Anderson et al., 2019). In mining regions where residues are stockpiled (i.e., mine tailings) and surface rocks are exposed to weathering, heavy rain events can wash the salts into surrounding surface waters (Cañedo-Argüelles et al., 2012). This leads to sharp salinity increases that are usually brief and not captured by conventional water quality monitoring programmes (Cañedo-Argüelles et al., 2017; Liu et al., 2021). At the same time, saline effluents generated as a by-product of resource extraction might be disposed directly to surface waters (Cormier et al., 2013b; Vengosh et al., 2014; Sauer et al., 2016; Yusta-García et al., 2017) and diffuse salt pollution can generate from leaks in the waste management infrastructure (Gorostiza & Sauri, 2019). Finally, mining can lead to the salt pollution of groundwaters (Xinwei et al. 2009; Kaushal et al. 2018; Bondu et al. 2021), which can enter rivers and streams at different rates depending on complex geomorphological processes that are difficult to predict (Dahl et al., 2007; Sun & Sun, 2013). In cold regions, salts are often applied to roads to keep them ice-free and ensure road safety and transportation efficiency. For example, salt application has exponentially increased in the US since 1940 (Jackson & Jobbagy, 2005), with around 25 million metric tons of salts applied to roads in 2019 (USGS, 2020). Also, 13.4 tons of sodium chloride are applied annually to each kilometer of roads affected by ice in the Alpine region of Tyrol (Niedrist et al., 2020). Commonly, rivers and streams close to roads in cold regions experience an increase in salinity during early spring (when the snow is melted and flows into the surrounding streams) and during periods of snow-removal from the roads (Crowther & Hynes, 1977; Ruth, 2003; Kaushal et al., 2005; Corsi et al., 2015; Nava et al.,

M. Cañedo-Argüelles
FEHM-Lab (Freshwater Ecology, Hydrology and Management), Departament de Biologia Evolutiva, Ecologia i Ciències Ambientals, Facultat de Biologia, Institut de Recerca de l'Aigua (IdRA), Universitat de Barcelona, Barcelona, Spain

2020; Dugan et al., 2020; Niedrist, 2020). Cities generate a large amount of wastewaters that contributes to the salinization of surface waters (Venkatesan et al., 2011) and groundwaters (Li et al., 2021). Salinity attributed to urban areas can be determined by the quantity and type of products used by consumers (Hoekstra, 2015), and the climatic conditions that influence the dilution capacity of rivers and streams (Tiyasha et al., 2020). Also, the efficiency of wastewater treatment plants (WWTP) modulates the salt load of their effluents. For example, Levlin (2014) monitored two WWTP in Stockholm and found no significant reduction in conductivity by the preliminary treatment, and less than a 30% reduction by the activated sludge process (Moyano-Salcedo et al., 2021). Overall, the salt pollution associated with wastewater discharges depends on the WWTP configuration (Gonçalves et al., 2019; Salcedo et al., 2021) and might be highest during the summer, when the dilution capacity of rivers and streams is reduced (Dinçer & Kargi, 2001; Van Vliet & Zwolsman, 2008).

Understanding the temporal dynamics of FS is important because they can affect the structure and functioning of biological communities. For example, Kefford et al. (2007a, b, c) found that the eggs of some freshwater invertebrates were more sensitive to salt pollution than their larval stages. Thus, FS might have a greater effect for macroinvertebrates during oviposition than during larval development or during summer, when many species have emerged from the water. Also, many invertebrates that feed on leaf litter are especially sensitive to salinization (Kefford et al., 2011). This can also have implications for ecosystem functioning, since aquatic invertebrates contribute to carbon cycling through leaf litter decomposition (Canhoto et al., 2021).The aim of this study was to analyze how human activities might disrupt the temporal dynamics of electrical conductivity (EC, a proxy to salinity) in Spanish rivers using long-term data at high temporal resolution. Although previous studies have analyzed long-term salinity trends in rivers (Kaushal et al., 2005; Jiang et al., 2022), this is the first study focusing on the temporal fluctuations of salinity at an interannual scale and a high temporal resolution. We hypothesized that rivers under low human pressure would have low and constant ECs, whereas rivers strongly affected by human activities would have high and variable ECs throughout the year. We expected that the temporal dynamics of EC in Spanish rivers would be mainly driven by (I) agricultural activity, leading to EC peaks during the crops' growing season; (II) mining, leading to high ECs near mine tailings during heavy rainfall events; (III) transportation in cold regions, with high ECs during snowmelt and precipitation events in spring; and (IV) wastewater discharge in urban areas that would lead to maximum ECs during the summer due to low river flows.

Materials and methods

Study area

We studied 13 river catchments covering a wide range of land reliefs (i.e., valleys and mountains) and geological formations (e.g., carbonated rocks the eastern and southern regions and igneous metamorphic and rocks in the western regions) (Morán-Tejeda et al., 2019), and differing in size (from 900 to more than 90 000 km^2) (Estévez et al., 2019). They also covered diverse climatic conditions: the central, southern, and eastern regions present a Mediterranean climate, whereas the northern border is dominated by a temperate oceanic climate (Rivas et al., 2011). Finally, these heterogeneous environmental conditions result in a gradient of hydrological conditions, with some rivers drying during the summer (Peñas & Barquín, 2019; Estévez et al., 2019).

Electrical conductivity measurements

We used daily measures of electrical conductivity (EC) for the period 2007–2011 from 91 stations of the Automatic Water Quality Information System (SAICA, 2020). Using these data, a set of 24 ecologically meaningful conductivity indices (CIs) (Table S1 in Online Resource 1) were calculated based on hydrological indices (Richter et al., 1996; Peñas & Barquín, 2019). These indices were divided into three groups regarding (1) the mean annual and monthly conductivity, (2) the magnitude and duration of annual conductivity extremes, and (3) the timing of extreme conductivity events.

Environmental and human drivers

We selected relevant variables that could drive the change in the temporal dynamics of EC (Table S2 in

Online Resource 1), which were related to land use ($n=8$), geologic characteristics ($n=2$), and anthropogenic pressures ($n=4$). Distance to the nearest mine (P_DMN) and distance to the nearest icy road (P_DIR) were computed in R (R Core Team, 2021) according to the information available from the Spanish National Geographic Institute (2020). To calculate P_DMN, all mines with operating permits were located. Only the mines exploiting ferrous, non-ferrous, precious, non-metallic (e.g., salt), industrial rocks, and coal mines were considered. To calculate P_DIR, areas with a minimum of 30 days of snow were selected. Then, to determine the roads where salt was likely added, the selected areas were intersected with a road map. The intersected roads were checked using information provided by the Spanish General Direction of Traffic (2020). Finally, the distances of each SAICA station to mines (P_DMN) and icy roads (P_DIR) were calculated. The rest of the variables were computed by Estevéz et al. (2019).

Assessment of the drivers of changes in the temporal dynamics of EC

First, principal components (PCA) and clustering (Lemenkova, 2018) analyses were performed to group the samples according to their CIs. The multicollinearity of CIs was calculated using the Variance Inflation Factor (VIF) function in the R package "car," and the CIs with highly collinearity (VIF > 5) were removed. Then, Random forests (RF) were performed to assess the relative importance of the environmental drivers for explaining the variation in EC within each group using the function "rfsrc" in the package "randomForestSRC" (Ishwaran et al., 2022). ANOVA and Tukey's tests were used to assess the differences in CI between clusters. Then, generalized additive models (GAMs) were used to assess the relationship between EC and the different drivers selected by the RF using the function "gam" in the package "mgcv" (Wood, 2021). The GAMs incorporated independent smooths for each cluster and time step (i.e., each day at which conductivity was measured) and they were built using a default Gaussian distribution. To obtain model diagnostics, we used the "gam.check" and "appraise" functions in the package gratia (Pedersen et al., 2019). We assessed the differences between GAMs (i.e., differences in the temporal behavior of EC between groups) by looking at the confidence intervals. If the difference between the confidence intervals of the fitted smooths between two sets of data (i.e., cluster groups in our study) was non-zero, a strong difference was assumed (Pedersen et al., 2019). Linear regressions between EC and precipitation were built. All the statistical analyses were performed in R (R Core Team, 2021). Finally, the nomenclature proposed by Muff et al. (2022) was used to report the results from statistical analyses in the language of evidence.

Results

The minimum EC was always above 100 µS/cm and the maximum EC value was 5989 µS/cm. Overall, we found a strong decrease in mean EC ($R2=0.001$; P value <0.001) at a rate of 17 µS/cm per year (Fig. S1 in Online Resource 2).

Variations in temporal dynamics of EC among Spanish rivers

Five indices related to the annual coefficient of variation (CVA), twelve to the monthly coefficient of variation (CVM), and ten indices related to the timing of extreme EC events (JMax and JMin) were selected to classify the rivers because of having a VIF lower than 5 (Tables S3, S3a and S3b; Online Resource 1). The first two axes of the PCA (Fig. 1) explained 56.7% of the variance in the different CIs, and the cluster analysis resulted in four groups of stations (SCI1, SCI2, SCI3, and SCI4; Fig. 2). The first axis of the PCA was mainly related to the coefficient of variation of the mean annual EC (CVA) and the coefficient of variation of the mean monthly EC (CVM from month 1 to 12). The groups were arranged along this axis as follows (from positive to negative values): SCI1, SCI4, SCI3, and SCI2. The second axis of the PCA was positively related to the Julian day of annual maximum EC per year (JMax) and negatively to the Julian day of annual minimum EC per year (JMin). All the groups contained stations with both positive and negative values of this axis, but the group SC1 showed the widest dispersion (i.e., a highest temporal variation in EC). SCI1 included 9 stations with the highest mean EC and standard deviation (2500 ± 930 µS/cm); group SCI2 included 37 stations with the lowest mean EC and standard deviation (374 ± 185 µS/cm); group SCI3 included 26 stations with moderate-low

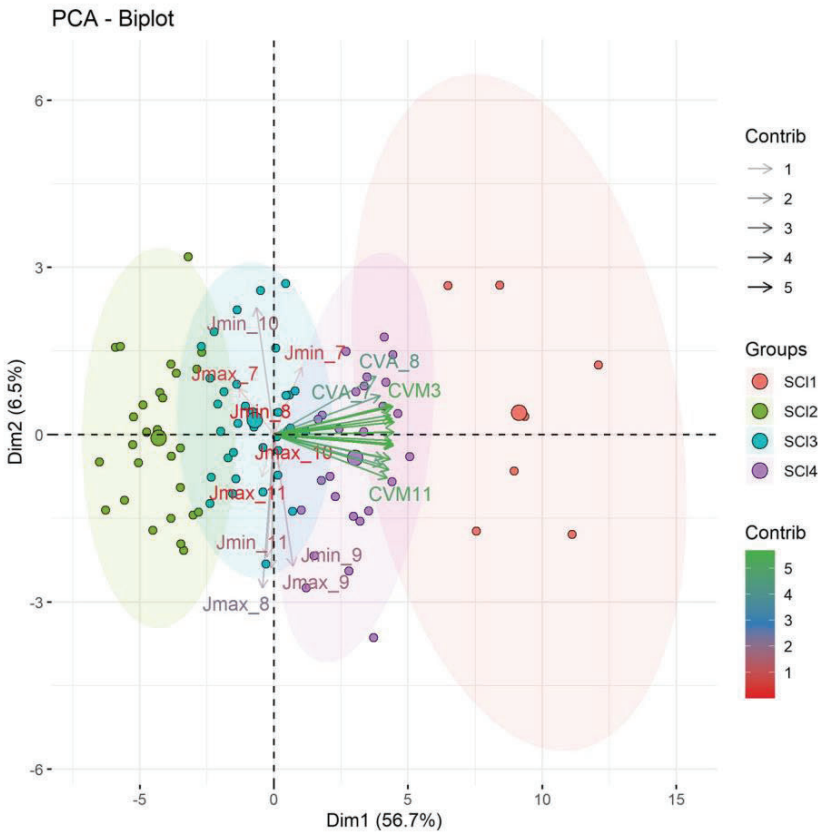


Fig. 1 Plot representing PCA and clustering of Synthetized Conductivity Indices (SCIs). The points and arrows represent the number of SAICA stations by cluster and the CIs, respectively

mean EC and standard deviation (850 ± 268 µS/cm); and group SCI4 included 19 stations with moderate-high mean EC and standard deviation (1300 ± 473 µS/cm). Figure 3 shows the EC variations by SCIs for the study period. In agreement with the PCA analysis, SCI1 showed the highest EC variations, followed by SCI4, SCI3, and SCI2. According to the comparison of GAMs, SCI1 showed strong differences (i.e., confidence intervals in pairwise comparisons for GAMs smooth terms was non-zero) from the rest of the groups in terms of temporal variations in EC (Fig. S2 in Online Resource 2). According to the Random Forest ($R2 = 0.52$), the temporal variation in EC was mainly driven by agriculture (MN_AGR), distance to the nearest icy road (P_DIR) and mining site (P_DMN) in SCI1; distance to the nearest icy road (P_DIR), area occupied by moors, heathland, scrub and shrubs (MN_SSH), agriculture (MN_AGR), and pasture (MN_PAS) in SCI2; mining (P_DMN) and urban areas (MN_UHD) in SCI3; and by pasture cultivation (MN_PAS), agriculture (MN_AGR) and, in some cases, the area occupied by coniferous forest (MN_CNF) in SCI4 (Fig. 4).

According to ANOVA, there was strong evidence of differences between groups (P value < 0.001 in all cases) for several of the drivers analyzed (Fig. 5). SCI1 was the most subjected to human activities, with the highest values of agricultural land, mining, and urban areas, and the lowest values of forest cover and calcareous and siliceous soils. On the opposite extreme of the anthropogenic disturbance gradient, SCI2 and SCI3 were characterized by the highest forest and pasture cover and the lowest urban cover, although SCI2 showed the closest distance to roads affected by snow, and SCI3 showed the closest distance to mining sites. SCI4 presented intermediate values for most drivers. Finally, geological conditions showed a weak relation to temporal EC variations in all SCIs and had the lowest relevance to explain EC variations in SCI1 (the most impacted

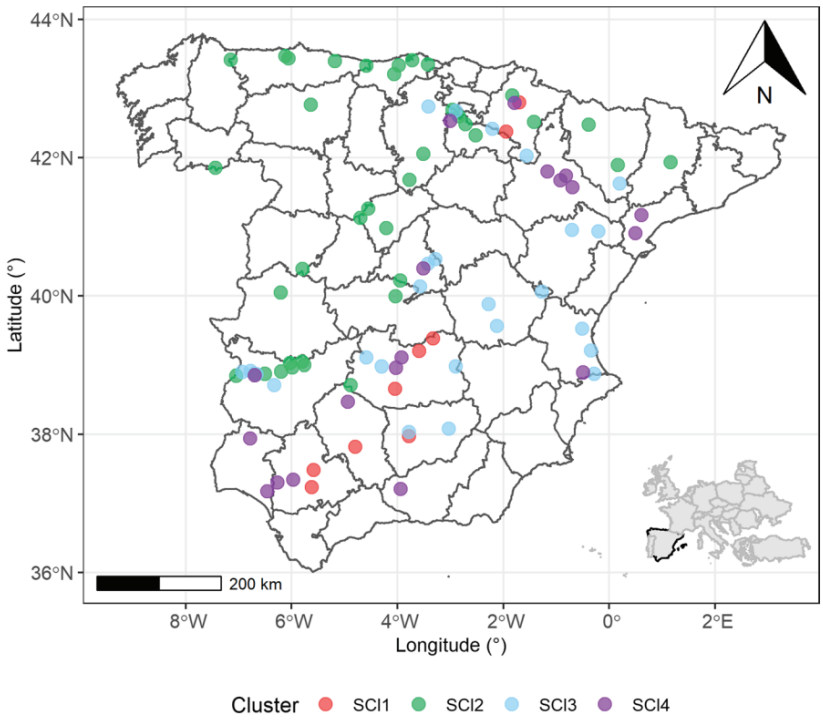


Fig. 2 Geographical map showing a spatial representation of the obtained cluster groups of Synthetized Conductivity Indices (SCIs). The points represent the number of SAICA stations by cluster

by human activities) (Fig. 4). Also, according to the ANOVA test, there was no evidence (P value = 0.738) for differences in EC between calcareous (mean EC = 920 ± 300 µS/cm) and siliceous (mean EC = 800 ± 279 µS/cm) catchments (Fig. S3, Online Resource 2). We found strong positive linear relationships between precipitation and EC during February (P value = 0.012) and November (P value = 0.007) in SCI1. In SCI2, EC was strongly associated with precipitation in March (P value = 0.027), July (P value < 0.001), August (P value < 0.001), October (P value = 0.002), and December (P value < 0.001). In SCI3, EC was strongly related to precipitation in February (P value < 0.001), October (P value = 0.019), and November (P value < 0.001). In SCI4, EC was very strongly related to precipitation in August (P value < 0.001), November (P value < 0.001), and December (P value < 0.035). Finally, EC was strongly related to heavy rainfall events in SCI3 (P value = 0.05), and to low rainfall events (< 10 mm) in SCI1 (P value < 0.019), SC2 (P value < 0.001), and SCI3 (P value < 0.001). The R-squared values of the linear models are shown in Table S4 (Online Resource 1).

Discussion

Overall, we found strong evidence for an amplification of the temporal variability in EC in Spanish rivers due to human activities. The EC was relatively constant along the year in rivers dominated by pasture and forests, whereas it experienced frequent and strong fluctuations in rivers subjected to high human pressure. Also, the group of sites most affected by anthropogenic disturbance (SCI1) showed mean EC values above the current Spanish water quality standards set to protect aquatic ecosystems (1000 µS/cm; Real Decreto 670, 2013) and human health (2500 µS/cm; Real Decreto 140, 2003). This aligns with previous studies showing that water quality standards in Europe are failing to protect aquatic biodiversity from salinization (Schuler et al., 2019; Hintz et al., 2022a, b). Contrary to our expectations, we found that the grouping of sites according to the temporal variability in EC did not respond to unique human drivers, but to a combination of them. Therefore, we cannot claim that each human activity has its own "temporal signature." This is likely related with regional differences in the human drivers of FS (e.g., different crops

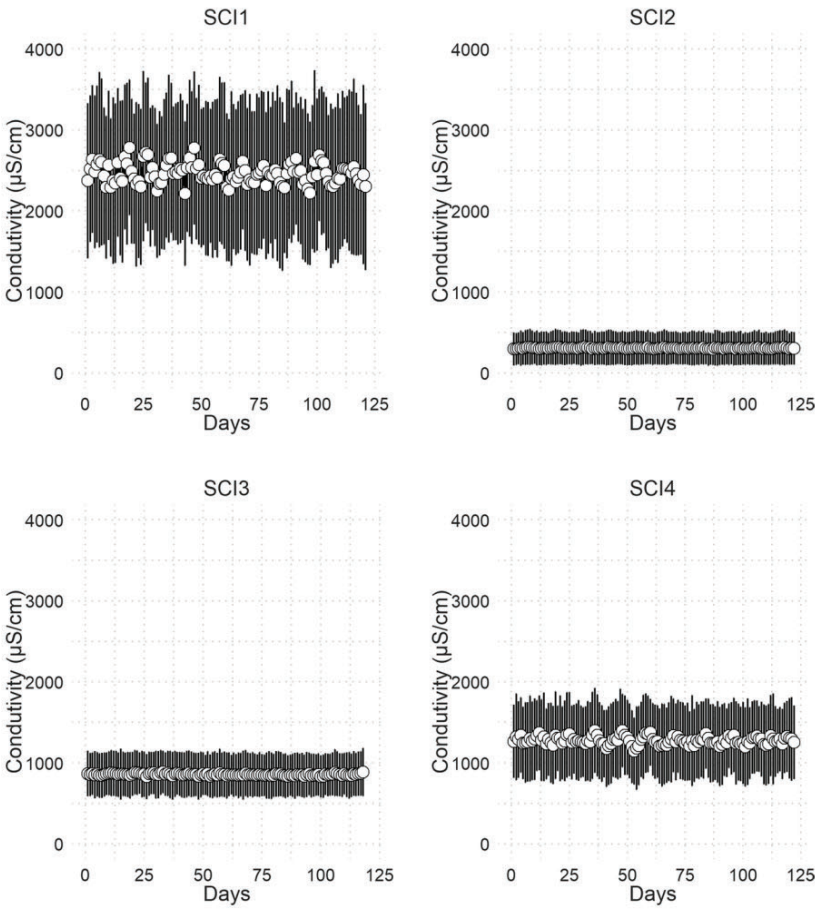


Fig. 3 Plot representing the mean value and variability in conductivity of each group with Synthetized Conductivity Indices (SCIs). The point and the irregular line represent the mean value and standard deviation, respectively

have different growing seasons) and in the natural drivers that modulate natural salinity (e.g., hydrology). Overall, the range of EC values reported in our study matches those reported by previous studies in Spanish rivers (Table S5 in Online Resource 3). We found strong evidence that the EC trends decreased from 2007 to 2011 for the whole set of rivers analyzed. These EC trends could be linked to technology improvements and the increase in the number of wastewater treatment plants (Fuentes et al., 2017; Rufí-Salís et al., 2022; Pompa-Pernía et al., 2022). Although a decrease in EC has also been reported for other regions (Jiang et al., 2022), it is important to notice that many freshwater ecosystems are getting saltier (Kaushal et al., 2005; Dugan et al., 2017) and this trend might be amplified by climate change (Le et al., 2019; Olson, 2019).

Agriculture was the main variable that differentiated sites with high mean EC and EC variability (SC1 and SCI4) from sites with low-moderate mean EC and EC variability (SCI2 and SCI3). This is in alignment with previous studies at the global (Kaushal et al., 2018; Thorslund et al., 2021) and the Spanish (Estévez et al., 2019) level, which identified agriculture as the main driver of FS. Our study reveals that agriculture is not only increasing the salt concentration of rivers, but also disrupting the natural temporal dynamics of salinity. Although the proximity of icy roads was not as important as agriculture, the ANOVA tests showed very strong evidence for differences between groups according to this variable. So far, road salt pollution of rivers and streams has been almost exclusively studied in Canada and the US (Cunillera-Montcusí et al., 2022). Our results suggest

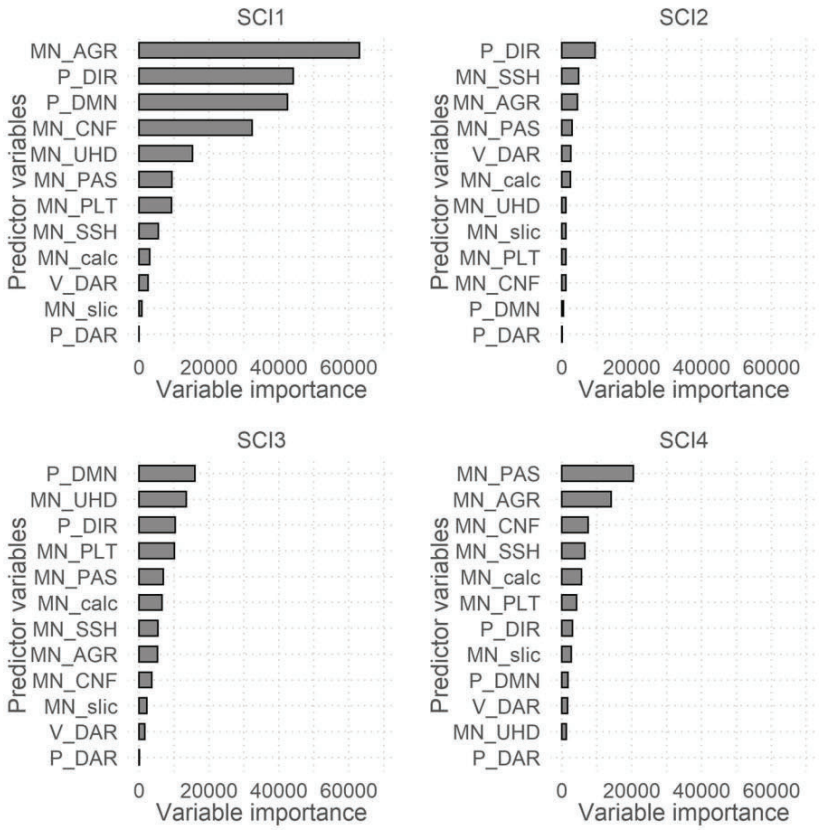


Fig. 4 Random forests (RF) plot representing the relative importance of the environmental drivers for explaining variation in conductivity within each SCIs. P_DMN: Distance to the nearest mining. P_DIR: Distance to the nearest icy road. P_DAR: Distance to the nearest dam upstream. V_DAR: Distance to the nearest effluent discharge upstream. MN_UHD: Area occupied by urban areas in the draining catchment. MN_AGR: Area occupied by agricultural land in the draining catchment. MN_CNF: Area occupied by coniferous forest in the draining catchment. MN_PLT: Area occupied by plantations in the draining catchment. MN_SSH: Area occupied by moors, heathland, scrub, and shrubs in the draining catchment. MN_PAS: Area occupied by pasture in the draining catchment. MN_calc: Area occupied by calcareous rocks in the draining catchment. MN_slic: Area occupied by siliceous rocks in the draining catchment

that this activity is partly responsible for the increase in EC and the alteration of EC dynamics in Spanish rivers, as it has been found for the Alps (Niedrist et al., 2020). Thus, we suggest that road salt pollution of rivers and streams deserves to be further studied in Europe. Despite wastewater treatment plants having a weak effect on EC variability, these also deserve attention due to the potential interacting effect of salinity with other chemical cocktails that compose the so-called freshwater salinization syndrome (Kaushal et al., 2018, 2019, 2021, 2022). Finally, we found weak differences in EC between rivers according to their geological composition. This suggests that human activities are overriding the influence of geology, which is the main driver of changes in salinity in pristine rivers and streams (Meybeck, 2003).

Temporal changes in EC were very strongly affected by precipitation during some of the studied months. The fact that the months that showed a strong linear relationship between precipitation and EC were different for each group suggests that human activities and climatic drivers interact to modulate the temporal dynamics of salt pollution. For instance, in the case of

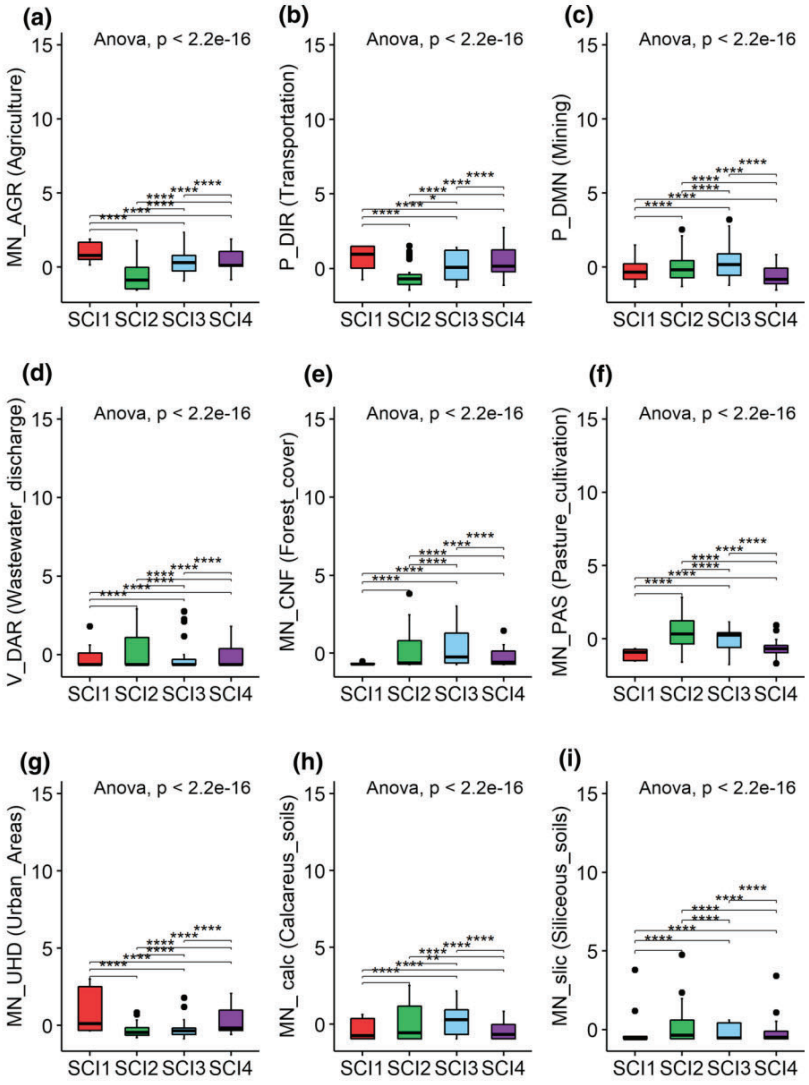


Fig. 5 Results of the relevant environmental variables (according to RF) and differences between SCIs (Standardized Values). **A** MN_AGR: Area occupied by agricultural land in the draining catchment. **B** P_DIR: Distance to the nearest icy road. **C** P_DMN: Distance to the nearest mining. **D** V_DAR: Distance to the nearest effluent discharge upstream. Limitation of 5000 m. **E** MN_CNF: Area occupied by coniferous forest in the draining catchment. **F** MN_PAS: Area occupied by pasture in the draining catchment. **G** MN_UHD: Area occupied by urban areas in the draining catchment. **H** MN_calc: Area occupied by calcareous rocks in the draining catchment. **I** MN_slic: Area occupied by siliceous rocks in the draining catchment

agriculture (which was most important in SCI1), daily EC and precipitation were strongly related during August–November, suggesting that salts could build up in the soil during the summer and then enter the rivers as runoff. Concordantly, Merchant et al. (2020) found that EC significantly increased in the Cidacos river (included in our study) during July–November due to crop irrigation. In SCI2, where road-de-icing and wastewater discharge were among the most important predictors according to RF, EC was related to precipitation during winter, spring, and summer. These are the months when there were roads affected by snow, salt could be washed into the rivers due to ice melting and river flows were low, respectively. The potential influence of road salt application on the EC of rivers enclosed in SCI2 aligns with a previous study (Asensio et al., 2017) that found salinized soils 3 m away from roads affected by snow during winter in some of the rivers belonging to this group (Aragon, Araquil, and Arga). Concordantly, in our study, these rivers showed higher mean and standard deviation EC (670 ± 155 µS/cm) than the rest of the

rivers belonging to the same group (280 ± 104 µS/cm). In SCI3, which had the greatest impact from mining, EC was strongly related to heavy precipitation in autumn. Heavy rainfalls and flash floods are common in Spain during autumn, especially in the Mediterranean region (Belmonte & Beltrán, 2001; Machado et al., 2011; Camarasa, 2016; Ribas et al., 2020), where important mining areas exist (Spanish National Geographic Institute, 2020). These heavy rain events are associated with EC peaks in mining areas due to the washing of salts that are stockpiled in mine tailings (Cañedo-Argüelles et al., 2012, 2017; Ladrera et al., 2017; Gorostiza & Sauril, 2019). Finally, it is important to take into account that the rivers included in this study are relatively large (mean water level = 0.76 ± 0.97 m), thereby having a high salt dilution capacity (Turunen et al., 2020). Thus, our results need to be taken with caution, as the magnitude of salt pollution and the disruption of the temporal salinity dynamics in smaller rivers and streams might be higher than those reported here. The disruption of the temporal dynamics of EC can have serious consequences for aquatic biodiversity. For example, we found EC peaks higher than 3500 µS/cm in SC1. These EC values are lethal to many riverine organisms according to field studies and laboratory assays (Kefford et al., 2003; Horrigan et al., 2007; Cañedo-Argüelles et al., 2013). However, it is not only the magnitude of the EC peaks that matter, but also their timing. For example, during winter, many macroinvertebrate species are at early development stages, which tend to be more sensitive to salinization than the older stages (Kefford et al., 2004, 2007a, b, c). Also, during summer, many taxa lay their eggs, which might not hatch at high EC (Bailey et al., 2004; Kefford et al., 2007a, b, c; Lawson et al., 2021). Also, the existence of unpredictable and frequent EC peaks along the year could difficult the adaptation of the species to salinization and have deleterious effects on both biodiversity and ecosystems functioning (Cañedo-Argüelles et al., 2014; Oliveira et al., 2021).

Conclusions

This study is the first to analyze how the combination of natural and human drivers (agriculture, mining, wastewater, transportation, and urban areas) influences the temporal dynamics of EC in Spanish rivers. We found strong evidence for a disruption of the temporal dynamics of EC due to human activities during the period study (2007–2011). We obtained four groups (SCI1, SCI2, SCI3, and SCI4) of rivers separated according to EC variability and the timing of extreme EC events. We found different EC patterns throughout the year, with some rivers showing high mean EC and EC variability (SCI1 and SCI4) and others lower and less variable ECs (SCI2 and SCI3). The disruption of the temporal dynamics of EC did not show a clear separation between stations according to the dominance of different human activities. Instead, we found that EC variations were determined by a combination of multiple environmental and human drivers. Agriculture was the main driver of FS, but de-icing roads, mining, and wastewater discharges were also important to some extent. Also, there was very strong evidence for relationships between precipitation and EC that could be related to different human activities (e.g., crop irrigation or road salt application). Overall, our results call for more studies analyzing the ecological implications of increased variability of EC as a result of human activities. According to our results, it seems advisable to measure EC multiple times throughout the year and establish monitoring periodicity according to the human pressures that are operating on rivers and the natural seasonal EC dynamics. For example, in agricultural watersheds dominated by agriculture, information on the timing of pesticide and fertilizer application, irrigation, and harvesting could be very useful to anticipate changes in ECs in the rivers. Also, more studies on the ecological impacts of EC fluctuations are needed to implement effective management responses that protect freshwater biodiversity from salinization.

Acknowledgements AM was supported in part by a doctoral grant from the Ministerio de Ciencia, Tecnología e innovación y Colfuturo (Colombia). MC was supported by a Ramón y Cajal contract funded by the Spanish Ministry of Science and Innovation (RYC2020-029829-I).

Author contributions All authors contributed to the study conception and design. Material preparation, data collection, and analysis were performed by AJMS, EE, JB, and MC-AI. The first draft of the manuscript was written by AJMS and MC-AI. All authors commented on previous versions of the manuscript. All authors read and approved the final manuscript. MC-AI and HS contributed to funding acquisition, and supervision.

Funding Open Access funding provided thanks to the CRUE-CSIC agreement with Springer Nature. AM was supported in part by a doctoral grant from the Ministerio de Ciencia, Tecnología e innovación y Colfuturo (Colombia). MC was supported by a Ramón y Cajal contract funded by the Spanish Ministry of Science and Innovation (RYC2020-029829-I).

Data availability All data produced from this study are provided in this manuscript (and its supplementary information files). The information on environmental drivers of freshwater salinization was downloaded from Sistema de Información de Ocupación de Suelos de España (SIOSE, https://www.siose.es/usos-de-suelo) and Instituto Geográfico Nacional, Spain (ING, 1 https://www.ign.es/web/ign/portal). Conductivity measurements were downloaded from the Water Quality Information System (SAICA network, http:// www.mapama.gob.es). Other datasets generated (e.g., R scripts) during the current study are available from the corresponding author upon request.

Declarations

Conflict of interest The authors declare there is no conflict of interest.

Ethical approval The research complies with ethical standards.

Consent for publication Not applicable.

Open Access This article is licensed under a Creative Commons Attribution 4.0 International License, which permits use, sharing, adaptation, distribution and reproduction in any medium or format, as long as you give appropriate credit to the original author(s) and the source, provide a link to the Creative Commons licence, and indicate if changes were made. The images or other third party material in this article are included in the article's Creative Commons licence, unless indicated otherwise in a credit line to the material. If material is not included in the article's Creative Commons licence and your intended use is not permitted by statutory regulation or exceeds the permitted use, you will need to obtain permission directly from the copyright holder. To view a copy of this licence, visit http://creativecommons.org/licenses/by/4.0/.

References

Alcalá, F. J. & E. Custodio, 2008. Using the Cl/Br ratio as a tracer to identify the origin of salinity in aquifers in Spain and Portugal. Journal of Hydrology 359(1–2): 0022–1694. https://doi.org/10.1016/j.jhydrol.2008.06.028.

Anderson, T. A., E. A. Bestland, I. Wallis, H. D. Guan & T. A. Anderson, 2019. Salinity balance and historical flushing quantified in a high-rainfall catchment (Mount Lofty Ranges, South Australia). Hydrogeology Journal 27: 1229–1244.

Arenas-Sánchez, A., S. Dolédec, M. Vighi & A. Rico, 2021. Effects of anthropogenic pollution and hydrological variation on macroinvertebrates in Mediterranean rivers: a case-study in the upper Tagus river basin (Spain). Science of the Total Environment 766: 144044. https://doi.org/10.1016/j.scitotenv.2020.144044.

Asensio, E., V. J. Ferreira, G. Gil, T. García-Armingol, A. M. López-Sabirón & G. Ferreira, 2017. Accumulation of deicing salt and leaching in Spanish soils surrounding roadways. International Journal of Environmental Research and Public Health 14(12): 1498. https://doi.org/10.3390/ijerph14121498.

Belmonte, A. M. C. & F. S. Beltrán, 2001. Flood events in Mediterranean ephemeral streams (ramblas) in Valencia region, Spain. CATENA 45(3): 229–249. https://doi.org/10.1016/S0341-8162(01)00146-1.

Besemer, K., 2015. Biodiversity, community structure and function of biofilms in stream ecosystems. Research in Microbiologoy 166(10): 774–781. https://doi.org/10.1016/j.resmic.2015.05.006.

Berger, E., O. Frör, & R. B. Schäfer, 2019. Salinity impacts on river ecosystem processes: A critical mini-review. Philosophical Transactions of the Royal Society B: Biological Sciences. Royal Society Publishing.

Birk, S., D. Chapman, L. Carvalho, et al., 2020. Impacts of multiple stressors on freshwater biota across spatial scales and ecosystems. Nature Ecology & Evolution 4: 1060–1068. https://doi.org/10.1038/s41559-020-1216-4.

Bondu, R., W. Kloppmann, M. O. Naumenko-Dèzes, P. Humez & B. Mayer, 2021. Potential impacts of shale gas development on inorganic groundwater chemistry: implications for environmental baseline assessment in shallow aquifers. Environmental Science and Technology 55(14): 9657–9671. https://doi.org/10.1021/acs.est.1c01172.

Boutron, O., C. Paugam, E. Luna-Laurent, P. Chauvelon, D. Sous, V. Rey & E. Migne, 2021. Hydro-saline dynamics of a shallow mediterranean coastal lagoon: complementary information from short and long term monitoring. Journal of Marine Science and Engineering 9(7): 701. https://doi.org/10.3390/jmse9070701.

Camarasa-Belmonte, A. M., 2016. Flash floods in Mediterranean ephemeral streams in Valencia Region (Spain). Journal of Hydrology 541: 0022–1694. https://doi.org/10.1016/j.jhydrol.2016.03.019.

Cañedo-argüelles, M., 2020. A review of recent advances and future challenges in freshwater salinization. Limnetica 39(1): 185–211. https://doi.org/10.23818/limn.39.13.

Canhoto, C., F. Bärlocher, M. Cañedo-Argüelles, R. Gómez, & A. L. Gonçalves, 2021. Salt modulates plant litter decomposition in stream ecosystems. In The Ecology of Plant Litter Decomposition in Stream Ecosystems. Springer, Cham: 323–345

Cañedo-Argüelles, M., T. E. Grantham, I. Perrée, M. Rieradevall, R. Céspedes-Sánchez & N. Prat, 2012. Response of stream invertebrates to short-term salinization: a mesocosm approach. Environmental Pollution 166: 144–151. https://doi.org/10.1016/j.envpol.2012.03.027.

Cañedo-Argüelles, M., B. J. Kefford, C. Piscart, N. Prat, R. B. Schäfer & C. J. Schulz, 2013. Salinisation of rivers: an

urgent ecological issue. Environmental Pollution 173: 157–167.
Cañedo-Argüelles, M., M. Bundschuh, C. Gutiérrez-Cánovas, B. J. Kefford, N. Prat, R. Trobajo & R. B. Schäfer, 2014. Effects of repeated salt pulses on ecosystem structure and functions in a stream mesocosm. Science of the Total Environment 476–477: 634–642. https://doi.org/10.1016/j.scitotenv.2013.12.067.
Cañedo-Argüelles, M., S. Brucet, S. Carrasco, N. Flor-Arnau, M. Ordeix, S. Ponsá & E. Coring, 2017. Effects of potash mining on river ecosystems: an experimental study. Environmental Pollution 224(2017): 759–770. https://doi.org/10.1016/j.envpol.2016.12.072.
Canedo-Arguelles, M., C. Hawkins, B. Kefford, R. Schäfer, B. Dyack, S. Brucet, D. B. Buchwalter, J. Dunlop, O. Fror, J. M. Lazorchak, E. Coring, H. R. Fernandez, W. Goodfellow, A. L. G. Achem, S. Hatfield-Dodds, B. K. Karimov, P. Mensah, J. R. Olson, C. Piscart, et al., 2016. Saving freshwater from salts: ion-specific standards are needed to protect biodiversity. Science 351(6276): 914–916. https://doi.org/10.1126/science.aad3488.
Casquin, A., S. Gu, R. Dupas, P. Petitjean, G. Gruau & P. Durand, 2020. River network alteration of C-N-P dynamics in a mesoscale agricultural catchment. Science of the Total Environment 749: 141551. https://doi.org/10.1016/j.scitotenv.2020.141551.
Cochero, J., M. Licursi & N. Gómez, 2017. Effects of pulse and press additions of salt on biofilms of nutrient-rich streams. Science of the Total Environment 579: 0048–9697. https://doi.org/10.1016/j.scitotenv.2016.11.152.
Corsi, S. R., L. A. De Cicco, M. A. Lutz & R. M. Hirsch, 2015. River chloride trends in snow-affected urban watersheds: increasing concentrations outpace urban growth rate and are common among all seasons. Science of the Total Environment 508: 488–497. https://doi.org/10.1016/j.scitotenv.2014.12.012.
Crosa, G., J. Froebrich, V. Nikolayenko, F. Stefani, P. Galli & D. Calamari, 2006. Spatial and seasonal variations in the water quality of the Amu Darya River (Central Asia). Water Research 40(11): 2237–2245. https://doi.org/10.1016/j.watres.2006.04.004.
Crowther, R. A. & H. B. N. Hynes, 1977. The effect of road deicing salt on the drift of stream benthos. Environmental Pollution 14(2): 113–126. https://doi.org/10.1016/0013-9327(77)90103-3.
Cunillera-Montcusí, D., M. Beklioğlu, M. Cañedo-Argüelles, E. Jeppesen, R. Ptacnik, C. A. Amorim, S. E. Arnott, S. A. Berger, S. Brucet, H. A. Dugan, M. Gerhard, Z. Horváth, S. Langenheder, J. C. Nejstgaard, M. Reinikainen, M. Striebel, P. Urrutia-Cordero, C. F. Vad, E. Zadereev & M. Matias, 2022. Freshwater salinisation: a research agenda for a saltier world. Trends in Ecology & Evolution 37(5): 0169–5347. https://doi.org/10.1016/j.tree.2021.12.005.
Dahl, M., B. Nilsson, J. H. Langhoff & J. C. Refsgaard, 2007. Review of classification systems and new multi-scale typology of groundwater-surface water interaction. Journal of Hydrology 344(1–2): 1–16. https://doi.org/10.1016/j.jhydrol.2007.06.027.
David, C.-M., M. Beklioğlu, M. Cañedo-Argüelles, Erik Jeppesen, R. Ptacnik, C. A. Amorim, S. E. Arnott, S. A. Berger, S. Brucet, H. A. Dugan, M. Gerhard, Z. Horváth, S. Langenheder, J. C. Nejstgaard, M. Reinikainen, M. Striebel, P. Urrutia-Cordero, C. F. Vad, E. Zadereev & M. Matias, 2022. Freshwater salinisation: a research agenda for a saltier world. Trends in Ecology & Evolution. https://doi.org/10.1016/j.tree.2021.12.005.
Dinçer, A. R. & F. Kargi, 2001. Salt inhibition kinetics in nitrification of synthetic saline wastewater. Enzyme and Microbial Technology 28(7–8): 661–665. https://doi.org/10.1016/S0141-0229(01)00312-X.
Dirección General de Tráfico (DGT), 2020. https://www.dgt.es/inicio/
Dugan, H. A., S. L. Bartlett, S. M. Burke, J. P. Doubek, F. E. Krivak-Tetley, N. K. Skaff, J. C. Summers, K. J. Farrell, I. M. McCullough, A. M. Morales-Williams, D. C. Roberts, Z. Ouyang, F. Scordo, P. C. Hanson & K. C. Weathers, 2017. Salting our freshwater lakes. Proceedings of the National Academy of Sciences of the United States of America 114: 4453–4458.
Dugan, H. A., N. K. Skaff, J. P. Doubek, S. L. Bartlett, S. M. Burke, F. E. Krivak-Tetley, et al., 2020. Lakes at risk of chloride contamination. Environmental Science and Technology 54(11): 6639–6650. https://doi.org/10.1021/acs.est.9b07718.
Estevéz, E., T. Rodríguez-Castillo, A. González-Ferrera, M. Cañedo-Arguelles & J. Barquín, 2019. Drivers of spatio-temporal patterns of salinity in Spanish rivers : a nationwide assessment. Philosophical Transactions of the Royal Society B 374(1764): 20180022.
Ferrarin, C., M. Bajo, D. Bellafiore, A. Cucco, F. De Pascalis, M. Ghezzo & G. Umgiesser, 2014. Toward homogenization of Mediterranean lagoons and their loss of hydrodiversity. Geophysical Research Letters 41(16): 5935–5941. https://doi.org/10.1002/2014GL060843.
Fuentes, R., T. Torregrosa-Martí & F. Hernández-Sancho, 2017. Productivity of wastewater treatment plants in the Valencia Region of Spain. Utilities Policy 46: 58–70.
Gonçalves, J., A. A. Baldovi, B. Chyoshi, L. Zanata, A. M. Salcedo, E. L. Subtil & L. H. Coelho, 2019. Effect of aluminum sulfate and cationic polymer addition in the mixed liquor of a submerged membrane bioreactor (SMBR): sludge characteristics and orthophosphate removal in batch experiments. Brazilian Journal of Chemical Engineering 36: 693–703. https://doi.org/10.1590/0104-6632.20190362s20180128.
Gardner, R. L., & R. A. Young, 1988. Assessing Strategies for Control of Irrigation-Induced Salinity in the Upper Colorado River Basin. , http://ajae.oxfordjournals.org/.
González Alonso, S., M. Catalá, R. R. Maroto, J. L. R. Gil, Á. G. de Miguel & Y. Valcárcel, 2010. Pollution by psychoactive pharmaceuticals in the Rivers of Madrid metropolitan area (Spain). Environment International Elsevier Ltd 36: 195–201. https://doi.org/10.1016/j.envint.2009.11.004.
Gorostiza, S. & D. Saurí, 2019. Naturalizing pollution: a critical social science view on the link between potash mining and salinization in the Llobregat river basin, northeast Spain. Philosophical Transactions of the Royal Society B: Biological Sciences. https://doi.org/10.1098/rstb.2018.0006.

Heimhuber, V., M. G. Tulbure, M. Broich, Z. Xie & M. Hurriyet, 2019. The role of GRACE total water storage anomalies, streamflow and rainfall in stream salinity trends across Australia is Murray-Darling Basin during and post the Millennium Drought. International Journal of Applied Earth Observation and Geoinformation 83(2018): 101927. https://doi.org/10.1016/j.jag.2019.101927.

Herbert, E. R., P. Boon, A. J. Burgin, S. C. Neubauer, R. B. Franklin, M. Ardón, K. N. Hopfensperger, L. P. Lamers & P. Gell, 2015. A global perspective on wetland salinization: *ecological consequences of a growing threat to freshwater wetlands*. Ecosphere 6(10): 206. https://doi.org/10.1890/ES14-00534.1.

Hintz, W. D. & R. A. Relyea, 2019. A review of the species, community, and ecosystem impacts of road salt salinisation in fresh waters. Freshwater Biology 64: 1081–1097. https://doi.org/10.1111/fwb.13286.

Hintz, W. D., S. E. Arnott, C. C. Symons, D. A. Greco, A. McClymont, J. A. Brentrup, M. Cañedo-Argüelles, A. M. Derry, A. L. Downing, D. K. Gray, S. J. Melles, R. A. Relyea, J. A. Rusak, C. L. Searle, L. Astorg, H. K. Baker, B. E. Beisner, K. L. Cottingham, Z. Ersoy, C. Espinosa, J. Franceschini, A. T. Giorgio, N. Göbeler, E. Hassal, M. P. Hébert, M. Huynh, S. Hylander, K. L. Jonasen, A. E. Kirkwood, S. Langenheder, O. Langvall, H. Laudon, L. Lind, M. Lundgren, L. Proia, M. S. Schuler, J. B. Shurin, C. F. Steiner, M. Striebel, S. Thibodeau, P. Urrutia-Cordero, L. Vendrell-Puigmitja & G. A. Weyhenmeyer, 2022a. Current water quality guidelines across North America and Europe do not protect lakes from salinization. Proceedings of the National Academy of Sciences of the United States of America. https://doi.org/10.1073/pnas.2115033119.

Hintz, W. D., L. Fay & R. A. Relyea, 2022b. Road salts, human safety, and the rising salinity of our fresh waters. Frontiers in Ecology and the Environment 20: 1540–9295. https://doi.org/10.1002/fee.2433.

Horrigan, N., J. E. Dunlop, B. J. Kefford & F. Zavahir, 2007. Acute toxicity largely reflects the salinity sensitivity of stream macroinvertebrates derived using field distributions. Marine and Freshwater Research 58(2): 178–186.

Hoekstra, A. Y., 2015. The water footprint: The relation between human consumption and water use The Water We Eat: Combining Virtual Water and Water Footprints. Springer International Publishing: 35–48.

Iglesias, A., C. Nebot, B. I. Vázquez, J. M. Miranda, C. M. F. Abuín & A. Cepeda, 2014. Detection of veterinary drug residues in surface waters collected nearby farming areas in Galicia, North of Spain. Environmental Science and Pollution Research 21: 2367–2377.

Spanish National Geographic Institute (IGN), (2020). https://www.ign.es/web/ign/portal

Ishwaran, H. & U. Kogalur, 2022. *Fast Unified Random Forests for Survival, Regression, and Classification (RF-SRC)*. R package version 3.0.0, https://cran.r-project.org/package=randomForestSRC.

Jackson, R. B. & E. G. Jobbágy, 2005. From icy roads to salty streams. Proceedings of the National Academy of Sciences of the United States of America 102(41): 14487–14488. https://doi.org/10.1073/pnas.0507389102.

Jiang, S., X. Wu, S. Du, Q. Wang & D. Han, 2022. Are UK rivers getting saltier and more alkaline? Water (switzerland) 14: 2813.

Kaushal, S. S., P. M. Groffman, G. E. Likens, K. T. Belt, W. P. Stack, V. R. Kelly & G. T. Fisher, 2005. Increased salinization of freshwater in the Northeastern United States. Proceedings of the National Academy of Sciences of the United States of America 102(38): 13517–13520. https://doi.org/10.1073/pnas.0506414102.

Kaushal, S. S., G. E. Likens, M. L. Pace, R. M. Utz, S. Haq, J. Gorman & M. Grese, 2018. Freshwater salinization syndrome on a continental scale. Proceedings of the National Academy of Sciences of the United States of America 115: E574–E583. https://doi.org/10.1073/pnas.1711234115.

Kaushal, S. S., G. E. Likens, M. L. Pace, S. Haq, K. L. Wood, J. G. Galella, C. Morel, T. R. Doody, B. Wessel, P. Kortelainen, A. Räike, V. Skinner, R. Utz & N. Jaworski, 2019. Novel 'chemical cocktails' in inland waters are a consequence of the freshwater salinization syndrome. Philosophical Transactions of the Royal Society B: Biological Sciences 374(1764): 8. https://doi.org/10.1098/rstb.2018.0017.

Kaushal, S. S., G. E. Likens, M. L. Pace, et al., 2021. Freshwater salinization syndrome: from emerging global problems to managing risks. Biogeochemistry 154: 255–292. https://doi.org/10.1007/s10533-021-00784-w.

Kaushal, S. S., 2016. Increased Salinization Decreases Safe Drinking Water. Environmental Science and Technology. American Chemical Society, 2765–2766.

Kaushal, S. S., P. M. Mayer, G. E. Likens, J. E. Reimer, C. M. Maas, M. A. Rippy, S. B. Grant, I. Hart, R. M. Utz, R. R. Shatkay, B. M. Wessel, C. E. Maietta, M. L. Pace, S. Duan, W. L. Boger, A. M. Yaculak, J. G. Galella, K. L. Wood, C. J. Morel, W. Nguyen, S. E. C. Querubin, R. A. Sukert, A. Lowien, A. W. Houde, A. Roussel, A. J. Houston, A. Cacopardo, C. Ho, H. Talbot-Wendlandt, J. M. Widmer, J. Slagle, J. A. Bader, J. H. Chong, J. Wollney, J. Kim, L. Shepherd, M. T. Wilfong, M. Houlihan, N. Sedghi, R. Butcher, S. Chaudhary & W. D. Becker, 2022. Five state factors control progressive stages of freshwater salinization syndrome. Limnology and Oceanography Letters. https://doi.org/10.1002/lol2.10248.

Kefford, B. J., P. J. Papas & D. Nugegoda, 2003. Relative salinity tolerance of macroinvertebrates from the Barwon River, Victoria, Australia. Marine and Freshwater Research 54(6): 755–765.

Kefford, B. J., A. Dalton, C. G. Palmer, et al., 2004. The salinity tolerance of eggs and hatchlings of selected aquatic macroinvertebrates in southeast Australia and South Africa. Hydrobiologia 517: 179–192. https://doi.org/10.1023/B:HYDR.0000027346.06304.bc.

Kefford, B. J., D. Nugegoda, L. Zalizniak, E. J. Fields & K. L. Hassell, 2007a. The salinity tolerance of freshwater macroinvertebrate eggs and hatchlings in comparison to their older life-stages: a diversity of responses. Aquatic Ecology 41(2): 335–348.

Kefford, B. J., D. Nugegoda, L. Zalizniak, E. J. Fields & K. L. Hassell, 2007b. The salinity tolerance of freshwater macroinvertebrate eggs and hatchlings in comparison to their older life-stages: A diversity of responses – The

salinity tolerance of freshwater macroinvertebrate eggs and hatchlings. Aquatic Ecology 41(2): 335–348. https://doi.org/10.1007/s10452-006-9066-y.

Kefford, B. J., D. Nugegoda, L. Zalizniak, et al., 2007c. The salinity tolerance of freshwater macroinvertebrate eggs and hatchlings in comparison to their older life-stages: a diversity of responses. Aquatic Ecology 41: 335–348. https://doi.org/10.1007/s10452-006-9066-y.

Kefford, B. J., R. Marchant, R. B. Schäfer, L. Metzeling, J. E. Dunlop, S. C. Choy & P. Goonan, 2011. The definition of species richness used by species sensitivity distributions approximates observed effects of salinity on stream macroinvertebrates. Environmental Pollution 159(1): 302–310. https://doi.org/10.1016/j.envpol.2010.08.025.

Kulmatov, R., J. Mirzaev, J. Abuduwaili & B. Karimov, 2020. Challenges for the sustainable use of water and land resources under a changing climate and increasing salinization in the Jizzakh irrigation zone of Uzbekistan. Journal of Arid Land 12(1): 90–103. https://doi.org/10.1007/s40333-020-0092-8.

Laceby, J. P., J. G. Kerr, D. Zhu, C. Chung, Q. Situ, S. Abbasi & J. F. Orwin, 2019. Chloride inputs to the North Saskatchewan River watershed: the role of road salts as a potential driver of salinization downstream of North America's northern most major city (Edmonton, Canada). Science of the Total Environment 688: 0048–9697. https://doi.org/10.1016/j.scitotenv.2019.06.208.

Ladrera, R., M. Cañedo-Argüelles & N. Prat, 2017. Impact of potash mining in streams: The Llobregat basin (northeast Spain) as a case study. Journal of Limnology 76: 343–354.

Lagarias, A. & A. Stratigea, 2021. High-resolution spatial data analysis for monitoring urban Sprawl in Coastal Zones: a case study in Crete Island. In Lecture Notes in Computer Science (including subseries Lecture Notes in Artificial Intelligence and Lecture Notes in Bioinformatics). https://doi.org/10.1007/978-3-030-87016-4_6

Lawson, L., D. A. Jackson & J. P. Smol, 2021. Salty summertime streams—road salt contaminated watersheds and estimates of the proportion of impacted species. FACETS 6: 317–333. https://doi.org/10.1139/facets-2020-0068.

Le, T. D. H., M. Kattwinkel, K. Schützenmeister, J. R. Olson, C. P. Hawkins & R. B. Schäfer, 2019. Predicting current and future background ion concentrations in German surface water under climate change. Philosophical Transactions of the Royal Society B: Biological Sciences 374: 20180004.

Leng, P., Q. Zhang, F. Li, R. Kulmatov, G. Wang, Y. Qiao & H. Hirwa, 2021. Agricultural impacts drive longitudinal variations of riverine water quality of the Aral Sea basin (Amu Darya and Syr Darya Rivers), Central Asia ☆. Environmental Pollution 284(February): 117405. https://doi.org/10.1016/j.envpol.2021.117405.

Lemenkova, Polina, 2018. R script to perform the Principal Component Analysis (PCA) to model impact factors affecting geomorphological structure of the Mariana Trench. 10.13140/RG.2.2.29003.85289.

Li, X., Y. Zhang, Z. Li & R. Wang, 2021. Response of the groundwater environment to rapid urbanization in Hohhot, the provincial capital of western China. Journal of Hydrology 603(PC): 127033. https://doi.org/10.1016/j.jhydrol.2021.127033.

Liu, Y., P. Wang, B. Gojenko, J. Yu, L. Wei & D. Luo, 2021. A review of water pollution arising from agriculture and mining activities in Central Asia: facts, causes and effects ☆. Environmental Pollution 291(September): 118209. https://doi.org/10.1016/j.envpol.2021.118209.

Llamas, M. I., P. Jiménez-Gavilán, J. A. Luque-Espinar, J. Benavente-Herrera, L. Candela, M. Sanmiguel-Martí, J. Rambla-Nebot, J. L. Aranda-Mares & I. Vadillo-Pérez, 2022. Hydrogeological, hydrodynamic and anthropogenic factors affecting the spread of pharmaceuticals and pesticides in water resources of the Granada plain (Spain). Journal of Hydrology 610: 127791.

Machado, M. J., G. Benito, M. Barriendos & F. S. Rodrigo, 2011. 500 Years of rainfall variability and extreme hydrological events in southeastern Spain drylands. Journal of Arid Environments 75: 0140–1963. https://doi.org/10.1016/j.jaridenv.2011.02.002.

Mendiguchía, C., C. Moreno & M. García-Vargas, 2007. Evaluation of natural and anthropogenic influences on the Guadalquivir River (Spain) by dissolved heavy metals and nutrients. Chemosphere 69: 1509–1517.

Merchán, D., L. Sanz, A. Alfaro, I. Pérez, M. Goñi, F. Solsona, I. Hernández-García, C. Pérez & J. Casalí, 2020. Irrigation implementation promotes increases in salinity and nitrate concentration in the lower reaches of the Cidacos River (Navarre, Spain). Science of the Total Environment 706: 135701. https://doi.org/10.1016/j.scitotenv.2019.135701.

Meybeck, M., 2003. Global occurrence of major elements in rivers. Treatise on Geochemistry 5–9: 207–223.

Ministerio de Agricultura, A. y M. A., 2013. Real Decreto 670/2013, de 6 de septiembre, por el que se modifica el Reglamento del Dominio Público Hidráulico aprobado por el Real Decreto 849/1986, de 11 de abril, en materia de registro de aguas y criterios de valoración de daños al dominio público hid. Boletín Oficial del Estado 1–42, https://www.boe.es/boe/dias/2013/09/21/pdfs/BOE-A-2013-9775.pdf.

Ministerio de la Presidencia, 2003. Real Decreto 140/2003, de 7 de feb, criterios sanitarios de la calidad del agua de consumo humano. Ministerio de la Presidencia Gobierno de España. Boletin oficial del estado 7228–7245, http://www.boe.es/boe/dias/2003/02/21/pdfs/A07228-07245.pdf.

R Core Team, 2021. R: A Language and Environment for Statistical Computing. R Foundation for Statistical Computing, Vienna, Austria. https://www.R-project.org/.

Monteiro, M. T. F., S. M. Oliveira, F. J. Luizão, L. A. Cândido, F. Y. Ishida & J. Tomasella, 2014. Dissolved organic carbon concentration and its relationship to electrical conductivity in the waters of a stream in a forested Amazonian blackwater catchment. Plant Ecology and Diversity Taylor & Francis 7: 205–213. https://doi.org/10.1080/17550874.2013.820223.

Morán-Tejeda, E., S. R. Fassnacht, J. Lorenzo-Lacruz, J. I. López-Moreno, C. García, E. Alonso-González & A.-J. Collados-Lara, 2019. Hydro-meteorological

characterization of major floods in Spanish Mountain Rivers. Water 11: 2641. https://doi.org/10.3390/w11122641.

Moyano-Salcedo, A. J., F. D. Cuadros-Segura, A. M. Pabon Laverde, & J. V. Trujillo Arias, 2021. Environmental Impact of Sewage Discharge Into Illegal UrbanAgglomerates in Villavicencio, Colombia. Tecnura Universidad Distrital Francisco Jose de Caldas 25: 43–62.

Muff, S., E. B. Nilsen, R. B. O'Hara & C. R. Nater, 2022. Rewriting results sections in the language of evidence. Trends in Ecology and Evolution 37: 203–210.

Nava, V., M. Patelli, T. Bonomi, G. A. Stefania, C. Zanotti, L. Fumagalli & B. Leoni, 2020. Chloride balance in freshwater system of a highly anthropized subalpine area: load and source quantification through a watershed approach. Water Resources Research 56(1): 26024. https://doi.org/10.1029/2019WR026024.

Newton, A., J. Icely, S. Cristina, A. Brito, A. C. Cardoso, F. Colijn & J. M. Zaldívar, 2014. An overview of ecological status, vulnerability and future perspectives of European large shallow, semi-enclosed coastal systems, lagoons and transitional waters. Estuarine, Coastal and Shelf Science 140(January 2017): 95–122. https://doi.org/10.1016/j.ecss.2013.05.023.

Niedrist, G. H., M. Cañedo-Argüelles & S. Cauvy-Fraunié, 2020. Salinization of Alpine rivers during winter months. Environmental Science and Pollution Research 28: 7295–7306. https://doi.org/10.1007/s11356-020-11077-4.

Official Website of the United States Government (UGS), 2020. 41,000 2018. *Pubs Warehouse,* (703), 2019–2020.

Olías, M., J. M. Nieto, A. M. Sarmiento, J. C. Cerón & C. R. Cánovas, 2004a. Seasonal water quality variations in a river affected by acid mine drainage: the Odiel River (South West Spain). Science of the Total Environment 333(1–3): 267–281. https://doi.org/10.1016/j.scitotenv.2004.05.012.

Olías, M., J. M. Nieto, A. M. Sarmiento, J. C. Cerón & C. R. Cánovas, 2004b. Seasonal water quality variations in a river affected by acid mine drainage: the Odiel River (South West Spain). Science of the Total Environment 333: 267–281.

Oliveira, R., A. Martínez, A. L. Gonçalves, E. S. Almeida Júnior & C. Canhoto, 2021. Salt pulses effects on in-stream litter processing and recovery capacity depend on substrata quality. Science of the Total Environment 783: 147013. https://doi.org/10.1016/j.scitotenv.2021.147013.

Olson, J. R., 2019. Predicting combined effects of land use and climate change on river and stream salinity. Philosophical Transactions of the Royal Society B: Biological Sciences 374: 20180005.

Ouyang, Y., P. Nkedi-Kizza, Q. T. Wu, D. Shinde & C. H. Huang, 2006. Assessment of seasonal variations in surface water quality. Water Research 40: 3800–3810.

Pedersen, E. J., D. L. Miller, G. L. Simpson, & N. Ross, 2019. Hierarchical generalized additive models in ecology: An introduction with mgcv.

Peñas, F. J. & J. Barquín, 2019. Assessment of large-scale patterns of hydrological alteration caused by dams. Journal of Hydrology 572(2018): 706–718. https://doi.org/10.1016/j.jhydrol.2019.03.056.

Piñon-Flores, M. A., I. Suazo-Ortuño, J. P. Ramírez-Herrejón, R. Moncayo-Estrada & E. del-Val, 2021. Habitat, water quality or geomorphological degradation in the streams: which is most important for conserving an endemic amphibian of Central Mexico? Journal for Nature Conservation. https://doi.org/10.1016/j.jnc.2021.126063.

Pompa-Pernía, A., S. Molina, A. Lejarazu-Larrañaga, J. Landaburu-Aguirre & E. García-Calvo, 2022. Validation of recycled nanofiltration and anion-exchange membranes for the treatment of urban wastewater for crop irrigation. Membranes 12: 746.

Ribas, A., J. Olcina & D. Sauri, 2020. More exposed but also more vulnerable? Climate change, high intensity precipitation events and flooding in Mediterranean Spain. Disaster Prevention and Management: an International Journal 29: 229.

Rincón, P. A. & J. Lobón-Cerviá, 1997. Temporal patterns in macroinvertebrate drift in a northern Spanish stream. Marine and Freshwater Research 48(5): 455–464. https://doi.org/10.1071/MF97037.

Richter, B. D., J. v Baumgartner, J. Powell, & D. P. Braun, 1996. A Method for Assessing Hydrologic Alteration within Ecosystems. conservation Biology.

Rivas-Martınez, S., S. Rivas-Saenz & M. A. Penas, 2011. Worldwide bioclimatic classification system. Global Geobotany 1: 1–634.

Rufí-Salís, M., A. Petit-Boix, S. Leipold, G. Villalba, J. Rieradevall, E. Moliné, X. Gabarrell, J. Carrera & M. E. Suárez-Ojeda, 2022. Increasing resource circularity in wastewater treatment: Environmental implications of technological upgrades. Science of the Total Environment 838: 156422.

Ruth, O., 2003. The effects of de-icing in Helsinki urban streams, Southern Finland. Water Science and Technology 48(9): 33–43. https://doi.org/10.2166/wst.2003.0486.

Salcedo Moyano, A. J., T. P. Delforno & E. L. Subtil, 2021. Simultaneous nitrification-denitrification (SND) using a thermoplastic gel as support: pollutants removal and microbial community in a pilot-scale biofilm membrane bioreactor. Environmental Technology. https://doi.org/10.1080/09593330.2021.1950843.

Sarmiento, A. M., A. DelValls, J. M. Nieto, M. J. Salamanca & M. A. Caraballo, 2011. Toxicity and potential risk assessment of a river polluted by acid mine drainage in the Iberian Pyrite Belt (SW Spain). Science of the Total Environment 409: 4763–4771. https://doi.org/10.1016/j.scitotenv.2011.07.043.

Sauer, F. G., M. Bundschuh, J. P. Zubrod, R. B. Schäfer, K. Thompson & B. J. Kefford, 2016. Effects of salinity on leaf breakdown: dryland salinity versus salinity from a coalmine. Aquatic Toxicology 177(June): 425–432. https://doi.org/10.1016/j.aquatox.2016.06.014.

Schäfer, R. B., M. Bundschuh, D. A. Rouch, E. Szöcs, P. C. von der Ohe, V. Pettigrove & B. J. Kefford, 2012. Effects of pesticide toxicity, salinity and other environmental variables on selected ecosystem functions in streams and the relevance for ecosystem services. Science of the Total Environment 415: 69–78. https://doi.org/10.1016/j.scitotenv.2011.05.063.

Schreiber, E. S. G., 1995. Long-term patterns of invertebrate stream drift in an Australian temperate stream.

Freshwater Biology 33: 13–25. https://doi.org/10.1111/j.1365-2427.1995.tb00382.x.

Schuler, M. S., M. Cañedo-Argüelles, W. D. Hintz, B. Dyack, S. Birk & R. A. Relyea, 2019. Regulations are needed to protect freshwater ecosystems from salinization. Philosophical Transactions of the Royal Society B: Biological Sciences 374: 20180019.

Sistema Automático de Información de Calidad de las Aguas (SAICA), 2020. www.mapama.gob.es

Bailey, S. A., I. C. Duggan, C. D. van Overdijk, T. H. Johengen, D. F. Reid & H. J. MacIsaac, 2004. Salinity tolerance of diapausing eggs of freshwater zooplankton. Freshwater Biology 49(3): 286–295.

Sun, N.-Z. & A. Sun, 2013. Mathematical modeling of groundwater pollution. *Civil and Environmental Engineering Department University of CaliforniaLos Angeles USA*, 1–289.https://doi.org/10.1007/978-1-4757-2558-2

Szklarek, S., A. Górecka & A. Wojtal-Frankiewicz, 2022. The effects of road salt on freshwater ecosystems and solutions for mitigating chloride pollution – a review. Science of the Total Environment. https://doi.org/10.1016/j.scitotenv.2021.150289.

Thorslund, J., M. F. P. Bierkens, G. H. P. Oude Essink, E. H. Sutanudjaja, & M. T. H. van Vliet, 2021. Common irrigation drivers of freshwater salinisation in river basins worldwide. Nature Communications Nature Research 12:1.

Timpano, A. J., C. E. Zipper, D. J. Soucek & S. H. Schoenholtz, 2018. Seasonal pattern of anthropogenic salinization in temperate forested headwater streams,. Water Research 133: 0043–1354. https://doi.org/10.1016/j.watres.2018.01.012.

Tiyasha, T. M. Tung, & Z. M. Yaseen, 2020. A survey on river water quality modelling using artificial intelligence models: 2000–2020. Journal of Hydrology. Elsevier B.V.

Tornabene, B. J., C. W. Breuner & B. R. Hossack, 2020. Relative toxicity and sublethal effects of NaCl and energy-related saline wastewaters on prairie amphibians. Aquatic Toxicology 228(August): 105626. https://doi.org/10.1016/j.aquatox.2020.105626.

Turunen, K., T. Räsänen, E. Hämäläinen, et al., 2020. Analyzing contaminant mixing and dilution in river waters influenced by mine water discharges. Water Air, & Soil Pollution 231: 317. https://doi.org/10.1007/s11270-020-04683-y.

United Nations. 2019. World Population Prospects 2019. In *Department of Economic and Social Affairs. World Population Prospects 2019.* Retrieved from http://www.ncbi.nlm.nih.gov/pubmed/12283219

USGS (U.S. Geological Survey, M. C. S.), 2020. Pubs Warehouse, official website of the United States government 2019–2020.

Van Vliet, M. T. H. & J. J. G. Zwolsman, 2008. Impact of summer droughts on the water quality of the Meuse River. Journal of Hydrology 353(1–2): 1–17. https://doi.org/10.1016/j.jhydrol.2008.01.001.

Van Vliet, M. T. H., M. Florke, & Y. Wada, 2017. Quality matters for water scarcity. Nature Geoscience. Nature Publishing Group, 800–802.

Vandersande, M. W., E. P. Glenn & J. L. Walworth, 2001. Tolerance of five riparian plants from the lower Colorado River to salinity drought and inundation. Journal of Arid Environments 49(1): 147–159. https://doi.org/10.1006/jare.2001.0839.

Vaughan, I. P. & N. J. Gotelli, 2019. Water quality improvements offset the climatic debt for stream macroinvertebrates over twenty years. Nature Communications 10: 1–8. https://doi.org/10.1038/s41467-019-09736-3.

Vengosh, A., R. B. Jackson, N. Warner, T. H. Darrah, & A. Kondash, 2014. A critical review of the risks to water resources from unconventional shale gas development and hydraulic fracturing in the United States. Environmental Science and Technology. American Chemical Society, 8334–8348.

Venkatesan, A. K., S. Ahmad, W. Johnson & J. R. Batista, 2011. Systems dynamic model to forecast salinity load to the Colorado River due to urbanization within the Las Vegas Valley. Science of the Total Environment 409(13): 2616–2625. https://doi.org/10.1016/j.scitotenv.2011.03.018.

Williams, W. D., 2001. Salinization: unplumbed salt in a parched landscape. Water Science and Technology 43(4): 85–91.

Wood, S. N., 2021. Generalized additive models: An introduction with R, second edition. Generalized Additive Models: An Introduction with R, Second Edition. CRC Press.

Xinwei, W., Z. Ningning, H. Xiyun, H. Dianming & G. Xiangbin, 2009. Pollution effect of inorganic salt from coal gangue piles on groundwater. Technology, China University of Petroleum 3: 120.

Yusta-García, R., M. Orta-Martínez, P. Mayor, C. González-Crespo & A. Rosell-Melé, 2017. Water contamination from oil extraction activities in Northern Peruvian Amazonian rivers. Environmental Pollution 225: 370–380.

Publisher's Note Springer Nature remains neutral with regard to jurisdictional claims in published maps and institutional affiliations.

3.4. Chapter III: What happens when salinization meets eutrophication? A test using stream microcosms

Article published in Science of The Total Environment on February 20, 2024.

Science of the Total Environment 912 (2024) 168824

Contents lists available at ScienceDirect

Science of the Total Environment

journal homepage: www.elsevier.com/locate/scitotenv

What happens when salinization meets eutrophication? A test using stream microcosms

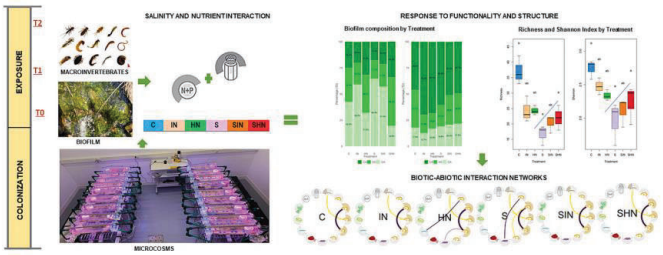
Alvaro Javier Moyano Salcedo [a,b,d,*], Narcís Prat [a], Lluís Bertrans-Tubau [c], Martí Piñero-Fernandez [a], David Cunillera-Montcusí [a,e], Julio C. López-Doval [c], Meritxell Abril [c], Lorenzo Proia [c], Miguel Cañedo-Argüelles [d]

[a] FEHM-Lab (Freshwater Ecology, Hydrology and Management), Departament de Biologia Evolutiva, Ecologia i Ciències Ambientals, Facultat de Biologia, Universitat de Barcelona, Barcelona, Spain
[b] Geohazards and Civil Engineering Research Group, Department of Civil Engineering, Saint Thomas Villavicencio University, C/22 No 1a, 500003 Villavicencio, Colombia
[c] BETA Technological Center, University of Vic–Central University of Catalonia (UVic–UCC), Vic, Barcelona, Spain
[d] Institute of Environmental Assessment and Water Research (IDAEA), CSIC, Carrer de Jordi Girona, 18-26, 08034 Barcelona, Spain
[e] WasserCluster Lunz - Biologische Station GmbH, Lunz am See, Austria

HIGHLIGHTS

- The study explored how nutrient and salt pollution interact in freshwater ecosystems using microcosms with biofilm and macroinvertebrates.
- We found a negative effect of salinity on biofilm function and cyanobacteria.
- We found a strong negative effect of salinity on macroinvertebrate richness and diversity.
- Nutrient addition weakly ameliorated salt toxicity to aquatic macroinvertebrates.

GRAPHICAL ABSTRACT



ARTICLE INFO

Editor: Sergi Sabater

Keywords:
Nutrient pollution
Salt pollution
Freshwater ecosystems
Microcosms
Biofilm
Macroinvertebrates

ABSTRACT

Nutrient and salt pollution often co-occur in rivers and streams due to human activities (e.g., agriculture, urbanization). Thus, understanding the interactive effects of nutrients and salinity on freshwater ecosystems is critical for environmental management. We experimentally assessed the interactive effects of nutrient and salt pollution on stream microcosms using biofilm and macroinvertebrates as model systems. Six treatments were performed in triplicate: control (C: N-NH_4+ = 0.05; P- PO_4^{3-} = 0.037; Cl- = 33.5 mg L^{-1}), intermediate nutrient (IN: N-NH_4+ = 0.4; P- PO_4^{3-} = 0.271; Cl- = 33. 5 mg L^{-1}), high nutrient (HN: N-NH_4+ = 0.84; P- PO_4^{3-} = 0.80; Cl- = 33.5 mg L^{-1}), salt (S: N-NH_4+ = 0.05; P- PO_4^{3-} = 0.037; Cl- = 3000 mg L^{-1}), salt with intermediate nutrient (SIN: N-NH_4+ = 0.4; P- PO_4^{3-} = 0.27; Cl- = 3000 mg L^{-1}) and salt with high nutrient (SHN: N-NH_4+ = 0.84; P- PO_4^{3-} = 0.80; Cl- = 3000 mg L^{-1}). After 14 days of exposure, biofilm chlorophyll-a increased across all

Abbreviations: C, Control treatment; IN, Intermediate Nutrient treatment; HN, High Nutrient treatment; S, Salt treatment; SIN, Salt with Intermediate Nutrient treatment; SHN, Salt with High Nutrient treatment.

* Corresponding author at: Institute of Environmental Assessment and Water Research (IDAEA), CSIC, Carrer de Jordi Girona, 18-26, 08034 Barcelona, Spain.
E-mail address: alvaromoyano@ub.edu (A.J. Moyano Salcedo).

https://doi.org/10.1016/j.scitotenv.2023.168824
Received 8 August 2023; Received in revised form 25 October 2023; Accepted 22 November 2023
Available online 27 November 2023
0048-9697/© 2023 The Authors. Published by Elsevier B.V. This is an open access article under the CC BY-NC-ND license (http://creativecommons.org/licenses/by-nc-nd/4.0/).

treatments, with cyanobacteria replacing diatoms and green algae. Treatments with no added nutrients (C and S) had more P uptake capacity than the rest. The indicator species analysis showed 8 significant taxa, with *Orthocladius (Orthocladius) gr. Wetterensis* and *Virganytarsus* significantly associated with the salinity treatment. Overall, salt pollution led to a very strong decline in macroinvertebrate richness and diversity. However, salt toxicity seemed to be ameliorated by nutrient addition. Finally, both structural equation models and biotic-abiotic interaction networks showed that complex biological interactions could be modulating the response of the biological communities to our treatments. Thus, our study calls for species-level assessments of salt and nutrient effects on river ecosystems and advocates for better management of co-occurring pollutants.

1. Introduction

Human activities are increasing the salt concentration of rivers and streams around the world (i.e., freshwater salinization, FS). There is strong evidence that FS can lead to drastic reductions in aquatic biodiversity (Kefford et al., 2006, 2012; Cañedo-Argüelles et al., 2013; Cañedo-Argüelles et al., 2016a, b; Cunillera-Montcusí et al., 2022) and alterations of ecosystem functioning (Herbert et al., 2015; Vendrell-Puigmitja et al., 2022). However, FS often co-occurs with multiple stressors (Kaushal et al., 2022) and the potential interactive effects of salinity and such stressors (e.g., climate change, eutrophication, pesticide pollution) is still poorly understood (Velasco et al., 2018). For example, salt and nutrient pollution are both frequent in rivers and streams subjected to the discharge of urban wastewater and irrigation return flows (Cañedo-argüelles, 2020; Thorslund et al., 2021). Although agriculture is the main driver of elevated NaCl and nitrogen (N) and phosphorus (P) concentrations in rivers and streams (Estévez et al., 2019; Thorslund et al., 2021), wastewater discharge is an important driver of FS when rivers flow through urban areas and most river catchments are impacted by a combination of both activities (Meybeck, 2003; Blaas and Kroeze, 2016; Bhide et al., 2021). Moreover, several industrial processes (e.g., ethanol, agro-food industries) generate by-products that release high concentrations of both nutrients and salts, strongly increasing freshwater and soil salinization (Christofoletti et al., 2013; Marinho et al., 2014). For example, in the ethanol industry, sugarcane vinasse is a massive and continuous by-product with elevated nutrient levels (e.g., pure vinasse has a total N: 639 mg L^{-1}, total P: 150 mg L^{-1}) and salinity (e.g., sodium: 60 mg L^{-1}, conductivity: 8420 μS cm^{-1}) that is difficult to manage and use as fertilizer, potentially affecting the surrounding aquatic and terrestrial biodiversity (Dreux Fraga, 2023). Finally, salt and nutrient load into freshwater ecosystems may vary depending on the agricultural and industrial practices (e.g., irrigation requirements, type of fertilizers), climate and meteorological factors and the efficiency of the wastewater treatment plants (e.g., nutrient and salt removal) (Merchán et al., 2020, Salcedo Moyano et al., 2022).

The vast majority of studies addressing the effects of FS in combination with multiple stressors in rivers have focused on the interaction of salts with temperature (Jackson and Funk, 2019; Serrano et al., 2020; Torregroza-Espinosa et al., 2021), pesticides (Szöcs et al., 2012; Stoler et al., 2017; Dornelas et al., 2021) and metals (Baysoy et al., 2012; Velasco et al., 2018), whereas the interaction between salt and nutrients enrichment has received less attention (Lind et al., 2018; Osburn et al., 2023) and has been much more studied in lakes (Lind et al., 2018; Greco et al., 2023, Wang et al., 2023; Ersoy et al., 2022) than in rivers (Pace et al., 1999; Kurle and Cardinale, 2011). Available studies suggest that both synergistic and antagonistic relationships between nutrients and salts are possible, depending on the tolerance of the community to NaCl and the triggering of cascading effects. For example, in the planktonic compartment, the abundance of algal species may be promoted through the reduction in the abundance of large cladocerans due to salt pollution, leading to an increase in chlorophyll-a concentration (Hintz et al., 2017). At the same time, nutrient pollution promotes algal growth, contributing to increased chlorophyll-a concentration (Carpenter et al., 2001; Dodds et al., 2002; Bennett et al., 2021). As a result, there is a synergistic effect that may promote primary production through a combination of increased resource availability and a relaxation of grazing pressure due to cladocerans loss (Lind et al., 2018; Osburn et al., 2023; Zadereev et al., 2023). However, this might not always be the case, since some groups of planktonic algae are subsidized by the N availability and can withstand wide ranges of salinity (e.g., cyanobacteria) whereas others in the benthic zone (e.g., *Nitella*, *Enteromorpha intestinalis*) do not (Lind et al., 2018; Greco et al., 2023; Borburema et al., 2022). Thus, eutrophication and salinization can also have antagonistic effects on the composition of algal communities. The changes in the trophic structure might have consequences for the entire ecosystem. For example, some planktonic cyanobacteria species are capable of releasing toxins (e.g., *Microcystis aeruginosa*) that make water resources unsafe for animals and humans (Gaillard et al., 2021; Georges Des Aulnois et al., 2019; Osburn et al., 2023).

The changes in primary production can determine the response of aquatic invertebrates, some of which feed on algae, to nutrient and salt pollution. For example, some studies evaluating the interactive effects of chloride (Cl) and nutrients have suggested that the toxic effects of increased salts on aquatic organisms such as copepods and snails may be ameliorated by nutrient enrichment, which increases food availability and consequently the available energy to cope with metabolic demands (Hintz et al., 2017; Lind et al., 2018; Greco et al., 2023, Silver and Donini, 2021). Concordantly, Brown and Yan (2015) showed that cladocerans (e.g., *Daphnia pulex* and *D. pulicaria*) were more tolerant to chloride when higher quality food resources were available (Isanta-Navarro et al., 2021). Also, Greco et al. (2023) suggested that organisms living in lakes with high nutrient concentrations could be more tolerant to chloride due to higher food quality and availability. The few available studies on the interactive effects of salt and nutrient pollution on stream invertebrates offer contradictory information. For example, a decline and shift in benthic macroinvertebrate composition has been documented in sections of the Molco River (Araucanía, Chile) where fish farms discharge their effluents. This phenomenon was attributed to the synergistic effects of nutrient enrichment and salinity, mainly due to the toxic effects of elevated salinity on taxa, and to community drift associated with habitat alteration (Encina-Montoya et al., 2020). On the contrary, some studies suggest that nutrients and salts might have antagonistic effects due to the above mentioned increase in food resources (Braukmann and Böhme, 2011; Schröder et al., 2015).

The aim of this study was to examine the interactive effects of nutrient and salt pollution on stream ecosystems by using microcosms (i.e., small artificial channel systems). These microcosms were used to test three treatments: nutrient addition, salt addition, and nutrient + salt addition. This setup allowed the experiment to be carried out under controlled conditions, including flow rate, temperature, light, nutrient levels, and salt, as performed in similar studies (Cochero et al., 2017; Vendrell-Puigmitja et al., 2022; Bertrans-Tubau et al., 2023). Also, the microcosms were adapted to take into account the geographic scale and the community being assessed, with the aim of addressing certain limitations (Martin, 2001; Menczelesz et al., 2020), although the representation of large-scale conditions remains one of these limitations. Benthic microbial communities dominated by primary producers (biofilms) and macroinvertebrates were focused on due to their importance as ecological indicators of rivers' health and because their interaction

can be affected by both stressors and lead to cascading effects (Pace et al., 1999; Kurle and Cardinale, 2011; Ersoy et al., 2022). Finally, it was hypothesized that: (1) Nutrient addition would increase chlorophyll-a concentration, photosynthetic efficiency and phosphorus uptake rate of biofilm communities due to a subsidy effect. This should have indirect positive effects on aquatic macroinvertebrate richness and abundance as a result of higher food availability; (2) Salt addition would have toxic effects both on biofilms and macroinvertebrates. Also, it would drive significant changes in the structure of both communities; and (3) The interaction between salt and nutrients would have an antagonistic effect on algae and macroinvertebrates, with the former being toxic and the latter subsidizing energy demands associated with osmoregulation.

2. Material and methods

2.1. Experimental design and operating

The study was performed in a set of 18 microcosms consisting of 6-L methacrylate channels (length × width × height 26 × 15 × 17 cm) installed in a temperature-controlled chamber at a constant temperature of 18 °C (Fig. 1). Each microcosm contained 15 stream cobbles (previously scraped and autoclaved), 1 large glass plate (220 cm^2) and 6 small glass plates (9 cm^2) used as substrates for natural biofilm colonization that also provided habitat for macroinvertebrates.

The microcosms were connected to a 5-L tank filled with 3 L of dechlorinated water, with an initial chemical composition of 0.05 mg L^{-1} N-NH_4+, 0.0375 mg L^{-1} P- PO_4^{3-} and 33.5 mg L^{-1} Cl. Water was recirculated in each microcosm by a submerged pump (EDEN 105, Eden Water Paradise, Italy) configured to maintain the same flow rate in each microcosm. The water was completely renewed every 3 days to avoid nutrient depletion. The photo-period was set out at 12 h light: 12 h dark using LEDs (LENB 135-lm, LENB/14.97/11.98). During the experiment, the irradiance reaching the substrata was 12 μmol photons m^{-2} s^{-1}.

Natural biofilms were inoculated in each microcosm to promote colonization. Diatoms and algae communities were obtained by scraping cobbles collected from a section of the Llobregat River at Balsareny (sampling point L68 in Prat and Rieradevall (2006)), Spain. This sampling site was selected because it had already been used in previous experiments exploring the effects of salinization on aquatic macroinvertebrates (Cañedo-Argüelles et al., 2012, 2014). The biofilm samples were collected 7 March 2022 and transported in 5 L bottles to the microcosms within 1 h of collection. To remove organic matter and excess of filamentous algae, the samples were filtered through a 500 μm mesh. Finally, 250 mL of this inoculum was added uniformly to each channel, and this procedure was repeated each time water was renewed during the colonization period. The colonization period lasted for three weeks, during which photosynthetic efficiency became appreciable (i.e., measurements indicating chlorophyll presence and biofilm maturity). Throughout this period, the photosynthetic activity and community composition of the biofilm was monitored and measured by means of the analysis of fluorescence response using Benthotorch (BTo-09-048 GPS bbe Moldaenke) and MiniPAM (Pulse Amplitude Modulated) chlorophyll fluorimeter (Heinz Walz GmbH) to assess its adaptation to each microcosm. Aquatic macroinvertebrates were collected at the same sampling point (L68) at the end of the biofilm colonization period (From 7 to 25 March 2022) by kicking all available habitats and using a hand net of 250 μm mesh size. They were transported inside coolers to the microcosms also within 1 h of collection. Each cooler was filled with river water collected at the sampling point. Finally, a 500 mL aliquot of the macroinvertebrate sample was collected from a tray where the community had been homogenized by gently agitating the water. This community sample was collected using a calibrated jar and inoculated into each microcosm. The colonization phase of macroinvertebrates overlapped with the final week of the three-week biofilm colonization period. During a 48 h period, we conducted observations to confirm the establishment and acclimatization of the benthic community within each microcosm (e.g., distribution of taxa within preferential habitats, low mortality and drift).

After the colonization and conditioning of the community, the exposure period started with the addition of salt and nutrients to each microcosm. The salt concentration was chosen at two different levels: low, corresponding to the average minimum concentration of the Llobregat River in the study section (ACA, 2023), and high. This higher salinity has been widely reported in freshwaters (Thorslund et al., 2021), especially within the study area where rivers and streams have high salt concentrations associated with the dissolution of salts that naturally occur in rocks (Prat and Rieradevall, 2006). Furthermore,

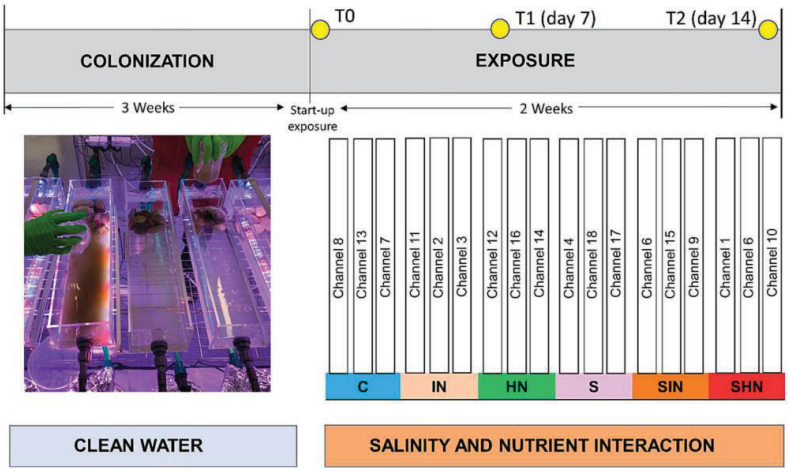


Fig. 1. Experimental design and sampling times (yellow circles) during the exposure period. The biofilm community was measured at T0, T1 and T2. The macroinvertebrate community was inoculated at the start of the exposure period (T0) and collected for identification at the end of the experiment (T2). Control treatment (C), salt (S), intermediate nutrients concentration (IN), high nutrients concentration (HN), salt treatment in combination with intermediate nutrients concentration (SIN) and salt treatment in combination with high nutrients concentration (SHN).

previous studies conducted using mesocosms and communities collected from the same river have consistently shown that a concentration of 3 g L^{-1} NaCl is sufficient to induce significant changes in aquatic macroinvertebrate communities (Cañedo-Argüelles et al., 2012, 2014).

Nitrogen and phosphorus concentrations mimicked those of streams affected by wastewater treatment plant discharges within the study area (Lorenzo Proia, personal communication based on water quality monitoring data collected by the BETA research center). The control was related to the average nutrient levels upstream the WWTPs, intermediate nutrient concentrations corresponded to sites located around 20 and 40 m downstream of the WWTP, and the high nutrient concentrations corresponded to the discharge point of the WWTPs.

The experimental design included 6 treatments in triplicate: control treatment (C: $N\text{-}NH_4+ = 0.05$; $P\text{-}PO_4^{3-} = 0.037$; Cl- = 33.5 mg L^{-1}), intermediate nutrient concentration (IN: $N\text{-}NH_4+ = 0.4$; $P\text{-}PO_4^{3-} = 0.271$; Cl- = 33. 5 mg L^{-1}), high nutrient concentration (HN: $N\text{-}NH_4+ = 0.84$; $P\text{-}PO_4^{3-} = 0.80$; Cl- = 33.5 mg L^{-1}), salt (S: $N\text{-}NH_4+ = 0.05$; $P\text{-}PO_4^{3-} = 0.037$; Cl- = 3000 mg L^{-1}), salt treatment in combination with intermediate nutrient concentration (SIN: $N\text{-}NH_4+ = 0.4$; $P\text{-}PO_4^{3-} = 0.27$; Cl- = 3000 mg L^{-1}) and salt treatment in combination with high nutrient concentration (SHN: $N\text{-}NH_4+ = 0.84$; $P\text{-}PO_4^{3-} = 0.80$; Cl- = 3000 mg L^{-1}). The experimental water used in the microcosms was dechlorinated tap water with high nitrate and nitrite concentrations (3.7 ± 0.2 $N\text{-}NO_3$- and < 0.1 ± 0.1 $N\text{-}NO_2$- mg L^{-1}). The biofilms and macroinvertebrate communities were exposed to the treatments during 14 days (From 25 to 7 April 2022) and the treatments were randomly distributed across the microcosms (Fig. 1).

2.2. Physical and chemical water conditions

Dissolved oxygen (DO) concentration and saturation, temperature, pH, and conductivity were measured directly in the microcosms using sensor probes (YSI professional plus, YSI Incorporated, USA). Also, triplicate water samples for each treatment (one random sample per treatment) were collected 3 times a week after each water change and filtered through a 0.22 um nylon filter (Merck) to analyze nutrient concentrations. Water samples were frozen immediately and kept at −20 °C until analysis. Finally, $N\text{-}NH_4^+$ and $P\text{-}PO_4^{3-}$ were analyzed following APHA (1992).

2.3. Biofilm sampling

Biofilms were sampled immediately before (T0) and 7 (T1) and 14 (T2) days after nutrient and salt addition. At each biofilm-sampling day, one random small glass plate (9 cm^2) was collected from each microcosm and scraped using a blunt spatula. Aliquots of 10 mL of biofilm were then sub-sampled to analyze chlorophyll-a concentration and ash-free dry mass (AFDM). Chlorophyll-a concentration and AFDM samples were stored at −20 °C until analysis.

2.3.1. Chlorophyll-a concentration and AFDM

Chlorophyll-a was measured using spectrophotometric techniques following standard methods (APHA, 1992). To calculate AFDM (ash-free dry mass), the biofilm suspension was filtered through filters (0.7 μm pore size), then dried for 72 h at 60 °C and combusted at 550 °C for 4 h obtaining algal dry mass (DM) and finally AFDM (1 g dry mass ≈ 0.9 g AFDM).

2.3.2. Photosynthetic efficiency and community composition in the biofilm

The photosynthetic efficiency (Yeff) was measured with a Mini-PAM (Pulse Amplitude Modulated) chlorophyll fluorimeter (Heinz Walz GmbH). The main photosynthetic groups' densities (diatoms, cyanobacteria and green algae) covering the colonized glass plates were measured using BenthoTorch probe (BTo-09-048 GPS bbe Moldaenke).

2.3.3. Phosphorus uptake rate of biofilm

Biofilm phosphorus uptake rate was determined directly on the colonized glass plates in each microcosm measuring the temporal decay of phosphorus in water after a controlled spike (Proia et al., 2017). The initial phosphorus concentration was determined, and the corresponding amount was added in each channel to quadruple the background concentration. Then, the biofilms were incubated under these conditions for 240 min and water was sampled in 10 mL tubes at 0, 120, and 240 min after the addition through a 0.22 um nylon filter (Merck) and stored at −20 °C until analysis. The biofilm phosphorus uptake rate was calculated as:

$$U = \frac{Po - Pf}{AxTf}$$

where P0 = the initial mass of P after the spike (μg); Pf = the final mass of P at the end of incubation (μg); A = the area colonized by biofilm (cm^2) and Tf = the time of incubation (h).

2.4. Sampling of macroinvertebrates

Macroinvertebrates were sampled from each microcosm at the end of the experiment by emptying the microcosms and scraping and washing all artificial substrates. The resulting sample (which contained water, sediment and algae) was filtered through a 250 μm mesh and preserved in 90 % ethanol at −5 °C. Then, at the laboratory, macroinvertebrates were sorted and identified at the genus level following Tachet et al. (2000), except for Chironomidae which were identified to the genus/species level using local taxonomic keys (Prat et al., 2014) because of being the dominant group in terms of relative abundance.

2.5. Data analysis

All statistical analyses were performed in R (R Core Team, 2002) and the nomenclature proposed by Muff et al. (2022) was used to report our results in the language of evidence (very strong evidence: P Value between 0.0001 and 0.001; strong evidence: P value between 0.001 and 0.01; moderate evidence: p value between 0.01 and 0.05; weak evidence: p value between 0.05 and 0.1; little or no evidence p value between 0.1 and 1). Two-way ANOVA was used to assess biofilm both the structural parameters (i.e., chlorophyll-a concentration, AFDM, and relative composition and abundance of each algal group) and functional parameters (i.e., photosynthetic efficiency, nutrient uptake capacity) across treatments. First, all interactions (e.g., time:salinity:nutrients) were examined. Then, in the absence of a strong relationship, variables without supporting evidence were systematically removed from the analysis to streamline the model, ultimately arriving at a representation of the most important interactions (e.g., Time + Salinity+Nutrients). In cases where moderate to strong differences were observed based on the two-way ANOVA model (P value <0.05), pairwise comparisons were performed using the Bonferroni test.

Macroinvertebrate richness and Shannon diversity indices were calculated using the "vegan" package (Oksanen et al., 2009) and differences between treatments were analyzed using the same procedure (two-way ANOVA + Bonferroni test). An Indicator Species Analysis (IndVal) was performed to identify indicator taxa for each treatment using the "labdsv" package (Roberts et al., 2023). Non-metric multidimensional scaling (NMDS) was used to visualize differences in community composition between treatments (Oksanen et al., 2009), and these differences were tested through an ADONIS test using the "labdsv" package (Roberts et al., 2023).

A structural equation model (SEM) was built to assess the interactions and effects between salinity, nutrients, algal communities and macroinvertebrates at the end of the exposure period using the "lavaan" package. SEM is based on the variance-covariance matrices between predictor and response variables and interactively assesses direct and

indirect causal pathways using correlations between these variables and their statistical significance (Grace, 2006; Frainer et al., 2014). The model contained 198 sampling units which included all sampling events (i.e., six treatments × three replicates × average of three sampling times for biofilm per replicate treatment; T1, T2 and T3) and 11 variables: salinity, nutrients, chlorophyll-a, photosynthetic yield, P-uptake rate, the concentration of cyanobacteria, diatoms and green algae, and the abundance, richness and Shannon diversity of macroinvertebrates. Before building the model, variables with a Spearman correlation higher than 0.9 were excluded (Taylor, 1990). Salinity and nutrients (i.e., sum of concentration of N-NH_4+ and P-PO_4^{3-} mg L^{-1}) were set as the predictor variables.

Finally, the interaction strength between the different taxa (focusing on those associated to any of the treatments according to IndVal analysis) in relation to abiotic variables was assessed using biotic-abiotic interaction networks (BAINs). The global interaction network of the experiment was obtained, and it was modulated by each treatment to compare their structure (i.e., number and strength of links; Hernández-Carrasco et al., 2023). BAINs were calculated using mixed graphical models (mgm; Haslbeck and Waldorp, 2020; Momal et al., 2020), which used a sparse penalized maximum likelihood estimator (LASSO) GLM to generate undirected graphs based on the distribution between variables without any previous assumptions about their dependencies (Ohlmann et al., 2018; García-Girón et al., 2020; Haslbeck and Waldorp, 2020). Since the aim was to describe the main BAIN structure for each treatment and not to focus on its predictive strength, cross-validation was employed as the procedure for selecting the tuning parameter (lambdasel = "CV"), allowing for a less restrictive selection of significant interactions. The mixed graphical model was moderated according to the six treatments, and the corresponding conditioned BAIN was obtained for each treatment.

3. Results

During the colonization period, pH, conductivity, DO and temperature remained stable with no differences between microcosms (Table S1). Once the exposure period started, there was no evidence of variability in DO, water temperature and pH, but conductivity changed as expected with the addition of salts (Table S2, Table S3).

There was very strong evidence (two- way ANOVA, P value <0.001, Table S4) that the chlorophyll-a concentration in the biofilms increased progressively during the exposure period in T0-T2 and T1-T2 (Fig. 2, pairwise comparison Table S5). At the end of the exposure time (T2), IN and SHN had the highest (T2, Max = 0.10 μg cm^{-2}, Min = 0.02 μg cm^{-2}) and lowest (T2, Max = 0.04 μg cm^{-2}, Min = 0.004 μg cm^{-2}) concentrations of chlorophyll-a, respectively. There was no evidence of changes in chlorophyll-a influenced by nutrients and salinity across treatments (Table S4).

AFDM increased throughout the experimental period in C channels (T0 = 0.38 ± 0.06 mg cm^{-2}), reaching a concentration of 0.77 (± 0.14) mg cm^{-2} by the end of the experiment (T2). In S, IN and SIN treatments there was also a steady mean increase of AFDM, whereas in HN and SHN it increased from T0 to T1 but then decreased from T1 to T2 (Fig. 2). Two-way ANOVA showed very strong change in AFDM during the

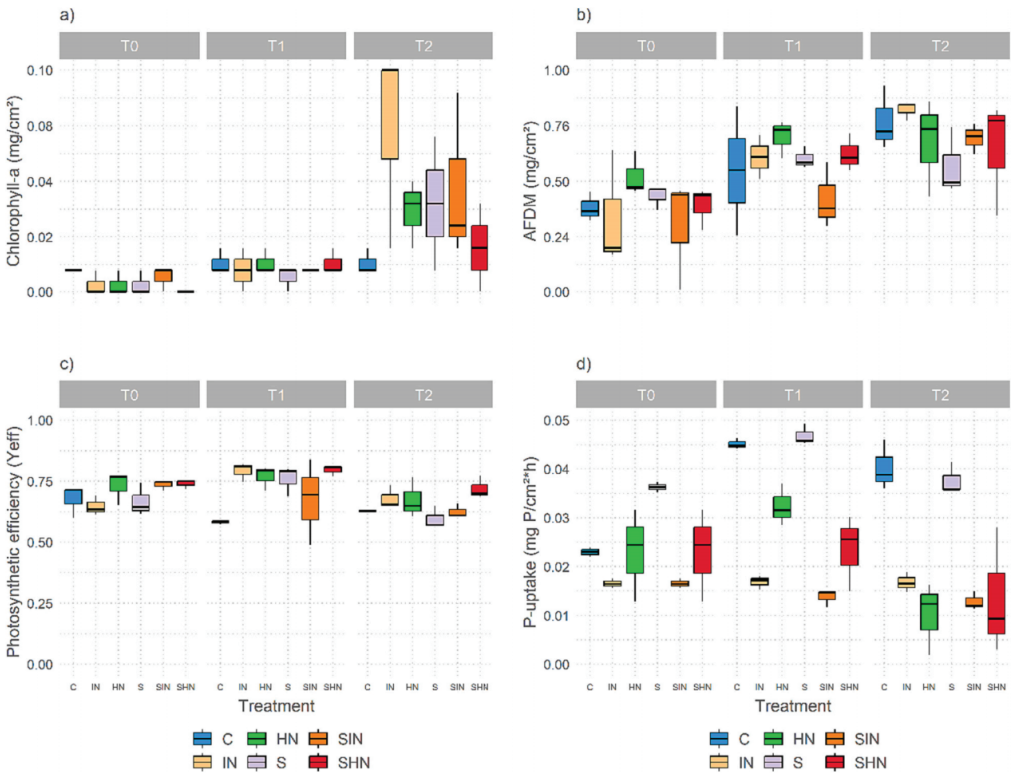


Fig. 2. Changes in the biofilm functioning during the exposure period for each treatment. a) Chlorophyll-a concentration; b) Ash-free dry mass (AFDM) c) Photosynthetic efficiency (Yeff); d) Phosphorus uptake rate.

exposure time (Table S6) for both T0-T1 and T0-T2 (pairwise comparison, Table S7). In spite of these differing trends, there were no significant differences in AFDM among salinity and nutrients levels (Table S6).

Yeff of the biofilm did not change strongly in the control treatment during the exposure period (Fig. 2). After 7 days of exposure (T1) Yeff increased in the IN, HN, S and SHN, whereas it decreased in C and SIN (Fig. 2). At the end of the exposure period (T2) Yeff decreased in all treatments except the control (C). The lowest Yeff was observed in the S treatment followed by SIN (Fig. 2). Also, there was no evidence of a change in Yeff due to salinity and nutrients across the treatments (Two-way ANOVA, Table S8).

P uptake rate showed a decrease in all treatments compared to the C at T2 (Fig. 2). Overall, the addition of nutrients, including the interactive salt-nutrient treatments (IN, HN, SIN, and SHN), resulted in a decrease in P uptake by the end of the experiment, whereas the treatments without nutrient addition (C and S) showed an increasing P uptake capacity from T0 to T2 (Fig. 2). According to two-way ANOVA, there was a very strong change in biofilm P uptake rate over time (T0-T1 and T1-T2) influenced by nutrients (P value <0.001, Table S9, Table S10, Table S11). Moreover, pairwise comparisons from the two-way ANOVA P uptake model further demonstrated differences in P uptake based on nutrient and time combinations (Table S12). Salinity did not have a strong effect on P uptake, as all low nutrient treatments (C and S) had high P uptake. The highest P uptake for both low and high nutrient concentrations treatments (C, S, HN, SHN) was found at exposure time T1. Contrarily, P uptake did not experience strong temporal fluctuations in the intermediate nutrient treatments (IN, SIN).

The biofilm community was mainly composed of green algae in C (42 %), IN (60 %), S (64 %) and SIN (57 %), while diatoms dominated in HN (37 %) and SHN (46 %) at the beginning of the experiment (T0, Fig. 3, Fig. S1). However, over time (T0-T2 and T1-T2), the biofilm community showed very strong changes (P value <0.001, two-way

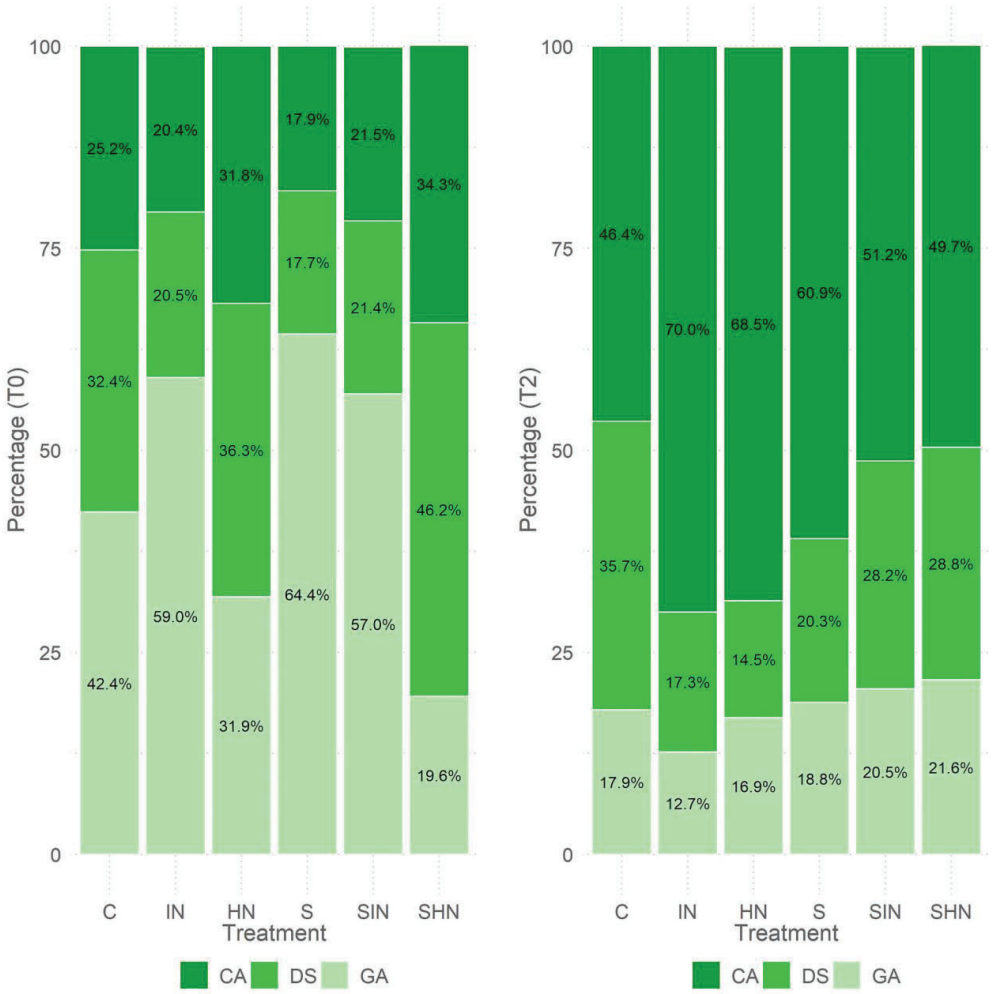


Fig. 3. Plot representing biofilm community composition at the beginning and end of the exposure period (T0 and T2) of each treatment. CA: Cyanobacteria, DS: Diatoms and GA: Green Algae. a) C: Control, b) IN: intermediate nutrients, c) NH: high nutrients, d) S: salt, e) SIN: salt in combination with intermediate nutrients and f) SHN: salt in interaction with high nutrients.

ANOVA, Table S13. Table S14), with cyanobacteria becoming dominant in all treatments (T2, Fig. 3). Pairwise comparisons showed that CA strongly differed from DS and GA in T0 and T1 when compared to T2 (Table S15). We found no evidence of differences in biofilm assemblages based on nutrient and salinity concentrations (Table S13). Although cyanobacteria were most abundant in the nutrient treatments (IN and HN, Fig. 3), they also dominated in the salt treatments (e.g., 61 % in S at T2). Also, in the salt treatments S and SIN green algae showed the greatest reduction (e.g., from 64 % in T0 to 19 % in T2 in the S treatment), whereas diatom concentrations weakly increased (e.g., from 21 % in T1 to 28 % in T2 in the SIN treatment) (Fig. S1). In contrast to S and SIN, there was a decrease in diatom concentration in SHN from T1 (46%) to T2 (29%), while green algae concentrations remained fairly constant along time (Fig. 3, Fig. S1).

Macroinvertebrate richness and abundance were dominated by chironomids (Fig. S2, Table S16), with small representation from other families such as *Baetidae, Oligochetae* and *Caenidae* (Table S16). The macroinvertebrate richness and Shannon diversity index were higher in the C than in the rest of the treatments (Fig. 4). The salinity (S) treatment showed the lowest values for both macroinvertebrate richness and diversity (Fig. 4). Macroinvertebrate richness showed a very strong change as a result of salinity (P value <0.001, two-way ANOVA, Table S17, Table S18), with moderate evidence of interaction between nutrients and salinity (Table S19). At the same time, Shannon diversity showed a very strong decrease in response to salinity (P value <0.001, two-way ANOVA, Table S20), but weak evidence of interactive effects between salinity and nutrients (Table S21). The decline in richness and Shannon diversity with salt addition seemed to be ameliorated by nutrient addition, since both increased along the nutrient addition gradient (from S to SIN and SHN; Fig. 4).

Eight macroinvertebrate taxa strongly associated with two different treatments were detected according to the IndVal analysis (Table S22). The predatory chironomids *Ablabesmyia* and *Conchapelopia* were found exclusively in C, whereas the chironomids *Cricotopus bicinctus* and *Virgatanytarsus* were exclusively found in S. The MDS and ADONIS analyses showed a strong dissimilarity between treatments in terms of community composition, with S, SIN, and SHN being the most different to C (Fig. S3; Table S23).

The SEM analysis (CFI = 0.90, RMSEA <0.05) (Fig. 5) revealed a strong negative effect of salt addition on cyanobacteria and the diversity and richness of aquatic macroinvertebrates, and a positive effect on macroinvertebrate abundance (Fig. S2) that was mainly related with an increase in *Orthocladius* (*Orthocladius*) gr. *wetterensis*, *Tanytarsus* and *Virgatanytarsus* (Table S24, Table S25). On the contrary, nutrients showed a weak to moderate positive effect on the concentration of all algal groups and on the richness, diversity and abundance of macroinvertebrates, and they had a strong positive effect on the photosynthetic yield. Therefore, nutrients and salt addition showed antagonistic effects on the concentration of the different algal groups and on the macroinvertebrate richness and diversity, but the effect of nutrients was

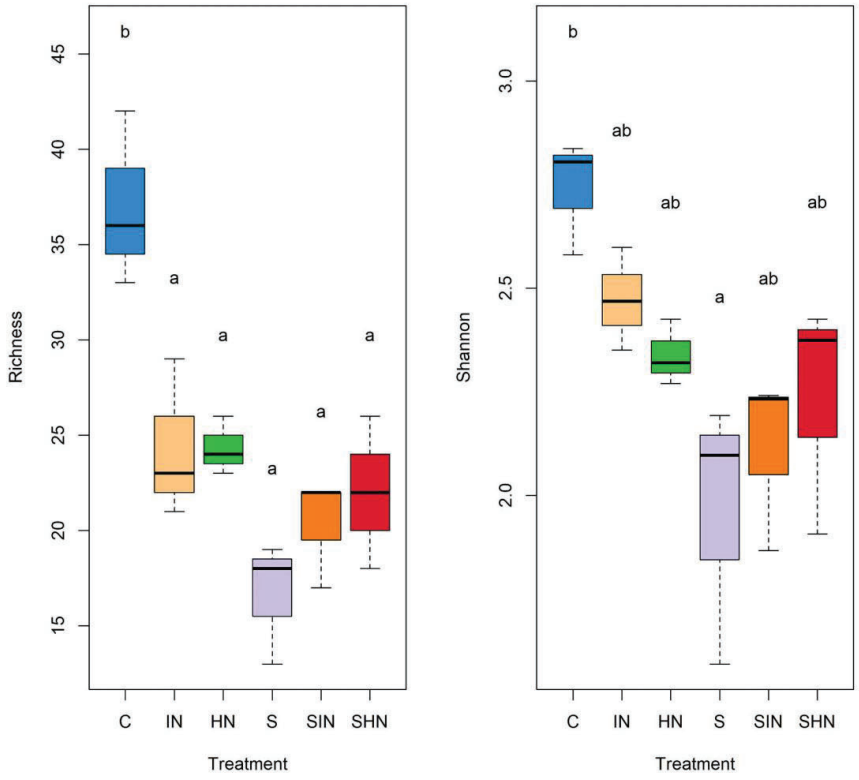


Fig. 4. Boxplot of the macroinvertebrate richness and Shannon diversity for each treatment at the end of the experiment: control treatment (C), salt treatment (S), intermediate nutrients concentration (IN), high nutrients concentration (HN), salt treatment in combination with intermediate nutrients concentration (SIN) and salt treatment in combination with high nutrients concentration (SHN). Differences between treatments are according to Bonferroni tests are shown with letters (i.e., different letters imply strong differences).

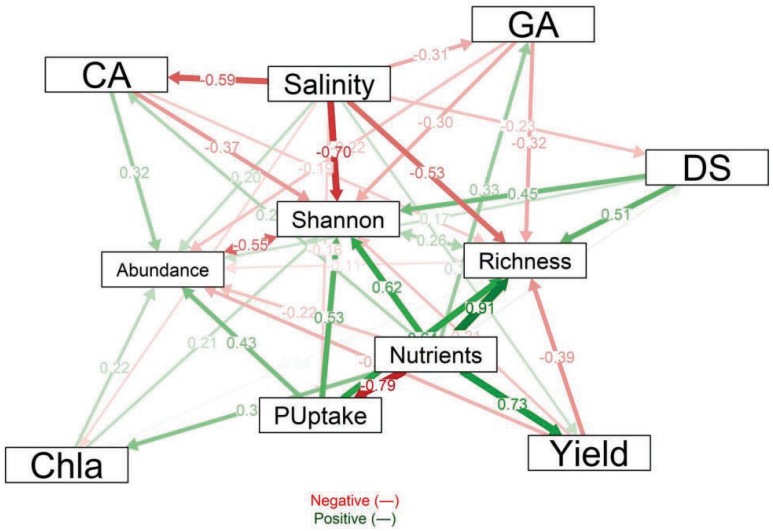


Fig. 5. Structural equation model showing the effects of nutrient and salt addition on the biofilm and aquatic macroinvertebrate communities. Salinity: salinity (mg L^{-1}); Nutrients: N-NH_4+ and P- PO_4^{3-} (mg L^{-1}); Chla: chlorophyll-a concentration (µg cm^{-2}); Yield: photosynthetic efficiency; PUptake: Phosphorus uptake (mg P $cm^{2}*h^{-1}$); DS: diatom concentration (µg cm^{-2}); GA: Green algae concentration (µg cm^{-2}); CA: Cyanobacteria concentration (µg cm^{-2}); Richness: taxa richness of aquatic macroinvertebrates; Shannon: Shannon Diversity of aquatic macroinvertebrates. Abundance: abundance of aquatic macroinvertebrates (total number of individuals). The red and green lines indicate negative and positive relationships, respectively. Model fit indices were set at CFI ≥ 0.90 and RMSEA ≤0.05.

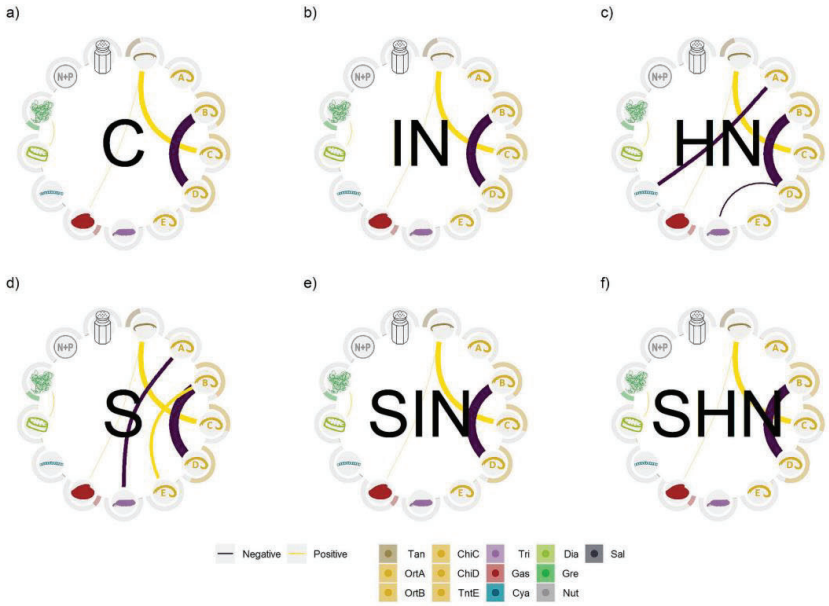


Fig. 6. Biotic-abiotic interaction networks corresponding to the conditioned main model for each experimental treatment: control treatment (C), salt (S), intermediate nutrients concentration (IN), high nutrients concentration (HN), salt treatment in combination with intermediate nutrients concentration (SIN) and salt treatment in combination with high nutrients concentration (SHN). Network nodes corresponds to the taxa strongly associated to treatments according to IndVal analysis, the concentration of the different algal groups and the abiotic variables: Tan (*Conchapelopia* sp.), OrtA (*Cricotopus bicinctus*), OrtB (*Orthocladius* gr. *wetterensis*), ChiC (*Phaenopsectra* sp.), ChiD (*Polypedilum* sp.), TntE (*Virgatanytarsus* sp.), Tri (*Hydroptila* sp.), Gas (*Bacillus* sp.), Cya (Cyanobacteria), Dia (Diatoms), Gre (Green Algae), Nut (Nutrient addition), Sal (Salt addition). Colored links indicate the sign of the covariation value (blue = negative, red = positive). The complete BAIN including all samples can be found in Fig. S4.

rather weak.

The global BAIN (i.e., including all the treatments) detected two interactions between some of the selected Chironomidae species (Fig. S4 and Table S26) indicating that covariation of the selected species was mostly explained by biotic interactions (all biotic-abiotic interactions are presented separately from Fig. S5 to Fig. S10). Once the model was conditioned for each one of the six treatments, the two main interactions were preserved along all the treatments (Fig. 6 and Table S27), but the model detected additional interactions for the HN and the S treatments (Fig. 6 C & D).

4. Discussion

Overall, it was found that nutrient addition strongly reduced the P uptake by the biofilm whereas salt addition had a strong negative effect on the richness and diversity of aquatic macroinvertebrates, with some taxa such as *Orthocladius* (*Orthocladius*) gr. *wetterensis* becoming clearly dominant. Although there was weak evidence of interactive effects between nutrients and salinity at the concentrations used in this study, the toxic effects of salt addition on aquatic macroinvertebrates seemed to be ameliorated by nutrients in a concentration-dependent manner (i.e., the higher the nutrient concentration the higher the ameliorating effect). Also, after natural succession, nutrients seemed to promote cyanobacteria growth, whereas salt seemed to prevent it, thereby suggesting potential interactive effects on algal communities that deserve further attention.

Nutrient addition was primarily responsible for the increase in chlorophyll-a concentrations, as shown in previous studies (Dodds et al., 2002; Dodds and Smith, 2017). However, it should be noted that this increase may be limited at high nutrient loads (Bennett et al., 2021), as it happened in our study (i.e., chlorophyll-a was much higher at intermediate than at higher nutrient concentrations). Our results suggest that while nutrient addition can promote chlorophyll-a concentration, it may also limit it during cyanobacterial blooms (Kane et al., 2014; Xu et al., 2015). This may be attributed to factors other than N limitation, as indicated by the N:P ratio (i.e., N:P ratio close to 5:1 in HN), such as the presence of biofilm communities that do not respond to variations in N and P levels, possibly due to nutrient saturation or other associated factors (e.g., limited available light, alteration of herbivores) (Bennett et al., 2021).

Furthermore, since cyanobacterial species are often dominant during blooms, it is possible that some of these species do not contain as much chlorophyll-a as other algal groups (Torregroza-Espinosa et al., 2021). Our results suggest that nutrients and salinity could have antagonistic effects on the composition of the biofilm. Cyanobacteria clearly became dominant along time in all treatments (including control), however its growth was promoted by nutrients and prevented by salts (i.e., the salt addition treatments had lower cyanobacteria biomass than the control treatment at the end of the study). It is important to note that dominance of cyanobacterial species could have strong implications for the entire aquatic ecological network because of the release of cytotoxins, which may affect other species, human health, and limit river uses (Gaillard et al., 2021; Osburn et al., 2023).

The shift in dominance from green algae to cyanobacteria found in our study could be related to a competition for resources (Vendrell-Puigmitja et al., 2022; Kimambo et al., 2019). However, the fact that only the biomass of the main algal groups was measured limits our ability to understand the effects of nutrients and salts on community composition, since the response to salt and nutrient addition might be species-specific. For example, there are different species within each algal group (i.e., cyanobacteria, diatoms, and green algae), with some species being able to tolerate high salinities (Arnott et al., 2023; Balycheva et al., 2023) and accumulate high concentrations of nutrients (Ardón et al., 2021; Bennett et al., 2021). Based on our results (e.g., photosynthetic efficiency increased along the nutrient addition gradient in the salt treatments) and previous studies (Li et al., 2021; Osburn et al., 2023; Arnott et al., 2023), it is hypothesized that nutrients might help some algal species to cope with salt stress by making more energy available. However, this might not always be the case. For example, *Aphanizomenon*, a genus of freshwater cyanobacteria, was sensitive to salt stress regardless of nitrogen availability in a previous study (Osburn et al., 2023). These changes in biofilms may not only have direct effects on various species, such as macroinvertebrates (Kurle and Cardinale, 2011), thereby disrupting the dynamics of subsequent trophic levels (Pace et al., 1999), but may also have far-reaching effects on various aspects, such as the decomposition of organic matter and changes in the carbon cycle, which are essential for the maintenance of ecosystem services (Pettorelli et al., 2018; Berger et al., 2019).

The macroinvertebrate communities in our study were dominated by Chironomidae. This is consistent with previous mesocosm studies performed in the region (Cañedo-Argüelles et al., 2012; Cañedo-Argüelles et al., 2014), and it is very likely related to the high dominance of the group in the studied streams and the adaptation of Chironomid species to experimental conditions (which might be stressful to some sensitive groups with specific habitat requirements such as EPT taxa). This group is not only abundant, it is also rich in species and therefore covers wide environmental gradients and represent multiple ecological traits (Cañedo-Argüelles et al., 2016a, b; Armitage et al., 2012; Serra et al., 2017). Taking this into account, the decision was made to identify Chironomidae at the genus/species level, which is rarely done in ecological studies involving aquatic macroinvertebrates (Bazzanti et al., 2008; Cañedo-Argüelles et al., 2016a, b). It was found that different Chironomidae taxa strongly responded to the treatments, with a replacement of taxa that could be partly driven by trophic interactions. This aligns with previous studies at the global (Serra et al., 2017; Martins et al., 2021; Hampel et al., 2023) and at the Spanish level (Bonada et al., 2006, 2007; Cañedo-Argüelles et al., 2012; Prat et al., 2013; Munne et al., 2021), which have identified chironomids as the main indicators of the ecological status of rivers. Another abundant group, Oligochaeta, showed a high tolerance to salt and nutrient pollution, also aligning with previous studies (Blinn and Ruiter, 2006; Wallace and Biastoch, 2016; Paul et al., 2018; Edegbene et al., 2023).

The low abundance of predatory chironomids (< 5 %, Table S24) exclusively associated with the control treatment (e.g., *Ablabesmyia* and *Conchapelopia*), suggests that they were affected by both nutrient and salt addition. Concordantly, several studies have found that these taxa were highly sensitive to salt pollution (Marshall and Bailey, 2004; Cañedo-Argüelles et al., 2012; Rico-Sánchez et al., 2022) and some studies have associated *Ablabesmyia* and *Conchapelopia* with low-intermediate nutrient concentrations (e.g., $N\text{-}NH_4^+ < 0.25$ mg L^{-1}) and low conductivities (273 µS cm^{-1}; 75 µS cm^{-1}, respectively) (Cañedo-Argüelles and Rieradevall, 2009; Rossaro et al., 2022). The reduced presence of predatory chironomids in the microcosms rules out the possibility of top-down control on the rest of the subfamilies (*Orthocladiinae*, *Chironominii* and *Tanytarsinii*) (Sánchez-Montoya et al., 2007; Cañedo-Argüelles et al., 2016a, b). The abundance of non-predators such as the tribe *Tanytarsinii* and the subfamily *Orthocladiinae* (total abundance >50 % and 38 %, respectively, Table S24) highlights not only the wide range of nutrient and salinity conditions that they can tolerate (Prat et al., 1983), but also the importance of these subfamilies in Mediterranean streams (Munoz and Prat, 1994). Also, factors such as lack of top-down control, plasticity in feeding habits and adaptation to artificial habitat conditions could partly explain the observed abundances (Rodríguez-Lozano et al., 2014; Rodríguez-Lozano et al., 2016). For example, previous studies have reported that the abundance and diversity of taxa such as *Tanytarsinii*, which exhibit a filter-feeding strategy and can become collector-gatherers under low or no current conditions, were unaffected by salt pollution (Marshall and Bailey, 2004). Also, *Tanytarsinii* show a preference for inhabiting the sides or bottom of cobbles and some species even construct tubes from small grains of sand or organic material for shelter (Puntí et al., 2009; Serra et al., 2017), providing additional protection from predators and

adverse environmental conditions (Caro-Borrero and Carmona-Jiménez, 2018). In the case of scrapers, strong reductions in abundance and diversity have been reported at salinities above 1500 mg L^{-1} (Marshall and Bailey, 2004). This is consistent with the reduction in Orthocladiinae taxa (except for *Orthocladius* (*Orthocladius*) gr. *wetterensis*) in the salinity treatments in our study (Table S5).

The reduction in macroinvertebrate richness and diversity caused by the salt treatment is in line with previous studies (Kefford et al., 2012; Cañedo-Argüelles et al., 2013; Feld et al., 2023). However, the toxic effect of salt addition was ameliorated by nutrient addition in a dose-dependent manner. Nutrients might have compensated for the toxic effects of salt addition on the biofilm, ultimately favoring macroinvertebrate richness and diversity. Our results do not strongly support this hypothesis (i.e., only cyanobacteria biomass and photosynthetic efficiency showed responded strongly to our treatments), but a deeper analysis of the algal communities at the species level would be needed to accept it or reject this hypothesis. For example, an increase in algal community diversity could mean a greater quantity and better quality of resources for macroinvertebrates, thereby increasing their fitness and their tolerance to salt stress (Guo et al., 2016; Isanta-Navarro et al., 2021). Although preferences may vary among subfamilies depending on their traits (e.g., feeding modes), high-quality green algae have been reported as the most important food source for all stream macroinvertebrates, followed by diatoms and cyanobacteria (Krivosheina, 2008; Guo et al., 2016). Indeed, the quality of the feeding resources can modulate salinity tolerance (Isanta-Navarro et al., 2021), with primary producers' quantity and quality being key for consumers' performance under salinity stress (Torres-Ruiz et al., 2007; Torres-Ruiz and Wehr, 2010; Guo et al., 2016).

Finally, our BAIN analysis suggested an increase in biotic interactions in the salt and high nutrient treatments. This means that species interactions could be playing a role in the response of the macroinvertebrate communities to our treatments. Concordantly, Arnott et al. (2023) found that differences in community composition could partly explain the differences in the sensitivity to salinity of zooplankton species of aquatic communities to salt and nutrient pollution. Also, Moniruzzaman et al. (2021) showed that community composition and biotic-abiotic interactions influence species segregation and aggregation, as well as the adaptation of a species to a particular set of conditions and resources in its environment and the life strategies of aquatic species. In fact, there are many studies showing that species interactions may be an important factor modulating the response of aquatic biodiversity to pollution (Clements et al., 2012; Gessner and Tlili, 2016). We encourage future studies to manipulate trophic interactions under experimental conditions to further explore the potential modulating effect of trophic interactions on the sensitivity of aquatic biodiversity to nutrient and salt pollution. Also, we call for more studies addressing not only the interaction between salts and nutrients resulting from several activities (e.g., agriculture, ethanol industry), but also their combined interaction with other commonly co-occurring pollutants such as pesticides (Schäfer et al., 2011; Markert et al., 2022; Dreux Fraga, 2023).

5. Conclusions

This study provides insights into the responses of algae and macroinvertebrates to the combined effects of salt and nutrients in Mediterranean river ecosystems. Nutrient addition increased chlorophyll-a levels, primarily due to cyanobacterial proliferation, but this increase was limited under nutrient saturation conditions. Nutrient addition affected P uptake by the biofilm, whereas salinity negatively impacted the diversity and richness of the entire aquatic macroinvertebrate community but favored the abundance of resistant chironomid taxa. Although there was weak evidence for an interactive effect between nutrients and salinity, the toxic effects of salt addition on aquatic macroinvertebrates appeared to be mitigated by nutrients in a concentration-dependent manner (i.e., higher nutrient concentrations resulted in stronger mitigating effects). This mitigation could be related to the recovery of green algae and diatom groups. Overall, nutrients promoted algal growth while salt appeared to inhibit it, suggesting potential interactive effects that deserve further attention through biofilm species-level analysis. At the same time, biofilm response may have had direct effects on macroinvertebrate communities, as greater food variety and quality may provide more energy to withstand the toxic effects of salinity. Finally, our results indicate that the feeding quality and preferences of macroinvertebrates and potential ecological interactions among different trophic levels could be key to understanding the effects of nutrients and salinity on the evaluated communities. These findings highlight the complexity of ecological responses to nutrient and salt pollution and have important implications for the management of the freshwater salinization syndrome.

Funding

This work was supported by a doctoral grant from the Ministerio de Ciencia, Tecnología e innovación y Colfuturo (Colombia) and IDAEA-CSIC contract associated to Ramón y Cajal (RYC2020-029829-I) for Alvaro Moyano. Miguel Cañedo- Argüelles Iglesias was supported by a Ramón y Cajal contract funded by the Spanish Ministry of Science and Innovation (RYC2020-029829-I). Lorenzo Proia was supported by a Ramón y Cajal contract funded by the Spanish Ministry of Science and Innovation (RYC2020-029829-I). David Cunillera-Montcusí was supported by European Union-NextGenerationEU, Ministry of Universities and Recovery, Transformation and Resilience Plan, through a call from Universitat de Girona.

CRediT authorship contribution statement

Alvaro Javier Moyano Salcedo: Conceptualization, Methodology, Formal analysis, Investigation, Writing – original draft & editing, Visualization, Project administration. **Narcís Prat:** Macroinvertebrate identification, Formal analysis, Investigation. **Lluís Bertrans-Tubau:** Conceptualization, Methodology, Investigation. **Martí Piñero Fernández:** Conceptualization, Methodology, Investigation. **David Cunillera-Montcusí:** Formal analysis, Investigation, Writing – review. **Julio C. López-Doval:** Methodology, Investigation, Writing – review. **Meritxell Abril Cuevas:** Conceptualization, Methodology, Investigation, Writing – review. **Lorenzo Proia:** Conceptualization, Methodology, Investigation, Writing – review. **Miguel Cañedo-Argüelles:** Conceptualization, Methodology, Formal analysis, Investigation, Writing – final draft & editing, Visualization, Supervision, Project administration.

Declaration of competing interest

The authors declare that they have no known competing financial interests or personal relationships that could have appeared to influence the work reported in this paper.

Data availability

Data will be made available on request.

Acknowledgements

We thank the Ministry of Science, Technology and Innovation of Colombia, the FHEM group of the University of Barcelona, the Beta Group of the University of Vic and the IDAEA-CSIC for the support provided to Alvaro Moyano.

Appendix A. Supplementary data

Supplementary data to this article can be found online at https://doi.org/10.1016/j.scitotenv.2023.168824.

References

Agència Catalana de l'aigua (ACA), 2023. Catalunya, Generalitat.

APHA, 1992. Standard Methods of the Examination of Water And Wastewater, 18th edition. American Public Health Association, American Water Works Association, Washington, DC.

Ardón, M., Zeglin, L.H., Utz, R.M., Cooper, S.D., Dodds, W.K., Bixby, R.J., Burdett, A.S., Follstad Shah, J., Griffiths, N.A., Harms, T.K., Johnson, S.L., Jones, J.B., Kominoski, J.S., McDowell, W.H., Rosemond, A.D., Trentman, M.T., Van Horn, D., Ward, A., 2021. Experimental nitrogen and phosphorus enrichment stimulates multiple trophic levels of algal and detrital-based food webs: a global meta-analysis from streams and rivers. Biol. Rev. 96, 692–715. https://doi.org/10.1111/brv.12673.

Arnott, S.E., Fugère, V., Symons, C.C., Melles, S.J., Beisner, B.E., Cañedo-Argüelles, M., Hébert, M.P., Brentrup, J.A., Downing, A.L., Gray, D.K., Greco, D., Hintz, W.D., McClymont, A., Relyea, R.A., Rusak, J.A., Searle, C.L., Astorg, L., Baker, H.K., Ersoy, Z., Espinosa, C., Franceschini, J.M., Giorgio, A.T., Göbeler, N., Hassal, E., Huynh, M., Hylander, S., Jonasen, K.L., Kirkwood, A., Langenheder, S., Langvall, O., Laudon, H., Lind, L., Lundgren, M., Moffett, E.R., Proia, L., Schuler, M.S., Shurin, J. B., Steiner, C.F., Striebel, M., Thibodeau, S., Cordero, P.U., Vendrell-Puigmitja, L., Weyhenmeyer, G.A., Derry, A.M., 2023. Widespread variation in salt tolerance within freshwater zooplankton species reduces the predictability of community-level salt tolerance. Limnol. Oceanogr. Lett. 8, 8–18. https://doi.org/10.1002/lol2.10277.

Balycheva, D., Anufriieva, E., Lee, R., Prazukin, A., Shadrin, N., 2023. Salinity-dependent species richness of Bacillariophyta in hypersaline environments. Water (Basel) 15, 2252. https://doi.org/10.3390/w15122252.

Baysoy, E., Atli, G., Gürler, C.Ö., Dogan, Z., Eroglu, A., Kocalar, K., Canli, M., 2012. The effects of increased freshwater salinity in the biodisponibility of metals (Cr, Pb) and effects on antioxidant systems of Oreochromis niloticus. Ecotoxicol. Environ. Saf. 84, 249–253. https://doi.org/10.1016/j.ecoenv.2012.07.017.

Bennett, M.G., Lee, S.S., Schofield, K.A., Ridley, C.E., Washington, B.J., Gibbs, D.A., 2021. Response of chlorophyll a to total nitrogen and total phosphorus concentrations in lotic ecosystems: a systematic review. Environ. Evid. https://doi.org/10.1186/s13750-021-00238-8.

Berger, E., Frör, O., Schäfer, R.B., 2019. Salinity impacts on river ecosystem processes: a critical mini-review. Philos. Trans. R. Soc. B. https://doi.org/10.1098/rstb.2018.0010.

Bertrans-Tubau, L., Menard, Y., Batisson, I., Creusot, N., Mazzella, N., Millan-Navarro, D., Moreira, A., Morin, S., Ponsá, S., Abril, M., Proia, L., Romaní, A.M., Artigas, J., 2023. Dissipation of pesticides by stream biofilms is influenced by hydrological histories. FEMS Microbiol. Ecol. 99 https://doi.org/10.1093/femsec/fiad083.

Bhide, S.V., Grant, S.B., Parker, E.A., Rippy, M.A., Godrej, A.N., Kaushal, S., Prelewicz, G., Saji, N., Curtis, S., Vikesland, P., Maile-Moskowitz, A., Edwards, M., Lopez, K.G., Birkland, T.A., Schenk, T., 2021. Addressing the contribution of indirect potable reuse to inland freshwater salinization. Nat. Sustain. 4, 699–707. https://doi.org/10.1038/s41893-021-00713-7.

Bazzanti, M., Grezzi, F., Della Bella, V., 2008. Chironomids (Diptera) of temporary and permanent ponds in central Italy: a neglected invertebrate group in pond ecology and conservation. Freshw. Ecol. 23, 219–229.

Blaas, H., Kroeze, C., 2016. Excessive nitrogen and phosphorus in European rivers: 2000-2050. Ecol. Indic. 67, 328–337. https://doi.org/10.1016/j.ecolind.2016.03.004.

Blinn, D.W., Ruiter, D.E., 2006. Tolerance values of stream caddisflies (trichoptera) in the lower Colorado River Basin, USA. Southwest. Nat. 51, 326–337. https://doi.org/10.1894/0038-4909(2006)51[326:TVOSCT]2.0.CO;2.

Bonada, N., Prat, N., Resh, V.H., Statzner, B., 2006. Developments in aquatic insect biomonitoring: a comparative analysis of recent approaches. Annu. Rev. Entomol. https://doi.org/10.1146/annurev.ento.51.110104.151124.

Bonada, N., Dolédec, S., Statzner, B., 2007. Taxonomic and biological trait differences of stream macroinvertebrate communities between mediterranean and temperate regions: implications for future climatic scenarios. Glob. Chang. Biol. 13, 1658–1671. https://doi.org/10.1111/j.1365-2486.2007.01375.x.

Borburema, H.D.S., Yokoya, N.S., Soares, L.P., de Souza, J.M.C., Nauer, F., Fujii, M.T., Pasqualetti, C.B., de Miranda, G.E.C., Marinho-Soriano, E., 2022. Mangrove macroalgae increase their growth under ocean acidification: a study with Bostrychia (Rhodophyta) haplotypes from different biogeographic provinces. J. Exp. Mar. Biol. Ecol. 552 https://doi.org/10.1016/j.jembe.2022.151740.

Braukmann, U., Böhme, D., 2011. Salt pollution of the middle and lower sections of the river Werra (Germany) and its impact on benthic macroinvertebrates. Limnologica 41, 113–124. https://doi.org/10.1016/j.limno.2010.09.003.

Brown, A.H., Yan, N.D., 2015. Food quantity affects the sensitivity of Daphnia to road salt. Environ. Sci. Technol. 49, 4673–4680. https://doi.org/10.1021/es5061534.

Cañedo-argüelles, M., 2020. A review of recent advances and future challenges in freshwater salinization. Limnetica 39, 185–211. https://doi.org/10.23818/limn.39.13.

Cañedo-Argüelles, M., Rieradevall, M., 2009. Quantification of environment-driven changes in epiphytic macroinvertebrate communities associated to Phragmites australis. J. Limnol. 68 (2), 229–241.

Cañedo-Argüelles, M., Grantham, T.E., Perrée, I., Rieradevall, M., Céspedes-Sánchez, R., Prat, N., 2012. Response of stream invertebrates to short-term salinization: a mesocosm approach. Environ. Pollut. 166, 144–151. https://doi.org/10.1016/j.envpol.2012.03.027.

Cañedo-Argüelles, M., Kefford, B.J., Piscart, C., Prat, N., Schäfer, R.B., Schulz, C.J., 2013. Salinisation of rivers: an urgent ecological issue. Environ. Pollut. https://doi.org/10.1016/j.envpol.2012.10.011.

Cañedo-Argüelles, M., Bundschuh, M., Gutiérrez-Cánovas, C., Kefford, B.J., Prat, N., Trobajo, R., Schäfer, R.B., 2014. Effects of repeated salt pulses on ecosystem structure and functions in a stream mesocosm. Sci. Total Environ. 476–477, 634–642. https://doi.org/10.1016/j.scitotenv.2013.12.067.

Cañedo-Argüelles, M., Bogan, M.T., Lytle, D.A., Prat, N., 2016a. Are Chironomidae (Diptera) good indicators of water scarcity? Dryland streams as a case study. Ecol. Indic. 71, 155–162. https://doi.org/10.1016/j.ecolind.2016.07.002.

Cañedo-Argüelles, M., Sala, M., Peixoto, G., Prat, N., Faria, M., Soares, A.M.V.M., Barata, C., Kefford, B., 2016b. Can salinity trigger cascade effects on streams? A mesocosm approach. Sci. Total Environ. 540, 3–10. https://doi.org/10.1016/j.scitotenv.2015.03.039.

Caro-Borrero, A., Carmona-Jiménez, J., 2018. Habitat preferences in freshwater benthic macroinvertebrates: algae as substratum and food resource in high mountain rivers from Mexico. Limnologica 69, 10–17. https://doi.org/10.1016/j.limno.2017.10.002.

Carpenter, S.R., Cole, J.J., Hodgson, J.R., Kitchell, J.F., Pace, M.L., Bade, D., Cottingham, K.L., Essington, T.E., Houser, J.N., Schindler, D.E., 2001. Trophic Cascades, Nutrients, and Lake Productivity: Whole-Lake Experiments. Source: Ecological Monographs.

Christofoletti, C.A., Escher, J.P., Correia, J.E., Marinho, J.F.U., Fontanetti, C.S., 2013. Sugarcane vinasse: environmental implications of its use. Waste Manag. 33, 2752–2761. https://doi.org/10.1016/j.wasman.2013.09.005.

Clements, W.H., Hickey, C.W., Kidd, K.A., 2012. How do aquatic communities respond to contaminants? It depends on the ecological context. Environ. Toxicol. Chem. https://doi.org/10.1002/etc.1937.

Cochero, J., Licursi, M., Gómez, N., 2017. Effects of pulse and press additions of salt on biofilms of nutrient-rich streams. Sci. Total Environ. 579, 1496–1503. https://doi.org/10.1016/j.scitotenv.2016.11.152.

Cunillera-Montcusí, D., Beklioğlu, M., Cañedo-Argüelles, M., Jeppesen, E., Ptacnik, R., Amorim, C.A., Arnott, S.E., Berger, S.A., Brucet, S., Dugan, H.A., Gerhard, M., Horváth, Z., Langenheder, S., Nejstgaard, J.C., Reinikainen, M., Striebel, M., Urrutia-Cordero, P., Vad, C.F., Zadereev, E., Matias, M., 2022. Freshwater salinisation: a research agenda for a saltier world. Trends Ecol. Evol. https://doi.org/10.1016/j.tree.2021.12.005.

Dodds, W.K., Smith, V.H., 2017. Nitrogen, phosphorus, and eutrophication in streams. Inland Waters 6, 155–164. https://doi.org/10.5268/IW-6.2.909.

Dodds, W.K., Smith, V.H., Lohman, K., 2002. Nitrogen and phosphorus relationships to benthic algal biomass in temperate streams. Can. J. Fish. Aquat. Sci. 59, 865–874. https://doi.org/10.1139/f02-063.

Dornelas, A.S.P., Sarmento, R.A., Saraiva, A.S., Barbosa, R.S., Vieira, M.M., Gravato, C., Soares, A.M.V.M., 2021. Effects of two biopesticides and salt on behaviour, regeneration and sexual reproduction of the freshwater planarian Girardia tigrina. J. Hazard. Mater. 404 https://doi.org/10.1016/j.jhazmat.2020.124089.

Dreux Fraga, P., 2023. Sugarcane Vinasse Provokes Acute and Chronic Responses and Bioaccumulation of Metals in Benthic Macroinvertebrates. https://doi.org/10.21203/rs.3.rs-2140305/v1.

Edegbene, A.O., Elakhame, L.A., Arimoro, F.O., Osimen, E.C., Akamagwuna, F.C., Ovie, T.T.E., Akumabor, E.C., Njuguna, C.W., 2023. Preliminary studies on macroinvertebrate biomonitoring of freshwater systems in the Afrotropics: a case study of the Chanchaga River in the Lower Niger-Benue Ecoregion of Nigeria. Biologia (Bratisl). https://doi.org/10.1007/s11756-023-01445-z.

Encina-Montoya, F., Boyero, L., Tonin, A.M., Aguayo, M.F., Esse, C., Vega, R., Correa-Araneda, F., Oberti, C., Nimptsch, J., 2020. Relationship between salt use in fish farms and drift of macroinvertebrates in a freshwater stream. Aquac. Environ. Interact. 12, 205–213. https://doi.org/10.3354/AEI00357.

Ersoy, Z., Abril, M., Cañedo-Argüelles, M., Espinosa, C., Vendrell-Puigmitja, L., Proia, L., 2022. Experimental assessment of salinization effects on freshwater zooplankton communities and their trophic interactions under eutrophic conditions. Environ. Pollut. 313 https://doi.org/10.1016/j.envpol.2022.120127.

Estévez, E., Rodríguez-Castillo, T., González-Ferreras, A.M., Cañedo-Argüelles, M., Barquín, J., 2019. Drivers of spatio-temporal patterns of salinity in Spanish rivers: a nationwide assessment. Philos. Trans. R. Soc. Lond., B, Biol. Sci. 374 https://doi.org/10.1098/rstb.2018.0022.

Feld, C.K., Lorenz, A.W., Peise, M., Fink, M., Schulz, C.J., 2023. Direct and indirect effects of salinisation on riverine biota: a case study from river Wipper, Germany. Hydrobiologia 850, 3043–3059. https://doi.org/10.1007/s10750-023-05229-z.

Frainer, A., McKie, B.G., Malmqvist, B., 2014. When does diversity matter? Species functional diversity and ecosystem functioning across habitats and seasons in a field experiment. J. Anim. Ecol. 83, 460–469. https://doi.org/10.1111/1365-2656.12142.

Gaillard, S., Réveillon, D., Danthu, C., Hervé, F., Sibat, M., Carpentier, L., Hégaret, H., Séchet, V., Hess, P., 2021. Effect of a short-term salinity stress on the growth, biovolume, toxins, osmolytes and metabolite profiles on three strains of the Dinophysis acuminata-complex (Dinophysis cf. sacculus). Harmful Algae 107. https://doi.org/10.1016/j.hal.2021.102009.

García-Girón, J., Heino, J., García-Criado, F., Fernández-Aláez, C., Alahuhta, J., 2020. Biotic interactions hold the key to understanding metacommunity organisation. Ecography 43, 1180–1190. https://doi.org/10.1111/ecog.05032.

Georges Des Aulnois, M., Roux, P., Caruana, A., Réveillon, D., Briand, E., Hervé, F., Savar, V., Bormans, M., Amzil, Z., 2019. Physiological and Metabolic Responses of Freshwater and Brackish-Water Strains of *Microcystis aeruginosa* Acclimated to a Salinity Gradient: Insight into Salt Tolerance. https://doi.org/10.1128/AEM.

Gessner, M.O., Tlili, A., 2016. Fostering integration of freshwater ecology with ecotoxicology. In: Freshwater Biology. Blackwell Publishing Ltd, pp. 1991–2001. https://doi.org/10.1111/fwb.12852.

Grace, J.B., 2006. Structural equation modeling and natural systems. In: Structural Equation Modeling and Natural Systems. Cambridge University Press. https://doi.org/10.1017/CBO9780511617799.

Greco, D.A., Arnott, S.E., Fournier, I.B., Schamp, B.S., 2023. Effects of chloride and nutrients on freshwater plankton communities. Limnol. Oceanogr. Lett. https://doi.org/10.1002/lol2.10202.

Guo, F., Kainz, M.J., Sheldon, F., Bunn, S.E., 2016. The importance of high-quality algal food sources in stream food webs - current status and future perspectives. Freshw. Biol. https://doi.org/10.1111/fwb.12755.

Hampel, H., Vázquez, R.F., González, H., Acosta, R., 2023. Evaluating the ecological status of fluvial networks of tropical Andean catchments of Ecuador. Water (Switzerland) 15. https://doi.org/10.3390/w15091742.

Haslbeck, J.M.B., Waldorp, L.J., 2020. mgm: estimating time-varying mixed graphical models in high-dimensional data. J. Stat. Soft. VV 1–49.

Herbert, E.R., Boon, P., Burgin, A.J., Neubauer, S.C., Franklin, R.B., Ardon, M., Hopfensperger, K.N., Lamers, L.P.M., Gell, P., Langley, J.A., 2015. A global perspective on wetland salinization: ecological consequences of a growing threat to freshwater wetlands. Ecosphere. https://doi.org/10.1890/ES14-00534.1.

Hernández-Carrasco, D., Cunillera-Montcusí, D., Antón-Pardo, M., Cañedo-Argüelles, M., Bas-Silvestre, M., Compte, J., Gascón, S., Quintana, X.D., Boix, D., 2023. Ecological restoration promotes zooplankton network complexity in Mediterranean coastal lagoons. Restor. Ecol. https://doi.org/10.1111/rec.13920.

Hintz, W.D., Mattes, B.M., Schuler, M.S., Jones, D.K., Stoler, A.B., Lind, L., Relyea, R.A., 2017. Salinization triggers a trophic cascade in experimental freshwater communities with varying food-chain length. Ecol. Appl. 27, 833–844. https://doi.org/10.1002/eap.1487.

Isanta-Navarro, J., Arnott, S.E., Klauschies, T., Martin-Creuzburg, D., 2021. Dietary lipid quality mediates salt tolerance of a freshwater keystone herbivore. Sci. Total Environ. 769 https://doi.org/10.1016/j.scitotenv.2020.144657.

Jackson, J.K., Funk, D.H., 2019. Temperature affects acute mayfly responses to elevated salinity: implications for toxicity of road de-icing salts. Philos. Trans. R. Soc. B 374. https://doi.org/10.1098/rstb.2018.0081.

Kane, D.D., Conroy, J.D., Peter Richards, R., Baker, D.B., Culver, D.A., 2014. Re-eutrophication of Lake Erie: correlations between tributary nutrient loads and phytoplankton biomass. J. Great Lakes Res. 40, 496–501. https://doi.org/10.1016/j.jglr.2014.04.004.

Kaushal, S.S., Reimer, J.E., Mayer, P.M., Shatkay, R.R., Maas, C.M., Nguyen, W.D., Boger, W.L., Yaculak, A.M., Doody, T.R., Pennino, M.J., Bailey, N.W., Galella, J.G., Weingrad, A., Collison, D.C., Wood, K.L., Haq, S., Newcomer-Johnson, T.A., Duan, S., Belt, K.T., 2022. Freshwater salinization syndrome alters retention and release of chemical cocktails along flowpaths: from stormwater management to urban streams. Freshw. Sci. 41, 420–441. https://doi.org/10.1086/721469.

Kefford, B.J., Nugegoda, D., Zalizniak, L., Fields, E.J., Hassell, K.L., 2006. The salinity tolerance of freshwater macroinvertebrate eggs and hatchlings in comparison to their older life-stages: a diversity of responses - the salinity tolerance of freshwater macroinvertebrate eggs and hatchlings. Aquat. Ecol. 41, 335–348. https://doi.org/10.1007/s10452-006-9066-y.

Kefford, B.J., Hickey, G.L., Gasith, A., Ben-David, E., Dunlop, J.E., Palmer, C.G., Allan, K., Choy, S.C., Piscart, C., 2012. Global scale variation in the salinity sensitivity of riverine macroinvertebrates: eastern Australia, France, Israel and South Africa. PLoS One 7. https://doi.org/10.1371/journal.pone.0035224.

Kimambo, O.N., Gumbo, J.R., Chikoore, H., 2019. The occurrence of cyanobacteria blooms in freshwater ecosystems and their link with hydro-meteorological and environmental variations in Tanzania. Heliyon e01312. https://doi.org/10.1016/j.heliyon.2019.

Krivosheina, M.G., 2008. On insect feeding on cyanobacteria. Paleontol. J. https://doi.org/10.1134/S003103010806004X.

Kurle, C.M., Cardinale, B.J., 2011. Ecological factors associated with the strength of trophic cascades in streams. Oikos 120, 1897–1908. https://doi.org/10.1111/j.1600-0706.2011.19465.x.

Li, C., Li, Y., Li, X., Ma, L., Xiao, Y., Zhang, C., 2021. Differential responses of plant primary productivity to nutrient addition in natural and restored alpine grasslands in the Qinghai Lake Basin. Front. Plant Sci. 12 https://doi.org/10.3389/fpls.2021.792123.

Lind, L., Schuler, M.S., Hintz, W.D., Stoler, A.B., Jones, D.K., Mattes, B.M., Relyea, R.A., 2018. Salty fertile lakes: how salinization and eutrophication alter the structure of freshwater communities. Ecosphere 9. https://doi.org/10.1002/ecs2.2383.

Marinho, J.F.U., Correia, J.E., Marcato, A.C. de C., Pedro-Escher, J., Fontanetti, C.S., 2014. Sugar cane vinasse in water bodies: impact assessed by liver histopathology in tilapia. Ecotoxicol. Environ. Saf. 110, 239–245. https://doi.org/10.1016/j.ecoenv.2014.09.010.

Markert, N., Guhl, B., Feld, C.K., 2022. The hierarchy of multiple stressors' effects on benthic invertebrates: a case study from the rivers Erft and Niers, Germany. Environ. Sci. Eur. 34 https://doi.org/10.1186/s12302-022-00679-z.

Marshall, N.A., Bailey, P.C.E., 2004. Impact of secondary salinisation on freshwater ecosystems: effects of contrasting, experimental, short-term releases of saline wastewater on macroinvertebrates in a lowland stream. Mar. Freshw. Res. 55, 509–523. https://doi.org/10.1071/MF03018.

Martin, L.E., 2001. Limitations on the Use of Impermeable Mesocosms for Ecological Experiments Involving Aurelia Sp. (Scyphozoa:Semaeostomeae). Oxford University Press.

Martins, I., Castro, D.M.P., Macedo, D.R., Hughes, R.M., Callisto, M., 2021. Anthropogenic impacts influence the functional traits of Chironomidae (Diptera) assemblages in a neotropical savanna river basin. Aquat. Ecol. 55, 1081–1095. https://doi.org/10.1007/s10452-021-09884-z.

Menczelesz, N., Szivák, I., Schmera, D., 2020. How do we construct and operate experimental streams? An overview of facilities, protocols, and studied questions. Hydrobiologia. https://doi.org/10.1007/s10750-019-04093-0.

Merchán, D., Sanz, L., Alfaro, A., Pérez, I., Goñi, M., Solsona, F., Hernández-García, I., Pérez, C., Casalí, J., 2020. Irrigation implementation promotes increases in salinity and nitrate concentration in the lower reaches of the Cidacos River (Navarre, Spain). Sci. Total Environ. 706 https://doi.org/10.1016/j.scitotenv.2019.135701.

Meybeck, M., 2003. Global analysis of river systems: from earth system controls to Anthropocene syndromes. Philos. Trans. R. Soc. Lond., B, Biol. Sci. https://doi.org/10.1098/rstb.2003.1379.

Momal, R., Robin, S., Ambroise, C., 2020. Tree-based inference of species interaction networks from abundance data. Methods Ecol. Evol. 11, 621–632. https://doi.org/10.1111/2041-210X.13380.

Moniruzzaman, M., Bhowmick, A.R., Karan, S., Mukherjee, J., 2021. Spatial heterogeneity within habitat indicates the community assemblage pattern and life strategies. Ecol. Indic. 123 https://doi.org/10.1016/j.ecolind.2021.107365.

Muff, S., Nilsen, E.B., O'Hara, R.B., Nater, C.R., 2022. Rewriting results sections in the language of evidence. Trends Ecol. Evol. https://doi.org/10.1016/j.tree.2021.10.009.

Munne, A., Bonada, N., Cid, N., Gallart, F., Sola, C., Bardina, M., Rovira, A., Sierra, C., Soria, M., Fortuno, P., Llorens, P., Latron, J., Estrela, T., Fidalgo, A., Serrano, I., Jimenez, S., Vega, R., Prat, N., 2021. A proposal to classify and assess ecological status in mediterranean temporary rivers: research insights to solve management needs. Water (Switzerland) 13. https://doi.org/10.3390/w13060767.

Munoz, I., Prat, N., 1994. Macroinvertebrate community in the lower Ebro river (NE Spain). Hydrobiologia 286, 65–78.

Ohlmann, M., Mazel, F., Chalmandrier, L., Bec, S., Coissac, E., Gielly, L., Pansu, J., Schilling, V., Taberlet, P., Zinger, L., Chave, J., Thuiller, W., 2018. Mapping the imprint of biotic interactions on β-diversity. Ecol. Lett. https://doi.org/10.1111/ele.13143.

Oksanen, J., Kindt, R., Simpson, G.L., 2009. The vegan Package.

Osburn, F.S., Wagner, N.D., Taylor, R.B., Chambliss, C.K., Brooks, B.W., Scott, J.T., 2023. The effects of salinity and N : P on N-rich toxins by both an N-fixing and non-N-fixing cyanobacteria. Limnol. Oceanogr. Lett. https://doi.org/10.1002/lol2.10234.

Pace, M.L., Cole, J.J., Carpenter, S.R., Kitchell, J.F., 1999. Throhic Cascades Revealed in Diverse Ecosystems, 14. TREE Elsevier Science Ltd, pp. 483–488.

Paul, W.L., Cook, R.A., Suter, P.J., Clarke, K.R., Shackleton, M.E., McInerney, P.J., Hawking, J.H., 2018. Long-term monitoring of macroinvertebrate communities over 2,300 km of the Murray River reveals ecological signs of salinity mitigation against a backdrop of climate variability. Water Resour. Res. 54, 7004–7028. https://doi.org/10.1029/2018WR022976.

Pettorelli, N., Schulte to Bühne, H., Tulloch, A., Dubois, G., Macinnis-Ng, C., Queirós, A. M., Keith, D.A., Wegmann, M., Schrodt, F., Stellmes, M., Sonnenschein, R., Geller, G. N., Roy, S., Somers, B., Murray, N., Bland, L., Geijzendorffer, I., Kerr, J.T., Broszeit, S., Leitão, P.J., Duncan, C., El Serafy, G., He, K.S., Blanchard, J.L., Lucas, R., Mairota, P., Webb, T.J., Nicholson, E., 2018. Satellite remote sensing of ecosystem functions: opportunities, challenges and way forward. Remote Sens. Ecol. Conserv. 4, 71–93. https://doi.org/10.1002/rse2.59.

Prat, N., Rieradevall, M., 2006. 25-years of biomonitoring in two mediterranean streams (Llobregat and Besòs basins, NE Spain). Limnetica 25, 541–550. https://doi.org/10.23818/limn.25.37.

Prat, N., Puig, M.-A., Gonazalez, G., Millet, X., 1983. Chironomid Longitudinal Distribution and Macroinvertebrate Diversity along the Llobregat River (NE Spain).

Prat, N., Rieradevall, M., Barata, C., Munné, A., 2013. The combined use of metrics of biological quality and biomarkers to detect the effects of reclaimed water on macroinvertebrate assemblages in the lower part of a polluted Mediterranean river (Llobregat River, NE Spain). Ecol. Indic. 24, 167–176. https://doi.org/10.1016/j.ecolind.2012.06.010.

Prat, N., David González-Trujillo, J., Ospina-Torres, R., 2014. Clave para la determinación de exuvias pupales de los quironómidos (Diptera: Chironomidae) de ríos altoandinos tropicales. Rev. Biol. Trop. (Int. J. Trop. Biol.) 62, 1385–1406. ISSN.

Proia, L., Romaní, A., Sabater, S., 2017. F phosphorus uptake capacity as a tool for the assessment of pollutant effects in river ecosystems. Ecotoxicology 26, 271–282. https://doi.org/10.1007/s10646-017-1761-z.

Puntí, T., Rieradevall, M., Prat, N., 2009. Environmental factors, spatial variation, and specific requirements of chironomidae in mediterranean reference streams. J. North Am. Benthol. Soc. 28, 247–265. https://doi.org/10.1899/07-172.1.

R Core Team, 2002. A Language and Environment for Statistical Computing. R Foundation for Statistical Computing.

Rico-Sánchez, A.E., Rodríguez-Romero, A.J., Sedeño-Díaz, J.E., López-López, E., Sundermann, A., 2022. Aquatic macroinvertebrate assemblages in rivers influenced by mining activities. Sci. Rep. 12 https://doi.org/10.1038/s41598-022-06869-2.

Roberts, D.W., David, M., Roberts, W., 2023. Package "Labdsv" Title Ordination and Multivariate Analysis for Ecology.

Rodríguez-Lozano, P., Verkaik, I., Rieradevall, M., Prat, N., 2014. Efectes potencials de la reintroduccio del barb de muntanya, 1. VIII Trobada d'Estudiosos de Sant Llorenç del Munt i l'Obac, Diputació de Barcelona, pp. 146–155.

Rodríguez-Lozano, P., Verkaik, I., Maceda-Veiga, A., Monroy, M., de Sostoa, A., Rieradevall, M., Prat, N., 2016. A trait-based approach reveals the feeding selectivity of a small endangered Mediterranean fish. Ecol. Evol. 6, 3299–3310. https://doi.org/10.1002/ece3.2117.

Rossaro, B., Marziali, L., Boggero, A., 2022. Response of chironomids to key environmental factors: perspective for biomonitoring. Insects 13. https://doi.org/10.3390/insects13100911.

Salcedo Moyano, A.J., Delforno, T.P., Subtil, E.L., 2022. Simultaneous nitrification-denitrification (SND) using a thermoplastic gel as support: pollutants removal and

microbial community in a pilot-scale biofilm membrane bioreactor. Environ. Technol. 43, 4411–4425. https://doi.org/10.1080/09593330.2021.1950843.
Sánchez-Montoya, M.D.M., Puntí, T., Suárez, M.L., Vidal-Abarca, M.D.R., Rieradevall, M., Poquet, J.M., Zamora-Muñoz, C., Robles, S., Álvarez, M., Alba-Tercedor, J., Toro, M., Pujante, A.M., Munné, A., Prat, N., 2007. Concordance between ecotypes and macroinvertebrate assemblages in Mediterranean streams. Freshw. Biol. 52, 2240–2255. https://doi.org/10.1111/j.1365-2427.2007.01826.x.
Schäfer, R.B., Kefford, B.J., Metzeling, L., Liess, M., Burgert, S., Marchant, R., Pettigrove, V., Goonan, P., Nugegoda, D., 2011. A trait database of stream invertebrates for the ecological risk assessment of single and combined effects of salinity and pesticides in South-East Australia. Sci. Total Environ. 409, 2055–2063. https://doi.org/10.1016/j.scitotenv.2011.01.053.
Schröder, M., Sondermann, M., Sures, B., Hering, D., 2015. Effects of salinity gradients on benthic invertebrate and diatom communities in a German lowland river. Ecol. Indic. 57, 236–248. https://doi.org/10.1016/j.ecolind.2015.04.038.
Serra, S.R.Q., Graça, M.A.S., Dolédec, S., Feio, M.J., 2017. Chironomidae traits and life history strategies as indicators of anthropogenic disturbance. Environ. Monit. Assess. 189 https://doi.org/10.1007/s10661-017-6027-y.
Serrano, M.A., Cobos, M., Magaña, P.J., Díez-Minguito, M., 2020. Sensitivity of Iberian estuaries to changes in sea water temperature, salinity, river flow, mean sea level, and tidal amplitudes. Estuar. Coast. Shelf Sci. 236 https://doi.org/10.1016/j.ecss.2020.106624.
Silver, S., Donini, A., 2021. Physiological responses of freshwater insects to salinity: molecular-, cellular- and organ-level studies. J. Exp. Biol. https://doi.org/10.1242/jeb.222190.
Stoler, A.B., Walker, B.M., Hintz, W.D., Jones, D.K., Lind, L., Mattes, B.M., Schuler, M.S., Relyea, R.A., 2017. Combined effects of road salt and an insecticide on wetland communities. Environ. Toxicol. Chem. 36, 771–779. https://doi.org/10.1002/etc.3639.
Szőcs, E., Kefford, B.J., Schäfer, R.B., 2012. Is there an interaction of the effects of salinity and pesticides on the community structure of macroinvertebrates? Sci. Total Environ. 437, 121–126. https://doi.org/10.1016/j.scitotenv.2012.07.066.
Tachet, H., Richoux, P., Bournaud, M., Usseglio-Polatera, P., 2000. Invertébrés deau douce. Systématique, biologie, écologie. CNRS Éditions, Paris.
Taylor, R.E.R., 1990. Interpretation of the correlation coefficient: a basic review. J. Diagn. Med. Sonogr. 30–39.
Thorslund, J., Bierkens, M.F.P., Oude Essink, G.H.P., Sutanudjaja, E.H., van Vliet, M.T. H., 2021. Common irrigation drivers of freshwater salinisation in river basins worldwide. Nat. Commun. 12 https://doi.org/10.1038/s41467-021-24281-8.
Torregroza-Espinosa, A.C., Restrepo, J.C., Escobar, J., Pierini, J., Newton, A., 2021. Spatial and temporal variability of temperature, salinity and chlorophyll-a in the Magdalena River mouth, Caribbean Sea. J. S. Am. Earth Sci. 105 https://doi.org/10.1016/j.jsames.2020.102978.
Torres-Ruiz, M., Wehr, J.D., 2010. Changes in the nutritional quality of decaying leaf litter in a stream based on fatty acid content. Hydrobiologia 651, 265–278. https://doi.org/10.1007/s10750-010-0305-9.
Torres-Ruiz, M., Wehr, J.D., Perrone, A.A., 2007. Trophic relations in a stream food web: importance of fatty acids for macroinvertebrate consumers. J. North Am. Benthol. Soc. 26, 509–522. https://doi.org/10.1899/06-070.1.
Velasco, J., Gutiérrez-Cánovas, C., Botella-Cruz, M., Sánchez-Fernández, D., Arribas, P., Carbonell, J.A., Millán, A., Pallarés, S., 2018. Effects of salinity changes on aquatic organisms in a multiple stressor context. Philos. Trans. R. Soc. Lond., B, Biol. Sci. https://doi.org/10.1098/rstb.2018.0011.
Vendrell-Puigmitja, L., Proia, L., Espinosa, C., Barral-Fraga, L., Cañedo-Argüelles, M., Osorio, V., Casas, C., Llenas, L., Abril, M., 2022. Hypersaline mining effluents affect the structure and function of stream biofilm. Sci. Total Environ. 843 https://doi.org/10.1016/j.scitotenv.2022.156966.
Wallace, A.M., Biastoch, R.G., 2016. Detecting changes in the benthic invertebrate community in response to increasing chloride in streams in Toronto, Canada. In: Freshwater Science. University of Chicago Press, pp. 353–363. https://doi.org/10.1086/685297.
Wang, Y., Jiang, X., Li, Y.L., Yang, L.J., Li, Y.H., Liu, Y., Zhou, L., Wang, P.Z., Zhao, X., Wang, H.J., Jeppesen, E., Xie, P., 2023. Interactive effects of nutrients and salinity on phytoplankton in subtropical plateau Lakes of contrasting water depths. Water (Switzerland) 15. https://doi.org/10.3390/w15010069.
Xu, H., Paerl, H.W., Qin, B., Zhu, G., Hall, N.S., Wu, Y., 2015. Determining critical nutrient thresholds needed to control harmful cyanobacterial blooms in eutrophic Lake Taihu, China. Environ. Sci. Technol. 49, 1051–1059. https://doi.org/10.1021/es503744q.
Zadereev, E., Lopatina, T., Ovchinnikov, S., Tolomeev, A., 2023. Grazing rate and feeding selectivity of small and large bodied cladocerans in waters from lakes with different salinity and phytoplankton structure. J. Oceanol. Limnol. https://doi.org/10.1007/s00343-022-2158-2.

3.5. Chapter IV: Assessing the effects of salinity on microbial communities and pollutant removal in urban wastewater treatment plants

Article published in the Journal of Water Process Engineering on August 16, 2024.

Journal of Water Process Engineering 66 (2024) 105974

Contents lists available at ScienceDirect

Journal of Water Process Engineering

journal homepage: www.elsevier.com/locate/jwpe

Assessing the effects of salinity on microbial communities and pollutant removal in urban wastewater treatment plants

Alvaro Javier Moyano Salcedo [a,b,d,*], Miguel Cañedo-Argüelles [a], Sujay S. Kaushal [c], Eva Maria Ciriero-Cebrián [d], Adrià Perez-Blanco [d], Humbert Salvadó [d]

[a] FEHM-Lab (Freshwater Ecology, Hydrology and Management), SHE-2, Institute of Environmental Assessment and Water Research (IDAEA), CSIC, Carrer de Jordi Girona, 18-26, 08034 Barcelona, Spain
[b] Geohazards and Civil Engineering Research Group, Department of Civil Engineering, Saint Thomas Villavicencio University, C/22 No 1a, 500003 Villavicencio, Colombia
[c] Department of Geology & Earth System Science Interdisciplinary Center, University of Maryland, College Park, MD, USA
[d] Department of Evolutive Biology, Ecology and Environmental Sciences, University of Barcelona, 08028 Barcelona, Spain

ARTICLE INFO

Editor: Li Gao

Keywords:
Wastewater treatment plants
Electrical conductivity
Salinity effects
protozoa communities
Pollutant removal efficiency

ABSTRACT

This study assessed the impact of electrical conductivity (EC) on the microeukaryotic community and pollutant removal efficiency in full-scale wastewater treatment plants (WWTPs) in Catalonia, Spain. Monthly samples from seven WWTPs (2010–2021) were collected, with microbial communities identified by microscopy and effluent quality parameters measured. Linear mixed-effects models (LMER), indicator species analysis (IndVal), and structural equation modeling (SEM) were used to evaluate the effects of EC on WWTP operation and microbial communities. EC levels varied widely among WWTPs (800 to 15,000 μS cm^{-1}), with mean removal rates generally low, not exceeding 26 %. EC removal was inversely correlated with organic matter removal ($p < 0.05$). IndVal analysis revealed distinct microbial communities associated with each WWTPs along the EC gradient (e.g., *Beggiatoa* spp. and *Epistylis* sp. were associated with high and low EC, respectively). High EC and peaks negatively affected the abundance of certain microorganisms (e.g., *Acineria uncinata*) ($p < 0.05$). Ciliate genera were most affected by EC peaks, with different species showing different salinity tolerance ranges (e.g. *Holophyra discolor* was affected by EC > 3000 μS cm^{-1}). Seasonal variations did not significantly alter community sensitivity to salinity ($p > 0.05$). LMER and SEM analyses revealed strong adverse effects of high EC and EC peaks on microbial diversity, richness, and the efficiency of organic matter and TKN removal ($p < 0.05$). This highlights the importance of monitoring and controlling EC levels in WWTP influent to maintain optimal treatment performance and the need for effective technologies or biological processes to mitigate saline discharges into rivers.

1. Introduction

Wastewater treatment plants (WWTPs) continuously receive saline wastewater from cities, which can adversely impact their operational conditions and overall functioning [1]. This saline influx can affect physical (e.g., accelerated corrosion), chemical (e.g., coagulation efficiency), and biological processes (e.g., inhibition of microbial communities) within WWTPs [2–4]. For example, the accumulation of saline influent in treatment units (e.g., activated sludge tanks) [5–7] can limit their ability to effectively remove pollutants (e.g., organic matter, nutrients) [8–10]. However, the resistance and resilience of microeukaryotic communities (e.g., protozoan) to increased salinity is still poorly understood, particularly in full-scale WWTPs. Also, the vast majority of experiments simulating activated sludge conditions have used indirect measures, such as the oxygen uptake rate (OUR), to assess community responses (Table S1). Therefore, the direct effects of salt on these communities in a practical operational setting remains unexplored [2,11]. Understanding salinity dynamics within WWTPs is necessary to maintain overall pollutant removal efficiency [12] and safeguard water quality for ecosystems and human consumption [13,14].

Salinity levels in urban wastewater depend not only on domestic activities [15,16] but also on contributions from construction (e.g.,

* Corresponding author at: FEHM-Lab (Freshwater Ecology, Hydrology and Management), SHE-2, Institute of Environmental Assessment and Water Research (IDAEA), CSIC, Carrer de Jordi Girona, 18-26, 08034 Barcelona, Spain.
E-mail address: alvaromoyano@ub.edu (A.J.M. Salcedo).

https://doi.org/10.1016/j.jwpe.2024.105974
Received 12 June 2024; Received in revised form 30 July 2024; Accepted 10 August 2024
Available online 16 August 2024
2214-7144/© 2024 The Authors. Published by Elsevier Ltd. This is an open access article under the CC BY-NC-ND license (http://creativecommons.org/licenses/by-nc-nd/4.0/).

highway paving and building expansion wastes), transportation (e.g., road de-icers, salts from asphalt wear), and industrial facilities (e.g., food additive and cleaning product industries) [17–20]. The latter occur when treated discharges connect to sewage systems, and ion removal is inefficient (e.g., due to poor regulation and lack of specific salt removal processes) [13,21]. Also, salinity concentrations in the urban environment can vary between regions and seasons. For instance, ion levels in wastewater may increase due to the use of water softeners in areas with hard water [22,23], and the application of salts for ice prevention in municipalities with combined sewage systems can lead to seasonal salinity peaks during winter months [16,19]. In coastal areas, variations in salinity can also occur due to seawater intrusion during high tide seasons [24,25]. Since salt removal efficiency depends on the treatment type [26], the operating conditions, the bacterial communities involved [27], and their adaptation to salinity [28–30], salt removal in WWTPs might require advanced treatments, which are usually lacking in WTTPs located in small and medium size cities [4,31]. Moreover, treatments like reverse osmosis or membrane systems are costly, energy-intensive, and produce by-products (e.g., brines), limiting their adoption [32,33]. Consequently, most urban WWTPs rely on indirect salt removal processes (e.g., conventional physicochemical and biological reactions) and rarely monitor salinity variations and their effects on microbial communities [34,35].

According to laboratory experiments, salinity can negatively impact microbial communities growing in activated sludge, but the salinity tolerance varies among groups, families, genera, and species [2,11,36,37]. However, there are barely no studies testing the response of microbial communities to increased salinity under real conditions (i.e., full-scale WWTPs), especially for microeukaryotic groups (e.g., ciliates, flagellates) [2]. The few available studies show that salinity primarily affects protozoa and metazoa, with less pronounced effects on bacterial activity [38]. Indeed, a strong negative effect of salinity has been observed for some protozoan communities (e.g., rotifers and nematodes), leading to their reduction or even disappearance when salinity exceeds a certain threshold (> 20 g/L NaCl) [2,39,40]. This negative response might depend on the species considered. For example, it has been shown that ciliates such as *Vorticella* spp. and *Opercularia articulata* can survive wide NaCl gradients (from 3 to 40 g/L NaCl) depending on their body size and the exposure time [2]. Understanding the response of protozoans to salinity is important because they play a major role in wastewater treatment and because their mortality has been shown to trigger trophic cascades in other food webs (e.g., reduced ciliate grazing leading to increased bacterial populations and potential effluent quality issues) [41,42].

Overall, there is little information on how salinity can affect the structure and seasonal dynamics of microbial communities involved in water treatment [43–47]. For example, sudden saline water inflows during storm events lead to temporary salinity peaks that can alter the structure of microbial communities [16,25]. At the same time, the response of the microbial communities to increased salinity might depend on the time of the year at which the event occurs. For example, seasonal temperature variations can cause shifts in microbial community composition, with certain taxa becoming more dominant in warmer months while others thrive in cooler conditions [46–48].

Understanding how microbial communities are modulated by EC is important because it can affect pollutant removal, although the available studies provide conflicting information (Table S1). It has been reported that pollutant removal efficiency is reduced under high saline conditions [1,49–51] due to inhibition of microbial enzyme activity or the mortality of microorganisms [52–55]. Conversely, some studies have not observed significant effects of saline wastewater on pollutant removal [56,57], provided that there is no impact on the colonization of microeukaryotic species (e.g., yeast *Meyerozyma*) associated with efficient contaminant removal [8,58]. Moreover, the vast majority of the studies addressing the effects of salinity on WWTPs employed pilot systems simulating high NaCl levels (30–60 g/L) with advanced treatments (e.g., MBBR) [59,60]. Thus, the typical salinity of full-scale conventional plants (< 20 g/L NaCl) [49], which can vary between cities and climates, has been overlooked [4,13,61].

In this study, we focused on the protozoa community due to its crucial role as a filtering community responsible for the elimination of suspended solids, as well as a bioindicator used to monitor effluent quality [36,62–66]. Also, the loss of protozoa can affect the entire microbial community through cascade effects, negatively impacting the wastewater treatment process [38,42,65,66]. We assessed the electrical conductivity (EC, used as a proxy for salinity) dynamics within seven urban WWTPs and their effects on the protozoa communities, with a special emphasis on salinity peaks and their implications for pollutant removal efficiency. The specific objectives of this study were to: (i) assess the effects of salinity on protozoan diversity and richness in full-scale urban WWTPs; (ii) identify the impact of EC peaks on microbial abundance and community dynamics; and (iii) evaluate the effect of increased salinity and salinity peaks on pollutant removal efficiency within WWTPs.

2. Materials and methods

2.1. Description and operating conditions of WWTPs

The study included seven WWTPs located in the Mediterranean region of Catalonia, Spain. These WWTPs, specifically located in the municipalities of Roses (WWTPRSS), Llançà (WWTPLLN), Castelló d'Empúries (WWTPCES), Reus (WWTPRUS), Amposta (WWTPAMP), Les Cases d'Alcanar (WWTPALC) and Sant Carles de la Ràpita (WWTPSCR), were selected for their local relevance, data availability, accessibility, and the use of biological systems for the removal of organic matter and, in some cases, nutrients. A detailed description of each WWTP is shown in Table S2 [67]. During the study period (2010–2021) samples were collected monthly from the WWTP biological treatment processes. These samples were analyzed for the identification of microeukaryotic and filamentous communities. Also, a comprehensive dataset of operational parameters and effluent quality measurements was compiled monthly for the specified study period. An approach of profiling each WWTP is presented (Table S2), based on site visits and data collection from the Catalan Water Agency [67], to show the main design and operating conditions.

2.2. Physical and chemical wastewater conditions

Influent and effluent quality parameters such as EC, pH, temperature, dissolved oxygen (DO) in the aeration tank, organic matter (biochemical oxygen demand, BOD_5, chemical oxygen demand, COD), nitrogen (total nitrogen (TN), Total Kjeldahl Nitrogen (TKN), ammonium, nitrate, and nitrite) and total phosphorus (TP) were measured for each WWTP during monthly sampling days. The EC values used were taken directly from the activated sludge process. All laboratory analyses were performed using sensors (EC, pH, temperature,DO) and following the methodology prescribed in the Standard Methods (BOD_5, COD, TN, TKN, ammonium, nitrate, nitrite and TP) [68]. These analyses were performed and reported by each WWTP. The microbiological community in the activated sludge tanks of the WWTPs was identified under stable operating conditions on the monthly days throughout the period of this study. The mean and standard deviation of the physicochemical characteristics of the effluent in the secondary treatment (i.e., the biological process) of each WWTP are presented in Table S3. Moreover, the variations in water quality parameters in the activated sludge tank of the WWTPs were evaluated using the coefficient of variation (CV) [69].

2.3. Microeukaryotic and filamentous microorganisms sampling, counts and identification

Activated sludge samples from each WWTP were used to identify the

microeukaryotic and filamentous bacterial communities. Monthly visits were made to each WWTP during the study period to collect activated sludge process samples. The activated sludge tank sampling protocol was the same at each plant. Samples were collected from the well mixed areas of the tanks. Sterile 0.5 L bottles were filled to 50 % capacity to avoid rapid depletion of DO during transport. Samples were transported to the University of Barcelona laboratory except for those from WWTPRSS, WWTPLLN and WWTPCES which were counted and identified within each WWTP following the same protocol as used in the university laboratory. Each sample was cooled, and protected from direct sunlight, where they were stored under refrigerated conditions (4 °C) until analysis within 2 h of arrival. Then, using optical microscopy (Zeiss Axioskop 40 microscope), microorganisms were sorted, identified, and counted every sample day at the family and genus/species levels, depending on the specific microeukaryotic and filamentous groups. Abundance of filamentous microorganisms was measured at 400× following Salvadó [70]. Counts of microeukaryotes larger than 20 μm were conducted following the method described by Madoni [71], which involved analyzing three 25 μL replicates at 100× magnification. For microeukaryotes smaller than 20 μm (such as small flagellates and amoebae), counts were performed at 400× magnification. Specifically, 15 microscopic fields on the coverslip (20 × 20 mm) were analyzed for each replicate. All counts were conducted in vivo using well-homogenized samples.

Filamentous microorganisms were identified at the morphotype level using the guidelines provided by Eikelboom [72] and Jenkins et al. [73]. Species-level determination of ciliates was carried out according to the methods outlined by Curds et al. [62] and Foissner et al. [74], using the ammoniacal silver carbonate impregnation [75] and dry silver nitrate techniques for accurate identification of morphologically similar species [76]. Also, based on the recommendations of Foissner et al. [77], certain species of peritrich ciliates were identified. Flagellated protists were identified following the protocols described by Jeuck and Arndt [78] and Lee et al. [79]. Amoebae were categorized based on size into small (<20 μm) and large (>20 μm) categories. Taxonomic classification of microeukaryotes followed the guidelines outlined by Adl et al. [80]. However, it is important to note that the terms 'flagellates' and 'amoebae' are not formal taxonomic ranks but are used to describe organisms possessing conspicuous flagella or pseudopodia, respectively, as commonly employed in bioindication analyses.

2.4. Microbial biodiversity indices

Four key indices were calculated to assess microbial diversity in activated sludge from wastewater treatment plants. These indices were calculated for both the total microbial community and specifically for Ciliates, allowing for a more focused analysis at genus/species resolution of this particular group. Richness was determined by counting the species present using the apply() function in R. The Shannon index was calculated considering the abundance and evenness of the species using the diversity() function from the "vegan" package. The Margalef index was calculated based on species richness and total abundance according to Margalef [81]. Heip's Evenness (HeipE) was evaluated for evenness using the equations proposed by Heip [82]. These indices provided a comprehensive understanding of the diversity and structure of microbial communities in WWTPs.

2.5. Electrical conductivity measurements

The effect of EC on the microbial community was determined using the monthly EC data for the study period for each WWTP. EC peaks were identified using the "findpeaks" function in the time series data. The monthly average EC values and EC peaks for each WWTP were used to assess the effect of EC on pollutant removal and the seasonal salinity effects on the communities.

2.6. Data analysis

All statistical analyses were performed in R Core Team [83], and the nomenclature proposed by Muff et al. [84] was used to report our results in the language of evidence. One-way Kruskal-Wallis tests were performed for each sampling month to assess variation in richness, Margalef, Shannon, and HeipE indices, and physicochemical parameters of effluent across WWTPs. When significant differences were detected following the Kruskal-Wallis test (p value < 0.05), post hoc comparisons were conducted using Mann-Whitney U test (p value < 0.05). Linear mixed-effects models (lmer) were constructed using the 'lme4' package to examine the relationship between EC concentrations and protozoan diversity and richness indices for each WWTP (included as a random factor) [85]. These models allowed us to assess both fixed effects (EC concentrations) and random effects (variance associated with each WWTP) on protozoan diversity and richness. Bacterial and protozoan indices were calculated using the "vegan" package [86]. Furthermore, Spearman correlation analyses were conducted to assess the relationships between EC and each diversity index (richness, Shannon, Margalef, Simpson, and HeipE), as well as environmental and water quality parameters. We interpreted the Spearman correlation as follows: (0 to 0.19) Very Weak or None, (0.20 to 0.39) Weak, (0.40 to 0.59) Moderate, (0.60 to 0.79) Strong, (0.80 to 1.0) Very Strong [87]. Indicator species analysis (IndVal) [88] was performed to identify indicator taxa for each WWTP using the 'labdsv' package [89]. These analyses were used to determine species according to each WWTP condition and EC level. Variance Inflation Factors (VIF) were used to determine collinearity between EC and environmental and water quality parameters [90].

The 'findpeaks' function from the 'pracma' package was used to identify EC peaks [91]. Significant peaks were defined as those exceeding the minimum detected peak value, capturing extreme variations in EC observed at each WWTP. The impact of these EC peaks on microbial species was assessed through pairwise comparisons between each EC peak and the immediately preceding non-peak value, using a binary flag system. Microorganisms were flagged as either 1 or 0 based on the presence or absence of EC peaks. These comparisons were conducted separately for each pair of groups (i.e., 0, 1), with each group consisting of two samples: one corresponding to a value of 0 and the other to a value of 1, as determined by the temporal variability of EC. The Mann-Whitney U test was then used to evaluate if there was a significant difference in microbial community abundance between samples associated with EC peaks and non-peaks. Subsequently, a Bonferroni correction was applied to mitigate Type I errors due to multiple testing. This approach accounted for the temporal proximity of the data, comparing months or days where data were available (e.g., samples taken monthly during periods of high or low EC, such as January - no EC peak, February - EC peak). The temporal variability of EC was also assessed in relation to the Margalef index over the year, examining the relationship between these two variables through a Spearman correlation analysis. Seasonal diversity associated with EC peaks and non-peaks was separately analyzed for WWTPRSS, WWTPLLN, and WWTPRUS. These plants were selected to represent WWTPs with high, intermediate, and low EC levels, respectively, and also had sufficient seasonal data to correlate the Margalef index with EC peaks per season.

Finally, a structural equation model (SEM) was built to assess the interactions between salinity, bacterial and protozoan communities, and pollutant removal efficiency using the "lavaan" package [92]. SEM is based on the variance-covariance matrices between predictor and response variables and interactively assesses direct and indirect causal pathways using correlations between these variables and their statistical significance [93]. The global model contained 305 sampling units which included all WWTP samples (i.e., WWTPRSS: 59 samples; WWTPLLN: 52 samples; WWTPCES: 52 samples; WWTPRUS 86 samples; WWTPAMP: 19 samples; WWTPALC: 9 samples; WWTPSCR: 27 samples) and variables (EC, percent removal of COD, BOD_5, NTK, NO_3^- and TP), as well as the abundance, richness, Margalef and Shannon indices of bacterial and

protozoan communities. Also, a global SEM was computed specifically for EC peak samples identified (i.e., WWTPRSS: 19 samples; WWTPLLN: 14 samples; WWTPCES: 13 samples; WWTPRUS: 18 samples; WWTPAMP: 4 samples; WWTPSCR: 10 samples), along with individual SEM models calculated for each WWTP. Before building the models, variables with a Spearman correlation higher than 0.9 were excluded [94]. Salinity was set as the predictor variable. Similar SEM models were computed individually for each WWTP.

3. Results

3.1. EC levels and operational conditions among WWTPs

Strong differences in EC were observed among the WWTPs evaluated. These differences were very strong between WWTPRSS and WWTPRUS, and between WWTPRSCR and WWTPRUS (Kruskal-Wallis p value <0.05, Table S3, Table S4, Table S5). WWTPRSS had the highest mean EC compared to the other WWTPs, followed by WWTPSCR and WWTPCES, while WWTPLLN and WWTPALC had intermediate to low EC values. Conversely, WWTPRUS had the lowest mean EC, followed by WWTPAMP (Table S3, Fig. 1).

Based on the CV and the range of water quality parameters in the activated sludge tank, variations were low to moderate (Table S3). The highest CVs for EC were observed in WWTPLLN (41 %) and WWTPSCR (45 %), followed by WWTPALC (39 %) and WWTPCES (30 %); and the lowest in WWTPRSS (21 %) and WWPTRUS (16 %). For DO, CVs were below 37 %, with WWTPRSS showing the lowest variation (20 %). COD and BOD_5 CVs ranged from 16 % to 44 %, with WWTPLLN having the highest CVs (COD = 39 %, BOD_5 = 44 %). For TN, CVs were highest in WWTPLLN (45 %), followed by WWTPRSS (39 %) and WWTPCES (37 %). The Kruskal-Wallis test showed no evidence of strong changes in physicochemical variables (EC, pH, temperature, DO, COD, BOD_5, TN, TP) during the operational period (p-value >0.05, Tables S6).

3.2. Microbial community composition and taxa associated with WWTP EC levels

Microbial community composition among WWTPs showed strong similarity (Fig. S1, NMDS analyses), dominated by different groups (Table S7). WWTPRSS showed the lowest values for the Shannon, Margalef, Richness, and HeipE indices, followed by WWTPALC and WWTPSCR. Conversely, WWTPRUS exhibited the highest values for the Shannon, Margalef, and Richness indices (Fig. S2). IndVal analysis (Table S8) identified five taxa associated with WWTPs with contrasting EC values (i.e., WWTPRSS and WWTPSCR, which have the highest average EC, and WWTPRUS, which has the lowest average EC). *Beggiatoa* spp. and *Choanoflagellates*, were found exclusively in WWTPRSS, while *Arcella* sp. was strongly associated with WWTPSCR. Finally, *Vorticella infusionum*, and *Epistylis* sp. were associated with WWTPRUS.

3.3. Effects of EC on microbial diversity and richness indices

The linear mixed effects model showed a very strong negative effect of EC on the richness (p value <0.05, Table S9), Shannon (p value <0.05, Table S10), and Margalef (p value <0.05, Table S11) indices for ciliates (Fig. 2). The global linear mixed effects model showed a similar strong

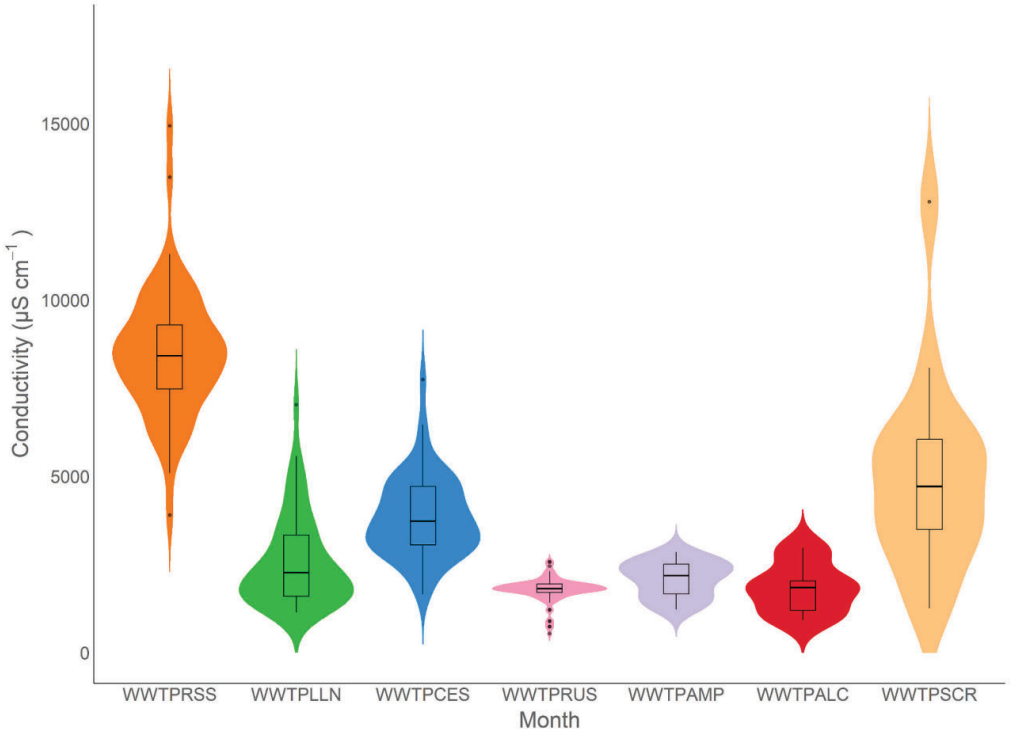


Fig. 1. Violin plots grouping monthly conductivity values by WWTP. WWTPRSS: Roses wastewater treatment plant. WWTPLLN: Llançà wastewater treatment plant. WWTPCES: Castelló d'Empúries wastewater treatment plant. WWTPRUS: Reus wastewater treatment plant. WWTPAMP: Amposta Wastewater Treatment Plant. WWTPALC: Les Cases d'Alcanar Wastewater Treatment Plant. WWTPSCR: Sant Carles de la Ràpita Wastewater Treatment Plant.

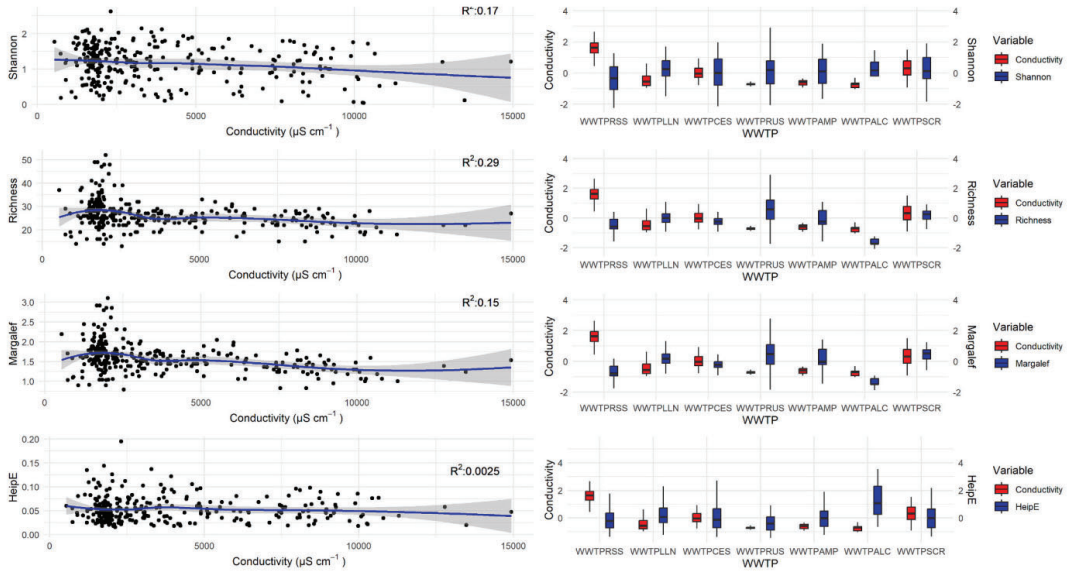


Fig. 2. On the left: linear mixed models of Shannon, richness, Margalef and HeipE indices for ciliates as a function of conductivity for each WWTP. On the right: box plot comparing conductivity and biodiversity indices for each WWTP. WWTPRSS: Roses wastewater treatment plant. WWTPLLN: Llançà wastewater treatment plant. WWTPCES: Castelló d'Empúries wastewater treatment plant. WWTPRUS: Reus wastewater treatment plant. WWTPAMP: Amposta Wastewater Treatment Plant. WWTPALC: Les Cases d'Alcanar Wastewater Treatment Plant WWTPSCR: Sant Carles de la Ràpita Wastewater Treatment Plant.

negative effect of EC on richness, Shannon, and Margalef indices for the total microbial community (Fig. S3).

Spearman rank correlation showed no evidence of strong relationships between EC and the other measured environmental and water quality variables (pH, DO, temperature, COD, BOD_5, TN, TP) within the evaluated WWTPs (Fig. S4). This suggests that EC levels in WWTPs did not exhibit strong collinearity with these parameters and independently influenced WWTP microbial community dynamics. Furthermore, VIF analysis for EC in relation to pH, DO, temperature, COD, BOD_5, TN, and PT were all within acceptable limits (ranging from 1.04 to 2.95, Fig. S5), indicating no substantial multicollinearity issues.

3.4. Impact of EC peaks on microbial communities and seasonal diversity response

EC peaks were identified in each of the WWTPs except WWTPALC (Table S12), which was not considered for this analysis due to its low number of samples. The temporal trend of EC and Margalef index by WWTP is shown in Fig. 3. The highest range in EC peaks was observed in WWTPRSS (i.e., EC from 6500 to 15,000 µS cm^{-1}) and WWTPSCR (EC from 3400 to 13,000 µS cm^{-1}), followed by WWTPCES (i.e., from EC 3700 to 8000 µS cm^{-1}) and WWTPLLN (i.e., EC from 1500 to 7000 µS cm^{-1}), which had moderately higher EC peaks (Table S12). In contrast, the conductivity in WWTPRUS (i.e., EC from 1800 to 2600 µS cm^{-1}) and WWTPAMP (i.e., EC from 2400 to 2700 µS cm^{-1}) remained fairly stable throughout the study period, with few peaks when compared to the other WWTPs (Table S12, Fig. 3).

Strong evidence of changes in total abundance of microorganisms in response to EC peaks was observed only in WWTPRSS and WWTPSCR (Kruskal-Wallis *p* value <0.05, Table S13). The microbial taxa that showed strong responses to EC peaks is shown in Table 1 (Mann-Whitney, p value <0.05, Table S14). Among them, *Acineria uncinata* and *Holophyra discolor* were the most sensitive. Moreover, a moderate negative correlation between EC and the Margalef index (Spearman, *p*-value <0.05) was found in WWTPRSS and WWTPSCR (Table S15, Fig. 3). Finally, Kruskal-Wallis analysis showed no evidence of seasonal changes (i.e., no clear differences in EC levels and community diversity between seasons) in the evaluated WWTPs (i.e., WWTPRSS, Fig. S6; WWTPLLN, Fig. S7; and WWTPRUS, Fig. S8; Table S16).

3.5. EC removal rates in urban WWTPs and salinity effects on pollutant removal efficiency

A relatively low mean EC removal, ranging from 9 to 26 %, was observed in all WWTPs (Fig. S9). We found strong evidence of an inverse relationship between EC removal and organic matter removal (COD, BOD_5, Fig. S10, *P* value <0.05, Table S17), but no evidence of a relationship between EC removal and nutrient removal (TN, TP, Fig. S11, *P* value >0.05, Table S17). EC removal reached a maximum of 60 % in WWTPSCR, but generally remained below 45 %. During the periods of worst efficiency in EC removal, all WWTPs had efficiencies below 5 %, implying high salinity discharges into the environment.

Furthermore, lmer models showed a negative effect of EC on pollutant removal efficiency (COD, BOD_5, TKN, NO_3^-, TP) (Fig. S12, lmer, Table S18 to Table S22). For BOD_5, COD and TKN, a strong inverse relationship with EC was observed (lmer, *P* value <0.05), indicating that removal efficiency of these pollutants decreased with increasing EC (Fig. S12, lmer, Table S18, Table S19, Table S20). Conversely, we found no strong negative effect of EC on nitrate and TP removal efficiency (lmer, P value <0.05, Fig. S12, Table S21, Table S22). These findings remained consistent across individual plants when analyzed separately using simple linear models (Fig. S13).

The global SEM model provided further evidence for EC as a primary driver of microbial abundance and community composition, thereby affecting pollutant removal (Fig. S14, Table S23 provides a summary of the global SEM). This finding was observed both for the overall microbial community and the ciliate community indices (Fig. S15). Strong negative regression coefficients show that EC can strongly affect

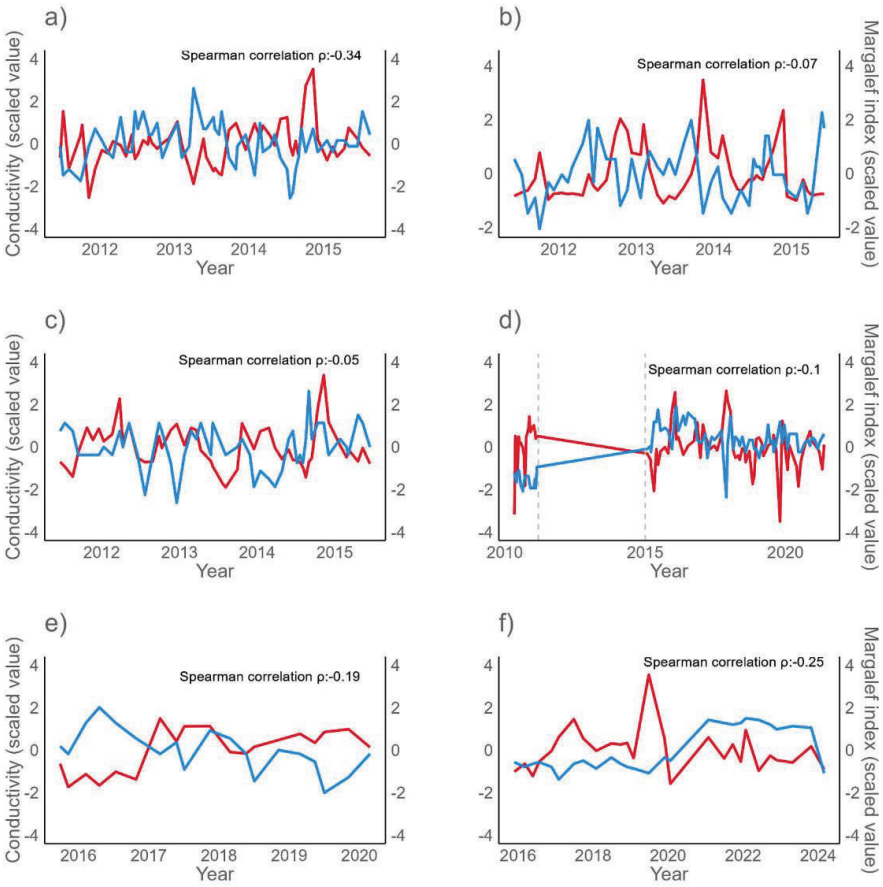


Fig. 3. Temporal variations in electrical conductivity (μS cm^{-1}) and Margalef index by WWTP. The red line represents electrical conductivity, and the blue line represents the Margalef index. In section c), the interval delimited by dashed lines represents a period for which there is no data a) WWTPRSS: Roses wastewater treatment plant. b) WWTPLLN: Llançà wastewater treatment plant. c). WWTPCES: Castelló d'Empúries wastewater treatment plant. d) WWTPRUS: Reus wastewater treatment plant. e) WWTPAMP: Amposta Wastewater Treatment Plant. f) WWTPSCR: Sant Carles de la Ràpita Wastewater Treatment Plant. (For interpretation of the references to colour in this figure legend, the reader is referred to the web version of this article.)

richness (p Value <0.001), the Margalef index (p value <0.001), the Shannon index (p Value <0.05) and the percentage of BOD_5 removal (p Value <0.001). We also found moderate negative effects of EC on TKN and nitrate, and no evidence of effects on the percentage of TP removal (p Value >0.05). Strong covariances were also observed between the latent richness variables, Margalef and Shannon, indicating a positive association between these diversity measures. When the global SEM model was run with only the EC peaks using ciliates abundance and diversity indices, it revealed an increased effect of EC on the measured variables in the WWTPs (Fig. 4, Table S24). This was particularly evident for the richness and Margalef indices (Fig. 4), accompanied by the intensification of the negative relationship on BOD_5 and TKN, resulting in decreased removal efficiencies associated with EC peaks (Fig. S16).

Finally, when the SEM analysis was individually built for each plant, we found strong evidence that EC can affect the microbial community when it reaches a certain level (Fig. S17). WWTPs with higher EC levels showed a stronger negative effect of EC on the microbial community. There was considerable variability in the correlation between EC and pollutant removal among WWTPs, revealing specific effects for each WWTP that also appeared to be influenced by EC levels. Although BOD_5 and COD removal was affected by EC at most sites, these relationships varied among WWTPs. For instance, a positive relationship was observed between EC and the removal of COD, BOD_5, and TP in WWTPRUS (which had the lowest EC values).

4. Discussion

Overall, the effects of EC on microbial communities varied between WWTPs, although specific taxa were associated with different EC levels. Microbial diversity and abundance strongly decrease along EC gradients in WWTPs with moderate to high EC ranges. In contrast, WWTPs with low EC levels showed weak to negligible response of the microbial communities to changes in EC. Ciliate abundance was strongly reduced by EC peaks, which also caused a moderate reduction in ciliate diversity. All these effects were consistent across seasons and EC removal rates remained low (they ranged between 10 % and 26 %) across WWTPs, showing no correlation with nutrient removal rates. The efficiency of

Table 1
Effect of EC peaks on the abundance of microorganisms in WWTPs.

WWTP	Genus/ Species	EC Peaks effects	EC peak intervals	Reference EC values of salinity tolerance (Foissner, 1995)
WWTPRSS	*Acineria uncinata*	Strongly Reduced	Min: 6435; Max: 14935 µS cm^{-1}	0–400 mg L^{-1} Cl^-
	Chilodonella uncinata	Strongly Reduced		433–54,000 µS cm^{-1}
	Holophyra discolor	Strongly Reduced		0–5000 mg L^{-1} Cl-
	Metacineta sp.	Strongly Reduced		570–23,000 µS cm^{-1}
	Trochilia minuta	Moderately Reduced		405–1700 µS cm^{-1}
	Tokophrya sp.	Moderately Reduced		0–800 mg L^{-1} Cl^-
	Vorticella aquadulcis	Moderately Reduced		395–1100 µS cm^{-1}
WWTPSCR	*Acineta* sp.	Strongly Reduced	Min: 3370; Max: 12780 µS cm^{-1}	0–800 mg L^{-1} Cl^-
	Acineria uncinata	Strongly Reduced		0–400 mg L^{-1} Cl^-
	Holophyra discolor	Moderately Reduced		0–5000 mg L^{-1} Cl^-
	Opercularia sp.	Moderately Reduced		0–400 mg L^{-1} Cl^-

Strongly Reduced and Moderately Reduced categorize the impact of EC peaks on microorganisms abundance. This impact was determined by the difference in average abundance between peak and non-peak periods (Mann-Whitney test, Table S17). 'Strongly Reduced' indicates a highly significant decrease ($p < 0.001$), while 'Moderately Reduced' indicates a significant decrease ($p < 0.05$).

organic matter and nitrogen removal was affected at high EC levels, potentially driven by disruptions in both biological interactions and physicochemical processes.

4.1. Specific taxa responses to EC

The community of protozoa and filamentous bacteria associated with WWTPs with high EC, such as WWTPRSS and WWTPSCR, was dominated by *Beggiatoa* sp., *choanoflagellates*, and *Arcella* sp. (as indicated by IndVal analysis), aligning with findings from previous studies [95–99]. For example, *Beggiatoa* sp. is known to be resilient to environmental changes in extreme aquatic environments, including hypersaline lakes such as Chiprana in Spain, being present in effluents rich in sulfide and nitrate, anoxic conditions, and even in the absence of oxygen [95,100,101]. Similarly, several species of *choanoflagellates* such as *Salpingoeca crinita* have adapted to the salt flats of the Atacama Desert in Chile [97–99]. Higher salinity has also been shown to increase *choanoflagellate* abundance in WWTPs [11]. Moreover, Roe and Patterson [102] reported a strong association between species within the *Arcella sp*, particularly *Arcella vulgaris*, and lakes affected by salt runoff from road deicing and agricultural areas (i.e., fertilizer and pesticide runoff with elevated salt and nutrients). Therefore, the abundance of these species in both aquatic environments and WWTPs, as reported in our study, suggest that they could be used as bioindicators of salinization, not only in these areas, but also in wastewater treatment processes [11,97,102].

Among the ciliate protozoa, peritrich ciliates such as *Vorticella infusionum* were associated with WWTPRUS (i.e., the WWTP with the lowest EC). Concordantly, Salvadó et al. [2] found that the abundance of *Vorticella infusionum* was reduced at high salt concentrations. Also, *Epistylis* sp. seemed to be very sensitive to salinity according to our results. This aligns with Foissner [74], who showed that *Epistylis* spp. was associated with low EC ranges (i.e., between 500 and 1500 µS cm^{-1}). Moreover, other studies showed that its abundance declines at high salinities (i.e., > 5 g/L) in both experimental setups and natural aquatic environments [2,103,104]. These responses appear to depend on factors such as the duration of the salinity exposure, acclimation to different salinities, specific species traits (e.g., size, feeding), and interactions among

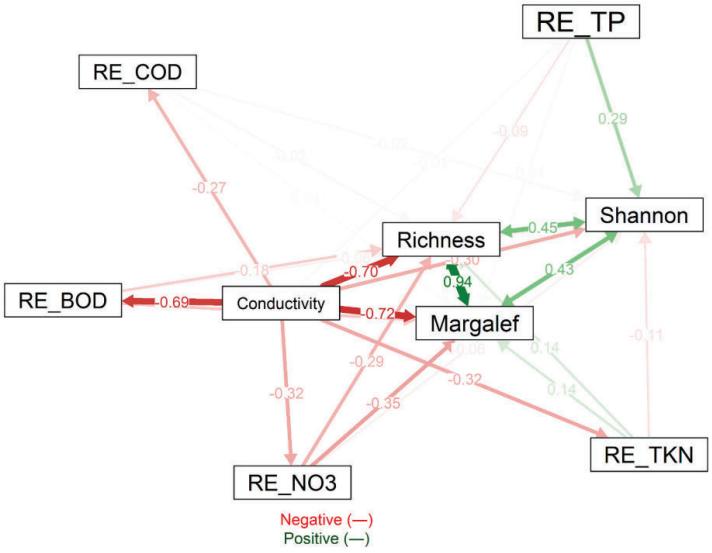


Fig. 4. Structural equation model showing the effects of electrical conductivity peaks on protozoan community indices for ciliates and percent pollutant removal. Conductivity: conductivity (µS cm^{-1}); RE_BOD: biochemical oxygen demand removal percentage; RE_COD: chemical oxygen demand removal percentage; RE_TKN: nitrogen total Kjeldahl removal percentage; RE_NO_3^-: nitrate removal percentage; RE_TP: total phosphorus removal percentage; Richness: Taxa richness of ciliates in the activated sludge process; Shannon: Shannon diversity of ciliates in the activated sludge process. Margalef: Margalef richness of ciliates in the activated sludge process. Red and green lines indicate negative and positive relationships, respectively. Model fit indices were set at CFI ≥ 0.90 and RMSEA ≤0.05. (For interpretation of the references to colour in this figure legend, the reader is referred to the web version of this article.)

protozoa within assemblages [40,104,105]. For example, Jones et al. [104] found that gradual acclimation to salinity strongly improved the survival of *Epistylis* sp. under laboratory conditions.

4.2. EC effects on the protozoa communities

The increase in EC was mainly responsible for the negative effects on community diversity and abundance indices. These findings are consistent with previous studies that have reported negative effects of high EC on aquatic communities not only in freshwater [106–110] but also in microorganisms from activated sludge experiments [2,111,112] (Table S1). This could be explained by the influence of EC on factors such as nutrient availability, osmolarity, and environmental toxicity, thereby potentially modulating the activity and composition of microbial communities [113–115]. In our WWTPs, the response of microorganisms appears to be codependent on EC concentration (i.e., as EC increases, biodiversity indices decrease). However, other factors, such as microbial adaptation to high salinity in activated sludge [5,116], operational factors (e.g., low COD and high salinity), environmental factors [46,117], and species interactions [118,119], also might play important roles in their response to salinity.

Although establishing links between resilience to toxic EC levels (e.g., at the species level), community interactions (e.g., individually, and collectively), and the resulting impact on pollutant removal efficiency is challenging [2,111,120], especially when analyzing data at a real scale (i.e., under uncontrolled conditions). It is important to consider the constant decrease in microbial diversity and richness indices at elevated EC concentrations, which could result in the loss of taxa crucial for WWTP processes and the disruption of community interactions. For example, it has been reported that interactions between protozoa such as *Paramecium* sp. *Vorticella* sp. *Epistylis* sp. and *Opercularia* sp. have been shown to increase their collective ability to degrade pollutants (e.g., COD, petroleum hydrocarbons) and better withstand adverse conditions compared to when they act individually [105,121,122]. This synergy among protozoa in a consortium may be a key factor in their efficiency to remove contaminants.

4.3. EC peaks effects on the ciliate communities

It is important to note that in our study the ciliate group was most negatively affected by EC peaks. Species such as *Acineria uncinata*, along with other species negatively correlated with EC (*Trochilia minuta*, *Opercularia sp*), may indicate not only the potential importance of ciliates as salinity indicators in WWTPs, but also that the changes in the structure of their assemblages may potentially affect pollutant removal [41,65,71]. We hypothesize that the moderate decrease in BOD_5 removal efficiency obtained in our study may be related to the negative effects of increased EC on *Acineria uncinata* and other ciliates (*Trochilia minuta*, *Vorticella* spp., *Opercularia* spp.). This aligns with several studies that have linked crawling ciliates, such as *Acineria uncinata*, with organic matter removal, not only individually but also acting in consortia with other communities [105,123,124]. Also, *Acineria uncinata* is considered an indicator of deficient sludge settlement conditions, playing a crucial role in the identification of disruptions in WWTP [66]. However, regression models only showed that EC primarily affected both ciliate species and pollutant removal efficiency separately. A clear relationship between ciliate group abundance and effects on COD and BOD_5 removal was not found. Furthermore, we ruled out any direct or indirect effects on N removal by species such as *Acineria uncinata*, in agreement with other studies that found no evidence of a relationship between ciliates such as *Acineria* spp. and N removal [64,66,125]. However, this is not always the case within the ciliate group, as other ciliates, like *Trochilia minuta*, have been associated with nitrifying conditions [126].

Comparisons between samples associated with EC peaks and non-peaks were influenced by both the magnitude of the peak and the stability of EC levels within WWTPs [2,127,128]. WWTPs with lower EC levels and greater EC stability (e.g., WWTPRUS) exhibit higher abundance and diversity of microbial communities, which are distinctly separated from WWTPs characterized by higher EC concentrations and variability (e.g., WWTPRSS) [2,127]. Consequently, WWTPs with higher EC levels also tend to experience higher EC peaks (i.e., WWTPRSS), resulting in pronounced effects not only on species diversity, as indicated by the negative correlation between EC peaks and the Margalef index (Fig. 3), but also on specific species such as *Holophyra discolor and Metacineta* sp. These effects extended to other diversity indices such as richness and Shannon diversity (according to EC peak SEM model, Fig. 4). However, the impact of salinity on community dynamics did not vary with the seasons. This could be explained by the lack of a strong correlation between salinity and temperature (i.e., salinity did not consistently and predictably align with seasonal changes in community dynamics). Finally, it has been reported that salt peaks negatively impact several parameters of activated sludge and contribute to the corrosion of equipment, including a reduction in floc size by approximately two-thirds, which affects the activity of this process in WWTPs [127–129]. This trend is particularly evident in the context of COD and BOD_5 removal efficiency, where a stronger negative interaction is observed between EC peaks and the efficiency of organic matter removal, as shown in the comparisons between SEM models.

4.4. EC removal in WWTPs and salinity effects on pollutant removal efficiency

A notable finding of our study is that we observed a relatively low EC removal, with an average never exceeding 26 % across all WWTPs evaluated. Furthermore, for these percentages of EC removal in WWTPs, we found evidence of a relationship with organic matter removal and no evidence of a relationship with nutrient removal (i.e., WWTPs with N removal by nitrification and denitrification). This positive association suggests that the processes involved in removing organic matter also contribute to reducing EC. However, a high elimination of organic matter does not ensure a high removal of EC. This observation could be explained by the decomposition of organic matter, which can produce organic acids and soluble salts (e.g., chloride, sulfate, nitrate) as byproducts of the removal process [130–132], thereby increasing the concentration of dissolved ions in the effluent. Also, the decomposition of organic matter can consume dissolved oxygen in the biological process, leading to anaerobic conditions and the production of ions through chemical reactions [133–135]. The absence of a relationship with nutrient elimination may suggest that, while some salinity is likely utilized in processes converting nitrogen from wastewater to gaseous nitrogen, the portion of EC removed as ammonium and alkalinity (e.g., estimated between 14 and 33 % of total EC) may not constitute a significant fraction of the total EC [136,137]. This could potentially explain the lack of a noticeable reduction in conductivity attributed to nitrogen removal processes. It is likely that the majority of EC was eliminated through physical processes (e.g., filtration due to adsorption of the cations on the colloids negatively charged) and chemical processes (e.g., flocculation, coagulation), as well as biological treatment (i.e., communities utilizing dissolved ions in the effluent to some extent) in the evaluated WWTPs [138–140].

BOD_5 and TKN removal efficiencies showed a strong negative response to elevated EC levels (lmer model), but we found no compelling evidence for changes in NO_3^- and TP removal efficiencies (individual lmer for each plant as well as the global lmer). This is consistent with numerous studies focused on WWTP exposed to extremely high salinity concentrations (e.g., 60 g/L NaCl) [9,47,124] (Table S1). However, a few studies have established correlations between low to moderate salinities (0.1 to 5 g/L NaCl) and reductions in contaminant removal (e.g., BOD_5, COD) due to the inhibition of microbial communities [7,38] (Table S1). According to our results, this negative effect of EC on the removal of organic matter and TKN could be related to the sensitivity to salinity of certain communities responsible for this process. The

alteration of microeukaryotic communities, such as ciliates, may have significant repercussions on the functioning of the treatment system [41,65,141,142]. For example, ciliates play a crucial role in regulating bacterial populations through predation and the release of essential nutrients [141,142]. If the ciliate population is affected, this could disturb the biological balance of the system (i.e., cascade effects), which in turn could impact the ability of ammonium-oxidizing (AOB) and denitrifying bacteria to effectively carry out their functions [65,142]. This disruption in microbial interactions could have serious implications for the overall efficiency of wastewater treatment in WWTPs.

Although we did not observe strong effects on nitrate and TP removal, our results (lmer and SEM), suggest that nitrate removal could be reduced during EC peaks. We hypothesize that in WWTPs with higher EC conditions (e.g., > 15,000), nitrate and TP removal may be more affected. These results are also consistent with previous studies, which highlight the variability in nutrient removal reductions depending on EC levels and the type of wastewater treatment system used (Table S1). Therefore, although EC might not be the main determinant of wastewater treatment efficiency, the effects of elevated EC levels and EC peaks on wastewater treatment processes should be monitored and controlled, especially in municipal WWTPs with salt-rich influents or salt intrusion [24,25,143]. Moreover, as we have highlighted, the relationship between EC and the biological processes involved in wastewater treatment can strongly vary from one WWTP to another and deserve further research.

5. Conclusions

This study is the first to analyze EC dynamics in WWTPs at a real scale and their effects on microeukaryotic communities and pollutant removal. We found strong evidence of negative effects of high EC levels and EC peaks on WWTP microbial communities, particularly affecting the ciliate group, as well as inverse relationships with organic matter and TKN removal. These effects are consistent across seasons and are evident at high concentrations and peaks of EC (i.e., EC levels to which both communities and WWTP processes are not acclimated). The response of microorganisms is related to EC concentration, although it is difficult to determine clear responses at the genus and species level. WWTPs with high EC levels harbor microbial communities dominated by species resistant to saline environments, such as *Beggiatoa* sp., *choanoflagellates*, and *Arcella* sp., which could serve as bioindicators of salinization in WWTPs. Disruption of ciliate communities could have significant implications for organic matter removal and overall WWTP performance. EC removal rates in conventional WWTPs, which lack advanced treatments, are relatively low, with a maximum mean observed removal of 26 %, and are not significantly correlated with nutrient removal efficiency. In summary, although EC is not the sole determinant of WWTP efficiency, its effects on WWTP functioning must be considered in the design of effective monitoring and management strategies to mitigate the adverse effects of EC fluctuations and ensure optimal wastewater treatment performance.

Funding

This work was supported by a doctoral grant from the Ministerio de Ciencia, Tecnología e innovación y Colfuturo (Colombia) and IDAEA-CSIC contract associated to Ramón y Cajal (RYC2020-029829-I) for Alvaro Moyano.

CRediT authorship contribution statement

Alvaro Javier Moyano Salcedo: Writing – review & editing, Writing – original draft, Visualization, Validation, Methodology, Investigation, Formal analysis, Data curation, Conceptualization. **Miguel Cañedo-Argüelles:** Writing – review & editing, Supervision, Methodology, Investigation, Formal analysis, Conceptualization. **Sujay S. Kaushal:** Writing – review & editing, Methodology, Investigation, Formal analysis, Conceptualization. **Eva Maria Ciriero-Cebrián:** Methodology, Investigation, Formal analysis, Conceptualization. **Adrià Perez-Blanco:** Methodology, Investigation, Formal analysis, Conceptualization. **Humbert Salvadó:** Writing – review & editing, Writing – original draft, Visualization, Validation, Supervision, Project administration, Methodology, Investigation, Formal analysis, Conceptualization.

Declaration of competing interest

The authors declare that they have no known competing financial interests or personal relationships that could have appeared to influence the work reported in this paper.

Data availability

Data will be made available on request.

Acknowledgements

We thank Consorci d'aigües Costa Brava Girona, Empresa Mixta d'Aigües de la Costa Brava S.A, EMACBSA- Roses WWTP, especially Anna Maria Huguet, Consell Comarcal del Montsià, Acciona Agua, and Aigües de Catalunya (the current entity managing the WWTP operations in the South Ebro Delta), and Aigües de Reus for their support in providing access to treatment plants, samples, and information. We also thank Oriol Canals for his general support during the process of sample collection and identification.

Appendix A. Supplementary data

Supplementary data to this article can be found online at https://doi.org/10.1016/j.jwpe.2024.105974.

References

[1] A. Uygur, F. Kargi, Salt inhibition on biological nutrient removal from saline wastewater in a sequencing batch reactor, Enzym. Microb. Technol. 34 (2004) 313–318, https://doi.org/10.1016/j.enzmictec.2003.11.010.
[2] H. Salvadó, M. Mas, S. Menéndez, P. Gracia, Effects of shock loads of salt on protozoan communities of activated sludge, Acta Protozool. 40 (2001) 177–185.
[3] J. Wang, Q. Liu, B. Wu, H. Hu, D. Dong, J. Yin, H. Ren, Effect of salinity on mature wastewater treatment biofilm microbial community assembly and metabolite characteristics, Sci. Total Environ. 711 (2020), https://doi.org/10.1016/j.scitotenv.2019.134437.
[4] A. Srivastava, V.K. Parida, A. Majumder, B. Gupta, A.K. Gupta, Treatment of saline wastewater using physicochemical, biological, and hybrid processes: insights into inhibition mechanisms, treatment efficiencies and performance enhancement, J. Environ. Chem. Eng. 9 (2021), https://doi.org/10.1016/j.jece.2021.105775.
[5] Y. Zhao, H.D. Park, J.H. Park, F. Zhang, C. Chen, X. Li, D. Zhao, F. Zhao, Effect of different salinity adaptation on the performance and microbial community in a sequencing batch reactor, Bioresour. Technol. 216 (2016) 808–816, https://doi.org/10.1016/j.biortech.2016.06.032.
[6] M.J. García-Ruiz, A. Castellano-Hinojosa, J. González-López, F. Osorio, Effects of salinity on the nitrogen removal efficiency and bacterial community structure in fixed-bed biofilm CANON bioreactors, Chem. Eng. J. 347 (2018) 156–164, https://doi.org/10.1016/j.cej.2018.04.067.
[7] Y. Chen, H. He, H. Liu, H. Li, G. Zeng, X. Xia, C. Yang, Effect of salinity on removal performance and activated sludge characteristics in sequencing batch reactors, Bioresour. Technol. 249 (2018) 890–899, https://doi.org/10.1016/j.biortech.2017.10.092.
[8] H. Wen, K. Xiong, H. Yang, P. Zhang, X. Wang, Dynamic mechanism of the microbiota of high-salinity organic wastewater with salt-tolerant yeast and its application, J. Environ. Chem. Eng. 10 (2022), https://doi.org/10.1016/j.jece.2022.107377.
[9] T. Ya, Z. Wang, J. Liu, M. Zhang, L. Zhang, X. Liu, Y. Li, X. Wang, Responses of microbial interactions to elevated salinity in activated sludge microbial community, Front. Environ. Sci. Eng. 17 (2023), https://doi.org/10.1007/s11783-023-1660-x.
[10] M.F. Hashad, Surabhi Sharma, Loring F. Nies, James E. Alleman, Study of Salt Wash Water Toxicity on Wastewater Treatment, Joint Transportation Research Program vol. 1, Indiana Department of Transportation and Purdue University, West Lafayette, Indiana, 2006, pp. 1–55.

[11] D. Correa-Galeote, A. Roibás, A. Mosquera-Corral, B. Juárez-Jiménez, J. González-López, B. Rodelas, Salinity is the major driver of the global eukaryotic community structure in fish-canning wastewater treatment plants, J. Environ. Manag. 290 (2021), https://doi.org/10.1016/j.jenvman.2021.112623.

[12] Y. Zhao, X. Zhuang, S. Ahmad, S. Sung, S.Q. Ni, Biotreatment of high-salinity wastewater: current methods and future directions, World J. Microbiol. Biotechnol. 36 (2020), https://doi.org/10.1007/s11274-020-02815-4.

[13] J. Hughes, K. Cowper-Heays, E. Olesson, R. Bell, A. Stroombergen, Impacts and implications of climate change on wastewater systems: a New Zealand perspective, Clim. Risk Manag. 31 (2021), https://doi.org/10.1016/j.crm.2020.100262.

[14] A. Zimmer, I.T. Winkler, C. De Albuquerque, Governing wastewater, curbing pollution, and improving water quality for the realization of human rights, Waterlines 33 (2014) 337–356, https://doi.org/10.3362/2046-1887.2014.034.

[15] J. Thorslund, M.T.H. van Vliet, A global dataset of surface water and groundwater salinity measurements from 1980–2019, Sci. Data 7 (2020), https://doi.org/10.1038/s41597-020-0562-z.

[16] A.J. Moyano Salcedo, E. Estévez, H. Salvadó, J. Barquín, M. Cañedo-Argüelles, Human activities disrupt the temporal dynamics of salinity in Spanish rivers, Hydrobiologia 850 (2023) 4531–4546, https://doi.org/10.1007/s10750-022-05063-9.

[17] A.J. Moyano-Salcedo, F.D. Cuadros-Segura, A.M. Pabon Laverde, J.V. Trujillo Arias, Environmental impact of sewage discharge into illegal urban agglomerates in Villavicencio, Colombia, Tecnura 25 (2021) 43–62, https://doi.org/10.14483/22487638.16273.

[18] N. Singh, T. Poonia, S.S. Siwal, A.L. Srivastav, H.K. Sharma, S.K. Mittal, Challenges of Water Contamination in Urban Areas, 2022, pp. 173–202, https://doi.org/10.1016/b978-0-323-91838-1.00008-7.

[19] C.M. Maas, S.S. Kaushal, M.A. Rippy, P.M. Mayer, S.B. Grant, R.R. Shatkay, J. T. Malin, S.V. Bhide, P. Vikesland, L. Krauss, J.E. Reimer, A.M. Yaculak, Freshwater salinization syndrome limits management efforts to improve water quality, Front. Environ. Sci. 11 (2023), https://doi.org/10.3389/fenvs.2023.1106581.

[20] S.S. Kaushal, J.E. Reimer, P.M. Mayer, R.R. Shatkay, C.M. Maas, W.D. Nguyen, W. L. Boger, A.M. Yaculak, T.R. Doody, M.J. Pennino, N.W. Bailey, J.G. Galella, A. Weingrad, D.C. Collison, K.L. Wood, S. Haq, T.A. Newcomer-Johnson, S. Duan, K.T. Belt, Freshwater salinization syndrome alters retention and release of chemical cocktails along flowpaths: from stormwater management to urban streams, Freshw. Sci. 41 (2022) 420–441, https://doi.org/10.1086/721469.

[21] S. Linke, B. Lehner, C. Ouellet Dallaire, J. Ariwi, G. Grill, M. Anand, P. Beames, V. Burchard-Levine, S. Maxwell, H. Moidu, F. Tan, M. Thieme, Global hydro-environmental sub-basin and river reach characteristics at high spatial resolution, Sci. Data 6 (2019), https://doi.org/10.1038/s41597-019-0300-6.

[22] V.R. Kelly, G.M. Lovett, K.C. Weathers, S.E.G. Findlay, D.L. Strayer, D.J. Burns, G. E. Likens, Long-term sodium chloride retention in a rural watershed: legacy effects of road salt on streamwater concentration, Environ. Sci. Technol. 42 (2008) 410–415, https://doi.org/10.1021/es071391l.

[23] A. Venkatesan, P.C. Wankat, Simulation of ion exchange water softening pretreatment for reverse osmosis desalination of brackish water, Desalination 271 (2011) 122–131, https://doi.org/10.1016/j.desal.2010.12.022.

[24] M. Berde, D. Jolis, Effect of saltwater intrusion on activated sludge flocculation, Water Environ. Res. 93 (2021) 750–761, https://doi.org/10.1002/wer.1455.

[25] A. Egea-Corbacho, P. Romero-Pareja, C. Aragón Cruz, C. Pavón, M.D. Coello, Effect of seawater intrusion using real wastewater on an attached biomass system operating a nitrogen and phosphorus removal process, J. Environ. Chem. Eng. 9 (2021), https://doi.org/10.1016/j.jece.2020.104927.

[26] S. Begmatov, A.G. Dorofeev, V.V. Kadnikov, A.V. Beletsky, N.V. Pimenov, N. V. Ravin, A.V. Mardanov, The structure of microbial communities of activated sludge of large-scale wastewater treatment plants in the city of Moscow, Sci. Rep. 12 (2022), https://doi.org/10.1038/s41598-022-07132-4.

[27] S. Sivaprakasam, S. Mahadevan, S. Sekar, S. Rajakumar, Biological treatment of tannery wastewater by using salt-tolerant bacterial strains, Microb. Cell Factories 7 (2008), https://doi.org/10.1186/1475-2859-7-15.

[28] Z. Wang, M.C.M. van Loosdrecht, P.E. Saikaly, Gradual adaptation to salt and dissolved oxygen: strategies to minimize adverse effect of salinity on aerobic granular sludge, Water Res. 124 (2017) 702–712, https://doi.org/10.1016/j.watres.2017.08.026.

[29] M. Hou, W. Li, H. Li, C. Li, X. Wu, Y. di Liu, Performance and bacterial characteristics of aerobic granular sludge in response to alternating salinity, Int. Biodeterior. Biodegradation 142 (2019) 211–217, https://doi.org/10.1016/j.ibiod.2019.05.007.

[30] S. Navada, O. Vadstein, Salinity acclimation strategies in nitrifying bioreactors, Front. Mar. Sci. 9 (2022), https://doi.org/10.3389/fmars.2022.867592.

[31] J. Honey-Rosés, D.W. Schneider, N. Brozović, Changing ecosystem service values following technological change, Environ. Manag. 53 (2014) 1146–1157, https://doi.org/10.1007/s00267-014-0270-6.

[32] L. Malaeb, G.M. Ayoub, Reverse osmosis technology for water treatment: state of the art review, Desalination 267 (2011) 1–8, https://doi.org/10.1016/j.desal.2010.09.001.

[33] A. Pérez-González, A.M. Urtiaga, R. Ibáñez, I. Ortiz, State of the art and review on the treatment technologies of water reverse osmosis concentrates, Water Res. 46 (2012) 267–283, https://doi.org/10.1016/j.watres.2011.10.046.

[34] A.J. Salcedo Moyano, T.P. Delforno, E.L. Subtil, Simultaneous nitrification-denitrification (SND) using a thermoplastic gel as support: pollutants removal and microbial community in a pilot-scale biofilm membrane bioreactor, Environ. Technol. (United Kingdom) 43 (2022) 4411–4425, https://doi.org/10.1080/09593330.2021.1950843.

[35] M. Sheikh, H.R. Harami, M. Rezakazemi, J.L. Cortina, T.M. Aminabhavi, C. Valderrama, Towards a sustainable transformation of municipal wastewater treatment plants into biofactories using advanced NH3-N recovery technologies: a review, Sci. Total Environ. 904 (2023), https://doi.org/10.1016/j.scitotenv.2023.166077.

[36] P. Madoni, Protozoa in wastewater treatment processes: a minireview, Ital. J. Zool. 78 (2011) 3–11, https://doi.org/10.1080/11250000903373797.

[37] D. Chen, L. Zhao, Z. Wang, Y. Li, Y. Li, M. Yin, X. Wang, Y. Yang, Successional dynamics of low C/N activated sludge system under salinity shock: performance, nitrogen removal pathways, microbial community, and assembly, Chemosphere 307 (2022), https://doi.org/10.1016/j.chemosphere.2022.135703.

[38] M.S. Moussa, D.U. Sumanasekera, S.H. Ibrahim, H.J. Lubberding, C. M. Hooijmans, H.J. Gijzen, M.C.M. Van Loosdrecht, Long term effects of salt on activity, population structure and floc characteristics in enriched bacterial cultures of nitrifiers, Water Res. 40 (2006) 1377–1388, https://doi.org/10.1016/j.watres.2006.01.029.

[39] S.S.S. Sarma, B. Elguea-Sánchez, S. Nandini, Effect of Salinity on Competition between the Rotifers Brachionus Rotundiformis Tschugunoff and *Hexarthra jenkinae* (De Beauchamp) (Rotifera), 2002.

[40] J.P. Bassin, R. Kleerebezem, G. Muyzer, A.S. Rosado, M.C.M. Van Loosdrecht, M. Dezotti, Effect of different salt adaptation strategies on the microbial diversity, activity, and settling of nitrifying sludge in sequencing batch reactors, Appl. Microbiol. Biotechnol. 93 (2012) 1281–1294, https://doi.org/10.1007/s00253-011-3428-7.

[41] W. Pauli, K. Jax, S. Berger, Protozoa in wastewater treatment: function and importance, in: The Handbook of Environmental Chemistry, Berlin, 2001, pp. 205–251.

[42] J. Julia, C. Yossef, de L. Marina, K. Ariel, J. Edouard, C. Antonis, Multiple micro-predators controlling bacterial communities in the environment, Curr. Opin. Biotechnol. 27 (2014) 185–190, https://doi.org/10.1016/j.copbio.2014.02.003.

[43] G.F. Wells, C.H. Wu, Y.M. Piceno, B. Eggleston, E.L. Brodie, T.Z. DeSantis, G. L. Andersen, T.C. Hazen, C.A. Francis, C.S. Criddle, Microbial biogeography across a full-scale wastewater treatment plant transect: evidence for immigration between coupled processes, Appl. Microbiol. Biotechnol. 98 (2014) 4723–4736, https://doi.org/10.1007/s00253-014-5564-3.

[44] S.F. Corsino, M. Capodici, M. Torregrossa, G. Viviani, A comprehensive comparison between halophilic granular and flocculent sludge in withstanding short and long-term salinity fluctuations, J. Water Process Eng. 22 (2018) 265–275, https://doi.org/10.1016/j.jwpe.2018.02.013.

[45] Y. Xia, X. Wen, B. Zhang, Y. Yang, Diversity and assembly patterns of activated sludge microbial communities: a review, Biotechnol. Adv. 36 (2018) 1038–1047, https://doi.org/10.1016/j.biotechadv.2018.03.005.

[46] C. Sun, B. Zhang, D. Ning, Y. Zhang, T. Dai, L. Wu, T. Li, W. Liu, J. Zhou, X. Wen, Seasonal dynamics of the microbial community in two full-scale wastewater treatment plants: diversity, composition, phylogenetic group based assembly and co-occurrence pattern, Water Res. 200 (2021), https://doi.org/10.1016/j.watres.2021.117295.

[47] M. Peces, G. Dottorini, M. Nierychlo, K.S. Andersen, M.K.D. Dueholm, P. H. Nielsen, Microbial communities across activated sludge plants show recurring species-level seasonal patterns, ISME Commun. 2 (2022), https://doi.org/10.1038/s43705-022-00098-4.

[48] A.A. Al Ali, V. Naddeo, S.W. Hasan, A.F. Yousef, Correlation between bacterial community structure and performance efficiency of a full-scale wastewater treatment plant, J. Water Process. Eng. 37 (2020), https://doi.org/10.1016/j.jwpe.2020.101472.

[49] J.-L. Wang, X.-M. Zhan, Y.-C. Feng, Y.I. Qian, Effect of salinity variations on the performance of activated sludge system, Biomed. Environ. Sci. 18 (2005) 5–8 (PMID: 15861771).

[50] G. Wu, Y. Guan, X. Zhan, Effect of salinity on the activity, settling and microbial community of activated sludge in sequencing batch reactors treating synthetic saline wastewater, Water Sci. Technol. 58 (2008) 351–358, https://doi.org/10.2166/wst.2008.675.

[51] S. Aslan, E. Simsek, Influence of salinity on partial nitrification in a submerged biofilter, Bioresour. Technol. 118 (2012) 24–29, https://doi.org/10.1016/j.biortech.2012.05.057.

[52] M. Pernetti, L. Di Palma, Experimental evaluation of inhibition effects of saline wastewater on activated sludge, Environ. Technol. 26 (2005) 695–704, https://doi.org/10.1080/09593330.2001.9619509.

[53] M. Ji, W. Kong, L. Yue, J. Wang, Y. Deng, L. Zhu, Salinity reduces bacterial diversity, but increases network complexity in Tibetan Plateau lakes, FEMS Microbiol. Ecol. 95 (2019), https://doi.org/10.1093/femsec/fiz190.

[54] Y. Li, J. Jiang, Y. Chen, W. Qie, W. Zhu, N. Xu, J. Zhao, Effects of salinity on the performance, microbial community, and functional genes among 4-chlorophenol wastewater treatment, Bioresour. Technol. 384 (2023), https://doi.org/10.1016/j.biortech.2023.129282.

[55] C. Li, Y. Li, X. Li, L. Ma, Y. Xiao, C. Zhang, Differential responses of plant primary productivity to nutrient addition in natural and restored alpine grasslands in the Qinghai Lake Basin, Front. Plant Sci. 12 (2021), https://doi.org/10.3389/fpls.2021.792123.

[56] Y. Zhang, M. Kuroda, S. Arai, F. Kato, D. Inoue, M. Ike, Biological treatment of selenate-containing saline wastewater by activated sludge under oxygen-limiting conditions, Water Res. 154 (2019) 327–335, https://doi.org/10.1016/j.watres.2019.01.059.

[57] M.F. Hamoda, I.M.S. Al-attar, Effects of hihg sodium chloride concentrations on activated sludge treatment, Water Sci. Technol. 31 (1995) 61–72, https://doi.org/10.1016/0273-1223(95)00407-E.

[58] A. Figler, V. B-Béres, D. Dobronoki, K. Márton, S.A. Nagy, I. Bácsi, Salt tolerance and desalination abilities of nine common green microalgae isolates, Water (Switzerland) 11 (2019), https://doi.org/10.3390/w11122527.

[59] H. Chen, Y. Wang, Z. Chen, Z. Wu, X. Chu, S. Qing, L. Xu, K. Yang, Q. Meng, H. Cheng, W. Zhan, Y. Wang, H. Zhou, Effects of salinity on anoxic–oxic system performance, microbial community dynamics and co-occurrence network during treating wastewater, Chem. Eng. J. 461 (2023), https://doi.org/10.1016/j.cej.2023.141969.

[60] J. Wang, Q. Liu, B. Wu, H. Hu, D. Dong, J. Yin, H. Ren, Effect of salinity on mature wastewater treatment biofilm microbial community assembly and metabolite characteristics, Sci. Total Environ. 711 (2020), https://doi.org/10.1016/j.scitotenv.2019.134437.

[61] Y.J. Wu, L.M. Whang, T. Fukushima, S.H. Chang, Responses of ammonia-oxidizing archaeal and betaproteobacterial populations to wastewater salinity in a full-scale municipal wastewater treatment plant, J. Biosci. Bioeng. 115 (2013) 424–432, https://doi.org/10.1016/j.jbiosc.2012.11.005.

[62] C.R. Curds, A. Cockburn, Protozoa in biological sewage-treatment processes-i. A survey of the protozoan fauna of british percolating filters and activated-sludge plants, Water Res. 4 (1970) 225–236, https://doi.org/10.1016/0043-1354(70)90069-2.

[63] H. Salvado, M.P. Gracia, J.M. Amigo, Capability of ciliated protozoa as indicators of effluent quality in activated sludge plants, Water Res. 29 (1995) 1041–1050, https://doi.org/10.1016/0043-1354(94)00258-9.

[64] M. Martin-Cereceda, S. Serrano, A. Guinea, A Comparative Study of Ciliated protozoa Communities in Activated-Sludge Plants, 1996.

[65] H. Salvadó, O. Canals, B. Pérez-Uz, L. Arregui, S. Serrano, Deactivation of internal recirculation in a full-scale Biological Nutrient Removal (BNR) Wastewater Treatment Plant (WWTP) reveals outstanding microeukaryotic bioindicators, J. Water Process Eng. 57 (2024), https://doi.org/10.1016/j.jwpe.2023.104669.

[66] M. Martfn-Cereceda, S. Serrano, A. Guinea, Occurrence of Acineria Uncinata in Activated Sludge Plants: Morphology and Relationship with Physico-Chemical Plant Parameters, 1995.

[67] Generalitat de Catalonya, L'Agència Catalana de l'Aigua, The Catalan Water Agency, 2023, pp. 1–13.

[68] R. Baird, A.D. Eaton, E.W. Rice, L. Bridgewater, American Public Health Association, American Water Works Association, Water Environment Federation, Standard Methods for the Examination of Water and Wastewater, American Public Health Association, American Water Works Association, Water Environment Federation, Wash. D.C., 2017, https://doi.org/10.2105/SMWW.2882.

[69] H. Abdi, Coefficient of Variation, University of Texas at Dallas Ed, 2010, pp. 1–5.

[70] H. Salvadó, Improvement of the intersection method for the quantification of filamentous organisms: basis and practice for bulking and foaming bioindication purposes, Water Sci. Technol. 74 (2016) 1274–1282, https://doi.org/10.2166/wst.2016.302.

[71] P. Madoni, A sludge biotic index (SBI) for the evaluation of the biological performance of activated sludge plants based on the microfauna analysis, Water Res. 28 (1994) 67–75, https://doi.org/10.1016/0043-1354(94)90120-1.

[72] Dick H. Eikelboom, Process Control of Activated Sludge Plants by Microscopic Investigation, 1st ed., IWA, UK, 2000.

[73] D. Jenkins, M.G. Richard, G.T. Daigger, D. Jenkins, Manual on the Causes and Control of Activated Sludge Bulking, Foaming, and Other Solids Separation Problems, Lewis Publishers, 2004.

[74] W. Foissner, H. Berger, H. Blatterer, F. Kohmann, Taxonomische und ökologische Revision der Ciliaten des Saprobien systems – Band IV: Gymnostomatea, Loxodes, Suctoria. Informations berichte des Bayer, Bayerisches Landesamt für Wasserwirtschaft, 1995.

[75] D. Fernández-Galiano, The ammoniacal silver carbonate method as a general procedure in the study of protozoa from sewage (and other) waters, Water Res. 28 (1994) 495–496, https://doi.org/10.1016/0043-1354(94)90288-7.

[76] B. Klein, Über eine neue Eigentümlichkeit der Pellicula von Chilodon uncinatus, 1926.

[77] W. Foissner, N. Blake, K. Wolf, H.-W. Breiner, T. Stoeck, Morphological and molecular characterization of some peritrichs (Ciliophora: Peritrichida) from tank bromeliads, including two new genera: Orborhabdostyla and vorticellides, Acta Protozool. 48 (2009) 291–319.

[78] A. Jeuck, H. Arndt, A short guide to common heterotrophic flagellates of freshwater habitats based on the morphology of living organisms, Protist 164 (2013) 842–860, https://doi.org/10.1016/j.protis.2013.08.003.

[79] J.J. Lee, S.H. Seymour, H. Hutner, E.C. Bovee, An Illustrated Guide to the Protozoa, Society of Protozoologists, 1985.

[80] S.M. Adl, D. Bass, C.E. Lane, J. Lukeš, C.L. Schoch, A. Smirnov, S. Agatha, C. Berney, M.W. Brown, F. Burki, P. Cárdenas, I. Čepička, L. Chistyakova, J. del Campo, M. Dunthorn, B. Edvardsen, Y. Eglit, L. Guillou, V. Hampl, A.A. Heiss, M. Hoppenrath, T.Y. James, A. Karnkowska, S. Karpov, E. Kim, M. Kolisko, A. Kudryavtsev, D.J.G. Lahr, E. Lara, L. Le Gall, D.H. Lynn, D.G. Mann, R. Massana, E.A.D. Mitchell, C. Morrow, J.S. Park, J.W. Pawlowski, M.J. Powell, D.J. Richter, S. Rueckert, L. Shadwick, S. Shimano, F.W. Spiegel, G. Torruella, N. Youssef, V. Zlatogursky, Q. Zhang, Revisions to the classification, nomenclature, and diversity of eukaryotes, J. Eukaryot. Microbiol. 66 (2019) 4–119, https://doi.org/10.1111/jeu.12691.

[81] R. Margalef, Diversidad de especies en las comunidades naturales, P. Inst. Biol. Apl. IX (1951) 5–27.

[82] C. Heip, A new index measuring evenness, J. Mar. Biol. Assoc. U. K. 54 (1974) 555–557, https://doi.org/10.1017/S0025315400022736.

[83] R Core Team, R: a language and environment for statistical computing, in: R Foundation for Statistical Computing, 2023, pp. 1–50. https://www.R-project.org/.

[84] S. Muff, E.B. Nilsen, R.B. O'Hara, C.R. Nater, Rewriting results sections in the language of evidence, Trends Ecol. Evol. 37 (2022) 203–210, https://doi.org/10.1016/j.tree.2021.10.009.

[85] D. Bates, M. Mächler, B.M. Bolker, S.C. Walker, Fitting linear mixed-effects models using lme4, J. Stat. Softw. 67 (2015), https://doi.org/10.18637/jss.v067.i01.

[86] J. Oksanen, R. Kindt, G.L. Simpson, The vegan package. http://cran.r-project.org/, 2009.

[87] P. Schober, L.A. Schwarte, Correlation coefficients: appropriate use and interpretation, Anesth. Analg. 126 (2018) 1763–1768, https://doi.org/10.1213/ANE.0000000000002864.

[88] M. Dufrêne, D. Dufrêne, P. Legendre, Species assemblages and indicator species: the need for a flexible asymmetrical approach, Ecol. Monogr. 67 (1997) 345–366, https://doi.org/10.1890/0012-9615(1997)067[0345:SAAIST]2.0.CO;2.

[89] D.W. Roberts, M. David, W. Roberts, Package "labdsv" Title Ordination and Multivariate Analysis for Ecology, 2023.

[90] R.M. O'Brien, A caution regarding rules of thumb for variance inflation factors, Qual. Quant. 41 (2007) 673–690, https://doi.org/10.1007/s11135-006-9018-6.

[91] M.W. Hans Borchers, Title Practical Numerical Math Functions Depends R (>= 3.1.0), 2023.

[92] Y. Rosseel, Journal of Statistical Software lavaan: An R Package for Structural Equation Modeling. http://www.jstatsoft.org/, 2012.

[93] J.B. Grace, Structural equation modeling and natural systems, Cambridge Univ. Press (2006), https://doi.org/10.1017/CBO9780511617799.

[94] R.E.R. Taylor, Interpretation of the correlation coefficient: a basic review, J. Diagnost. Med. Sonogr. (1990) 30–39.

[95] S. Hinck, T.R. Neu, G. Lavik, M. Mussmann, D. De Beer, H.M. Jonkers, Physiological adaptation of a nitrate-storing Beggiatoa sp. to diel cycling in a phototrophic hypersaline mat, Appl. Environ. Microbiol. 73 (2007) 7013–7022, https://doi.org/10.1128/AEM.00548-07.

[96] C. Wylezich, S.A. Karpov, A.P. Mylnikov, R. Anderson, K. Jürgens, Ecologically Relevant Choanoflagellates Collected from Hypoxic Water Masses of the Baltic Sea Have Untypical Mitochondrial Cristae. http://www.biomedcentral.com/1471-2180/12/271, 2012.

[97] S. Schiwitza, H. Arndt, F. Nitsche, Four new choanoflagellate species from extreme saline environments: indication for isolation-driven speciation exemplified by highly adapted Craspedida from salt flats in the Atacama Desert (Northern Chile), Eur. J. Protistol. 66 (2018) 86–96, https://doi.org/10.1016/j.ejop.2018.08.001.

[98] S. Schiwitza, H. Arndt, F. Nitsche, First description of an euryoecious acanthoecid choanoflagellate species, Enibas tolerabilis gen. et sp. nov. from a salar in the Chilean Andes based on morphological and transcriptomic data, Eur. J. Protistol. 67 (2019) 106–113, https://doi.org/10.1016/j.ejop.2018.11.004.

[99] S. Schiwitza, L. Gutsche, E. Freches, H. Arndt, F. Nitsche, Extended divergence estimates and species descriptions of new craspedid choanoflagellates from the Atacama Desert, northern Chile, Eur. J. Protistol. 79 (2021), https://doi.org/10.1016/j.ejop.2021.125798.

[100] D.C. Nelson, N.P. Revsbech, B.O. Barker, Microoxic-Anoxic Niche of Beggiatoa spp.: Microelectrode Survey of Marine and Freshwater Strains. https://journals.asm.org/journal/aem, 1986.

[101] R. Dunker, H. Røy, A. Kamp, B.B. Jørgensen, Motilitypatterns of lamentous sulfur bacteria, Beggiatoa spp, FEMS Microbiol. Ecol. 77 (2011) 176–185, https://doi.org/10.1111/j.1574-6941.2011.01099.x.

[102] H.M. Roe, R.T. Patterson, Arcellacea (testate amoebae) as bio-indicators of road salt contamination in lakes, Microb. Ecol. 68 (2014) 299–313, https://doi.org/10.1007/s00248-014-0408-3.

[103] L.R.P. Utz, D.W. Coats, Spatial and temporal patterns in the occurrence of peritrich ciliates as epibionts on calanoid copepods in the Chesapeake Bay, USA, J. Eukaryot. Microbiol. 52 (2005) 236–244, https://doi.org/10.1111/j.1550-7408.2005.00025.x.

[104] E. Jones, M.T.H. van Vliet, Drought impacts on river salinity in the southern US: implications for water scarcity, Sci. Total Environ. 644 (2018) 844–853, https://doi.org/10.1016/j.scitotenv.2018.06.373.

[105] L. Kachieng'a, M.N.B. Momba, The synergistic effect of a consortium of protozoan isolates (Paramecium sp., Vorticella sp., Epistylis sp. and Opercularia sp.) on the biodegradation of petroleum hydrocarbons in wastewater, J. Environ. Chem. Eng. 6 (2018) 4820–4827, https://doi.org/10.1016/j.jece.2018.07.005.

[106] B.J. Kefford, G.L. Hickey, A. Gasith, E. Ben-David, J.E. Dunlop, C.G. Palmer, K. Allan, S.C. Choy, C. Piscart, Global scale variation in the salinity sensitivity of riverine macroinvertebrates: Eastern Australia, France, Israel and South Africa, PLoS One 7 (2012), https://doi.org/10.1371/journal.pone.0035224.

[107] M. Cañedo-Argüelles, M. Bundschuh, C. Gutiérrez-Cánovas, B.J. Kefford, N. Prat, R. Trobajo, R.B. Schäfer, Effects of repeated salt pulses on ecosystem structure and functions in a stream mesocosm, Sci. Total Environ. 476–477 (2014) 634–642, https://doi.org/10.1016/j.scitotenv.2013.12.067.

[108] A.J. Moyano Salcedo, N. Prat, L. Bertrans-Tubau, M. Piñero-Fernandez, D. Cunillera-Montcusí, J.C. López-Doval, M. Abril, L. Proia, M. Cañedo-Argüelles, What happens when salinization meets eutrophication? A test using stream microcosms, Sci. Total Environ. 912 (2024), https://doi.org/10.1016/j.scitotenv.2023.168824.

[109] E. Berger, O. Frör, R.B. Schäfer, Salinity impacts on river ecosystem processes: a critical mini-review, Philos. Trans. R. Soc. B 374 (2019), https://doi.org/10.1098/rstb.2018.0010.

[110] R.B. Schäfer, M. Bundschuh, D.A. Rouch, E. Szöcs, P.C. von der Ohe, V. Pettigrove, R. Schulz, D. Nugegoda, B.J. Kefford, Effects of pesticide toxicity, salinity and other environmental variables on selected ecosystem functions in streams and the relevance for ecosystem services, Sci. Total Environ. 415 (2012) 69–78, https://doi.org/10.1016/j.scitotenv.2011.05.063.

[111] C. Cortés-Lorenzo, A. González-Martínez, H. Smidt, J. González-López, B. Rodelas, Influence of salinity on fungal communities in a submerged fixed bed bioreactor for wastewater treatment, Chem. Eng. J. 285 (2016) 562–572, https://doi.org/10.1016/j.cej.2015.10.009.

[112] A. Rodriguez-Sanchez, J.C. Leyva-Diaz, B. Muñoz-Palazon, J.M. Poyatos, J. Gonzalez-Lopez, Influence of salinity cycles in bioreactor performance and microbial community structure of membrane-based tidal-like variable salinity wastewater treatment systems, Environ. Sci. Pollut. Res. 26 (2019) 514–527, https://doi.org/10.1007/s11356-018-3608-4.

[113] G.K. Bielmyer, S.J. Klaine, J.R. Tomasso, W.R. Arnold, Changes in water quality after addition of sea salts to fresh water: implications during toxicity testing, Chemosphere 57 (2004) 1707–1711, https://doi.org/10.1016/j.chemosphere.2004.05.040.

[114] T.P. Thuy Pham, C.W. Cho, Y.S. Yun, Environmental fate and toxicity of ionic liquids: a review, Water Res. 44 (2010) 352–372, https://doi.org/10.1016/j.watres.2009.09.030.

[115] E. Bremer, R. Krämer, Responses of Microorganisms to Osmotic Stress, 2019, https://doi.org/10.1146/annurev-micro-020518.

[116] L. Lin, S. Pratt, Z. Li, L. Ye, Adaptation and evolution of freshwater Anammox communities treating saline/brackish wastewater, Water Res. 207 (2021), https://doi.org/10.1016/j.watres.2021.117815.

[117] Y. Le Deng, Y.J. Ruan, S.M. Zhu, X.S. Guo, Z.Y. Han, Z.Y. Ye, G. Liu, M.M. Shi, The impact of do and salinity on microbial community in poly(Butylene succinate) denitrification reactors for recirculating aquaculture system wastewater treatment, AMB Express 7 (2017) 1–11, https://doi.org/10.1186/s13568-017-0412-3.

[118] J. Cao, Q. Zhu, T. Zhang, Y. Wu, Q. Zhang, B. Fu, F. Fang, Q. Feng, J. Luo, Distribution patterns of microbial community and functional characteristics in full-scale wastewater treatment plants: focusing on the influent types, Chemosphere 281 (2021), https://doi.org/10.1016/j.chemosphere.2021.130899.

[119] Z. Feng, T. Li, Y. Lin, G. Wu, Microbial communities and interactions in full-scale A2/O and MBR wastewater treatment plants, J. Water Process Eng. 46 (2022), https://doi.org/10.1016/j.jwpe.2022.102660.

[120] H. He, Y. Chen, X. Li, Y. Cheng, C. Yang, G. Zeng, Influence of salinity on microorganisms in activated sludge processes: a review, Int. Biodeterior. Biodegradation 119 (2017) 520–527, https://doi.org/10.1016/j.ibiod.2016.10.007.

[121] A.V. Mboyi, I. Kamika, M. Momba, The ability of consortium wastewater protozoan and bacterial species to remove COD in the presence of nanomaterials under varying pH conditions, J. Environ. Sci. Health A Tox. Hazard. Subst. Environ. Eng. 52 (2017) 697–709, https://doi.org/10.1080/10934529.2017.1301744.

[122] M. Gad, M. Yosri, M.E. Fawzy, R.M. Moghazy, E.M.S. Elfeky, M.A. Marouf, M. A. El-Khateeb, Microeukaryotic communities diversity with a special emphasis on protozoa taxa in an integrated wastewater treatment system, Environ. Sci. Eur. 36 (2024), https://doi.org/10.1186/s12302-024-00907-8.

[123] J. Puigagut, J. García, H. Salvadó, Microfauna community as an indicator of effluent quality and operational parameters in an activated sludge system for treating piggery wastewater, Water Air Soil Pollut. 203 (2009) 207–216, https://doi.org/10.1007/s11270-009-0004-1.

[124] I.C.V. Siqueira-Castro, J.A. Greinert-Goulart, R. Rossetto, J.R. Guimarães, R.M. B. Franco, Ciliated protozoa community of a combined UASB–activated sludge system in southeastern Brazil, Environ. Sci. Pollut. Res. 23 (2016) 23804–23814, https://doi.org/10.1007/s11356-016-7591-3.

[125] D. Dubber, N.F. Gray, The influence of fundamental design parameters on ciliates community structure in Irish activated sludge systems, Eur. J. Protistol. 47 (2011) 274–286, https://doi.org/10.1016/j.ejop.2011.05.001.

[126] L. Arregui, R. Liébana, P. Calvo, H.A. Pérez-Uz, S. Serrano, Bioindication in activated sludge wastewater treatment plants, in: Cesaro J. Valdez, Enrique M. Maradona (Eds.), Handbook of Wastewater Treatment: Biological Methods, Technology and Environmental Impact, Nova Science Publishers, 2013, pp. 277–291.

[127] J. Tauber, B. Flesch, V. Parravicini, K. Svardal, J. Krampe, Influence of road salt thawing peaks on the inflow composition and activated sludge properties in municipal wastewater treatment, Water Sci. Technol. 84 (2021) 314–322, https://doi.org/10.2166/wst.2021.045.

[128] L. Guo, Y. Xie, W. Sun, Y. Xu, Y. Sun, Research progress of high-salinity wastewater treatment technology, Water (Switzerland) 15 (2023), https://doi.org/10.3390/w15040684.

[129] Y. Cui, H. Su, Y. Chen, Y. Chen, Y. Peng, Mechanism of activated sludge floc disintegration induced by excess addition of NaCl, Clean (Weinh) 43 (2015) 1197–1206, https://doi.org/10.1002/clen.201400219.

[130] B. Bolto, D. Dixon, R. Eldridge, S. King, K. Linge, Removal of Natural Organic Matter by Ion Exchange, 2002.

[131] D.A. Fearing, J. Banks, S. Guyetand, C.M. Eroles, B. Jefferson, D. Wilson, P. Hillis, A.T. Campbell, S.A. Parsons, Combination of ferric and MIEX® for the treatment of a humic rich water, Water Res. 38 (2004) 2551–2558, https://doi.org/10.1016/j.watres.2004.02.020.

[132] H. Humbert, H. Gallard, H. Suty, J.P. Croué, Natural organic matter (NOM) and pesticides removal using a combination of ion exchange resin and powdered activated carbon (PAC), Water Res. 42 (2008) 1635–1643, https://doi.org/10.1016/j.watres.2007.10.012.

[133] H.K. Shon, S. Vigneswaran, S.A. Snyder, Effluent organic matter (EfOM) in wastewater: constituents, effects, and treatment, Crit. Rev. Environ. Sci. Technol. 36 (2006) 327–374, https://doi.org/10.1080/10643380600580011.

[134] M.N. Gatti, F. García-Usach, A. Seco, J. Ferrer, Wastewater COD characterization: analysis of respirometric and physical-chemical methods for determining biodegradable organic matter fractions, J. Chem. Technol. Biotechnol. 85 (2010) 536–544, https://doi.org/10.1002/jctb.2325.

[135] N.H. Tran, H.H. Ngo, T. Urase, K.Y.H. Gin, A critical review on characterization strategies of organic matter for wastewater and water treatment processes, Bioresour. Technol. 193 (2015) 523–533, https://doi.org/10.1016/j.biortech.2015.06.091.

[136] S. Le Bonté, M.N. Pons, O. Potier, P. Rocklin, Relation between conductivity and ion content in urban wastewater, Revue Des Sci. de l'Eau 21 (2008) 429–438, https://doi.org/10.7202/019165ar.

[137] E. Levlin, Conductivity measurements for controlling municipal waste-water treatment, Land Water Resour. Eng. (2007) 51–62.

[138] R. Jarboui, F. Sellami, A. Kharroubi, N. Gharsallah, E. Ammar, Olive mill wastewater stabilization in open-air ponds: impact on clay-sandy soil, Bioresour. Technol. 99 (2008) 7699–7708, https://doi.org/10.1016/j.biortech.2008.01.074.

[139] M. Achak, L. Mandi, N. Ouazzani, Removal of organic pollutants and nutrients from olive mill wastewater by a sand filter, J. Environ. Manag. 90 (2009) 2771–2779, https://doi.org/10.1016/j.jenvman.2009.03.012.

[140] M. Achak, N. Ouazzani, A. Yaacoubi, L. Mandi, Modern olive mill effluent characterization and their treatment by coagulation-floculation using lime and aluminium sulphate, Revue Des Sci. de l'Eau 21 (2008) 53–67, https://doi.org/10.7202/017930ar.

[141] E. Neubacher, M. Prast, E.J. Cleven, U.G. Berninger, Ciliate grazing on Nitrosomonas europaea and Nitrospira moscoviensis: is selectivity a factor for the nitrogen cycle in natural aquatic systems? Hydrobiologia 596 (2008) 241–250, https://doi.org/10.1007/s10750-007-9100-7.

[142] R. Solomon, T. Wein, B. Levy, S. Eshed, R. Dror, V. Reiss, T. Zehavi, O. Furman, I. Mizrahi, E. Jami, Protozoa populations are ecosystem engineers that shape prokaryotic community structure and function of the rumen microbial ecosystem, ISME J. 16 (2022) 1187–1197, https://doi.org/10.1038/s41396-021-01170-y.

[143] M.A. Hummel, M.S. Berry, M.T. Stacey, Sea level rise impacts on wastewater treatment systems along the U.S. coasts, Earths Fut. 6 (2018) 622–633, https://doi.org/10.1002/2017EF000805.

4. OVERALL DISCUSSION

4.1. GlobSalt: A comprehensive global river salinity dataset and its implications for freshwater salinization studies

The first chapter introduces the GlobSalt dataset, which provides a comprehensive overview of river salinity on a global scale. This dataset not only fills spatial gaps in global FS, but also provides high temporal resolution for most of the basins included. Globsalt covers approximately 20% of the rivers worldwide, identifying potential FS hotspots and the temporal variations in salinity and associated ions. This information is highly valuable for conducting further studies on FS dynamics (Linke et al., 2019; Cunillera-Montcusí et al., 2022; Ehalt Macedo et al., 2022). For example, GlobSalt data combined with other global datasets, such as HydroAtlas (Linke et al., 2019), allowed us to evaluate the potential natural and anthropogenic drivers that explain FS on a global scale (Figure 4.1, Figure 4.2). Similarly, in the case of wastewater, by combining GlobSalt with HydroWaste (Ehalt Macedo et al., 2022) and calculating EC upstream and downstream of each available WWTP, preliminary results show a very strong variation (Figure 4.3, Figure 4.4) and increase in EC downstream of the evaluated WWTPs (Figure 4.6). Also, it was possible to distinguish the effect of EC on phytoplankton communities in some U.S. rivers based on the impact of human activities, comparing areas with greater interaction with other pollutants and more pristine areas (Figure 4.5) (WQP, 2018; Linke et al., 2019).

Along this discussion section, I will show the potential of GlobSalt to be used in FS research by relating it the different chapters of the present thesis: Chapter 1: Key drivers of FS: Insights from GlobSalt and HydroAtlas; Chapter 2: Assessing temporal variations in FS influenced by WWTPs using GlobSalt and HydroWaste Data; Chapter 3: Salinity influence on river phytoplankton using WQP and GlobSalt Data; Chapter 4:

Assessment wastewater discharges effect on FS: A Global Approach with HydroWaste and GlobSalt. These are all preliminary results that require further development, but they might help to guide future research efforts. It is also important to note the limitations of GlobSalt in terms of geographic and temporal representativeness, data quality, and observed FS patterns.

Geographic and temporal coverage

Geographic distribution and data density

GlobSalt reveals a skewed geographic distribution of observations, with a strong concentration in North America and Europe. This bias is a common issue in global databases, where more extensively studied regions dominate the available data (Meybeck M., 1987; Hartmann et al., 2014; Thorslund and van Vliet, 2020; Virro et al., 2021). Consequently, this imbalance can obscure or exaggerate global salinity trends, particularly in areas with limited observational data, such as Africa and Asia (Thorslund and van Vliet, 2020; Virro et al., 2021). To address these discrepancies and provide a more accurate understanding of FS, more detailed analyses at the basin level are essential (Kaushal et al., 2018; Cañedo-Argüelles et al., 2019; Cunillera-Montcusí et al., 2022). These discrepancies in the distribution of data across regions can be attributed to several factors. Many countries do not include salinity parameters in their monitoring programs, and some do not make their water quality data publicly available (Gutiérrez-Cánovas et al., 2019; Kelly et al., 2008, 2024). Moreover, the lack of economic and technical resources in certain regions, combined with challenges such as the difficulty of monitoring remote or conflict-prone areas, exacerbates the problem (Cuvelier et al., 2014; Blaen et al., 2016; Stoffels et al., 2024). As a result, despite improvements in data

collection in various regions through GlobSalt, significant information gaps remain globally, particularly in continents such as Asia, Africa, and parts of the Americas.

Country data (Table 2, Chapter 1) indicate a marked difference in data density across regions. For instance, countries such as the U.S. and Germany have a high density of salinity data, facilitating a comprehensive approach to FS (e.g. exploring the interaction between stressors). In contrast, large countries like Russia and Brazil have lower data densities, which may limit our ability to capture natural and anthropogenic gradients. Also, it is important to consider the methodology used to calculate data density relative to the area of each country, which may not be appropriate for all countries worldwide (Richter et al., 1996; Kumar et al., 2024; Messager et al., 2024). For example, there may be significant variability due to differences in country size and number of rivers, leading to proportionality issues. For instance, Australia may have a large amount of data but a low data density if it has fewer rivers or a smaller proportion of riverine area (Musie and Gonfa, 2023; Messager et al., 2024). Conversely, the U.S. might appear to have a higher data density. This is due to its greater number of rivers and comprehensive coverage, as well as a higher number of monitoring stations along individual rivers (McDowell et al., 2024; Vance et al., 2024). Therefore, it is important to analyze each river in as much detail as possible or at a local scale where feasible (Kaushal et al., 2018; Cañedo-Argüelles et al., 2019; Cunillera-Montcusí et al., 2022). This country-based data density indicator can be used as a starting point for interpreting FS in the basins of each country with available data. It is crucial that future studies expand coverage in underrepresented regions to obtain a more accurate picture of global FS patterns (McDowell et al., 2024; Vega et al., 2024).

Despite the spatial limitations of GlobSalt, it is important to note that it was possible to establish ranges and temporal variations of major ions and EC. This allowed

the identification of potential "hot spots" of river salinization, which could be related to human activities (e.g. agriculture, mining) or natural processes. Regions of high salinity such as the Mediterranean, the Midwestern USA, the arid zones of Argentina and Chile, and southwestern Australia are critical areas where the processes (Kaushal, 2016; Cañedo-Argüelles et al., 2012, 2013, 2014, 2016, 2017; Estevéz et al., 2019) and effects of salinization on aquatic ecosystems are stronger (Kefford et al., 2005, 2003; Hassell et al., 2006; Szöcs et al., 2012; Kefford, 2019). Therefore, the vast majority of efforts for understanding of FS have been concentrated in some of these areas (Kaushal et al., 2005, 2024, 2013, 2018; Kefford et al., 2016; Maas et al., 2023; Shelton et al., 2024). However, further studies are needed, not only on riverine ecosystems (e.g. trophic interactions and other salinization-related contaminants), but also on whole ecosystems and the economic (e.g. crop loss, infrastructure damage) and human (e.g. vector proliferation) sectors.

Temporal Coverage

Temporal analysis indicates that EC levels have generally remained stable from 1980 to 2023, with no significant increasing or decreasing trends observed over this period. However, the strongest FS variations were observed at sites with high mean EC, which is expected, as the drivers of salinization fluctuate over time. Temporal stability suggests that there have been no drastic changes in the factors driving FS, such as land use, agricultural practices, or large-scale climate conditions. However, this observation should be taken with caution as it could be explained by insufficient temporal coverage in some basins. It is also possible that most sampling stations in GlobSalt are located on large rivers with high salt dilution capacity, while there is limited data for smaller streams that are more severely affected by salinization (Richter et al., 1996; Kumar et al., 2024; Messager et al., 2024). For example, significant regional changes could be hidden by a

lack of data in certain areas. Also, the lack of temporal variation in the data could also be an artifact of changes in sampling methodology or data frequency (e.g., the number of sampling repetitions per day) (Kumar et al., 2024; Messager et al., 2024). A more detailed analysis of the evolution of measurement techniques and sampling frequency is necessary to confirm the observed temporal stability.

Despite the potential temporal limitations of GlobSalt, it provides valuable interannual data for thousands of rivers worldwide. This brings an opportunity to develop future studies of temporal variations in FS, such as how salinity fluctuations affect aquatic communities (Cañedo-Argüelles et al., 2012; Cunillera-Montcusí et al., 2022). Moreover, with finer temporal resolution (e.g., frequent measurements throughout the day), it may be possible to gain a better understanding of FS patterns and identify "signatures" associated with specific anthropogenic activities.

Data Quality and Validity: Identification and Handling of Erroneous Data

The percentage of potentially erroneous data (35%) highlights the importance of data quality validation. The method of identifying erroneous data by comparing theoretical and empirical ratios could be a suitable alternative, although it is limited by the extreme EC values (Ros Sum, 1946; Lxxen, 1977; McCleskey et al., 2012). Although extreme values (i.e. exceeding EC of 30000 μS cm^{-1}) in saline regions appear to be correct, additional analyses are needed to rule out potential systematic measurement errors (Zander and Kralisch, 2016; Brown et al., 2018). Continued validation and refinement of error detection methods is essential to improve data accuracy (Abrahart and See, 2002; Brown et al., 2018). These extreme EC values, if correct, indicate highly saline conditions, possibly in brackish influenced rivers or coastal regions (Gutiérrez-Cánovas

et al., 2019; Setiawan et al., 2023; Yang and Zhang, 2024). It is critical to validate these data as they may represent unique environments with high natural salinity or areas affected by human activities such as saline wastewater discharges. These values may also have significant ecological implications for local aquatic biodiversity and therefore deserve further attention (2020; Salvadó et al., 2001; Merbt et al., 2015; Pascual-Benito et al., 2020).

Correlation between EC and major ions

The correlation between EC and major ions on a global scale has allowed the identification of the ions that contribute most to FS. GlobSalt allowed the verification and establishment of strong correlations between EC and sodium and chloride ions based on extensive river data. According to GlobSalt, sodium and chloride are the primary ions contributing to spatial variations in EC globally. This may be primarily because these ions are highly soluble in water, are present in many surface rocks, and are the major ions in seawater (contributing to river salinity through atmospheric processes and seawater intrusion). However, in some regions, significantly high concentrations of other ions, such as sulfate or potassium, have also been observed. These elevated concentrations may be attributed to unique geological formations or human activities, such as mining. Finally, several recommendations are proposed to improve the utility of salinity data:

Improve sampling strategies: The salinity observations from GlobSalt highlight the need for sampling approaches tailored to local conditions. Efforts should be made to intensify data collection both spatially (by expanding geographic coverage at the basin scale) and temporally (by increasing measurement frequency) to better capture salinity gradients and temporal variability.

Expand global geographic coverage: It is essential to increase sampling in regions with low data density and to capture a wide range of environmental and climatic gradients to improve the global representativeness of the dataset.

Refine validation methods: Further development of methods for error detection and validation of extreme data points is needed to improve data quality.

Increase analysis of temporal ranges: Additional studies should focus on the temporal evolution of salinity data to identify seasonal trends, such as peaks and fluctuations in salinity levels, as well as any significant shifts that may occur.

Although the GlobSalt dataset provides a valuable foundation for studying river salinity on a global scale, its limitations in geographic coverage and data quality must be recognized. As research progresses, increasing coverage and refining analytical methods will enhance our understanding of patterns and trends in FS.

Key drivers of FS: Insights from GlobSalt and HydroAtlas

To assess the drivers of FS, first, the 260 variables from HydroAtlas, which include both anthropogenic and environmental information for basins worldwide, were integrated with the GlobSalt data (according to the methodology in Chapter 1). Then, Spearman correlations were performed to identify highly correlated variables. Correlation matrices were used to examine pairwise relationships, and variables with correlation coefficients greater than 0.8 were removed to reduce multicollinearity and improve model interpretability (Schober and Schwarte, 2018). As a result, 126 variables were selected from HydroAtlas. After eliminating redundancies and checking data quality, a Random Forest (RF) analysis was performed to evaluate the relative importance of the HydroAtlas drivers in explaining EC from GlobSalt rivers (Ishwaran et al. 2022). This analysis was

performed using the rfsrc function from the randomForestSRC package (Ishwaran et al. 2022). The RF analysis revealed that road density was the most important anthropogenic driver of river salinization, while precipitation and soil water content emerged as important natural determinants (Figure 4.1).

According to the RF analysis, soil water content (35%), precipitation (25%), and road density (12%) together accounted for over 70% of the variation in EC. Therefore, these variables were selected for inclusion in the Generalized Additive Model (GAM) (Simpson, 2021; Wood, 2021). The GAM provided further evidence of a very strong relationship between EC and the variables road density, precipitation, and soil water content (p value < 0.001) (Figure 4.2). The results indicate that variations in road density, precipitation, and soil water content are closely associated with pronounced changes in EC, underscoring the importance of these factors in explaining river salinity.

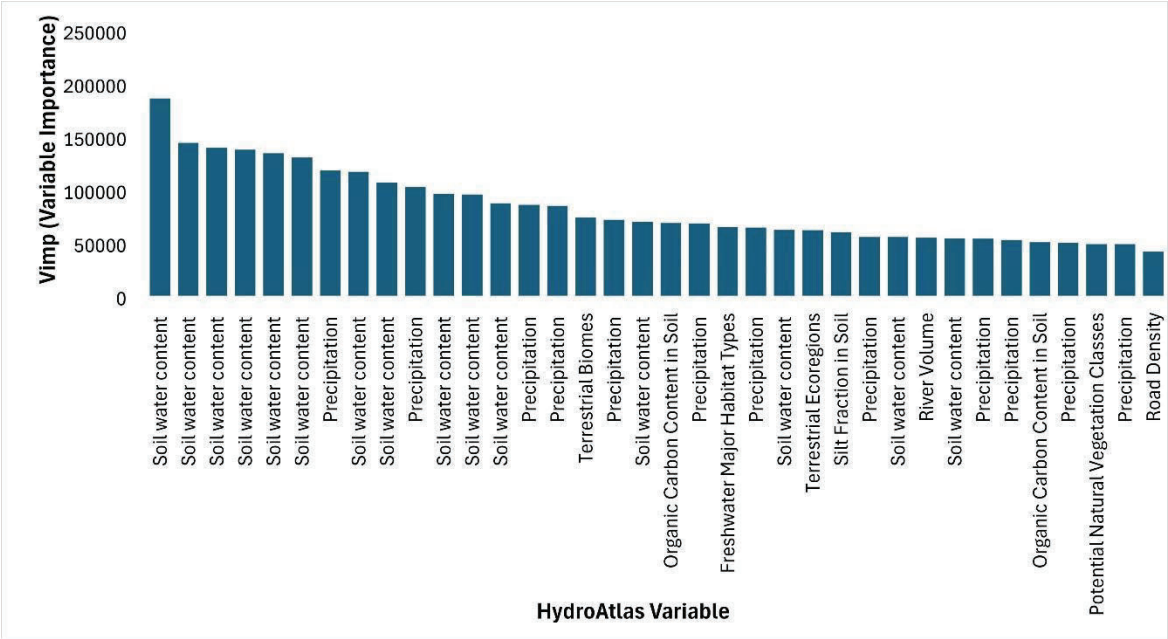


Figure 4. 1. Plot representing the main natural and anthropogenic variables from the HydroAtlas, according to the random forest analysis, that explain the conductivity of rivers included in GlobSalt. *Multiple variants of HydroAtlas variables (e.g., Soil Water Content) are included, defined by temporal scales (monthly averages for January to December or annual averages) and spatial extents (reach catchment or total watershed upstream).

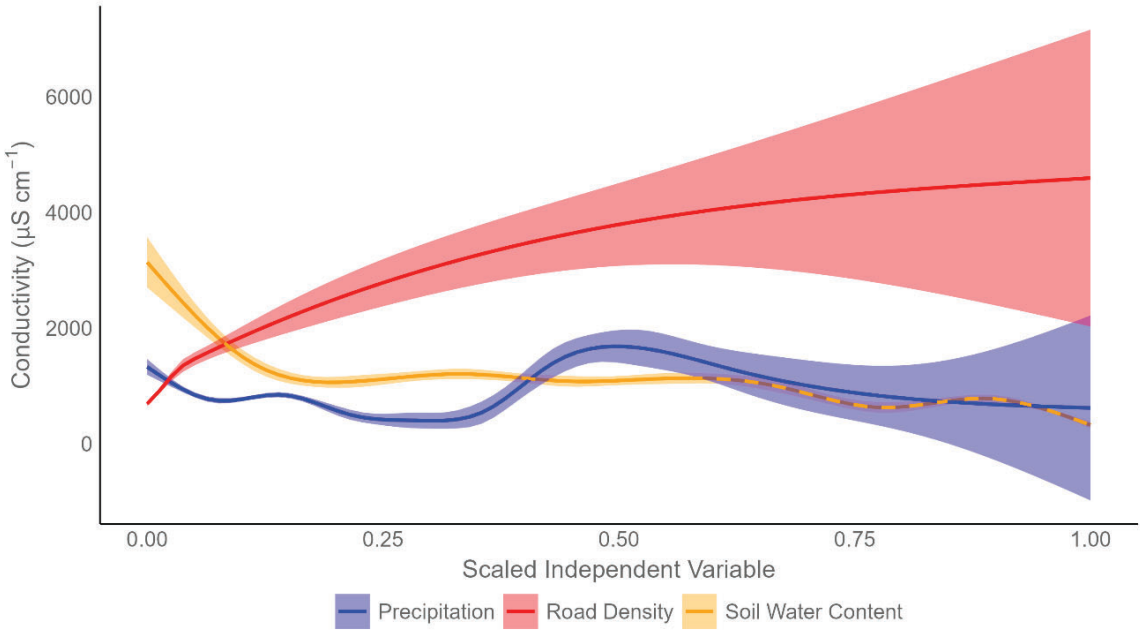


Figure 4. 2. Generalized Additive Model (GAM) plot with smooth terms presenting the relationship of soil water content, precipitation, and road density with conductivity.

The density of roads can serve as an indirect indicator (proxy) of urbanization and the intensity of human activities in a region (Watts et al., 2003; Leu et al., 2008; Meijer et al., 2018). Areas with high road density are typically associated with greater urbanization and higher concentrations of human activities. Such development tends to alter the natural landscape in various ways, affecting hydrology and water quality (Watts et al., 2003; Leu et al., 2008; Meijer et al., 2018). One of the most notable consequences of urbanization and road construction is the increase in impervious surfaces, which hinder water infiltration into the soil and promote greater surface runoff (Meijer et al., 2018; Gramaglia et al., 2024; Tang et al., 2024). This runoff can carry a variety of contaminants, including salts and nutrients, from urban areas (e.g., wastewater discharge), agricultural lands, and mining sites to rivers and streams (Cañedo-Argüelles et al., 2013; S. S. Kaushal et al., 2018). Additionally, the use of salts for road de-icing during winter directly impacts freshwater salinization dynamics. In many regions of the U.S. and Europe, de-icing salts dissolve in rainwater or runoff and are transported to rivers and streams, significantly contributing to freshwater salinization, as several studies have concluded (Ruth, 2003; Asensio et al., 2017; Jackson and Funk, 2019; Niedrist et al., 2021).

Furthermore, in many regions, particularly rural areas with less stringent environmental regulations and waste management controls, roads may be associated with improper disposal of debris and waste (Henry et al., 2006; Meijer et al., 2018; Mihai et al., 2022). The lack of adequate infrastructure (e.g., proper waste collection systems, landfill facilities) and robust waste management policies can lead to the accumulation of waste near roads, which can then be carried away by runoff into rivers (Henry et al., 2006; Meijer et al., 2018). These wastes may contain additional pollutants that exacerbate water salinity and affect the overall quality of the aquatic ecosystem.

Road density also may reflect the co-occurrence or interaction of human activities within a basin (e.g., basins with a higher degree of agriculture, industry or other activities tend to have greater road density) (Meijer et al., 2018; Tang et al., 2024; Zhang et al., 2024). These human activities can have cumulative effects on water quality. Therefore, high road density is associated not only with increased runoff of pollutants but also with changes in land use and resource management practices, which together can exacerbate river salinity (Meijer et al., 2018; Tang et al., 2024). This may explain why variables directly related to agriculture from HydroAtlas (such as crop or pasture density) have not emerged as primary drivers of freshwater salinization in our analysis, as reported in various studies (David et al., 2016; Estévez et al., 2019; Casquin et al., 2020; Liu et al., 2021; Luna Juncal et al., 2023; Thorslund et al., 2021). Instead, road density could serve as a more comprehensive indicator, capturing the combined effects of multiple human activities that alter and disrupt natural salinity dynamics, rather than agriculture alone.

Precipitation plays a critical role in modulating stream EC by influencing salinity concentrations through dilution and runoff processes, especially during extreme events and depending on the natural and anthropogenic characteristics of the watershed (Timpano et al., 2018; Kaushal et al., 2018; Olson, 2019; Ombadi and Varadharajan, 2022; Bolotin et al., 2023; Bolan et al., 2024). For example, in 259 watersheds across the U.S., salinity exhibited significant variability due to flood events caused by heavy precipitation (Ombadi and Varadharajan, 2022). During these floods, stream salinity decreased by up to 100% or increased by up to 34% compared to the long-term mean. Dilution, facilitated by the increase in river flow, was found to be the dominant mechanism that reduced salinity at most sites. However, in 6% of the flood events, other mechanisms caused an increase in salinity (Ombadi and Varadharajan, 2022). This

increase in salinity was related to pre-flood river salinity conditions and site characteristics such as climate, urbanization, and mining. For example, in temperate climates, urbanization increased salinity dilution (i.e., runoff tended to reduce salinity), whereas in arid climates, mining increased salinity (Camarasa-Belmonte, 2016; Ombadi and Varadharajan, 2022). Similarly, the dominant salinity regimes in other watersheds were characterized by an annual peak in summer-fall and a decline in spring, mainly explained by precipitation, stream slope, and soil salinity (Camarasa-Belmonte, 2016; Bolotin et al., 2023). Also, in watersheds affected by mining, salinity showed a minimum in winter and a maximum in late summer. This pattern was strongly responsive to seasonal dilution variations driven by catchment evapotranspiration, geology and terrestrial vegetation (Timpano et al., 2018). This highlights that while increased precipitation generally increases water volume and facilitates salt dilution, it can also increase runoff, which can transport salts from the soil and other sources into the stream (Kaushal et al., 2018; Bolan et al., 2024). Thus, the effect of precipitation on stream salinity depends not only on the dilution capacity and type of runoff, but also on the natural characteristics of each watershed (e.g., geology, soils, climate, vegetation). These natural characteristics can explain up to 78% of the variation in salinity (Olson, 2019).

Soil water content can influence the effects of precipitation on FS and the availability of salts for runoff (Perri et al., 2020; Gavrilescu, 2021; Ramos et al., 2023). High soil water content can amplify the effects of runoff by increasing the volume of water and salts that move from surrounding areas to water bodies (Perri et al., 2020; Ramos et al., 2023; Kaushal et al., 2023). This process is particularly important in regions with intense or frequent rainfall and depends on factors such as soil type (e.g., calcareous or siliceous), infiltration capacity (i.e., when the soil becomes saturated), and the level of

anthropogenic influence or dominant human activities (Perri et al., 2020; Ondrasek and Rengel, 2021; Kaushal et al., 2023). Consequently, both soil water content and precipitation have a significant impact on FS dynamics. Soil water content emerges as a key indicator by modulating the transfer of water and salts to rivers.

Finally, the GAM model provided strong evidence of interactions between road density, precipitation, and soil water content (p-value < 0.001). These interactions suggest co-variation among these drivers, which are crucial for understanding the complex processes influencing FS. For example, the combination of high soil water content or high road density with intense precipitation may exacerbate FS more than any of these factors alone (Kaushal et al., 2023). However, more detailed studies considering the anthropogenic, environmental, and climatic variability of different basins are needed.

4.2. Impact of human activity and environmental variables on temporal variability of conductivity in river ecosystems

In the second chapter, it was possible to separate sites based on the level of anthropization (i.e., anthropized areas versus less anthropized areas) and examine their relationship with variations in EC (Crosa et al., 2006; Puntí et al., 2009; Estévez et al., 2019). Overall, sites with greater intensity of human activities showed greater temporal variation in EC compared to less intervened sites. Although agriculture was the main activity driving the temporal variations in EC, mining, wastewater discharge, and road deicing also appeared as important variables (Le Bonté et al., 2008; Estévez et al., 2019; Liu et al., 2021; Vendrell-Puigmitja et al., 2022). Also, we found that these variations can be partially modulated by natural variables such as precipitation or geology, but in less anthropized areas, they do not represent significant disturbances or fluctuations in river

salinity (Kaushal et al., 2018). In contrast, in areas with multiple human activities, not only was greater variability observed, but factors such as precipitation appeared to amplify this variability (e.g., due to the anthropic salt cycle altering natural salt levels washed into rivers).

One area that warrants further exploration is the concept of ecological resilience in relation to the temporal variability of salinity (Hassell et al., 2006; Kefford et al., 2007; Garrido et al., 2013; Leslie and McCabe, 2013). Ecosystems typically have some capacity to absorb disturbances, but repeated or prolonged exposure to fluctuating salinity levels could reduce this resilience (Hassell et al., 2006; Kefford et al., 2007). Understanding how different ecosystems respond to temporal changes in salinity, particularly in terms of recovery after salinity spikes, could inform more sustainable land and water management practices (Cañedo-Argüelles and Rieradevall, 2009; Niedrist et al., 2021; Cunillera-Montcusí et al., 2022). Additionally, there may be thresholds beyond which ecosystems cannot recover, leading to irreversible damage or regime shifts (Scheffer et al., 2003; Jeppesen et al., 2007).

Furthermore, FS often occurs in tandem with other environmental stressors (e.g., nutrient pollution, climate change) (Tockner et al., 2010; Bremer and Krämer, 2019; Gutiérrez-Cánovas et al., 2019; Velasco et al., 2019), and the interaction between stressors can exacerbate the effects of temporal salinity variability on freshwater ecosystems (Benjankar et al., 2021; Velasco et al., 2019; En Guo et al., 2019). For example, increased temperatures due to climate change could exacerbate the effects of freshwater salinization by altering evaporation rates and reducing the water available for dilution (Velasco et al., 2019; Kaushal et al., 2018; Cunillera-Montcusí et al., 2022). Thus, the effects of salinity fluctuations or peaks on aquatic communities may differ depending

on whether they occur during a wet season or a drought (Kaushal et al., 2018; Kefford et al., 2007). It is important to evaluate salinity fluctuations in conjunction with other stressors throughout the year (Velasco et al., 2019; Bremer and Krämer, 2019; Cañedo-Argüelles, 2021). Therefore, there is a need for long-term, high-resolution monitoring of salinity and related stressor to capture the full extent of FS and its temporal dynamics (Benjankar et al., 2021). Such data could improve the accuracy of predictive models, which are essential for anticipating future changes in salinity under different land-use and climate scenarios (Melesse et al., 2020; Borovskaya et al., 2022). Advanced modeling techniques, incorporating machine learning and big data analytics, could help in identifying patterns and predicting the impacts of FS at both local and global scales (Brocca et al., 2024).

Assessing temporal variations in FS influenced by WWTPs using GlobSalt and HydroWaste data

The global data on WWTPs from HydroWaste, combined with GlobSalt, allowed an exploration of the potential effects of wastewater discharge on temporal variations in river salinity. Table 4.1 provides a summary of the main characteristics resulting from the integration of both datasets, including the maximum, minimum and standard deviation (SD) values of EC. EC data were obtained for over 6,000 WWTPs from HydroWaste associated with rivers from GlobSalt within a 500-meter radius. Data were collected from 35 countries in South America, North America, Europe, Africa, Asia and Oceania. However, 65% of the data comes from the U.S. and 25% from Europe (e.g. Germany 6%, Italy 5%, and France 4%), indicating lower representation from the remaining countries.

Table 4. 1. Attributes, structure and parameter statistics of the GlobSalt and HydroWaste integration. Variable names and descriptions, including reported units, of both databases.

Attribute	**Description**	**Unit**	**Number of total records by attribute**	**Number of sites/WWTP/ countries**	**Maximum, minimum and standard deviation value per water parameter**
HYBAS_ID	Basin ID HydroAtlas	#	759017	-	-
WASTE_ID	WWTP ID HydroWaste	#	759017	6239	-
x	Longitudinal coordinate of sample location	Decimal Degrees	759017	9807	-
y	Latitudinal coordinate of sample location	Decimal Degrees	759017	9807	-
year	Year of the sample in record	yyy	759017	-	-
month	Month of the sample in record	mm	759017	-	-
Station_ID	Sampling river point ID associated with each basin	#	759017	-	-
Country	Geographic location	Name	759017	35	-
Conductivity	Measurement of electrical EC in the surface water	µS cm^{-1} @25C	759017	9807	Max = 19115 Min= 19.6 SD = 1080
Conductivity Upstream WWTPs			374138	4830	Max = 6353 Min= 19.6 SD = 568
Conductivity Downstream WWTPs			384879	4977	Max = 19115 Min= 45.3 SD = 1753

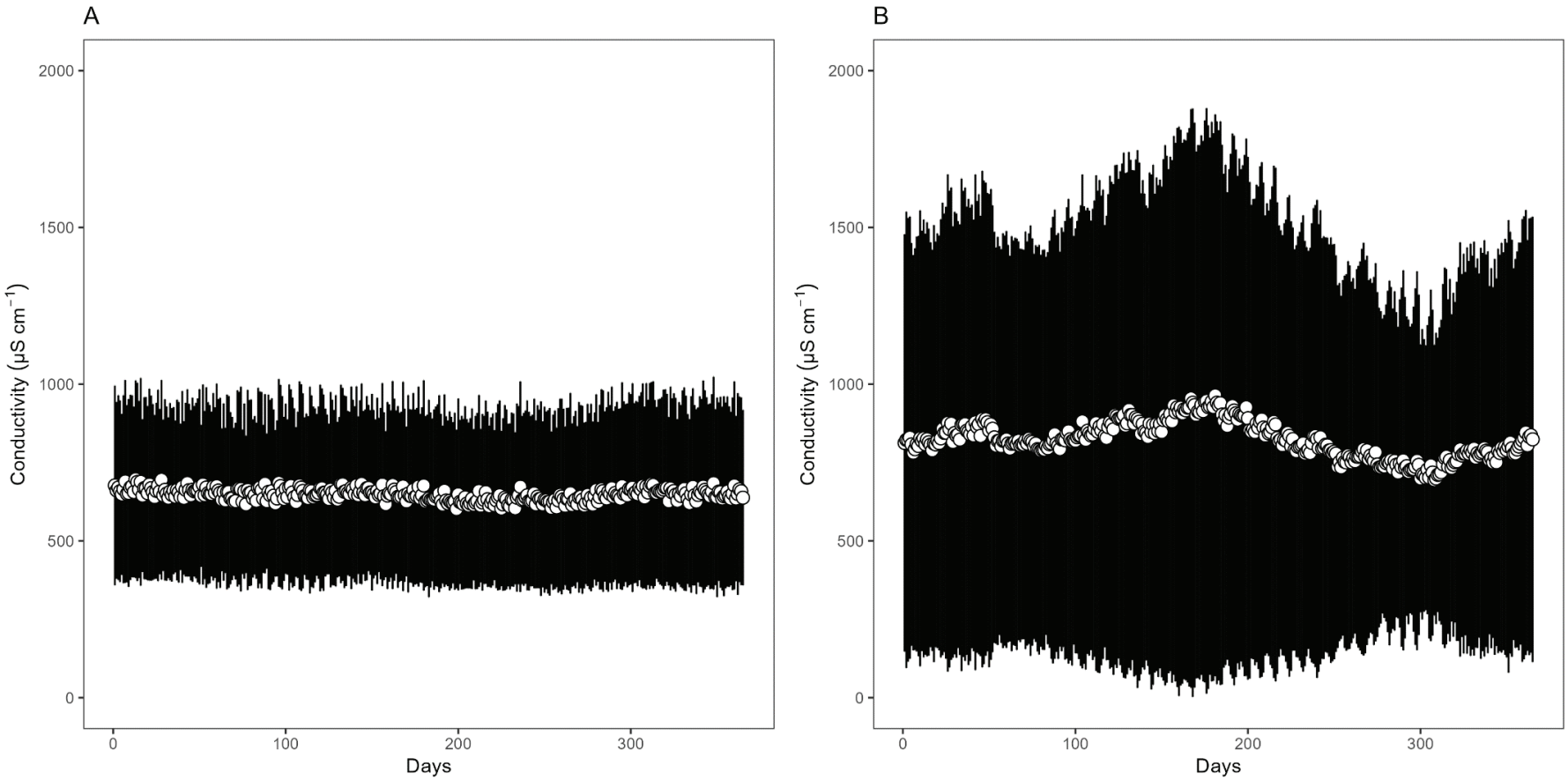


Figure 4. 3. Plot representing the mean value and variability in conductivity of river stations from GlobSalt, both upstream and downstream of WWTPs from HydroWaste. The point represents the mean value, and the irregular line represents the standard deviation. Panel A: river stations upstream of WWTPs; Panel B: river stations downstream of WWTPs.

Linear mixed-effects models (LMER) were used to evaluate the temporal variation of FS associated with interannual variations (i.e., the period from 1980 to 2024) (Bates et al., 2015) (Figure 4.3) in wastewater discharge from WWTPs and across different seasons (i.e., summer, spring, fall, and winter) (Figure 4.4). According to the LMER, the interannual standard deviation changed strongly at upstream river stations compared to downstream sites (p value < 0.05, Figure 4.3). This suggests an increase in variability and peaks in EC at downstream sites (Estévez et al., 2019; Tauber et al., 2021). This dynamic extends seasonally for river sites associated with downstream WWTPs compared to upstream stations (Figure 4.4). Strong differences in EC variability were observed at all downstream sites for each season (p value < 0.05, Figure 4.4). These EC fluctuations were higher compared to upstream sites. Also, consistent with the LMER model results, these variations appeared to be further exacerbated during summer and winter (Bolan et al., 2024; Bolotin et al., 2023; Kaushal et al., 2018; Olson, 2019; Ombadi and Varadharajan, 2022; Timpano et al., 2018) (Figure 4.4). However, no clear pattern was found depending on the time of the year when variation occurs (e.g., specific days of the season). Therefore, contrasting this information with other factors, including local and regional data, other drivers near the evaluated WWTPs, and climatic variables, may further explain these variations (Bolan et al., 2024; Bolotin et al., 2023; Kaushal et al., 2018).

To better understand temporal FS and its impact on aquatic ecosystems, it is crucial to adopt a multidisciplinary and long-term approach. A key strategy would be to establish high-resolution monitoring networks that integrate data on salinity, meteorological conditions, water quality, and other environmental variables (Linke et al., 2019; Lagarias and Stratigea, 2021; Guo et al., 2023). This would allow for a more precise

assessment of how salinity fluctuations interact with other environmental stressors. Moreover, advanced predictive models should be developed that utilize machine learning techniques and big data analytics to identify complex patterns and forecast the impacts of salinization under different land-use and climate scenarios. These models should be continuously validated and adjusted with empirical data to enhance their accuracy and utility (Melesse et al., 2020; Borovskaya et al., 2022; Brocca et al., 2024). Collaboration between scientists, water resource managers, and policymakers is essential to translate these findings into sustainable management practices that minimize the negative impacts of FS.

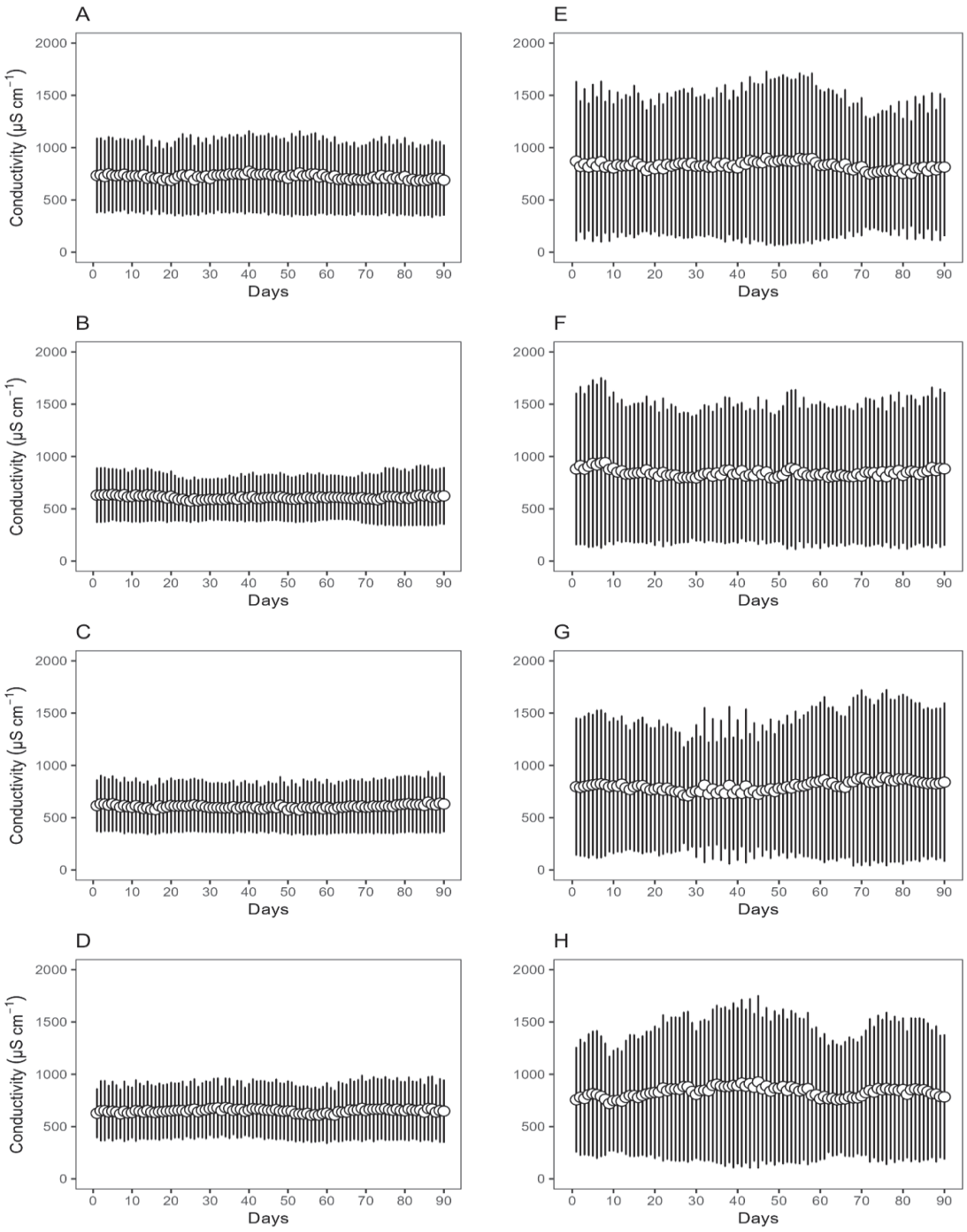


Figure 4. 4. Plot showing the mean value and variability in conductivity at river stations from GlobSalt across different seasons, both upstream and downstream of WWTPs from HydroWaste. Panels A-D display data for upstream stations in Winter (SD: 714 µS cm^{-1}), Spring (SD: 474 µS cm^{-1}), Summer (SD: 506 µS cm^{-1}), and Fall (SD: 552 µS cm^{-1}), respectively. Panels E-H display data for downstream stations in Winter (SD: 1724 µS cm^{-1}), Spring (SD: 1710 µS cm^{-1}), Summer (SD: 1859 µS cm^{-1}), and Fall (SD: 1754 µS cm^{-1}) respectively.

Finally, specific case studies in areas affected by multiple human activities (e.g., wastewater discharges, agriculture, road de-icing), seasonal variations, and extreme events should be conducted to develop mitigation and adaptation strategies that strengthen the resilience of aquatic ecosystems to changes in salinity.

4.3. Responses of aquatic communities to the interactive effects of salinization and nutrient enrichment: Additive and antagonistic effects

In the third chapter, the response of algal and macroinvertebrate communities to the combined effects of salinization and nutrient enrichment was additive to some extent (i.e., each stressor had independent effects on the communities) (Velasco et al., 2019; Greco et al., 2023), but nutrients were observed to ameliorate the effects of salinization (i.e. antagonistic effect), possibly by providing food and energy to the individuals. This response was primarily influenced by both salinization and nutrient levels (i.e., higher concentrations led to greater effects) (Larson and Belovsky, 2013; Greco et al., 2023; Wang et al., 2023). Overall, we found that salinization remains the main driver of toxic effects on aquatic communities and does not interact synergistically with nutrients.

An important aspect to emphasize is that biological information needs to be resolved at the species level to accurately understand the responses of salinization in interaction with other stressors (Munoz and Prat, 1994; Prat and Rieradevall, 2006; Puntí et al., 2009). Furthermore, experimental studies should be conducted under real river conditions and should include not only different species within the food web but also all relevant environmental variables in the study ecosystem (Linke et al., 2019; Cunillera-Montcusí et al., 2022; Ehalt MacEdo et al., 2022). A common limitation, with respect to effects on aquatic communities, remains the challenge of collecting data across different

levels of the food web (e.g., primary, secondary) at a fine scale (e.g., species level) while ensuring the inclusion of necessary anthropogenic and environmental variables for a comprehensive analysis (Linke et al., 2019; Cunillera-Montcusí et al., 2022).

Salinity influence on river phytoplankton using WQP and GlobSalt Data

Using available data from the Water Quality Portal (WQP) in the U.S., it was possible to match suspended phytoplankton concentration data with river data from GlobSalt. A total of 487 data points were collected from 65 river stations in the U.S. (e.g., Grand Calumet, Rock Creek Rivers) for the period between 2018 and 2019. Also, by utilizing variables from HydroAtlas (Human Footprint Index, HFI), rivers with low human intervention (i.e., referred to as "pristine", HFI < 100) were distinguished from rivers with high human impact (i.e., referred to as "impacted", HFI ≥ 101) (Figure 4.5). LMER were used to examine suspended phytoplankton concentration responses to EC in different rivers (Bates et al., 2015). River types were treated as random effects in the models to account for variability. This allowed for the evaluation of the effects of EC on phytoplankton levels across different rivers in the U.S., examining its relationship with salinity and distinguishing locations with potentially higher contaminant interactions, such as nutrients, from those with lower interactions.

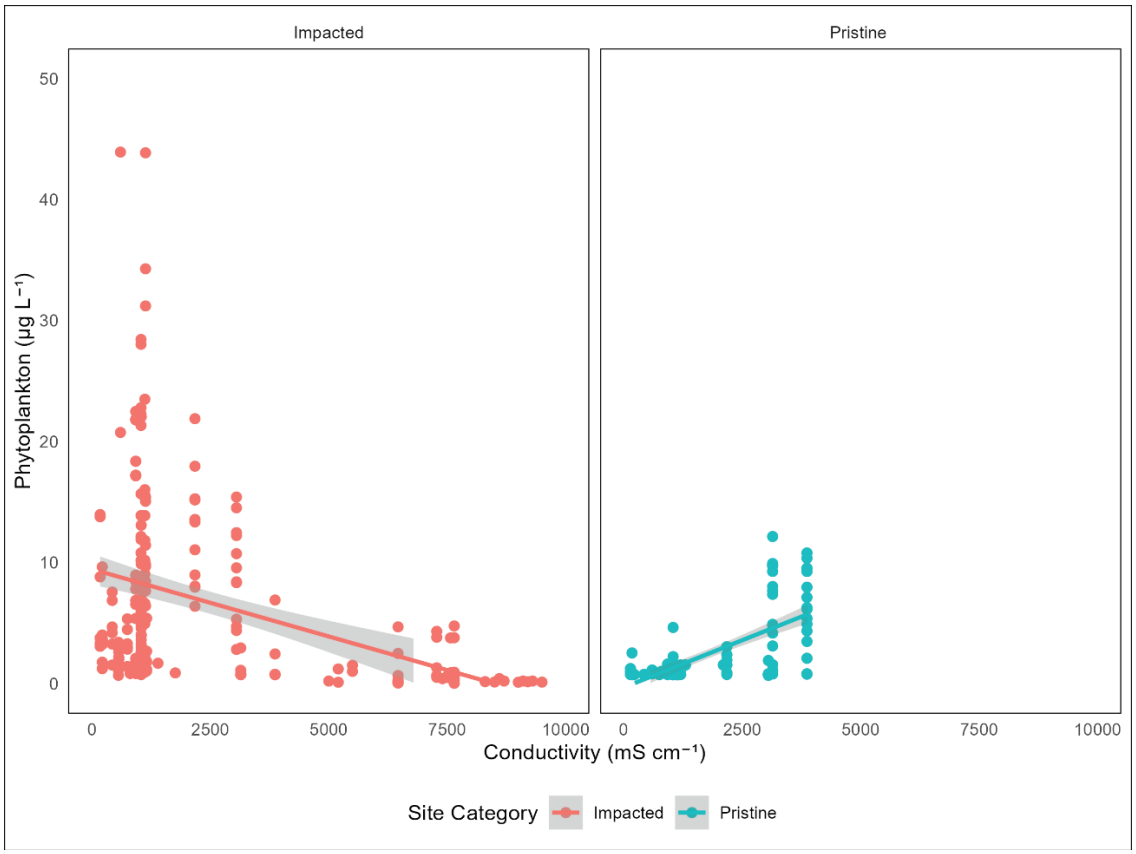


Figure 4. 5. Scatter plot showing the LMER model between phytoplankton and conductivity levels in U.S. rivers. Points and linear regression lines in orange and blue represent impacted and pristine areas, respectively. *Sites were separated based on the Human Footprint variable from HydroATLAS, which ranges from 0 to 500, with 500 indicating the most impacted areas. Sites were classified as "Pristine" with index values < 100, while those with values ≥ 101 were considered "Impacted".

LMER models reveal a complex interaction between EC and phytoplankton concentrations, showing significant differences between pristine and impacted sites ($p < 0.01$). In impacted sites, a strong negative relationship between EC and phytoplankton concentration was observed ($p < 0.01$). This result suggests that EC has a pronounced adverse effect on phytoplankton in these sites. Although nutrient concentration data were not available for the evaluated sites, the Human Footprint Index suggests that nutrient and other pollutant loads are likely high in impacted areas. Even though higher nutrient levels could potentially benefit phytoplankton growth, the strong negative relationship observed between EC and phytoplankton indicates that the negative impacts of high EC outweigh

any potential benefits from increased nutrients (Hintz et al., 2022, 2017; Schuler et al., 2019). Random effects in the LMER model account for variability between sites and show that, even when considering this site-to-site variation, the negative relationship between EC and phytoplankton remains strong in more anthropized sites.

In contrast, the analysis of pristine sites reveals a different relationship between EC and suspended phytoplankton. Although the coefficient for EC is negative, indicating a tendency for phytoplankton to decrease with increasing EC, this effect is considerably weaker and not strong (coefficient: -0.000805, p-value > 0.05). Moreover, the negative effect of EC in pristine sites is countered by a very strong positive interaction (p-value < 0.01), suggesting that in these sites, higher EC levels may have a beneficial effect on suspended phytoplankton (Larson and Belovsky, 2013; Wang et al., 2023; Zadereev et al., 2023). This finding could indicate that pristine ecosystems have higher resilience or adaptation capacity to variations in EC, or that EC in these environments is not associated with the same pollutant loads as in impacted sites. Moreover, it suggests that EC may have a positive effect on ecosystem processes and interactions to a certain extent. However, in pristine sites, increased conductivity likely leads to the loss of large-bodied cladocerans such as Daphnia, which reduces grazing pressure and allows phytoplankton biomass to increase (Hintz et al., 2022). In contrast, in impacted sites, where Daphnia populations are already diminished due to pollution, this grazing effect is less pronounced, and the main observed impact is the toxic effect of salts on the phytoplankton. Further data on phytoplankton community composition would be necessary to fully understand these dynamics.

Overall, these results highlight the importance of considering the environmental context when assessing the effects of EC on phytoplankton and other communities (Hintz

et al., 2017; Schuler et al., 2019). Impacted sites show a stronger response to EC, potentially reflecting higher pollution loads and disturbances in ecological balance, while pristine sites seem to maintain greater stability in their phytoplankton communities despite variations in EC (Lawsona and Jackson, 2021; Bolotin et al., 2023). This difference in responses suggests that water quality management strategies should be tailored to the specific characteristics of each site to mitigate negative impacts on aquatic ecosystems (Olson, 2019; Ombadi and Varadharajan, 2022).

Finally, in addition to the main findings presented in this third chapter, it is crucial to consider how biological community responses may vary over time and across different spatial contexts. Species adaptation to salinity and nutrient conditions could influence their long-term responses, as well as the spatial variability observed within and between rivers. Furthermore, interactions with other pollutants and climate change could significantly alter the observed dynamics, highlighting the need for future research to address these complexities. Similarly, the implications for resource management must be carefully considered, with strategies adapted to mitigate both salinization and eutrophication. Management recommendations should reflect the interaction between these factors and local needs. Finally, future research should delve deeper into these issues and also consider the potential impact on local communities and economic systems related to aquatic resources.

4.4. Disruption of the microbial community and reduced efficiency of pollutant removal due to high conductivity in WWTPs

In the fourth chapter, the effects of EC on microbial communities within WWTPs and the resulting impact on pollutant removal efficiency were examined. The findings indicate that the influence of EC on microbial communities varies significantly

across different WWTPs, with specific taxa showing distinct responses to varying EC levels. Notably, high EC and EC peaks had a pronounced effect on microbial communities, particularly ciliates, which experienced substantial reductions in both abundance and diversity (Salvadó et al., 2001). Furthermore, at such elevated salinity conditions, pollutant removal, particularly the elimination of organic matter and TKN, was strongly reduced (He et al., 2017; Xia et al., 2018). The effects of high EC levels and sudden salinity shocks suggest potential disruptions in both biological interactions and physicochemical processes in WWTPs, highlighting the critical need for managing EC levels to maintain treatment efficacy.

However, extending these findings to different urban scenarios presents challenges. It is crucial to assess these effects across various WWTPs and evaluate the relationships using bioindicators from different trophic levels within the systems (Pérez-Uz et al., 2010; Arregui et al., 2013). Understanding interspecific relationships within these trophic chains is also essential, as reductions in the abundance or loss of certain species can significantly impact the entire food web (Pauli et al., 2001; Julia et al., 2014). Furthermore, analyzing specific microbial groups responsible for contaminant removal, such as those involved in nutrient processing, will provide deeper insights into how EC affects treatment processes (Salvadó et al., 2001, 2024; Neubacher et al., 2008; Li et al., 2019). Also, zoning analyses of WWTPs could help identify the main drivers of salinity entering the plants (Linke et al., 2019; Ehalt MacEdo et al., 2022). For example, although a significant percentage of WWTPs are located in coastal areas (i.e., within approximately 10 km of the ocean, around 20% of plants globally), this issue is not confined to these regions (Newton et al., 2014; Hummel et al., 2018; Ehalt MacEdo et al., 2022). Major cities, in general, contribute more salinity due to higher pollution loads, and areas with

less stringent regulations and high industrial influence can also generate greater ion contributions (Moyano-Salcedo et al., 2021; Ehalt MacEdo et al., 2022; Tariq and Mushtaq, 2023). Future studies should aim to disentangle these complex interactions to better inform management strategies and optimize wastewater treatment performance.

Furthermore, it is essential for treatment plants to adopt advanced monitoring systems that not only measure EC in real time with higher frequency but also include periodic analysis for ion quantification (Malaeb and Ayoub, 2011; Sheikh et al., 2023). In WWTPs where these practices are already in place, it is crucial to evaluate and utilize these parameters for more effective control and monitoring. Understanding ion levels will enable a more accurate comprehension of how salinity interferes with biological communities, physicochemical reactions, and the removal of contaminants such as nutrients (Uygur and Kargi, 2004; Bolto et al., 2002; Li et al., 2022). Integrating this data into the WWTP management system not only improves the ability to anticipate and mitigate adverse effects, but also optimizes overall treatment performance by providing a more comprehensive view of ongoing processes. Furthermore, developing predictive models based on this data could offer new strategies for adjusting operations in real time, adapting processes to variations in salinity load, and improving treatment efficiency (Aghdam et al., 2023).

Sudden peaks in salinity can be difficult to control in some WWTPs, making it important to investigate this area of research more closely (Le Bonté et al., 2008; Tauber et al., 2021). For instance, in coastal regions, such salinity peaks may occur during high tides or at specific times of the year (Berde and Jolis, 2021; Egea-Corbacho et al., 2021; Setiawan et al., 2023). Similarly, in areas with industrial influence, salinity spikes may occur during operational periods when wastewater is discharged into the sewer system

(Lefebvre and Moletta, 2006; Duan et al., 2024). Modeling these events could aid in developing preventive control systems within WWTPs. Moreover, once an EC peak is detected, strategies could be implemented to chemically stabilize these salinity loads or to inoculate microbial communities that can sustain pollutant removal processes, although such measures may be costly and may not be feasible for all WWTPs. Furthermore, the transition and upgrade of primary and secondary treatment plants to advanced systems is an urgent need that requires increased attention and efforts to secure the necessary resources (Malaeb and Ayoub, 2011; Venkatesan and Wankat, 2011; Pérez-González et al., 2012). For example, worldwide it is estimated that 2% of wastewater treatment plants have only primary treatment, while 60% have secondary treatment and the remaining 38% have advanced treatment (Ehalt MacEdo et al., 2022). However, this distribution varies from country to country; for example, in Colombia, only 50% of municipalities have a wastewater treatment plant, and within this coverage, 60% are primary treatment plants, 30% have secondary treatment, and only 10% use advanced treatment (Ehalt MacEdo et al., 2022). Collaborative efforts to advance these technologies and address salinity challenges will be critical to improving the resilience and efficiency of wastewater treatment processes.

Monitoring and managing EC levels in WWTPs, particularly in systems exposed to high EC conditions or saline influent, can not only improve operational performance, but also mitigate the negative effects of wastewater discharges. Observations of low EC removal efficiencies in some WWTPs suggest that conventional systems may not effectively address salinity issues, highlighting the need for tailored management strategies. It is important to note that these systems were not originally designed with salinity effects in mind (i.e. salinity was not considered an environmental issue at the time

of their design, and in many places, it still is not) (Lefebvre and Moletta, 2006; Zimmer et al., 2014; Pereda et al., 2021). Therefore, improving indirect salinity removal processes is critical. WWTPs should be seen as an opportunity to more effectively manage salinity impacts from urban areas to rivers.

Assessment wastewater discharges effect on freshwater salinization: A global approach with HydroWaste and GlobSalt

To assess the increase in salinity associated with WWTPs and the dilution capacity of rivers, the data resulting from the integration of GlobSalt with HydroWaste was used (Table 4.1). LMER were employed to analyze salinity associated with wastewater discharge from WWTPs across different seasons (i.e., summer, spring, autumn, and winter). These models accounted for variability among different river types and evaluated the impact of wastewater discharge on salinity by comparing the EC at sites 500 meters upstream and downstream of each WWTP.

Overall, the LMER model showed very strong differences in EC between river stations upstream and downstream of WWTPs in all seasons ($p < 0.05$, Figure 4.5). In particular, mean EC concentrations were higher at downstream sites compared to upstream sites of the WWTPs studied. This effect appeared to be more pronounced during summer, with a moderate to high increase in EC (i.e., an increase in mean EC of 256 µS cm^{-1}), followed by fall and spring (Figure 4.6, Table 4.2). The increase in EC during winter was lower compared to the other seasons (Figure 4.6). This result supports the hypothesis that the effect of treated wastewater on river salinity is amplified during periods of low flow, such as in summer. During these periods, the river reduces its ability to disperse contaminants, leading to a strong increase in salinity downstream of WWTPs (Link et al., 2017; Folegot et al., 2018).

Table 4. 2. Mean, Maximum, and Minimum conductivity values upstream and downstream of WWTPs by Season according to the GlobSalt and HydroWaste integration.

Season	Location	Mean EC	Maximum EC	Minimum EC	EC increase
Winter	Upstream	727	3000	19	101
	Downstream	828	18010	43	
Spring	Upstream	658	2573	42	106
	Downstream	824	17534	56	
Summer	Upstream	606	4120	30	256
	Downstream	862	18870	47	
Fall	Upstream	650	3000	45	179
	Downstream	829	19115	63	

EC = Electrical conductivity µS cm⁻¹

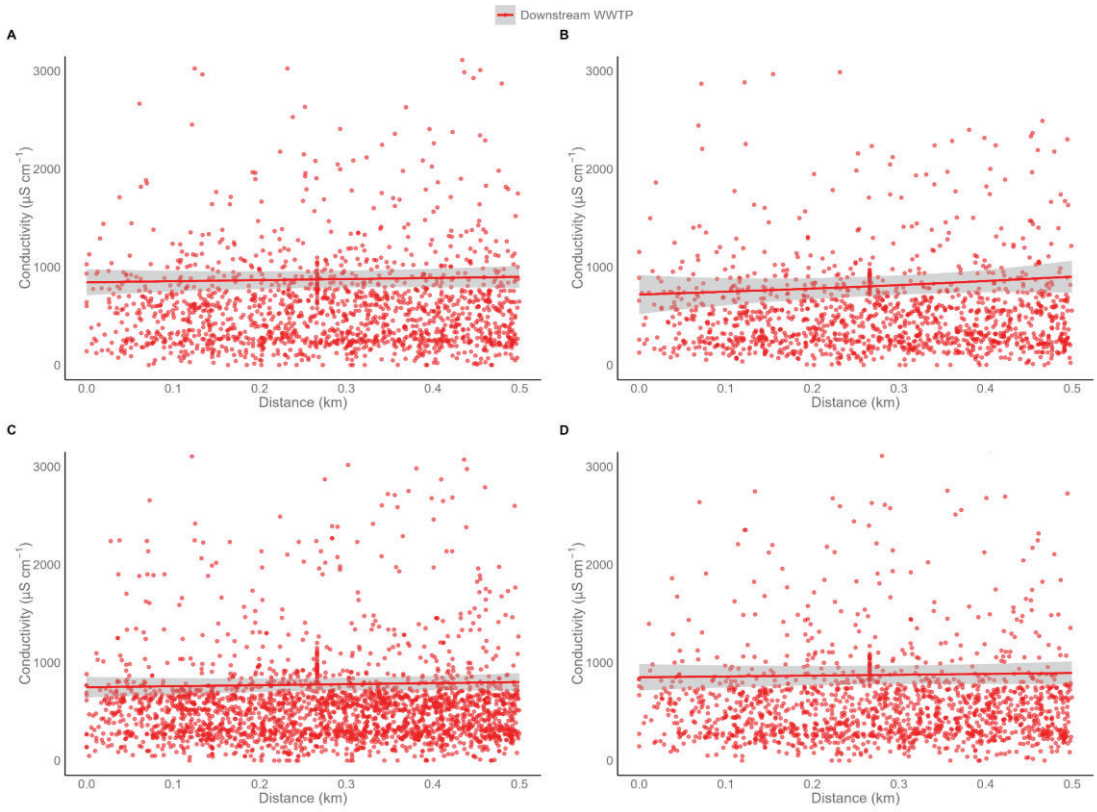


Figure 4. 6. Linear Mixed-Effects Regression (LMER) between conductivity and river station associated with upstream and downstream WWTPs by season. A: Winter, B: Spring, C: Summer, D: Fall.

The increase in EC downstream of WWTPs could be attributed to the limited capacity of some treatment systems to remove ions from wastewater. However, while a clear trend toward increased salinity from WWTP discharges is evident, further research is needed to better understand these dynamics. Preliminary results should be interpreted cautiously. For instance, the analysis included rivers from diverse regions globally, mainly from the U.S. and Europe but also from Africa and South America. This global approach might obscure regional differences due to several factors. For example, certain Mediterranean rivers, such as the Llobregat River in some sections, could have higher baseline EC compared to Canadian rivers (Sabater et al., 1990; Prat and Rieradevall, 2006; Pascual-Benito et al., 2020; Pereda et al., 2021). It is also possible to find rivers more affected by WWTPs with higher salt loads due to larger populations and industries, or proximity to coastal areas (Venâncio et al., 2022; Setiawan et al., 2023; Yang and Zhang, 2024). Another important aspect is that not all WWTPs have the same design, and this can modulate their contribution to FS: advanced treatment plants are expected to be more effective at removing ions compared to conventional treatment plants (Sher et al., 2020; Sheikh et al., 2023). Therefore, an analysis that considers the type of treatment could provide a more detailed understanding of the dynamics between WWTPs and EC. These factors may mask areas where WWTPs have little or no effect on river salinity.

No single trend was observed that applies to all distances in the LMER model for distinguishing the dilution potential of rivers by season. The EC can either increase or decrease with distance depending on the specific distance considered and the river flow influenced by factors such as rainfall events that cause significant fluctuations (Ort and Siegrist, 2009; Link et al., 2017; Turunen et al., 2020). Also, it is possible that some of the EC fluctuations near WWTP discharges may not be associated with them but rather

with illegal discharges or other unexpected sources of pollution (Ort and Siegrist, 2009; Turunen et al., 2020). The results indicate considerable variability in EC as it changes with distance. For an accurate interpretation, it is necessary to conduct independent analyses for each river to visualize the effects of distance on changes in EC. This could allow for the identification of specific patterns or trends.

Moreover, the rivers were not categorized by size (e.g., length, flow, volume), which might mean that the impact of wastewater on smaller rivers is overshadowed by larger rivers (Ort and Siegrist, 2009; Link et al., 2017). It is also important to consider the comparison between permanent and intermittent rivers. In cases like small rivers or intermittent rivers, during drought periods, decreased flow could exacerbate salinity by concentrating the wastewater discharge volumes (Bond et al., 2008; Cooper et al., 2013; Gómez et al., 2017). This potential effect on small and intermittent rivers might not be fully observed if larger rivers have more data, more monitoring stations, and possibly greater resilience to the effects of wastewater discharges (Cooper et al., 2013; Gómez et al., 2017). A notable example is the Mediterranean region, where, during summer, wastewater can represent over 90% of river flow or even the entirety of it in certain rivers (Molinos-Senante et al., 2011; Sebastiá et al., 2013). Considering how climate change might interact with wastewater discharge in the future is a critical point to highlight.

Spatial and Temporal Variability in WWTP Efficiency

In addition to seasonal variations in rivers, the efficiency of WWTPs may vary not only across different regions but also throughout the year. Factors such as plant load capacity (e.g., ion load during summer versus winter) and regular maintenance (e.g., cleaning or purging processes within the WWTP) can influence ion removal efficiency and, consequently, river salinity (Moglia, 2008; Ort and Siegrist, 2009). At the same time,

conducting specific temporal analyses could help identify WWTP efficiency in regions where treatment upgrades and improvements have been implemented. For example, comparing water quality in a region before and after such upgrades could help determine how these efforts have contributed to protecting rivers from salinization.

Interactions with other pollution sources

It is important to note that WWTPs do not operate in isolation and their impact on river salinity can be increased or decreased by the presence of other nearby sources of pollution. Activities such as agriculture or mining, which can release large amounts of salts in a diffuse and uncontrolled manner, may also contribute. In addition, natural processes (e.g., sediment transport, intense precipitation) may increase river salinity in certain regions as the river progresses (Cañedo-Argüelles et al., 2017; Estévez et al., 2019; Turunen et al., 2020; Thorslund et al., 2021).

In areas where human activities coexist with WWTPs, observed river salinity may not solely result from wastewater discharges but from a combination of sources. This could partly explain regional variations in salinity levels and underscores the need for more detailed and specific studies of each WWTP. An integrative approach considering various pollution sources could provide a more accurate picture of the relative role of WWTPs in increasing FS (Cunillera-Montcusí et al., 2022). To achieve this, detailed case studies in areas where such interactions are likely could be valuable. For example, evaluating intensive agricultural or mining regions near WWTPs could help delineate the contributions of each source to FS. This type of analysis would allow for clearer identification of where improvements in WWTP management or additional policies might be needed to mitigate pollution alongside other human activities.

Moreover, this highlights the importance of considering the local context when evaluating WWTP efficiency. Plants located in areas with high agricultural or mining activity might face additional challenges in maintaining low river salinity. In these cases, continuous monitoring and the implementation of adaptive management strategies that account for all pollution sources could be recommended to effectively protect aquatic ecosystems.

Implications for biodiversity, socioeconomic factors, and management perspectives

The increase in EC downstream of rivers influenced by WWTPs can have implications not only for surrounding biodiversity (Kefford et al., 2003; Hassell et al., 2006; Szöcs et al., 2012), but also for downstream socioeconomic activities and water use by nearby populations (e.g., for consumption) (Kaushal, 2016; Scheelbeek et al., 2016). Although numerous studies have made significant efforts to quantify the effects of increased salinity on species diversity and abundance, as well as on infrastructure damage, agricultural losses, and water access limitations, further research on salinity impacts near WWTPs is needed (Salvadó et al., 2001; Kefford et al., 2003; Hassell et al., 2006; Cañedo-Argüelles et al., 2014; Lind et al., 2018; Correa-Galeote et al., 2021; Vendrell-Puigmitja et al., 2022). This will enable more appropriate management decisions in these areas (e.g., urban ecosystems) and control biodiversity, which is crucial for maintaining river health. In this regard, water management policies should consider not only wastewater treatment and discharge but also their interaction with human activities and local ecosystems, to ensure a balance between socioeconomic development and environmental conservation.

5. GENERAL RECOMMENDATIONS

The prevention of salinity pollution in rivers requires a comprehensive approach, starting with the monitoring and development of environmental management plans for key activities driving FS. In agriculture, it is critical to understand farming practices at the watershed level, which involves monitoring and inventorying the products used and offering technical advice. The goal is to develop plans that optimize agricultural systems, including adjusting fertilizer application rates, collecting and treating irrigation water, and promoting the use of alternative products to agrochemicals. Furthermore, implementing and optimizing agricultural treatment systems is essential (e.g., in livestock and crop farming), with a special focus on the reuse of resources (e.g., water, nutrients) within farms. Promoting sustainable agricultural practices, such as organic farming, agroforestry, and crop rotation, can reduce chemical inputs, minimize runoff, and control salinization. Equally important is the proper management of solid and liquid waste in industries like mining, as well as controlling the use of salt products applied to roads during winter months. Optimizing storage, disposal, and on-site treatment systems can help prevent the runoff of contaminants into rivers.

Advanced monitoring systems play a crucial role in capturing real-time variations in salinity, not only by measuring EC but also by analyzing ions and other environmental variables multiple times throughout the year. These systems should be zoned according to anthropogenic pressures, such as in agricultural watersheds or areas with wastewater discharges, to provide targeted monitoring during critical periods, like road salting in winter or fertilizer application seasons. Moreover, more research is needed on the response of aquatic species to sudden salinity shocks, particularly across different times of the year and considering interactions with other stressors.

Another essential measure is the protection and restoration of riparian buffer zones, which act as natural barriers against the entry of salts and other contaminants into rivers. Similarly, controlling groundwater extraction is crucial, especially in coastal areas where excessive pumping leads to saline intrusion into rivers. Also, reforesting degraded areas can reduce FS by improving water infiltration and decreasing surface runoff, while plants help absorb excess salts from the soil. In regions facing severe water salinization, advanced technologies such as desalination and water reuse systems can convert brackish water into potable water and reduce pressure on freshwater resources. Education and awareness programs are also vital to empowering local communities and farmers to adopt best practices for salinization prevention and water conservation. An integrated watershed management approach is needed to address all sources of FS, both natural and anthropogenic, involving stakeholders across sectors to ensure coordinated management efforts.

Finally, effective governance frameworks are essential for addressing salinization. Strengthening regulations, ensuring compliance, and enforcing penalties for illegal discharges are key to reducing salinity loads. The social and economic dimensions of freshwater salinization must be assessed, considering its impacts on infrastructure, ecosystem services, and human health. Comprehensive governance requires collaborative decision-making and international cooperation to address transboundary salinization challenges, ensuring sustainable management of freshwater resources.

5.1. Recommendations for Spain

For policy makers and technical bodies

Review and Update of Legislation: Strengthening Regulations: Review and update existing regulations, such as Royal Decree 140/2003 and Royal Decree 665/2023, to include stricter and more specific conductivity limits that adequately protect aquatic ecosystems and their biodiversity.

Evidence-Based Decisions: Ensure that policies and reference values are grounded in the best available science. For example, studies are needed to predict current and future salinity conditions under different climate and socioeconomic change scenarios for each hydrological confederation in Spain (e.g., Duero, Segura, Ebro). Additionally, based on the specific realities of each basin, include studies on key drivers such as agriculture, mining, or wastewater discharges in urban areas. Ensure the adoption of regulations, making sure they are socioeconomically viable. Include an iterative approach that allows for the adaptation of standards as new information becomes available.

Characterization and monitoring of aquatic ecosystems

Establish Baseline Salinity: Set baseline natural salinity levels for each river type (e.g. mountain rivers, plains rivers, rivers with coastal influence), recognizing differences between ecosystems. For example, mountain rivers (which typically have low salinity) and Mediterranean rivers (with naturally higher salinity). Also, rivers in mountainous regions like the Guadalquivir basin, which have a significant flow year-round and well-developed riparian vegetation, may have naturally lower salinities compared to rivers in plain areas such as those in the Ebro basin, which may experience higher salinity due to agricultural runoff and urban influences. Additionally, streams in Mediterranean regions, such as the Júcar basin, might require different thresholds due to greater evaporation rates.

This should be done in line with the typologies defined in Spain's hydrological plans. Identifying human activities that affect each watershed, particularly those contributing to increased salinity, should be prioritized, and a thorough characterization of ionic composition in rivers should follow. Strengthen advisory programs focused on these specific regions to mitigate human-induced salinization and enhance technical efficiency in agriculture and industry.

Ongoing Monitoring: Implement continuous monitoring programs tailored to Spain's river typologies using bioassays and field studies to measure the impact of various salts. Periodic evaluations of the effects of anthropogenic activities on salinization (e.g., irrigated agriculture in the Segura basin or intensive industry along the Ebro basin) should guide adaptive management policies. Additionally, monitoring programs should focus on critical zones, such as transition waters near estuaries (e.g., Guadalquivir estuary), to better understand salinity dynamics in these mixed systems.

National Monitoring System: Establish a continuous monitoring system for salinity in rivers and freshwater bodies, with particular attention to the most affected regions. For example, expand the SAICA network and monitoring networks of each river basin committee and provinces to include ion and EC measurements at all stations. Ensure easy public access to this information. Create a national platform to gather and make this information available to the general public.

For businesses and the private sector

Improve agricultural management:

Efficient Irrigation Techniques: Promote drip irrigation to minimize salt accumulation in the soil. Monitor irrigation with reused water containing high levels of salinization, especially in halophytic crops (e.g., quinoa, barley, spinach). Additionally, expand soil

salinity monitoring and control through sensors in irrigated areas (15% of the total agricultural area in Spain) to prevent further FS. Due to drought conditions in some regions (e.g., Catalonia), avoid introducing irrigation for traditionally unirrigated crops such as olive trees or vineyards, as this could exacerbate FS. This practice could worsen the situation if saline wastewater or groundwater is used, further impacting the water cycle and river flow.

Sustainable Agriculture: Encourage reduced use of chemical fertilizers and adoption of crops that require less water.

Leaching Control: Implement practices such as crop rotation and cover crops to improve soil structure and control leaching of salts.

Agricultural Wastewater Collection: Expand and support the adoption of agricultural wastewater collection and storage systems, as seen in some regions of Spain (e.g., Levante and Murcia). These systems include channels and underground pipes to capture and redirect runoff water to storage ponds for subsequent treatment and reuse. This practice optimizes water use by allowing its reuse for irrigation, contributes to water conservation, and improves agricultural sustainability in water-scarce areas.

Regulate and supervise mining:

Strengthen Environmental Regulations: Require mining companies to implement more efficient containment systems to prevent the dissolution of saline waste into water bodies.

Rehabilitation of Affected Areas: Mandate companies to rehabilitate mining areas, including restoring contaminated watercourses.

Continuous Monitoring: Implement constant water quality monitoring programs in watersheds affected by mining and establish penalties for non-compliance.

Manage desalination plants:

Brine Treatment: Develop more sustainable methods for treating and disposing of brines, such as their reuse in industrial processes.

Strategic Location: Plan the location of new desalination plants in areas with minimal ecological impact and avoid sensitive zones.

Ecosystem Monitoring: Implement monitoring programs to assess the impact of brine discharges and take corrective measures if necessary.

Control use of road de-icing agents:

Research Alternatives: Promote the use of less contaminating materials or non-chemical techniques for de-icing.

Reduction in Sensitive Areas: Limit the use of de-icing agents in areas near vulnerable water bodies.

Awareness Campaigns: Develop campaigns to raise awareness about the environmental impacts of road salt use and promote more responsible practices.

Improve urban wastewater treatment:

Optimize Treatment Plants: Enhance technologies to increase efficiency in salt removal.

Reuse Treated Wastewater: Encourage reuse for agricultural irrigation and other uses without risks to health or the environment.

Monitoring and Control of Discharges: Establish a rigorous system for monitoring salinity in wastewater discharges and penalize non-compliance.

Protect coastal aquifers:

Control Over-exploitation: Regulate the use of coastal aquifers to prevent saline intrusion, promoting sustainable extraction practices.

Artificial Recharge: Implement artificial recharge techniques with treated waters to counteract marine intrusion.

Climate Change Adaptation: Develop water management plans considering the impacts of climate change on aquifer salinization.

For society

It is crucial for society to recognize salinization as an environmental issue caused by human activities, similar to eutrophication or climate change. Although scientific evidence has proven increased salinity, it is still not perceived as a severe problem. There is a call to include salinization in public discourse, raise awareness about its risks to social well-being and public health, and seek solutions through societal consensus.

5.2. Open questions

Do we need to understand the life cycle of salt, from cradle to grave, in water systems and in various processes involving water, extending to soil and air?

Is there "virtual salinity", i.e., the amount of salt that is indirectly introduced into water systems through various production and consumption processes in one place, but later exported and consumed elsewhere? There could be indirect salinity that producing countries should "charge" to consuming countries.

Can we calculate the Salinity Footprint based on virtual water and the production of goods and services with high salinity flows for a process, industry, or country?

How effectively can artificial intelligence and deep learning be trained to predict freshwater ecosystem salinization?

How do microplastics interact with salt and other chemicals in freshwater ecosystems, and what are the implications for ecosystem health and human well-being?

What are the long-term ecological and socio-economic impacts of desalination plants on coastal and marine environments?

How can traditional ecological knowledge complement scientific research in understanding and managing FS?

What are the synergistic effects of multiple stressors, such as climate change, pollution, and invasive species, on FS dynamics?

Is it possible to manage the effects of salt on WWTPs while simultaneously enhancing their capability to effectively remove salinity from urban wastewater?

How can innovative engineering solutions, such as bioengineering and green infrastructure, be utilized to mitigate and adapt to FS in urban and agricultural landscapes?

5.3. Future scenarios

Conducting field experiments or laboratory-scale studies is necessary to advance the definition of effects and thresholds specific to each region, particularly in regions where FS has been less studied (Latin America, Africa, Asia). Additionally, artificial intelligence offers promising opportunities for predicting current and future freshwater salinization (FS) scenarios using satellite data and historical records of water chemistry, climate factors, hydrogeology, economics, and societal dynamics. For example:

Global Scale:

Develop enhanced global databases that integrate salinity and biological data to delineate thresholds where aquatic communities undergo significant shifts.

Establish standardized methodologies for harmonizing salinity data across regions, facilitating large-scale assessments of FS impacts on ecosystem functions and global biogeochemical cycles.

Utilize satellite and drone technologies to monitor and predict FS dynamics alongside other environmental proxies, enhancing global-scale forecasting under diverse climate change scenarios.

Predicting directions and growth of global development, including areas transitioning to agricultural or mining use, population growth, increased wastewater discharge, or the use of saline agents in construction, industries, and transportation systems.

Identifying critical FS zones based on environmental and anthropogenic drivers.

Predicting scenarios of FS's relationship with human health and economic impacts of FS.

Using climate change predictions to determine areas at risk of water scarcity where FS may have a dramatic impact.

Regional Scale:

Identify community-specific salinity thresholds crucial for understanding species composition changes and ecosystem dynamics.

Assess basin-level characteristics such as geology and land use influencing FS and its ecological repercussions, emphasizing upstream-downstream connectivity and regional adaptation strategies.

Implement large-scale mesocosm experiments across climatic and land use gradients to elucidate salinity thresholds and ecological ramifications at regional scales.

Local Scale:

Explore FS impacts on less-studied trophic levels and their cascading effects on ecosystem functions like nutrient cycling and greenhouse gas emissions.

Investigate salinity tolerance traits in species and their implications for ecosystem resilience and adaptive capacities.

Integrate genomic and molecular approaches (e.g., eDNA, RNA-based sequencing) to assess microbial responses to FS, crucial for understanding microbial-driven ecosystem processes.

Temporal Scale:

Utilize long-term datasets and paleolimnological records to capture historical FS events and predict long-term ecological responses.

Apply high-frequency monitoring technologies to track short-term FS dynamics and ecosystem responses, providing insights into rapid evolutionary adaptations and ecosystem metabolism.

Examine regional adaptations to background salinities and their implications for community assembly and eco-evolutionary dynamics under varying FS regimes.

Multiscale and multidisciplinary perspectives:

Promote interdisciplinary collaborations to evaluate impacts of chemical cocktails (e.g., metal ions, nutrients) on trophic processes and ecosystem services under FS conditions.

Assess synergistic effects of multiple stressors on community structure and function within FS-affected ecosystems, integrating ecological, economic, social, and political perspectives.

Engage citizen science initiatives to enhance global participation in FS monitoring and data collection, fostering a comprehensive understanding and management strategies.

Social and economic implications:

Evaluate economic costs associated with FS impacts on freshwater ecosystems, including infrastructure damage, water treatment expenses, and loss of ecosystem services.

Integrate social dimensions like water potability, community health risks, and livelihood impacts dependent on freshwater resources.

Develop economic valuation frameworks to quantify the monetary value of ecosystem services affected by FS, aiding in conservation and management strategies' cost-benefit analyses.

Policy and governance:

Explore regulatory frameworks and policy interventions to mitigate FS impacts, including setting salinity thresholds and enforcing water quality standards.

Examine adaptive governance approaches fostering stakeholder engagement, community participation, and collaborative decision-making in FS management.

Evaluate international agreements and protocols addressing transboundary FS issues, promoting cooperation and information sharing among countries.

Technological innovations:

Advance sensor technologies for real-time monitoring of salinity levels and ecosystem responses, enhancing early warning systems for FS-induced ecological disturbances.

Apply emerging technologies such as AI, machine learning, and remote sensing to predict FS trends, identify hotspots, and optimize resource allocation for monitoring and management.

Integrate blockchain technology for secure data sharing and transparency in managing global-scale FS datasets and collaborative research efforts.

Educational and outreach initiatives:

Develop educational programs and public awareness campaigns about FS impacts on freshwater ecosystems and human well-being.

Engage local communities, schools, and citizen scientists in monitoring and reporting FS impacts, fostering a bottom-up approach to data collection and conservation efforts.

Establish capacity-building initiatives to empower researchers, practitioners, and policymakers in FS-affected regions with knowledge and skills for effective mitigation and adaptation strategies.

Ethical and equity considerations:

Explore ethical dimensions related to the distribution of FS impacts and vulnerabilities of marginalized communities and ecosystems.

Incorporate equity considerations into FS management strategies, ensuring fair access to freshwater resources and equitable distribution of ecosystem service benefits.

Promote inclusive approaches respecting indigenous knowledge systems and traditional practices in managing FS impacts, fostering culturally sensitive and effective conservation efforts.

6. CONCLUSIONS

1. The GlobSalt dataset is a valuable tool for studying FS on a global scale, as it provides significant spatial coverage and high temporal resolution across different watersheds. This database allowed the identification of several salinization "hotspots" worldwide and the temporal variation of FS, both explained by natural processes and anthropogenic activities. Factors such as road density, precipitation and soil water content were found to be the most influential variables in explaining these FS processes. However, the limitations of GlobSalt, particularly in terms of geographic and temporal representation, suggest the need to expand coverage to underrepresented regions such as Africa and Asia to improve the accuracy of understanding global salinization trends. The urgent need for basin-scale studies with specific environmental and anthropogenic data is also highlighted to gain a more detailed understanding of FS processes.
2. Although the analysis of GlobSalt data has revealed important patterns and key correlations between EC and major contributing ions (such as sodium and chloride), as well as the influence of anthropogenic and environmental variables, it is important to treat the presence of potentially erroneous data with caution. There is a need to improve sampling and data validation strategies. Moreover, the observed temporal variability should be validated with data at a finer temporal scale and considering different watershed characteristics, such as river size. Therefore, further studies are needed to enhance data quality, extend the temporal coverage of each river, and explore in greater detail the impacts of FS on aquatic ecosystems and its relationship with human activities and natural processes.
3. Temporal EC variation in rivers with higher levels of human activity, such as agriculture, mining, and wastewater discharge, showed greater salinity variability

compared to less anthropized sites. Although agriculture was the primary driver of this temporal variation, other factors such as mining, wastewater discharge, and road deicing also played a significant role. Natural variables such as precipitation and geology moderated these variations but were not major perturbations in less anthropized areas. In contrast, greater variability was observed in areas with multiple human activities, with factors such as precipitation appearing to amplify this variability, suggesting that anthropogenic activities significantly alter natural salinity patterns.

4. Temporal variation of EC in rivers upstream and downstream of WWTPs showed different patterns. The interannual standard deviation of EC was significantly higher at sites downstream of WWTPs than at sites upstream, indicating increased variability and peaks in EC at discharge points. This variability was also more pronounced during different seasons, with the most intense effects observed in summer. These results suggest that wastewater discharges contribute significantly to temporal salinity variability in rivers, and that the interaction between seasonal factors and wastewater discharges may exacerbate these effects. Therefore, it is crucial to establish high-resolution monitoring networks that integrate salinity data and other environmental stressors to better assess the impact of wastewater discharges on aquatic ecosystems and to develop effective management strategies.
5. The effects of the interaction between nutrients and salt on algae and macroinvertebrates in riverine ecosystems typical of the Mediterranean region showed both additive and antagonistic effects. Nutrient addition increased chlorophyll a levels, mainly due to the proliferation of cyanobacteria, although this increase was limited under nutrient saturation conditions. Salinization was the

main factor causing toxic effects on algae and macroinvertebrate communities, resulting in the dominance of resistant groups (such as resistant chironomid species). Although interactive effects between nutrients and salinity were weak, nutrients mitigated the toxic effects of salt on macroinvertebrates in a concentration-dependent manner. This mitigation may have been related to the recovery of green algae and diatom groups. Nutrients promoted algal growth while salt inhibited it, suggesting interactive effects that need to be further investigated at the biofilm species level. The biofilm response may have influenced macroinvertebrate communities by providing better food quality and diversity. These results highlight the complexity of ecological responses to nutrient and salt pollution and have important implications for the management of FS.

6. The influence of salinity on phytoplankton in U.S. rivers showed significant differences between pristine and impacted sites. In impacted sites, salinity had a strong negative relationship with phytoplankton concentration, likely due to high pollutant loads. Although nutrients in these areas might benefit phytoplankton growth, the adverse effects of salinity appeared to be dominant. In contrast, at pristine sites, although salinity also negatively affected phytoplankton, this effect was much weaker. This suggests that pristine ecosystems may have higher resilience to salinity changes, and higher salinity levels could even have a beneficial impact on phytoplankton in these areas. These findings highlight the importance of considering the specific conditions of each site when developing water management strategies to address both salinity and pollutant impacts effectively.

7. Salinity affects microbial communities and pollutant removal in urban WWTPs. High levels and peaks of EC were found to negatively impact microbial communities, particularly ciliates, and were inversely related to the removal of organic matter and nitrogen (TKN). These effects are consistent across seasons and are associated with EC concentrations that microbial communities and WWTP processes cannot adequately manage. WWTPs with high EC levels tend to harbor microbial communities dominated by salt-resistant species, which could serve as indicators of salinization. Disruption of ciliate communities may be linked to decreased organic matter removal and overall WWTP performance. The observed EC removal rates in conventional WWTPs were relatively low, as expected, since these plants are not designed for this process. Understanding the impact of EC is crucial for designing effective monitoring and management strategies to improve wastewater treatment performance. Also, improving treatment systems to better manage ion removal represents a significant opportunity to control salinity entering rivers from urban areas.
8. WWTPs have a strong impact on river EC concentrations. EC was significantly higher in river sections downstream of WWTPs, especially during the summer months when river dilution capacity is lower. These findings indicate that salinity increases are more pronounced during low-flow periods, which could exacerbate FS issues. The ion removal capacity of some WWTPs is limited, contributing to higher river salinity. However, regional differences and the specific characteristics of each treatment plant, such as the type of technology used, can influence these outcomes. Furthermore, the presence of other pollution sources, such as agriculture and mining, can amplify the impact of wastewater discharges

on salinization. Seasonal variability in WWTP efficiency and interactions with other pollution sources highlight the need for detailed, site-specific evaluations. Further studies should consider local contexts and the specific characteristics of each river to develop effective management strategies that mitigate salinization and protect aquatic ecosystems. It is also crucial to address impacts on biodiversity and socioeconomic implications to balance urban development with environmental conservation

7. REFERENCES

Abrahart, R.J., See, L., 2002. Multi-model data fusion for river flow forecasting: an evaluation of six alternative methods based on two contrasting catchments, Hydrology and Earth System Sciences. https://doi.org/10.5194/hess-6-655-2002

Aghdam, E., Mohandes, S.R., Manu, P., Cheung, C., Yunusa-Kaltungo, A., Zayed, T., 2023. Predicting quality parameters of wastewater treatment plants using artificial intelligence techniques. J Clean Prod. https://doi.org/10.1016/j.jclepro.2023.137019

Albert, N., 2005. How much sodium is in your diet? Am J Health Educ. https://doi.org/10.1080/19325037.2005.10608170

Almeida, J., Ribeiro, A.B., Silva, A.S., Faria, P., 2020. Overview of mining residues incorporation in construction materials and barriers for full-scale application. Journal of Building Engineering. https://doi.org/10.1016/j.jobe.2020.101215

Aristi, I., Casellas, M., Elosegi, A., Insa, S., Petrovic, M., Sabater, S., Acuña, V., 2016. Nutrients versus emerging contaminants-Or a dynamic match between subsidy and stress effects on stream biofilms. Environmental Pollution. https://doi.org/10.1016/j.envpol.2016.01.067

Arregui, L., Liébana, R., Calvo, P., A, Pérez-Uz, H., Serrano, S., 2013. Bioindication in activated sludge wastewater treatment plants, in: Cesaro J. Valdez Enrique M. Maradona (Ed.), Handbook of Wastewater Treatment: Biological Methods, Technology and Environmental Impac. Nova Science Publishers. https://doi.org/10.1111/j.1550-7408.2002.tb00376.x

Asensio, E., Ferreira, V.J., Gil, G., García-Armingol, T., López-Sabirón, A.M., Ferreira, G., 2017. Accumulation of de-icing salt and leaching in Spanish soils surrounding roadways. Int J Environ Res Public Health. https://doi.org/10.3390/ijerph14121498

Aslan, S., Simsek, E., 2012. Influence of salinity on partial nitrification in a submerged biofilter. Bioresour Technol. https://doi.org/10.1016/j.biortech.2012.05.057

Baberschke, N., Irob, K., Preuer, T., Meinelt, T., Kloas, W., 2019. Potash mining effluents and ion imbalances cause transient osmoregulatory stress, affect gill integrity and elevate chronically plasma sulfate levels in adult common roach, Rutilus rutilus. Environmental Pollution. https://doi.org/10.1016/j.envpol.2019.03.004

Bailey, S.A., Duggan, I.C., Van Overdijk, C.D.A., Johengen, T.H., Reid, D.F., Macisaac, H.J., 2004. Salinity tolerance of diapausing eggs of freshwater zooplankton. Freshw Biol. https://doi.org/10.1111/j.1365-2427.2004.01185.x

Bates, D., Mächler, M., Bolker, B.M., Walker, S.C., 2015. Fitting linear mixed-effects models using lme4. J Stat Softw. https://doi.org/10.18637/jss.v067.i01

Becerra-Castro, C., Lopes, A.R., Vaz-Moreira, I., Silva, E.F., Manaia, C.M., Nunes, O.C., 2015. Wastewater reuse in irrigation: A microbiological perspective on implications in soil

fertility and human and environmental health. Environ Int. https://doi.org/10.1016/j.envint.2014.11.001

Begmatov, S., Dorofeev, A.G., Kadnikov, V. V., Beletsky, A. V., Pimenov, N. V., Ravin, N. V., Mardanov, A. V., 2022. The structure of microbial communities of activated sludge of large-scale wastewater treatment plants in the city of Moscow. Sci Rep. https://doi.org/10.1038/s41598-022-07132-4

Benjankar, R., Kafle, R., Satyal, S., Adhikari, N., 2021. Analyses of spatial and temporal variations of salt concentration in waterbodies based on high resolution measurements using sensors. Hydrology. https://doi.org/10.3390/hydrology8020064

Berde, M., Jolis, D., 2021. Effect of saltwater intrusion on activated sludge flocculation. Water Environment Research. https://doi.org/10.1002/wer.1455

Bernhardt, E.S., Band, L.E., Walsh, C.J., Berke, P.E., 2008. Understanding, managing, and minimizing urban impacts on surface water nitrogen loading. Ann N Y Acad Sci. https://doi.org/10.1196/annals.1439.014

Bhide, S. V., Grant, S.B., Parker, E.A., Rippy, M.A., Godrej, A.N., Kaushal, S., Prelewicz, G., Saji, N., Curtis, S., Vikesland, P., Maile-Moskowitz, A., Edwards, M., Lopez, K.G., Birkland, T.A., Schenk, T., 2021. Addressing the contribution of indirect potable reuse to inland freshwater salinization. Nat Sustain. https://doi.org/10.1038/s41893-021-00713-7

Birk, S., Chapman, D., Carvalho, L., Spears, B.M., Andersen, H.E., Argillier, C., Auer, S., Baattrup-Pedersen, A., Banin, L., Beklioğlu, M., Bondar-Kunze, E., Borja, A., Branco, P., Bucak, T., Buijse, A.D., Cardoso, A.C., Couture, R.M., Cremona, F., de Zwart, D., Feld, C.K., Ferreira, M.T., Feuchtmayr, H., Gessner, M.O., Gieswein, A., Globevnik, L., Graeber, D., Graf, W., Gutiérrez-Cánovas, C., Hanganu, J., Işkın, U., Järvinen, M., Jeppesen, E., Kotamäki, N., Kuijper, M., Lemm, J.U., Lu, S., Solheim, A.L., Mischke, U., Moe, S.J., Nõges, P., Nõges, T., Ormerod, S.J., Panagopoulos, Y., Phillips, G., Posthuma, L., Pouso, S., Prudhomme, C., Rankinen, K., Rasmussen, J.J., Richardson, J., Sagouis, A., Santos, J.M., Schäfer, R.B., Schinegger, R., Schmutz, S., Schneider, S.C., Schülting, L., Segurado, P., Stefanidis, K., Sures, B., Thackeray, S.J., Turunen, J., Uyarra, M.C., Venohr, M., von der Ohe, P.C., Willby, N., Hering, D., 2020. Impacts of multiple stressors on freshwater biota across spatial scales and ecosystems. Nat Ecol Evol. https://doi.org/10.1038/s41559-020-1216-4

Blackburn, G., Mcleod, S., 1983. Salinity of Atmospheric Precipitation in the Murray-Darling Drainage Division, Australia, Aust. J. Soil Res. https://doi.org/10.1071/SR9830411

Blaen, P.J., Khamis, K., Lloyd, C.E.M., Bradley, C., Hannah, D., Krause, S., 2016. Real-time monitoring of nutrients and dissolved organic matter in rivers: Capturing event dynamics, technological opportunities and future directions. Science of the Total Environment. https://doi.org/10.1016/j.scitotenv.2016.06.116

Bolan, S., Padhye, L.P., Jasemizad, T., Govarthanan, M., Karmegam, N., Wijesekara, H., Amarasiri, D., Hou, D., Zhou, P., Biswal, B.K., Balasubramanian, R., Wang, H., Siddique, K.H.M., Rinklebe, J., Kirkham, M.B., Bolan, N., 2024. Impacts of climate change on the fate of contaminants through extreme weather events. Science of the Total Environment. https://doi.org/10.1016/j.scitotenv.2023.168388

Bolotin, L.A., Summers, B.M., Savoy, P., Blaszczak, J.R., 2023. Classifying freshwater salinity regimes in central and western U.S. streams and rivers. Limnol Oceanogr Lett. https://doi.org/10.1002/lol2.10251

Bolto, B., Dixon, D., Eldridge, R., King, S., Linge, K., 2002. Removal of natural organic matter by ion exchange, Water Research. https://doi.org/10.1016/S0043-1354(02)00231-2

Bond, N.R., Lake, P.S., Arthington, A.H., 2008. The impacts of drought on freshwater ecosystems: An Australian perspective. Hydrobiologia. https://doi.org/10.1007/s10750-008-9326-z

Borovskaya, R., Krivoguz, D., Chernyi, S., Kozhurin, E., Khorosheltseva, V., Zinchenko, E., 2022. Surface Water Salinity Evaluation and Identification for Using Remote Sensing Data and Machine Learning Approach. J Mar Sci Eng 10. https://doi.org/10.3390/jmse10020257

Boutron, O., Paugam, C., Luna-Laurent, E., Chauvelon, P., Sous, D., Rey, V., Meulé, S., Chérain, Y., Cheiron, A., Migne, E., 2021. Hydro-saline dynamics of a shallow mediterranean coastal lagoon: Complementary information from short and long term monitoring. J Mar Sci Eng 9, 222–227. https://doi.org/10.3390/jmse9070701

Bremer, E., Krämer, R., 2019. Responses of Microorganisms to Osmotic Stress. https://doi.org/10.1146/annurev-micro-020518

Brocca, L., Barbetta, S., Camici, S., Ciabatta, L., Dari, J., Filippucci, P., Massari, C., Modanesi, S., Tarpanelli, A., Bonaccorsi, B., Mosaffa, H., Wagner, W., Vreugdenhil, M., Quast, R., Alfieri, L., Gabellani, S., Avanzi, F., Rains, D., Miralles, D.G., Mantovani, S., Briese, C., Domeneghetti, A., Jacob, A., Castelli, M., Camps-Valls, G., Volden, E., Fernandez, D., 2024. A Digital Twin of the terrestrial water cycle: a glimpse into the future through high-resolution Earth observations. Frontiers in Science 1. https://doi.org/10.3389/fsci.2023.1190191

Brown, A.H., Yan, N.D., 2015. Food quantity affects the sensitivity of Daphnia to road salt. Environ Sci Technol. https://doi.org/10.1021/es5061534

Brown, A.W., Kaiser, K.A., Allison, D.B., 2018. Issues with data and analyses: Errors, underlying themes, and potential solutions. Proc Natl Acad Sci. https://doi.org/10.1073/pnas.1708279115

Camarasa Belmonte, A.M., Segura Beltrán, F., 2001. Flood events in Mediterranean ephemeral streams (ramblas) in Valencia region, Spain. Catena (Amst).https://doi.org/10.1016/S0341-8162(01)00146-1

Camarasa-Belmonte, A.M., 2016. Flash floods in Mediterranean ephemeral streams in Valencia Region (Spain). J Hydrol (Amst). https://doi.org/10.1016/j.jhydrol.2016.03.019

Canavan, R.W., Slomp, C.P., Jourabchi, P., Van Cappellen, P., Laverman, A.M., van den Berg, G.A., 2006. Organic matter mineralization in sediment of a coastal freshwater lake and response to salinization. Geochim Cosmochim Acta 70. https://doi.org/10.1016/j.gca.2006.03.012

Cañedo-argüelles, M., 2021. A review of recent advances and future challenges in freshwater salinization. Limnetica. https://doi.org/10.23818/limn.39.13

Cañedo-Argüelles, M., Brucet, S., Carrasco, S., Flor-Arnau, N., Ordeix, M., Ponsá, S., Coring, E., 2017. Effects of potash mining on river ecosystems: An experimental study. Environmental Pollution. https://doi.org/10.1016/j.envpol.2016.12.072

Cañedo-Argüelles, M., Bundschuh, M., Gutiérrez-Cánovas, C., Kefford, B.J., Prat, N., Trobajo, R., Schäfer, R.B., 2014. Effects of repeated salt pulses on ecosystem structure and functions in a stream mesocosm. Science of the Total Environment. https://doi.org/10.1016/j.scitotenv.2013.12.067

Cañedo-Argüelles, M., Grantham, T.E., Perrée, I., Rieradevall, M., Céspedes-Sánchez, R., Prat, N., 2012. Response of stream invertebrates to short-term salinization: A mesocosm approach. Environmental Pollution. https://doi.org/10.1016/j.envpol.2012.03.027

Cañedo-Argüelles, M., Hawkins, C.P., Kefford, B.J., Schäfer, R.B., Dyack, B.J., Brucet, S., Buchwalter, D., Dunlop, J., Frör, O., Lazorchak, J., Coring, E., Fernandez, H.R., Goodfellow, W., Achem, A.L.G., Hatfield-Dodds, S., Karimov, B.K., Mensah, P., Olson, J.R., Piscart, C., Prat, N., Ponsá, S., Schulz, C.J., Timpano, A.J., 2016. Saving freshwater from salts : Ion-specific standards are needed to protect biodiversity. Science. https://doi.org/10.1126/science.aad3488

Cañedo-Argüelles, M., Kefford, B.J., Piscart, C., Prat, N., Schäfer, R.B., Schulz, C.J., 2013. Salinisation of rivers: An urgent ecological issue. Environmental Pollution. https://doi.org/10.1016/j.envpol.2012.10.011

Cañedo-Argüelles, M., Rieradevall, M., 2009. Quantification of environment-driven changes in epiphytic macroinvertebrate communities associated to Phragmites australis, J. Limnol. https://doi.org/10.4081/jlimnol.2009.229

Cañedo-Argüelles, Miguel, Sala, M., Peixoto, G., Prat, N., Faria, M., Soares, A.M.V.M., Barata, C., Kefford, B., 2016. Can salinity trigger cascade effects on streams? A mesocosm approach. Science of the Total Environment. https://doi.org/10.1016/j.scitotenv.2015.03.039

Cañero, C., Vilariño, F., Mauri, J., Radeva, P., 2002. Predictive (Un)distortion model and 3-D reconstruction by biplane snakes. IEEE Trans Med Imaging. https://doi.org/10.1109/TMI.2002.804421

Canhoto Cristina, Felix Bärlocher, Miguel Cañedo-Argüelles, Rosa Gómez, Gonçalves, and A.L., 2021. The Ecology of Plant Litter Decomposition in Stream Ecosystems: An Overview. Springer, Cham. https://doi.org/10.1007/978-3-030-72854-0_1

Casquin, A., Gu, S., Dupas, R., Petitjean, P., Gruau, G., Durand, P., 2020. River network alteration of C-N-P dynamics in a mesoscale agricultural catchment. Science of The Total Environment. https://doi.org/10.1016/J.SCITOTENV.2020.141551

Chen, H., Wang, Yangyang, Chen, Z., Wu, Z., Chu, X., Qing, S., Xu, L., Yang, K., Meng, Q., Cheng, H., Zhan, W., Wang, Yuguang, Zhou, H., 2023. Effects of salinity on anoxic–oxic system performance, microbial community dynamics and co-occurrence network during treating wastewater. Chemical Engineering Journal. https://doi.org/10.1016/j.cej.2023.141969

Chen, Y., He, H., Liu, H., Li, H., Zeng, G., Xia, X., Yang, C., 2018. Effect of salinity on removal performance and activated sludge characteristics in sequencing batch reactors. Bioresour Technol. https://doi.org/10.1016/j.biortech.2017.10.092

Cochero, J., Licursi, M., Gómez, N., 2017. Effects of pulse and press additions of salt on biofilms of nutrient-rich streams. Science of the Total Environment. https://doi.org/10.1016/j.scitotenv.2016.11.152

Cooper, S.D., Lake, P.S., Sabater, S., Melack, J.M., Sabo, J.L., 2013. The effects of land use changes on streams and rivers in mediterranean climates. Hydrobiologia. https://doi.org/10.1007/s10750-012-1333-4

Correa-Galeote, D., Roibás, A., Mosquera-Corral, A., Juárez-Jiménez, B., González-López, J., Rodelas, B., 2021. Salinity is the major driver of the global eukaryotic community structure in fish-canning wastewater treatment plants. J Environ Manage. https://doi.org/10.1016/j.jenvman.2021.112623

Corsino, S.F., Capodici, M., Torregrossa, M., Viviani, G., 2018. A comprehensive comparison between halophilic granular and flocculent sludge in withstanding short and long-term salinity fluctuations. Journal of Water Process Engineering. https://doi.org/10.1016/j.jwpe.2018.02.013

Cortés-Lorenzo, C., González-Martínez, A., Smidt, H., González-López, J., Rodelas, B., 2016. Influence of salinity on fungal communities in a submerged fixed bed bioreactor for wastewater treatment. Chemical Engineering Journal. https://doi.org/10.1016/j.cej.2015.10.009

Cotta, C.P., Pinto, T.J.S., Yoshii, M.P.C., Silva, L.C.M., Ogura, A.P., Gabriel, G.V.M., Schiesari, L.C., Carmo, J.B., Montagner, C.C., Espíndola, E.L.G., Moreira, R.A., 2023.

Exposure to fipronil, 2,4-D and vinasse influences macroinvertebrate assemblage structure: An experimental mesocosm approach. Science of the Total Environment. https://doi.org/10.1016/j.scitotenv.2023.164259

Crosa, G., Froebrich, J., Nikolayenko, V., Stefani, F., Galli, P., Calamari, D., 2006. Spatial and seasonal variations in the water quality of the Amu Darya River (Central Asia). Water Res. https://doi.org/10.1016/j.watres.2006.04.004

Crowther, R.A., Hynes, H.B.N., 1977. The effect of road deicing salt on the drift of stream benthos. Environmental Pollution. https://doi.org/10.1016/0013-9327(77)90103-3

Cui, Y., Su, H., Chen, Yefei, Chen, Yongbao, Peng, Y., 2015. Mechanism of Activated Sludge Floc Disintegration Induced by Excess Addition of NaCl. Clean (Weinh). https://doi.org/10.1002/clen.201400219

Cunillera-Montcusí, D., Beklioğlu, M., Cañedo-Argüelles, M., Jeppesen, E., Ptacnik, R., Amorim, C.A., Arnott, S.E., Berger, S.A., Brucet, S., Dugan, H.A., Gerhard, M., Horváth, Z., Langenheder, S., Nejstgaard, J.C., Reinikainen, M., Striebel, M., Urrutia-Cordero, P., Vad, C.F., Zadereev, E., Matias, M., 2022. Freshwater salinisation: a research agenda for a saltier world. Trends Ecol Evol. https://doi.org/10.1016/j.tree.2021.12.005

Cuvelier, J., Vlassenroot, K., Olin, N., 2014. Resources, conflict and governance: A critical review. Extractive Industries and Society. https://doi.org/10.1016/j.exis.2014.07.006

Daliakopoulos, I.N., Tsanis, I.K., Koutroulis, A., Kourgialas, N.N., Varouchakis, A.E., Karatzas, G.P., Ritsema, C.J., 2016. The threat of soil salinity: A European scale review. Science of the Total Environment. https://doi.org/10.1016/j.scitotenv.2016.08.177

David, M.B., Mitchell, C.A., Gentry, L.E., Salemme, R.K., 2016. Chloride Sources and Losses in Two Tile-Drained Agricultural Watersheds. J Environ Qual. https://doi.org/10.2134/jeq2015.06.0302

Des, M., Fernández-Nóvoa, D., deCastro, M., Gómez-Gesteira, J.L., Sousa, M.C., Gómez-Gesteira, M., 2021. Modeling salinity drop in estuarine areas under extreme precipitation events within a context of climate change: Effect on bivalve mortality in Galician Rías Baixas. Science of the Total Environment. https://doi.org/10.1016/j.scitotenv.2021.148147

Di Giacomo, G., Romano, P., 2022. Evolution and Prospects in Managing Sewage Sludge Resulting from Municipal Wastewater Purification. Energies (Basel). https://doi.org/10.3390/en15155633

Duan, L., Yun, Q., Jiang, G., Teng, D., Zhou, G., Cao, Y., 2024. A review of chloride ions removal from high chloride industrial wastewater: Sources, hazards, and mechanisms. J Environ Manage. https://doi.org/10.1016/j.jenvman.2024.120184

Egea-Corbacho, A., Romero-Pareja, P., Aragón Cruz, C., Pavón, C., Coello, M.D., 2021. Effect of seawater intrusion using real wastewater on an attached biomass system operating

a nitrogen and phosphorus removal process. J Environ Chem Eng. https://doi.org/10.1016/j.jece.2020.104927

Ehalt MacEdo, H., Lehner, B., Nicell, J., Grill, G., Li, J., Limtong, A., Shakya, R., 2022. Distribution and characteristics of wastewater treatment plants within the global river network. Earth Syst Sci Data. https://doi.org/10.5194/essd-14-559-2022

En Guo, Q., Guo Li, B., Li Nan, L., Nan Nie, Z., Yu Cao, S., 2019. Spatial and temporal variation of salt ions in the surface water of Shule River Valley in Gansu Province, China. Water Sci Technol Water Supply. https://doi.org/10.2166/ws.2018.124

Entrekin, S.A., Clay, N.A., Mogilevski, A., Howard-Parker, B., Evans-White, M.A., 2019. Multiple riparian–stream connections are predicted to change in response to salinization. Philosophical Transactions of the Royal Society B: Biological Sciences. https://doi.org/10.1098/rstb.2018.0042

Ersoy, Z., Abril, M., Cañedo-Argüelles, M., Espinosa, C., Vendrell-Puigmitja, L., Proia, L., 2022. Experimental assessment of salinization effects on freshwater zooplankton communities and their trophic interactions under eutrophic conditions. Environmental Pollution. https://doi.org/10.1016/j.envpol.2022.120127

Estévez, E., Rodríguez-Castillo, T., González-Ferreras, A.M., Cañedo-Argüelles, M., Barquín, J., 2019. Drivers of spatio-temporal patterns of salinity in Spanish rivers: A nationwide assessment. Philosophical Transactions of the Royal Society B: Biological Sciences. https://doi.org/10.1098/rstb.2018.0022

Feth, J.H., 1981. Chloride in Natural Continental Water A Review. J. Water Supply. https://doi.org/10.3133/wsp2176

Folegot, S., Hannah, D.M., Dugdale, S.J., Kurz, M.J., Drummond, J.D., Klaar, M.J., Lee-Cullin, J., Keller, T., Martí, E., Zarnetske, J.P., Ward, A.S., Krause, S., 2018. Low flow controls on stream thermal dynamics. Limnologica. https://doi.org/10.1016/j.limno.2017.08.003

Gardner, R.L., Young, R.A., 1988. Assessing Strategies for Control of Irrigation-Induced Salinity in the Upper Colorado River Basin. American Journal of Agricultural Economics. https://doi.org/10.2307/1241974

Garrido, M., Lafabrie, C., Torre, F., Fernandez, C., Pasqualini, V., 2013. Resilience and stability of Cymodocea nodosa seagrass meadows over the last four decades in a Mediterranean lagoon. Estuar Coast Shelf Sci. https://doi.org/10.1016/j.ecss.2013.05.035

Gavrilescu, M., 2021. Water, soil, and plants interactions in a threatened environment. J. Water (Switzerland). https://doi.org/10.3390/w13192746

Gómez, R., Arce, M.I., Baldwin, D.S., Dahm, C.N., 2017. Water Physicochemistry in Intermittent Rivers and Ephemeral Streams, in: Intermittent Rivers and Ephemeral Streams:

Ecology and Management. Elsevier Inc. https://doi.org/10.1016/B978-0-12-803835-2.00005-X

Gómez-Coma, L., Ortiz-Martínez, V.M., Fallanza, M., Ortiz, A., Ibañez, R., Ortiz, I., 2020. Blue energy for sustainable water reclamation in WWTPs. Journal of Water Process Engineering. https://doi.org/10.1016/j.jwpe.2019.101020

Gorham E., 1958. The influence and importance of daily weather conditions in the supply of chloride, sulphate and other ions to fresh waters from atmospheric precipitation. Philos Trans R Soc Lond B Biol Sci. https://doi.org/10.1098/rstb.1958.0001

Gramaglia, C., Rio, M., Salles, C., Tournoud, M.G., 2024. Reducing the imperviousness of urban soils to enhance the quality of surface water: obstacles and levers to implementing ecological runoff management in the south of France. J Hydrol (Amst). https://doi.org/10.1016/j.jhydrol.2024.131168

Greco, D.A., Arnott, S.E., Fournier, I.B., Schamp, B.S., 2023. Effects of chloride and nutrients on freshwater plankton communities. Limnol Oceanogr Lett. https://doi.org/10.1002/lol2.10202

Guerzoni, S., Chester, R., Dulac, F., Herut, B., Loy¨eloy¨e-Pilot, M.-D., Measures, C., Migon, C., Molinaroli, E., Moulin, C., Rossini, P., Saydam, C., Soudine, A., Ziveri, P., 1999. The role of atmospheric deposition in the biogeochemistry of the Mediterranean Sea, Progress in Oceanography. https://doi.org/10.1016/S0079-6611(99)00024-5

Guo, L., Xie, Y., Sun, W., Xu, Y., Sun, Y., 2023. Research Progress of High-Salinity Wastewater Treatment Technology. Water (Switzerland). https://doi.org/10.3390/w15040684

Gutiérrez-Cánovas, C., Arribas, P., Naselli-Flores, L., Bennas, N., Finocchiaro, M., Millán, A., Velasco, J., 2019. Evaluating anthropogenic impacts on naturally stressed ecosystems: Revisiting river classifications and biomonitoring metrics along salinity gradients. Science of the Total Environment. https://doi.org/10.1016/j.scitotenv.2018.12.253

Hartmann, J., Lauerwald, R., Moosdorf, N., 2014. A Brief Overview of the GLObal RIver Chemistry Database, GLORICH. Procedia Earth and Planetary Science. https://doi.org/10.1016/j.proeps.2014.08.005

Hassell, K.L., Kefford, B.J., Nugegoda, D., 2006. Sub-lethal and chronic salinity tolerances of three freshwater insects: Cloeon sp. and Centroptilum sp. (Ephemeroptera: Baetidae) and Chironomus sp. (Diptera: Chironomidae). Journal of Experimental Biology. https://doi.org/10.1242/jeb.02457

Hatch, M., Munday, T., Heinson, G., 2010. A comparative study of in-river geophysical techniques to define variations in riverbed salt load and aid managing river salinization. Geophysics. https://doi.org/10.1190/1.3475706

He, H., Chen, Y., Li, X., Cheng, Y., Yang, C., Zeng, G., 2017. Influence of salinity on microorganisms in activated sludge processes: A review. Int Biodeterior Biodegradation. https://doi.org/10.1016/j.ibiod.2016.10.007

Henry, R.K., Yongsheng, Z., Jun, D., 2006. Municipal solid waste management challenges in developing countries - Kenyan case study. Waste Management. https://doi.org/10.1016/j.wasman.2005.03.007

Herbert, E.R., Boon, P., Burgin, A.J., Neubauer, S.C., Franklin, R.B., Ardon, M., Hopfensperger, K.N., Lamers, L.P.M., Gell, P., Langley, J.A., 2015. A global perspective on wetland salinization: Ecological consequences of a growing threat to freshwater wetlands. Ecosphere. https://doi.org/10.1890/ES14-00534.1

Hintz, W.D., Arnott, S.E., Symons, C.C., Greco, D.A., McClymont, A., Brentrup, J.A., Cañedo-Argüelles, M., Derry, A.M., Downing, A.L., Gray, D.K., Melles, S.J., Relyea, R.A., Rusak, J.A., Searle, C.L., Astorg, L., Baker, H.K., Beisner, B.E., Cottingham, K.L., Ersoy, Z., Espinosa, C., Franceschini, J., Giorgio, A.T., Göbeler, N., Hassal, E., Hébert, M.P., Huynh, M., Hylander, S., Jonasen, K.L., Kirkwood, A.E., Langenheder, S., Langvall, O., Laudon, H., Lind, L., Lundgren, M., Proia, L., Schuler, M.S., Shurin, J.B., Steiner, C.F., Striebel, M., Thibodeau, S., Urrutia-Cordero, P., Vendrell-Puigmitja, L., Weyhenmeyer, G.A., 2022. Current water quality guidelines across North America and Europe do not protect lakes from salinization. Proc Natl Acad Sci U S A 119. https://doi.org/10.1073/pnas.2115033119

Hintz, W.D., Mattes, B.M., Schuler, M.S., Jones, D.K., Stoler, A.B., Lind, L., Relyea, R.A., 2017. Salinization triggers a trophic cascade in experimental freshwater communities with varying food-chain length. Ecological Applications. https://doi.org/10.1002/eap.1487

Hintz, W.D., Relyea, R.A., 2019. A review of the species , community , and ecosystem impacts of road salt salinisation in fresh waters. https://doi.org/10.1111/fwb.13286

Hintz, W.D., Relyea, R.A., 2017. Impacts of road deicing salts on the early-life growth and development of a stream salmonid : Salt type matters. Environmental Pollution. https://doi.org/10.1016/j.envpol.2017.01.040

Honey-Rosés, J., Schneider, D.W., Brozović, N., 2014. Changing ecosystem service values following technological change. Environ Manage. https://doi.org/10.1007/s00267-014-0270-6

Horrigan, N., Dunlop, J.E., Kefford, B.J., Zavahir, F., 2007. Acute toxicity largely reflects the salinity sensitivity of stream macroinvertebrates derived using field distributions. Mar Freshw Res. https://doi.org/10.1071/MF05241

Hosseiniyan Khatibi, S.M., Zununi Vahed, F., Sharifi, S., Ardalan, M., Mohajel Shoja, M., Zununi Vahed, S., 2019. Osmolytes resist against harsh osmolarity: Something old something new. Biochimie. https://doi.org/10.1016/j.biochi.2019.01.002

Hou, M., Li, W., Li, H., Li, C., Wu, X., Liu, Y. di, 2019. Performance and bacterial characteristics of aerobic granular sludge in response to alternating salinity. Int Biodeterior Biodegradation. https://doi.org/10.1016/j.ibiod.2019.05.007

Hudec, M.R., Jackson, M.P.A., 2007. Terra infirma: Understanding salt tectonics. Earth Sci Rev. https://doi.org/10.1016/j.earscirev.2007.01.001

Hughes, J., Cowper-Heays, K., Olesson, E., Bell, R., Stroombergen, A., 2021. Impacts and implications of climate change on wastewater systems: A New Zealand perspective. Clim Risk Manag. https://doi.org/10.1016/j.crm.2020.100262

Hummel, M.A., Berry, M.S., Stacey, M.T., 2018. Sea Level Rise Impacts on Wastewater Treatment Systems Along the U.S. Coasts. Earths Future. https://doi.org/10.1002/2017EF000805

Irrgang, C., Boers, N., Sonnewald, M., Barnes, E.A., Kadow, C., Staneva, J., Saynisch-Wagner, J., 2021. Towards neural Earth system modelling by integrating artificial intelligence in Earth system science. Nat Mach Intell. https://doi.org/10.1038/s42256-021-00374-3

Ishwaran, A.H., Kogalur, U.B., Kogalur, M.U.B., Suggests, D., Openmp, D.F., Mahalanobis, N., Chrome, G., Gpl, L., Date, R.C., 2022. Package ‘ randomForestSRC ’. https://api.semanticscholar.org/CorpusID:2003897

Jackson, J.K., Funk, D.H., 2019. Temperature affects acute mayfly responses to elevated salinity: Implications for toxicity of road de-icing salts. Philosophical Transactions of the Royal Society B: Biological Sciences. https://doi.org/10.1098/rstb.2018.0081

Jackson, R.B., Jobbágy, E.G., 2005. From icy roads to salty streams. Proc Natl Acad Sci. https://doi.org/10.1073/pnas.0507389102

Ji, B., Zhang, H., Zhou, L., Yang, J., Zhang, K., Yuan, X., Ma, J., Qian, Y., 2021. Effect of the rapid increase of salinity on anoxic-oxic biofilm reactor for treatment of high-salt and high-ammonia–nitrogen wastewater. Bioresour Technol. https://doi.org/10.1016/j.biortech.2021.125363

Jin, Y., Ding, J., Zhan, W., Du, J., Wang, G., Pang, J., Ren, N., Yang, S., 2023. Effect of dissolved oxygen concentration on performance and mechanism of simultaneous nitrification and denitrification in integrated fixed-film activated sludge sequencing batch reactors. Bioresour Technol. https://doi.org/10.1016/j.biortech.2023.129616

Jones, E.R., Van Vliet, M.T.H., Qadir, M., Bierkens, M.F.P., 2021. Country-level and gridded estimates of wastewater production, collection, treatment and reuse. Earth Syst Sci Data. https://doi.org/10.5194/essd-13-237-2021

Jordán, M.M., Navarro-Pedreño, J., García-Sánchez, E., Mateu, J., Juan, P., 2004. Spatial dynamics of soil salinity under arid and semi-arid conditions: Geological and environmental implications. Environmental Geology. https://doi.org/10.1007/s00254-003-0894-y

Julia, J., Yossef, C., Marina, de L., Ariel, K., Edouard, J., Antonis, C., 2014. Multiple micro-predators controlling bacterial communities in the environment. Curr Opin Biotechnol. https://doi.org/10.1016/j.copbio.2014.02.003

Kaushal, Gold, A.J., Bernal, S., Tank, J.L., 2018. Diverse water quality responses to extreme climate events: an introduction. Biogeochemistry. https://doi.org/10.1007/s10533-018-0527-x

Kaushal, S.S., 2016. Increased Salinization Decreases Safe Drinking Water. Environ Sci Technol. https://doi.org/10.1021/acs.est.6b00679

Kaushal, S.S., Duan, S., Doody, T.R., Haq, S., Smith, R.M., Newcomer Johnson, T.A., Newcomb, K.D., Gorman, J., Bowman, N., Mayer, P.M., Wood, K.L., Belt, K.T., Stack, W.P., 2017. Human-accelerated weathering increases salinization, major ions, and alkalinization in fresh water across land use. Applied Geochemistry. https://doi.org/10.1016/j.apgeochem.2017.02.006

Kaushal, S.S., Groffman, P.M., Likens, G.E., Belt, K.T., Stack, W.P., Kelly, V.R., Band, L.E., Fisher, G.T., 2005. Increased salinization of fresh water in the Northeastern United States. Proc Natl Acad Sci. https://doi.org/10.1073/pnas.0506414102

Kaushal, S.S., Likens, G.E., Mayer, P.M., Shatkay, R.R., Shelton, S.A., Grant, S.B., Utz, R.M., Yaculak, A.M., Reimer, J.E., Bhide, S. V, Malin, J.T., 2023. The Anthropogenic Salt Cycle. Nature reviews earth & environment. https://doi.org/10.1038/s43017-023-00485-y

Kaushal, S.S., Likens, G.E., Pace, M.L., Reimer, J.E., Maas, C.M., Galella, J.G., Utz, R.M., Duan, S., Kryger, J.R., Yaculak, A.M., Boger, W.L., Bailey, N.W., Haq, S., Wood, K.L., Wessel, B.M., Park, C.E., Collison, D.C., Aisin, B.Y. 'aaqob I., Gedeon, T.M., Chaudhary, S.K., Widmer, J., Blackwood, C.R., Bolster, C.M., Devilbiss, M.L., Garrison, D.L., Halevi, S., Kese, G.Q., Quach, E.K., Rogelio, C.M.P., Tan, M.L., Wald, H.J.S., Woglo, S.A., 2021. Freshwater salinization syndrome: from emerging global problem to managing risks, Biogeochemistry. Springer International Publishing. https://doi.org/10.1007/s10533-021-00784-w

Kaushal, S.S., Likens, G.E., Pace, M.L., Utz, R.M., Haq, S., Gorman, J., Grese, M., 2018. Freshwater salinization syndrome on a continental scale. Biogeochemistry. https://doi.org/10.1073/pnas.1711234115

Kaushal, S.S., Likens, G.E., Utz, R.M., Pace, M.L., Grese, M., Yepsen, M., 2013. Increased river alkalinization in the eastern U.S. Environ Sci Technol. https://doi.org/10.1021/es401046s

Kaushal, S.S., Mayer, P.M., Shatkay, R.R., Maas, C.M., Cañedo-Argüelles, M., Hintz, W.D., Wessel, B.M., Tully, K., Rippy, M.A., Grant, S.B., 2024. Salinization of inland waters, in: Reference Module in Earth Systems and Environmental Sciences. Elsevier. https://doi.org/10.1016/b978-0-323-99762-1.00042-5

Kefford, B.J., 2019. Why are mayflies (Ephemeroptera) lost following small increases in salinity? Three conceptual osmophysiological hypotheses. Philosophical Transactions of the Royal Society B: Biological Sciences. https://doi.org/10.1098/rstb.2018.0021

Kefford, B.J., 1998. The relationship between electrical conductivity and selected macroinvertebrate communities in four river systems of south-west Victoria, Australia, International Journal of Salt Lake Research. KluwerAcademic Publishers. https://doi.org/10.1023/A:1009019404720

Kefford, B.J., Buchwalter, D., Cañedo-Argüelles, M., Davis, J., Duncan, R.P., Hoffmann, A., Thompson, R., 2016. Salinized rivers: Degraded systems or new habitats for salt-tolerant faunas? Biol Lett. https://doi.org/10.1098/rsbl.2015.1072

Kefford, B.J., Nugegoda, D., Zalizniak, L., Fields, E.J., Hassell, K.L., 2007. The salinity tolerance of freshwater macroinvertebrate eggs and hatchlings in comparison to their older life-stages: A diversity of responses - The salinity tolerance of freshwater macroinvertebrate eggs and hatchlings. Aquat Ecol. https://doi.org/10.1007/s10452-006-9066-y

Kefford, B.J., Palmer, C.G., Nugegoda, D., 2005. Relative salinity tolerance of freshwater macroinvertebrates from the south-east Eastern Cape, South Africa compared with the Barwon Catchment, Victoria, Australia, Marine and Freshwater Research. https://doi.org/10.1071/MF04098

Kefford, B.J., Papas, P.J., Nugegoda, D., 2003. Relative salinity tolerance of macroinvertebrates from the Barwon River , Victoria , Australia Arthur Rylah Institute for Environmental Research , Department of Natural Resources and Lethal salinity tolerance and selected field distr. Mar Freshw Res. https://doi.org/10.1071/MF04098

Kelly, M.G., Free, G., Kolada, A., Phillips, G., Warner, S., Wolfram, G., Poikane, S., 2024. Warding off freshwater salinization: Do current criteria measure up? Wiley Interdisciplinary Reviews: Water. https://doi.org/10.1002/wat2.1694

Kelly, V.R., Lovett, G.M., Weathers, K.C., Findlay, S.E.G., Strayer, D.L., Burns, D.J., Likens, G.E., 2008. Long-term sodium chloride retention in a rural watershed: Legacy effects of road salt on streamwater concentration. Environ Sci Technol. https://doi.org/10.1021/es0713911

Kirkham, C., Bertoni, C., Cartwright, J., Lensky, N.G., Sirota, I., Rodriguez, K., Hodgson, N., 2020. The demise of a ‘salt giant’ driven by uplift and thermal dissolution. Earth Planet Sci Lett. https://doi.org/10.1016/j.epsl.2019.115933

Kolesar, K.R., Mattson, C.N., Peterson, P.K., May, N.W., Prendergast, R.K., Pratt, K.A., 2018. Increases in wintertime PM2.5 sodium and chloride linked to snowfall and road salt application. Atmos Environ. https://doi.org/10.1016/j.atmosenv.2018.01.008

Kulmatov, R., Mirzaev, J., Abuduwaili, J., Karimov, B., 2020. Challenges for the sustainable use of water and land resources under a changing climate and increasing

salinization in the Jizzakh irrigation zone of Uzbekistan. J Arid Land. https://doi.org/10.1007/s40333-020-0092-8

Kumar, D., Kumar, R., Sharma, M., Awasthi, A., Kumar, M., 2024. Global water quality indices: Development, implications, and limitations. Total Environment Advances. https://doi.org/10.1016/j.teadva.2023.200095

Laceby, J.P., Kerr, J.G., Zhu, D., Chung, C., Situ, Q., Abbasi, S., Orwin, J.F., 2019. Chloride inputs to the North Saskatchewan River watershed: the role of road salts as a potential driver of salinization downstream of North America's northern most major city (Edmonton, Canada). Science of the Total Environment. https://doi.org/10.1016/j.scitotenv.2019.06.208

Lagarias, A., Stratigea, A., 2021. High-Resolution Spatial Data Analysis for Monitoring Urban Sprawl in Coastal Zones: A Case Study in Crete Island, Lecture Notes in Computer Science (including subseries Lecture Notes in Artificial Intelligence and Lecture Notes in Bioinformatics). Springer International Publishing. https://doi.org/10.1007/978-3-030-87016-4_6

Larson, C.A., Belovsky, G.E., 2013. Salinity and nutrients influence species richness and evenness of phytoplankton communities in microcosm experiments from Great Salt Lake, Utah, USA. J Plankton Res. https://doi.org/10.1093/plankt/fbt053

Lawsona, L., Jackson, D.A., 2021. Salty summertime streams—road salt contaminated watersheds and estimates of the proportion of impacted species. Facets. https://doi.org/10.1139/FACETS-2020-0068

Le Bonté, S., Pons, M.N., Potier, O., Rocklin, P., 2008. Relation between conductivity and ion content in urban wastewater. Revue des Sciences de l'Eau. https://doi.org/10.7202/019165ar

Le, T.D.H., Kattwinkel, M., Schützenmeister, K., Olson, J.R., Hawkins, C.P., Schäfer, R.B., 2019. Predicting current and future background ion concentrations in German surface water under climate change. Philosophical Transactions of the Royal Society B: Biological Sciences 374. https://doi.org/10.1098/rstb.2018.0004

Lee, J.J., Hutner, S.H. (Seymour H., Bovee, E.C., 1985. An Illustrated guide to the protozoa. Society of Protozoologists. https://api.semanticscholar.org/CorpusID:82687261

Lee, Y., Oleszkiewicz, J.A., 2003. Effects of predation and ORP conditions on the performance of nitrifiers in activated sludge systems. Water Res. https://doi.org/10.1016/S0043-1354(03)00341-5

Lefebvre, O., Moletta, R., 2006. Treatment of organic pollution in industrial saline wastewater: A literature review. Water Res. https://doi.org/10.1016/j.watres.2006.08.027

Leslie, P., McCabe, J.T., 2013. Response diversity and resilience in social-ecological systems. Curr Anthropol. https://doi.org/10.1086/669563

Leu, M., Hanser, S.E., Knick, S.T., 2008. The human foothprint in the west: a large-scale analysis of anthropogenic impacts applications. Ecol applications. https://doi.org/10.1890/07-0480.1

Levlin, E., 2007. Conductivity measurements for controlling municipal waste-water treatment. Land and Water Resources Engineering. https://doi.org/www.diva-portal.org/smash/record.jsf?pid=diva2%3A497628&dswid=-848

Li, S., Peng, C., Cheng, T., Wang, C., Guo, L., Li, D., 2019. Nitrogen-cycling microbial community functional potential and enzyme activities in cultured biofilms with response to inorganic nitrogen availability. J Environ Sci (China). https://doi.org/10.1016/j.jes.2018.03.029

Li, X., Guo, M., 2022. The Impact of Salinization and Wind Erosion on the Texture of Surface Soils: An Investigation of Paired Samples from Soils with and without Salt Crust. Land (Basel) 11. https://doi.org/10.3390/land11070999

Li, X. na, Zhang, W. wei, Wu, J. ying, Li, H. jie, Zhao, T. kai, Zhao, C. qiao, Shi, R. shuang, Li, Z. shuang, Wang, C., Li, C., 2021. Loss of nitrogen and phosphorus from farmland runoff and the interception effect of an ecological drainage ditch in the North China Plain—A field study in a modern agricultural park. Ecol Eng. https://doi.org/10.1016/j.ecoleng.2021.106310

Li, Y., Yang, Z., Yang, K., Wei, J., Li, Z., Ma, C., Yang, X., Wang, T., Zeng, G., Yu, G., Yu, Z., Zhang, C., 2022. Removal of chloride from water and wastewater: Removal mechanisms and recent trends. Science of the Total Environment. https://doi.org/10.1016/j.scitotenv.2022.153174

Lind, L., Schuler, M.S., Hintz, W.D., Stoler, A.B., Jones, D.K., Mattes, B.M., Relyea, R.A., 2018. Salty fertile lakes: how salinization and eutrophication alter the structure of freshwater communities. Ecosphere. https://doi.org/10.1002/ecs2.2383

Link, M., Voß, K., Schäfer, R.B., von der Ohe, P.C., 2017. Comparison of dilution factors for German wastewater treatment plant effluents in receiving streams to the fixed dilution factor from chemical risk assessment. Science of the Total Environment. https://doi.org/10.1016/j.scitotenv.2017.04.180

Linke, S., Lehner, B., Ouellet Dallaire, C., Ariwi, J., Grill, G., Anand, M., Beames, P., Burchard-Levine, V., Maxwell, S., Moidu, H., Tan, F., Thieme, M., 2019. Global hydro-environmental sub-basin and river reach characteristics at high spatial resolution. Sci Data. https://doi.org/10.1038/s41597-019-0300-6

Liu, Y., Wang, P., Gojenko, B., Yu, J., Wei, L., Luo, D., 2021. A review of water pollution arising from agriculture and mining activities in Central Asia : Facts , causes and effects. Environmental Pollution. https://doi.org/10.1016/j.envpol.2021.118209

Luna Juncal, M.J., Masino, P., Bertone, E., Stewart, R.A., 2023. Towards nutrient neutrality: A review of agricultural runoff mitigation strategies and the development of a decision-making framework. Science of the Total Environment. https://doi.org/10.1016/j.scitotenv.2023.162408

Laxen, D.P.H., 1977. A specific conductance method for quality control in water analysis. Pergamon Press. Water Research. https://doi.org/10.1016/0043-1354(77)90188-9

Maas, C.M., Kaushal, S.S., Rippy, M.A., Mayer, P.M., Grant, S.B., Shatkay, R.R., Malin, J.T., Bhide, S. V., Vikesland, P., Krauss, L., Reimer, J.E., Yaculak, A.M., 2023. Freshwater salinization syndrome limits management efforts to improve water quality. Front Environ Sci. https://doi.org/10.3389/fenvs.2023.1106581

Machado, M.J., Benito, G., Barriendos, M., Rodrigo, F.S., 2011. 500 Years of rainfall variability and extreme hydrological events in southeastern Spain drylands. J Arid Environ. https://doi.org/10.1016/j.jaridenv.2011.02.002

Malaeb, L., Ayoub, G.M., 2011. Reverse osmosis technology for water treatment: State of the art review. Desalination. https://doi.org/10.1016/j.desal.2010.09.001

Markert, N., Guhl, B., Feld, C.K., 2022. The hierarchy of multiple stressors' effects on benthic invertebrates: a case study from the rivers Erft and Niers, Germany. Environ Sci Eur. https://doi.org/10.1186/s12302-022-00679-z

Martin, L.E., 2001. Limitations on the use of impermeable mesocosms for ecological experiments involving Aurelia sp. (Scyphozoa:Semaeostomeae). Journal of Plankton Research. https://doi.org/10.1093/plankt/23.1.1

McCleskey, R.B., Nordstrom, D.K., Ryan, J.N., Ball, J.W., 2012. A new method of calculating electrical conductivity with applications to natural waters. Geochim Cosmochim Acta. https://doi.org/10.1016/j.gca.2011.10.031

McDowell, R.W., Noble, A., Kittridge, M., Ausseil, O., Doscher, C., Hamilton, D.P., 2024. Monitoring to detect changes in water quality to meet policy objectives. Sci Rep. https://doi.org/10.1038/s41598-024-52512-7

Meijer, J.R., Huijbregts, M.A.J., Schotten, K.C.G.J., Schipper, A.M., 2018. Global patterns of current and future road infrastructure. Environmental Research Letters. https://doi.org/10.1088/1748-9326/aabd42

Melesse, A.M., Khosravi, K., Tiefenbacher, J.P., Heddam, S., Kim, S., Mosavi, A., Pham, B.T., 2020. River water salinity prediction using hybrid machine learning models. Water (Switzerland) 12, 1–21. https://doi.org/10.3390/w12102951

Merbt, S.N., Auguet, J.C., Blesa, A., Martí, E., Casamayor, E.O., 2015. Wastewater Treatment Plant Effluents Change Abundance and Composition of Ammonia-Oxidizing Microorganisms in Mediterranean Urban Stream Biofilms. Microb. https://doi.org/10.1007/s00248-014-0464-8

Messager, M.L., Dickens, C.W.S., Eriyagama, N., Tharme, R.E., 2024. Limited comparability of global and local estimates of environmental flow requirements to sustain river ecosystems. Environmental Research Letters. https://doi.org/10.1088/1748-9326/ad1cb5

Meybeck, M., 2003. Global Occurrence of Major Elements in Rivers. Paris, France. Treatise on Geochemistry. https://doi.org/10.1016/B0-08-043751-6/05164-1

Meybeck M., 1987. Global chemical weathering of surficial rocks estimated from river dissolved loads. American Journal of Science 287, 401–428.

M.F. Hamoda, I. M. S. Al-attar, 1995. Effects of hihg sodium chloride concentrations on activated sludge treatment. Water Science and Technology. https://doi.org/10.1016/0273-1223(95)00407-E

Mihai, F.C., Gündogdu, S., Markley, L.A., Olivelli, A., Khan, F.R., Gwinnett, C., Gutberlet, J., Reyna-Bensusan, N., Llanquileo-Melgarejo, P., Meidiana, C., Elagroudy, S., Ishchenko, V., Penney, S., Lenkiewicz, Z., Molinos-Senante, M., 2022. Plastic Pollution, Waste Management Issues, and Circular Economy Opportunities in Rural Communities. Sustainability (Switzerland). https://doi.org/10.3390/su14010020

Moglia, M., 2008. Sources of critical contaminants in domestic wastewater: contaminant loads from household appliances. Environmental Nanotechnology, Monitoring & Management. https://doi.org/10.1016/j.enmm.2024.100894

Molinos-Senante, M., Hernández-Sancho, F., Sala-Garrido, R., 2011. Assessing disproportionate costs to achieve good ecological status of water bodies in a Mediterranean river basin. Journal of Environmental Monitoring. https://doi.org/10.1039/c1em10209e

Mondal, N.C., Singh, V.P., Singh, V.S., Saxena, V.K., 2010. Determining the interaction between groundwater and saline water through groundwater major ions chemistry. J Hydrol (Amst). https://doi.org/10.1016/j.jhydrol.2010.04.032

Moreira-Nordemann, L.M., 1984. Salinity and weathering rate of rocks in a semi-arid region, Journal of Hydrology. https://doi.org/10.1016/0022-1694(84)90074-X

Moussa, M.S., Sumanasekera, D.U., Ibrahim, S.H., Lubberding, H.J., Hooijmans, C.M., Gijzen, H.J., Van Loosdrecht, M.C.M., 2006. Long term effects of salt on activity, population structure and floc characteristics in enriched bacterial cultures of nitrifiers. Water Res. https://doi.org/10.1016/j.watres.2006.01.029

Moyano Salcedo, A.J., Estévez, E., Salvadó, H., Barquín, J., Cañedo-Argüelles, M., 2023. Human activities disrupt the temporal dynamics of salinity in Spanish rivers. Hydrobiologia 850, 4531–4546. https://doi.org/10.1007/s10750-022-05063-9

Moyano-Salcedo, A.J., Cuadros-Segura, F.D., Pabon Laverde, A.M., Trujillo Arias, J.V., 2021. Environmental Impact of Sewage Discharge Into Illegal UrbanAgglomerates in Villavicencio, Colombia. J. Tecnura. https://doi.org/10.14483/22487638.16273

Munoz, I., Prat, N., 1994. Macroinvertebrate community in the lower Ebro river (NE Spain), Hydrobiologia. https://doi.org/10.1007/BF00008498

Musie, W., Gonfa, G., 2023. Fresh water resource, scarcity, water salinity challenges and possible remedies: A review. Heliyon. https://doi.org/10.1016/j.heliyon.2023.e18685

Neave, M., Rayburg, S., 2006. Salinity and erosion: a preliminary investigation of soil erosion on a salinized hillslope. IAHS Publ. https://api.semanticscholar.org/CorpusID:128564900

Neubacher, E., Prast, M., Cleven, E.J., Berninger, U.G., 2008. Ciliate grazing on Nitrosomonas europaea and Nitrospira moscoviensis: Is selectivity a factor for the nitrogen cycle in natural aquatic systems? Hydrobiologia. https://doi.org/10.1007/s10750-007-9100-7

Newton, A., Icely, J., Cristina, S., Brito, A., Cardoso, A.C., Colijn, F., Riva, S.D., Gertz, F., Hansen, J.W., Holmer, M., Ivanova, K., Leppäkoski, E., Canu, D.M., Mocenni, C., Mudge, S., Murray, N., Pejrup, M., Razinkovas, A., Reizopoulou, S., Pérez-Ruzafa, A., Schernewski, G., Schubert, H., Carr, L., Solidoro, C., Viaroli, P., Zaldívar, J.M., 2014. An overview of ecological status, vulnerability and future perspectives of European large shallow, semi-enclosed coastal systems, lagoons and transitional waters. Estuar Coast Shelf Sci. https://doi.org/10.1016/j.ecss.2013.05.023

Niedrist, G.H., Cañedo-Argüelles, M., Cauvy-Fraunié, S., 2021. Salinization of Alpine rivers during winter months. Environmental Science and Pollution Research. https://doi.org/10.1007/s11356-020-11077-4

Obaideen, K., Shehata, N., Sayed, E.T., Abdelkareem, M.A., Mahmoud, M.S., Olabi, A.G., 2022. The role of wastewater treatment in achieving sustainable development goals (SDGs) and sustainability guideline. Energy Nexus. https://doi.org/10.1016/j.nexus.2022.100112

Olías, M., Nieto, J.M., Sarmiento, A.M., Cerón, J.C., Cánovas, C.R., 2004. Seasonal water quality variations in a river affected by acid mine drainage: The Odiel River (South West Spain). Science of the Total Environment. https://doi.org/10.1016/j.scitotenv.2004.05.012

Olson, J.R., 2019. Predicting combined effects of land use and climate change on river and stream salinity. Philosophical Transactions of the Royal Society B: Biological Sciences. https://doi.org/10.1098/rstb.2018.0005

Ombadi, M., Varadharajan, C., 2022. Urbanization and aridity mediate distinct salinity response to floods in rivers and streams across the contiguous United States. Water Res. https://doi.org/10.1016/j.watres.2022.118664

Ondrasek, G., Rengel, Z., 2021. Environmental salinization processes: Detection, implications & solutions. Science of the Total Environment. https://doi.org/10.1016/j.scitotenv.2020.142432

Ort, C., Siegrist, H., 2009. Assessing wastewater dilution in small rivers with high resolution conductivity probes. Water Science and Technology. https://doi.org/10.2166/wst.2009.174

Pascual-Benito, M., Nadal-Sala, D., Tobella, M., Ballesté, E., García-Aljaro, C., Sabaté, S., Sabater, F., Martí, E., Gracia, C.A., Blanch, A.R., Lucena, F., 2020. Modelling the seasonal impacts of a wastewater treatment plant on water quality in a Mediterranean stream using microbial indicators. J Environ Manage. https://doi.org/10.1016/j.jenvman.2020.110220

Paul, W.L., Cook, R.A., Suter, P.J., Clarke, K.R., Shackleton, M.E., McInerney, P.J., Hawking, J.H., 2018. Long-Term Monitoring of Macroinvertebrate Communities Over 2,300 km of the Murray River Reveals Ecological Signs of Salinity Mitigation Against a Backdrop of Climate Variability. Water Resour Res. https://doi.org/10.1029/2018WR022976

Pauli, W., Jax, K., Berger, S., 2001. Protozoa in Wastewater Treatment: Function and Importance, in: The Handbook of Environmental Chemistry. B Springer. https://doi.org/10.1007/10508767_3

Peces, M., Dottorini, G., Nierychlo, M., Andersen, K.S., Dueholm, M.K.D., Nielsen, P.H., 2022. Microbial communities across activated sludge plants show recurring species-level seasonal patterns. ISME Communications. https://doi.org/10.1038/s43705-022-00098-4

Pereda, O., von Schiller, D., García-Baquero, G., Mor, J.R., Acuña, V., Sabater, S., Elosegi, A., 2021. Combined effects of urban pollution and hydrological stress on ecosystem functions of Mediterranean streams. Science of the Total Environment. https://doi.org/10.1016/j.scitotenv.2020.141971

Pérez-González, A., Urtiaga, A.M., Ibáñez, R., Ortiz, I., 2012. State of the art and review on the treatment technologies of water reverse osmosis concentrates. Water Res. https://doi.org/10.1016/j.watres.2011.10.046

Pérez-Uz, B., Arregui, L., Calvo, P., Salvadó, H., Fernández, N., Rodríguez, E., Zornoza, A., Serrano, S., 2010. Assessment of plausible bioindicators for plant performance in advanced wastewater treatment systems. Water Res. https://doi.org/10.1016/j.watres.2010.07.024

Perri, S., Molini, A., Hedin, L.O., Porporato, A., 2022. Contrasting effects of aridity and seasonality on global salinization. Nat Geosci. https://doi.org/10.1038/s41561-022-00931-4

Perri, S., Suweis, S., Holmes, A., Marpu, P.R., Entekhabi, D., Molini, A., 2020. River basin salinization as a form of aridity. Proc Natl Acad Sci U S A 117, 17635–17642. https://doi.org/10.1073/pnas.2005925117

Pettorelli, N., Schulte to Bühne, H., Tulloch, A., Dubois, G., Macinnis-Ng, C., Queirós, A.M., Keith, D.A., Wegmann, M., Schrodt, F., Stellmes, M., Sonnenschein, R., Geller, G.N., Roy, S., Somers, B., Murray, N., Bland, L., Geijzendorffer, I., Kerr, J.T., Broszeit, S., Leitão, P.J., Duncan, C., El Serafy, G., He, K.S., Blanchard, J.L., Lucas, R., Mairota, P.,

Webb, T.J., Nicholson, E., 2018. Satellite remote sensing of ecosystem functions: opportunities, challenges and way forward. Remote Sens Ecol Conserv. https://doi.org/10.1002/rse2.59

Prat, N., Rieradevall, M., 2006. 25-years of biomonitoring in two mediterranean streams (Llobregat and Besòs basins, NE Spain). Limnetica. https://doi.org/10.23818/limn.25.37

Prosser, I.P., Rutherfurd, I.D., Olley, J.M., Young, W.J., Wallbrink, P.J., Moran, C.J., 2001. Large-scale patterns of erosion and sediment transport in river networks, with examples from Australia, in: Marine and Freshwater Research. https://doi.org/10.1071/MF00033

Puntí, T., Rieradevall, M., Prat, N., 2009. Environmental factors, spatial variation, and specific requirements of chironomidae in mediterranean reference streams. J North Am Benthol Soc. https://doi.org/10.1899/07-172.1

Radwanur, M., Talukder, R., Rutherford, S., Chu, C., 2015. Salinization of Drinking Water in the Context of Climate Change and Sea Level Rise A Public Health Priority for Coastal Bangladesh. The International Journal of Climate Change: Impacts and Responses. https://doi.org/10.18848/1835-7156/CGP/v08i01/37260

Rahman, A.K.M.M., Ahmed, K.M., Butler, A.P., Hoque, M.A., 2018. Influence of surface geology and micro-scale land use on the shallow subsurface salinity in deltaic coastal areas: a case from southwest Bangladesh. Environ Earth Sci. https://doi.org/10.1007/s12665-018-7594-0

Ramos, T.B., Darouich, H., Oliveira, A.R., Farzamian, M., Monteiro, T., Castanheira, N., Paz, A., Alexandre, C., Gonçalves, M.C., Pereira, L.S., 2023. Water use, soil water balance and soil salinization risks of Mediterranean tree orchards in southern Portugal under current climate variability: Issues for salinity control and irrigation management. Agric Water Manag. https://doi.org/10.1016/j.agwat.2023.108319

Reichstein, M., Camps-Valls, G., Stevens, B., Jung, M., Denzler, J., Carvalhais, N., Prabhat, 2019. Deep learning and process understanding for data-driven Earth system science. Nature. https://doi.org/10.1038/s41586-019-0912-1

Richter, B.D., Baumgartner, J. V, Powell, J., Braun, D.P., 1996. A Method for Assessing Hydrologic Alteration within Ecosystems, conservation Biology. https://doi.org/10.1046/j.1523-1739.1996.10041163.x

Rico-Sánchez, A.E., Rodríguez-Romero, A.J., Sedeño-Díaz, J.E., López-López, E., Sundermann, A., 2022. Aquatic macroinvertebrate assemblages in rivers influenced by mining activities. Sci Rep. https://doi.org/10.1038/s41598-022-06869-2

Rodriguez-Sanchez, A., Leyva-Diaz, J.C., Muñoz-Palazon, B., Poyatos, J.M., Gonzalez-Lopez, J., 2019. Influence of salinity cycles in bioreactor performance and microbial community structure of membrane-based tidal-like variable salinity wastewater treatment

systems. Environmental Science and Pollution Research. https://doi.org/10.1007/s11356-018-3608-4

Roe, H.M., Patterson, R.T., 2014. Arcellacea (Testate Amoebae) as Bio-indicators of Road Salt Contamination in Lakes. Microb Ecol. https://doi.org/10.1007/s00248-014-0408-3

Romero, F., Acuña, V., Font, C., Freixa, A., Sabater, S., 2019. Effects of multiple stressors on river biofilms depend on the time scale. Sci Rep. https://doi.org/10.1038/s41598-019-52320-4

Rossum, J.R., 1946. Conductance method for checking accuracy of water analyses. J. Anal Chem. https://doi.org/10.1021/ac60029a034

Roveri, M., Franco, V.M., Lucchi, R., Rogledi, S., 2003. Sedimentary and tectonic evolution of the Vena del Gesso basin (Northern Apennines, Italy): Implications for the onset of the Messinian salinity crisis, GSA Bulletin. https://doi.org/10.1130/0016-7606(2003)115<0387:SATEOT>2.0.CO;2

Russoniello, C.J., Fernandez, C., Bratton, J.F., Banaszak, J.F., Krantz, D.E., Andres, A.S., Konikow, L.F., Michael, H.A., 2013. Geologic effects on groundwater salinity and discharge into an estuary. J Hydrol (Amst) 498, 1–12. https://doi.org/10.1016/j.jhydrol.2013.05.049

Ruth, O., 2003. The effects of de-icing in Helsinki urban streams, Southern Finland. Water Science and Technology. https://doi.org/10.2166/wst.2003.0486

Sabater, F., Sabater, S., Armengol, J., 1990. Chemical characteristics of a mediterranean river as influenced by land uses in the watershed, War. Res. https://doi.org/10.1016/0043-1354(90)90097-P

Salcedo Moyano, A.J., Delforno, T.P., Subtil, E.L., 2022. Simultaneous nitrification-denitrification (SND) using a thermoplastic gel as support: pollutants removal and microbial community in a pilot-scale biofilm membrane bioreactor. Environmental Technology. https://doi.org/10.1080/09593330.2021.1950843

Salvadó, H., Canals, O., Pérez-Uz, B., Arregui, L., Serrano, S., 2024. Deactivation of internal recirculation in a full-scale Biological Nutrient Removal (BNR) Wastewater Treatment Plant (WWTP) reveals outstanding microeukaryotic bioindicators. Journal of Water Process Engineering. https://doi.org/10.1016/j.jwpe.2023.104669

Salvadó, H., Mas, M., Menéndez, S., Gracia, P., 2001. Effects of Shock Loads of Salt on Protozoan Communities of Activated Sludge. Acta Protozool. https://api.semanticscholar.org/CorpusID:6777365

Sampedro, T., Tristán, C., Gómez-Coma, L., Rioyo, J., Sainz, M., Ortiz, I., Ibañez, R., 2023. SWRO concentrates for more efficient wastewater reclamation. Desalination. https://doi.org/10.1016/j.desal.2022.116156

Sauer, F.G., Bundschuh, M., Zubrod, J.P., Schäfer, R.B., Thompson, K., Kefford, B.J., 2016. Effects of salinity on leaf breakdown: Dryland salinity versus salinity from a coalmine. Aquatic Toxicology. https://doi.org/10.1016/j.aquatox.2016.06.014

Scheelbeek, P.F.D., Khan, A.E., Mojumder, S., Elliott, P., Vineis, P., 2016. Drinking Water Sodium and Elevated Blood Pressure of Healthy Pregnant Women in Salinity-Affected Coastal Areas. Hypertension. https://doi.org/10.1161/HYPERTENSIONAHA.116.07743

Schober, P., Schwarte, L.A., 2018. Correlation coefficients: Appropriate use and interpretation. Anesth Analg. https://doi.org/10.1213/ANE.0000000000002864

Schuler, M.S., Cañedo-Argüelles, M., Hintz, W.D., Dyack, B., Birk, S., Relyea, R.A., 2019. Regulations are needed to protect freshwater ecosystems from salinization. Philosophical Transactions of the Royal Society B: Biological Sciences. https://doi.org/10.1098/rstb.2018.0019

Schulz, C.J., Cañedo-Argüelles, M., 2019. Lost in translation: The German literature on freshwater salinization. Philosophical Transactions of the Royal Society B: Biological Sciences. https://doi.org/10.1098/rstb.2018.0007

Sebastiá, M.T., Rodilla, M., Falco, S., Sanchis, J.A., 2013. Analysis of the effects of wet and dry seasons on a Mediterranean river basin: Consequences for coastal waters and its quality management. Ocean Coast Manag. https://doi.org/10.1016/j.ocecoaman.2013.03.012

Serra, S.R.Q., Graça, M.A.S., Dolédec, S., Feio, M.J., 2017. Chironomidae traits and life history strategies as indicators of anthropogenic disturbance. Environ Monit Assess. https://doi.org/10.1007/s10661-017-6027-y

Serraj, R., Pingali, P., 2019. Agriculture & Food Systems to 2050 Global Trends, Challenges and Opportunities, World Scientific P. ed. World Scientific P., London. https://doi.org/10.1142/11212

Setiawan, I., Morgan, L.K., Doscher, C., 2023. Saltwater intrusion from an estuarine river: A field investigation. J Hydrol (Amst) 617. https://doi.org/10.1016/j.jhydrol.2022.128955

Sheikh, M., Harami, H.R., Rezakazemi, M., Cortina, J.L., Aminabhavi, T.M., Valderrama, C., 2023. Towards a sustainable transformation of municipal wastewater treatment plants into biofactories using advanced NH3-N recovery technologies: A review. Science of the Total Environment. https://doi.org/10.1016/j.scitotenv.2023.166077

Shelton, S.A., Kaushal, S.S., Mayer, P.M., Shatkay, R.R., Rippy, M.A., Grant, S.B., Newcomer-Johnson, T.A., 2024. Salty chemical cocktails as water quality signatures: Longitudinal trends and breakpoints along different U.S. streams. Science of the Total Environment. https://doi.org/10.1016/j.scitotenv.2024.172777

Sher, F., Hanif, K., Iqbal, S.Z., Imran, M., 2020. Implications of advanced wastewater treatment: Electrocoagulation and electroflocculation of effluent discharged from a

wastewater treatment plant. Journal of Water Process Engineering. https://doi.org/10.1016/j.jwpe.2019.101101

Shon, H.K., Vigneswaran, S., Snyder, S.A., 2006. Effluent organic matter (EfOM) in wastewater: Constituents, effects, and treatment. Crit Rev Environ Sci Technol. https://doi.org/10.1080/10643380600580011

Silver, S., Donini, A., 2021. Physiological responses of freshwater insects to salinity: molecular-, cellular- And organ-level studies. Journal of Experimental Biology. https://doi.org/10.1242/jeb.222190

Simões, M., Simões, L.C., Vieira, M.J., 2010. A review of current and emergent biofilm control strategies. LWT. https://doi.org/10.1016/j.lwt.2009.12.008

Simpson, 2017. Comparing smooths to factor-smooth interactions I by-variable smooths. R rep. https://gavinsimpson.github.io/gratia/

Singh, A.K., Mondal, G.C., Kumar, S., Singh, T.B., Tewary, B.K., Sinha, A., 2008. Major ion chemistry, weathering processes and water quality assessment in upper catchment of Damodar River basin, India. Environmental Geology. https://doi.org/10.1007/s00254-007-0860-1

Singh, N., Poonia, T., Siwal, S.S., Srivastav, A.L., Sharma, H.K., Mittal, S.K., 2022. Challenges of water contamination in urban areas. https://doi.org/10.1016/b978-0-323-91838-1.00008-7

Srivastava, A., Parida, V.K., Majumder, A., Gupta, B., Gupta, A.K., 2021. Treatment of saline wastewater using physicochemical, biological, and hybrid processes: Insights into inhibition mechanisms, treatment efficiencies and performance enhancement. J Environ Chem Eng. https://doi.org/10.1016/j.jece.2021.105775

Stoffels, R.J., Booker, D.J., Franklin, P.A., Holmes, R., 2024. Monitoring for the adaptive management of rivers. J Environ Manage. https://doi.org/10.1016/j.jenvman.2023.119787

Stoler, A.B., Walker, B.M., Hintz, W.D., Jones, D.K., Lind, L., Mattes, B.M., Schuler, M.S., Relyea, R.A., 2017. Combined effects of road salt and an insecticide on wetland communities. Environ Toxicol Chem. https://doi.org/10.1002/etc.3639

Sun, C., Zhang, B., Ning, D., Zhang, Y., Dai, T., Wu, L., Li, T., Liu, W., Zhou, J., Wen, X., 2021. Seasonal dynamics of the microbial community in two full-scale wastewater treatment plants: Diversity, composition, phylogenetic group based assembly and co-occurrence pattern. Water Res. https://doi.org/10.1016/j.watres.2021.117295

Szklarek, S., Górecka, A., Wojtal-Frankiewicz, A., 2022. The effects of road salt on freshwater ecosystems and solutions for mitigating chloride pollution - A review. Science of the Total Environment. https://doi.org/10.1016/j.scitotenv.2021.150289

Szöcs, E., Kefford, B.J., Schäfer, R.B., 2012. Is there an interaction of the effects of salinity and pesticides on the community structure of macroinvertebrates? Science of the Total Environment. https://doi.org/10.1016/j.scitotenv.2012.07.066

Tang, J., Liu, D., Shang, C., Niu, J., 2024. Impacts of land use change on surface infiltration capacity and urban flood risk in a representative karst mountain city over the last two decades. J Clean Prod. https://doi.org/10.1016/j.jclepro.2024.142196

Tariq, A., Mushtaq, A., 2023. Untreated Wastewater Reasons and Causes: A Review of Most Affected Areas and Cities, IJCBS. Tariq and Mushtaq. https://doi.org/10.1016/j.jclepro.2023.1359892

Tauber, J., Flesch, B., Parravicini, V., Svardal, K., Krampe, J., 2021. Influence of road salt thawing peaks on the inflow composition and activated sludge properties in municipal wastewater treatment. Water Science and Technolog. https://doi.org/10.2166/wst.2021.045

Thorslund, J., Bierkens, M.F.P., Oude Essink, G.H.P., Sutanudjaja, E.H., van Vliet, M.T.H., 2021. Common irrigation drivers of freshwater salinisation in river basins worldwide. Nat Commun. https://doi.org/10.1038/s41467-021-24281-8

Thorslund, J., van Vliet, M.T.H., 2020. A global dataset of surface water and groundwater salinity measurements from 1980–2019. Sci Data 7. https://doi.org/10.1038/s41597-020-0562-z

Timpano, A.J., Zipper, C.E., Soucek, D.J., Schoenholtz, S.H., 2018. Seasonal pattern of anthropogenic salinization in temperate forested headwater streams. Water Res 133, 8–18.

Tiyasha, Tung, T.M., Yaseen, Z.M., 2020. A survey on river water quality modelling using artificial intelligence models: 2000–2020. J Hydrol (Amst). https://doi.org/10.1016/j.jhydrol.2020.124670

Tockner, K., Pusch, M., Borchardt, D., Lorang, M.S., 2010. Multiple stressors in coupled river-floodplain ecosystems. Freshw Biol. https://doi.org/10.1111/j.1365-2427.2009.02371.x

Tortajada, S., David, V., Brahmia, A., Dupuy, C., Laniesse, T., Parinet, B., Pouget, F., Rousseau, F., Simon-Bouhet, B., Robin, F.X., 2011. Variability of fresh- and salt-water marshes characteristics on the west coast of France: A spatio-temporal assessment. Water Res. https://doi.org/10.1016/j.watres.2011.05.024

Turunen, K., Räsänen, T., Hämäläinen, E., Hämäläinen, M., Pajula, P., Nieminen, S.P., 2020. Analysing Contaminant Mixing and Dilution in River Waters Influenced by Mine Water Discharges. Water Air Soil Pollut. https://doi.org/10.1007/s11270-020-04683-y

Uygur, A., Kargi, F., 2004. Salt inhibition on biological nutrient removal from saline wastewater in a sequencing batch reactor. Enzyme Microb Technol. https://doi.org/10.1016/j.enzmictec.2003.11.010

van Vliet, M.T.H., Zwolsman, J.J.G., 2008. Impact of summer droughts on the water quality of the Meuse river. J Hydrol (Amst). https://doi.org/10.1016/j.jhydrol.2008.01.001

Vance, T.C., Huang, T., Butler, K.A., 2024. Big data in Earth science: Emerging practice and promise. Science. https://doi.org/10.1126/science.adh9607

Vega, S.P., Gutierrez, R.R., Maturana, A.Y., Escusa, F., 2024. Data limitations in developing countries make river restoration planning challenging. Study case of the Cesar River, Colombia. Ecohydrology and Hydrobiology. https://doi.org/10.1016/j.ecohyd.2024.01.012

Velasco, J., Gutiérrez-Cánovas, C., Botella-Cruz, M., Sánchez-Fernández, D., Arribas, P., Carbonell, J.A., Millán, A., Pallarés, S., 2019. Effects of salinity changes on aquatic organisms in a multiple stressor context. Philosophical Transactions of the Royal Society B: Biological Sciences. https://doi.org/10.1098/rstb.2018.0011

Venâncio, C., Ribeiro, R., Lopes, I., 2022. Seawater intrusion: an appraisal of taxa at most risk and safe salinity levels. Biological Reviews. https://doi.org/10.1111/brv.12803

Vendrell-Puigmitja, L., Proia, L., Espinosa, C., Barral-Fraga, L., Cañedo-Argüelles, M., Osorio, V., Casas, C., Llenas, L., Abril, M., 2022. Hypersaline mining effluents affect the structure and function of stream biofilm. Science of the Total Environment. https://doi.org/10.1016/j.scitotenv.2022.156966

Vengosh, A., Jackson, R.B., Warner, N., Darrah, T.H., Kondash, A., 2014. A critical review of the risks to water resources from unconventional shale gas development and hydraulic fracturing in the United States. Environ Sci Technol. https://doi.org/10.1021/es405118y

Venkatesan, A., Wankat, P.C., 2011. Simulation of ion exchange water softening pretreatment for reverse osmosis desalination of brackish water. Desalination. https://doi.org/10.1016/j.desal.2010.12.022

Venkatesan, A.K., Ahmad, S., Johnson, W., Batista, J.R., 2011. Systems dynamic model to forecast salinity load to the Colorado River due to urbanization within the Las Vegas Valley. Science of the Total Environment. https://doi.org/10.1016/j.scitotenv.2011.03.018

Vineis, P., Chan, Q., Khan, A., 2011. Climate change impacts on water salinity and health. J Epidemiol Glob Health. https://doi.org/10.1016/j.jegh.2011.09.001

Virro, H., Amatulli, G., Kmoch, A., Shen, L., Uuemaa, E., 2021. GRQA: Global River Water Quality Archive. Earth Syst Sci Data. https://doi.org/10.5194/essd-13-5483-2021

Walker, R.H., Belvin, A.C., Mouser, J.B., Pennino, A., Plont, S., Robinson, C.D., Smith, L.B., Thapa, J., Zipper, C.E., Angermeier, P.L., Entrekin, S.A., 2023. Global review reveals how disparate study motivations, analytical designs, and focal ions limit understanding of salinization effects on freshwater animals. Science of the Total Environment. https://doi.org/10.1016/j.scitotenv.2023.164061

Wallace, T.C., Cowan, A.E., Bailey, R.L., 2019. Current sodium intakes in the United States and the modelling of glutamate's incorporation into select savory products. Nutrients. https://doi.org/10.3390/nu11112691

Wang, J., Liu, Q., Wu, B., Hu, H., Dong, D., Yin, J., Ren, H., 2020. Effect of salinity on mature wastewater treatment biofilm microbial community assembly and metabolite characteristics. Science of the Total Environment. https://doi.org/10.1016/j.scitotenv.2019.134437

Wang, J.-L., Zhan, X.-M., Feng, Y.-C., Qian, Y.I., 2005. Effect of Salinity Variations on the Performance of Activated Sludge System. Biomedical and environmental sciences. https://doi.org/10.1013/j.evsc.1312.11.002

Wang, Y., Jiang, X., Li, Y.L., Yang, L.J., Li, Y.H., Liu, Y., Zhou, L., Wang, P.Z., Zhao, X., Wang, H.J., Jeppesen, E., Xie, P., 2023. Interactive Effects of Nutrients and Salinity on Phytoplankton in Subtropical Plateau Lakes of Contrasting Water Depths. Water (Switzerland). https://doi.org/10.3390/w15010069

Watts, R.D., Compton, R.W., Mccammon, J.H., Ouren, D.S., 2003. Intensity of human use, backcountry roads, and analysis of human accessibility. Escholasp. https://escholarship.org/uc/item/764725mt

Weinberger, R., Lyakhovsky, V., Baer, G., Begin, Z.B., 2006. Mechanical modeling and InSAR measurements of Mount Sedom uplift, Dead Sea basin: Implications for effective viscosity of rock salt. Geochemistry, Geophysics, Geosystems 7. https://doi.org/10.1029/2005GC001185

Wells, G.F., Wu, C.H., Piceno, Y.M., Eggleston, B., Brodie, E.L., DeSantis, T.Z., Andersen, G.L., Hazen, T.C., Francis, C.A., Criddle, C.S., 2014. Microbial biogeography across a full-scale wastewater treatment plant transect: Evidence for immigration between coupled processes. Appl Microbiol Biotechnol. https://doi.org/10.1007/s00253-014-5564-3

Wen, H., Xiong, K., Yang, H., Zhang, P., Wang, X., 2022. Dynamic mechanism of the microbiota of high-salinity organic wastewater with salt-tolerant yeast and its application. J Environ Chem Eng. https://doi.org/10.1016/j.jece.2022.107377

Wood, S.N., 2021. Generalized additive models: An introduction with R, second edition, Generalized Additive Models: An Introduction with R, Second Edition. CRC Press. https://doi.org/10.1201/9781315370279

Wu, G., Guan, Y., Zhan, X., 2008. Effect of salinity on the activity, settling and microbial community of activated sludge in sequencing batch reactors treating synthetic saline wastewater. Water Science and Technology. https://doi.org/10.2166/wst.2008.675

Wu, Y.J., Whang, L.M., Fukushima, T., Chang, S.H., 2013. Responses of ammonia-oxidizing archaeal and betaproteobacterial populations to wastewater salinity in a full-scale

municipal wastewater treatment plant. J Biosci Bioeng. https://doi.org/10.1016/j.jbiosc.2012.11.005

Xia, Y., Wen, X., Zhang, B., Yang, Y., 2018. Diversity and assembly patterns of activated sludge microbial communities: A review. Biotechnol Adv. https://doi.org/10.1016/j.biotechadv.2018.03.005

Ya, T., Wang, Z., Liu, J., Zhang, M., Zhang, L., Liu, X., Li, Y., Wang, X., 2023. Responses of microbial interactions to elevated salinity in activated sludge microbial community. Front Environ Sci Eng 17. https://doi.org/10.1007/s11783-023-1660-x

Yang, J., Gao, L., Liu, Q., Guo, Z., 2024. Assessing environmental impacts of response strategies for sustainable food system transformation. Sustainable Development. https://doi.org/10.1002/sd.2795

Yang, J., Zhang, W., 2024. Storm-induced saltwater intrusion responds divergently to sea level rise in a complicated estuary. Environmental Research Letters. https://doi.org/10.1088/1748-9326/ad0e32

Zadereev, E., Lopatina, T., Ovchinnikov, S., Tolomeev, A., 2023. Grazing rate and feeding selectivity of small and large bodied cladocerans in waters from lakes with different salinity and phytoplankton structure. J Oceanol Limnol. https://doi.org/10.1007/s00343-022-2158-2

Zander, F., Kralisch, S., 2016. River basin information system: Open environmental data management for research and decision making. ISPRS Int J Geoinf 5. https://doi.org/10.3390/ijgi5070123

Zhang, C., Wang, Y., Chang, J., Li, J., Pan, S., Yang, B., Zhan, X., Dai, Q., 2024. Global patterns of human–wildlife spatial associations and implications for differentiating conservation strategies. Conservation Biology 38. https://doi.org/10.1111/cobi.14279

Zhao, Y., Park, H.D., Park, J.H., Zhang, F., Chen, C., Li, X., Zhao, D., Zhao, F., 2016. Effect of different salinity adaptation on the performance and microbial community in a sequencing batch reactor. Bioresour Technol. https://doi.org/10.1016/j.biortech.2016.06.032

Zhao, Y., Zhuang, X., Ahmad, S., Sung, S., Ni, S.Q., 2020. Biotreatment of high-salinity wastewater: current methods and future directions. World J Microbiol Biotechnol. https://doi.org/10.1007/s11274-020-02815-4

Zimmer, A., Winkler, I.T., De Albuquerque, C., 2014. Governing wastewater, curbing pollution, and improving water quality for the realization of human rights. Waterlines. https://doi.org/10.3362/2046-1887.2014.034

8. APPENDICES



Supplementary material: Chapter I

GLOBal river SALiniTy and associated ions (GlobSalt)

Alvaro Javier Moyano Salcedo*[1,2,9], Theresa Piana[4], Julie Crabot[9], Ben J. Kefford[3], Elisabeth Berger[4], Shelley E. Arnott[5], Josefin Thorslund[6], Michel Meybeck[7], Sujay S. Kaushal[8], Ralf B. Schäfer[4], Miguel Cañedo-Argüelles Iglesias*[9]

1 FEHM-Lab (Freshwater Ecology, Hydrology and Management), Departament de Biologia Evolutiva, Ecologia i Ciències Ambientals, Facultat de Biologia, Universitat de Barcelona, Barcelona, Spain.

2 Geohazards and Civil Engineering Research Group, Department of Civil Engineering, Saint Thomas Villavicencio University, C/22 No 1a, 500003, Villavicencio, Colombia.

3 Centre for Applied Water Science, Institute for Applied Ecology, University of Canberra, ACT, Australia

4 RPTU Kaiserslautern-Landau, iES - Institute for Environmental Sciences, Landau, Germany

5 Department of Biology, Queen's University, Kingston, Ontario, Canada K7L 3N6

6 Department of Physical Geography and the Bolin Centre for Climate Research, Stockholm University, Stockholm, Sweden. Department of Physical Geography, Utrecht University, Utrecht, The Netherlands.

7 UMR 7619 METIS, Sorbonne Université-CNRS-EPHE, Paris, France

8 Department of Geology & Earth System Science Interdisciplinary Center, University of Maryland, College Park, MD, USA

9 FEHM-Lab (Freshwater Ecology, Hydrology and Management), SHE-2, Institute of Environmental Assessment and Water Research (IDAEA), CSIC, Carrer de Jordi Girona, 18-26, 08034, Barcelona, Spain.

*Corresponding authors: Alvaro Javier Moyano Salcedo, alvaromoyano@ub.edu

Miguel Cañedo-Argüelles Iglesias, mcahse@cid.csic.es

Table S1. Description of the sources used to compile the GlobSalt dataset.

Country/Continent /Global	Source	Description	Number of river station by source	Start Year	End Year
África	Ministère de l'Environnement, de l'Eau et de l'Assainissement - Direction Nationale de l'Hydraulique du Mali	Water quality in African rivers, government institute	14	1987	2015
	Ministry of Agriculture - General Directorate for Water Resources	Water quality in African rivers, government institute	2	1980	1982
	Ministry of Environment, Water and Natural Resources - Central Water Testing Laboratory	Water quality in African rivers, government institute	33	1980	2015
	Ministry of Health - National Chemical Laboratories	Water quality in African rivers, government institute	2	1980	1992
	Ministry of Water & Environment - Directorate of Water Resources Management	Water quality in African rivers, government institute	4	1980	1980
	Ministry of Water and Livestock - Water Laboratories Unit	Water quality in African rivers, government institute	4	1980	2012
	Ministry of Water Resources and Irrigation - National Water Research Center	Water quality in African rivers, government institute	7	1980	1980

Country/Continent /Global	Source	Description	Number of river station by source	Start Year	End Year
	Water Research Institute	Water quality in African rivers, government institute	11	1991	2012
Argentina	Instituto Nacional de Agua - Centro de Tecnología del Uso del Agua	Water quality in Argentine rivers, government institute	12	1980	2013
	Ministerio de Obras Públicas - Subsecretario de Planificación y Gestión Operativa de Proyectos Hídricos	Water quality in Argentine rivers, government institute	132	1980	2023
Asia	Ministry of Environment & Natural Resources - Central Environment Authority	Water quality in Asian rivers, government institute	12	1980	2015
	Ministry of Environmental Protection of the People's Republic of China - China National Environmental Monitoring Center	Water quality in Asian rivers, government institute	10	1980	1997
	Ministry of Public Works - Research Institute for Water Resources Development	Water quality in Asian rivers, government institute	10	1980	1994
	National Institute for Environmental Studies - Center for Global Environment Research	Water quality in Asian rivers, government institute	17	1980	2022
	National Institute of Environmental Research - Environmental Diagnostics Research Department	Water quality in Asian rivers, government institute	3	1982	2022

Country/Continent /Global	Source	Description	Number of river station by source	Start Year	End Year
	University of Engineering and Technology - Institute of Environmental Engineering and Research	Water quality in Asian rivers, government institute	4	1979	2003
	Mekong River Commission - Mekong Secretariat	Water quality in Asian rivers, government institute	96	1985	2009
Australia	QLD AU Gov	Water quality in Australian rivers, government institute	12	1993	2013
	Waterconnect	Water Connect data portal - Australia	6	1980	2018
	Waternws	Water Connect data portal - New South Wales government, Australia	413	1900	2023
	Watervic	Water Connect data portal - Victoria government, Australia	259	1980	2023
	AU Gov	Water quality in Australian rivers, government institute	1198	1980	2018
	Department of the Environment and Heritage - Water Policy Section	Water quality in Australian rivers, government institute	8	1980	1987
Bangladesh	Department of Environment	Water quality in Bangladesh rivers, government institute	5	1980	1995

Country/Continent /Global	Source	Description	Number of river station by source	Start Year	End Year
Brazil	Brazilian Institute of Environment, Renewable and Natural Resources	Water quality in Brazilian rivers, government institute	81	1980	2013
Canada	CA Gov	Water quality in Canadian rivers	111	2000	2023
	Ontario Gov	Water quality in Canadian rivers	423	2000	2016
Chile	General Directorate of Water	Water quality in Chilean rivers, government institute	737	1980	2018
Colombia	Instituto de Hidrología, Meteorología y Estudios Ambientales	Water quality in Colombian rivers, government institute	140	2005	2013
	Instituto Nacional de Salud - Laboratorio Salud Ambiental	Water quality in Colombian rivers, government institute	2	1981	1988
	Red de Calidad Hídrica de Bogotá Tradicional (RCHB-T)	Water quality in Colombian rivers, Bogotá, government institute	30	2006	2023
Ecuador	Ministerio de Desarrollo Urbano y Vivienda - Subsecretaría de Agua Potable, Saneamiento y Residuos Sólidos	Water quality in Ecuadorian rivers, government institute	3	1979	1986
Europe	Waterbase	European Water Quality. European Environment Agency	13765	1969	2021

Country/Continent /Global	Source	Description	Number of river station by source	Start Year	End Year
French	Office National de l¿Eau Potable - Laboratoire de la Qualité des Eaux	Water quality in French rivers, government institute	4	1987	2012
	SIEAdour-Garonne	Water quality in French rivers, government institute	2968	1980	2023
Germany	Daten- und Kartendienst der LUBW	Water quality data, state of Baden-Württemberg Germany	179	2000	2022
	Bavaria (BY): Bayrisches Landesamt für Umwel (LfU)	Water quality data, state of Bavaria Germany	1180	1980	2023
	Berlin (BE): Senatsverwaltung für Mobilität, Verkehr, Klimaschutz und Umwelt (Berlin)	Water quality data, state of Berlin Germany	64	1954	2023
	Bremen (HB): Freie Hansestadt Bremen	Water quality data, state of Bremen Germany	13	2001	2020
	Hamburg (HH): Behörde für Umwelt, Klima, Energie und Agrarwirtschaft	Water quality data, state of Hamburg Germany	9	2000	2024
	Lower-Saxony (NI): Niedersächsischer Landesbetrieb für Wasserwirtschaft, Küsten- und Naturschutz (NLWKN)	Water quality data, state of Lower-Saxony Germany	2951	2000	2020

Country/Continent /Global	Source	Description	Number of river station by source	Start Year	End Year
Global	GEMStat	Global Freshwater Quality for Water Resources Database and Global Change	4420	1980	2022
	Glorich	GLObal RIver Chemistry of the University database of Hamburg	27873	1942	2011
Guatemala	Ministerio de Comunicaciones Infraestructura Y Vivienda - Instituto Nacional de Sismología, Volcánología, Meteorología e Hidrologia	Water quality in Guatemala rivers, government institute	92	1981	2012
India	India-WRIS	Water quality in Indian rivers, government institute	2407	1990	2018
Mexico	Comisión Nacional del Agua	Water quality data for surface locations in Mexico, government institute	2111	2012	2021
	National Commission of Water - General Subdivision of Administration of Water	Water quality in Mexican rivers, government institute	10	1980	1996
New Zealand	National Institute of Water and Atmospheric Research	Water quality in New Zealand rivers, government institute	80	1980	2021
	NIWA	Water quality in New Zealand rivers, government institute	33	1989	2019

Country/Continent /Global	Source	Description	Number of river station by source	Start Year	End Year
Panama	Ministerio de Ambiente Autoridad Nacional del Ambiente	Water quality in Panamanian rivers, government institute	1	1980	1985
	Unidad de Calidad de Agua - Autoridad del Canal de Panamá	Water quality in Panamanian rivers, government institute	53	2003	2010
Peru	General Directorate of Environmental Health	Water quality in Peruvian rivers, government institute	8	1980	1983
Philippines	Department of Environment and Natural Resources - Environmental Management Bureau	Water quality in Philippines rivers, government institute	2	1980	1999
	Department of Health - Bureau of Environmental Health	Water quality in Philippines rivers, government institute	5	1981	1987
Romania	ICPDR	International Commission for the Protection of the Danube River (ICPDR), Romania Europe	117	1989	2018
Senegal	Sénégalaise des Eaux	Water quality in Senegal rivers, government institute	5	1986	2000
South Africa	Department of Water Affairs and Forestry - Institute for Water Quality Studies	Water quality in South Africa rivers, government institute	273	1990	2010

Country/Continent /Global	Source	Description	Number of river station by source	Start Year	End Year
	Department of Water and Sanitation - DWS	Water quality in South Africa rivers, government institute	1710	1960	2022
	Institute for Research Development - Project Hydro-Geodynamics of the Amazon Basin	Water quality in South American rivers, government institute	4	2003	2006
	Organización Panamericana de la Salud	Water quality in South American rivers, government institute	2	1980	1982
Spain	SAICA network	Water Quality Information System of Spanish rivers, government institute	1231	2001	2023
Uruguay	Department of Environmental Evaluation	Water quality in Uruguayan rivers, government institute	5	1980	1994
USA	WQP	USGS Water Quality Portal for surface and groundwaters across the US	37388	1980	2023

Table S2. Examples of unit conversion from parameters form in source data to the GlobSalt version; x1 and x2 are observation values before and after conversion, respectively.

Parameter	Source	Source form Unit	Unit GlobSalt	x1	n	Mx1	Mx2	x2
Nitrate	GLORICH	NO3N µmol L^{-1}	mg L^{-1}	210.268	1000	62.004	14.007	0.0475
Ammonium	GLORICH	NH4N µmol L^{-1}	mg L^{-1}	1.5	1000	18.039	14.007	0.0011
Calcium	GLORICH	Ca µmol L^{-1}	mg L^{-1}	12,154	1000	40.078	40.078	12.154
Magnesium	GLORICH	Mg µmol L^{-1}	mg L^{-1}	12,081	1000	24.305	24.305	12.081
Sodium	GLORICH	Na µmol L^{-1}	mg L^{-1}	11,802	1000	22.99	22.99	11.802
Potassium	GLORICH	K µmol L^{-1}	mg L^{-1}	11,642	1000	39.098	39.098	11.642
Silica	GLORICH	SiO2 µmol L^{-1}	mg L^{-1}	9,880	1000	60.086	28.086	4.618
Chloride	GLORICH	Cl µmol L^{-1}	mg L^{-1}	12,600	1000	35.453	35.453	12.6
Sulphate	GLORICH	SO4 µmol L^{-1}	mg L^{-1}	12	1000	96.062	32.06	0.0040

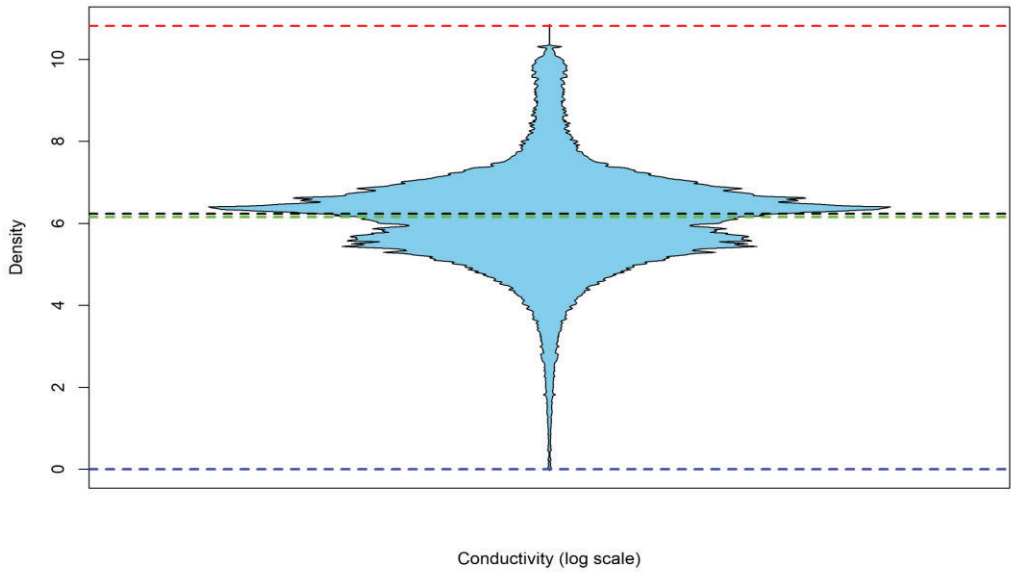


Figure S1. Beanplot of the Conductivity Distribution in GlobSalt. The distribution was adjusted for a log-normal fit, including quartiles and outliers as per this method. The black, green, blue, and red lines represent the median, mean, minimum, and maximum of the data.

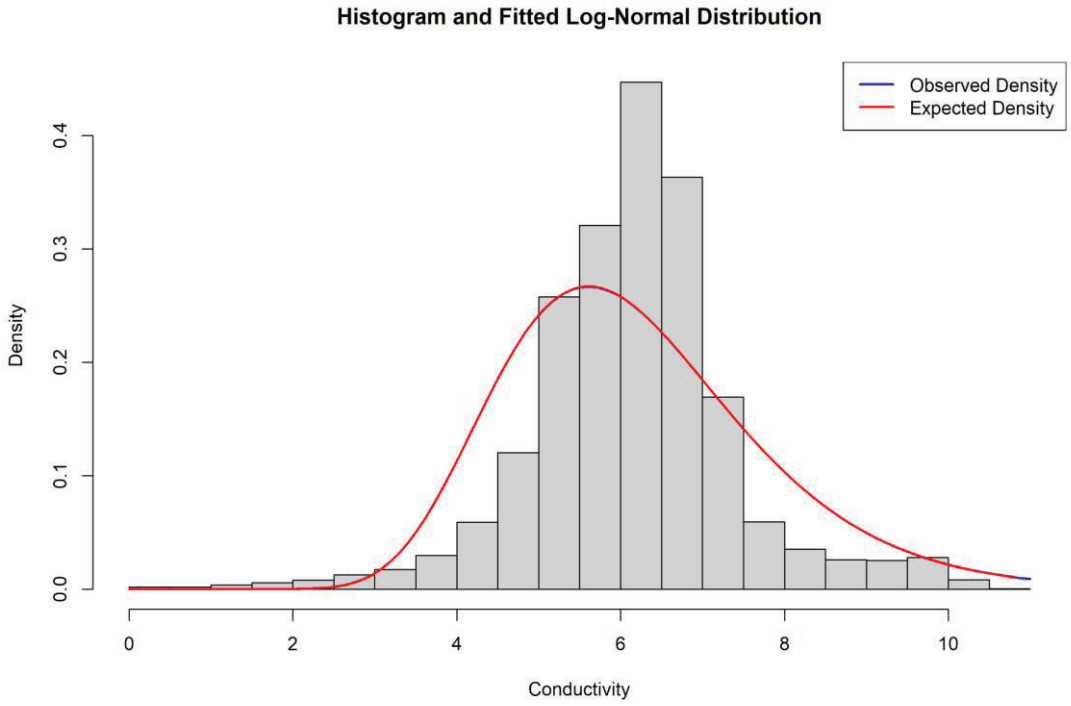


Figure S2. Histogram plot showing both the observed density (blue line) and the expected density (red line) of the conductivity distribution in GlobSalt, along with the fitted log-normal distribution.

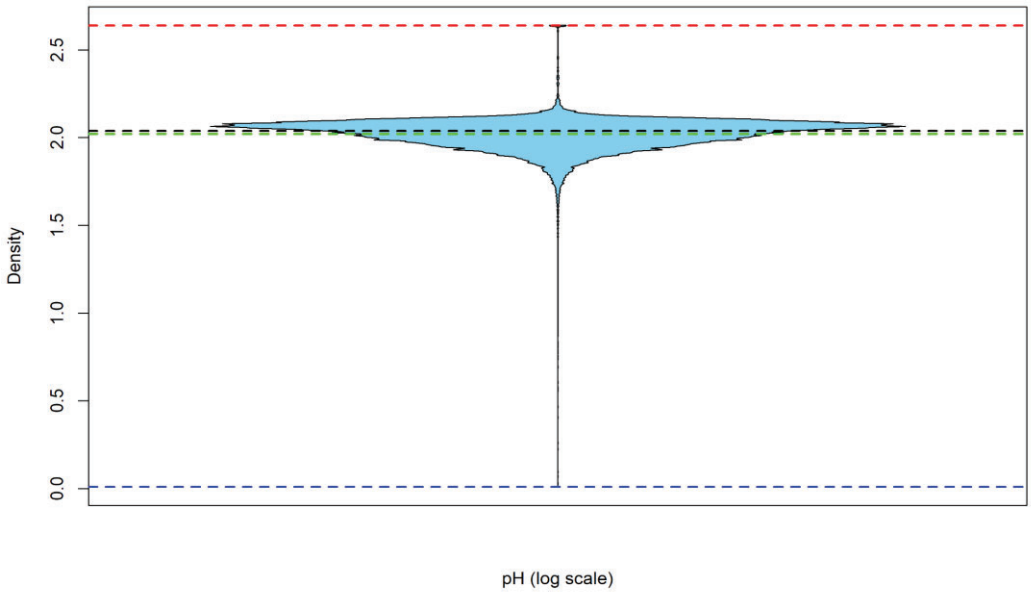


Figure S3. Beanplot of the pH Distribution in GlobSalt. The distribution was adjusted for a log-normal fit, including quartiles and outliers as per this method. The black, green, blue, and red lines represent the median, mean, minimum, and maximum of the data.

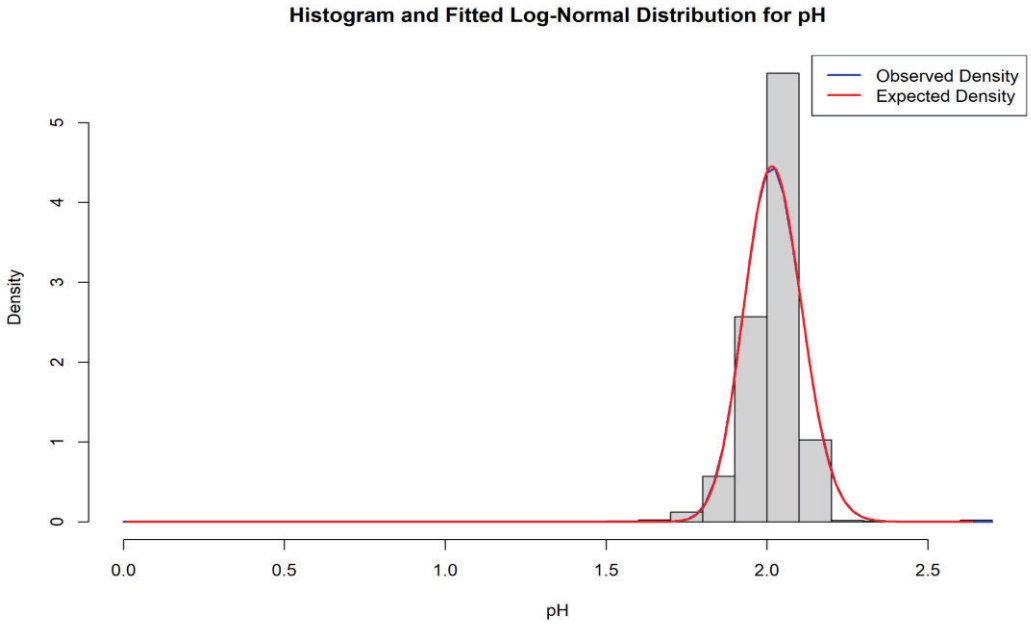


Figure S4. Histogram plot showing both the observed density (blue line) and the expected density (red line) of the pH distribution in GlobSalt, along with the fitted log-normal distribution.

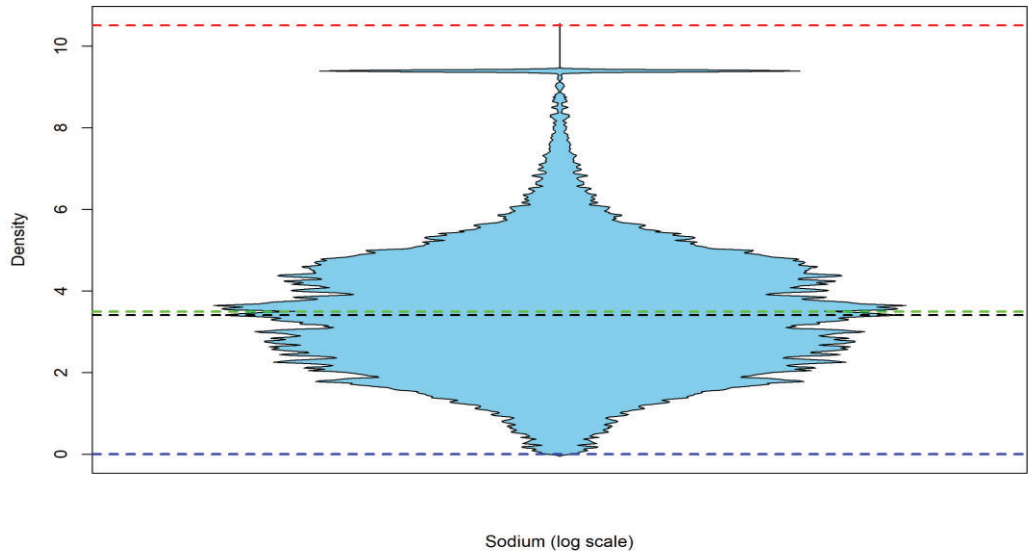


Figure S5. Beanplot of the sodium Distribution in GlobSalt. The distribution was adjusted for a log-normal fit, including quartiles and outliers as per this method. The black, green, blue, and red lines represent the median, mean, minimum, and maximum of the data.

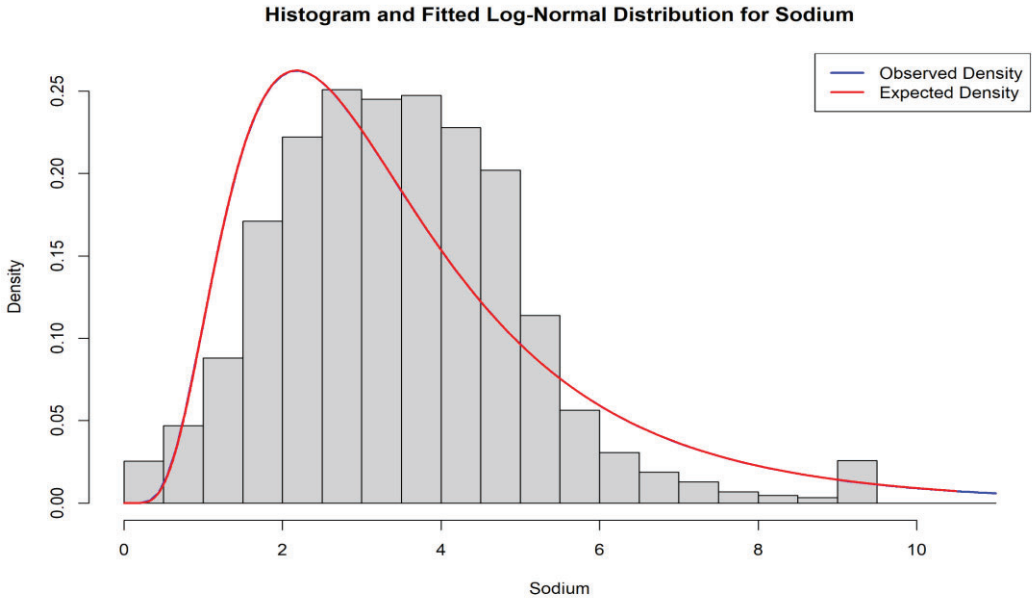


Figure S6. Histogram plot showing both the observed density (blue line) and the expected density (red line) of the sodium distribution in GlobSalt, along with the fitted log-normal distribution.

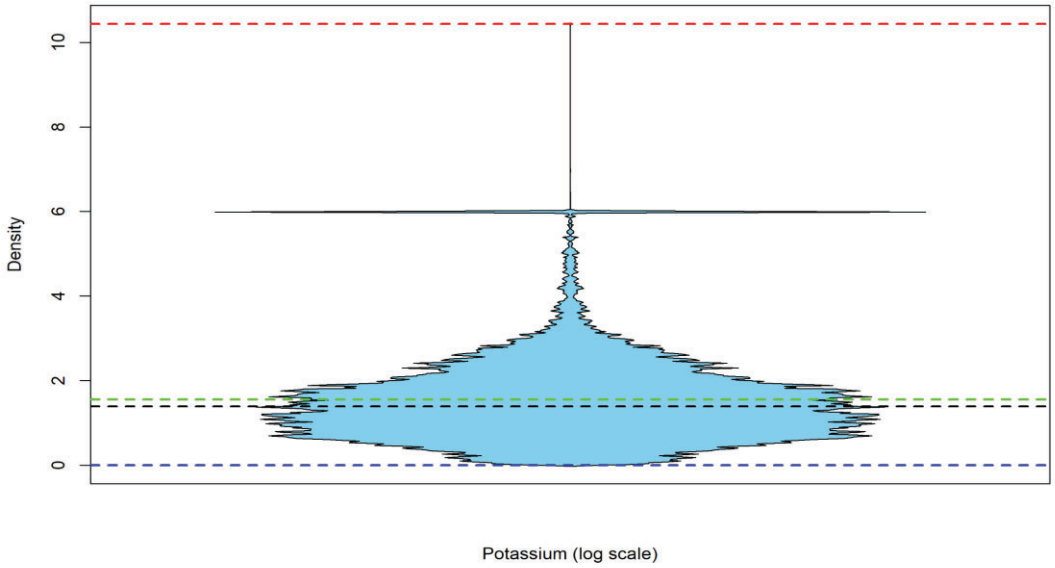


Figure S7. Beanplot of the potassium Distribution in GlobSalt. The distribution was adjusted for a log-normal fit, including quartiles and outliers as per this method. The black, green, blue, and red lines represent the median, mean, minimum, and maximum of the data.

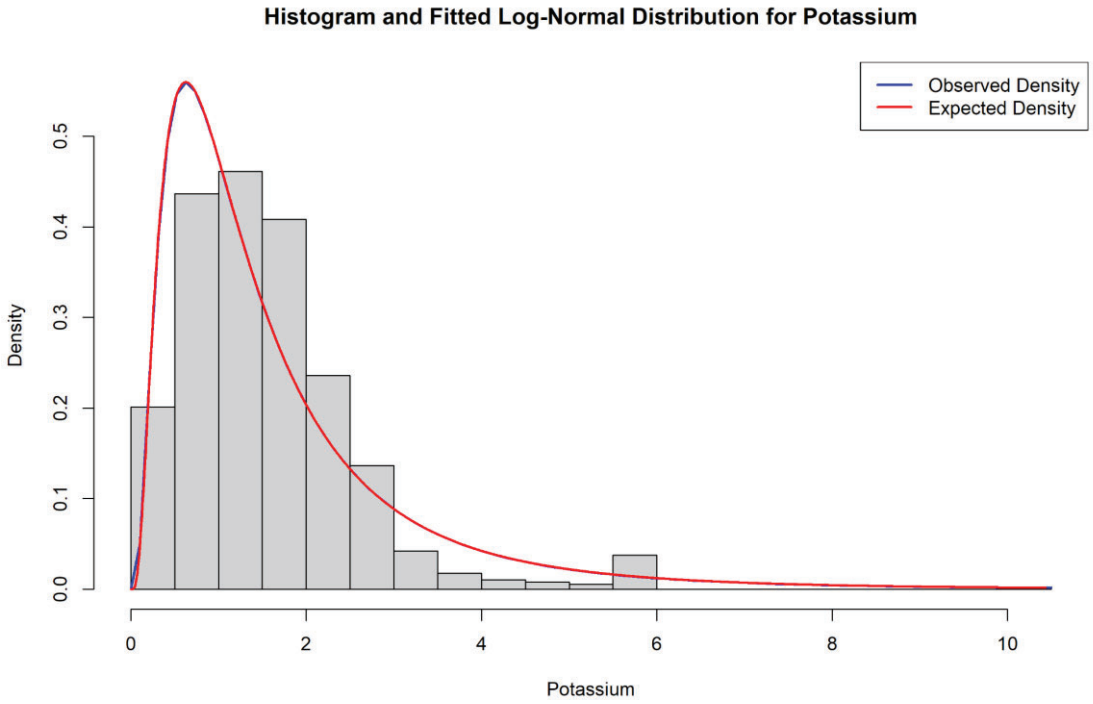


Figure S8. Histogram plot showing both the observed density (blue line) and the expected density (red line) of the potassium distribution in GlobSalt, along with the fitted log-normal distribution.

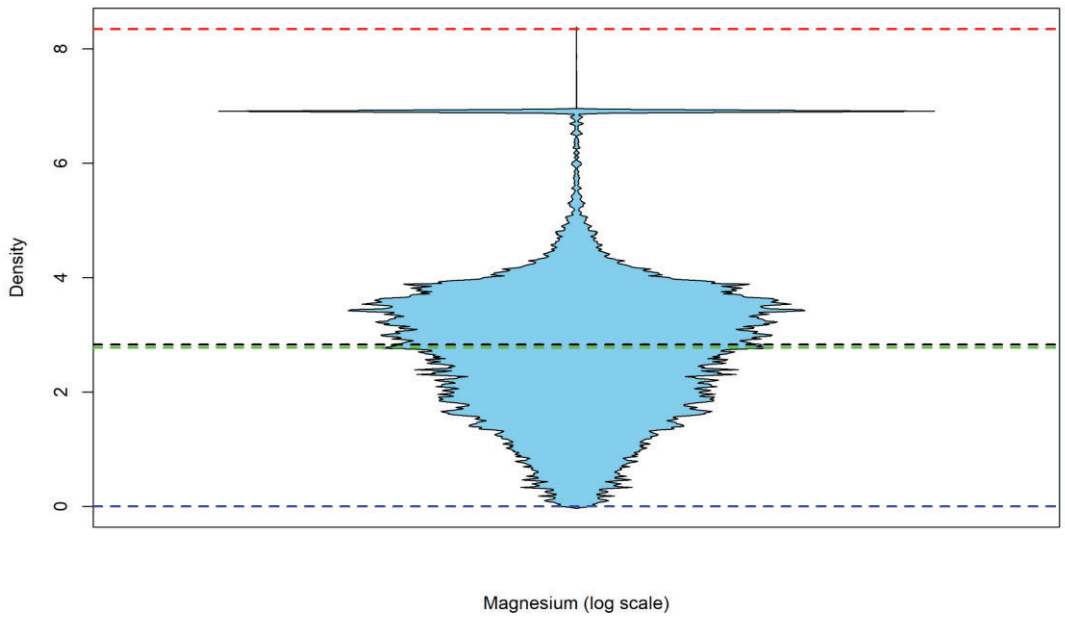


Figure S9. Beanplot of the magnesium Distribution in GlobSalt. The distribution was adjusted for a log-normal fit, including quartiles and outliers as per this method. The black, green, blue, and red lines represent the median, mean, minimum, and maximum of the data.

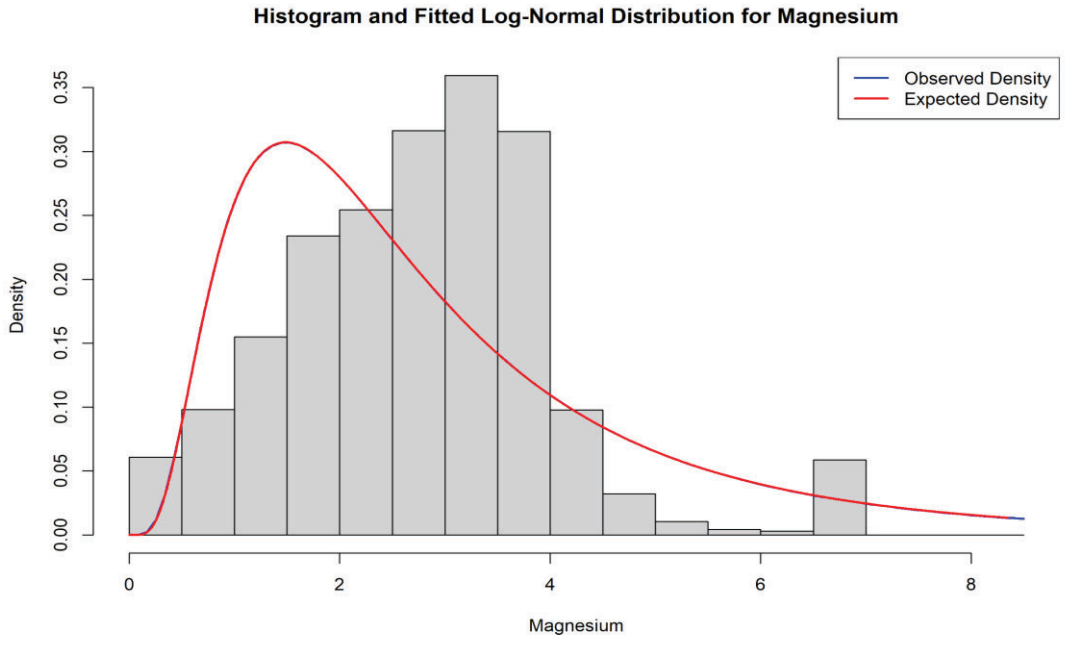


Figure S10. Histogram plot showing both the observed density (blue line) and the expected density (red line) of the magnesium distribution in GlobSalt, along with the fitted log-normal distribution.

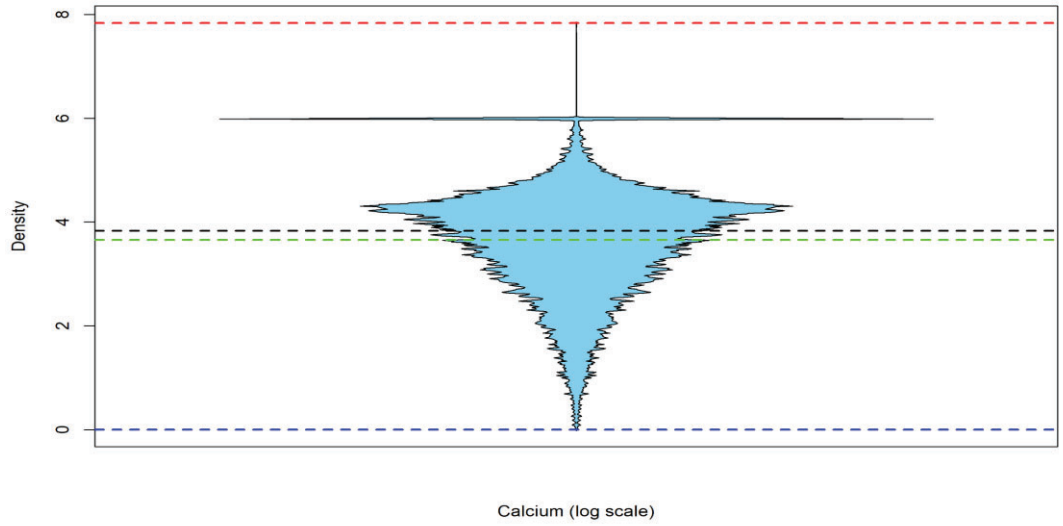


Figure S11. Beanplot of the Calcium Distribution in GlobSalt. The distribution was adjusted for a log-normal fit, including quartiles and outliers as per this method. The black, green, blue, and red lines represent the median, mean, minimum, and maximum of the data.

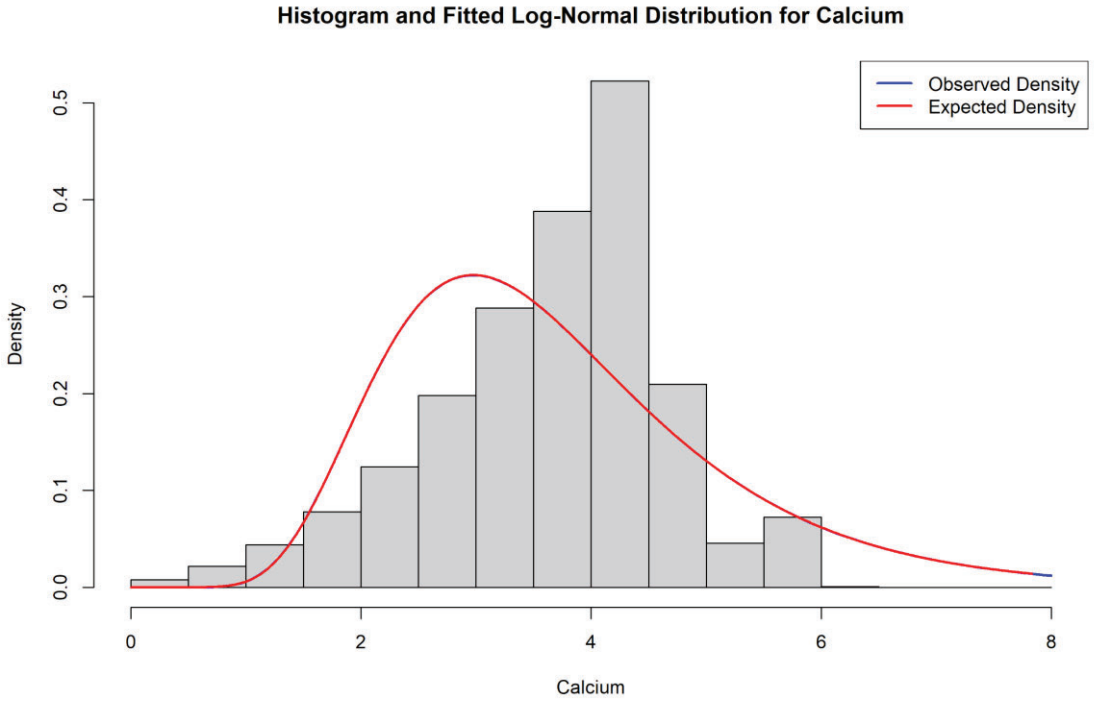


Figure S12. Histogram plot showing both the observed density (blue line) and the expected density (red line) of the calcium distribution in GlobSalt, along with the fitted log-normal distribution.

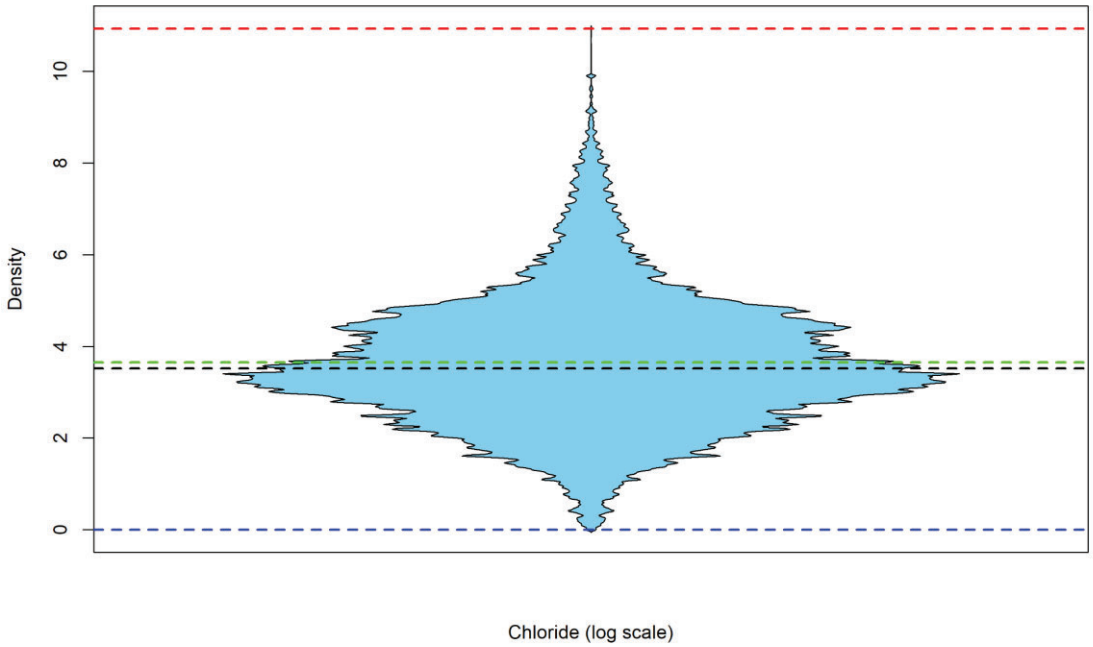


Figure S13. Beanplot of the Chloride Distribution in GlobSalt. The distribution was adjusted for a log-normal fit, including quartiles and outliers as per this method. The black, green, blue, and red lines represent the median, mean, minimum, and maximum of the data.

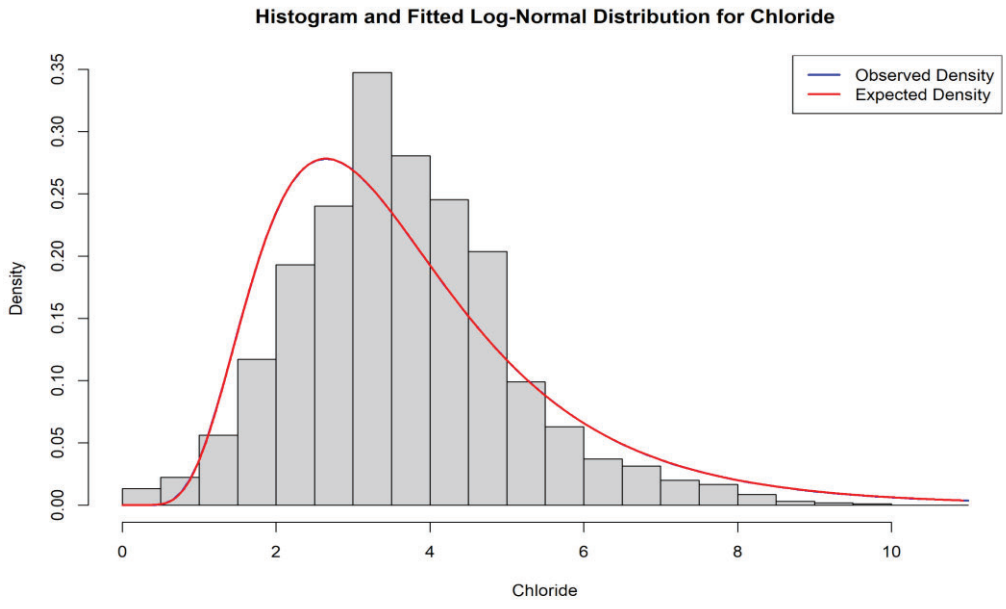
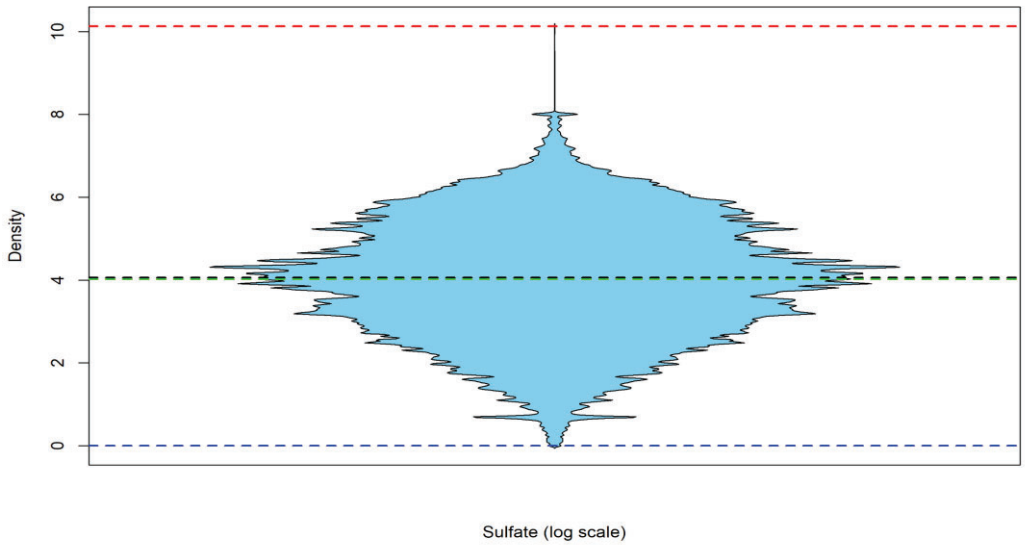


Figure S14. Histogram plot showing both the observed density (blue line) and the expected density (red line) of the chloride distribution in GlobSalt, along with the fitted log-normal distribution.



Figure

S15. Beanplot of the Sulphate Distribution in GlobSalt. The distribution was adjusted for a log-normal fit, including quartiles and outliers as per this method. The black, green, blue, and red lines represent the median, mean, minimum, and maximum of the data.

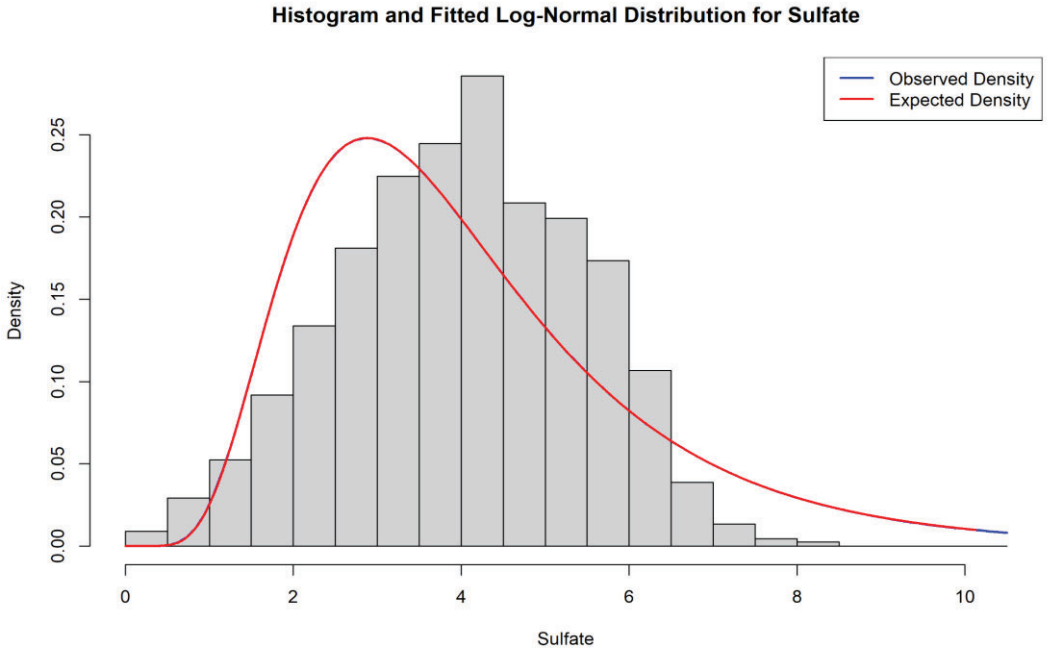


Figure S16. Histogram plot showing both the observed density (blue line) and the expected density (red line) of the sulphate distribution in GlobSalt, along with the fitted log-normal distribution.

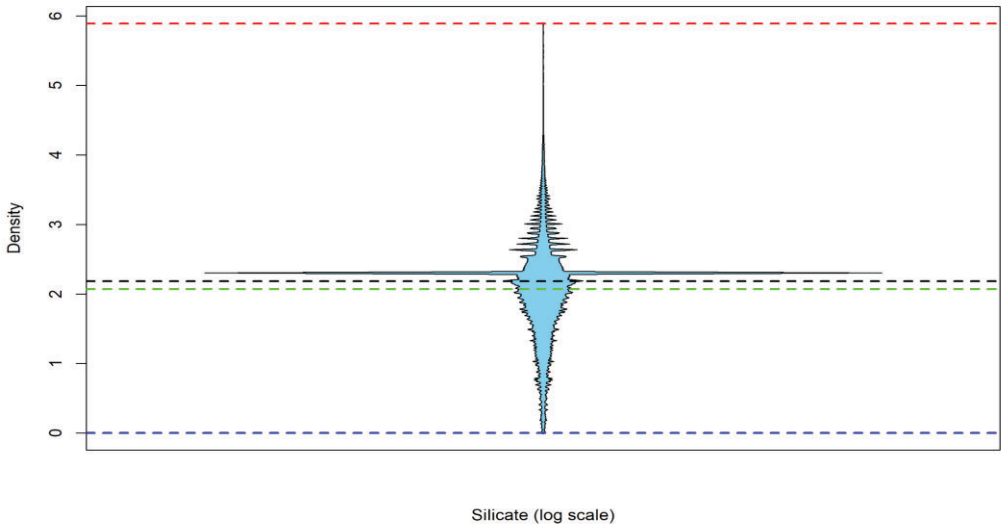


Figure S17. Beanplot of the Silicate Distribution in GlobSalt. The distribution was adjusted for a log-normal fit, including quartiles and outliers as per this method. The black, green, blue, and red lines represent the median, mean, minimum, and maximum of the data.

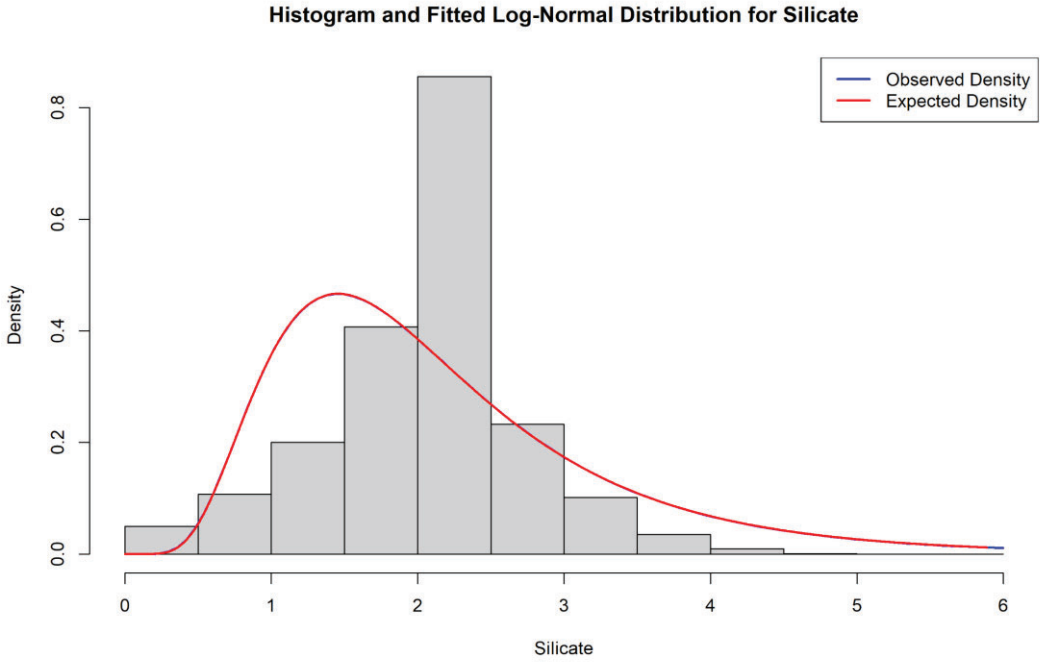


Figure S18. Histogram plot showing both the observed density (blue line) and the expected density (red line) of the silicate distribution in GlobSalt, along with the fitted log-normal distribution.

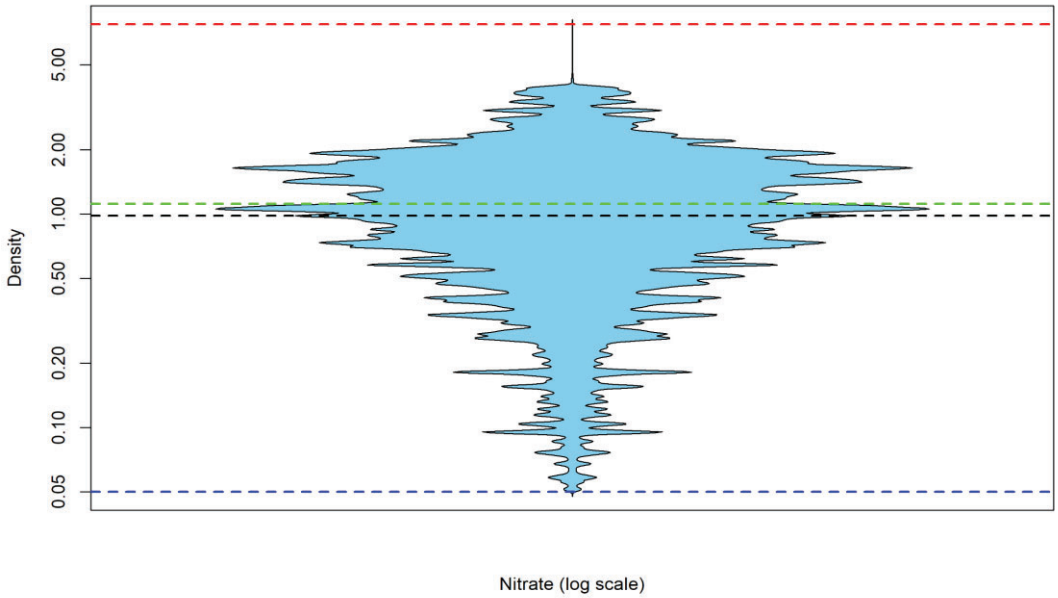


Figure S19. Beanplot of the Nitrate Distribution in GlobSalt. The distribution was adjusted for a log-normal fit, including quartiles and outliers as per this method. The black, green, blue, and red lines represent the median, mean, minimum, and maximum of the data.

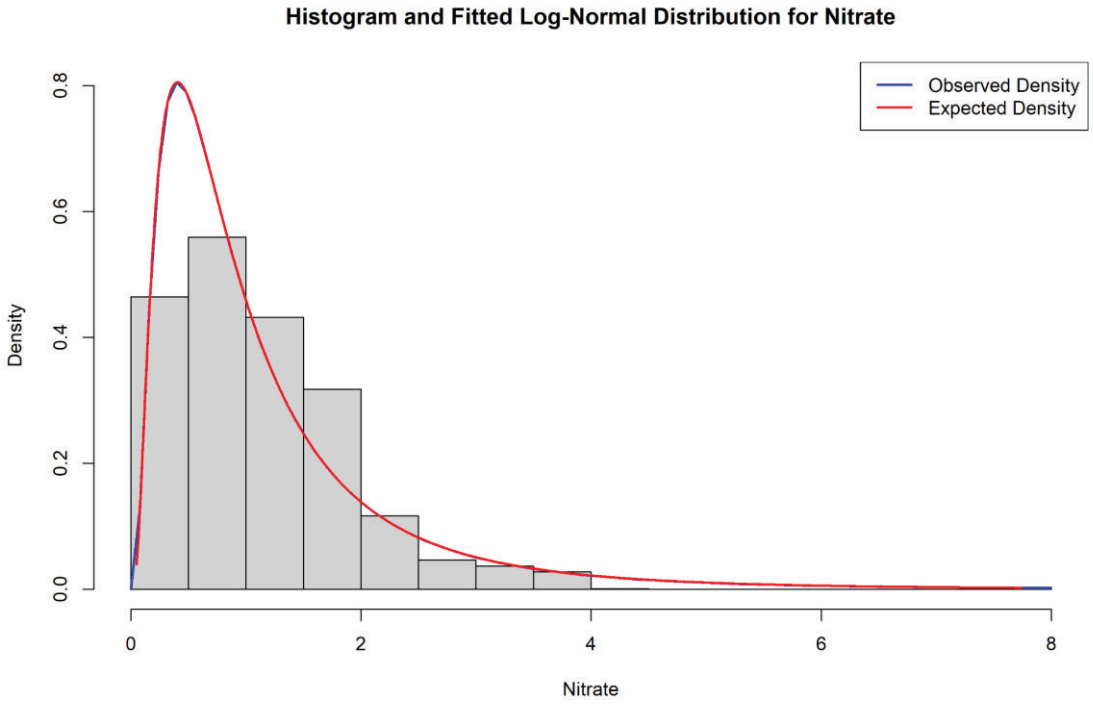


Figure S20. Histogram plot showing both the observed density (blue line) and the expected density (red line) of the nitrate distribution in GlobSalt, along with the fitted log-normal distribution.

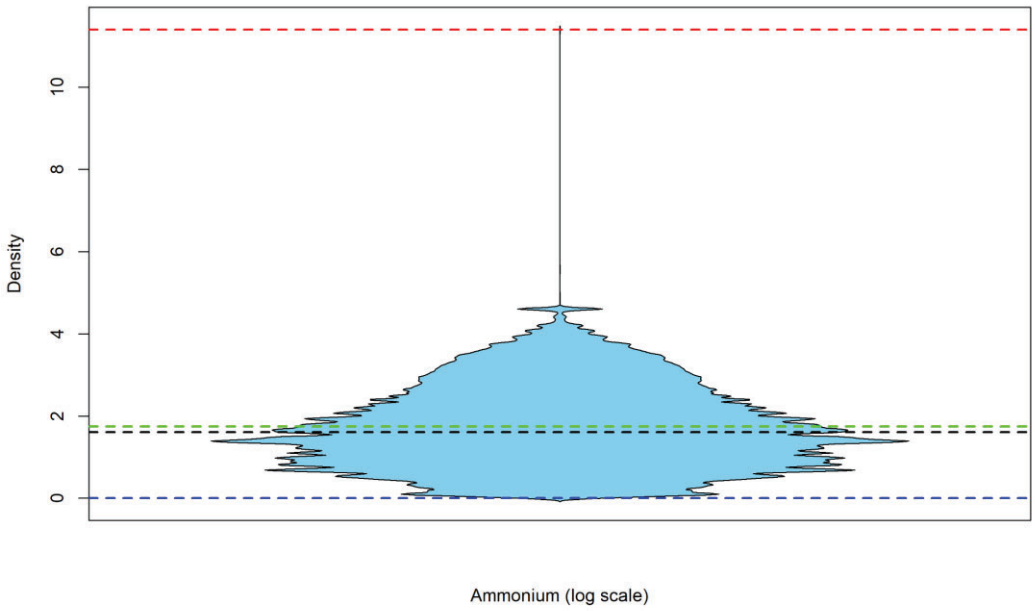


Figure S21. Beanplot of the Ammonium Distribution in GlobSalt. The distribution was adjusted for a log-normal fit, including quartiles and outliers as per this method. The black, green, blue, and red lines represent the median, mean, minimum, and maximum of the data.

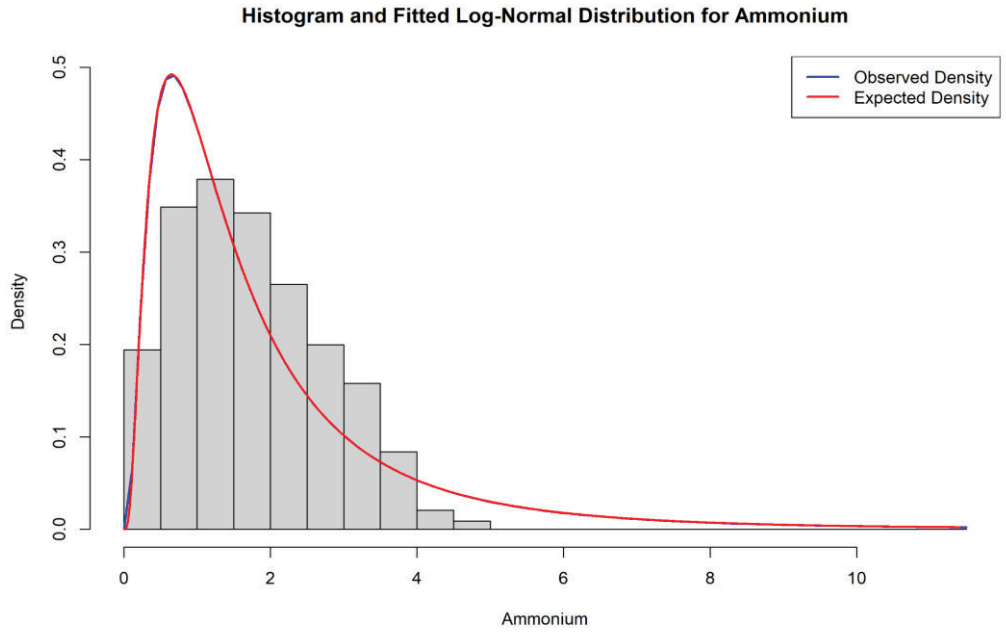


Figure S22. Histogram plot showing both the observed density (blue line) and the expected density (red line) of the ammonium distribution in GlobSalt, along with the fitted log-normal distribution.

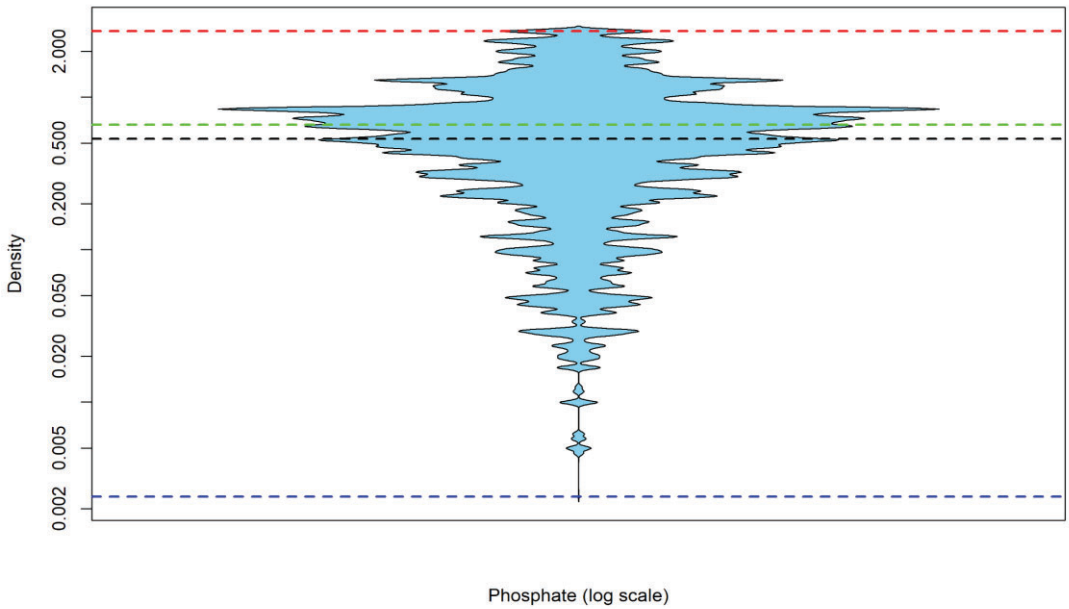


Figure S23. Beanplot of the Phosphate Distribution in GlobSalt. The distribution was adjusted for a log-normal fit, including quartiles and outliers as per this method. The black, green, blue, and red lines represent the median, mean, minimum, and maximum of the data.

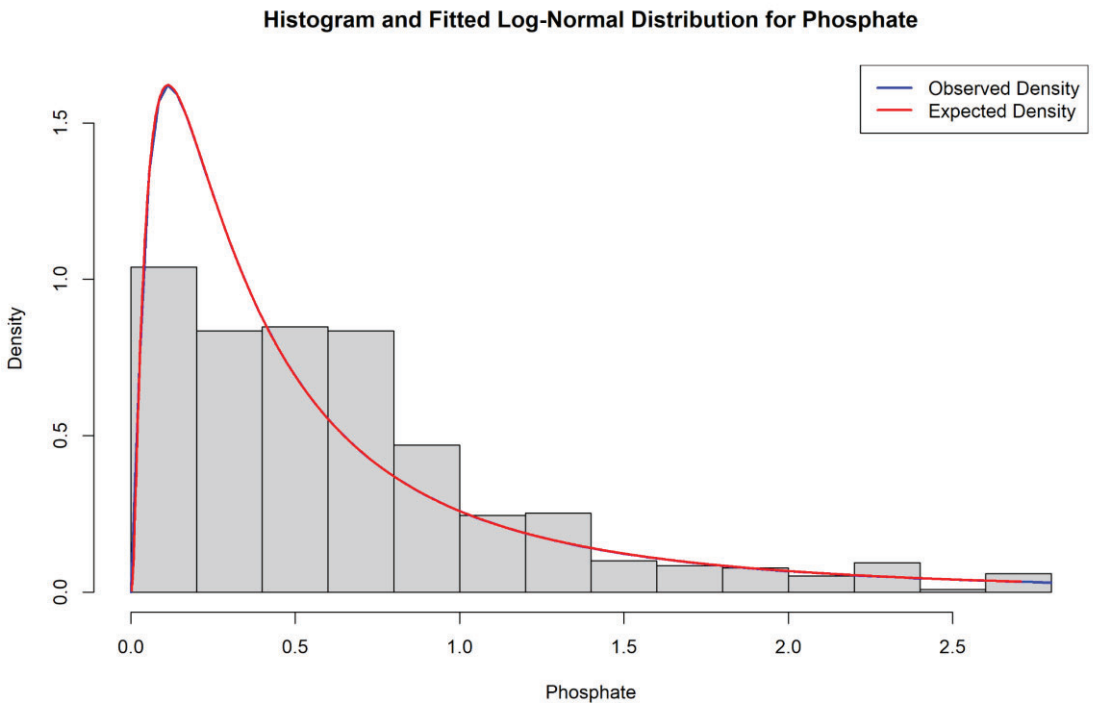


Figure S24. Histogram plot showing both the observed density (blue line) and the expected density (red line) of the phosphate distribution in GlobSalt, along with the fitted log-normal distribution.

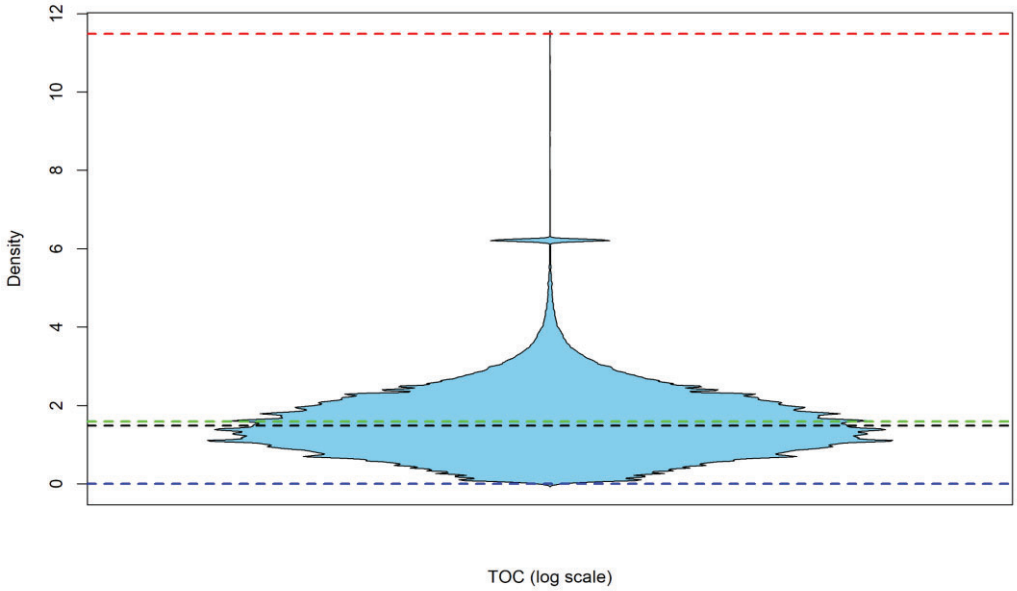


Figure S25. Beanplot of the Total Organic Carbon (TOC) Distribution in GlobSalt. The distribution was adjusted for a log-normal fit, including quartiles and outliers as per this method. The black, green, blue, and red lines represent the median, mean, minimum, and maximum of the data.

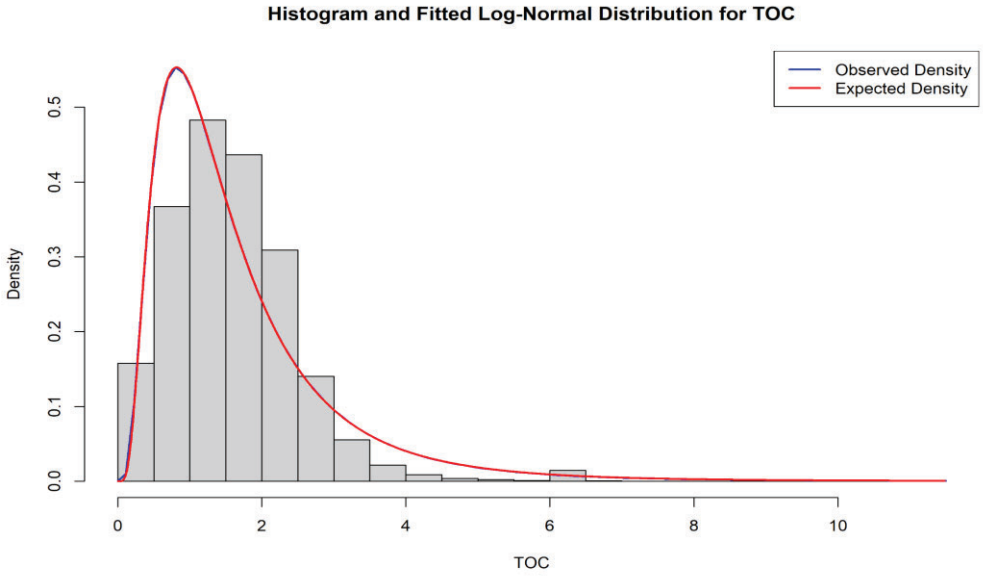


Figure S26. Histogram plot showing both the observed density (blue line) and the expected density (red line) of the Total Organic Carbon (TOC) distribution in GlobSalt, along with the fitted log-normal distribution.

GlobSalt data catalog

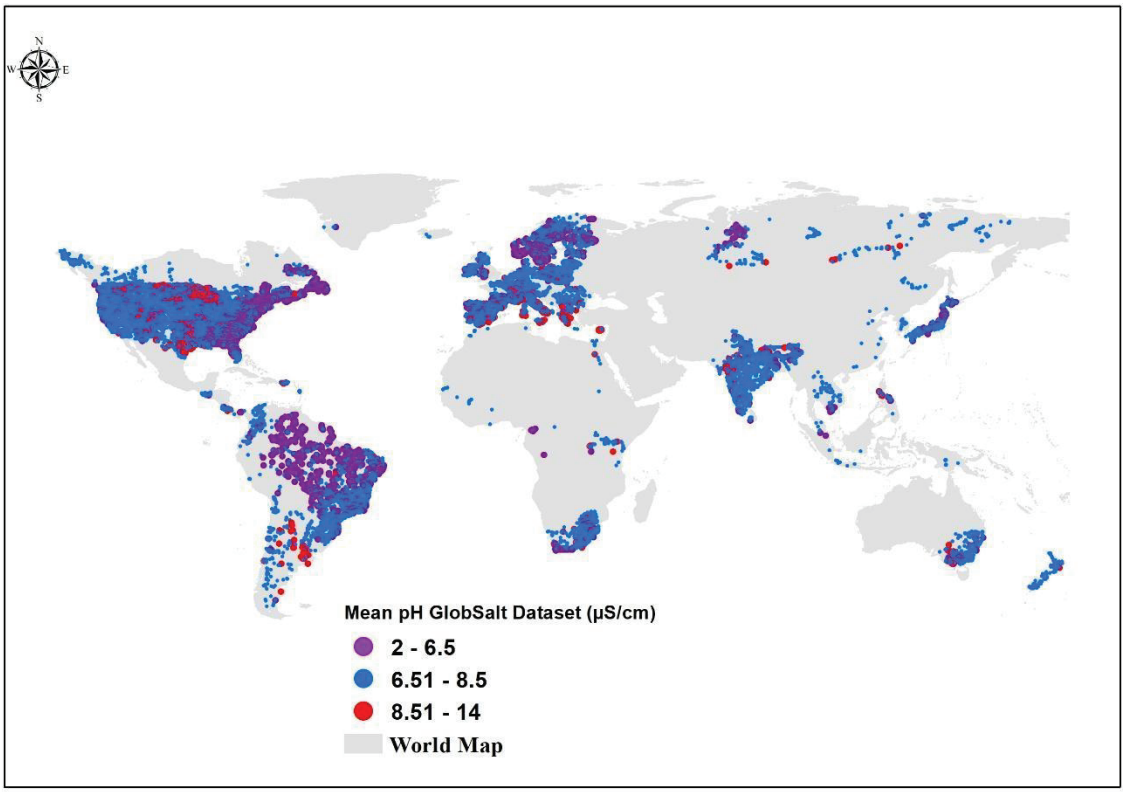


Figure C1. Global distribution of measured mean pH and station density. The global map in the panel shows the measured mean pH values per river in each country, based on observations included in the GlobSalt database, over the entire data period (1980-2023). Purple, blue, and red dots represent pH levels as follows: purple for acidic (low) pH (2-6.5), blue for neutral to slightly alkaline pH (6.5-8.5), and red for basic (high) pH (8.5-14), respectively.

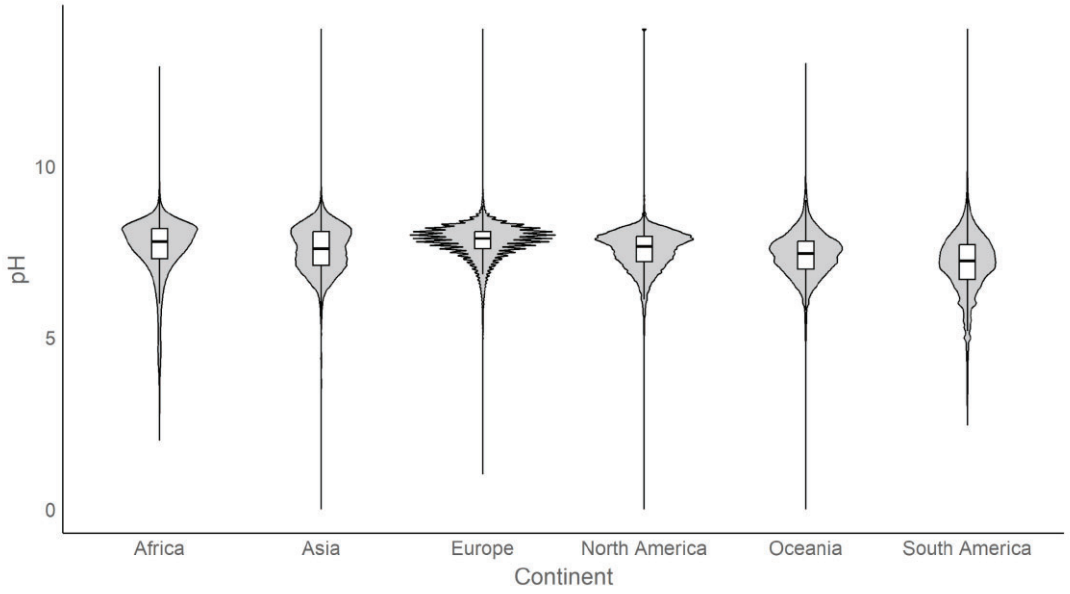


Figure C2. Global violin plot of pH by continent. Global Violin Plot of pH by Continent. EC observations are included in the GlobSalt database, over the entire data period (1980-2023). Each gray violin plot represents the available data set according to the number (n) of observations per continent (Africa n = 222081, Asia n= 146318, Europe n = 862589, North America n = 9657892, Oceania n = 94118, South America n = 67352).

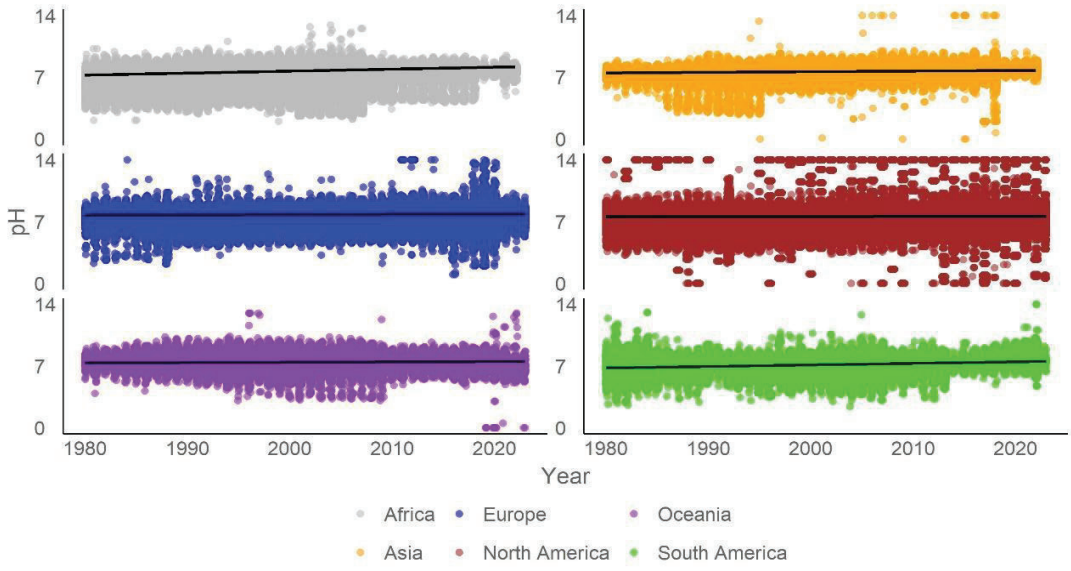


Figure C3. Global temporal dispersion plot pH by continent. pH observations are included in the GlobSalt database over the entire data period (1980-2023). Each color point (gray, yellow, blue, brown, purple, and green) represents the number (n) of observations per continent (Africa n = 222081, Asia n= 146318, Europe n = 862589, North America n = 9657892, Oceania n = 94118, South America n = 67352).

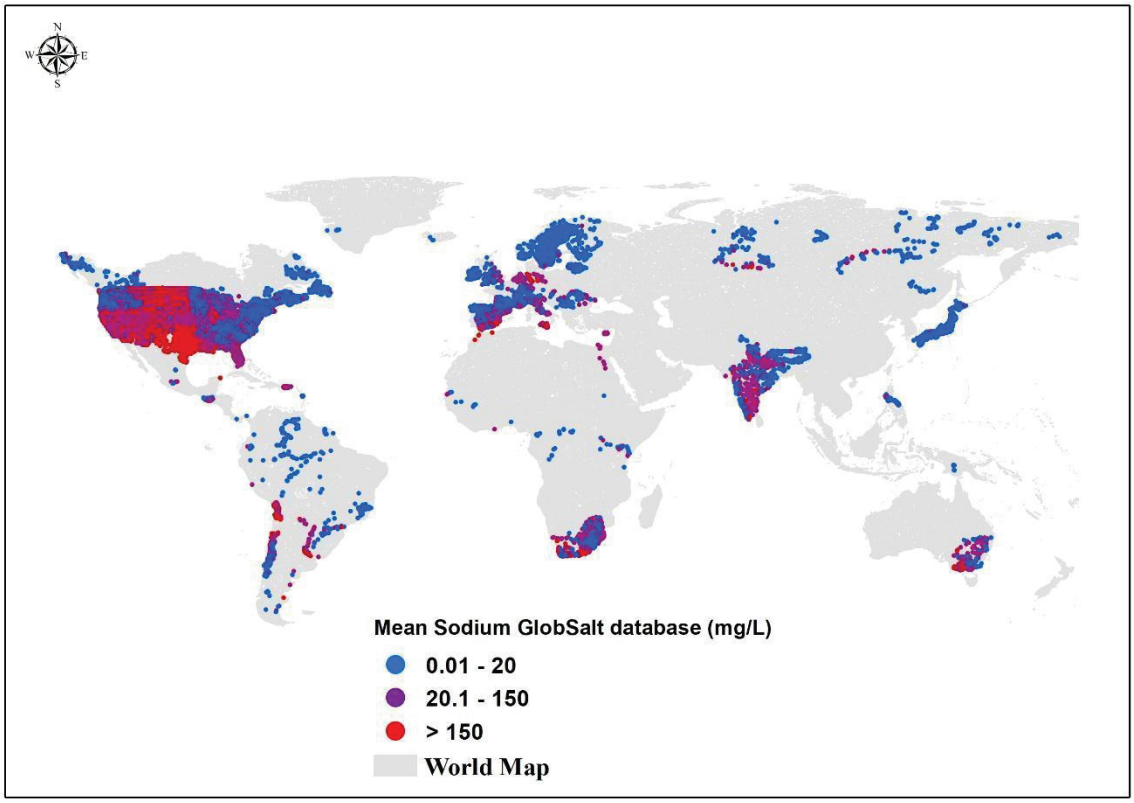


Figure C4. Global distribution of measured mean dissolved sodium and station density. The global map in the panel shows the measured mean sodium values per river in each country, based on observations included in the GlobSalt database, over the entire data period (1980-2023). Ble, purple, and red dots represent low, moderate, and high sodium, respectively.

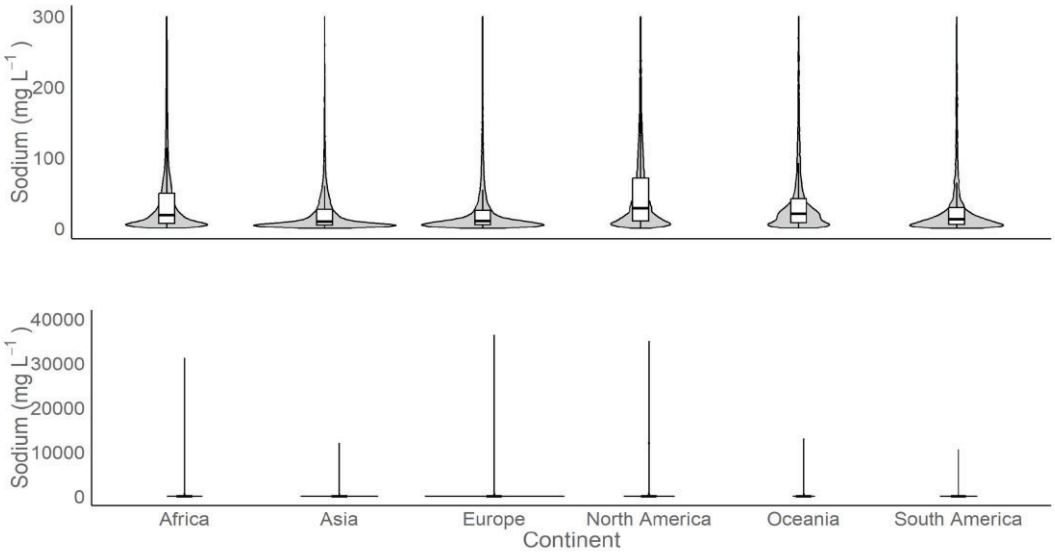


Figure C5. Global violin plot of dissolved sodium by continent. Top: Global Violin Plot of sodium by Continent with Zoom to 300 mg L^{-1}. Bottom: Global Violin Plot sodium across entire scale by Continent. Sodium observations are included in the GlobSalt database, over the entire data period (1980-2023). Each gray violin plot represents the available data set according to the number (n) of observations per continent (Africa n = 133687, Asia n= 100698, Europe n = 204582, North America n = 5029090, Oceania n = 9797, South America n = 15582).

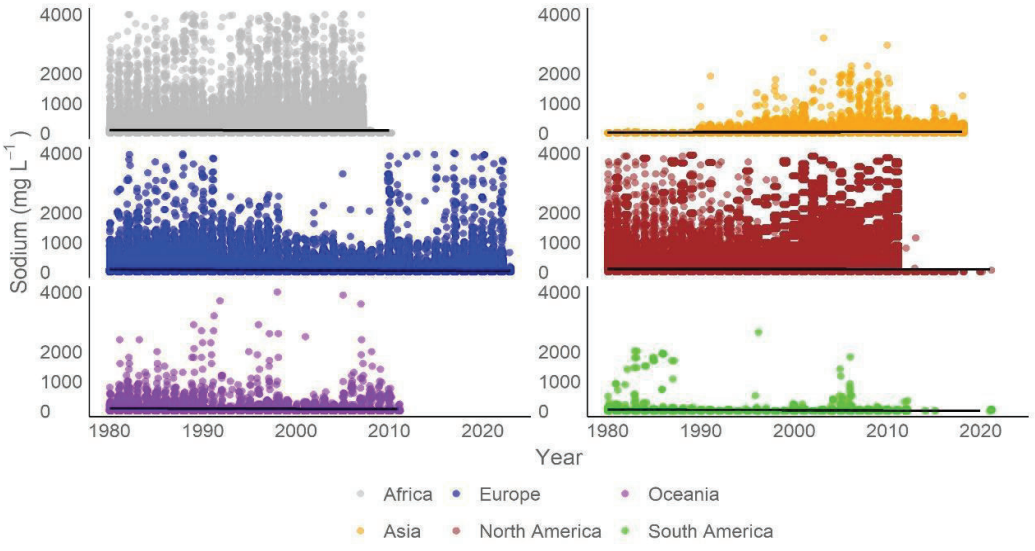


Figure C6. Global temporal dispersion plot of dissolved sodium by continent. Sodium observations are included in the GlobSalt database over the entire data period (1980-2023). Each color point (gray, yellow, blue, brown, purple, and green) represents the number (n) of observations per continent (Africa n = 133687, Asia n= 100698, Europe n = 204582, North America n = 5029090, Oceania n = 9797, South America n = 15582).

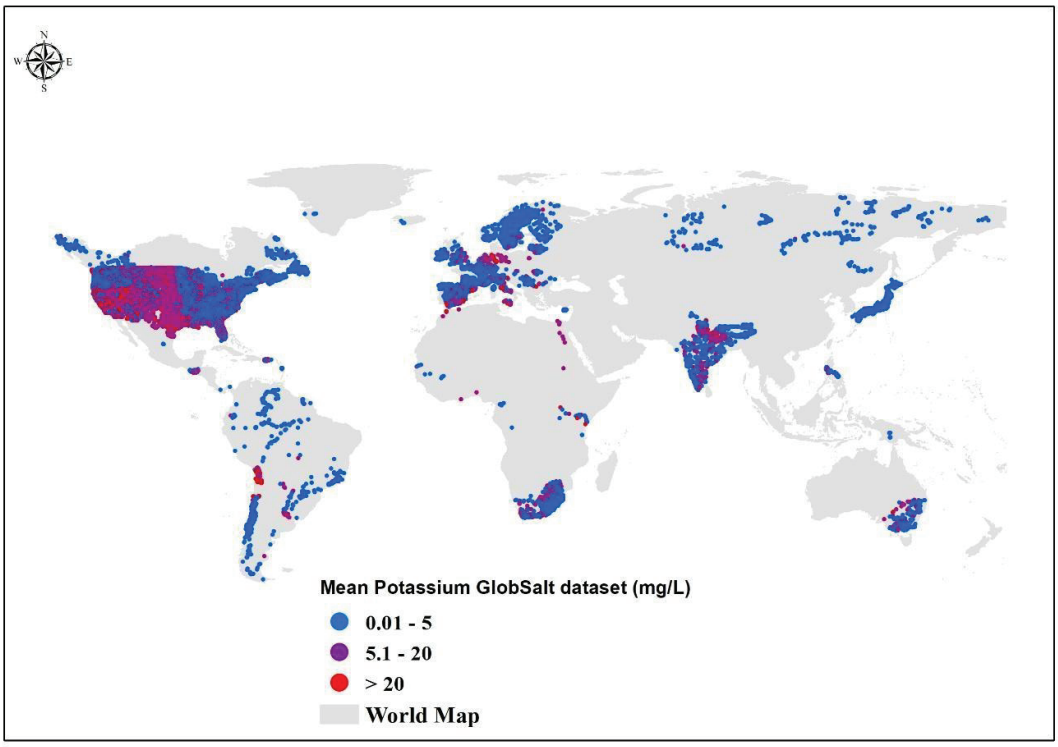


Figure C7. Global distribution of measured mean dissolved potassium and station density. The global map in the panel shows the measured mean potassium values per river in each country, based on observations included in the GlobSalt database, over the entire data period (1980-2023). Blue, purple, and red dots represent low, moderate, and high potassium levels, respectively.

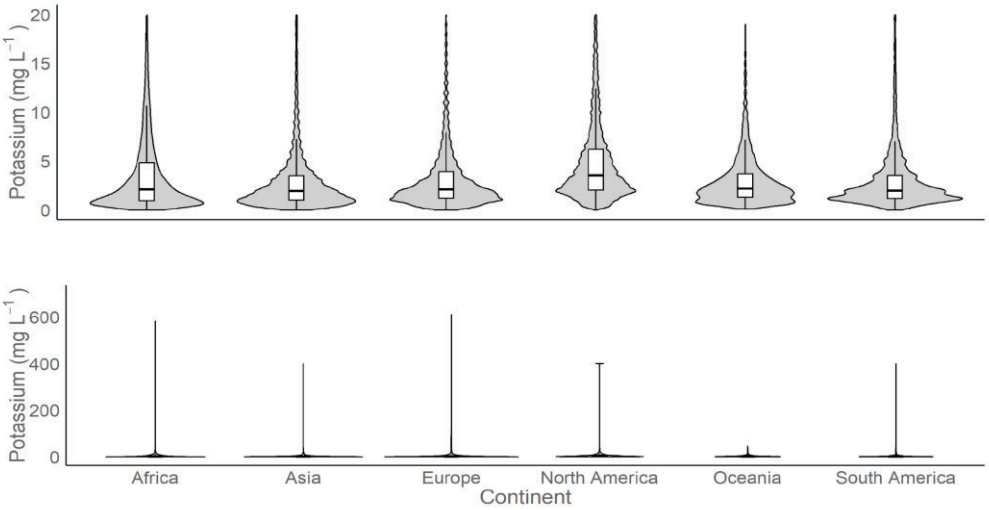


Figure C8. Global violin plot of dissolved potassium by continent. Top: Global Violin Plot of potassium by Continent with Zoom to 20 mg L^{-1}. Bottom: Global Violin Plot of potassium across the entire scale by Continent. Potassium observations are included in the GlobSalt database, over the entire data period (1980-2023). Each gray violin plot represents the available data set according to the number (n) of observations per continent (Africa n = 130020, Asia n = 100855, Europe n = 154423, North America n = 4794390, Oceania n = 9706, South America n = 16667).

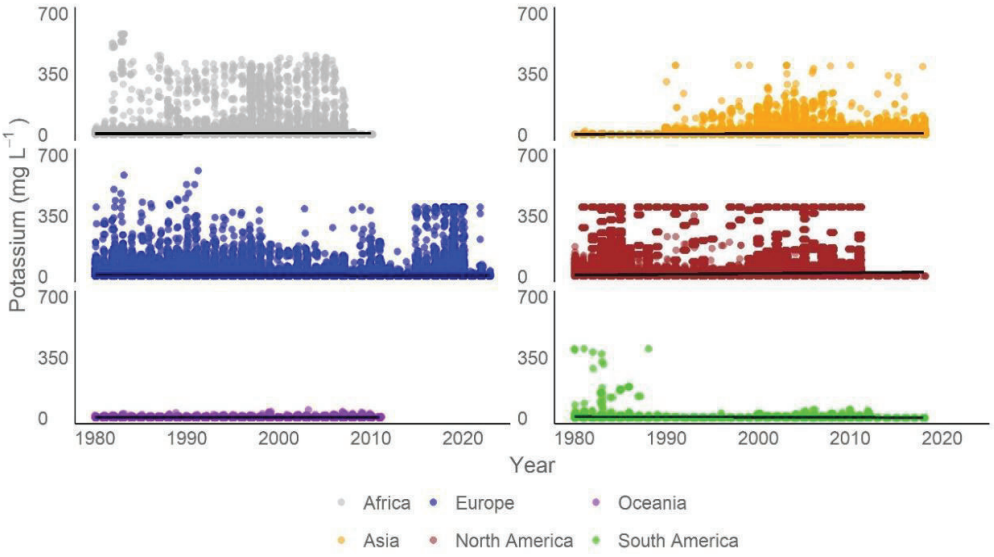


Figure C9. Global temporal dispersion plot of dissolved potassium by continent. Potassium observations are included in the GlobSalt database over the entire data period (1980-2023). Each color point (gray, yellow, blue, brown, purple, and green) represents the number (n) of observations per continent (Africa n = 130020, Asia n = 100855, Europe n = 154423, North America n = 4794390, Oceania n = 9706, South America n = 16667).

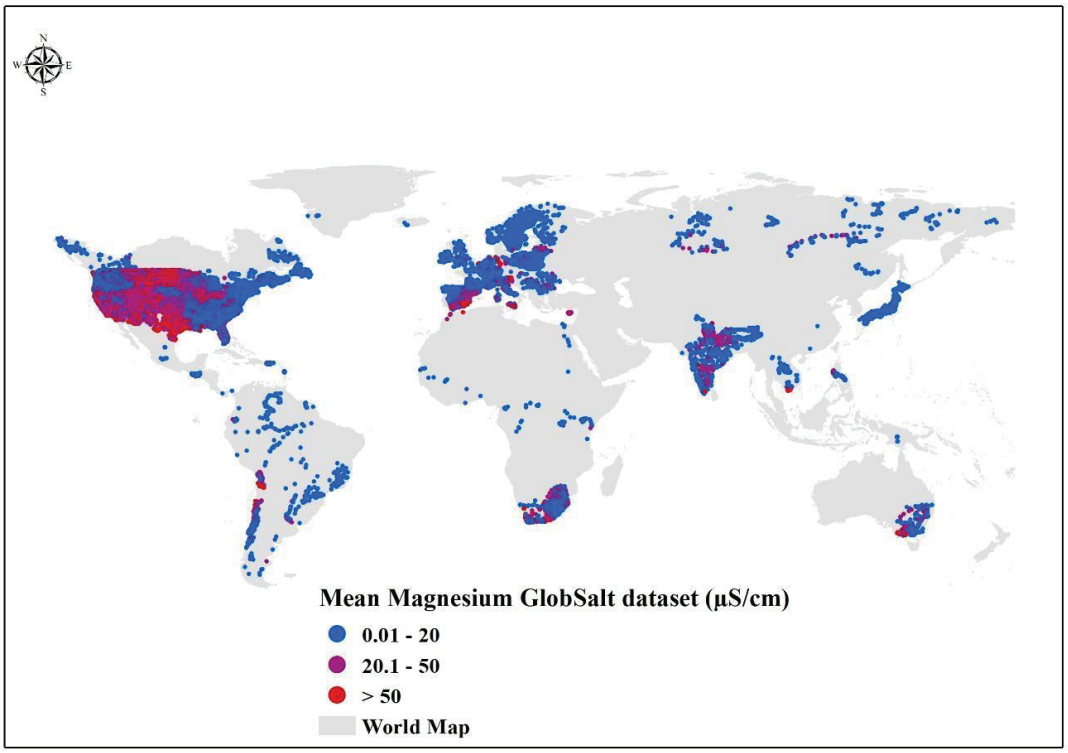


Figure C10. Global distribution of measured mean dissolved magnesium and station density. The global map in the panel shows the measured mean magnesium values per river in each country, based on observations included in the GlobSalt database, over the entire data period (1980-2023). Blue, purple, and red dots represent low, moderate, and high magnesium levels, respectively.

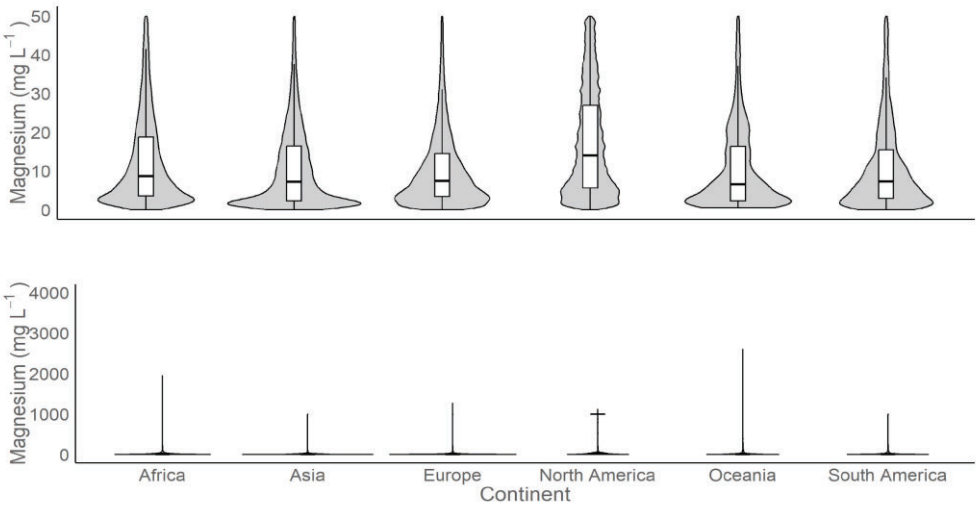


Figure C11. Global violin plot of dissolved magnesium by continent. Top: Global Violin Plot of magnesium by Continent with Zoom to 50 mg L^{-1}. Bottom: Global Violin Plot of magnesium across the entire scale by Continent. Magnesium observations are included in the GlobSalt database, over the entire data period (1980-2023). Each gray violin plot represents the available data set according to the number (n) of observations per continent (Africa n = 133816, Asia n = 111565, Europe n = 193759, North America n = 5489267, Oceania n = 9807, South America n = 15678).

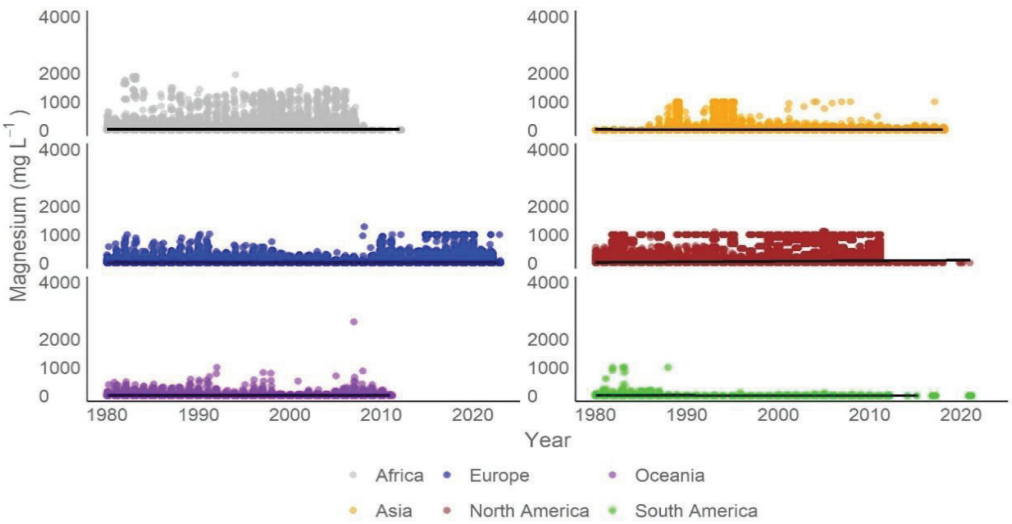


Figure C12. Global temporal dispersion plot of dissolved magnesium by continent. Magnesium observations are included in the GlobSalt database over the entire data period (1980-2023). Each color point (gray, yellow, blue, brown, purple, and green) represents the number (n) of observations per continent (Africa n = 133816, Asia n = 111565, Europe n = 193759, North America n = 5489267, Oceania n = 9807, South America n = 15678).

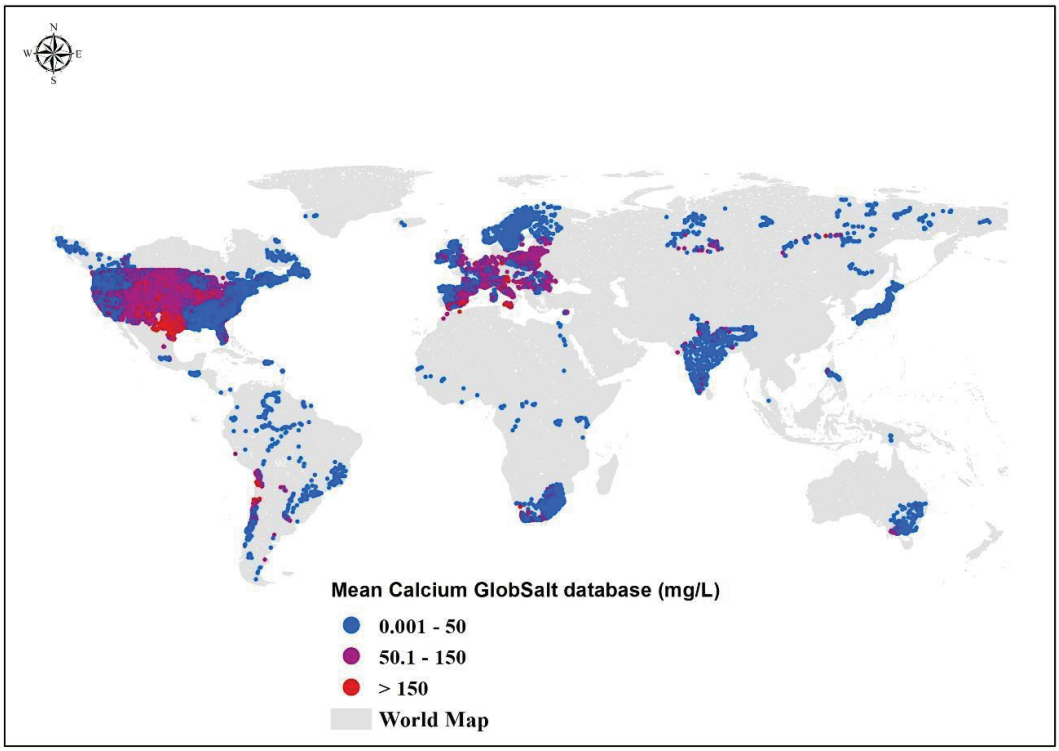


Figure C13. Global distribution of measured mean dissolved calcium and station density. The global map in the panel shows the measured mean calcium values per river in each country, based on observations included in the GlobSalt database, over the entire data period (1980-2023). Blue, purple, and red dots represent low, moderate, and high calcium levels, respectively.

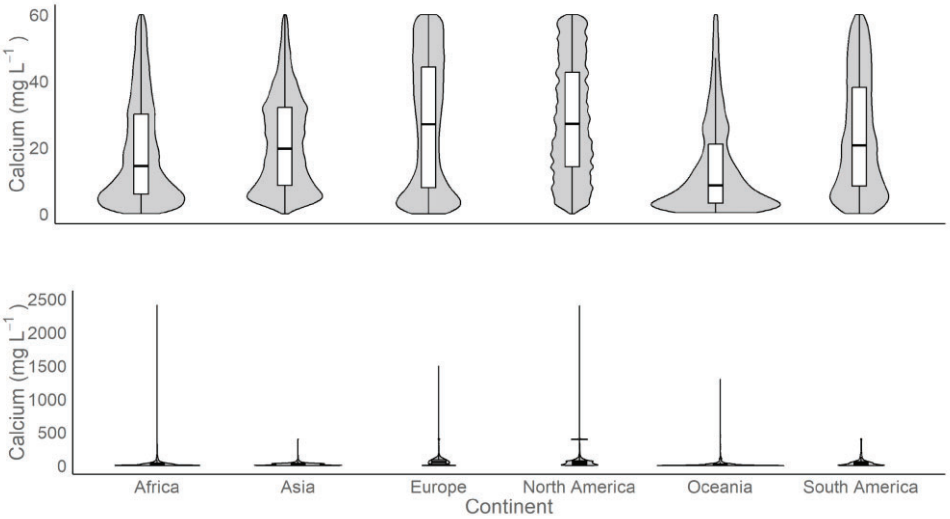


Figure C14. Global violin plot of dissolved calcium by continent. Top: Global Violin Plot of calcium by Continent with Zoom to 60 mg L^{-1}. Bottom: Global Violin Plot of calcium across the entire scale by Continent. Calcium observations are included in the GlobSalt database, over the entire data period (1980-2023). Each gray violin plot represents the available data set according to the number (n) of observations per continent (Africa n = 133361, Asia n = 105402, Europe n = 262310, North America n = 5559902, Oceania n = 9463, South America n = 15644).

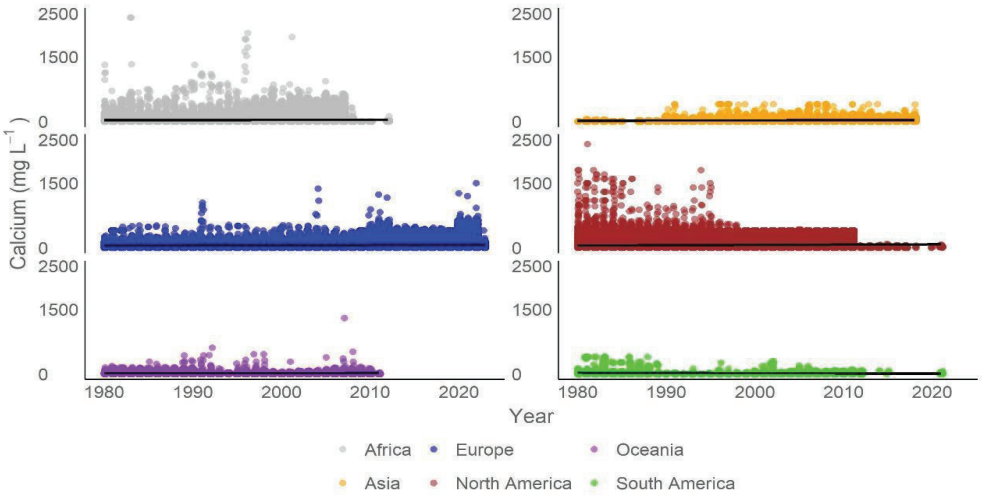


Figure C15. Global temporal dispersion plot of dissolved calcium by continent. Calcium observations are included in the GlobSalt database over the entire data period (1980-2023). Each color point (gray, yellow, blue, brown, purple, and green) represents the number (n) of observations per continent (Africa n = 133361, Asia n = 105402, Europe n = 262310, North America n = 5559902, Oceania n = 9463, South America n = 15644).

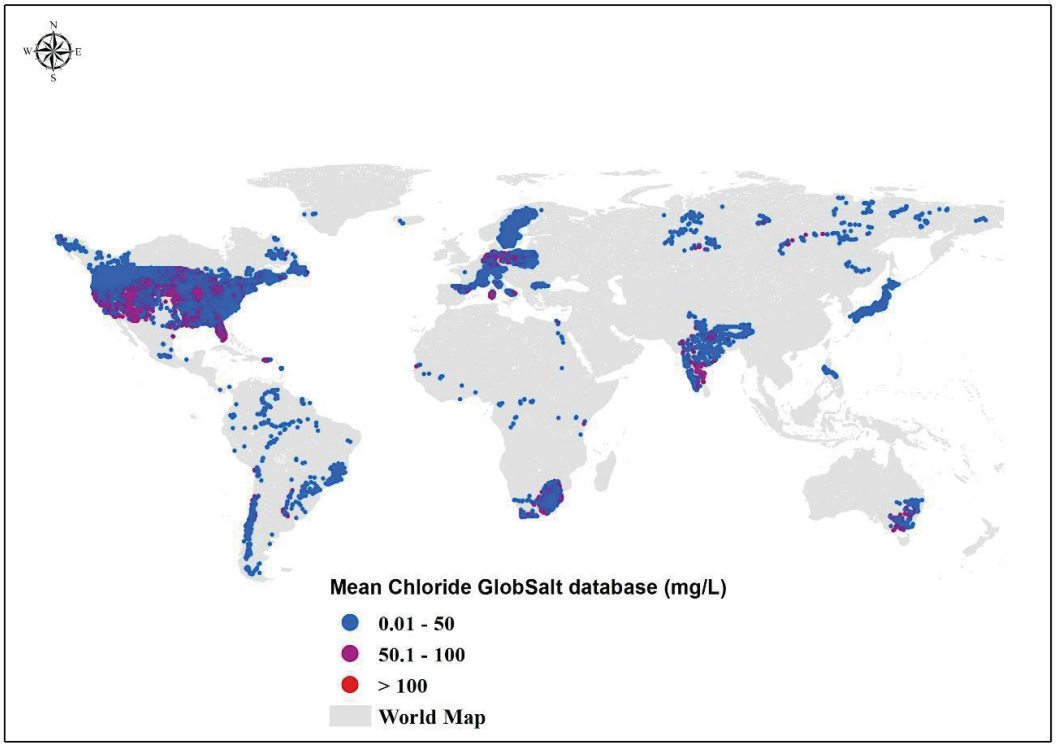


Figure C16. Global distribution of measured mean dissolved chloride and station density. The global map in the panel shows the measured mean chloride values per river in each country, based on observations included in the GlobSalt database, over the entire data period (1980-2023). Blue, purple, and red dots represent low, moderate, and high chloride levels, respectively.

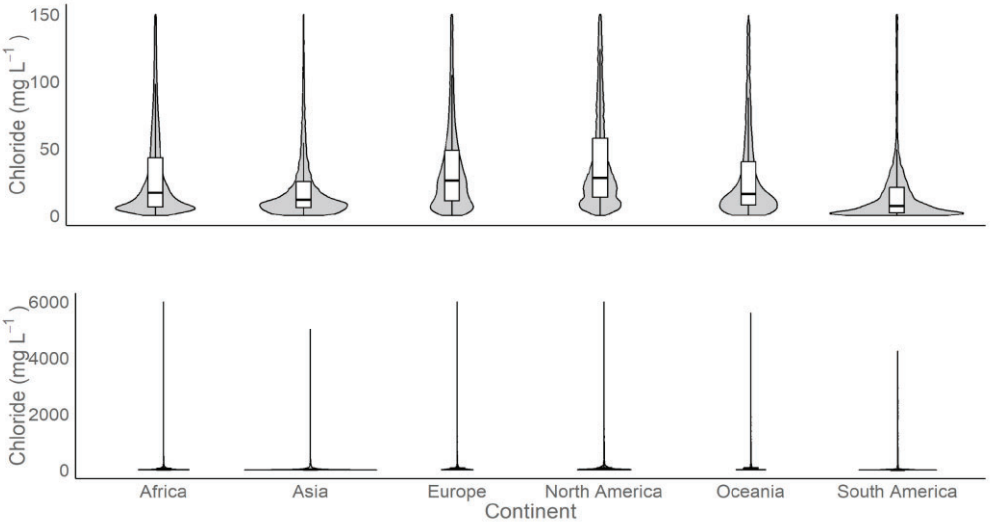


Figure C17. Global violin plot of dissolved chloride by continent. Top: Global Violin Plot of chloride by Continent with Zoom to 150 mg L^{-1}. Bottom: Global Violin Plot of chloride across the entire scale by Continent. Chloride observations are included in the GlobSalt database, over the entire data period (1980-2023). Each gray violin plot represents the available data set according to the number (n) of observations per continent (Africa n = 135515, Asia n = 106452, Europe n = 175926, North America n = 5373355, Oceania n = 9488, South America n = 17769).

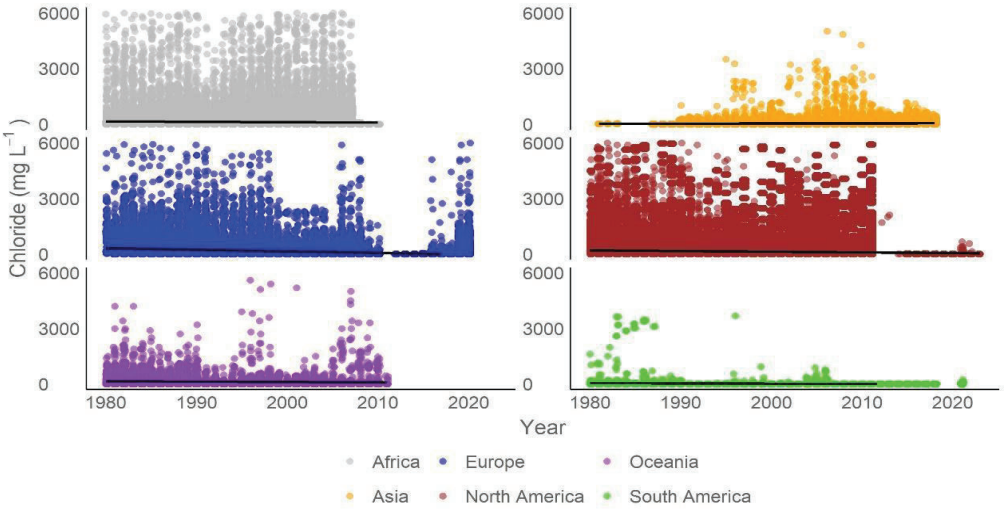


Figure C18. Global temporal dispersion plot of dissolved chloride by continent. Chloride observations are included in the GlobSalt database over the entire data period (1980-2023). Each color point (gray, yellow, blue, brown, purple, and green) represents the number (n) of observations per continent (Africa n = 135515, Asia n = 106452, Europe n = 175926, North America n = 5373355, Oceania n = 9488, South America n = 17769).

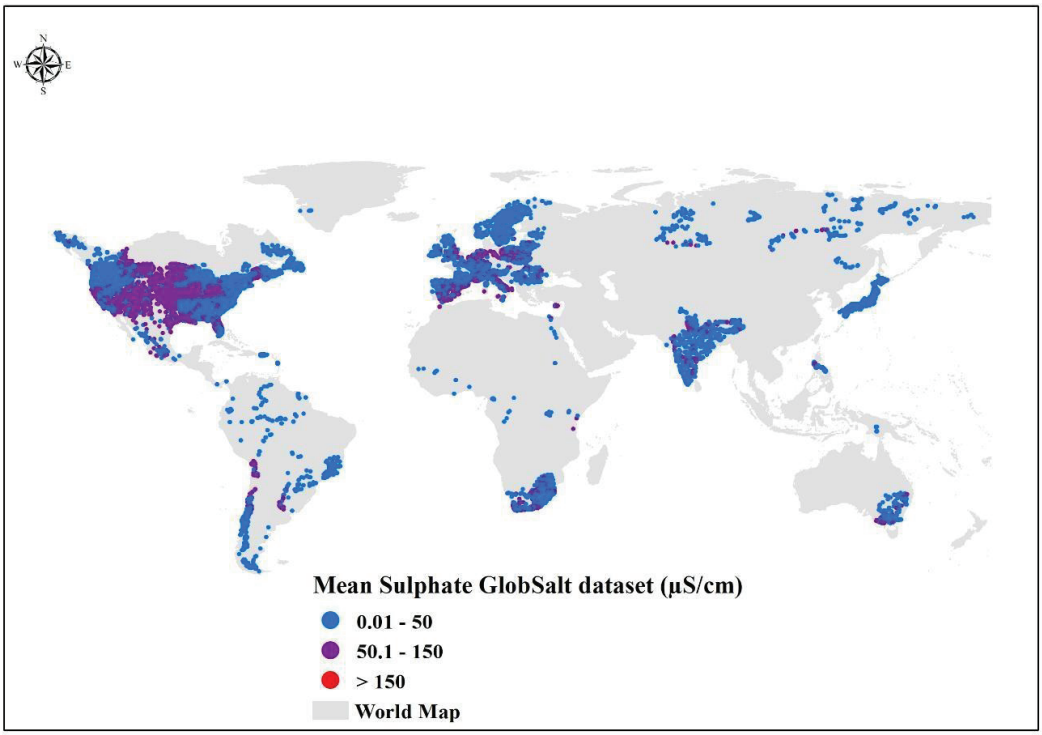


Figure C19. Global distribution of measured mean sulphate and station density. The global map in the panel shows the measured mean sulphate values per river in each country, based on observations included in the GlobSalt database, over the entire data period (1980-2023). Blue, purple, and red dots represent low, moderate, and high sulphate levels, respectively.

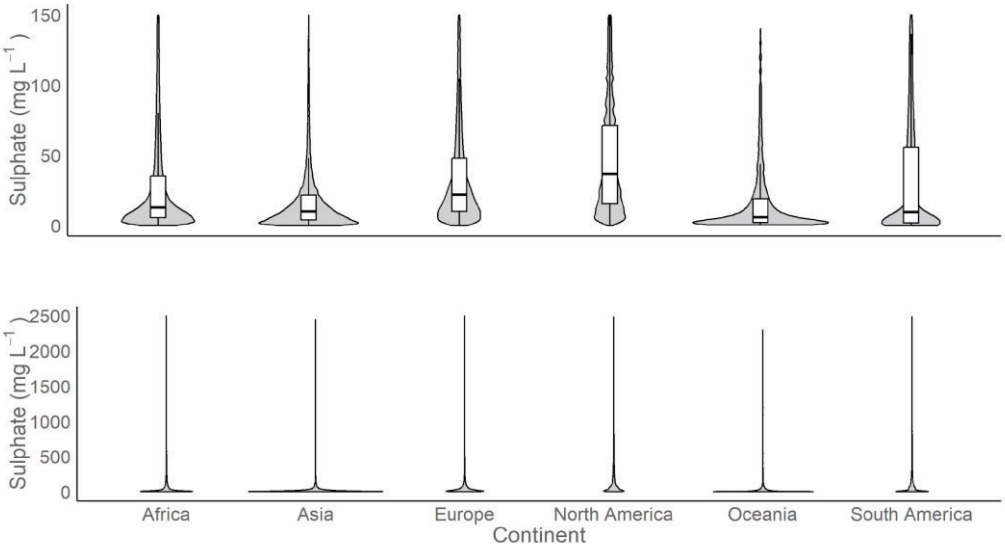


Figure C20. Global violin plot of dissolved sulphate by continent. Top: Global Violin Plot of sulphate by Continent with Zoom to 150 mg L^{-1}. Bottom: Global Violin Plot of sulphate across entire scale by Continent. Sulphate observations are included in the GlobSalt database, over the entire data period (1980-2023). Each gray violin plot represents the available data set according to the number (n) of observations per continent (Africa n = 136929, Asia n = 97109, Europe n = 239298, North America n = 4803213, Oceania n = 8153, South America n = 17114).

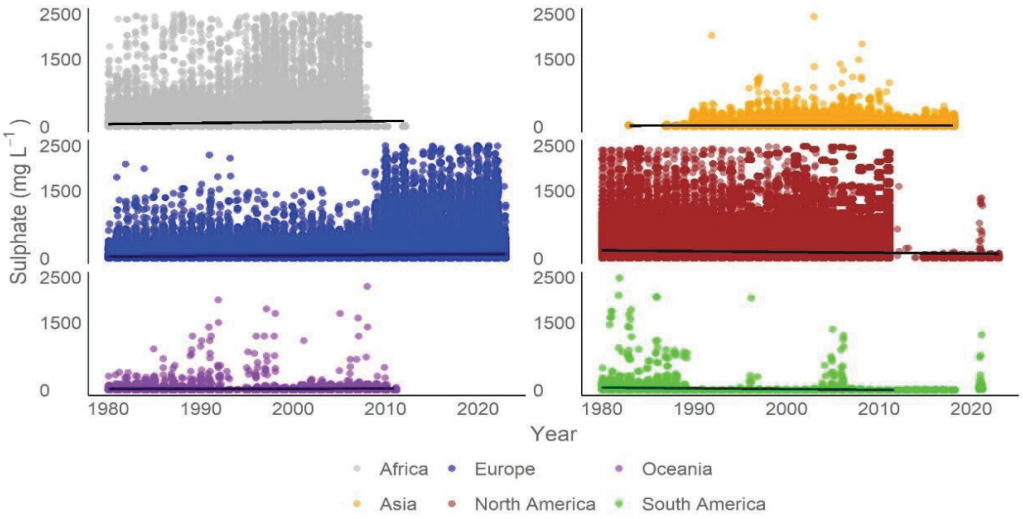


Figure C21. Global temporal dispersion plot of dissolved sulphate by continent. Sulphate observations are included in the GlobSalt database over the entire data period (1980-2023). Each color point (gray, yellow, blue, brown, purple, and green) represents the number (n) of observations per continent (Africa n = 136929, Asia n = 97109, Europe n = 394531, North America n = 4803213, Oceania n = 8153, South America n = 17114).

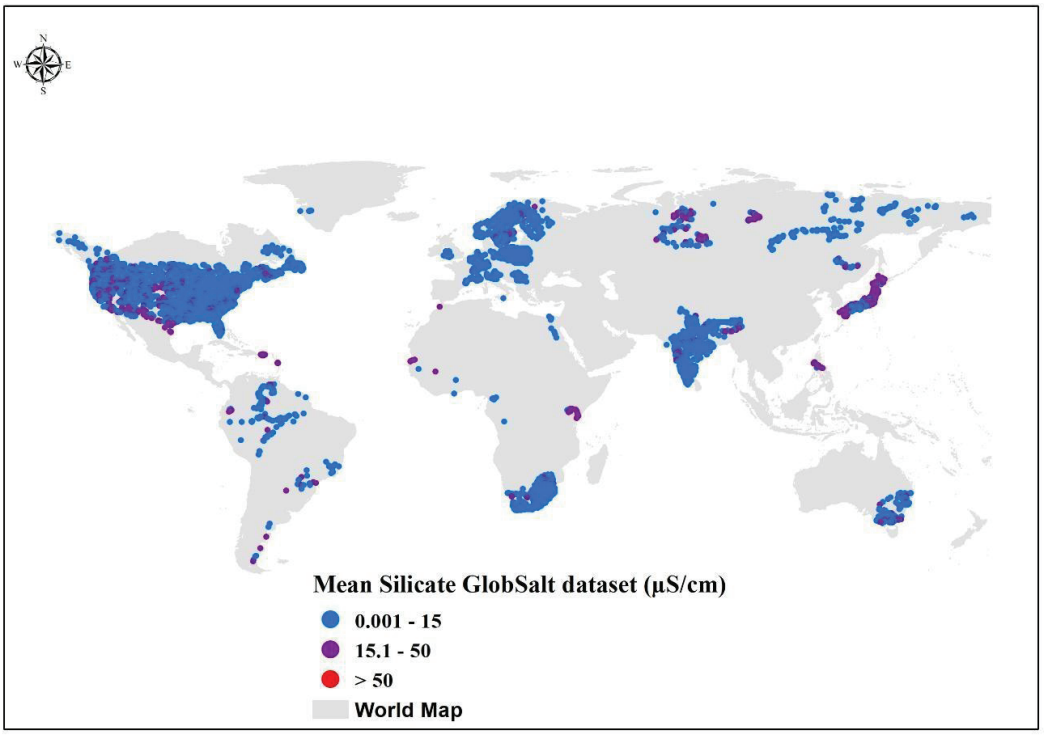


Figure C22. Global distribution of measured mean dissolved silicate and station density. The global map in the panel shows the measured mean silicate values per river in each country, based on observations included in the GlobSalt database, over the entire data period (1980-2023). Blue, purple, and red dots represent low, moderate, and high silicate levels, respectively.

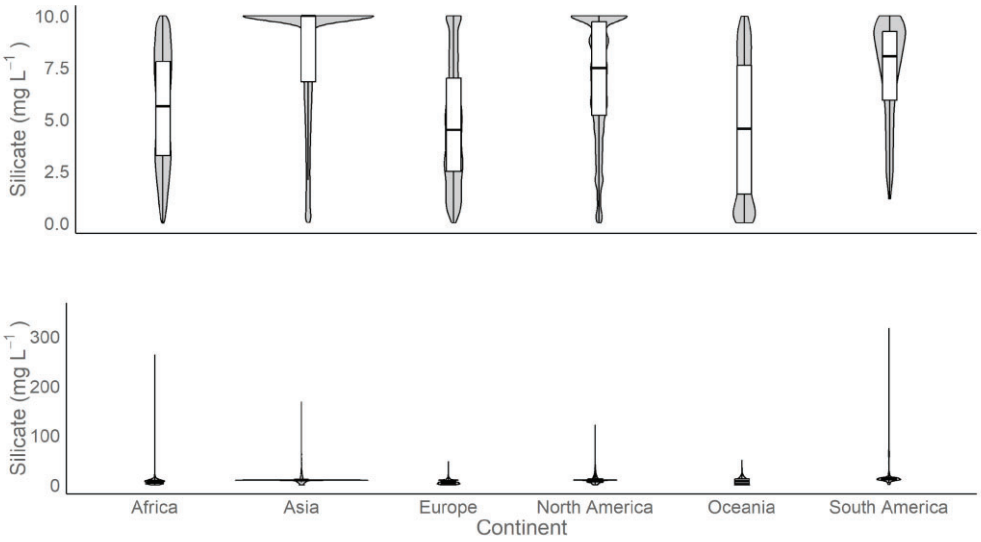


Figure C23. Global violin plot of dissolved silicate by continent. Top: Global Violin Plot of silicate by Continent with Zoom to 10 mg L^{-1}. Bottom: Global Violin Plot of silicate across the entire scale by Continent. Silicate observations are included in the GlobSalt database, over the entire data period (1980-2023). Each gray violin plot represents the available data set according to the number (n) of observations per continent (Africa n = 125842, Asia n = 79112, Europe n = 34883, North America n = 175049, Oceania n = 11055, South America n = 1992).

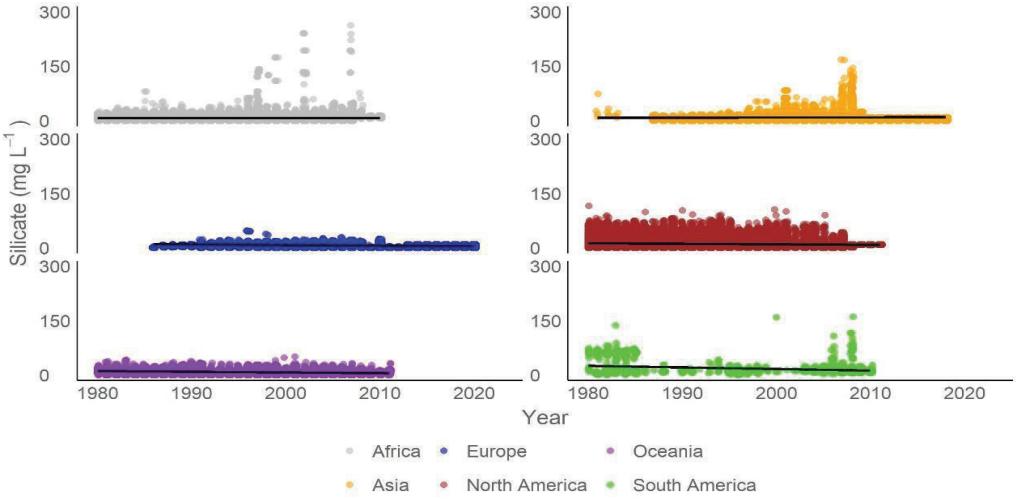


Figure C24. Global temporal dispersion plot of dissolved silicate by continent. Silicate observations are included in the GlobSalt database over the entire data period (1980-2023). Each color point (gray, yellow, blue, brown, purple, and green) represents the number (n) of observations per continent (Africa n = 125842, Asia n = 79112, Europe n = 34883, North America n = 175049, Oceania n = 11055, South America n = 1992).

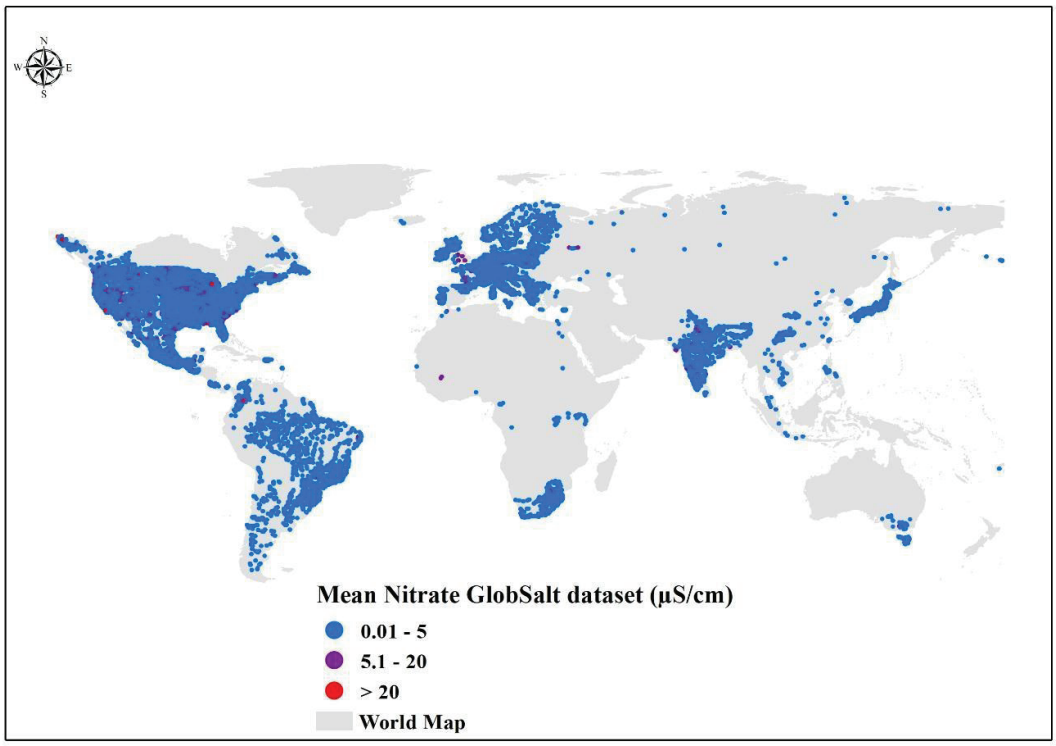


Figure C25. Global distribution of measured mean nitrate and station density. The global map in the panel shows the measured mean nitrate values per river in each country, based on observations included in the GlobSalt database, over the entire data period (1980-2023). Blue, purple, and red dots represent low, moderate, and high nitrate levels, respectively.

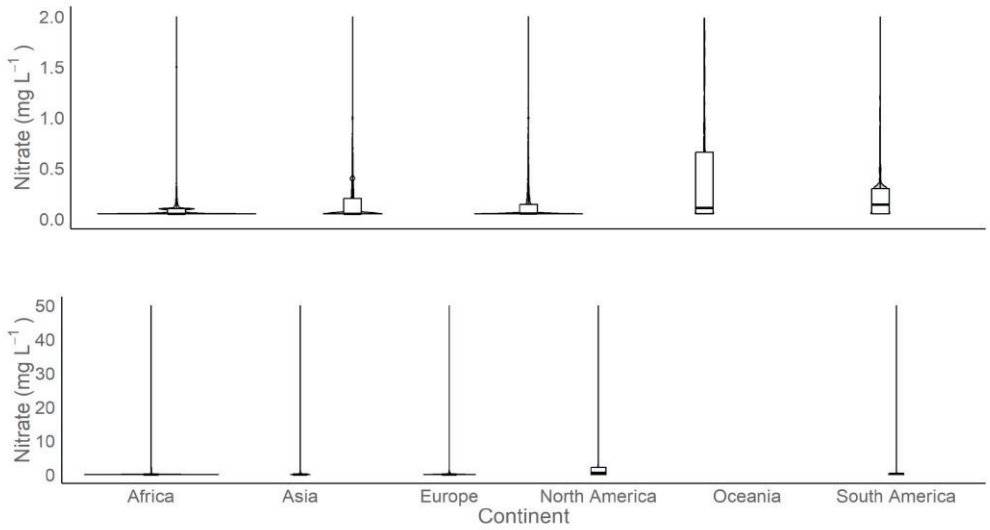


Figure C26. Global violin plot of nitrate by continent. Top: Global Violin Plot of nitrate by Continent with Zoom to 20 mg L^{-1}. Bottom: Global Violin Plot of nitrate across the entire scale by Continent. Nitrate observations are included in the GlobSalt database, over the entire data period (1980-2023). Each gray violin plot represents the available data set according to the number (n) of observations per continent (Africa n = 69429, Asia n = 68447, Europe n = 478303, North America n = 1147316, Oceania n = 6180, South America n = 25707).

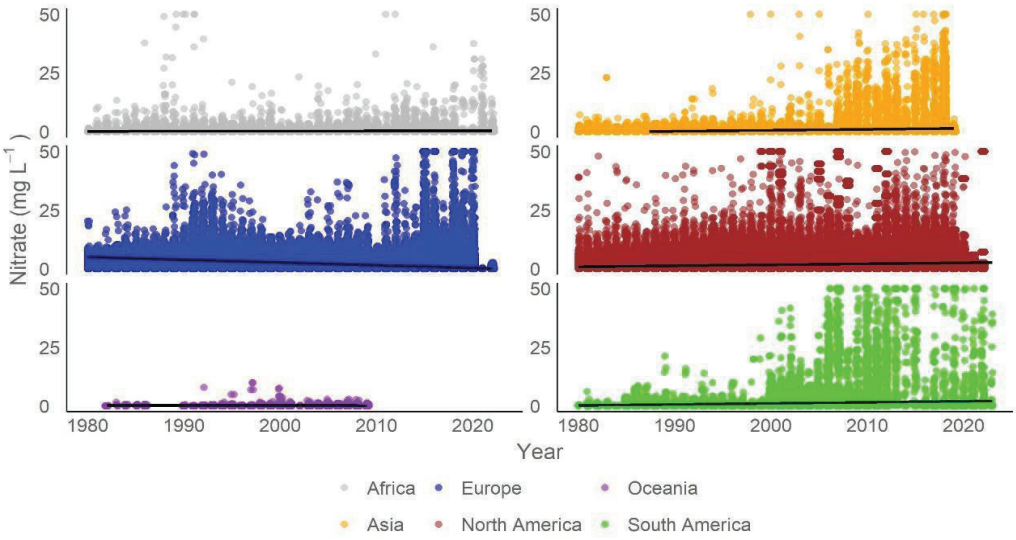


Figure C27. Global temporal dispersion plot of nitrate by continent. Nitrate observations are included in the GlobSalt database over the entire data period (1980-2023). Each color point (gray, yellow, blue, brown, purple, and green) represents the number (n) of observations per continent (Africa n = 69429, Asia n = 68447, Europe n = 478303, North America n = 1147316, Oceania n = 6180, South America n = 25707).

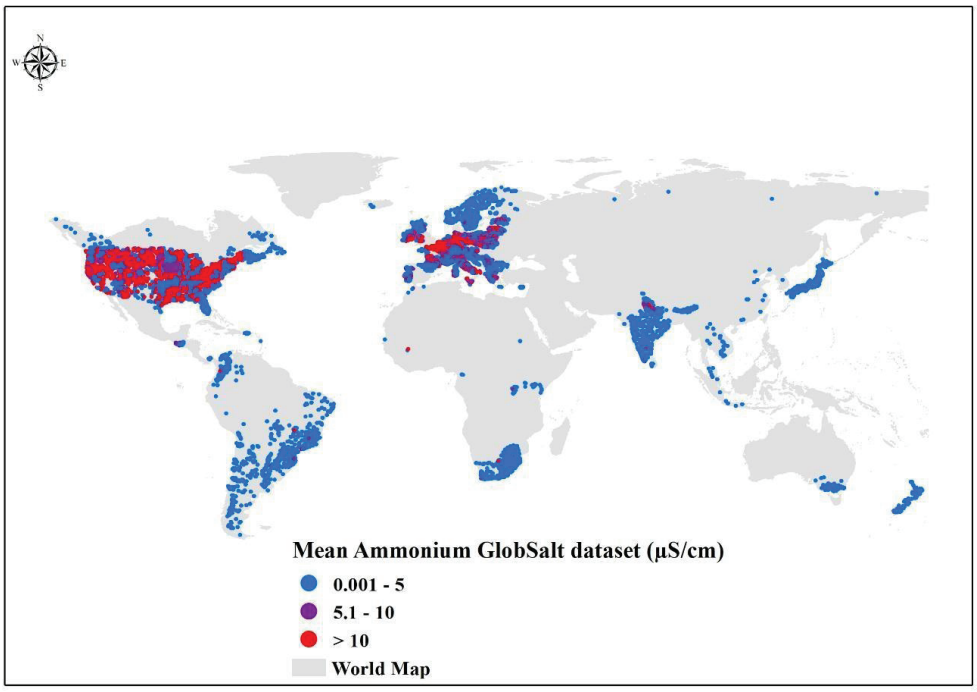


Figure C28. Global distribution of measured mean ammonium and station density. The global map in the panel shows the measured mean ammonium values per river in each country, based on observations included in the GlobSalt database, over the entire data period (1980-2023). Blue, purple, and red dots represent low, moderate, and high ammonium levels, respectively.

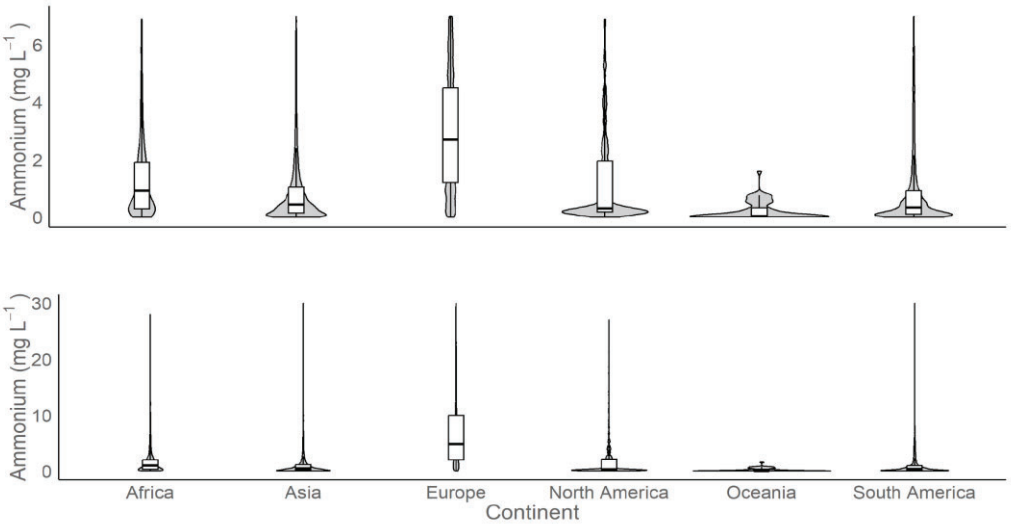


Figure C29. Global violin plot of ammonium by continent. Top: Global Violin Plot of ammonium by Continent with Zoom to 6 mg L^{-1}. Bottom: Global Violin Plot of ammonium across the entire scale by Continent. Ammonium observations are included in the GlobSalt database, over the entire data period (1980-2023). Each gray violin plot represents the available data set according to the number (n) of observations per continent (Africa n = 140913, Asia n = 66527, Europe n = 747967, North America n = 371981, Oceania n = 3541, South America n = 27876).

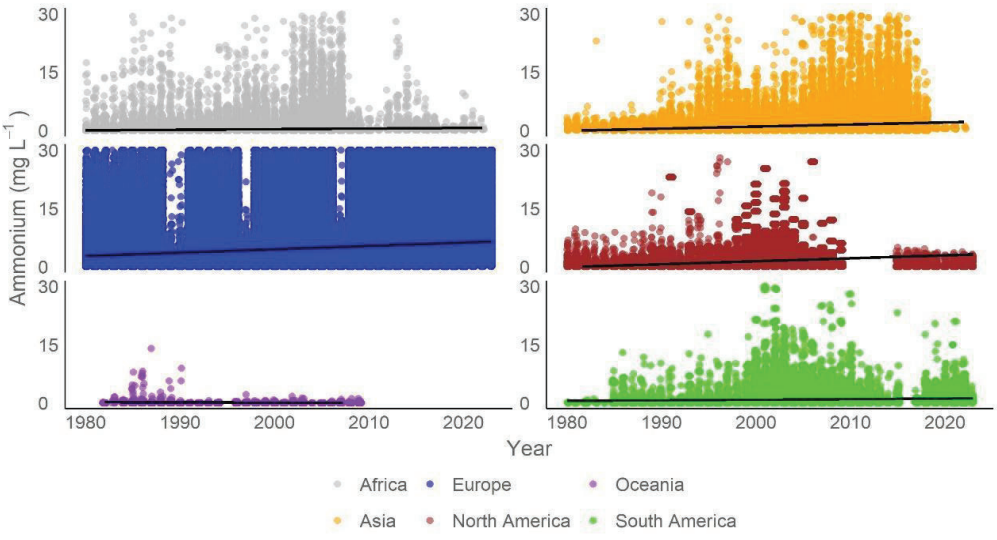


Figure C30. Global temporal dispersion plot of ammonium by continent. Ammonium observations are included in the GlobSalt database over the entire data period (1980-2023). Each color point (gray, yellow, blue, brown, purple, and green) represents the number (n) of observations per continent (Africa n = 140913, Asia n = 66527, Europe n = 747967, North America n = 371981, Oceania n = 3541, South America n = 27876).

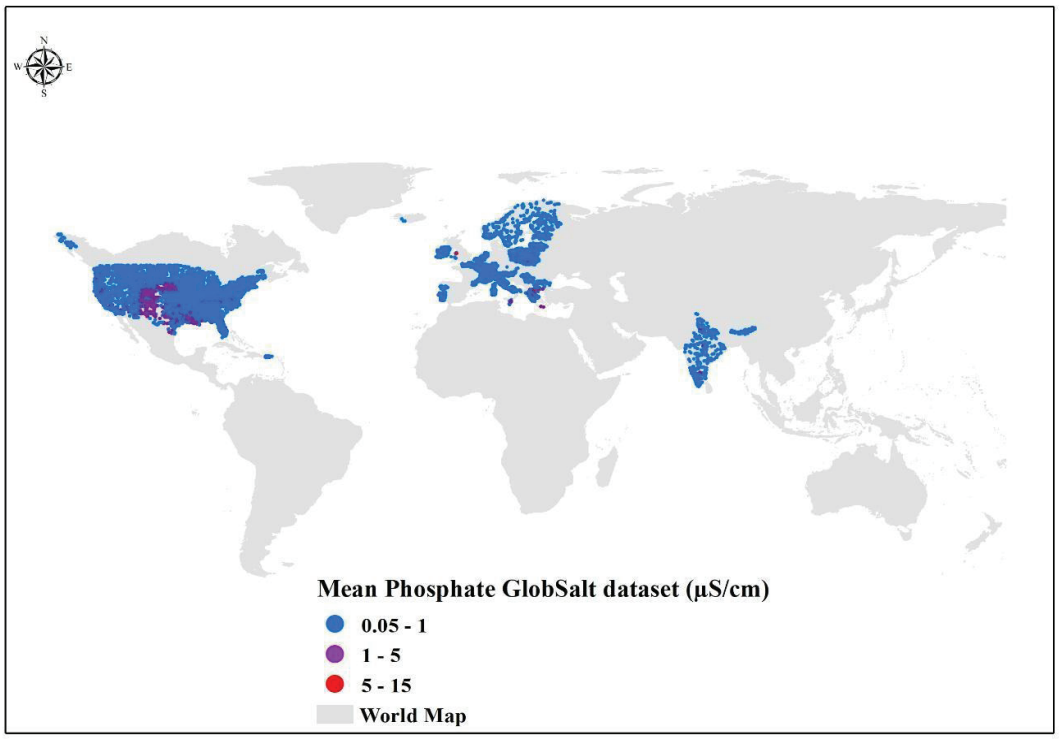


Figure C31. Global distribution of measured mean phosphate and station density. The global map in the panel shows the measured mean phosphate values per river in each country, based on observations included in the GlobSalt database, over the entire data period (1980-2023). Blue, purple, and red dots represent low, moderate, and high phosphate levels, respectively.

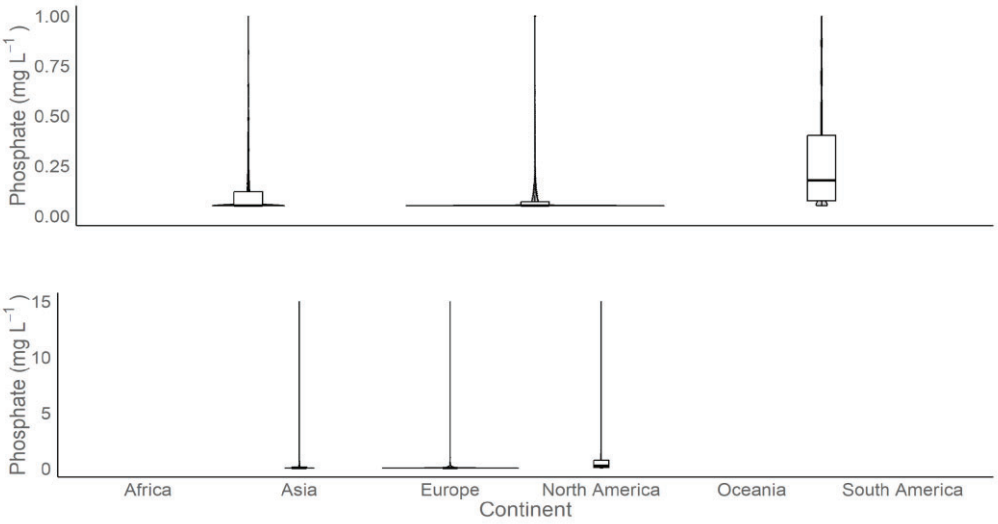


Figure C32. Global violin plot of phosphate by continent. Top: Global Violin Plot of phosphate by Continent with Zoom to 20 mg L-1. Bottom: Global Violin Plot of phosphate across entire scale by Continent. Phosphate observations are included in the GlobSalt database, over the entire data period (1980-2023). Each gray violin plot represents the available data set according to the number (n) of observations per continent (Asia n = 33641, Europe n = 174630, North America n = 748642).

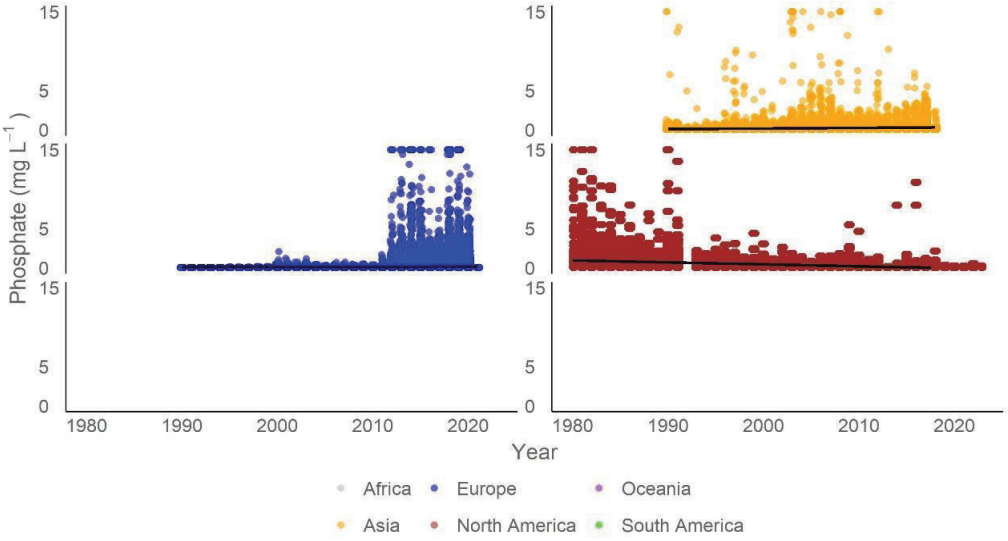


Figure C33. Global temporal dispersion plot of phosphate by continent. Phosphate observations are included in the GlobSalt database over the entire data period (1980-2023). Each color point (gray, yellow, blue, brown, purple, and green) represents the number (n) of observations per continent (Asia n = 33641, Europe n = 174630, North America n = 748642).

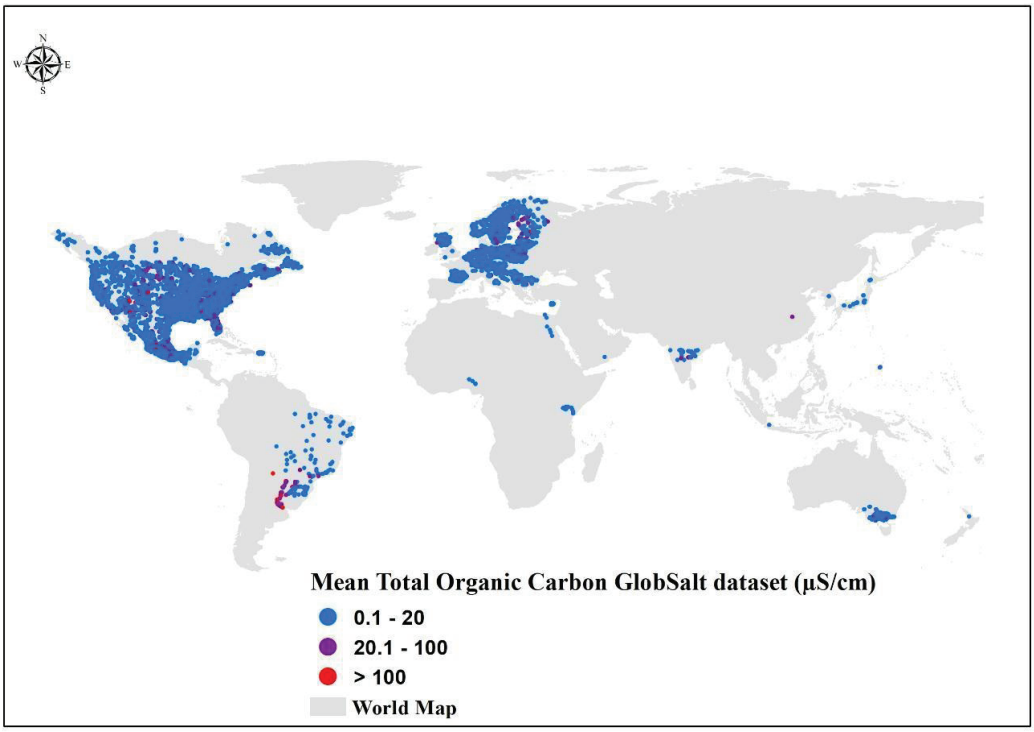


Figure C34. Global distribution of measured mean total organic carbon (TOC) and station density. The global map in the panel shows the measured mean TOC values per river in each country, based on observations included in the GlobSalt database, over the entire data period (1980-2023). Blue, purple, and red dots represent low, moderate, and high TOC levels, respectively.

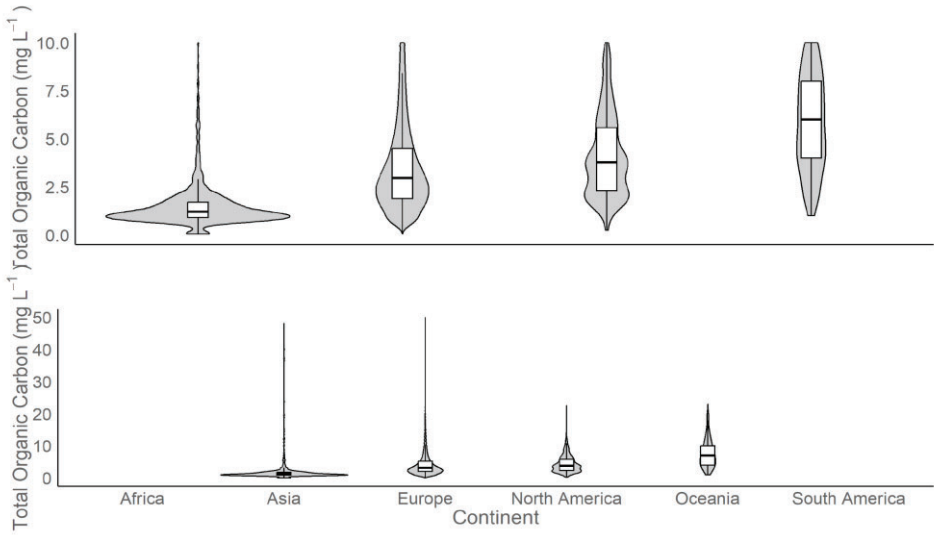


Figure C35. Global violin plot of total organic carbon (TOC) by continent. Top: Global Violin Plot of total organic carbon (TOC) by Continent with Zoom to 20 mg L-1. Bottom: Global Violin Plot of total organic carbon (TOC) across the entire scale by Continent. Total organic carbon (TOC) observations are included in the GlobSalt database, over the entire data period (1980-2023). Each gray violin plot represents the available data set according to the number (n) of observations per continent (Africa n = 63, Asia n = 3804, Europe n = 499640, North America n = 313367, Oceania n = 4010, South America n = 310).

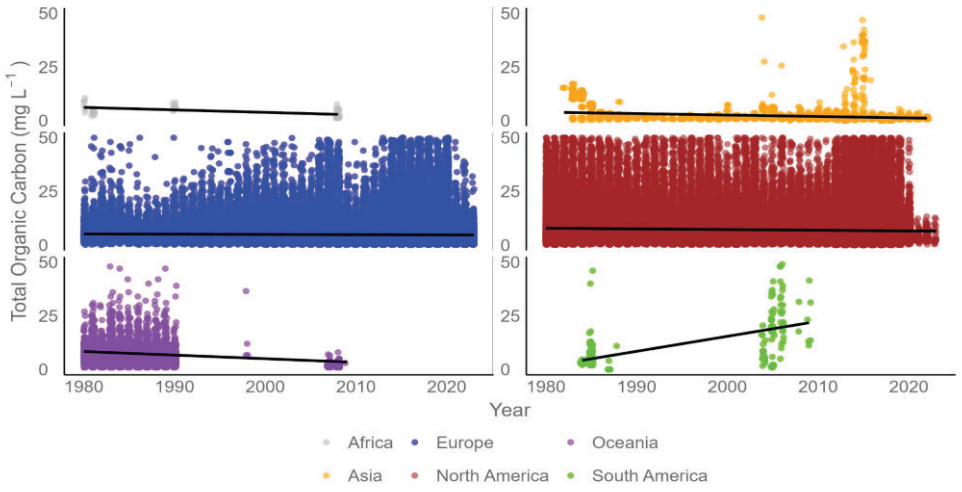


Figure C36. Global temporal dispersion plot of total organic carbon (TOC) by continent. Total organic carbon (TOC) observations are included in the GlobSalt database over the entire data period (1980-2023). Each color point (gray, yellow, blue, brown, purple, and green) represents the number (n) of observations per continent (Africa n = 63, Asia n = 3804, Europe n = 499640, North America n = 313367, Oceania n = 4010, South America n = 310).

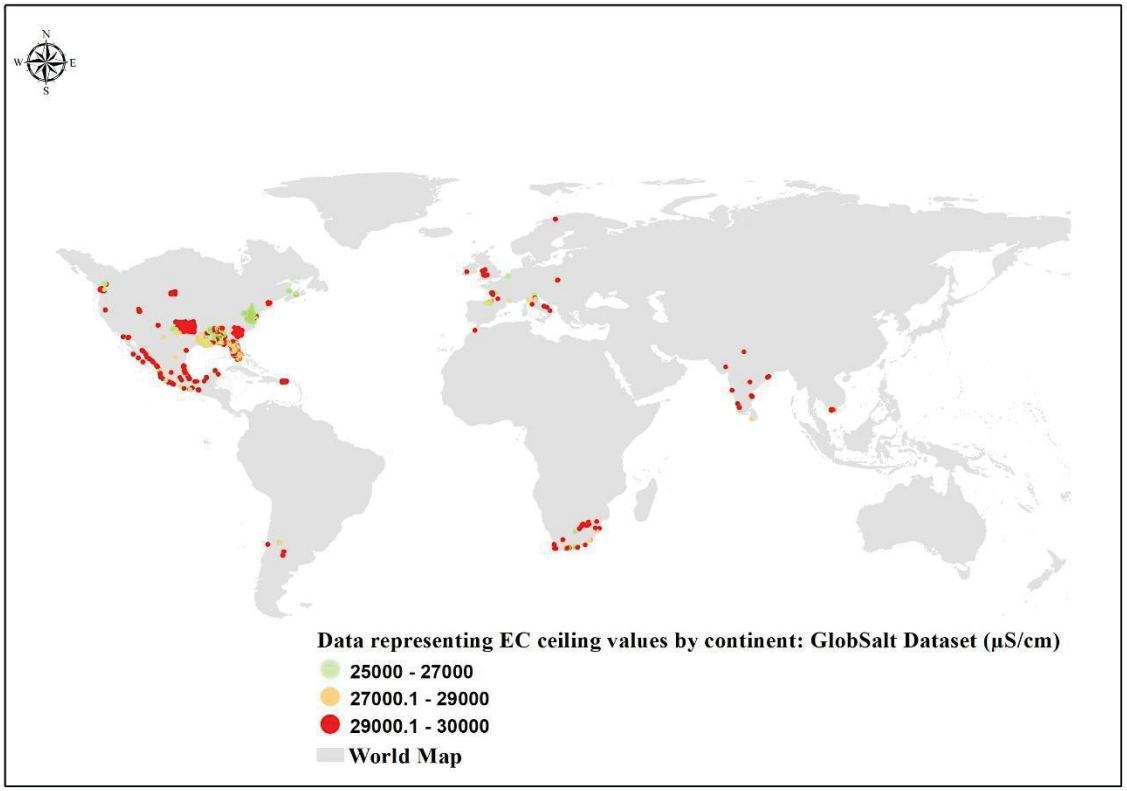


Figure C37. Ceiling values of electrical conductivity by continent. The map illustrates the ceiling EC values that have been consistently observed across multiple stations within each continent, based on data from the GlobSalt database spanning the entire period (1980-2023). Green, orange, and red dots indicate low, moderate, and high ceiling values, respectively, providing insights into the presence of consistently ceiling EC levels across continents (Africa n = 426, Asia n = 328, Europe n = 934, North America n = 19081, South America n = 574).

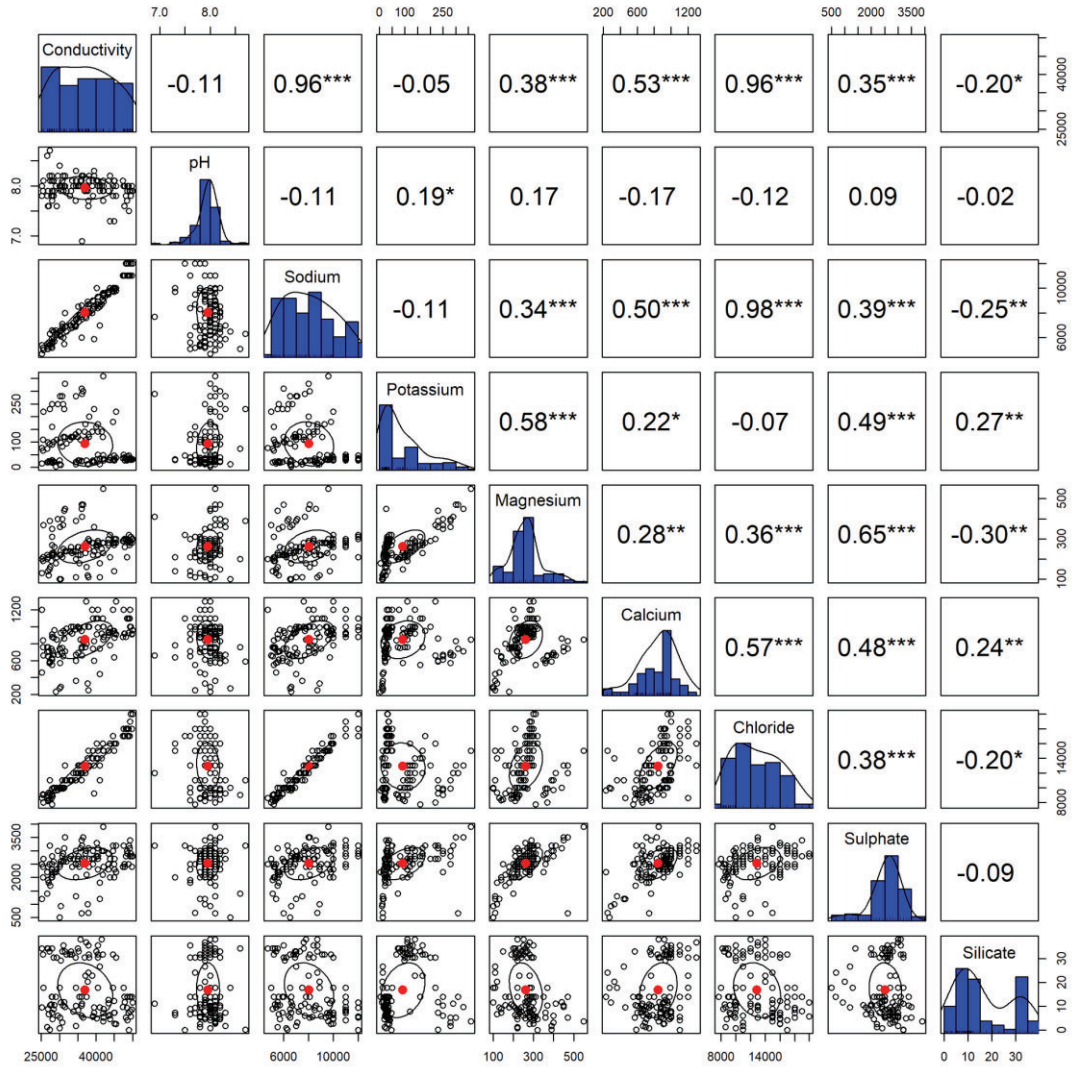


Figure C38. Correlation plot of electrical conductivity (EC) ceiling values and ion concentrations in the GlobSalt dataset, including inter-ion correlations. Red dots indicate the strength of correlation between variables (stronger intensity represents higher correlation, while weaker intensity represents lower correlation).

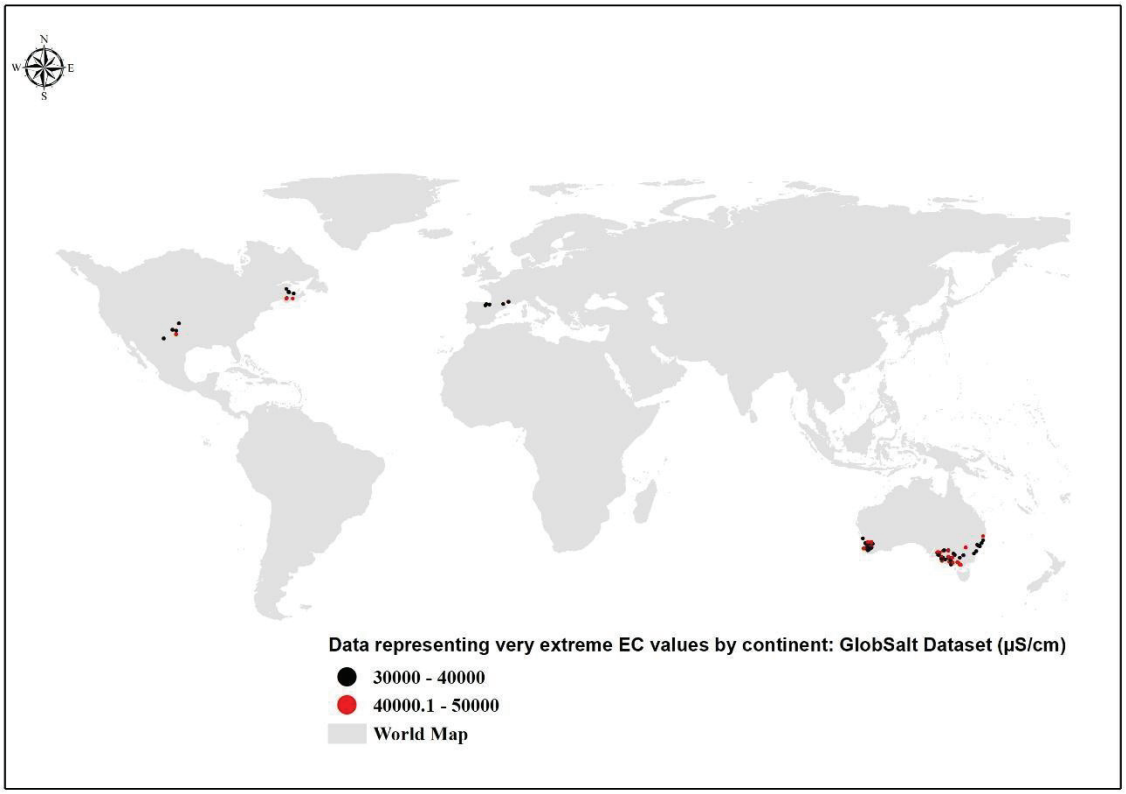


Figure C39. Extreme values of electrical conductivity by continent. The map illustrates the highest and moderately high EC values measured per continent, based on observations included in the GlobSalt database, over the entire data period (1980-2023). Black dots indicate very high EC values, while red dots indicate the highest EC values. Both black and red dots represent extreme EC values, providing insights into the range of EC across continents (Europe n = 39, North America n = 160, South America n = 1895).

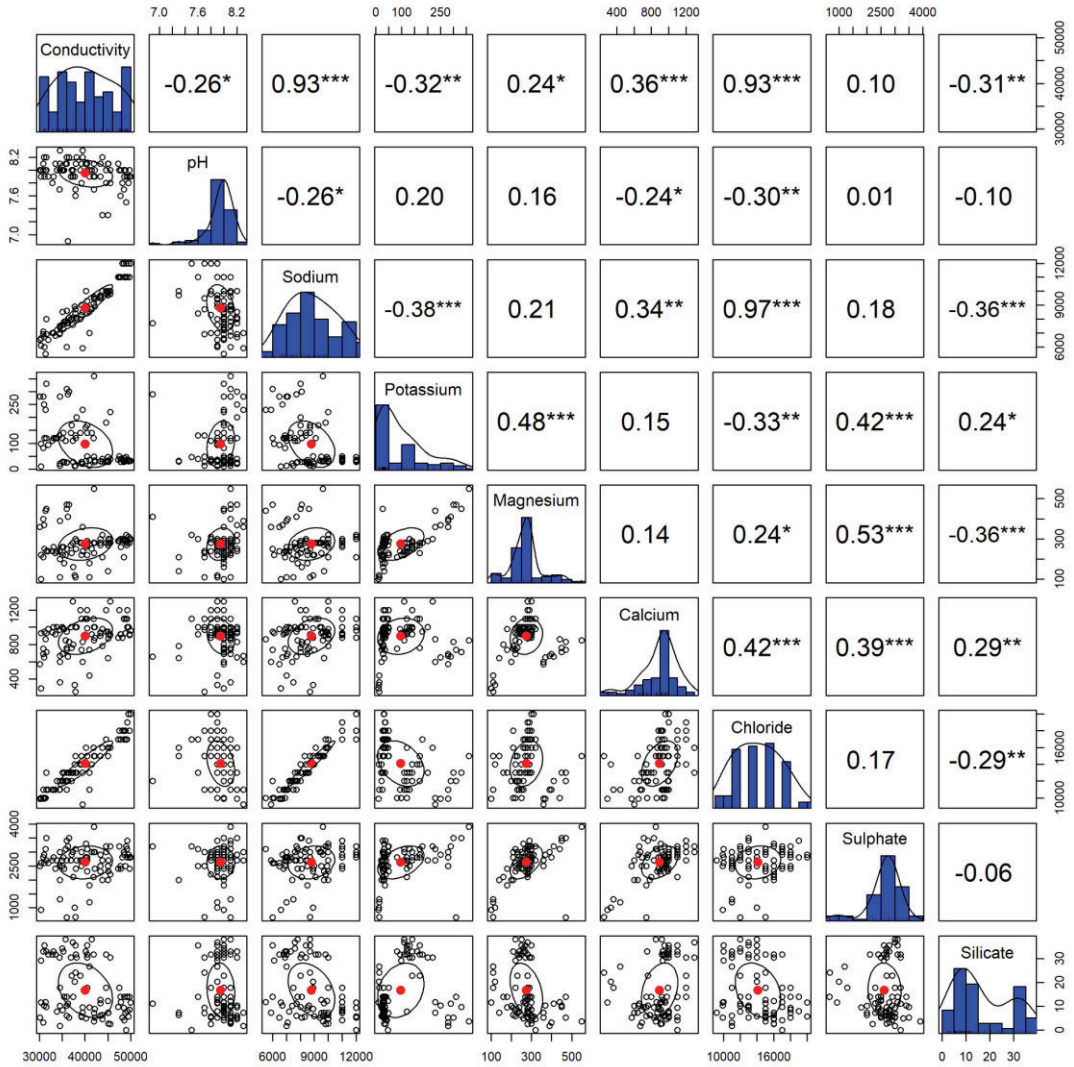


Figure C40. Correlation plot of electrical conductivity (EC) extreme values and ion concentrations in the GlobSalt dataset, including inter-ion correlations. Red dots indicate the strength of correlation between variables (stronger intensity represents higher correlation, while weaker intensity represents lower correlation).

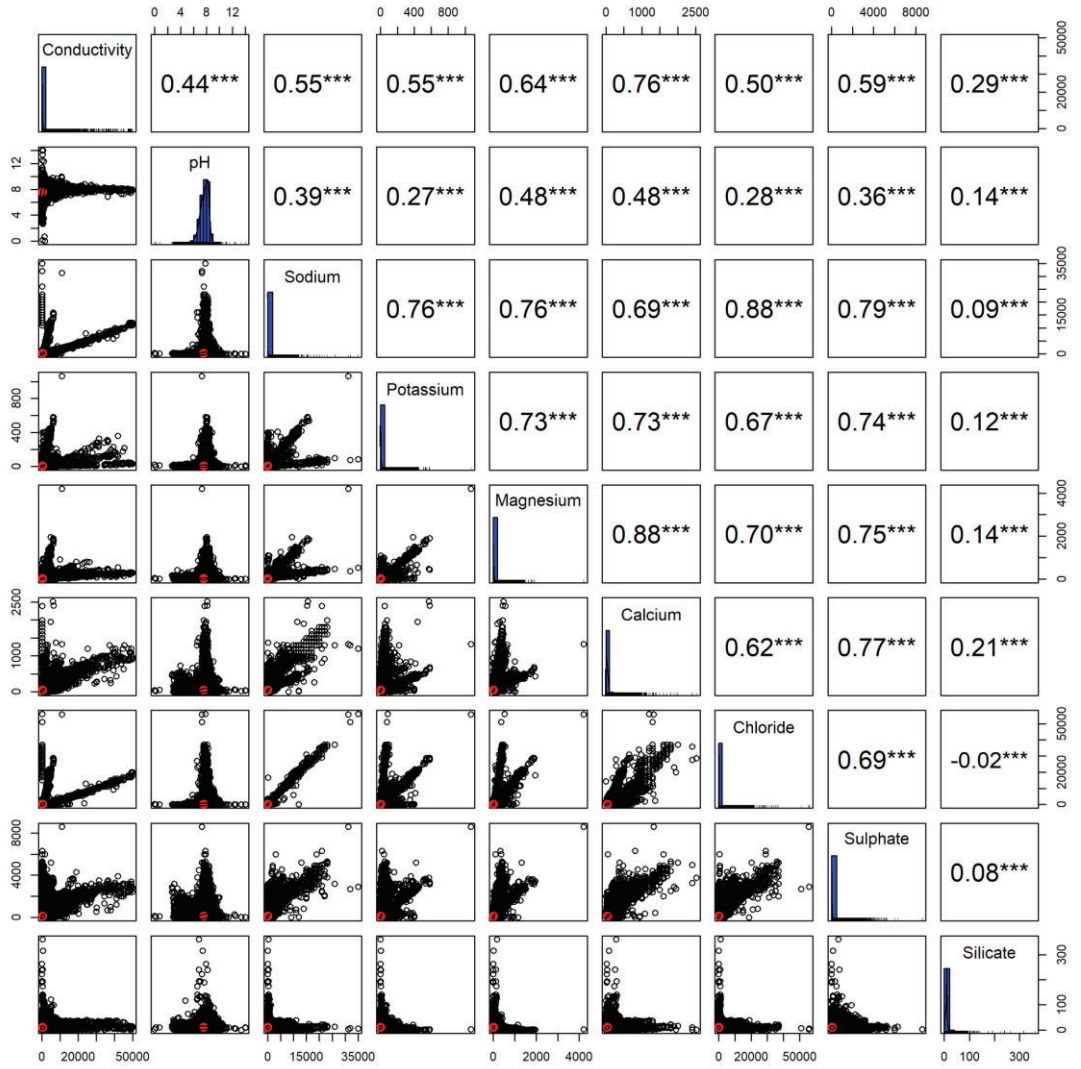


Figure C41. Correlation plot of electrical conductivity (EC) and ion concentrations in the GlobSalt dataset (unfiltered potential data errors), including inter-ion correlations (ions unit, mg L^{-1}). Red dots indicate the strength of correlation between variables. The location and intensity of the red dots can provide further insights into the relationship between the variables (e.g., stronger intensity of red color represents higher correlation, while weaker intensity suggests lower correlation).

Supplementary material: Chapter II

Online Resource 1

Tittle: Human activities disrupt the temporal dynamics of salinity in Spanish rivers

Journal name: Hydrobiologia

- **Author information: The name(s) of the author(s):**

Alvaro Javier Moyano Salcedo 1,2, Edurne Estévez 3, Humbert Salvadó 4, José Barquín 5, Miguel Cañedo-Argüelles Iglesias 6,7

9. **The affiliation(s) of the author(s), i.e. institution, (department), city, (state), country**

1 FEHM-Lab (Freshwater Ecology, Hydrology and Management), Departament de Biologia Evolutiva, Ecologia i Ciències Ambientals, Facultat de Biologia, Universitat de Barcelona, Barcelona, Spain.

2 Geohazards and Civil Engineering Research Group, Department of Civil Engineering, Saint Thomas Villavicencio University, C/22 No 1a, 500003, Villavicencio, Colombia.

3 Department of Ecology, University of Innsbruck, Innsbruck, Austria.

4 Department of Evolutive Biology, Ecology and Environmental Sciences, University of Barcelona, 08028 Barcelona, Spain

5 Environmental Hydraulics Institute 'IH Cantabria', University of Cantabria, PCTCAN. C/ Isabel Torres 15, 39011 Santander, Spain

6 Institute of Environmental Assessment and Water Research (IDAEA-CSIC), Carrer de Jordi Girona, 18-26, 08034, Barcelona, Spain.

7 FEHM-Lab (Freshwater Ecology, Hydrology and Management), Departament de Biologia Evolutiva, Ecologia i Ciències Ambientals, Facultat de Biologia, Institut de Recerca de l'Aigua (IdRA), Universitat de Barcelona, Barcelona, Spain.

10. **e-mail address of the corresponding author**

1 A Moyano Salcedo, alvaromoyano@ub.edu

3 E Estévez, Edurne.Estevez-Cano@uibk.ac.at

4 H Salvadó, hsalvado@ub.edu

5 J Barquín, jose.barquin@unican.es

Table S1. Conductivity indices (CIs) computed from daily measures of conductivity from 91 stations of the Automatic Water Quality Information System. Indices were computed annually from 2007 to 2011.

Group	Code	Description
1) Magnitude of annual and monthly conductivity	MMC7-11[1]*	Mean monthly (1-12) conductivity for all years (7-11) (i.e. mean of all Januaries from 2007 to 2011, and so on respectively for all months until December)
	SDM7-11*	Standard deviation of mean monthly (1-12) conductivity for all years (7-11)
	CIM7-11*	Confidence interval of mean monthly (1-12) conductivity for all years (7-11)
	CVM7-11*	Coefficient of variation of mean monthly (1-12) conductivity for all years (7-11)
	MAC7-11	Mean annual conductivity per year
	SDA7-11	Standard deviation of mean annual conductivity per year
	CIA7-11	Confidence interval of mean annual conductivity per year
	CVA7-11	Coefficient of variation of mean annual conductivity per year
2) Magnitude and duration of annual conductivity extremes	1MC7-11	Magnitude of minimum annual conductivity of 1-day duration per year
	3MC7-11	Magnitude of minimum annual conductivity of 3-day duration per year
	7MC7-11	Magnitude of minimum annual conductivity of 7-day duration per year
	30MC7-11	Magnitude of minimum annual conductivity of 30-day duration per year
	90MC7-11	Magnitude of minimum annual conductivity of 90-day duration per year

Group	Code	Description
	1MMC7-11	Magnitude of maximum annual conductivity of 1-day duration per year
	3MMC7-11	Magnitude of maximum annual conductivity of 3-day duration per year
	7MMC7-11	Magnitude of maximum annual conductivity of 7-day duration per year
	30MMC7-11	Magnitude of maximum annual conductivity of 30-day duration per year
	90MMC7-11	Magnitude of maximum annual conductivity of 90-day duration per year
	75M7-11	Mean magnitude of conductivity that exceeded 75% of the mean annual conductivity per year
	95M7-11	Mean magnitude of conductivity that exceeded 95% of the mean annual conductivity per year
	25M7-11	Mean magnitude of conductivity that exceeded 25% of the mean annual conductivity per year
	5M7-11	Mean magnitude of conductivity that exceeded 5% of the mean annual conductivity per year
3) Timing of extreme conductivity events	JMax7-11	Julian day of annual maximum conductivity per year
	JMin7-11	Julian day of annual minimum conductivity per year

[1]7-11 (data by year from 2007 to 2011); *an index per month and year

Table S2. Environmental variables used to investigate the most important drivers of temporal variability of salinity.

Environmental variable	Source	Code	Definition	Units
Land uses	SIOSE	MN_UHD	Area occupied by urban areas in the draining catchment	Parts per unit (º/1)
		MN_AGR	Area occupied by agricultural land in the draining catchment	Parts per unit (º/1)
		MN_PAS	Area occupied by pasture in the draining catchment	Parts per unit (º/1)
		MN_BLF	Area occupied by broadleaf forest in the draining catchment	Parts per unit (º/1)
		MN_CNF	Area occupied by coniferous forest in the draining catchment	Parts per unit (º/1)
		MN_PLT	Area occupied by plantations in the draining catchment	Parts per unit (º/1)

Environmental variable	Source	Code	Definition	Units
		MN_SSH	Area occupied by moors, heathland, scrub and shrubs in the draining catchment	Parts per unit (º/1)
Geologic IGME	SIOSE	MN_calc	Area occupied by calcareous rocks in the draining catchment	Parts per unit (º/1)
		MN_slic	Area occupied by siliceous rocks in the draining catchment	Parts per unit (º/1)
Anthropic pressures	Instituto Geográfico Nacional (2020)	P_DMN	Distance to the nearest mining.	m
	Dirección General de Tránsito (2020)	P_DIR	Distance to the nearest icy road.	m

Environmental variable	Source	Code	Definition	Units
	Hydrographic confederations & water agencies	P_DAR	Distance to the nearest dam upstream. Limitation of 5000 m.	m
	Hydrographic confederations & water agencies	V_DAR	Distance to the nearest effluent discharge upstream. Limitation of 5000 m.	m

Table S3. Values of conductivity indices (CIs) selected according to variance inflation factor: Coefficient of variation of mean annual from 2007 to 2011.

SAICA station	**CVA_7**	**CVA_8**	**CVA_9**	**CVA_10**	**CVA_11**
1	7.76	9.18	7.14	7.91	11.00
2	22.49	25.85	24.06	25.29	27.50
3	17.30	16.84	16.48	17.86	18.26
4	43.21	36.17	46.28	43.78	42.72
5	23.08	19.59	18.72	21.62	21.10
6	22.86	21.08	25.05	22.92	22.21
7	29.86	27.84	27.66	19.59	18.38
8	9.66	11.79	9.90	11.43	12.60
9	21.76	23.53	20.22	20.88	22.77
10	10.50	10.06	11.26	11.01	10.60
11	22.73	24.28	26.78	32.58	29.40
12	28.24	30.97	29.63	34.43	33.78
13	22.75	24.47	31.34	39.23	35.65
14	22.60	25.78	22.51	23.78	20.56
15	19.84	19.39	21.61	19.28	13.71
16	19.84	19.39	30.32	29.64	40.21
17	15.24	17.12	8.50	9.33	16.23
18	17.31	15.31	19.74	18.95	13.27
19	14.81	16.57	14.63	14.19	18.19
20	14.61	13.54	14.90	12.95	16.29
21	22.13	26.02	27.41	33.34	30.94
22	21.85	31.94	33.42	38.00	23.49
23	51.12	45.57	49.59	24.12	16.94
24	6.87	7.56	7.08	9.06	13.54
25	16.00	13.53	9.80	9.51	15.36

SAICA station	CVA_7	CVA_8	CVA_9	CVA_10	CVA_11
26	24.18	25.23	24.11	25.04	31.55
27	26.55	28.04	27.72	26.81	34.59
28	16.77	14.57	17.67	19.65	26.01
29	25.54	28.19	28.28	35.12	41.45
30	19.58	15.75	18.19	21.93	25.38
31	19.58	15.75	58.30	49.16	52.50
32	9.00	8.42	6.32	7.79	7.15
33	14.32	8.42	31.07	7.79	39.47
34	22.72	21.19	22.75	23.82	32.10
35	24.88	24.51	20.26	17.33	25.63
36	21.46	21.67	23.04	21.23	37.28
37	17.38	8.80	24.27	29.24	42.39
38	19.28	20.71	16.81	21.83	22.16
39	16.94	34.76	31.97	26.24	36.80
40	19.09	16.55	21.86	22.97	27.02
41	21.74	23.76	31.42	30.47	37.95
42	44.06	45.96	43.20	39.86	51.08
43	16.98	17.88	19.33	20.09	27.55
44	17.77	17.18	15.74	16.77	18.43
45	16.12	18.87	16.47	16.29	21.93
46	18.15	16.24	15.15	14.80	20.68
47	15.29	20.73	18.95	12.81	21.81
48	21.61	19.39	24.55	25.14	25.83
49	3.41	3.61	6.08	16.03	26.84
50	24.21	18.84	26.39	24.05	20.47
51	19.89	18.20	17.16	23.71	30.62
52	13.82	12.84	10.27	9.88	19.04

SAICA station	CVA_7	CVA_8	CVA_9	CVA_10	CVA_11
53	29.80	25.22	25.85	20.64	32.29
54	25.21	23.92	21.28	21.62	34.13
55	20.44	20.32	11.73	8.82	10.74
56	37.00	17.27	28.56	23.76	35.19
57	13.20	14.66	14.21	19.66	24.98
58	22.79	22.35	23.67	30.63	36.35
59	6.37	7.78	5.61	4.82	8.97
60	17.57	18.48	18.87	18.65	18.83
61	9.98	10.78	9.16	7.99	5.42
62	10.59	13.13	11.31	11.01	13.74
63	16.08	16.37	14.12	16.36	19.27
64	21.65	23.53	16.65	8.28	14.51
65	9.48	5.14	10.58	12.44	14.68
66	13.10	18.82	18.69	20.57	19.68
67	25.85	24.39	23.19	22.30	24.82
68	37.10	30.54	33.36	41.06	35.65
69	22.55	26.75	18.96	24.11	21.53
70	34.60	34.83	28.05	35.34	35.45
71	28.47	31.38	30.14	29.92	27.50
72	11.93	15.65	17.41	19.19	18.38
73	20.23	19.64	21.40	21.17	18.52
74	34.20	36.28	22.99	32.16	33.04
75	24.98	26.62	27.45	29.42	26.98
76	10.11	7.08	10.91	11.27	10.00
77	18.13	19.15	19.13	17.99	20.24
78	21.38	19.37	23.67	24.24	20.43
79	34.70	32.74	29.97	29.44	26.75

SAICA station	CVA_7	CVA_8	CVA_9	CVA_10	CVA_11
80	14.24	15.21	14.27	18.36	13.93
81	39.81	43.79	38.51	32.96	41.57
82	13.55	12.47	18.56	16.40	16.06
83	49.62	53.84	46.67	50.38	59.66
84	6.54	6.02	8.34	7.74	5.11
85	27.58	29.23	27.38	28.34	28.93
86	24.87	27.93	23.53	28.34	18.05
87	13.62	10.58	11.05	16.10	11.25
88	15.34	15.43	13.22	10.32	11.25
89	7.27	7.70	6.35	6.98	5.57
90	49.75	43.84	47.92	41.89	44.80
91	37.03	35.07	29.40	31.79	33.51

Table S3a. Values of conductivity indices (CIs) selected according to variance inflation factor: Coefficient of variation of mean conductivity for the months of January (CVM1) to December (CVM12) from 2007 to 2011.

SAICA station	CVM1	CVM2	CVM3	CVM4	CVM5	CVM6	CVM7	CVM8	CVM9	CVM10	CVM11	CVM12
1	8.37	7.74	7.62	7.45	7.61	8.32	9.19	10.95	11.57	10.65	11.73	11.15
2	25.22	27.19	25.42	23.83	24.64	25.77	23.35	23.31	23.66	24.06	24.69	25.04
3	16.80	17.53	17.37	17.43	17.00	17.16	16.54	17.29	17.13	17.45	17.08	17.90
4	44.33	41.04	41.71	41.23	39.96	39.06	41.17	39.16	39.43	43.02	44.52	44.89
5	22.41	22.04	20.47	20.64	23.21	22.15	22.69	22.86	22.49	22.39	22.90	23.11
6	23.21	21.96	23.37	22.95	22.56	22.03	20.56	20.86	21.58	23.55	24.33	24.00
7	28.15	27.14	27.42	27.33	25.55	24.90	24.58	22.78	24.19	25.82	26.76	27.15
8	10.89	10.75	11.06	10.77	10.99	11.26	11.27	11.23	11.43	11.44	11.67	11.95
9	22.71	21.71	21.99	22.32	21.53	21.51	22.13	21.60	21.59	21.85	21.72	23.20
10	10.72	10.94	11.15	10.95	11.24	11.34	11.23	10.49	10.72	11.02	12.13	12.22
11	28.21	27.97	27.74	27.02	24.35	24.64	24.89	28.30	28.15	27.96	29.21	30.21
12	32.01	33.39	31.07	29.28	29.03	29.50	29.67	29.09	32.41	31.62	30.75	32.35
13	29.90	30.12	31.06	29.59	29.81	30.37	30.36	31.03	32.50	32.04	31.35	31.20
14	23.64	23.80	23.82	23.64	23.62	23.28	23.32	22.51	22.17	22.67	22.70	22.52

SAICA station	CVM1	CVM2	CVM3	CVM4	CVM5	CVM6	CVM7	CVM8	CVM9	CVM10	CVM11	CVM12
15	20.57	20.47	20.75	20.14	20.34	20.18	20.06	19.18	18.60	19.45	20.58	21.10
16	34.04	34.16	33.68	35.65	34.44	40.02	41.06	41.57	37.77	38.89	37.60	37.55
17	16.57	16.92	16.92	16.87	16.23	15.35	15.34	14.82	15.34	14.53	14.61	16.35
18	17.12	17.23	17.10	17.82	17.29	16.49	17.77	15.84	18.21	16.38	13.85	17.16
19	15.07	16.91	16.39	18.78	15.52	16.28	15.93	13.62	13.84	14.67	15.20	15.60
20	14.09	13.76	14.05	14.13	13.71	13.28	17.50	15.42	16.94	17.34	17.36	17.13
21	28.82	27.25	26.44	34.37	26.91	24.65	28.81	33.73	29.28	29.32	30.44	30.57
22	30.60	35.95	40.71	38.94	37.55	32.13	30.94	38.29	38.29	35.91	32.15	29.65
23	47.46	47.20	47.08	47.86	46.93	47.84	49.14	45.42	47.00	46.05	45.90	45.48
24	8.52	8.25	7.74	8.12	7.55	8.56	9.00	12.29	13.02	12.10	12.14	12.84
25	11.96	12.03	12.27	12.20	13.74	14.01	14.25	13.91	13.82	14.05	14.62	14.24
26	23.50	24.01	24.41	24.47	26.64	26.36	28.01	28.18	27.49	27.16	28.11	27.78
27	26.63	26.95	27.19	27.37	29.18	29.59	29.81	29.37	28.59	28.47	29.47	29.63
28	18.14	22.75	20.43	16.39	18.92	18.45	21.39	14.99	20.94	23.01	21.60	19.93
29	32.12	31.44	29.38	27.76	31.70	31.56	32.19	29.32	29.88	33.57	36.30	34.70
30	19.23	19.24	19.81	20.26	23.06	24.50	25.81	24.39	23.58	23.53	23.58	24.19

SAICA station	CVM1	CVM2	CVM3	CVM4	CVM5	CVM6	CVM7	CVM8	CVM9	CVM10	CVM11	CVM12
31	49.62	45.66	41.40	45.77	49.35	57.68	67.71	63.09	57.67	61.89	67.35	66.35
32	8.39	7.79	7.30	6.35	6.59	6.95	7.56	8.16	9.02	9.04	8.31	8.25
33	36.64	36.65	37.64	38.49	38.54	35.90	28.93	34.50	34.31	36.76	36.72	38.05
34	23.15	22.44	22.12	22.34	23.43	24.33	25.81	27.28	28.54	34.26	33.01	32.04
35	22.73	20.98	21.74	22.23	23.44	24.47	24.01	25.53	24.87	24.53	24.38	24.78
36	23.48	22.20	22.71	21.51	23.43	24.23	26.27	28.22	28.30	28.91	29.60	30.52
37	25.83	27.61	24.16	26.50	32.68	34.38	37.79	31.16	33.69	37.93	38.99	41.47
38	20.25	20.90	18.62	17.31	18.89	19.58	21.58	19.44	21.90	22.50	22.72	22.81
39	29.28	29.13	31.43	32.58	31.78	32.15	30.30	32.81	33.55	36.54	38.65	38.16
40	17.72	17.90	20.58	20.86	22.82	21.21	25.63	28.79	29.80	30.71	30.16	29.33
41	26.77	27.32	26.21	25.99	28.97	30.23	32.81	35.05	34.36	34.34	33.91	33.09
42	43.13	43.65	42.33	43.66	43.79	43.82	46.50	46.74	48.12	49.28	50.55	47.91
43	25.19	18.08	17.44	16.94	20.58	21.33	22.54	24.14	26.56	22.90	22.89	22.54
44	16.26	16.61	16.48	16.46	17.24	17.97	18.53	18.87	19.02	19.71	19.89	19.43
45	15.49	15.28	15.84	17.96	19.57	20.93	20.36	21.65	20.49	19.71	20.03	20.48
46	15.20	36.15	15.61	15.80	17.38	18.59	18.79	16.40	16.48	16.65	16.58	16.52

SAICA station	CVM1	CVM2	CVM3	CVM4	CVM5	CVM6	CVM7	CVM8	CVM9	CVM10	CVM11	CVM12
47	17.07	16.02	16.34	17.10	19.02	19.07	19.23	20.56	21.07	22.73	21.48	20.79
48	23.59	21.46	22.11	23.00	23.81	24.41	19.77	23.52	25.73	24.23	23.66	24.22
49	13.91	11.97	11.39	11.19	10.73	11.46	12.23	17.70	18.97	17.54	15.98	17.47
50	22.24	23.23	22.46	22.83	25.19	24.77	25.64	28.38	28.52	22.28	25.05	24.03
51	25.19	24.41	24.94	27.12	26.26	26.06	27.59	23.84	26.13	23.58	25.37	25.07
52	11.96	12.19	12.17	12.43	12.09	12.18	14.54	17.69	17.92	17.28	17.61	17.75
53	35.07	34.89	33.30	31.40	33.25	35.75	37.81	34.46	34.95	38.70	41.16	40.28
54	25.14	24.29	24.45	22.52	22.92	25.40	24.82	21.63	20.77	23.80	24.87	24.54
55	12.46	12.31	19.72	15.59	16.25	14.56	17.20	15.52	20.29	18.88	16.94	19.91
56	27.20	29.96	25.84	25.17	25.34	33.43	34.30	35.83	35.13	37.43	46.85	50.62
57	15.14	19.02	15.66	15.86	15.50	15.28	18.35	19.79	20.01	20.34	20.39	24.44
58	27.23	26.93	27.41	27.93	23.91	27.06	26.66	29.26	26.63	25.83	27.29	29.00
59	8.34	10.56	12.71	11.22	7.28	8.89	8.59	7.33	7.25	7.78	7.31	8.51
60	23.37	22.30	25.68	26.31	26.93	22.63	23.52	27.00	27.40	32.33	30.69	29.71
61	9.97	10.10	10.16	9.82	9.98	10.96	13.57	9.02	13.10	10.77	9.40	9.49
62	11.32	11.86	14.15	11.56	11.76	11.81	11.65	13.44	12.60	13.13	13.08	13.05

SAICA station	CVM1	CVM2	CVM3	CVM4	CVM5	CVM6	CVM7	CVM8	CVM9	CVM10	CVM11	CVM12
63	18.70	19.57	19.89	18.50	16.22	15.10	13.39	19.11	16.98	16.73	16.03	20.09
64	19.88	19.48	20.05	20.67	19.36	21.45	19.35	19.84	20.64	21.67	22.09	22.92
65	8.39	11.18	12.57	11.26	10.83	15.97	11.69	15.12	10.77	14.44	15.61	11.48
66	19.81	21.16	19.69	19.01	16.29	17.93	18.93	20.15	19.76	20.70	19.66	18.77
67	23.74	22.49	25.57	24.48	23.41	25.28	27.84	23.98	22.76	24.43	23.61	25.31
68	37.17	34.00	51.89	32.91	33.10	32.80	34.66	32.65	31.08	32.50	34.84	37.93
69	21.67	23.22	23.36	24.49	25.81	27.83	25.68	27.52	25.93	25.33	23.91	23.38
70	35.22	33.25	34.42	36.28	35.01	34.32	35.66	37.27	34.92	34.74	32.98	32.75
71	29.15	29.20	29.56	29.94	30.23	30.71	30.76	28.81	28.67	28.90	29.35	28.87
72	17.25	16.46	16.43	18.27	17.25	16.02	14.77	18.22	17.79	17.76	17.61	18.21
73	19.99	21.63	22.51	20.61	21.84	21.38	18.02	19.36	20.48	19.95	22.75	21.51
74	31.36	30.93	37.92	38.10	33.66	34.70	35.11	35.49	32.35	31.79	29.96	32.27
75	26.50	26.61	26.32	26.64	26.88	27.14	28.70	27.51	26.63	26.69	27.15	27.02
76	9.89	10.02	9.53	10.05	9.55	9.89	11.48	11.02	10.13	9.23	9.74	10.15
77	19.84	19.51	19.89	22.22	20.98	19.72	19.99	20.01	19.78	19.23	18.68	19.88
78	20.90	20.21	21.80	24.28	21.18	20.39	22.87	24.03	21.10	23.03	22.31	21.49

SAICA station	CVM1	CVM2	CVM3	CVM4	CVM5	CVM6	CVM7	CVM8	CVM9	CVM10	CVM11	CVM12
79	30.62	30.02	30.28	31.30	29.84	30.08	30.95	30.87	30.97	30.93	30.76	30.42
80	15.75	16.25	16.64	16.93	16.55	16.23	16.93	15.79	15.92	15.77	15.36	15.83
81	37.43	38.98	40.95	39.80	38.64	38.03	37.06	42.41	41.25	41.35	40.78	40.55
82	15.62	16.07	15.94	16.35	15.40	14.98	15.55	14.70	14.71	15.41	15.21	15.54
83	53.53	54.91	52.55	51.38	50.88	54.03	53.20	53.42	52.65	53.43	54.70	57.45
84	7.00	6.83	6.73	6.69	6.75	6.30	6.94	6.81	7.46	7.54	7.07	7.48
85	28.53	28.73	29.09	27.99	26.64	27.32	28.47	28.75	29.87	29.82	29.41	28.75
86	25.49	25.28	25.18	25.08	23.64	23.98	23.32	25.16	24.94	26.31	24.63	24.62
87	14.07	13.37	16.55	15.72	14.49	16.00	15.67	15.96	15.75	15.04	14.33	14.24
88	14.22	13.92	14.46	14.42	14.04	14.03	12.95	12.78	13.16	13.55	13.73	13.53
89	7.86	7.61	8.23	7.79	7.43	7.33	8.03	6.56	7.03	7.01	7.42	7.47
90	48.45	39.23	50.96	45.49	45.47	46.39	45.47	48.37	50.74	46.49	45.37	47.37
91	34.78	34.27	36.49	37.44	33.32	33.11	37.02	32.76	33.31	31.24	32.41	32.60

Table S3b. Values of conductivity indices (CIs) selected according to variance inflation factor: Julian day of annual maximum (JMax) and minimum (JMin) conductivity from 2001 to 2011.

SAICA station	JMax_7	JMax_8	JMax_9	JMax_10	JMax_11	JMin_7	JMin_8	JMin_9	JMin_10	JMin_11
1	345	342	222	224	161	214	154	35	11	316
2	41	342	222	283	160	37	155	63	93	284
3	191	100	99	99	67	34	276	61	346	345
4	128	129	343	160	313	214	338	315	3	284
5	8	250	220	188	313	122	154	337	3	306
6	128	68	188	127	96	214	338	337	3	60
7	312	99	66	340	37	276	308	315	11	316
8	342	68	283	129	343	93	339	94	339	246
9	345	164	102	41	222	336	154	33	335	1
10	346	12	101	182	192	125	278	308	162	335
11	67	40	314	10	10	93	125	315	336	92
12	40	9	190	189	253	336	254	42	41	152
13	41	336	214	61	11	93	33	338	63	91
14	285	347	32	316	101	345	163	11	186	32

SAICA station	JMax_7	JMax_8	JMax_9	JMax_10	JMax_11	JMin_7	JMin_8	JMin_9	JMin_10	JMin_11
15	346	133	132	152	346	91	159	343	344	10
16	346	133	222	343	342	91	159	224	193	215
17	335	1	32	281	128	186	340	5	346	32
18	192	103	122	255	222	69	340	247	5	285
19	94	223	41	343	9	340	158	5	125	60
20	98	99	215	184	185	100	255	247	5	346
21	284	102	99	223	101	305	32	216	4	224
22	346	72	215	93	42	189	310	278	279	193
23	313	11	189	182	39	184	340	5	153	43
24	250	249	65	338	155	306	347	213	306	222
25	274	1	152	253	154	161	313	158	217	122
26	33	336	306	345	91	189	313	342	8	122
27	61	256	305	61	91	251	221	98	67	336
28	40	342	161	223	344	69	248	214	316	132
29	70	69	313	314	11	69	4	5	346	336
30	155	338	185	184	154	282	191	159	189	336

SAICA station	JMax_7	JMax_8	JMax_9	JMax_10	JMax_11	JMin_7	JMin_8	JMin_9	JMin_10	JMin_11
31	155	338	221	188	37	282	191	216	316	285
32	253	10	217	190	9	280	343	8	127	121
33	157	128	96	187	341	341	67	186	340	96
34	161	316	344	316	278	275	2	247	38	336
35	224	12	215	224	217	155	4	247	155	122
36	91	336	312	189	11	275	35	247	346	336
37	121	183	341	219	344	306	246	314	185	43
38	183	93	33	12	346	155	40	314	346	275
39	335	345	100	162	155	336	33	277	4	336
40	345	163	282	335	1	100	255	247	316	285
41	335	345	274	224	315	275	184	341	97	336
42	12	285	276	305	32	245	342	7	97	275
43	213	43	71	6	252	41	161	98	189	336
44	346	12	276	62	60	282	191	128	189	346
45	244	103	71	224	70	69	191	343	189	336
46	305	194	132	3	41	100	161	189	33	193

SAICA station	JMax_7	JMax_8	JMax_9	JMax_10	JMax_11	JMin_7	JMin_8	JMin_9	JMin_10	JMin_11
47	223	286	122	345	11	275	285	247	61	336
48	184	34	309	214	92	69	283	336	255	162
49	160	341	310	250	278	248	125	254	340	190
50	123	1	182	156	217	161	255	130	41	254
51	3	33	338	307	3	130	69	152	255	183
52	161	254	12	345	274	188	67	96	157	282
53	158	67	7	62	281	275	35	276	346	43
54	279	158	66	157	66	335	337	2	335	32
55	252	67	97	342	311	185	158	6	305	343
56	5	336	343	160	343	161	346	340	4	316
57	7	66	218	279	37	245	40	32	345	246
58	3	93	346	12	244	100	158	191	344	41
59	60	72	335	1	245	344	154	10	338	63
60	98	281	97	188	188	346	347	123	282	121
61	12	133	338	35	68	8	275	152	183	188
62	275	125	222	314	68	216	344	60	282	252

SAICA station	JMax_7	JMax_8	JMax_9	JMax_10	JMax_11	JMin_7	JMin_8	JMin_9	JMin_10	JMin_11
63	285	12	122	33	281	306	33	216	222	9
64	343	9	157	99	182	344	347	12	193	160
65	158	38	97	251	158	63	100	313	275	213
66	284	275	153	9	36	276	184	345	154	187
67	128	343	8	100	161	276	62	216	154	187
68	281	8	342	65	67	316	338	315	3	284
69	284	102	163	161	91	8	158	280	218	36
70	8	160	8	342	188	4	276	255	154	60
71	224	163	11	345	11	338	217	63	125	187
72	345	336	214	68	253	276	215	345	123	218
73	11	132	314	10	101	307	215	34	123	249
74	345	42	253	342	158	337	93	224	70	182
75	131	224	245	315	70	277	217	310	125	187
76	335	245	152	132	61	63	184	154	221	284
77	246	247	93	132	102	128	2	220	219	193
78	94	217	277	92	92	7	311	187	186	39

SAICA station	JMax_7	JMax_8	JMax_9	JMax_10	JMax_11	JMin_7	JMin_8	JMin_9	JMin_10	JMin_11
79	132	103	12	93	342	36	156	279	95	5
80	279	127	37	193	277	343	9	311	312	8
81	132	71	71	122	12	64	248	4	339	36
82	2	277	60	285	343	63	338	315	11	121
83	128	8	129	342	39	307	246	345	154	1
84	346	255	346	12	32	36	62	247	338	190
85	315	132	344	10	41	1	215	247	63	187
86	222	284	10	152	65	337	2	33	1	193
87	276	306	306	193	65	64	217	4	4	193
88	63	286	102	95	314	339	279	5	248	126
89	344	346	344	161	3	61	64	182	67	159
90	69	250	68	100	219	246	2	216	64	71
91	98	40	129	281	188	307	93	62	154	182

Table S4. R-squared from linear regression between conductivity and precipitation per SCIs. (-) Represents that there was no evidence of a relationship between EC and precipitation

Months / Heavy and low rainfal (Conductivity related to precipitation)	**SCI1**	**SCI2**	**SCI3**	**SCI4**
	R^2 linear regression			
January	-	-	-	-
February	0.01748904	-	0.00690385	-
March	-	0.00263840	-	-
April	-	-	-	-
May	-	-	-	-
June	-	-	-	-
July	-	0.00536620	-	-
August	-	0.00526948	-	0.01555295
September	-	-	-	-
October	-	0.00501223	0.00694434	-
November	0.01992045	-	0.01243113	0.02055223
December	-	0.01488893	-	0.004584923
Heavy rainfall	-	-	0.04596652	-
Low rainfall	0.00128	0.00310293	0.000666860	-

Online Resource 2

Tittle: Human activities disrupt the temporal dynamics of salinity in Spanish rivers

Journal name: Hydrobiologia

- **Author information: The name(s) of the author(s):**

Alvaro Javier Moyano Salcedo 1,2, Edurne Estévez 3, Humbert Salvadó 4, José Barquín 5, Miguel Cañedo-Argüelles Iglesias 6,7

- **The affiliation(s) of the author(s), i.e. institution, (department), city, (state), country**

1 FEHM-Lab (Freshwater Ecology, Hydrology and Management), Departament de Biologia Evolutiva, Ecologia i Ciències Ambientals, Facultat de Biologia, Universitat de Barcelona, Barcelona, Spain.

2 Geohazards and Civil Engineering Research Group, Department of Civil Engineering, Saint Thomas Villavicencio University, C/22 No 1a, 500003, Villavicencio, Colombia.

3 Department of Ecology, University of Innsbruck, Innsbruck, Austria.

4 Department of Evolutive Biology, Ecology and Environmental Sciences, University of Barcelona, 08028 Barcelona, Spain

5 Environmental Hydraulics Institute 'IH Cantabria', University of Cantabria, PCTCAN. C/ Isabel Torres 15, 39011 Santander, Spain

6 Institute of Environmental Assessment and Water Research (IDAEA-CSIC), Carrer de Jordi Girona, 18-26, 08034, Barcelona, Spain.

7 FEHM-Lab (Freshwater Ecology, Hydrology and Management), Departament de Biologia Evolutiva, Ecologia i Ciències Ambientals, Facultat de Biologia, Institut de Recerca de l'Aigua (IdRA), Universitat de Barcelona, Barcelona, Spain.

- **e-mail address of the corresponding author**

1 A Moyano Salcedo, alvaromoyano@ub.edu

3 E Estévez, Edurne.Estevez-Cano@uibk.ac.at

4 H Salvadó, hsalvado@ub.edu

5 J Barquín, jose.barquin@unican.es

6 M Cañedo-Argüelles, miguel.canedo@idaea.csic.es

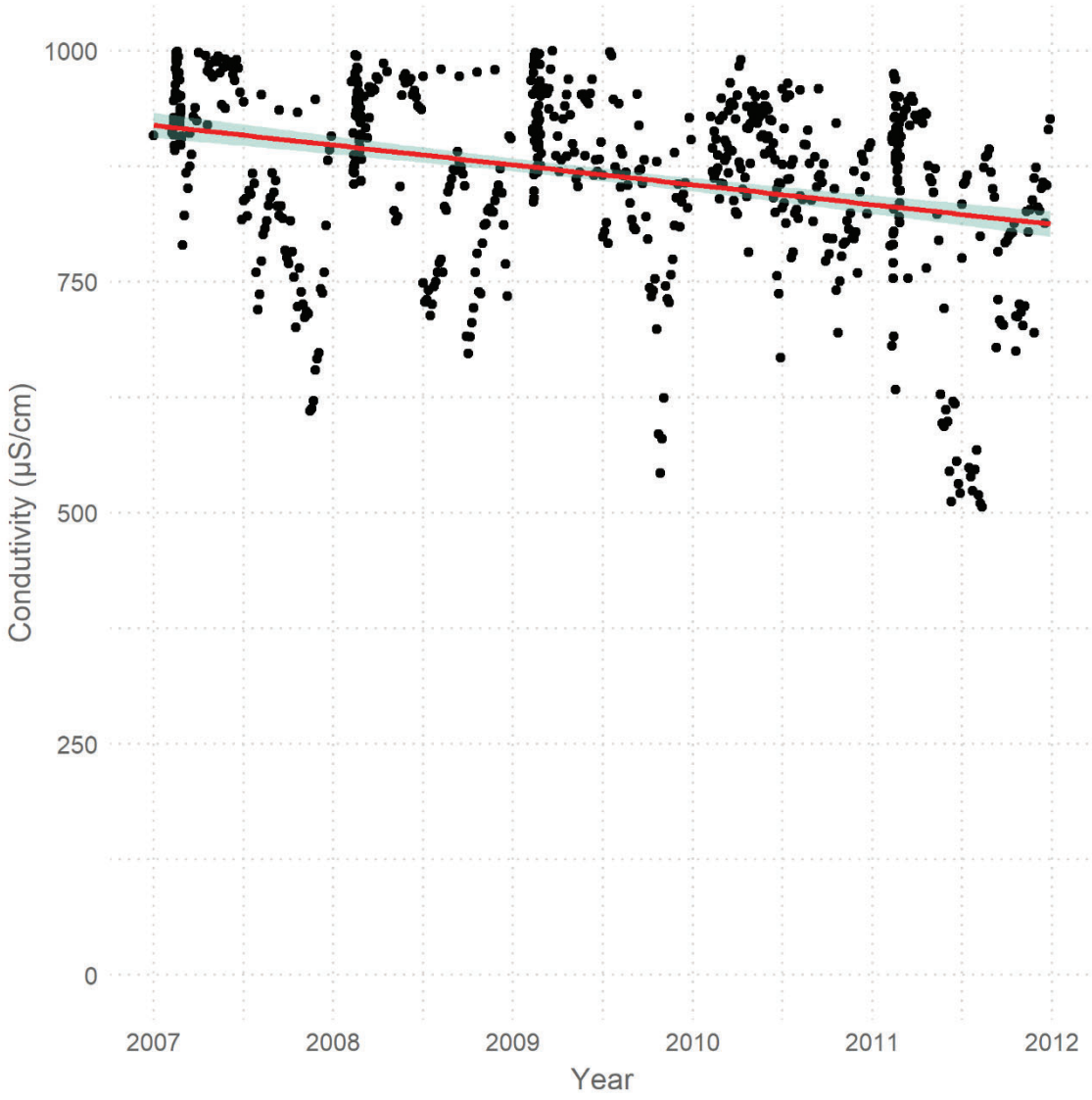


Figure S1. Scatterplot and linear model between electrical conductivity and time for the period 2007 to 2011 for the whole set of rivers analyzed. Red lines represent the electrical conductivity trends and the gray area the smoothing fit with confidence intervals. Points represent mean values of electrical conductivity per day for all rivers.

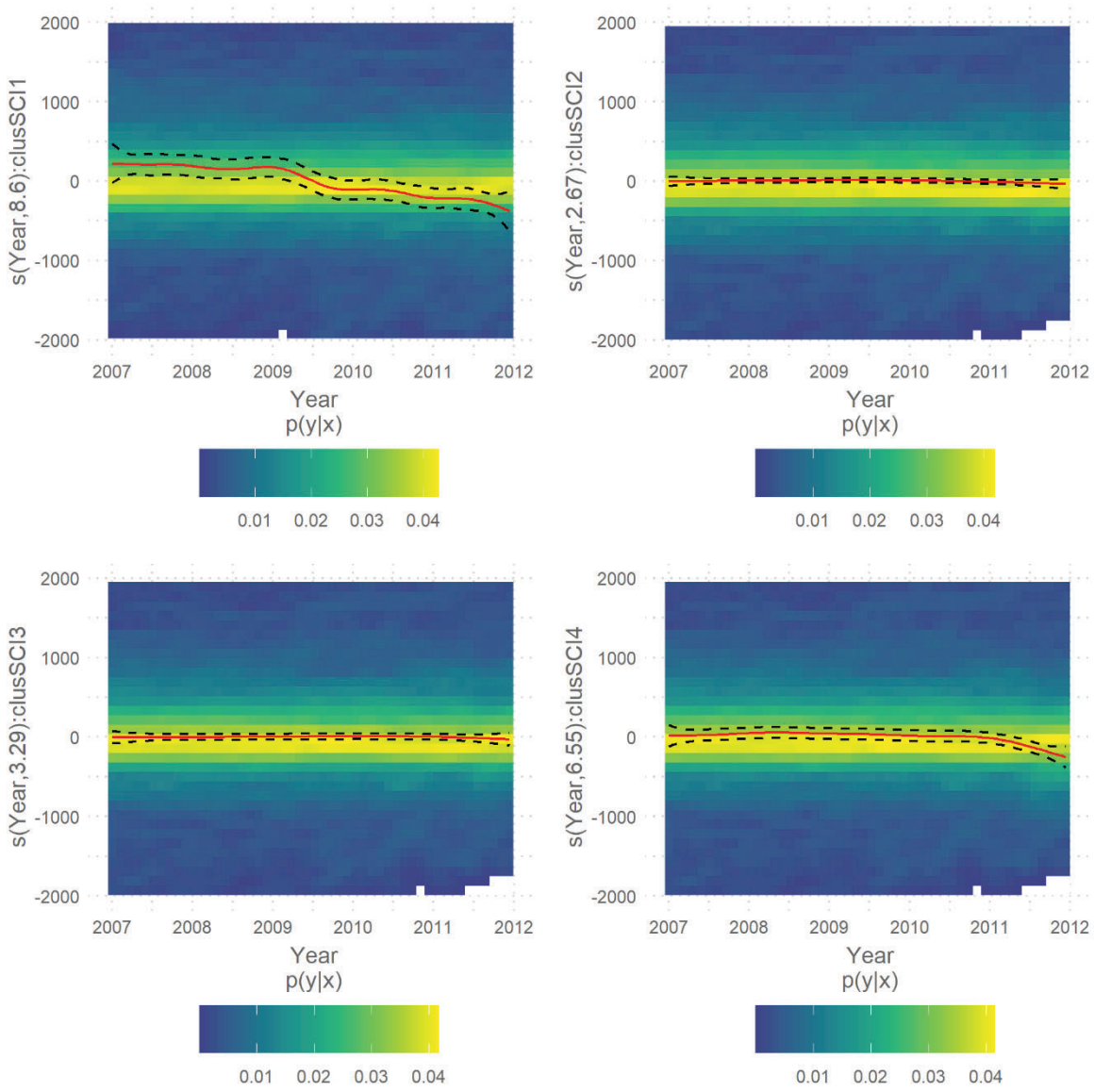


Figure S2. GAM models with smoothing spline fits to explain the conductivity variation within each group of sites (SCI1, SCI2, SCI3 and SCI4) for the period 2007–2011. Dashed lines areas represent the smoothing fit with confidence intervals.

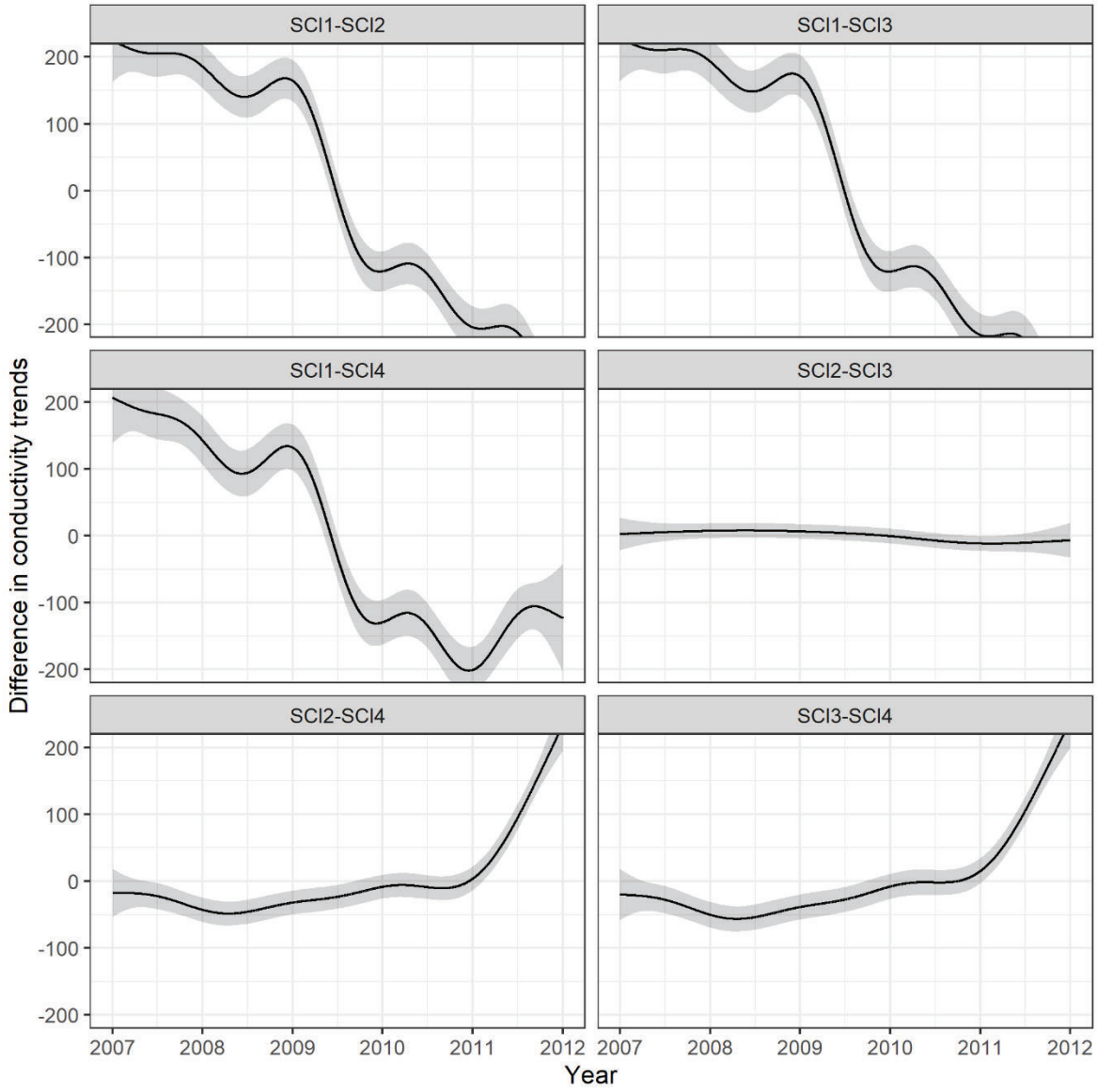


Figure S3. Pairwise comparisons for GAMs smooth terms to assess the significance of the differences in conductivity variation between groups (SCI1, SCI2, SCI3 and SCI4) for the period 2007–2011. Dashed lines represent the smoothing fit with confidence intervals.

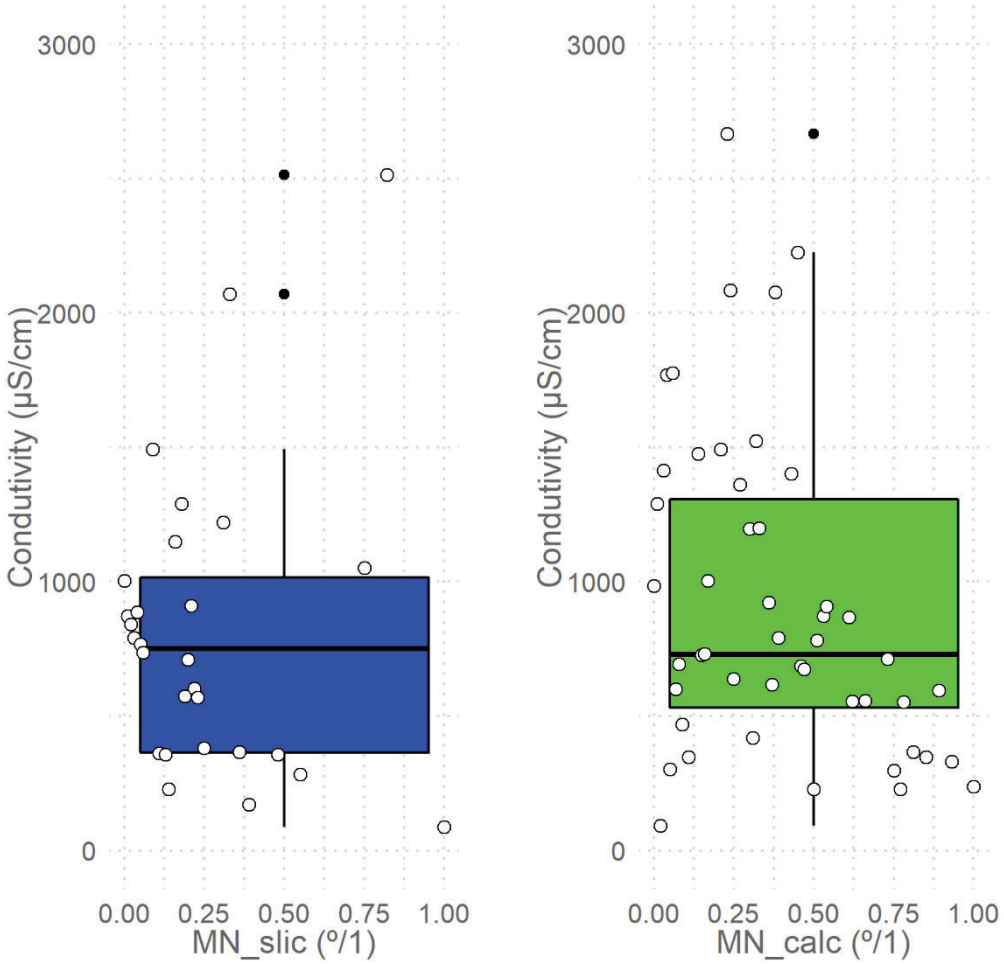


Figure S4. Boxplot of the electrical conductivity for sites divided into siliceous (MN_slic) and calcareous (MN_calc) catchments. MN_slic: Area occupied by calcareous rocks in the draining catchment. MN_calc: Area occupied by siliceous rocks in the draining catchment. The x-axis represents soil type dominance (in parts per unit (º/1)). The y-axis represents the mean conductivity calculated according to soil dominance including all rivers analyzed. The white dots represent the mean conductivity according to soil magnitude.

Online Resource 3

Tittle: Human activities disrupt the temporal dynamics of salinity in Spanish rivers

Journal name: Hydrobiologia

- **Author information: The name(s) of the author(s):**

Alvaro Javier Moyano Salcedo 1,2, Edurne Estévez 3, Humbert Salvadó 4, José Barquín 5, Miguel Cañedo-Argüelles Iglesias 6,7

- **The affiliation(s) of the author(s), i.e. institution, (department), city, (state), country**

1 FEHM-Lab (Freshwater Ecology, Hydrology and Management), Departament de Biologia Evolutiva, Ecologia i Ciències Ambientals, Facultat de Biologia, Universitat de Barcelona, Barcelona, Spain.

2 Geohazards and Civil Engineering Research Group, Department of Civil Engineering, Saint Thomas Villavicencio University, C/22 No 1a, 500003, Villavicencio, Colombia.

3 Department of Ecology, University of Innsbruck, Innsbruck, Austria.

4 Department of Evolutive Biology, Ecology and Environmental Sciences, University of Barcelona, 08028 Barcelona, Spain

5 Environmental Hydraulics Institute 'IH Cantabria', University of Cantabria, PCTCAN. C/ Isabel Torres 15, 39011 Santander, Spain

6 Institute of Environmental Assessment and Water Research (IDAEA-CSIC), Carrer de Jordi Girona, 18-26, 08034, Barcelona, Spain.

7 FEHM-Lab (Freshwater Ecology, Hydrology and Management), Departament de Biologia Evolutiva, Ecologia i Ciències Ambientals, Facultat de Biologia, Institut de Recerca de l'Aigua (IdRA), Universitat de Barcelona, Barcelona, Spain.

- **e-mail address of the corresponding author**

1 A Moyano Salcedo, alvaromoyano@ub.edu

3 E Estévez, Edurne.Estevez-Cano@uibk.ac.at

4 H Salvadó, hsalvado@ub.edu

5 J Barquín, jose.barquin@unican.es

6 M Cañedo-Argüelles, miguel.canedo@idaea.csic.es

Table S5. Electrical conductivity (mean, maximum and minimum values) reported in Spanish rivers affected by different human activities.

Study	River	Human drivers of salinization	Mean conductivity (mS/cm)	Minimum conductivity (mS/cm)	Maximum conductivity (mS/cm)	Reference
Seasonal water quality variations in a river affected by acid mine drainage: the Odiel River (Southwest Spain)	Odiel River	Mining	1.4	0.16	4.8	Oliás et al., 2004
Evaluation of natural and anthropogenic influences on the Guadalquivir River (Spain) by dissolved heavy metals and nutrients	Guadalquivir River	Sewage Agriculture	8.8	0.68	50.7	Mendiguchía et al., 2007.
Trend study and assessment of surface water quality in the Ebro River (Spain)	Ebro river	Low pollution regions (low population density)	0.5	0.2	0.7	Bouza-Deaño et al., 2008
		High pollution zones (sewage, agriculture)	1.1	0.8	1.3	
		Moderate pollution (downstream region)	0.9	0.8	1	
Hydrochemical characteristics and seasonal influence on the pollution by acid mine drainage	Odiel river Basin (including	Mining	2.9	0.1	18.5	Sarmiento et al., 2009

Study	River	Human drivers of salinization	Mean conductivity (mS/cm)	Minimum conductivity (mS/cm)	Maximum conductivity (mS/cm)	Reference
in the Odiel river Basin (SW Spain)	the Tinto river)					
Pollution by psychoactive pharmaceuticals in the Rivers of Madrid metropolitan area (Spain)	Jarama river	Sewage	0.03	-	-	González-Alonso et al., 2010
	Bodonal stream		0.6	0.5	0.8	
	Manzanres river		0.6	0.3	0.9	
	Guadarrama river		0.2	0.02	0.3	
	Soto Stream		0.8	-	-	
	Henares river		0.7	0.5	0.8	
	Tajo river		1.1	1	1.3	
Toxicity and potential risk assessment of a river polluted by	Villar stream	Mining	-	2.9	3.3	Sarmiento et al., 2011

Study	River	Human drivers of salinization	Mean conductivity (mS/cm)	Minimum conductivity (mS/cm)	Maximum conductivity (mS/cm)	Reference
acid mine drainage in the Iberian Pyrite Belt (SW Spain)						
Detection of veterinary drug residues in surface waters collected nearby farming areas in Galicia, North of Spain	Miño river	Agriculture Pasture Urban	0.12	0.09	0.17	Iglesias et al., 2013.
	Asma River		0.06	0.04	0.08	
Impact of potash mining in streams: The Llobregat basin (northeast Spain) as a case study	d´Or Stream	Mining	6.2	1.4	11	Ladrera et al., 2016.
	Llobregat River		-	-	2.5	
	Conangle Stream		-	-	4..5	
	Soldevila Stream		-	-	132.4	
Effects of anthropogenic pollution and hydrological	Upper Tagus river basin	Natural	1.8	-	-	

Study	River	Human drivers of salinization	Mean conductivity (mS/cm)	Minimum conductivity (mS/cm)	Maximum conductivity (mS/cm)	Reference
variation on macroinvertebrates in Mediterranean rivers: A case-study in the upper Tagus river basin (Spain)		Agriculture	5	-	-	Arenas-Sánchez et al., 2021
		Urban	1.4	-	-	
Hydrogeological, hydrodynamic and anthropogenic factors affecting the spread of pharmaceuticals and pesticides in water resources of the Granada plain (Spain)	Genil river	Agriculture (irrigation) Urban area	1.1	0.7	1.3	Llamas et al., 2022

Supplementary material: Chapter III

Table S1: Physico-chemical conditions on each treatment (3 microcosms per treatment) during the colonization and exposure period (mean ± SD). C: Control, IN: intermediate nutrients, NH: high nutrients, S: salt, e) SIN: salt in combination with intermediate nutrients and SHN: salt in interaction with high nutrients.

Period	Treatment	Physico-chemical parameters				
		pH	Conductivity ($\mu S\ cm^{-1}$)	Dissolved Oxygen ($mg\ L^{-1}$)	Dissolved Oxygen (%)	Temperature (°C)
				T0		
Colonization	C	8.26 (±0.02)	270.33 (±2.51)	8.99 (±0.26)	90.36 (±2.75)	15.66 (±0.05)
	IN	8.37 (±0.21)	259.66 (±13.57)	9.09 (±0.06)	90.83 (±0.66)	15.33 (±0.15)
	HN	8.31 (±0.10)	265.66 (±4.93)	8.95 (±0.17)	89.90 (±1.58)	15.63 (±0.20)
	S	8.57 (±0.35)	252.33 (±25.79)	9.44 (±0.44)	94.96 (±4.67)	15.50 (±0.17)
	SIN	8.23 (±0.01)	271.33 (±2.08)	8.97 (±0.20)	90.30 (±1.90)	15.66 (±0.11)
	SHN	8.27 (±0.11)	278 (±15.62)	9.20 (±0.37)	91.70 (±2.88)	15.20 (±0.40)
				T1		
Exposure	C	7.95 (±0.16)	291.66 (±8.32)	8.22 (±0.93)	81.90 (±9.36)	15.16 (±0.05)
	IN	8.21 (±0.13)	298.33 (±10.69)	9.10 (±0.06)	90 (±0.34)	14.96 (±0.05)
	HN	8.34 (±0.04)	307 (±3.60)	9.23 (±0.25)	92.06 (±2.65)	15.23 (±0.11)
	S	8.18 (±0.13)	3574.33 (±71.71)	8.95 (±0.31)	89.33 (±3.43)	15.26 (±0.15)
	SIN	8.23 (±0.10)	3630.66 (±24.00)	9.03 (±0.30)	90.26 (±3.25)	15.33 (±0.15)
	SHN	8.19 (±0.08)	3575 (±101.86)	9.02 (±0.32)	89.06 (±2.58)	14.96 (±0.30)

Period	Treatment	Physico-chemical parameters				
		pH	Conductivity ($\mu S\ cm^{-1}$)	Dissolved Oxygen ($mg\ L^{-1}$)	Dissolved Oxygen (%)	Temperature (°C)
				T2		
	C	8.53 (±0.13)	302.66 (±68.80)	9.55 (±0.33)	95.20 (±2.17)	15.73 (±0.11)
	IN	8.61 (±0.28)	289 (±38.22)	10.10 (±0.58)	100.93 (±5.57)	15.26 (±0.15)
	HN	8.61 (±0.07)	312 (±26)	9.62 (±0.21)	97.16 (±1.06)	15.56 (±0.25)
	S	8.34 (±0.07)	3720 (±18.33)	9.59 (±0.27)	98.26 (±2.22)	15.83 (±0.20)
	SIN	8.30 (±0.04)	3732 (±74.33)	9.46 (±0.31)	95.50 (±3.31)	15.80 (±0.10)
	SHN	8.36 (±0.29)	3747 (±44.13)	10.27 (±0.82)	102.26 (±7.58)	15.23 (±0.32)

Table S2: Repeated measures two-way ANOVA of conductivity, salinity and nutrients during the exposure period

	numDF	denDF	F-value	p-value
(Intercept)	1	35	32187.08	<.0001
Salinity	1	14	23529.82	<.0001
Nutrients	2	14	0.23	0.8002
Time	1	35	6.73	0.0137

Table S3: Pairwise comparisons of conductivity of two-way ANOVA Conductivity model and salinity using the Bonferroni test.

Salinity	lsmean	SE	df	lower.CL	upper.CL	.group
33.5	290.6296	15.80011	14	250.9781	330.2811	a
3000	3718.1852	15.80011	14	3678.5337	3757.8367	b

* Nutrients = Sum of individual values of $N\text{-}NH_4+$ and $P\text{-}PO_4^{3-}$. (C: $N\text{-}NH_4+ = 0.05$; $P\text{-}PO_4^{3-} = 0.037$; Cl = 33.5 mg/L), intermediate nutrient (IN: $N\text{-}NH_4+ = 0.4$; $P\text{-}PO_4^{3-} = 0.271$; Cl = 33. 5 mg/L), high nutrient (HN: $N\text{-}NH_4+ = 0.84$; $P\text{-}PO_4^{3-} = 0.80$; Cl = 33.5 mg/L), salt (S: $N\text{-}NH_4+ = 0.05$; $P\text{-}PO_4^{3-} = 0.037$; Cl = 3000 mg/L), salt with intermediate nutrient (SIN: $N\text{-}NH_4+ = 0.4$; $P\text{-}PO_4^{3-} = 0.27$; Cl = 3000 mg/L) and salt with high nutrient (SHN: $N\text{-}NH_4+ = 0.84$; $P\text{-}PO_4^{3-} = 0.80$; Cl = 3000 mg/L).

Table S4: Repeated measures two-way ANOVA Chlorophyll-a concentration of biofilm, salinity and nutrients during the exposure period

	numDF	denDF	F-value	p-value
(Intercept)	1	30	56.5105102	<.0001
Nutrients	2	14	2.1681682	0.1512
Salinity	1	14	0.4864865	0.4969
Time	2	30	18.8168168	<.0001
Nutrients: Time	4	30	2.4474475	0.0678

Table S5. Pairwise comparisons of Two-way ANOVA Chlorophyll-a model and times using the Bonferroni test. T0 represents the beginning of the exposure time, T1 corresponds to 7 days after, and T2 represents 14 days after the addition of nutrients and salt treatments.

Time	lsmean	SE	df	lower.CL	upper.CL	.group
T0	0.004444444	0.004138796	14	-0.0068037889	0.01569268	a
T1	0.011111111	0.004138796	14	-0.0001371222	0.02235934	a
T2	0.038333333	0.004138796	14	0.0270851000	0.04958157	b

Table S6: Repeated measures two-way ANOVA AFDM concentration of biofilm and salinity, nutrients during the exposure period.

	numDF	denDF	F-value	p-value
(Intercept)	1	30	549.6897052	<.0001
Nutrients	2	14	0.5960105	0.5644
Salinity	1	14	2.5502457	0.1325
Time	2	30	21.0345427	<.0001
Nutrients:Time	4	30	1.5244861	0.2202

Table S7: Pairwise comparisons of Two-way ANOVA AFDM model and times using the Bonferroni test. T0 represents the initial exposure time after colonization of the communities, T1 corresponds to 7 days after, and T2 represents 14 days after the addition of nutrients and salt treatments.

Time	lsmean	SE	df	lower.CL	upper.CL	.group
T0	0.3943222	0.03610922	14	0.2961862	0.4924583	a
T1	0.5839667	0.03610922	14	0.4858306	0.6821027	b
T2	0.6960444	0.03610922	14	0.5979084	0.7941805	b

Table S8: Repeated measures two-way ANOVA Yeff of biofilm and salinity, nutrients during the exposure period.

	numDF	denDF	F-value	p-value
(Intercept)	1	32	3087.0972847	0.0000000
Nutrients	2	32	1.3329337	0.2779499
Salinity	1	16	0.7384886	0.4028376
Time	2	32	2.1400248	0.1341880

Table S9. Repeated measures two-way ANOVA P uptake of biofilm and salinity, nutrients during the exposure period.

	numDF	denDF	F-value	p-value
(Intercept)	1	30	6.447175e+02	<.0001
Nutrients	2	14	4.863017e+01	<.0001
Salinity	1	14	6.435526e-05	0.9937
Time	2	30	1.202452e+01	0.0001
Nutrients: Time	4	30	9.175890e+00	0.0001

Table S10. Pairwise comparisons of Two-way ANOVA P uptake and times using the Bonferroni test. T0 represents the initial exposure time after colonization of the communities, T1 corresponds to 7 days after, and T2 represents 14 days after the addition of nutrients and salt treatments.

Times	lsmean	SE	df	lower.CL	upper.CL	.group
T0	0.002306976	0.0001400489	14	0.001926358	0.002687595	a
T1	0.002974620	0.0001400489	14	0.002594001	0.003355239	b
T2	0.002185844	0.0001400489	14	0.001805226	0.002566463	a

Table S11. Pairwise comparisons of Two-way ANOVA P uptake and nutrients using the Bonferroni test.

Nutrients	lsmean	SE	df	lower.CL	upper.CL	.group
0.0875	0.003820813	0.0001697956	14	0.003359350	0.004282276	b
0.671	0.001554924	0.0001697956	14	0.001093461	0.002016387	a
1.65	0.002091704	0.0001697956	14	0.001630241	0.002553167	a

* Nutrients = Sum of individual values of $N\text{-}NH_4+$ and $P\text{-}PO_4^{3-}$. (C: $N\text{-}NH_4+ = 0.05$; $P\text{-}PO_4^{3-} = 0.037$; Cl = 33.5 mg/L), intermediate nutrient (IN: $N\text{-}NH_4+ = 0.4$; $P\text{-}PO_4^{3-} = 0.271$; Cl = 33. 5 mg/L), high nutrient (HN: $N\text{-}NH_4+ = 0.84$; $P\text{-}PO_4^{3-} = 0.80$; Cl = 33.5 mg/L), salt (S: $N\text{-}NH_4+ = 0.05$; $P\text{-}PO_4^{3-} = 0.037$; Cl = 3000 mg/L), salt with intermediate nutrient (SIN: $N\text{-}NH_4+ = 0.4$; $P\text{-}PO_4^{3-} = 0.27$; Cl = 3000 mg/L) and salt with high nutrient (SHN: $N\text{-}NH_4+ = 0.84$; $P\text{-}PO_4^{3-} = 0.80$; Cl = 3000 mg/L).

Table S12. Pairwise comparisons of Two-way ANOVA P uptake and nutrients:times using the Bonferroni test. T0 represents the initial exposure time after colonization of the communities, T1 corresponds to 7 days after, and T2 represents 14 days after the addition of nutrients and salt treatments.

Nutrients	Times	lsmean	SE	df	lower.CL	upper.CL	.group
1.65	T2	0.001178150	0.0002425719	14	0.0003842746	0.001972025	a
0.671	T2	0.001478954	0.0002425719	14	0.0006850788	0.002272830	ab
0.671	T1	0.001529089	0.0002425719	14	0.0007352131	0.002322964	ab
0.671	T0	0.001656729	0.0002425719	14	0.0008628533	0.002450604	abc
1.65	T0	0.002299482	0.0002425719	14	0.0015056063	0.003093357	bc
1.65	T1	0.002797480	0.0002425719	14	0.0020036043	0.003591355	bcd
0.0875	T0	0.002964719	0.0002425719	14	0.0021708431	0.003758594	cd

Nutrients	Times	lsmean	SE	df	lower.CL	upper.CL	.group
0.0875	T2	0.003900429	0.0002425719	14	0.0031065533	0.004694304	de
0.0875	T1	0.004597292	0.0002425719	14	0.0038034166	0.005391167	e

* Nutrients = Sum of individual values of $N\text{-}NH_4+$ and $P\text{-}PO_4^{3-}$. (C: $N\text{-}NH_4+ = 0.05$; $P\text{-}PO_4^{3-} = 0.037$; Cl = 33.5 mg/L), intermediate nutrient (IN: $N\text{-}NH_4+ = 0.4$; $P\text{-}PO_4^{3-} = 0.271$; Cl = 33. 5 mg/L), high nutrient (HN: $N\text{-}NH_4+ = 0.84$; $P\text{-}PO_4^{3-} = 0.80$; Cl = 33.5 mg/L), salt (S: $N\text{-}NH_4+ = 0.05$; $P\text{-}PO_4^{3-}= 0.037$; Cl = 3000 mg/L), salt with intermediate nutrient (SIN: $N\text{-}NH_4+ = 0.4$; $P\text{-}PO_4^{3-} = 0.27$; Cl = 3000 mg/L) and salt with high nutrient (SHN: $N\text{-}NH_4+ = 0.84$; $P\text{-}PO_4^{3-} = 0.80$; Cl = 3000 mg/L).

Table S13: Repeated measures two-way ANOVA of Photosynthetic Community Composition of biofilm, salinity and nutrients during the exposure period.

	numDF	denDF	F-value	p-value
(Intercept)	1	135	386.912888	0.000000e+00
Nutrients	2	14	2.327447	1.340746e-01
Salinity	1	14	1.193438	2.930801e-01
Time	2	135	6.788153	0.0016
Biofilm	2	135	2.058481	1.316357e-01
Biofilm:Time	4	135	23.776776	<.0001

Table S14: Pairwise comparisons of Two-way ANOVA model of Photosynthetic Community Composition of Biofilm and times using the Bonferroni test. T0 represents the initial exposure time after colonization of the communities, T1 corresponds to 7 days after, and T2 represents 14 days after the addition of nutrients and salt treatments.

Times	lsmean	SE	df	lower.CL	upper.CL	.group
T0	1.095370	0.1003212	14	0.822722	1.368019	a
T1	1.109444	0.1003212	14	0.836796	1.382093	a
T2	1.521976	0.1012466	14	1.246813	1.797140	b

Table S15. Pairwise comparisons of Two-way ANOVA model of Photosynthetic Community Composition of Biofilm and biofilm:times using the Bonferroni test. T0 represents the initial exposure time after colonization of the communities, T1 corresponds to 7 days after, and T2 represents 14 days after the addition of nutrients and salt treatments.

Biofilm	Time	lsmean	SE	df	lower.CL	upper.CL	.group
CA	T1	0.7200000	0.1682384	14	0.1693990	1.270601	a
CA	T0	0.7927778	0.1682384	14	0.2421768	1.343379	a
GA	T2	0.8081510	0.1731556	14	0.2414571	1.374845	a
DS	T0	0.8927778	0.1682384	14	0.3421768	1.443379	ab
DS	T2	1.0672222	0.1682384	14	0.5166213	1.617823	ab
GA	T1	1.1500000	0.1682384	14	0.5993990	1.700601	ab
DS	T1	1.4583333	0.1682384	14	0.9077324	2.008934	ab
GA	T0	1.6005556	0.1682384	14	1.0499546	2.151157	b
CA	T2	2.6905556	0.1682384	14	2.1399546	3.241157	c

CA: Cyanobacteria; DS: Diatoms; GA: Green Algae.

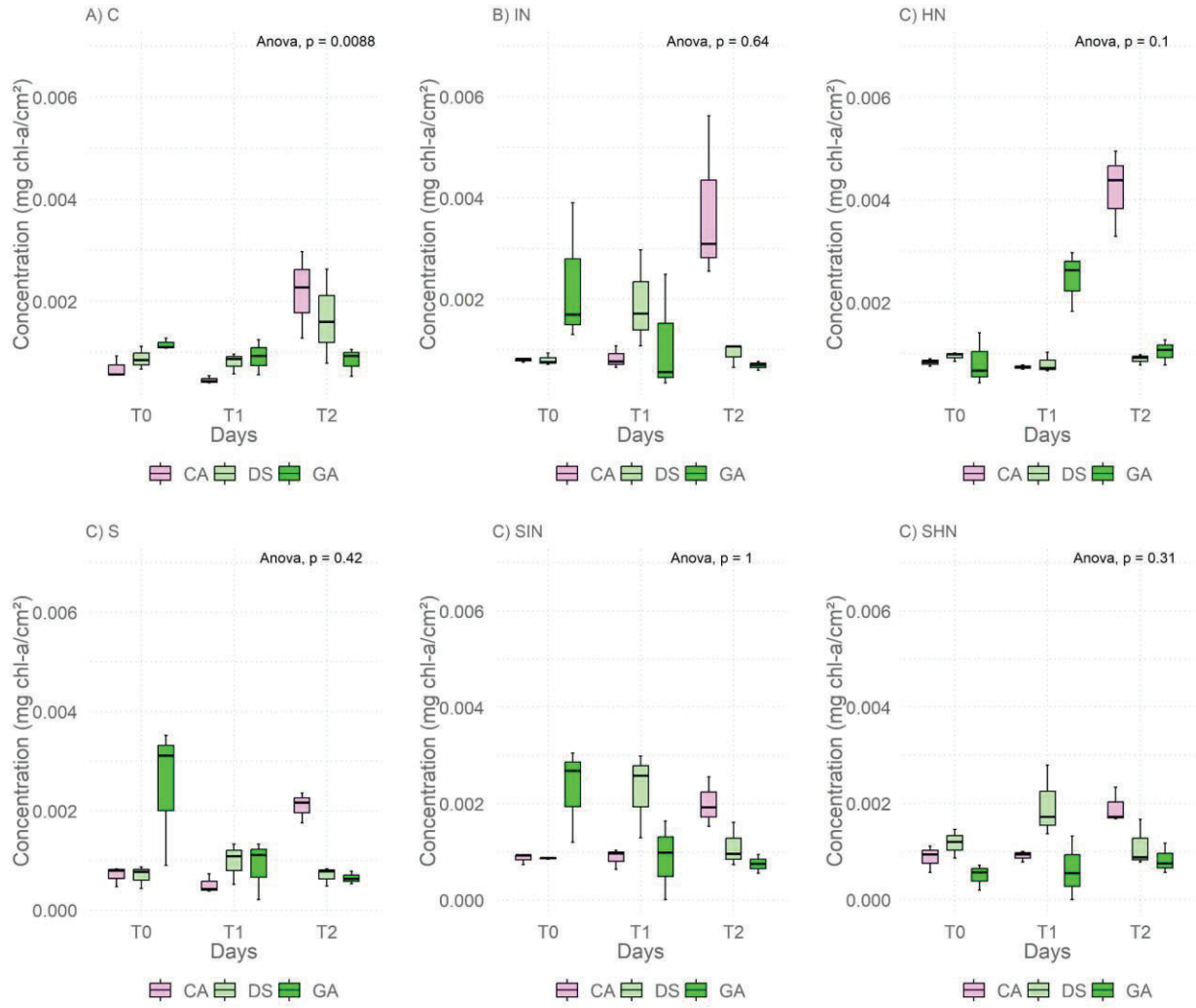


Figure S1. Changes in the biofilm community composition over the exposure period (T0, T1, T2) for each treatment. CA: Cyanobacteria; DS: Diatoms; GA: Green Algae. a) C: Control, b) IN: intermediate nutrients, c) HN: high nutrients, d) S: salt, e) SIN: salt in combination with intermediate nutrients and f) SHN: salt in combination with high nutrients. ANOVA represents the comparison of the communities (CA+DS+GA) during the exposure time (T0, T1, T2). T0 represents the initial exposure time after colonization of the communities, T1 corresponds to 7 days after, and T2 represents 14 days after the addition of nutrients and salt treatments.

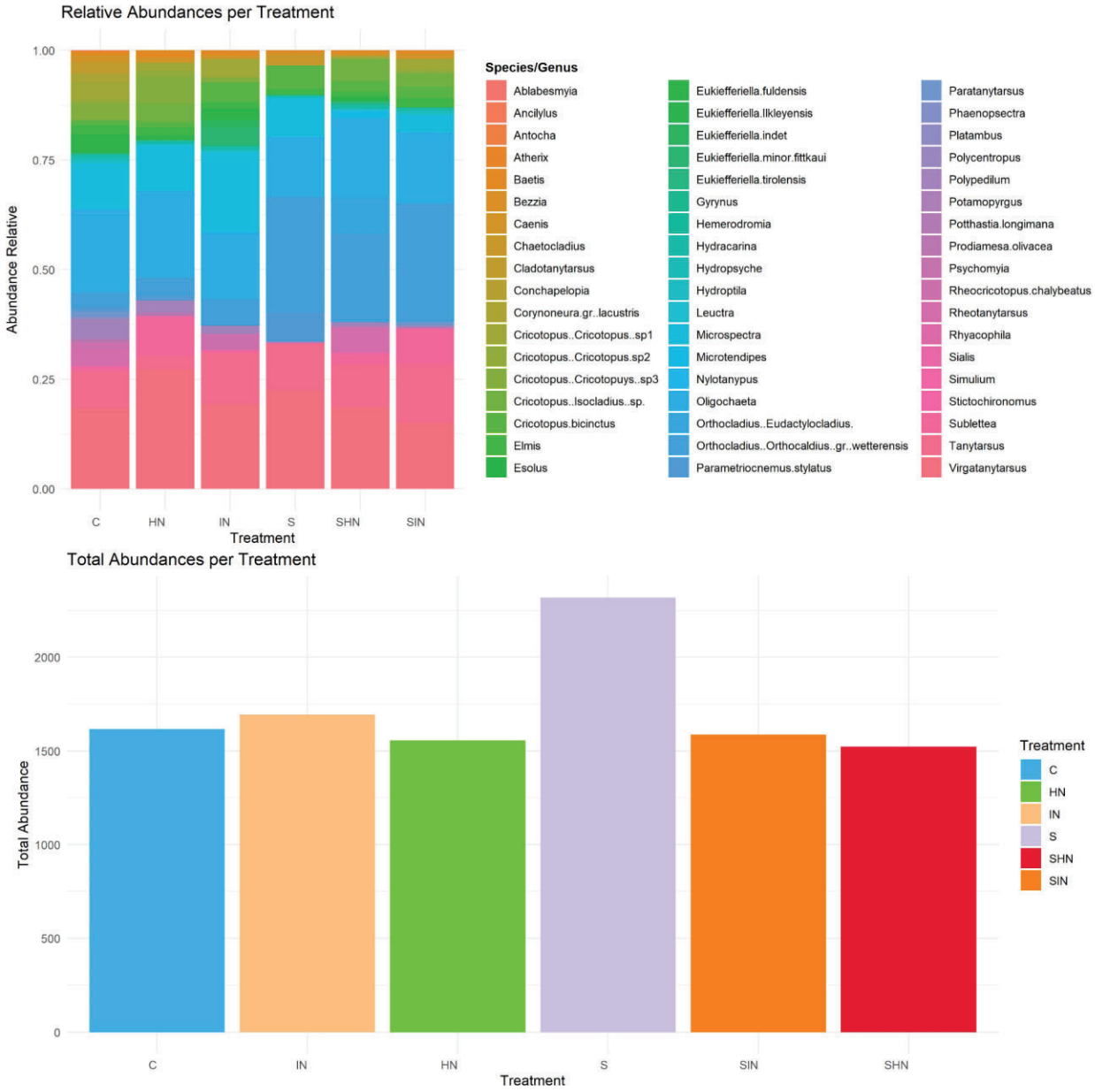


Figure S2. Plot representing total and relative abundance of macroinvertebrates of each treatment. a) C: Control, b) IN: intermediate nutrients, c) NH: high nutrients, d) S: salt, e) SIN: salt in combination with intermediate nutrients and f) SHN: salt in interaction with high nutrients.

Table S16. Total Macroinvertebrate community in each treatment. C: Control, b) IN: intermediate nutrients, c) NH: high nutrients, d) S: salt, e) SIN: salt in combination with intermediate nutrients and f) SHN: salt in interaction with high nutrients.

Channel/individuals	**C**	**IN**	**HN**	**S**	**SIN**	**SHN**
Ablabesmyia	9 ± 0	0 ± 0	0 ± 0	0 ± 0	0 ± 0	0 ± 0
Conchapelopia	9 ± 0	0 ± 0	0 ± 0	0 ± 0	0 ± 0	0 ± 0
Nylotanypus	27 ± 1	31 ± 4	22 ± 22	0 ± 0	0 ± 0	0 ± 0
Potthastia longimana	33 ± 11	71 ± 21	0 ± 0	45 ± 44	6	72 ± 72
Prodiamesa olivacea	10 ± 9	0 ± 0	9 ± 9	0 ± 0	0 ± 0	0 ± 0
Chaetocladius	0 ± 0	0 ± 0	0 ± 0	44 ± 44	0 ± 0	0 ± 0
Corynoneura gr. lacustris	30 ± 30	0 ± 0	0 ± 0	0 ± 0	0 ± 0	0 ± 0
Cricotopus (Cricotopus)sp2	11 ± 11	0 ± 0	18 ± 18	0 ± 0	12 ± 12	0 ± 0
Cricotopus (Cricotopus) sp3	56 ± 56	15 ± 15	84 ± 59	0 ± 0	0 ± 0	0 ± 0
Cricotopus (Cricotopus) sp1	61 ± 28	65 ± 64	24 ± 24	0 ± 0	38 ±37	10 ± 9
Cricotopus (Isocladius) sp.	0 ± 0	0 ± 0	54 ± 6	0 ± 0	50 ± 37	71 ± 71
Cricotopus bicinctus	17 ± 6	70 ± 39	18 ± 18	107 ± 15	37 ± 37	36
Eukiefferiella fuldensis	60 ± 60	32 ± 31	13 ± 12	0 ± 0	0 ± 0	12 ± 11
Eukiefferiella Ilkleyensis	0 ± 0	9 ± 9	0 ± 0	0 ± 0	0 ± 0	0 ± 0
Eukiefferiella indet	0 ± 0	24 ± 23	0 ± 0	0 ± 0	0 ± 0	0 ± 0
Eukiefferiella minor-fittkaui	5 ± 5	63 ± 63	0 ± 0	0 ± 0	0 ± 0	0 ± 0
Eukiefferiella tirolensis	0 ± 0	0 ± 0	0 ± 0	0 ± 0	0 ± 0	12 ± 11
Orthocladius (Eudactylocladius)	0 ± 0	0 ± 0	0 ± 0	0 ± 0	0 ± 0	119 ± 119

Channel/individuals	**C**	**IN**	**HN**	**S**	**SIN**	**SHN**
Orthocladius (Orthocladius) gr. wetterensis	47 ± 22	92 ± 1	54 ± 5	522 ± 32	418 ± 106	285 ± 69
Parametriocnemus stylatus	16 ± 16	0 ± 0	15 ± 15	132 ± 132	0 ± 0	0 ± 0
Rheocricotopus chalybeatus	22 ± 22	55 ± 55	0 ± 0	0 ± 0	0 ± 0	0
Microtendipes	0 ± 0	0 ± 0	0 ± 0	0 ± 0	0 ± 0	23 ± 22
Phaenopsectra	4 ± 4	0 ± 0	0 ± 0	0 ± 0	0 ± 0	0 ± 0
Polypedilum	66 ± 32	27 ± 18	36 ± 18	0 ± 0	6 ±6	8 ± 8
Stictochironomus	0 ± 0	0 ± 0	0 ± 0	0 ± 0	0 ± 0	5 ± 5
Cladotanytarsus	39 ± 39	0 ± 0	0 ± 0	0 ± 0	0 ± 0	0 ± 0
Microspectra	157 ± 53	278 ± 44	139 ± 76	175 ± 175	62 ± 61	0 ± 0
Paratanytarsus	18 ± 18	0 ± 0	0 ± 0	0 ± 0	13 ± 12	0 ± 0
Rheotanytarsus	57 ± 57	0 ± 0	0 ± 0	0 ± 0	0 ± 0	81 ± 81
Sublettea	13 ± 13	9 ± 9	122 ± 8	0 ± 0	124 ± 123	32 ± 32
Tanytarsus	125 ± 32	177 ± 32	40 ± 31	214 ± 10	206 ± 97	136 ± 79
Virgatanytarsus	277 + 6	295 ± 37	366 ± 15	445 ± 94	235 ± 50	267 ± 123
Hydroptila	14 ± 1	7 ± 2	3 ± 3	4 ± 1	11 ± 1	5 ± 2
Rhyacophila	1 ± 0	2 ± 1	1 ± 1	1 ± 2	3 ± 3	1 ± 1
Bezzia	3 ± 1	1 ± 1	0 ± 1	1 ± 1	2 ± 2	1 ± 1
Elmis	31 ± 8	24 ± 3	26 ± 7	24 ± 5	34 ± 8	18 ± 4
Esolus	2 ± 1	1 ± 1	1 ± 1	0 ± 0	0 ± 1	1 ± 1

Channel/individuals	**C**	**IN**	**HN**	**S**	**SIN**	**SHN**
Baetis	12 ± 1	15 ± 9	22 ± 18	10 ± 3	11 ± 2	9 ± 3
Caenis	22 ± 4	14 ± 7	15 ± 6	13 ± 5	16 ± 7	9 ± 4
Oligochaeta	285 ± 3	234 ± 68	267 ± 19	271 ± 9	252 ± 16	259 ± 27
Leuctra	2 ± 2	2 ± 3	1 ± 1	0 ± 1	1 ± 1	4 ± 3
Potamopyrgus	3 ± 2	0 ± 0	2 ± 2	0 ± 0	2 ± 1	4 ± 5
Antocha	1 ± 1	1 ± 1	0 ± 0	0 ± 0	0 ± 1	0 ± 0
Atherix	0 ± 0	0 ± 0	0 ± 0	0 ± 1	0 ± 0	1 ± 1
Hemerodromia	3 ± 1	3 ± 3	2 ± 2	1 ± 1	1 ± 2	1 ± 1
Gyrynus	1 ± 1	0 ± 0	0 ± 1	1 ± 1	0 ± 0	0 ± 0
Polycentropus	4 ± 1	2 ± 2	1 ± 2	3 ± 4	0 ± 1	3 ± 2
Simulium	3 ± 3	1 ± 1	1 ± 1	0 ± 0	0 ± 0	0 ± 0
Hydracarina	10 ± 3	11 ± 2	9 ± 4	10 ± 1	13 ± 1	11 ± 2
Platambus	1 ± 1	0 ± 0	0 ± 0	0 ± 0	0 ± 0	0 ± 0
Sialis	1 ± 1	0 ± 0	0 ± 0	0 ± 0	0 ± 0	0 ± 0
Psychomyia	1 ± 1	0 ± 0	0 ± 0	1 ± 1	0 ± 0	2 ± 3
Hydropsyche	1 ± 1	0 ± 0	0 ± 0	0 ± 0	0 ± 0	0 ± 0
Ancilylus	2 ± 0	0 ± 0	0 ± 0	0 ± 0	1 ± 2	0 ± 0

Table S17. Two-way ANOVA of macroinvertebrate richness, salinity and nutrients during the exposure time.

	numDF	denDF	F-value	p-value
(Intercept)	1	12	833.433628	<.0001
Salinity	1	12	28.318584	0.0002
Salinity:Nutrients	4	12	7.278761	0.0032

Table S18. Pairwise comparisons of Two-way ANOVA model of macroinvertebrate richness and salinity using the Bonferroni test.

Salinity	lsmean	SE	df	lower.CL	upper.CL	.group
3000	19.66667	1.181127	12	16.64294	22.69039	a
33.5	28.55556	1.181127	12	25.53183	31.57928	b

* Salinity expressed as Cl. Control (C: Cl = 33.5 mg/L), intermediate nutrient (IN: Cl = 33. 5 mg/L), high nutrient (HN: Cl = 33.5 mg/L), salt (S: Cl = 3000 mg/L), salt with intermediate nutrient (SIN: Cl = 3000 mg/L) and salt with high nutrient (SHN: Cl = 3000 mg/L).

Table S19. Pairwise comparisons of Two-way ANOVA model of macroinvertebrate richness and nutrients:salinity using the Bonferroni test.

Nutrients	Salinity	lsmean	SE	df	lower.CL	upper.CL	.group
0.0875	3000	16.66667	2.045773	12	10.21700	23.11634	a
0.671	3000	20.33333	2.045773	12	13.88366	26.78300	a
1.65	3000	22.00000	2.045773	12	15.55033	28.44967	a
0.671	33.5	24.33333	2.045773	12	17.88366	30.78300	a
1.65	33.5	24.33333	2.045773	12	17.88366	30.78300	a
0.0875	33.5	37.00000	2.045773	17	30.89533	43.10467	b

* Nutrients = Sum of individual values of $N\text{-}NH_4+$ and $P\text{-}PO_4^{3-}$ .Salinity expressed as Cl. Control (C: $N\text{-}NH_4+ = 0.05$; $P\text{-}PO_4^{3-} = 0.037$; Cl = 33.5 mg/L), intermediate nutrient (IN: $N\text{-}NH_4+ = 0.4$; $P\text{-}PO_4^{3-} = 0.271$; Cl = 33. 5 mg/L), high nutrient (HN: $N\text{-}NH_4+ = 0.84$; $P\text{-}PO_4^{3-} = 0.80$; Cl = 33.5 mg/L), salt (S: $N\text{-}NH_4+ = 0.05$; $P\text{-}PO_4^{3-}= 0.037$; Cl = 3000 mg/L), salt with intermediate nutrient (SIN: $N\text{-}NH_4+ = 0.4$; $P\text{-}PO_4^{3-} = 0.27$; Cl = 3000 mg/L) and salt with high nutrient (SHN: $N\text{-}NH_4+ = 0.84$; $P\text{-}PO_4^{3-} = 0.80$; Cl = 3000 mg/L).

Table S20: Two-way ANOVA of Shannon macroinvertebrate index, salinity and nutrients during the exposure time

	numDF	denDF	F-value	p-value
(Intercept)	1	14	1504.5326	<.0001
Salinity	1	14	12.0638	0.001
Nutrients	2	14	0.1166	0.8908
Salinity:Nutrients	2	12	3.8582	0.0508

Table S21. Pairwise comparisons of Two-way ANOVA model of Shannon macroinvertebrate index and salinity using the Bonferroni test

Salinity	lsmean	SE	df	lower.CL	upper.CL	.group
3000	2.103639	0.08424168	14	1.892229	2.315050	a
33.5	2.517434	0.08424168	14	2.306023	2.728844	b

* Salinity expressed as Cl. Control (C: Cl = 33.5 mg/L), intermediate nutrient (IN: Cl = 33. 5 mg/L), high nutrient (HN: Cl = 33.5 mg/L), salt (S: Cl = 3000 mg/L), salt with intermediate nutrient (SIN: Cl = 3000 mg/L) and salt with high nutrient (SHN: Cl = 3000 mg/L).

Table S22: Results of IndVal analysis for macroinvertebrates

Taxa	Treatment	IndVal	P Value (<0.05)
Conchapelopia	C	1	0.009
Phaenopsectra	C	1	0.007
Ancylus	C	0.67	0.034
Polypedilum	C	0.46	0.026
Hydroptila	C	0.32	0.004
Orthocladius (Orthocladius) gr. wetterensis	S	0.36	0.027
Cricotopus bicinctus	S	0.37	0.022
Virganytarsus	S	0.26	0.035

IndVal indicator values range from 0 to 1. Control (C), intermediate nutrient (IN), high nutrient (HN), salt (S), salt with intermediate nutrient (SIN) and salt with high nutrient (SHN).

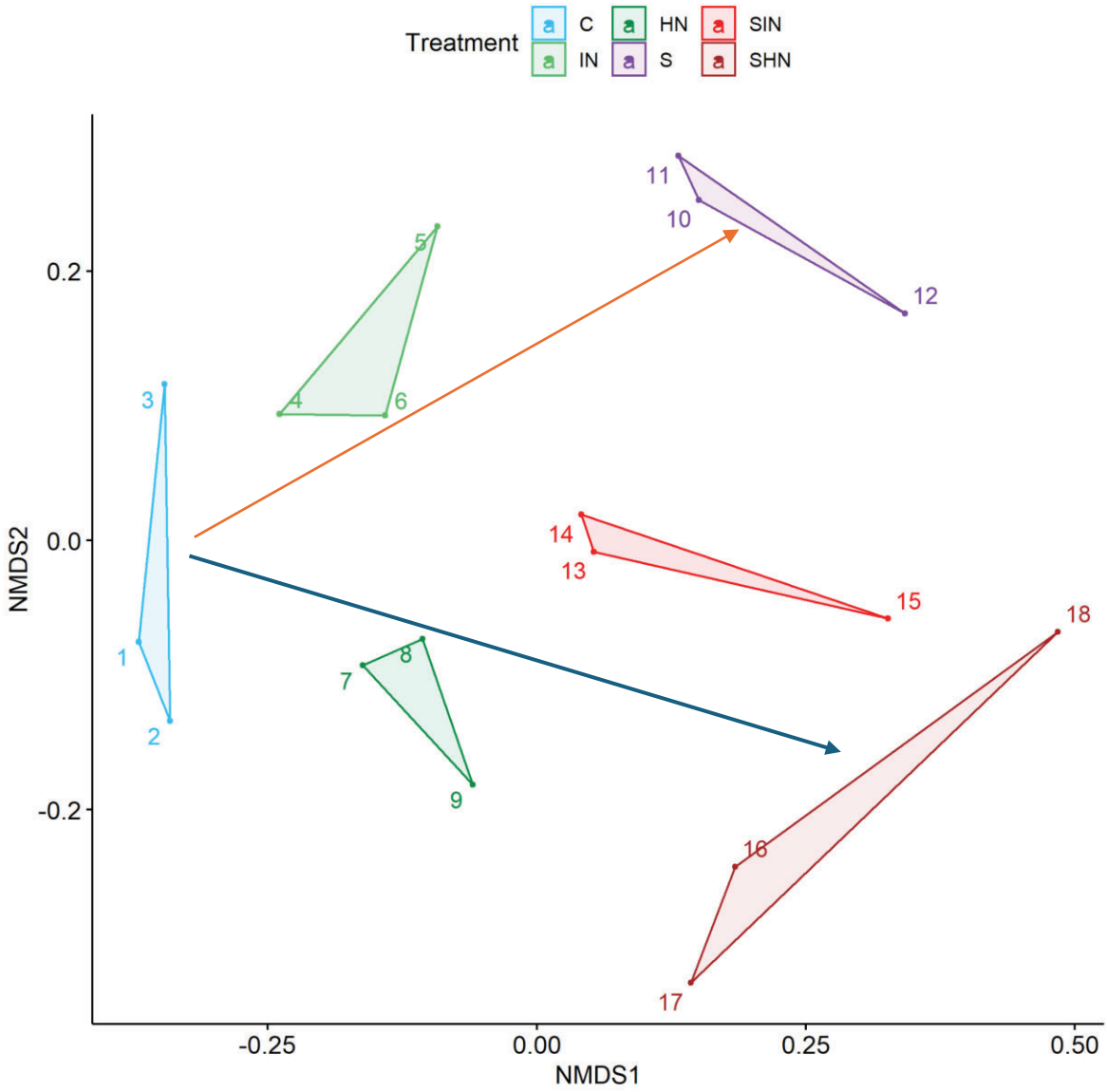


Figure S3. Results of NMDS for each treatment. Control (C), intermediate nutrient (IN), high nutrient (HN), salt (S), salt with intermediate nutrient (SIN) and salt with high nutrient (SHN). Orange line: Effects of salt and low nutrients, direct effects, salt and low nutrients do not allow antagonistic effects. Blue line: Antagonistic effects, and high nutrients do compensate for the effects of salt. SIN= Low nutrients do not have enough antagonistic power to Salt.

Table S23: Results of ADONIS analysis for the whole macroinvertebrate community in relation to nutrients and salinity treatment

Source of variance	Df	Sums of squares	Mean squares	F	R^2	P
Total community						
Nutrients	1	0.172	0.172	6.890	0.138	0.001**
Salinity	1	0.425	0.425	16.995	0.341	0.001**
Nutrients: Salinity	1	0.297	0.297	11.869	0.238	0.001**
Residuals	14	0.350	0.025		0.281	
Total	17	1.245			1	

Table S24: Total abundance of chironomidae genera in each treatment.

Code	Subfamily tribe	Channel/individuals	C	IN	HN	S	SIN	SHN	Total	% Abundance
1	Tanypodinae	Ablabesmyia	9 ± 0	0 ± 0	0 ± 0	0 ± 0	0 ± 0	0 ± 0	9 ± 4	0.12
1	Tanypodinae	Conchapelopia	9 ± 0	0 ± 0	0 ± 0	0 ± 0	0 ± 0	0 ± 0	9 ± 4	0.12
1	Tanypodinae	Nylotanypus	27 ± 1	31 ± 4	22 ± 22	0 ± 0	0 ± 0	0 ± 0	81 ± 15	1.07
2	Diamesinae	Potthastia longimana	33 ± 11	71 ± 21	0 ± 0	45 ± 44	6.00	72 ± 72	227 ± 31	3.00
2	Prodiamesinae	Prodiamesa olivacea	10 ± 9	0 ± 0	9 ± 9	0 ± 0	0 ± 0	0 ± 0	19 ± 5	0.25
3	Orthocladiinae	Chaetocladius	0 ± 0	0 ± 0	0 ± 0	44 ± 44	0 ± 0	0 ± 0	44 ± 18	0.58
3	Orthocladiinae	Corynoneura gr. lacustris	30 ± 30	0 ± 0	0 ± 0	0 ± 0	0 ± 0	0 ± 0	30 ± 12	0.40
3	Orthocladiinae	Cricotopus (Cricotopus)sp2	11 ± 11	0 ± 0	18 ± 18	0 ± 0	12 ± 12	0 ± 0	42 ± 8	0.55
3	Orthocladiinae	Cricotopus (Cricotopus) sp3	56 ± 56	15 ± 15	84 ± 59	0 ± 0	0 ± 0	0 ± 0	155 ± 36	2.06
3	Orthocladiinae	Cricotopus (Cricotopus) sp1	61 ± 28	65 ± 64	24 ± 24	0 ± 0	38 ±37	10 ± 9	198 ±27	2.62
3	Orthocladiinae	Cricotopus (Isocladius) sp.	0 ± 0	0 ± 0	54 ± 6	0 ± 0	50 ± 37	71 ± 71	175 ± 33	2.31
3	Orthocladiinae	Cricotopus bicinctus	17 ± 6	70 ± 39	18 ± 18	107 ± 15	37 ± 37	36.00	286 ± 35	3.78
3	Orthocladiinae	Eukiefferiella fuldensis	60 ± 60	32 ± 31	13 ± 12	0 ± 0	0 ± 0	12 ± 11	115 ± 23	1.52
3	Orthocladiinae	Eukiefferiella Ilkleyensis	0 ± 0	9 ± 9	0 ± 0	0 ± 0	0 ± 0	0 ± 0	9 ± 4	0.12
3	Orthocladiinae	Eukiefferiella indet	0 ± 0	24 ± 23	0 ± 0	0 ± 0	0 ± 0	0 ± 0	23 ± 9	0.31

Code	Subfamily tribe	Channel/individuals	C	IN	HN	S	SIN	SHN	Total	% Abundance
3	Orthocladiinae	Eukiefferiella minor-fittkaui	5 ± 5	63 ± 63	0 ± 0	0 ± 0	0 ± 0	0 ± 0	68 ± 25	0.91
3	Orthocladiinae	Eukiefferiella tirolensis	0 ± 0	0 ± 0	0 ± 0	0 ± 0	0 ± 0	12 ± 11	12 ± 5	0.15
3	Orthocladiinae	Orthocladius (Eudactylocladius)	0 ± 0	0 ± 0	0 ± 0	0 ± 0	0 ± 0	119 ± 119	119 ± 49	1.57
3	Orthocladiinae	Orthocladius (Orthocladius) gr. wetterensis	47 ± 22	92 ± 1	54 ± 5	**522 ± 32**	**418 ± 106**	**285 ± 69**	1419 ± 203	18.75
3	Orthocladiinae	Parametriocnemus stylatus	16 ± 16	0 ± 0	15 ± 15	132 ± 132	0 ± 0	0 ± 0	164 ± 52	2.17
3	Orthocladiinae	Rheocricotopus chalybeatus	22 ± 22	55 ± 55	0 ± 0	0 ± 0	0 ± 0	0.00	78 ± 23	1.03
4	Chironominii	Microtendipes	0 ± 0	0 ± 0	0 ± 0	0 ± 0	0 ± 0	23 ± 22	22 ± 9	0.30
4	Chironominii	Phaenopsectra	4 ± 4	0 ± 0	0 ± 0	0 ± 0	0 ± 0	0 ± 0	4 ± 2	0.06
4	Chironominii	Polypedilum	66 ± 32	27 ± 18	36 ± 18	0 ± 0	6 ±6	8 ± 8	143 ± 25	1.90
4	Chironominii	Stictochironomus	0 ± 0	0 ± 0	0 ± 0	0 ± 0	0 ± 0	5 ± 5	5 ± 2	0.07
5	Tanytarsinii	Cladotanytarsus	39 ± 39	0 ± 0	0 ± 0	0 ± 0	0 ± 0	0 ± 0	39 ± 16	0.52
5	Tanytarsinii	Microspectra	157 ± 53	278 ± 44	139 ± 76	175 ± 175	62 ± 61	0 ± 0	813 ± 96	10.74
5	Tanytarsinii	Paratanytarsus	18 ± 18	0 ± 0	0 ± 0	0 ± 0	13 ± 12	0 ± 0	31 ± 8	0.42
5	Tanytarsinii	Rheotanytarsus	57 ± 57	0 ± 0	0 ± 0	0 ± 0	0 ± 0	81 ± 81	138 ± 36	1.82

Code	Subfamily tribe	Channel/individuals	C	IN	HN	S	SIN	SHN	Total	% Abundance
5	Tanytarsinii	Sublettea	13 ± 13	9 ± 9	122 ± 8	0 ± 0	124 ± 123	32 ± 32	302 ± 58	3.98
5	Tanytarsinii	Tanytarsus	125 ± 32	177 ± 32	40 ± 31	214 ± 10	206 ± 97	136 ± 79	901 ±65	11.90
5	Tanytarsinii	Virgatanytarsus	277 + 6	295 ± 37	366 ± 15	445 ± 94	235 ± 50	267 ± 123	1888 ± 77	24.93
		Total	**1177 ± 206**	**1314 ± 233**	**1017 ± 185**	**1685± 310**	**1207 ± 222**	**1170 ± 209**	**7572 ± 1344**	100

*Colors highlight genera according to abundance associated with each treatment.

	Presence only in control, minority species
	Highly sensitive to salinity
xxx	Higher abundance in salinity treatments
	Presence in all salt and nutrient treatments and interactions

Table S25: Summary of Structural equation model showing the effects of nutrient and salt addition on the biofilm and aquatic macroinvertebrate communities. Salinity: salinity (mg L−1); Nutrients: N-NH4 and P-PO4 (mg L−1); Chla: chlorophyll-a concentration (µg cm−2); Yield: photosynthetic efficiency; PUptake: Phosphorus uptake (mg P cm²*h -1); DS: diatom concentration (µg cm−2); GA: Green algae concentration (µg cm−2); CA: Cyanobacteria concentration (µg cm−2); Richness: taxa richness of aquatic macroinvertebrates; Shannon: Shannon Diversity of aquatic macroinvertebrates Abundance: abundance of aquatic macroinvertebrates (total number of individuals). Lavaan 0.6.16 ended normally after 22 iterations

Estimator	ML	
Optimization method		NLMINB
Number of model parameters		48
Number of observations		18
Model Test User Model:		
Test statistic	36.368	
Degrees of freedom		15
P-value (Chi-square)		0.002
Model Test Baseline Model:		
Test statistic	197.355	
Degrees of freedom		54
P-value	0.000	
User Model versus Baseline Model:		
Comparative Fit Index (CFI)		0.891
Tucker-Lewis Index (TLI)		0.463
Loglikelihood and Information Criteria:		
Loglikelihood user model (H0)		-144.745
Loglikelihood unrestricted model (H1)		-126.561
Akaike (AIC)	385.489	
Bayesian (BIC)	428.227	
Sample-size adjusted Bayesian (SABIC)		280.738
Root Mean Square Error of Approximation:		
RMSEA	0.281	
90 Percent confidence interval - lower		0.166
90 Percent confidence interval - upper		0.399
P-value H_0: RMSEA <= 0.050		0.003
P-value H_0: RMSEA >= 0.080		0.995

Standardized Root Mean Square Residual:

SRMR	0.172

Parameter Estimates:

Standard errors	Standard
Information	Expected
Information saturated (h1) model	Structured

Regressions:

	Estimate	Std.Err	z-value	P(>|z|)	Std.lv	Std.all
Richness ~						
Salinity	-0.611	0.097	-6.323	0.000	-0.611	-0.528
Nutrients	1.056	0.146	7.225	0.000	1.056	0.914
Yield	-0.454	0.106	-4.279	0.000	-0.454	-0.393
Chla	0.043	0.076	0.565	0.572	0.043	0.037
CA	-0.214	0.091	-2.359	0.018	-0.214	-0.185
DS	0.585	0.071	8.214	0.000	0.585	0.507
GA	-0.370	0.078	-4.762	0.000	-0.370	-0.320
PUptake	0.744	0.116	6.390	0.000	0.744	0.644
Abundance ~						
Salinity	0.223	0.201	1.110	0.267	0.223	0.201
Nutrients	-0.241	0.304	-0.794	0.427	-0.241	-0.217
Yield	-0.310	0.220	-1.406	0.160	-0.310	-0.279
Chla	0.248	0.158	1.572	0.116	0.248	0.223
CA	0.354	0.188	1.880	0.060	0.354	0.319
DS	0.187	0.148	1.263	0.207	0.187	0.168
GA	-0.241	0.161	-1.491	0.136	-0.241	-0.217
PUptake	0.473	0.242	1.954	0.051	0.473	0.426
Shannon ~						
Salinity	-0.781	0.110	-7.124	0.000	-0.781	-0.695
Nutrients	0.695	0.166	4.188	0.000	0.695	0.619
Yield	-0.236	0.120	-1.956	0.050	-0.236	-0.210
Chla	0.234	0.086	2.718	0.007	0.234	0.209
CA	-0.414	0.103	-4.016	0.000	-0.414	-0.368
DS	0.510	0.081	6.294	0.000	0.510	0.453
GA	-0.338	0.088	-3.823	0.000	-0.338	-0.300
PUptake	0.600	0.132	4.536	0.000	0.600	0.534
Chla ~						
Salinity	-0.130	0.215	-0.605	0.545	-0.130	-0.130
Nutrients	0.385	0.215	1.790	0.074	0.385	0.385
Yield ~						
Salinity	0.182	0.154	1.181	0.237	0.182	0.182
Nutrients	0.734	0.154	4.766	0.000	0.734	0.734
PUptake ~						
Salinity	-0.161	0.140	-1.145	0.252	-0.161	-0.161
Nutrients	-0.787	0.140	-5.611	0.000	-0.787	-0.787
CA ~						
Salinity	-0.589	0.180	-3.269	0.001	-0.589	-0.589
Nutrients	0.262	0.180	1.456	0.145	0.262	0.262
DS ~						
Salinity	-0.225	0.229	-0.983	0.326	-0.225	-0.225
Nutrients	0.053	0.229	0.229	0.819	0.053	0.053
GA ~						

Salinity	-0.311	0.210	-1.479	0.139	-0.311	-0.311
Nutrients	0.328	0.210	1.561	0.119	0.328	0.328

Covariances:

	Estimate	Std.Err	z-value	P(>|z|)	Std.lv	Std.all
.Richness ~~						
.Abundance	-0.018	0.040	-0.447	0.655	-0.018	-0.106
.Shannon	0.025	0.023	1.084	0.278	0.025	0.264
.Abundance ~~						
.Shannon	-0.105	0.052	-2.035	0.042	-0.105	-0.547

Variances:

	Estimate	Std.Err	z-value	P(>|z|)	Std.lv	Std.all
.Richness	0.082	0.027	3.000	0.003	0.082	0.065
.Abundance	0.352	0.117	3.000	0.003	0.352	0.303
.Shannon	0.105	0.035	3.000	0.003	0.105	0.088
.Chla	0.788	0.263	3.000	0.003	0.788	0.835
.Yield	0.404	0.135	3.000	0.003	0.404	0.427
.PUptake	0.335	0.112	3.000	0.003	0.335	0.354
.CA	0.552	0.184	3.000	0.003	0.552	0.584
.DS	0.894	0.298	3.000	0.003	0.894	0.946
.GA	0.751	0.250	3.000	0.003	0.751	0.796

R-Square:

	Estimate		
Richness	0.935		
Abundance	0.697		
Shannon	0.912		
Chla	0.165		
Yield	0.573		
PUptake	0.646		
CA	0.416		
DS	0.054		
		GA	0.204

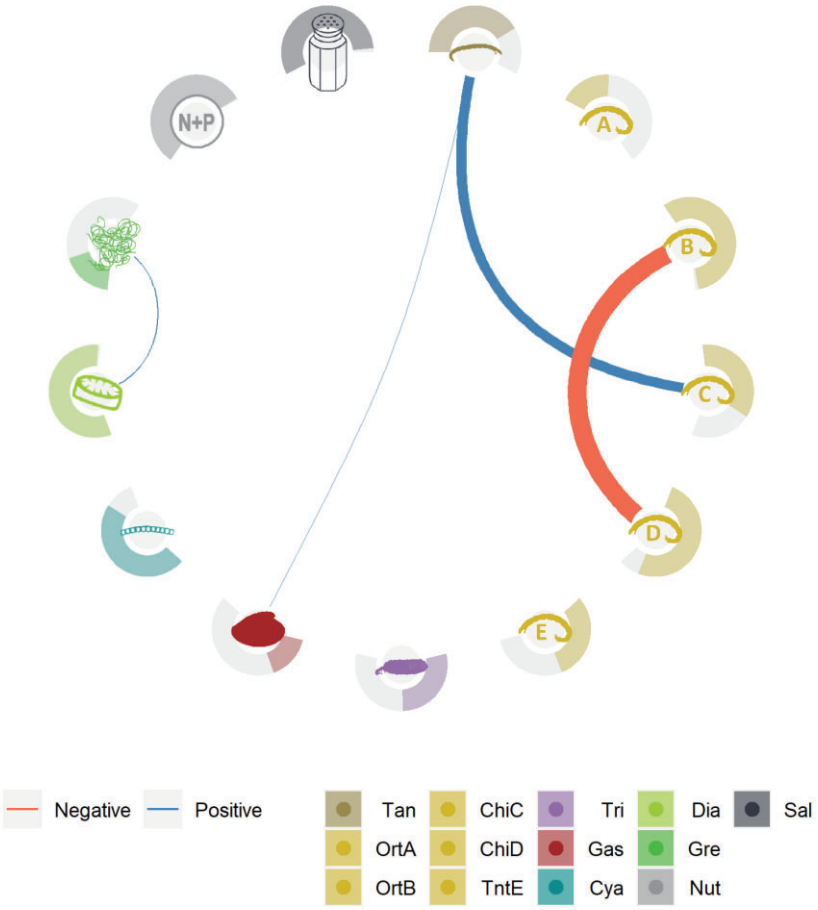


Figure S4. Main biotic-abiotic interaction network for all the experimental treatments and modulated by the treatment factor. Each network node corresponds to a determined biotic group (indVal species) or an abiotic feature. In a clockwise direction we can find: Tan (*Conchapelopia* sp.), OrtA (*Cricotopus bicinctus*), OrtB (*Orthocladius* gr. *wetterensis*), ChiC (*Phaenopsectra* sp.), ChiD (*Polypedilum* sp.), TntE (*Virgatanytarsus* sp.), Tri (*Hydroptila* sp.), Gas (*Ancylus* sp.), Cya (Cyanobacteria), Dia (Diatoms), Gre (Green Algae), Nut (Nutrient treatment concentration), Sal (Salinity treatment concentration). Colored links indicate the sign of the covariation value being blue negative covariation and red positive covariation.)

Table S26: Main BAIN weighted adjacency matrix with the estimated pairwise interactions informing about covariation between each pair of nodes which contain biotic and abiotic variables. Tan (*Conchapelopia* sp.), OrtA (*Cricotopus bicinctus*), OrtB (*Orthocladius* gr. *wetterensis*), ChiC (*Phaenopsectra* sp.), ChiD (*Polypedilum* sp.), TntE (*Virgatanytarsus* sp.), Tri (*Hydroptila* sp.), Gas (*Ancilylus* sp.), Cya (Cyanobateria), Dia (Diatoms), Gre (Green Algae), Nut (Nutrient treatment concentration), Sal (Salinity treatment concentration), Treat (categorical variable representing each treatment used as modulator of the BAIN). Each value represents a pairwise interaction in absolute value who defines the covariation strength between these two nodes of the BAIN.

	Tan	OrtA	OrtB	ChiC	ChiD	TntE	Tri	Gas	Cya	Dia	Ga	Nut	Sal	Treat
Tan	0.0	0.0	0.0	0.44	0.0	0.0	0.0	0.07	0.0	0.0	0.0	0.0	0.0	0.17
OrtA	0.0	0.0	0.0	0.0	0.0	0.0	0.0	0.0	0.0	0.0	0.0	0.0	0.0	0.0
OrtB	0.0	0.0	0.0	0.0	0.76	0.0	0.0	0.0	0.0	0.0	0.0	0.0	0.0	0.0
ChiC	0.44	0.0	0.0	0.0	0.0	0.0	0.0	0.0	0.0	0.0	0.0	0.0	0.0	0.0
ChiD	0.0	0.0	0.76	0.0	0.0	0.0	0.0	0.0	0.0	0.0	0.0	0.0	0.0	0.0
TntE	0.0	0.0	0.0	0.0	0.0	0.0	0.0	0.0	0.0	0.0	0.0	0.0	0.0	0.0
Tri	0.0	0.0	0.0	0.0	0.0	0.0	0.0	0.0	0.0	0.0	0.0	0.0	0.0	0.0
Gas	0.06	0.0	0.0	0.0	0.0	0.0	0.0	0.0	0.0	0.0	0.0	0.0	0.0	0.0

Cya	0.0	0.0	0.0	0.0	0.0	0.0	0.0	0.0	0.0	0.0	0.0	0.0	0.0	0.0
Dia	0.0	0.0	0.0	0.0	0.0	0.0	0.0	0.0	0.0	0.0	0.09	0.0	0.0	0.0
Ga	0.0	0.0	0.0	0.0	0.0	0.0	0.0	0.0	0.0	0.09	0.0	0.0	0.0	0.0
Nut	0.0	0.0	0.0	0.0	0.0	0.0	0.0	0.0	0.0	0.0	0.0	0.0	0.0	0.12
Sal	0.0	0.0	0.0	0.0	0.0	0.0	0.0	0.0	0.0	0.0	0.0	0.0	0.0	0.08
Treat	0.17	0.0	0.0	0.0	0.0	0.0	0.0	0.0	0.0	0.0	0.0	0.12	0.08	0.0

Table S27: Modulated BAINs weighted adjacency matrix with the estimated pairwise interactions informing about covariation between each pair of nodes which contain biotic and abiotic variables. Tan (*Conchapelopia* sp.), OrtA (*Cricotopus bicinctus*), OrtB (*Orthocladius* gr. *wetterensis*), ChiC (*Phaenopsectra* sp.), ChiD (*Polypedilum* sp.), TntE (*Virgatanytarsus* sp.), Tri (*Hydroptila* sp.), Gas (*Ancilylus* sp.), Cya (Cyanobateria), Dia (Diatoms), Gre (Green Algae), Nut (Nutrient treatment concentration), Sal (Salinity treatment concentration), Treat (categorical variable representing each treatment used as modulator of the BAIN). Each value represents a pairwise interaction in absolute value who defines the covariation strength between these two nodes of the BAIN.

C treatment													
	Tan	OrtA	OrtB	ChiC	ChiD	TntE	Tri	Gas	Cya	Dia	Ga	Nut	Sal
Tan	0.00	0.00	0.00	0.44	0.00	0.00	0.00	0.07	0.00	0.00	0.00	0.00	0.00

OrtA	0.00	0.00	0.00	0.00	0.00	0.00	0.00	0.00	0.00	0.00	0.00	0.00	0.00
OrtB	0.00	0.00	0.00	0.00	0.76	0.00	0.00	0.00	0.00	0.00	0.00	0.00	0.00
ChiC	0.44	0.00	0.00	0.00	0.00	0.00	0.00	0.00	0.00	0.00	0.00	0.00	0.00
ChiD	0.00	0.00	0.76	0.00	0.00	0.00	0.00	0.00	0.00	0.00	0.00	0.00	0.00
TntE	0.00	0.00	0.00	0.00	0.00	0.00	0.00	0.00	0.00	0.00	0.00	0.00	0.00
Tri	0.00	0.00	0.00	0.00	0.00	0.00	0.00	0.00	0.00	0.00	0.00	0.00	0.00
Gas	0.07	0.00	0.00	0.00	0.00	0.00	0.00	0.00	0.00	0.00	0.00	0.00	0.00
Cya	0.00	0.00	0.00	0.00	0.00	0.00	0.00	0.00	0.00	0.00	0.00	0.00	0.00
Dia	0.00	0.00	0.00	0.00	0.00	0.00	0.00	0.00	0.00	0.00	0.10	0.00	0.00
Ga	0.00	0.00	0.00	0.00	0.00	0.00	0.00	0.00	0.00	0.10	0.00	0.00	0.00
Nut	0.00	0.00	0.00	0.00	0.00	0.00	0.00	0.00	0.00	0.00	0.00	0.00	0.00
Sal	0.00	0.00	0.00	0.00	0.00	0.00	0.00	0.00	0.00	0.00	0.00	0.00	0.00
	HN treatment												

	Tan	OrtA	OrtB	ChiC	ChiD	TntE	Tri	Gas	Cya	Dia	Ga	Nut	Sal
Tan	0.00	0.00	0.00	0.44	0.00	0.00	0.00	0.07	0.00	0.00	0.00	0.00	0.00
OrtA	0.00	0.00	0.00	0.00	0.00	0.00	0.00	0.00	0.35	0.00	0.00	0.00	0.00
OrtB	0.00	0.00	0.00	0.00	0.76	0.00	0.00	0.00	0.00	0.00	0.00	0.00	0.00
ChiC	0.44	0.00	0.00	0.00	0.00	0.00	0.00	0.00	0.00	0.00	0.00	0.00	0.00
ChiD	0.00	0.00	0.76	0.00	0.00	0.00	0.16	0.00	0.00	0.00	0.00	0.00	0.00
TntE	0.00	0.00	0.00	0.00	0.00	0.00	0.00	0.00	0.00	0.00	0.00	0.00	0.00
Tri	0.00	0.00	0.00	0.00	0.16	0.00	0.00	0.00	0.00	0.00	0.00	0.00	0.00
Gas	0.07	0.00	0.00	0.00	0.00	0.00	0.00	0.00	0.00	0.00	0.00	0.00	0.00
Cya	0.00	0.35	0.00	0.00	0.00	0.00	0.00	0.00	0.00	0.00	0.00	0.00	0.00
Dia	0.00	0.00	0.00	0.00	0.00	0.00	0.00	0.00	0.00	0.00	0.10	0.00	0.00
Ga	0.00	0.00	0.00	0.00	0.00	0.00	0.00	0.00	0.00	0.10	0.00	0.00	0.00
Nut	0.00	0.00	0.00	0.00	0.00	0.00	0.00	0.00	0.00	0.00	0.00	0.00	0.00

Sal	0.00	0.00	0.00	0.00	0.00	0.00	0.00	0.00	0.00	0.00	0.00	0.00	0.00

IN treatment

	Tan	OrtA	OrtB	ChiC	ChiD	TntE	Tri	Gas	Cya	Dia	Ga	Nut	Sal
Tan	0.00	0.00	0.00	0.44	0.00	0.00	0.00	0.07	0.00	0.00	0.00	0.00	0.00
OrtA	0.00	0.00	0.00	0.00	0.00	0.00	0.00	0.00	0.00	0.00	0.00	0.00	0.00
OrtB	0.00	0.00	0.00	0.00	0.76	0.00	0.00	0.00	0.00	0.00	0.00	0.00	0.00
ChiC	0.44	0.00	0.00	0.00	0.00	0.00	0.00	0.00	0.00	0.00	0.00	0.00	0.00
ChiD	0.00	0.00	0.76	0.00	0.00	0.00	0.00	0.00	0.00	0.00	0.00	0.00	0.00
TntE	0.00	0.00	0.00	0.00	0.00	0.00	0.00	0.00	0.00	0.00	0.00	0.00	0.00
Tri	0.00	0.00	0.00	0.00	0.00	0.00	0.00	0.00	0.00	0.00	0.00	0.00	0.00
Gas	0.07	0.00	0.00	0.00	0.00	0.00	0.00	0.00	0.00	0.00	0.00	0.00	0.00
Cya	0.00	0.00	0.00	0.00	0.00	0.00	0.00	0.00	0.00	0.00	0.00	0.00	0.00
Dia	0.00	0.00	0.00	0.00	0.00	0.00	0.00	0.00	0.00	0.00	0.10	0.00	0.00

Ga	0.00	0.00	0.00	0.00	0.00	0.00	0.00	0.00	0.00	0.10	0.00	0.00	0.00
Nut	0.00	0.00	0.00	0.00	0.00	0.00	0.00	0.00	0.00	0.00	0.00	0.00	0.00
Sal	0.00	0.00	0.00	0.00	0.00	0.00	0.00	0.00	0.00	0.00	0.00	0.00	0.00

S treatment

	Tan	OrtA	OrtB	ChiC	ChiD	TntE	Tri	Gas	Cya	Dia	Ga	Nut	Sal
Tan	0.00	0.00	0.00	0.44	0.00	0.00	0.00	0.07	0.00	0.00	0.00	0.00	0.00
OrtA	0.00	0.00	0.00	0.00	0.00	0.00	0.35	0.00	0.00	0.00	0.00	0.00	0.00
OrtB	0.00	0.00	0.00	0.00	0.76	0.31	0.00	0.00	0.00	0.00	0.00	0.00	0.00
ChiC	0.44	0.00	0.00	0.00	0.00	0.00	0.00	0.00	0.00	0.00	0.00	0.00	0.00
ChiD	0.00	0.00	0.76	0.00	0.00	0.00	0.00	0.00	0.00	0.00	0.00	0.00	0.00
TntE	0.00	0.00	0.31	0.00	0.00	0.00	0.00	0.00	0.00	0.00	0.00	0.00	0.00
Tri	0.00	0.35	0.00	0.00	0.00	0.00	0.00	0.00	0.00	0.00	0.00	0.00	0.00
Gas	0.07	0.00	0.00	0.00	0.00	0.00	0.00	0.00	0.00	0.00	0.00	0.00	0.00

Cya	0.00	0.00	0.00	0.00	0.00	0.00	0.00	0.00	0.00	0.00	0.00	0.00	0.00
Dia	0.00	0.00	0.00	0.00	0.00	0.00	0.00	0.00	0.00	0.00	0.10	0.00	0.00
Ga	0.00	0.00	0.00	0.00	0.00	0.00	0.00	0.00	0.00	0.10	0.00	0.00	0.00
Nut	0.00	0.00	0.00	0.00	0.00	0.00	0.00	0.00	0.00	0.00	0.00	0.00	0.00
Sal	0.00	0.00	0.00	0.00	0.00	0.00	0.00	0.00	0.00	0.00	0.00	0.00	0.00

SHN treatment

	Tan	OrtA	OrtB	ChiC	ChiD	TntE	Tri	Gas	Cya	Dia	Ga	Nut	Sal
Tan	0.00	0.00	0.00	0.44	0.00	0.00	0.00	0.07	0.00	0.00	0.00	0.00	0.00
OrtA	0.00	0.00	0.00	0.00	0.00	0.00	0.00	0.00	0.00	0.00	0.00	0.00	0.00
OrtB	0.00	0.00	0.00	0.00	0.76	0.00	0.00	0.00	0.00	0.00	0.00	0.00	0.00
ChiC	0.44	0.00	0.00	0.00	0.00	0.00	0.00	0.00	0.00	0.00	0.00	0.00	0.00
ChiD	0.00	0.00	0.76	0.00	0.00	0.00	0.00	0.00	0.00	0.00	0.00	0.00	0.00
TntE	0.00	0.00	0.00	0.00	0.00	0.00	0.00	0.00	0.00	0.00	0.00	0.00	0.00

Tri	0.00	0.00	0.00	0.00	0.00	0.00	0.00	0.00	0.00	0.00	0.00	0.00	0.00
Gas	0.07	0.00	0.00	0.00	0.00	0.00	0.00	0.00	0.00	0.00	0.00	0.00	0.00
Cya	0.00	0.00	0.00	0.00	0.00	0.00	0.00	0.00	0.00	0.00	0.00	0.00	0.00
Dia	0.00	0.00	0.00	0.00	0.00	0.00	0.00	0.00	0.00	0.00	0.10	0.00	0.00
Ga	0.00	0.00	0.00	0.00	0.00	0.00	0.00	0.00	0.00	0.10	0.00	0.00	0.00
Nut	0.00	0.00	0.00	0.00	0.00	0.00	0.00	0.00	0.00	0.00	0.00	0.00	0.00
Sal	0.00	0.00	0.00	0.00	0.00	0.00	0.00	0.00	0.00	0.00	0.00	0.00	0.00

SIN treatment

	Tan	OrtA	OrtB	ChiC	ChiD	TntE	Tri	Gas	Cya	Dia	Ga	Nut	Sal
Tan	0.00	0.00	0.00	0.44	0.00	0.00	0.00	0.07	0.00	0.00	0.00	0.00	0.00
OrtA	0.00	0.00	0.00	0.00	0.00	0.00	0.00	0.00	0.00	0.00	0.00	0.00	0.00
OrtB	0.00	0.00	0.00	0.00	0.76	0.00	0.00	0.00	0.00	0.00	0.00	0.00	0.00
ChiC	0.44	0.00	0.00	0.00	0.00	0.00	0.00	0.00	0.00	0.00	0.00	0.00	0.00

ChiD	0.00	0.00	0.76	0.00	0.00	0.00	0.00	0.00	0.00	0.00	0.00	0.00	0.00
TntE	0.00	0.00	0.00	0.00	0.00	0.00	0.00	0.00	0.00	0.00	0.00	0.00	0.00
Tri	0.00	0.00	0.00	0.00	0.00	0.00	0.00	0.00	0.00	0.00	0.00	0.00	0.00
Gas	0.07	0.00	0.00	0.00	0.00	0.00	0.00	0.00	0.00	0.00	0.00	0.00	0.00
Cya	0.00	0.00	0.00	0.00	0.00	0.00	0.00	0.00	0.00	0.00	0.00	0.00	0.00
Dia	0.00	0.00	0.00	0.00	0.00	0.00	0.00	0.00	0.00	0.00	0.10	0.00	0.00
Ga	0.00	0.00	0.00	0.00	0.00	0.00	0.00	0.00	0.00	0.10	0.00	0.00	0.00
Nut	0.00	0.00	0.00	0.00	0.00	0.00	0.00	0.00	0.00	0.00	0.00	0.00	0.00
Sal	0.00	0.00	0.00	0.00	0.00	0.00	0.00	0.00	0.00	0.00	0.00	0.00	0.00

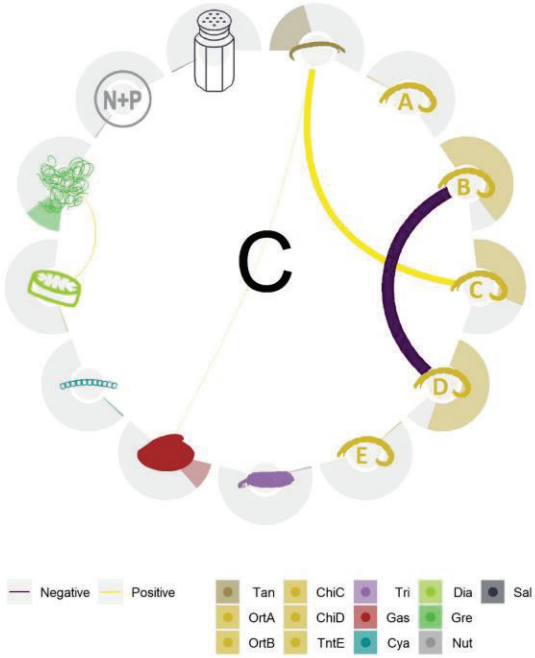


Figure S5. Biotic-abiotic interaction networks corresponding to the conditioned main model for C experimental treatment. control treatment (C). Network nodes corresponds to the taxa strongly associated to treatments according to IndVal analysis, the concentration of the different algal groups and the abiotic variables: Tan (*Conchapelopia* sp.), OrtA (*Cricotopus bicinctus*), OrtB (*Orthocladius* gr. *wetterensis*), ChiC (*Phaenopsectra* sp.), ChiD (*Polypedilum* sp.), TntE (*Virgatanytarsus* sp.), Tri (*Hydroptila* sp.), Gas (*Ancylus* sp.), Cya (Cyanobacteria), Dia (Diatoms), Gre (Green Algae), Nut (Nutrient addition), Sal (Salt addition). Colored links indicate the sign of the covariation value (blue = negative, red = positive). The complete BAIN including all samples can be found in Figure S4.

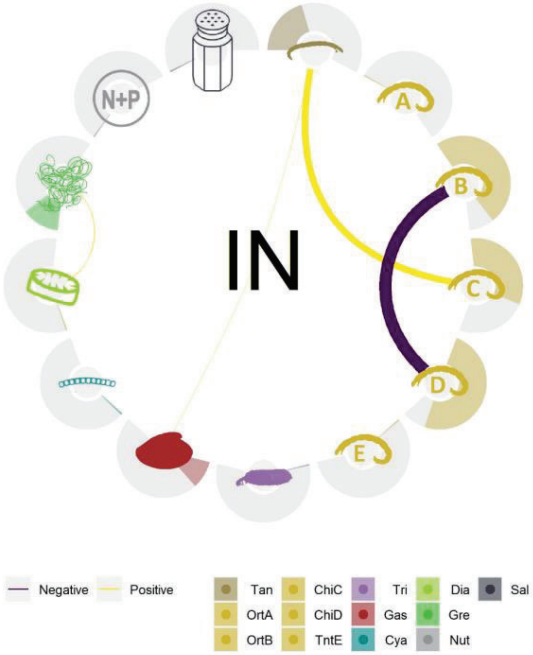


Figure S6. Biotic-abiotic interaction networks corresponding to the conditioned main model for IN experimental treatment: Intermediate nutrients concentration (IN). Network nodes corresponds to the taxa strongly associated to treatments according to IndVal analysis, the concentration of the different algal groups and the abiotic variables: Tan (*Conchapelopia* sp.), OrtA (*Cricotopus bicinctus*), OrtB (*Orthocladius* gr. *wetterensis*), ChiC (*Phaenopsectra* sp.), ChiD (*Polypedilum* sp.), TntE (*Virgatanytarsus* sp.), Tri (*Hydroptila* sp.), Gas (*Ancylus* sp.), Cya (Cyanobacteria), Dia (Diatoms), Gre (Green Algae), Nut (Nutrient addition), Sal (Salt addition). Colored links indicate the sign of the covariation value (blue = negative, red = positive). The complete BAIN including all samples can be found in Figure S4.

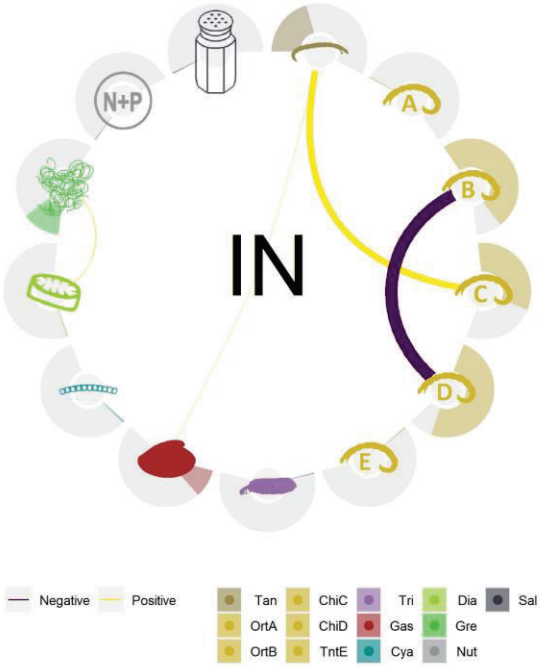


Figure S7. Biotic-abiotic interaction networks corresponding to the conditioned main model for HN experimental treatment: high nutrients concentration (HN). Network nodes corresponds to the taxa strongly associated to treatments according to IndVal analysis, the concentration of the different algal groups and the abiotic variables: Tan (*Conchapelopia* sp.), OrtA (*Cricotopus bicinctus*), OrtB (*Orthocladius* gr. *wetterensis*), ChiC (*Phaenopsectra* sp.), ChiD (*Polypedilum* sp.), TntE (*Virgatanytarsus* sp.), Tri (*Hydroptila* sp.), Gas (*Ancylus* sp.), Cya (Cyanobacteria), Dia (Diatoms), Gre (Green Algae), Nut (Nutrient addition), Sal (Salt addition). Colored links indicate the sign of the covariation value (blue = negative, red = positive). The complete BAIN including all samples can be found in Figure S4.

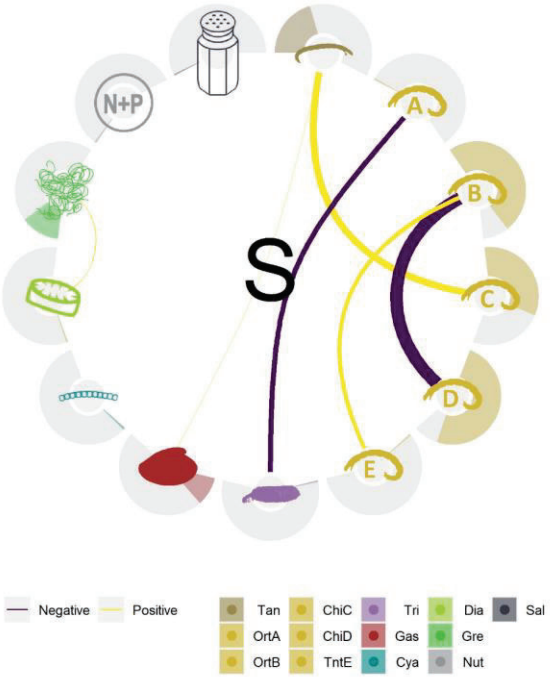


Figure S8: Biotic-abiotic interaction networks corresponding to the conditioned main model for S experimental treatment: salt (S). Network nodes corresponds to the taxa strongly associated to treatments according to IndVal analysis, the concentration of the different algal groups and the abiotic variables: Tan (*Conchapelopia* sp.), OrtA (*Cricotopus bicinctus*), OrtB (*Orthocladius* gr. *wetterensis*), ChiC (*Phaenopsectra* sp.), ChiD (*Polypedilum* sp.), TntE (*Virgatanytarsus* sp.), Tri (*Hydroptila* sp.), Gas (*Ancylus* sp.), Cya (Cyanobacteria), Dia (Diatoms), Gre (Green Algae), Nut (Nutrient addition), Sal (Salt addition). Colored links indicate the sign of the covariation value (blue = negative, red = positive). The complete BAIN including all samples can be found in Figure S4.

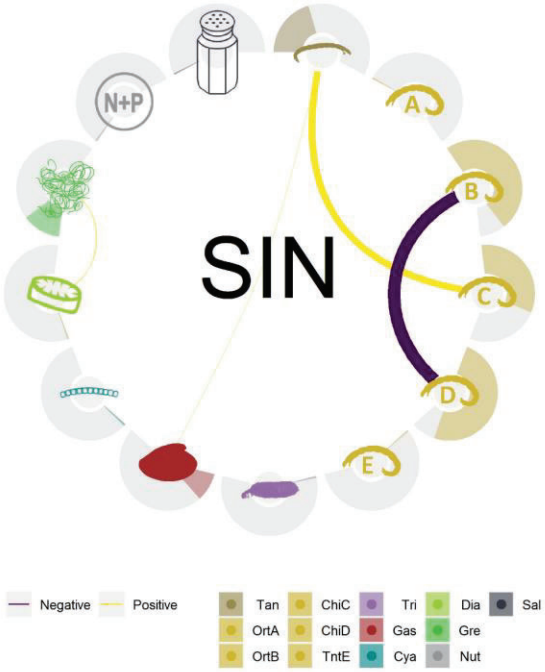


Figure S9: Biotic-abiotic interaction networks corresponding to the conditioned main model for SIN experimental treatment: salt treatment in combination with intermediate nutrients concentration (SIN). Network nodes corresponds to the taxa strongly associated to treatments according to IndVal analysis, the concentration of the different algal groups and the abiotic variables: Tan (*Conchapelopia* sp.), OrtA (*Cricotopus bicinctus*), OrtB (*Orthocladius* gr. *wetterensis*), ChiC (*Phaenopsectra* sp.), ChiD (*Polypedilum* sp.), TntE (*Virgatanytarsus* sp.), Tri (*Hydroptila* sp.), Gas (*Ancylus* sp.), Cya (Cyanobacteria), Dia (Diatoms), Gre (Green Algae), Nut (Nutrient addition), Sal (Salt addition). Colored links indicate the sign of the covariation value (blue = negative, red = positive). The complete BAIN including all samples can be found in Figure S4.



Figure S10: Biotic-abiotic interaction networks corresponding to the conditioned main model for SHN experimental treatment: salt treatment in combination with high nutrients concentration (SHN). Network nodes corresponds to the taxa strongly associated to treatments according to IndVal analysis, the concentration of the different algal groups and the abiotic variables: Tan (*Conchapelopia* sp.), OrtA (*Cricotopus bicinctus*), OrtB (*Orthocladius* gr. *wetterensis*), ChiC (*Phaenopsectra* sp.), ChiD (*Polypedilum* sp.), TntE (*Virgatanytarsus* sp.), Tri (*Hydroptila* sp.), Gas (*Ancylus* sp.), Cya (Cyanobacteria), Dia (Diatoms), Gre (Green Algae), Nut (Nutrient addition), Sal (Salt addition). Colored links indicate the sign of the covariation value (blue = negative, red = positive). The complete BAIN including all samples can be found in Figure S4.

Supplementary material: Chapter IV

Assessing the effects of salinity on microbial communities and pollutant removal in urban wastewater treatment plants

Alvaro Javier Moyano Salcedo*[1,2,5], Miguel Cañedo-Argüelles[1], Sujay S. Kaushal[3], Eva Maria Ciriero-Cebrián[4], Adrià Perez-Blanco[5], Humbert Salvadó[5]

1 FEHM-Lab (Freshwater Ecology, Hydrology and Management), SHE-2, Institute of Environmental Assessment and Water Research (IDAEA), CSIC, Carrer de Jordi Girona, 18-26, 08034, Barcelona, Spain

2 Geohazards and Civil Engineering Research Group, Department of Civil Engineering, Saint Thomas Villavicencio University, C/22 No 1a, 500003, Villavicencio, Colombia.

3 Department of Geology & Earth System Science Interdisciplinary Center, University of Maryland, College Park, MD, USA

4 Empresa Mixta d'Aigües de la Costa Brava S.A, EMACBSA- Roses WWTP, Camí Arenes s/n 17480 Roses, Girona, Spain.

5 Department of Evolutive Biology, Ecology and Environmental Sciences, University of Barcelona, 08028, Barcelona, Spain

***Corresponding autor:** Alvaro Javier Moyano Salcedo, alvaromoyano@ub.edu

Table S1. Salinity Effects on Wastewater Treatment Processes: A Comprehensive Review. Summary of studies on salinity effects in wastewater treatment.

Salinity wastewater level	Observed impact on WWTP process	Treatment mechanism	Reference
Salinity of 10 g/l NaCl and 30 g/l NaCl	Adding NaCl to acclimated biomass did not harm system efficiency; effluent salinity increased but did not hinder biomass growth, favoring salt-tolerant species.	Bench-scale, completely mixed reactors	Hamoda and Al-attar, 1995
Salinity of 0.4, 3, 5, 10, 20, and 40 g/L NaCl	Salt rising from 3 to 10 g/L over 96 hours impacted microbial communities, especially protozoa and metazoa. Some ciliates resisted high NaCl doses, but at 20 g/L, total ciliate abundance sharply dropped, potentially affecting activated sludge processes. By 40 g/L, no protozoa or metazoa survived after 24 hours. The study examines the short-term impact of NaCl on wastewater treatment microorganisms.	Sequencing-scale batch reactor (SBRs)	Salvadó et al., 2001
Salt between 0 and 6% (w/v) in the reactor	As the salt content increased, both the rate and efficiency of COD, NH_4-N, and PO_4-P removal decreased. Simultaneously, there were increases in effluent nutrient concentrations and the sludge volume index, indicating reductions in the efficiency of nutrient and organic matter removal	SBRs	Uygur and Kargi, 2004

Salinity wastewater level	Observed impact on WWTP process	Treatment mechanism	Reference
Salt between 0.1, 0.5, 2, 5, 10 and 20 g/L	No significant reduction in total organic carbon (TOC) removal and oxygen uptake rate (OUR) of activated sludge at 0.5 or 0.1 g/L salinity. TOC removal efficiency decreased significantly at high NaCl concentrations: 30% at 5 g/L, 45% at 10 g/L, and 72% at 20 g/L compared to the control. OUR decreased rapidly, especially at 2 g/L and 5 g/L, with reductions of 20% and 22%, respectively.	Completely mixed batch reactor operated in a batch-wise mode	Wang et al., 2005
Salinity 5 up to 40 g Cl^-/L	Ammonia oxidizers more sensitive than nitrite oxidizers; Both groups almost completely inhibited at 40 g Cl^-/L; No significant effect of sludge adaptation to salt over a one-year period; Salt stress led to less diverse microbial population; Sludges with different populations showed similar activities under identical conditions; High salt concentrations strongly inhibited higher organisms like protozoa; Better settling sludge evolved at higher salt contents.	SBRs	Moussa et al., 2006

Salinity wastewater level	Observed impact on WWTP process	Treatment mechanism	Reference
Three salinities (in terms of concentrations of NaCl)—10, 20 and 40 g NaCl/l	The microbial diversity decreased with increasing the salinity, and the microbial community structure was greatly influenced by the salinity. Bacteroidetes and Actinobacteria were the dominant phylums.	SBRs	Wu et al., 2008
Salt concentration of 0, 3.7, 24.1 and 44.1 g/L	Enzymatic activities (acid phosphatase, alkaline phosphatase, glucosidase, protease, and esterase) decreased with increasing salinity. Biotransformation of organic matter was significantly reduced. Redundancy analysis revealed a negative correlation between salinity and enzymatic activities. COD and BOD5 removal efficiencies reduced from 92% to 39.6% as NaCl concentrations increased.	Submerged fixed bed bioreactor	Cortés-Lorenzo et al., 2012
Salinity of 40 g/l	Salinity variations (0–40 g/l) in a submerged biofilter reactor affected partial nitrification. At 1 g/l NaCl, NH_4-N removal improved, but higher concentrations led to NH_4-N oxidation and inhibition. Total oxidized NH_4-N decreased from 0.754 to 0.322 kg/m^3 day without salt to 40 g/l salinity in the PNBR.	Submerged Biofilter Reactor	Aslan and Simsek, 2012

Salinity wastewater level	Observed impact on WWTP process	Treatment mechanism	Reference
Salinity of 1.93, 3,58 and 4.83 psu	Diversity and abundance of ammonia-oxidizing Betaproteobacteria and archaea increase with a decrease of waterwaste salinity.	Conventional activated sludge plant	Wu et al., 2013
Salinity concentrations of 0.02, 0.19, 0.27, 0.35, 0.69, 1.02, 2.02, and 3.02 % (W/V) NaCl	Elevated salinity concentrations significantly impacted all aerobic PAO metabolic processes. Upon reaching a threshold of 2%, the aerobic maintenance energy requirement increased. Furthermore, an increase in salinity from 0 to 0.18% resulted in substantial inhibition, with rates decreasing by 25% for O2, 46% for PO4, and 63% for NH4-uptake.	SBRs	Wells et al., 2014
Salinity from 0,2 to 6,6 g/L (Na^+)	Increased Na^+ in wastewater disrupts floc structure, reducing size, stability and increasing porosity in the EPS. Na^+ displacement of $Mg2^+$ weakens EPS bridges, forming more porous flocs. Accumulating in LB-EPS, Na^+ sorption diminishes EPS production, resulting in weak, highly porous flocs and decreased overall size.	SBRs	Cui et al., 2015

Salinity wastewater level	Observed impact on WWTP process	Treatment mechanism	Reference
Salinity ranging from 0 to 20 g/L	Richness and diversity of the microbial community were greatly affected by salinity. The removal rate of COD, NH_4-N, and PO_4-P gradually decreased (by approximately 45%) when the salinity increased to 20 g/L.	SBRs	Chen et al., 2018
Salinity of 30 and 70 g/L NaCl	Decreased BOD5 removal efficiency in reactors subjected to drastic salinity increase; Stable performances achieved after 18 days in AGS-R1 (90%) and 27 days in FAS-R1 (82%); Higher loss in nitritation efficiency in FAS reactors proportional to shock intensity; Nitritation and denitrification completely restored 5 days after salinity shock; No significant effects observed after moderate shock; Drastic shocks caused significant changes in EPS structure, with a 45% increase in loosely-bound EPS in AGS and 55% in FAS.	Aerobic granular sludge (AGS) and flocculent activated sludge (FAS)	Corsino et al., 2018

Salinity wastewater level	Observed impact on WWTP process	Treatment mechanism	Reference
Salinity of 0.6, 14 and 20 g/L.	Biofilm coverage rate decreased with increasing NaCl concentrations, affecting bacterial community variation and metabolomic pathways. Gammaproteobacteria dominated, exhibiting NaCl tolerance. Species like Pseudomonas and Planococcus showed NaCl sensitivity/tolerance.	Moving-scale Bed Biofilm Reactor (MBBR)	Wang et al., 2020
Intermittent salinity peaks (road salt), NaCl loads up to 1,147 t/d and PE-specific loads of 0.26–0.5 kg NaCl/(PE · y).	Intermittent salinity peaks revealing impacts on sludge parameters, floc size, and settling velocity. Respiration measurements indicated increased microbial activity below 1 g/L NaCl but up to 30% inhibition between 1 and 3 g NaCl/L.	Conventional activated sludge plant	Tauber et al., 2021
Increased salinity from 0 to 60 g/L	Outstanding NH_4-N removal (95%, 60 ~ 70 mg/(L-d)) was observed at 60 g/L salinity. Excess COD, not salinity, inhibited the nitrification capacity of the biofilm.	Anoxic–oxic (A/O) biofilm reactor (scale)	Ji et al., 2021

Salinity wastewater level	Observed impact on WWTP process	Treatment mechanism	Reference
Salinity of 20-60 g/L NaCl	Efficient removal of urea (99%) and COD (90%) were achieved under high salinity. Oxic microorganisms were more tolerant to salinity stress than the anoxic ones. Microbial alpha diversity decreased with increased salinity, as well as beta diversity also significantly changed. Clostridiales and Oceanospirillales played crucial roles in maintaining system stability.	Anoxic–oxic (A/O) reactor (scale)	Chen et al., 2023
Salinity of 0, 5, 10 and 20 g/L	Elevated salinity compromised the COD removal efficiency of AnMBR, but had a minimal impact on dye removal efficacy. Low salinity (5 g/L) enhanced biogas production, while high salinity (>10 g/L) had an adverse effect. Microbial analysis revealed a transition from salinity-sensitive to salinity-tolerant microbes.	Anaerobic membrane bioreactor (AnMBR) (scale)	Wang et al., 2023

Salinity wastewater level	Observed impact on WWTP process	Treatment mechanism	Reference
Salinity of 0%, 1%, 2%, and 3%	Higher salinity resulted in low microbial diversity, and small, complex, more competitive overall networks, leading to poor performance of the treatment process. Subnetworks of major phyla (Proteobacteria, Bacteroidetes, and Chloroflexi) and functional bacteria (such as AOB, NOB and denitrifiers) differed substantially under elevated salinity process.	SBRs	Ya et al., 2023
Salinity of 91.3 g/L	Salinity affected the composition and relative abundance of different microbial groups in response to environmental changes. However, despite changes in the microbial community due to salinity, the removal efficiency of pollutants such as COD, NH3-H and NT increased significantly as a result of bioaugmentation. This suggests that although salinity can affect the microbial community, the presence of salt-tolerant yeast (e.g. Meyerozyma) can offset these effects and improve treatment efficiency.	Activated sludge industrial wastewater plant	Wen et al., 2022

Table S2. Description of WWTPs, design and operating conditions. WWTPRSS: Roses wastewater treatment plant. WWTPLLN: Llançà wastewater treatment plant. WWTPCES: Castelló d'Empúries wastewater treatment plant. WWTPRUS: Reus wastewater treatment plant. WWTPAMP: Amposta Wastewater Treatment Plant. WWTPALC: Les Cases d'Alcanar Wastewater Treatment Plant WWTPSCR: Sant Carles de la Ràpita Wastewater Treatment Plant

Parameters/ WWTPs	WWTP RSS	WWTP LLN	WWTP CES	WWTP RUS	WWTP AMP	WWTP ALC	WWT PSCR
Latitude	42.276802	42.376328	42.245339	41.128068	40.704528	40.537421	40.62776
Longitude	3.175689	3.148548	3.102969	1.11873	0.610087	0.490024	0.62189
Design Flow (m3/day)	25,000	9,625	16,750	25,000	5,500	1,569	6,310
Population equivalent (PE) service capacity	114,583	43,000	67,000	195,833	27,500	6,799	28,921
Total Suspended Solids (TSS) Design (mg/l)	225	330	300	362	261	591	300
Biochemical Oxygen Demand (DBO5) Design (mg/l)	275	415	240	470	282	640	275
Nitrogen (N) Design (mg/l)	-	70	-	-	43	-	50
Ammonium (NH4) Design (mg/l)	-	-	-	-	-	-	-
Phosphorus (P) Design (mg/l)	-	-	-	-	-	-	15

Parameters/ WWTPs	WWTP RSS	WWTP LLN	WWTP CES	WWTP RUS	WWTP AMP	WWTP ALC	WWT PSCR
Pre-Treatment	Screening, Grit Removal	Screening, Grit Removal	Screening, Grit Removal	Screening, Grit Removal	Screening, Grit Removal	Screening	Screening, Grit Removal
Primary Treatment	-	-	-	Physical and chemical process	-	-	Homogenization tank and reactor
Secondary Treatment	Carousel System, Sedimentation, Diffuser Aeration	Carousel System, Sedimentation, Diffuser Aeration	Carousel System, Sedimentation, Diffuser Aeration	Piston Flow process	Carousel System, Sedimentation, Rotor Aeration	Sequential Batch Reactor (SBR), Sedimentation, Diffuser Aeration	Carousel System, Sedimentation, Diffuser Aeration
Tertiary Treatment	Chlorination, Sand Filtration, UV Radiation	Chlorination, Sand Filtration, UV Radiation	-	-	-	Sand Filtration, UV Disinfection	Filtration, UV Disinfection
Sludge treatment	-	-	Thickening, Centrifuge Dewatering	Anaerobic digestion and filter press dewatering	Gravity Thickening, Centrifugal Dewatering	Centrifugal Dewatering	-
Discharge Location	Mediterranean Sea	Mediterranean Sea, Llançà Stream	Riu Muga, Ampurdán Wetlands	Mas Calbó Intermittent Stream	Ebro River	Doña Manuela Intermittent Stream	Alfacs Bay

Table S3. Mean concentrations, coefficient of variation and ranges of wastewater quality parameters in each WWTPs. WWTPRSS: Roses wastewater treatment plant. WWTPLLN: Llançà wastewater treatment plant. WWTPCES: Castelló d'Empúries wastewater treatment plant. WWTPRUS: Reus wastewater treatment plant. WWTPAMP: Amposta Wastewater Treatment Plant. WWTPALC: Les Cases d'Alcanar Wastewater Treatment Plant WWTPSCR: Sant Carles de la Ràpita Wastewater Treatment Plant

Parameter / WWTPs	WWTPRSS	WWTPLLN	WWTPCES	WWTPRUS	WWTPAMP	WWTPALC	WWTPSCR
EC	8530 ± 1858 CV= 21% (3900-14935)	2561 ± 1080 CV= 41% (1141-7025)	3843 ± 1153 CV= 30% (1657-7740)	1782 ± 227 CV= 16% (800-2580)	1949 ± 477 CV= 24% (1221-2856)	2374 ± 1218 CV= 39% (921-2976)	4441 ± 2034 CV= 45% (1252-12780)
pH	7.2 ± 0.1 CV= 3% (7-8)	6.8 ± 0.1 CV= 3% (7-8)	7 ± 0.1 CV= 2% (7-8)	7.6 ± 0.1 CV= 4% (7-8)	7.2 ± 0.2 CV= 4% (7-8)	7.5 ± 0.2 CV= 7% (6-8)	7.3 ± 0.2 CV= 4% (7-8)
Temperature	21.2 ± 4 CV= 20% (13-28)	19.4 ± 4 CV= 23% (12-27)	20.5 ± 5 CV= 24% (11-28)	19 ± 5 CV= 19% (12-28)	21 ± 4 CV= 19% (15-27)	23 ± 3 CV= 13% (14-27)	20 ± 3 CV= 25% (9-28)
DO	2.5 ± 0.5 CV= 20% (1.5-4.5)	2.1 ± 0.6 CV= 28% (1.5-5)	1.6 ± 0.6 CV= 37% (1.5-4.5)	2.4 ± 0.8 CV= 33% (1.5-4)	2.3 ± 0.7 CV= 30% (1.5-5)	2.2 ± 0.8 CV= 36% (1.5-5)	2.3 ± 0.7 CV= 30% (1.5-4.5)
BOD5	146 ± 47 CV= 32% (84-474)	183 ± 82 CV= 44% (73-406)	221 ± 88 CV= 39% (72-501)	376 ± 82 CV= 21% (78-403)	302 ± 63 CV= 20% (200-402)	323 ± 53 CV= 16% (180-440)	256 ± 93 CV= 36% (64-462)
COD	407 ± 145 CV= 35% (166-681)	562 ± 224 CV= 39% (130-518)	600 ± 99 CV= 33% (134-677)	881 ± 145 CV= 16% (117-534)	542 ± 116 CV= 21% (330-478)	612 ± 99 CV= 16% (371-841)	636 ± 140 CV= 22% (101-561)
Total N	48 ± 19 CV= 39% (7-94)	64 ± 29 CV= 45% (10-162)	59 ± 22 CV= 37% (10-181)	101 ± 17 CV= 12% (67-128)	56 ± 17 CV= 30% (37-121)	49 ± 12 CV= 26% (37-86)	61 ± 19 CV= 31% (18-134)
Total P	5 ± 2 CV= 40% (2-10)	13 ± 2 CV= 15% (1-12)	8 ± 3 CV= 37% (2-22)	9.9 ± 2 CV= 20% (6-32)	7 ± 2 CV= 28% (5-18)	7 ± 1 CV= 14% (6-24)	6 ± 1 CV= 16% (3-10)

EC: Electrical conductivity µS cm^{-1}; DO: Dissolved oxygen mg L^{-1}; BOD_5: Biochemical oxygen demand mg L^{-1}; COD: chemical oxygen demand mg L^{-1}; Total N: Total Nitrogen mg L^{-1}; Total P: Total phosphorus mg L^{-1} () = represents Maximun and minimum values

Table S4: One-way Kruskal-Wallis tests of monthly electrical conductivity between WWTPs during the study period.

Comparison	chi-squared	df	p-value	method	Significance
Conductivity by WWTP	199.53	6	< 2.2e-16	Kruskal-Wallis rank sum test	***

Table S5: Pairwise comparison using Mann-Whitney U test of monthly EC concentration between WWTPs. WWTPCES: Castelló d'Empúries wastewater treatment plant. WWTPRUS: Reus wastewater treatment plant. WWTPAMP: Amposta Wastewater Treatment Plant. WWTPALC: Les Cases d'Alcanar Wastewater Treatment Plant WWTPSCR: Sant Carles de la Ràpita Wastewater Treatment Plant

Pairwise comparisons using Wilcoxon rank sum test with continuity correction

data: Data$Conductivity and Data$WWTP

P value adjustment method: bonferroni

	WWTPALC	WWTPAMP	WWTPCES	WWTPLLN	WWTPRSS	WWTPRUS
WWTPAMP	1.00	-	-	-	-	-
WWTPCES	0.00039	1.8e-07	-	-	-	-
WWTPLLN	1.00	1.00	3.1e-06	-	-	-
WWTPRSS	3.4e-05	1.5e-09	< 2e-16	< 2e-16	-	-
WWTPRUS	1.00000	0.41061	< 2e-16	0.20800	< 2e-16	-
WWTPSCR	0.00991	0.00131	1.00000	0.00615	3.3e-05	1.8e-05

Table S6: One-way Kruskal-Wallis tests of monthly environmental and water quality parameters (Conductivity, pH, T: temperature, DO, COD, BOD, TN, TP) across different WWTPs during the study period. WWTPRSS: Roses wastewater treatment plant. WWTPLLN: Llançà wastewater treatment plant. WWTPCES: Castelló d'Empúries wastewater treatment plant. WWTPRUS: Reus wastewater treatment plant. WWTPAMP: Amposta Wastewater Treatment Plant. WWTPALC: Les Cases d'Alcanar Wastewater Treatment Plant WWTPSCR: Sant Carles de la Ràpita Wastewater Treatment Plant

WWTP	chi-squared	df	p-value	method	Comparison	Significance
WWTPRSS	8.985772	11	0.6232	Kruskal-Wallis rank sum test	Conductivity by Month	ns
WWTPLLN	37.63792	11	9.00E-05	Kruskal-Wallis rank sum test	Conductivity by Month	ns
WWTPCES	7.47059	11	0.3928	Kruskal-Wallis rank sum test	Conductivity by Month	ns
WWTPRUS	9.75546	11	0.2633	Kruskal-Wallis rank sum test	Conductivity by Month	ns
WWTPAMP	7.7	7	0.35978	Kruskal-Wallis rank sum test	Conductivity by Month	ns
WWTPALC	6.666667	5	0.24663	Kruskal-Wallis rank sum test	Conductivity by Month	ns
WWTPSCR	9.625	7	0.21083	Kruskal-Wallis rank sum test	Conductivity by Month	ns
WWTPRSS	38	38	0.4695	Kruskal-Wallis rank sum test	pH by month	ns
WWTPLLN	27	27	0.4636	Kruskal-Wallis rank sum test	pH by month	ns
WWTPCES	27	27	0.4638	Kruskal-Wallis rank sum test	pH by month	ns
WWTPRUS	85	85	0.4796	Kruskal-Wallis rank sum test	pH by month	ns
WWTPAMP	18	18	0.4557	Kruskal-Wallis rank sum test	pH by month	ns
WWTPALC	8	8	0.4335	Kruskal-Wallis rank sum test	pH by month	ns
WWTPSCR	15	15	0.4514	Kruskal-Wallis rank sum test	pH by month	ns
WWTPRSS	43	43	0.4713	Kruskal-Wallis rank sum test	T by month	ns
WWTPLLN	36	36	0.4686	Kruskal-Wallis rank sum test	T by month	ns
WWTPCES	32	32	0.4667	Kruskal-Wallis rank sum test	T by month	ns
WWTPRUS	85	85	0.4796	Kruskal-Wallis rank sum test	T by month	ns
WWTPAMP	18	18	0.4557	Kruskal-Wallis rank sum test	T by month	ns
WWTPALC	8	8	0.4335	Kruskal-Wallis rank sum test	T by month	ns
WWTPSCR	15	15	0.4514	Kruskal-Wallis rank sum test	T by month	ns
WWTPRSS	41	41	0.4706	Kruskal-Wallis rank sum test	DO by month	ns
WWTPLLN	35	35	0.4682	Kruskal-Wallis rank sum test	DO by month	ns

WWTP	chi-squared	df	p-value	method	Comparison	Significance
WWTPCES	31	31	0.4662	Kruskal-Wallis rank sum test	DO by month	ns
WWTPRUS	77	77	0.4786	Kruskal-Wallis rank sum test	DO by month	ns
WWTPAMP	16	16	0.453	Kruskal-Wallis rank sum test	DO by month	ns
WWTPALC	3	3	0.406	Kruskal-Wallis rank sum test	DO by month	ns
WWTPSCR	13	13	0.4478	Kruskal-Wallis rank sum test	DO by month	ns
WWTPRSS	49.38	55	0.6883	Kruskal-Wallis rank sum test	COD by month	ns
WWTPLLN	50.336	49	0.4204	Kruskal-Wallis rank sum test	COD by month	ns
WWTPCES	47.068	43	0.3096	Kruskal-Wallis rank sum test	COD by month	ns
WWTPRUS	75.279	74	0.4367	Kruskal-Wallis rank sum test	COD by month	ns
WWTPAMP	18	18	0.4557	Kruskal-Wallis rank sum test	COD by month	ns
WWTPALC	8	8	0.4335	Kruskal-Wallis rank sum test	COD by month	ns
WWTPSCR	24.759	25	0.4759	Kruskal-Wallis rank sum test	COD by month	ns
WWTPRSS	55.761	55	0.446	Kruskal-Wallis rank sum test	BOD by month	ns
WWTPLLN	50.605	49	0.41	Kruskal-Wallis rank sum test	BOD by month	ns
WWTPCES	46.08	43	0.346	Kruskal-Wallis rank sum test	BOD by month	ns
WWTPRUS	76.468	74	0.3992	Kruskal-Wallis rank sum test	BOD by month	ns
WWTPAMP	18	18	0.4557	Kruskal-Wallis rank sum test	BOD by month	ns
WWTPALC	8	8	0.4335	Kruskal-Wallis rank sum test	BOD by month	ns
WWTPSCR	23.526	25	0.5469	Kruskal-Wallis rank sum test	BOD by month	ns
WWTPRSS	55.829	55	0.4435	Kruskal-Wallis rank sum test	TN by month	ns
WWTPLLN	50.594	49	0.4104	Kruskal-Wallis rank sum test	TN by month	ns
WWTPCES	45.497	43	0.3685	Kruskal-Wallis rank sum test	TN by month	ns
WWTPRUS	68.312	74	0.6645	Kruskal-Wallis rank sum test	TN by month	ns
WWTPAMP	18	18	0.4557	Kruskal-Wallis rank sum test	TN by month	ns
WWTPALC	8	8	0.4335	Kruskal-Wallis rank sum test	TN by month	ns
WWTPSCR	25.928	25	0.4114	Kruskal-Wallis rank sum test	TN by month	ns
WWTPRSS	57.461	55	0.3842	Kruskal-Wallis rank sum test	TP by month	ns
WWTPLLN	49.973	49	0.4345	Kruskal-Wallis rank sum test	TP by month	ns
WWTPCES	48.653	43	0.2559	Kruskal-Wallis rank sum test	TP by month	ns

WWTP	chi-squared	df	p-value	method	Comparison	Significance
WWTPRUS	79.428	74	0.312	Kruskal-Wallis rank sum test	TP by month	ns
WWTPAMP	18	18	0.4557	Kruskal-Wallis rank sum test	TP by month	ns
WWTPALC	8	8	0.4335	Kruskal-Wallis rank sum test	TP by month	ns
WWTPSCR	26	25	0.4076	Kruskal-Wallis rank sum test	TP by month	ns

DO: Dissolved oxygen mg L^{-1}; BOD_5: Biochemical oxygen demand mg L^{-1}; COD: chemical oxygen demand mg L^{-1} ; TN: Total Nitrogen mg L^{-1} ; TP: Total phosphorus mg L^{-1}

Tabla S7. Total microbial community in each WWTP. WWTPRSS: Roses wastewater treatment plant. WWTPLLN: Llançà wastewater treatment plant. WWTPCES: Castelló d'Empúries wastewater treatment plant. WWTPRUS: Reus wastewater treatment plant. WWTPAMP: Amposta Wastewater Treatment Plant. WWTPALC: Les Cases d'Alcanar Wastewater Treatment Plant WWTPSCR: Sant Carles de la Ràpita Wastewater Treatment Plant

Especie/genus	Clase	WWTPRSS	%	WWTPLLN	%	WWTPCES	%	WWTPRUS	%	WWTPAMP	%	WWTPALC	%	WWTPSCR	%
Arcella sp.	Amoebas	4	0.04	1554	5.7	2614	14.3	598	2.0	179	0.6	738	5.3	3055	17.0
Centropyxis sp.	Amoebas	1	0.01	23	0.1	18	0.1	0	0.0	0	0.0	0	0.0	0	0.0
Cochliopodium sp	Amoebas	0	0.00	0	0.0	0	0.0	1589	5.2	924	3.2	719	5.1	1643	9.1
Cryptodifflugia sp.	Amoebas	0	0.00	0	0.0	43	0.2	0	0.0	0	0.0	357	2.5	0	0.0
Euglypha sp.	Amoebas	1	0.01	58	0.2	88	0.5	0	0.0	6319	22.0	988	7.1	3022	16.8
Gymnamoebae	Amoebas	12415	98	15341	55.9	12387	67.8	26823	88.2	21278	74.1	11207	80.0	10262	57.1
Pyxidicula sp.	Amoebas	228	1.8	10447	38.1	3108	17.0	1414	4.6	0	0.0	0	0.0	0	0.0
Trinema sp.	Amoebas	1	0.0	10	0.0	3	0.0	0	0.0	0	0.0	0	0.0	0	0.0
Amoebas totales		12651	100.0	27434	100.0	18262	100.0	30424	100.0	28701	100.0	14009	100.0	17982	100.0
Acineria incurvata	Ciliates	0	0	3	0.1	7	0.1	0	0.0	0	0.0	0	0.0	0	0.0
Acineria uncinata	Ciliates	953	11	576	10.8	32	0.5	634	7.7	614	6.2	696	24.4	642	11.9
Acineta sp.	Ciliates	216	3	202	3.8	201	3.1	16	0.2	51	0.5	222	7.8	429	8.0
Amphileptus claparedei	Ciliates	0	0	0	0.0	0	0.0	9	0.1	0	0.0	0	0.0	0	0.0
Amphileptus sp.	Ciliates	2	0	14	0.3	0	0.0	0	0.0	0	0.0	0	0.0	0	0.0
Aspidisca cicada	Ciliates	704	8	732	13.7	440	6.9	723	8.8	182	1.8	236	8.3	603	11.2

Especie/genus	Clase	WWTPRSS	%	WWTPLLN	%	WWTPCES	%	WWTPRUS	%	WWTPAMP	%	WWTPALC	%	WWTPSCR	%
Aspidisca lynceus	Ciliates	0	0	312	5.8	933	14.6	2	0.0	1	0.0	0	0.0	3	0.0
Calyptotricha lanuginosa	Ciliates	0	0	165	3.1	2333	36.4	0	0.0	0	0.0	0	0.0	23	0.4
Chaetospira muelleri	Ciliates	0	0	1	0.0	47	0.7	0	0.0	0	0.0	0	0.0	108	2.0
Chillodonells	Ciliates	6	0	73	1.4	75	1.2	0	0.0	0	0.0	0	0.0	0	0.0
Chilodonella uncinata	Ciliates	0	0	0	0.0	0	0.0	8	0.1	0	0.0	0	0.0	8	0.1
Cinetochilum margaritaceum	Ciliates	128	2	0	0.0	13	0.2	0	0.0	0	0.0	0	0.0	0	0.0
Coleps sp.	Ciliates	0	0	0	0.0	0	0.0	0	0.0	0	0.0	0	0.0	0	0.0
Cyclidium sp.	Ciliates	0	0	1	0.0	0	0.0	0	0.0	0	0.0	4	0.2	0	0.0
Cyrtolophosis sp.	Ciliates	0	0	0	0.0	0	0.0	0	0.0	0	0.0	0	0.0	3	0.0
Dexiotricha sp.	Ciliates	188	2	30	0.6	94	1.5	0	0.0	3642	36.6	102	3.6	121	2.3
Discophrya elongata	Ciliates	0	0	0	0.0	0	0.0	14	0.2	9	0.1	0	0.0	4	0.1
Drepanomonas revoluta	Ciliates	1	0	0	0.0	0	0.0	0	0.0	0	0.0	0	0.0	20	0.4
Enchelys vermiformis	Ciliates	0	0	0	0.0	0	0.0	0	0.0	2	0.0	0	0.0	0	0.0
Endosphaera sp.	Ciliates	0	0	0	0.0	0	0.0	14	0.2	44	0.4	0	0.0	4	0.1
Epicarchesium sp	Ciliates	58	1	44	0.8	21	0.3	14	0.2	4	0.0	0	0.0	0	0.0
Epistylis sp.	Ciliates	61	1	362	6.8	74	1.2	2429	29.5	355	3.6	53	1.9	50	0.9
Euplotes sp.	Ciliates	111	1	1	0.0	117	1.8	7	0.1	0	0.0	0	0.0	3	0.0
Gastronauta membranaceus	Ciliates	0	0	0	0.0	0	0.0	62	0.7	0	0.0	0	0.0	0	0.0
Holophrya discolor	Ciliates	17	0	21	0.4	22	0.3	21	0.2	45	0.5	0	0.0	36	0.7
Litonotus lamella	Ciliates	21	0	7	0.1	1	0.0	117	1.4	6	0.1	0	0.0	4	0.1
Metacineta sp.	Ciliates	7	0	2	0.0	2	0.0	0	0.0	0	0.0	0	0.0	0	0.0
Metacystis sp.	Ciliates	1	0	93	1.8	132	2.1	0	0.0	12	0.1	1138	40.0	122	2.3
Metopus sp.	Ciliates	11	0	0	0.0	1	0.0	0	0.0	0	0.0	261	9.2	0	0.0
Microthorax pusillus	Ciliates	0	0	0	0.0	0	0.0	0	0.0	811	8.1	0	0.0	341	6.4
Opercularia sp	Ciliates	1061	13	178	3.3	148	2.3	694	8.4	2701	27.1	0	0.0	726	13.5
Oxitrichidae	Ciliates	1	0	0	0.0	0	0.0	69	0.8	0	0.0	0	0.0	3	0.0
Paramecium sp.	Ciliates	0	0	0	0.0	0	0.0	10	0.1	1	0.0	4	0.2	0	0.0

Especie/genus	Clase	WWTPRSS	%	WWTPLLN	%	WWTPCES	%	WWTPRUS	%	WWTPAMP	%	WWTPALC	%	WWTPSCR	%
Phialina sp.	Ciliates	7	0	157	2.9	96	1.5	0	0.0	0	0.0	0	0.0	0	0.0
Plagiocampa rouxi	Ciliates	47	1	30	0.6	168	2.6	5	0.1	139	1.4	98	3.4	87	1.6
Podophrya sp.	Ciliates	11	0	11	0.2	16	0.3	2	0.0	2	0.0	4	0.2	0	0.0
Pseudochilodonopsis fluviatilis	Ciliates	0	0	0	0.0	0	0.0	76	0.9	0	0.0	0	0.0	0	0.0
Pseudovorticella sp.	Ciliates	38	0	5	0.1	0	0.0	218	2.6	182	1.8	4	0.2	289	5.4
Sphatidium sp.	Ciliates	0	0	2	0.0	0	0.0	0	0.0	0	0.0	0	0.0	0	0.0
Spirostomum teres	Ciliates	0	0	44	0.8	0	0.0	0	0.0	133	1.3	0	0.0	0	0.0
Suctor sp.	Ciliates	0	0	0	0.0	0	0.0	2	0.0	0	0.0	0	0.0	0	0.0
Telotrochs	Ciliates	5	0	7	0.1	0	0.0	13	0.2	7	0.1	0	0.0	9	0.2
Thuricola sp.	Ciliates	0	0	0	0.0	50	0.8	0	0.0	0	0.0	0	0.0	0	0.0
Tokophrya spp	Ciliates	2	0	3	0.1	5	0.1	36	0.4	60	0.6	0	0.0	4	0.1
Trochilia minuta	Ciliates	2130	25	752	14.1	402	6.3	109	1.3	6	0.1	0	0.0	1328	24.7
Trochiliodes recta	Ciliates	15	0	8	0.1	0	0.0	0	0.0	0	0.0	0	0.0	0	0.0
Unidentified ciliate	Ciliates	1	0	0	0.0	0	0.0	0	0.0	2	0.0	18	0.6	0	0.0
Uronema nigricans	Ciliates	1494	18	5	0.1	262	4.1	210	2.5	0	0.0	0	0.0	25	0.5
Vorticella aquadulcis	Ciliates	326	4	1036	19.4	486	7.6	649	7.9	593	6.0	0	0.0	314	5.8
Vorticella convallaria	Ciliates	556	7	362	6.8	218	3.4	409	5.0	8	0.1	0	0.0	30	0.6
Vorticella infusionum	Ciliates	0	0	5	0.1	0	0.0	1502	18.2	284	2.9	0	0.0	8	0.1
Vorticella microstoma	Ciliates	3	0	4	0.1	2	0.0	84	1.0	0	0.0	0	0.0	0	0.0
Vorticella sp.	Ciliates	206	2	86	1.6	10	0.2	86	1.0	55	0.6	4	0.2	29	0.5
Zoothamnium sp.	Ciliates	19	0	0	0.0	0	0.0	0	0.0	0	0.0	0	0.0	0	0.0
Total Ciliates		8409	100	5334	100.0	6410	100.0	8245	100.0	9952	100.0	2846	100.0	5370	100.0
Actinomycetes Nocardioformes (ACNO)	Filamentous bacteria	0	0	0	0.0	0	0.0	22	5.1	35	6.8	0	0.0	0	0.0
Beggiatoa spp.	Filamentous bacteria	87	13	1	0.2	1	0.1	1	0.2	0	0.0	2	0.2	0	0.0
Candidatus Alysiosphaera europaea	Filamentous bacteria	0	0	0	0.0	0	0.0	0	0.0	0	0.0	8	0.7	13	2.3
Candidatus Monilobacter batavus	Filamentous bacteria	6	1	17	3.9	94	9.3	0	0.0	0	0.0	0	0.0	0	0.0

Especie/genus	Clase	WWTPRSS	%	WWTPLLN	%	WWTPCES	%	WWTPRUS	%	WWTPAMP	%	WWTPALC	%	WWTPSCR	%
Flexibacter sp.	Filamentous bacteria	0	0	0	0.0	0	0.0	0	0.0	2	0.4	1	0.1	0	0.0
Haliscomenobacter hydrossis	Filamentous bacteria	13	2	19	4.4	13	1.3	11	2.5	9	1.8	9	0.9	4	0.8
Isosphaera sp	Filamentous bacteria	0	0	0	0.0	0	0.0	4	1.0	0	0.0	0	0.0	8	1.4
Microthrix spp	Filamentous bacteria	252	38	116	26.6	597	59.2	7	1.7	129	25.3	283	27.8	110	19.2
Nostocoida limicola	Filamentous bacteria	24	4	16	3.6	8	0.8	13	3.0	29	5.8	113	11.1	61	10.7
Sphaerotilus natans	Filamentous bacteria	0	0	0	0.0	0	0.0	1	0.2	0	0.0	0	0.0	0	0.0
Streptococcus sp	Filamentous bacteria	1	0	0	0.0	0	0.0	1	0.3	1	0.2	0	0.0	1	0.2
Thiothrix	Filamentous bacteria	13	2	18	4.1	29	2.9	8	1.8	1	0.1	23	2.3	7	1.1
Type 0041	Filamentous bacteria	6	1	10	2.3	17	1.7	10	2.4	23	4.6	20	2.0	25	4.5
Type 0092	Filamentous bacteria	36	5	218	49.8	216	21.4	2	0.5	111	21.9	227	22.3	193	33.7
Type 021N	Filamentous bacteria	46	7	3	0.7	2	0.2	312	71.3	2	0.4	1	0.1	0	0.0
Type 0581	Filamentous bacteria	0	0	0	0.0	0	0.0	0	0.0	1	0.2	0	0.0	0	0.0
Type 0675	Filamentous bacteria	172	26	11	2.5	12	1.2	0	0.0	21	4.1	0	0.0	0	0.0
Type 0803	Filamentous bacteria	0	0	0	0.0	0	0.0	0	0.0	72	14.1	0	0.0	50	8.8
Type 0914	Filamentous bacteria	3	1	0	0.1	2	0.2	1	0.2	2	0.4	0	0.0	3	0.4
Type 0961	Filamentous bacteria	4	1	1	0.2	2	0.2	3	0.7	0	0.1	0	0.0	0	0.0
Type 1701	Filamentous bacteria	0	0	1	0.2	0	0.0	15	3.3	1	0.1	0	0.0	0	0.0
Type 1851	Filamentous bacteria	3	0	6	1.4	13	1.3	3	0.6	17	3.4	19	1.9	14	2.5
Type 1863	Filamentous bacteria	0	0	0	0.0	0	0.0	10	2.3	0	0.0	0	0.0	0	0.0
Unidentified Filamentous	Filamentous bacteria	0	0	0	0.0	0	0.0	13	3.0	52	10.2	313	30.7	82	14.4
Total filamentous bacteria		666	100	437		1008		437	100.0	509	100.0	1018	100.0	572	100.0
Astasia sp.	Flagellates	1	0	0	0.0	1	0.0	0	0.0	0	0.0	22	0.0	49	0.0

Especie/genus	Clase	WWTPRSS	%	WWTPLLN	%	WWTPCES	%	WWTPRUS	%	WWTPAMP	%	WWTPALC	%	WWTPSCR	%
Bicosoeca sp	Flagellates	0	0	0	0.0	0	0.0	0	0.0	0	0.0	0	0.0	1607	0.8
Bodonidos	Flagellates	129214	35	44551	73.9	118588	90.5	96127	79.6	122245	77.1	162128	87.6	180520	85.3
Choanoflagellates	Flagellates	216665	59	12781	21.2	10749	8.2	548	0.5	27855	17.6	3095	1.7	3067	1.4
Entosiphon sp.	Flagellates	1	0	58	0.1	0	0.0	8	0.0	0	0.0	0	0.0	0	0.0
Notosolenus sp	Flagellates	14586	4	66	0.1	475	0.4	0	0.0	42	0.0	0	0.0	79	0.0
Ochromonads	Flagellates	0	0	0	0.0	0	0.0	12114	10.0	1466	0.9	4381	2.4	8504	4.0
Other Flagellates	Flagellates	0	0	0	0.0	0	0.0	8790	7.3	0	0.0	0	0.0	0	0.0
Peranema sp.	Flagellates	111	0	744	1.2	60	0.0	36	0.0	74	0.0	13	0.0	83	0.0
Petalomonas sp.	Flagellates	159	0	90	0.1	102	0.1	2	0.0	118	0.1	89	0.0	221	0.1
Polytoma sp	Flagellates	0	0	0	0.0	0	0.0	0	0.0	0	0.0	9	0.0	4	0.0
Trepomonas sp.	Flagellates	3158	1	0	0.0	0	0.0	0	0.0	395	0.2	0	0.0	1608	0.8
Trimastix sp.	Flagellates	0	0	0	0.0	0	0.0	0	0.0	0	0.0	2857	1.5	0	0.0
Unidentified euglenids	Flagellates	0	0	0	0.0	0	0.0	3118	2.6	0	0.0	0	0.0	0	0.0
Unidentified flagellate g1	Flagellates	837	0	1986	3.3	993	0.8	0	0.0	0	0.0	0	0.0	3482	1.6
Unidentified flagellate g2	Flagellates	1	0	0	0.0	0	0.0	0	0.0	6373	4.0	12543	6.8	12454	5.9
Total flagellates		364733	100	60275	100.0	130968	100.0	120744	100.0	158567	100.0	185137	100.0	211677	100.0
Fungi	Others	0	0	0	0	0	0	0	0	0	0	0	1	0	0
Gastrotricha	Others	0	0	5	16	0	0	0	0	0	0	0	0	0	0
Lecanidae	Others	0	0	15	45	37	45	88	31	0	0	16	53	86	29
Nematodes	Others	24	100	9	27	19	23	56	20	19	4	2	8	13	4
Rotaria sp.	Others	0	0	4	12	27	32	136	49	484	95	11	38	201	67
Chlamydomonads (green)	Others	0	0	0	0	0	0	0	0	4	1	0	0	0	0
Total others		24	100	34	100.0	82	100.0	280	100.0	507	100.0	29	100.0	300	100.0

Unidentified flagellate g1: flagellates <20µm Ind./ml ; Unidentified flagellate g2: flagellates >20µm Ind./ml

Table S8. Results of IndVal analysis for microbial community. WWTPRSS: Roses wastewater treatment plant. WWTPRUS: Reus wastewater treatment plant. WWTPSCR: Sant Carles de la Ràpita Wastewater Treatment Plant

Species/genus	**WWTP**	**IndVal**	**P value**	**Frequence**
Beggiatoa spp.	WWTPRSS	0,93	0,001	86
Choanoflagellates	WWTPRSS	0,75	0,001	153
Vorticella infusionum	WWTPRUS	0,80	0,001	91
Epistylis sp.	WWTPRUS	0,71	0,001	160
Arcella sp.	WWTPSCR	0,4	0,018	201
IndVal for Conductivity > 8000 µS cm-1				
Species/genus	**WWTP**	**IndVal**	**P value**	**Frequence**
Beggiatoa spp.	WWTPRSS	0,97	0,003	37
Choanoflagellates	WWTPRSS	0,97	0,007	38
Arcella sp.	WWTPSCR	0.99	0.001	39

Table S9. Linear mixed model between Richness Index as a function of conductivity for each WWTP. WWTPRSS: Roses wastewater treatment plant. WWTPLLN: Llançà wastewater treatment plant. WWTPCES: Castelló d'Empúries wastewater treatment plant. WWTPRUS: Reus wastewater treatment plant. WWTPAMP: Amposta Wastewater Treatment Plant. WWTPALC: Les Cases d'Alcanar Wastewater Treatment Plant WWTPSCR: Sant Carles de la Ràpita Wastewater Treatment Plant

Models: Simple_model: Richness ~ (1 | WWTP) Mixed_model_Richness: Richness ~ Conductivity + (1 | WWTP)	npar	AIC	BIC	logLik	deviance	Chisq	Df	Pr(>Chisq)
Simple_model	3	2470.884	2482.525	-1232.442	2464.884			
Mixed_model_Richness	4	2465.881	2481.403	-1228.941	2457.881	7.002533	1	0.008139**

Linear mixed model fit by REML ['lmerMod']
Formula: Richness ~ Conductivity + (1 | WWTP)
Data: AllIndexes
REML criterion at convergence: 2453.2
Scaled residuals:
Min 1Q Median 3Q Max
-3.2708 -0.4375 0.0052 0.3722 5.1629
Random effects:
Groups Name Variance Std.Dev.
WWTP (Intercept) 34.38 5.864
Residual 52.74 7.262
Number of obs: 304, groups: WWTP, 7
Fixed effects:
Estimate Std. Error t value
(Intercept) 29.4603 2.2522 13.081
Conductivity -2.0184 0.7641 -2.642

Correlation of Fixed Effects:
(Intr)Conductivity 0.001

Confidence intervals:
2.5 % 97.5 %
.sig01 3.324253 10.2861454
.sigma 6.747306 7.8240316
(Intercept) 24.768285 34.1442341
Conductivity -3.507418 -0.5270591

Significance codes: 0 '***' 0.001 '**' 0.01 '*' 0.05 '.' 0.1 ' ' 1

Table S10. Linear mixed model between Shannon Index as a function of conductivity for each WWTP. WWTPRSS: Roses wastewater treatment plant. WWTPLLN: Llançà wastewater treatment plant. WWTPCES: Castelló d'Empúries wastewater treatment plant. WWTPRUS: Reus wastewater treatment plant. WWTPAMP: Amposta Wastewater Treatment Plant. WWTPALC: Les Cases d'Alcanar Wastewater Treatment Plant WWTPSCR: Sant Carles de la Ràpita Wastewater Treatment Plant

Models: Simple_model: Shannon ~ (1 | WWTP) Mixed_Model_Shannon: Shannon ~ Conductivity + (1 | WWTP)	npar	AIC	BIC	logLik	deviance	Chisq	Df	Pr(>Chisq)
Simple_model	3	547.3141	558.9557	-270.6571	541.3141			
Mixed_Model_Shannon:	4	544.0300	559.5521	-268.0150	536.0300	5.28410	1	0.00131 *

Linear mixed model fit by REML ['lmerMod']
Formula: Shannon ~ Conductivity + (1 | WWTP)
Data: AllIndexes
REML criterion at convergence: 406.2
Scaled residuals:

Min	1Q	Median	3Q	Max
-2.22563	-0.58896	0.05511	0.77424	2.02349

Random effects:

Groups	Name	Variance	Std.Dev.
WWTP	(Intercept)	0.0000	0.0000
Residual		0.2164	0.4652

Number of obs: 304, groups: WWTP, 7
Fixed effects:

	Estimate	Std. Error	t value
(Intercept)	1.10115	0.02668	41.274
Conductivity	-0.08671	0.02672	-3.245

Correlation of Fixed Effects:

	(Intr)
Conductivity	0.000

Confidence intervals:

	2.5 %	97.5 %
.sig01	0.0000000	0.17977449
.sigma	0.4729614	0.54855162
(Intercept)	1.1465639	1.32008602
Conductivity	-0.1624753	-0.01582463

Significance codes: 0 '***' 0.001 '**' 0.01 '*' 0.05 '.' 0.1 ' ' 1

Table S11. Linear mixed model between Margalef Index as a function of conductivity for each WWTP. WWTPRSS: Roses wastewater treatment plant. WWTPLLN: Llançà wastewater treatment plant. WWTPCES: Castelló d'Empúries wastewater treatment plant. WWTPRUS: Reus wastewater treatment plant. WWTPAMP: Amposta Wastewater Treatment Plant. WWTPALC: Les Cases d'Alcanar Wastewater Treatment Plant WWTPSCR: Sant Carles de la Ràpita Wastewater Treatment Plant

Models: Simple_Model: Margalef ~ (1 | WWTP) Mixed_model_Margalef: Margalef ~ Conductivity + (1 | WWTP)	npar	AIC	BIC	logLik	deviance	Chisq	Df	Pr(>Chisq)
Simple_Model	3	462.808	474.4496	-228.404	456.808			
Mixed_model_Margalef	4	457.106	472.6281	-224.553	449.106	7.70198	1	0.00551**

Linear mixed model fit by REML ['lmerMod']
Formula: Margalef ~ Conductivity + (1 | WWTP)
Data: AllIndexes
REML criterion at convergence: 455.7
Scaled residuals:
Min 1Q Median 3Q Max
-3.1848 -0.4571 0.0042 0.3784 5.0176
Random effects:
Groups Name Variance Std.Dev.
WWTP (Intercept) 0.1168 0.3417
Residual 0.1931 0.4395
Number of obs: 304, groups: WWTP, 7
Fixed effects:
Estimate Std. Error t value
(Intercept) 1.7613 0.1314 13.402
Conductivity -0.1276 0.0461 -2.768
Correlation of Fixed Effects:
(Intr)
Conductivity 0.001

Confidence intervals:
2.5 % 97.5 %
.sig01 0.1925735 0.60004015
.sigma 0.4083289 0.47349358
(Intercept) 1.4877058 2.03464466
Conductivity -0.2176780 -0.03789775

Significance codes: 0 '***' 0.001 '**' 0.01 '*' 0.05 '.' 0.1 ' '

Table S12. Electrical conductivity peak and sample time identified by WWTP. WWTPRSS: Roses wastewater treatment plant. WWTPLLN: Llançà wastewater treatment plant. WWTPCES: Castelló d'Empúries wastewater treatment plant. WWTPRUS: Reus wastewater treatment plant. WWTPAMP: Amposta Wastewater Treatment Plant. WWTPALC: Les Cases d'Alcanar Wastewater Treatment Plant WWTPSCR: Sant Carles de la Ràpita Wastewater Treatment Plant

Sample time	WWTPRSS EC peaks	Sample time	WWTPLLN EC peaks	Sample time	WWTPCES EC peaks	Sample time	WWTPRUS EC peaks	Sample time	WWTPAMP EC peaks	Sample time	WWTPSCR EC peaks
50	14935	30	7025	5	7740	47	2580	7	2856	14	12780
18	13480										
2	11300	45	5570	10	6460	29	2560	10	2673	7	8080
43	10795	17	5165	29	5120	13	2230	18	2600	21	6922
23	10430	21	4895	12	5105	71	2170	15	2490	17	6157
34	10290	33	4360	19	5090	37	2150	-	_	12	5571
37	10260	5	3550	5	4890	39	2120	-	_	10	5510
5	10130	12	2511	21	4880	15	2110	-	_	19	5407
39	10080	39	2470	33	4880	80	2030	-	_	26	5198
56	9890	37	2270	7	4830	68	1979	-	_	23	4217
13	9320	48	2265	16	4420	2	1965	-	_	2	3370
18	9260	8	1629	51	3790	18	1964	-	-	-	-
27	8950	10	1605	49	3710	5	1955	-	-	-	-
16	8820	51	1594	36	3700	31	1948	-	-	-	-
46	8760	25	1479	-	-	61	1945	-	-	-	-
10	8725	-	-	-	-	7	1871	-	-	-	-
53	8275	-	-	-	-	86	1848	-	-	-	-
8	7970	-	-	-	-	74	1840	-	-	-	-
30	6435	-	-	-	-	44	1831	-	-	-	-

Table S13: One-way Kruskal-Wallis tests of abundance associated with EC peak and non-peak periods in WWTPs during the study period. WWTPRSS: Roses wastewater treatment plant. WWTPLLN: Llançà wastewater treatment plant. WWTPCES: Castelló d'Empúries wastewater treatment plant. WWTPRUS: Reus wastewater treatment plant. WWTPAMP: Amposta Wastewater Treatment Plant. WWTPALC: Les Cases d'Alcanar Wastewater Treatment Plant WWTPSCR: Sant Carles de la Ràpita Wastewater Treatment Plant.

Comparison	chi-squared	df	p-value	method	Significance
Total abundance associated to EC peak and no EC peak in WWTPRSS	96.335	55	0.0004802	Kruskal-Wallis rank sum test	***
Total abundance associated to EC peak and no EC peak in WWTPLLN	112.3	65	0.725	Kruskal-Wallis rank sum test	ns
Total abundance associated to EC peak and no EC peak in WWTPCES	117.2	62	0.965	Kruskal-Wallis rank sum test	ns
Total abundance associated to EC peak and no EC peak in WWTPRUS	109.5	67	0.896	Kruskal-Wallis rank sum test	ns
Total abundance associated to EC peak and no EC peak in WWTPAMP	105.2	57	0.0789	Kruskal-Wallis rank sum test	ns
Total abundance associated to EC peak and no EC peak in WWTPALC	110.1	63	0.728	Kruskal-Wallis rank sum test	ns
Total abundance associated to EC peak and no EC peak in WWTPSCR	96.912	60	0.001795	Kruskal-Wallis rank sum test	**

Table S14: Pairwise Comparisons of species abundance associated with EC Peak and Non-Peak Periods in WWTPs. WWTPRSS: Roses wastewater treatment plant. WWTPLLN: Llançà wastewater treatment plant. WWTPCES: Castelló d'Empúries wastewater treatment plant. WWTPRUS: Reus wastewater treatment plant. WWTPAMP: Amposta Wastewater Treatment Plant. WWTPALC: Les Cases d'Alcanar Wastewater Treatment Plant WWTPSCR: Sant Carles de la Ràpita Wastewater Treatment Plant.

Pairwise comparisons using Mann-Whitney test with continuity correction

data: Species abundance associated with EC peak and non-peak

*P value adjustment method: bonferroni

Specie/Genus	Statistic W	WWTPRSS	WWTPLLN	WWTPCES	WWTPRUS	WWTPAMP	WWTPSCR
Acineria uncinata	115.3	0.0003***					
Chillodonella	172.2	0.0001***	-	-	-	-	-
Holophyra discolor	171.5	0.0004***	-	-	-	-	-
Metacineta sp	176.3	0.0002***	-	-	-	-	-
Trochilia minuta	102.8	0.045*	-	-	-	-	-
Tokophrya sp.	145.1	0.036*	-	-	-	-	-
Vorticella aquadulcis	147.2	0.041*	-	-	-	-	-
Acineta sp.	12.8	-	-	-	-	-	0.0003***
Acineria uncinata	113.5	-	-	-	-	-	0.0008**
Holophyra discolor	142.8	-	-	-	-	-	0.004**
Opercularia sp	119.2	-	-	-	-	-	0.002**

Significance codes: 0 '***' 0.001 '**' 0.01 '*' 0.05 '.' 0.1 ' ' 1

Table S15: Spearman Correlation between Electrical Conductivity and Margalef Trends across WWTPs. WWTPRSS: Roses wastewater treatment plant. WWTPLLN: Llançà wastewater treatment plant. WWTPCES: Castelló d'Empúries wastewater treatment plant. WWTPRUS: Reus wastewater treatment plant. WWTPAMP: Amposta Wastewater Treatment Plant. WWTPALC: Les Cases d'Alcanar Wastewater Treatment Plant WWTPSCR: Sant Carles de la Ràpita Wastewater Treatment Plant.

Variable 1	Variable 2	WWTP	S	p-value	rho
Conductivity	Margalef	WWTPRSS	45754	0.00904	-0.3511
Conductivity	Margalef	WWTPLLN	24324	0.7874	-0.0722
Conductivity	Margalef	WWTPCES	23525	0.9763	-0.0520
Conductivity	Margalef	WWTPRUS	118738	0.2702	-0.1202
Conductivity	Margalef	WWTPAMP	3573.5	0.0652	-0.1908
Conductivity	Margalef	WWTPSCR	1753.7	0.01742	-0.2538

Table S16. One-Kruskal-Wallis between EC and Margalef index per season of the year by WWTPs. WWTPRSS: Roses wastewater treatment plant. WWTPLLN: Llançà wastewater treatment plant. WWTPCES: Castelló d'Empúries wastewater treatment plant. WWTPRUS: Reus wastewater treatment plant. WWTPAMP: Amposta Wastewater Treatment Plant. WWTPALC: Les Cases d'Alcanar Wastewater Treatment Plant WWTPSCR: Sant Carles de la Ràpita Wastewater Treatment Plant.

WWTP	Season	Kruskal-Wallis chi-squared statistic	Degrees of Freedom	p-value
WWTPRSS	Autumn	3.6067	1	0.05755
	Winter	0.29167	1	0.5892
	Spring	3.125	1	0.0771
	Summer	1.3787	1	0.2403
WWTPLLN	Autumn	0.6	1	0.4386
	Spring	1.0331	1	0.3094
	Summer	0.23988	1	0.6243
	Winter	0.74074	1	0.3894
WWTPRUS	Summer	0.099387	1	0.7526
	Autumn	0.12295	1	0.7259
	Winter	0.075342	1	0.7837
	Spring	0.21	1	0.6468

Table S17. Global linear model regression of the relationship between electrical conductivity and organic matter and nutrient removal efficiencies in WWWPs.

Variable	Predictor	Estimate	Std_Error	t_value	Pr
RE_EC	RE_BOD	-0.2009	0.0817	-2.459	0.01453*
RE_EC	RE_COD	-0.8737	0.281	-3.109	0.00206*
RE_EC	RE_TKN	0.0435	0.0228	1.907	0.05745
RE_EC	RE_NO_3	-0.0235	0.0213	-1.101	0.27181
RE_EC	RE_TP	0.036	0.0361	0.997	0.31982

*RE: Removal efficienc

Table S18. Global linear mixed model between removal efficiency of biological oxygen demand (RE_BOD) as a function of conductivity for each WWTP. WWTPRSS: Roses wastewater treatment plant. WWTPLLN: Llançà wastewater treatment plant. WWTPCES: Castelló d'Empúries wastewater treatment plant. WWTPRUS: Reus wastewater treatment plant. WWTPAMP: Amposta Wastewater Treatment Plant. WWTPALC: Les Cases d'Alcanar Wastewater Treatment Plant WWTPSCR: Sant Carles de la Ràpita Wastewater Treatment Plant

Models: Mixed_Model: RE_BOD ~ Conductivity + (1 | WWTP) Null_Model: RE_BOD ~ 1 + (1 | WWTP)	npar	AIC	BIC	logLik	deviance	Chisq	Df	Pr(>Chisq)
Null_Model	3	2173	2183	-1083.6	2167.2			
Mixed_Model:	4	2768	2184	-1080.4	2160.8	6.4767	1	0.01093*

Linear mixed model fit by REML ['lmerMod']
Formula: RE_COD ~ Conductivity + (1 | EDAR)
Data: EDAR1
REML criterion at convergence: 2173.3
Scaled residuals:

Min	1Q	Median	3Q	Max
-10.2691	-0.2012	0.1809	0.4760	1.3678

Random effects:

Groups	Name	Variance	Std.Dev.
WWTP	(Intercept)	6.542	2.558
Residual		69.586	8.342

Number of obs: 304, groups: WWTP, 7
Fixed effects:

	Estimate	Std. Error	t value
(Intercept)	92.2242323	1.5898128	58.009
Conductivity	-0.0008394	0.0002970	-2.826

Correlation of Fixed Effects:

	(Intr)	Conductivity
Conductivity	-0.710	

Confidence intervals:

	2.5 %	97.5 %
.sig01	0.310489409	4.9346617837
.sigma	7.710064797	9.0626387621
(Intercept)	88.982113613	95.2563282433
Conductivity	-0.001478314	-0.0002240276

Significance codes: 0 '***' 0.001 '**' 0.01 '*' 0.05 '.' 0.1 ' ' 1

Table S19. Global linear mixed model between removal efficiency of chemical oxygen demand (RE_COD) as a function of conductivity for each WWTP. WWTPRSS: Roses wastewater treatment plant. WWTPLLN: Llançà wastewater treatment plant. WWTPCES: Castelló d'Empúries wastewater treatment plant. WWTPRUS: Reus wastewater treatment plant. WWTPAMP: Amposta Wastewater Treatment Plant. WWTPALC: Les Cases d'Alcanar Wastewater Treatment Plant WWTPSCR: Sant Carles de la Ràpita Wastewater Treatment Plant

Models: Mixed_Model: RE_COD~ Conductivity + (1 | WWTP) Null_Model: RE_COD ~ 1 + (1 | WWTP)	npar	AIC	BIC	logLik	deviance	Chisq	Df	Pr(>Chisq)
Null_Model	3	1423	2183	-708.6	1417.2			
Mixed_Model:	4	1424	2184	-708.1	1416.8	0.7096	1	0.03996*

Linear mixed model fit by REML ['lmerMod']
Formula: RE_COD ~ Conductivity + (1 | EDAR)
Data: EDAR1
REML criterion at convergence: 1433
Scaled residuals:
Min 1Q Median 3Q Max
-6.0604 -0.2168 0.2624 0.5653 1.3711
Random effects:
Groups Name Variance Std.Dev.
WWTP (Intercept) 1.027 1.013
Residual 5.944 2.438
Number of obs: 304, groups: WWTP, 7
Fixed effects:
Estimate Std. Error t value
(Intercept) 9.687e+01 5.484e-01 176.648
Conductivity -7.234e-05 9.425e-05 -0.767
Correlation of Fixed Effects:
(Intr)
Conductivity -0.645

Confidence intervals:

2.5 % 97.5 %
.sig01 0.447896679 1.843805e+00
.sigma 2.251720249 2.645162e+00
(Intercept) 95.759313947 9.792789e+01
Conductivity -0.000260213 1.113778e-04

Significance codes: 0 '***' 0.001 '**' 0.01 '*' 0.05 '.' 0.1 ' ' 1

Table S20. Global linear mixed model between removal efficiency of Total Kjeldahl Nitrogen (RE_TKN) as a function of conductivity for each WWTP. WWTPRSS: Roses wastewater treatment plant. WWTPLLN: Llançà wastewater treatment plant. WWTPCES: Castelló d'Empúries wastewater treatment plant. WWTPRUS: Reus wastewater treatment plant. WWTPAMP: Amposta Wastewater Treatment Plant. WWTPALC: Les Cases d'Alcanar Wastewater Treatment Plant WWTPSCR: Sant Carles de la Ràpita Wastewater Treatment Plant

Models: Mixed_Model: RE_TKN~ Conductivity + (1 | WWTP) Null_Model: RE_TKN ~ 1 + (1 | WWTP)	npar	AIC	BIC	logLik	deviance	Chisq	Df	Pr(>Chisq)
Null_Model	3	2804.6	2815.8	-1399.3	2798.6			
Mixed_Model:	4	2793.0	2807.9	-1392.5	2785.0	13.59	1	0.0002274 ***

Linear mixed model fit by REML ['lmerMod']
Formula: RE_TKN ~ Conductivity + (1 | WWTP)
Data: WWTP
REML criterion at convergence: 2790.5
Scaled residuals:

Min	1Q	Median	3Q	Max
-12.0080	-0.3130	0.0407	0.3584	2.3456

Random effects:

Groups	Name	Variance	Std.Dev.
WWTP	(Intercept)	764.5	27.65
Residual		512.1	22.63

Number of obs: 304, groups: WWTP, 7
Fixed effects:

	Estimate	Std. Error	t value
(Intercept)	6.039e+01	1.119e+01	5.395
Conductivity	3.891e-03	9.973e-04	3.902

Correlation of Fixed Effects:
(Intr) Conductivity -0.326

Confidence intervals:

	2.5 %	97.5 %
.sig01	15.59215773	48.716238492
.sigma	20.89302547	24.543857807
(Intercept)	37.00136917	83.042188298
Conductivity	0.00180489	0.005830173

Significance codes: 0 '***' 0.001 '**' 0.01 '*' 0.05 '.' 0.1 ' ' 1

Table S21. Global linear mixed model between removal efficiency of nitrate (RE_NO3) as a function of conductivity for each WWTP. WWTPRSS: Roses wastewater treatment plant. WWTPLLN: Llançà wastewater treatment plant. WWTPCES: Castelló d'Empúries wastewater treatment plant. WWTPRUS: Reus wastewater treatment plant. WWTPAMP: Amposta Wastewater Treatment Plant. WWTPALC: Les Cases d'Alcanar Wastewater Treatment Plant WWTPSCR: Sant Carles de la Ràpita Wastewater Treatment Plant

Models: Mixed_Model: RE_NO3 ~ Conductivity + (1 | WWTP) Null_Model: RE_NO3 ~ 1 + (1 | WWTP)	npar	AIC	BIC	logLik	deviance	Chisq	Df	Pr(>Chisq)
Null_Model	3	2854	6865	-1408.6	2848.2			
Mixed_Model:	4	2855	2870	-1408.1	2847.8	0.7096	1	0.7001

Linear mixed model fit by REML ['lmerMod']
Formula: RE_NO3 ~ Conductivity + (1 | WWTP)
Data: WWTP
REML criterion at convergence: 2853
Scaled residuals:
Min 1Q Median 3Q Max
-3.0505 -0.1653 -0.1036 0.0383 3.8877
Random effects:
Groups Name Variance Std.Dev.
WWTP (Intercept) 931.9 30.53
Residual 629.9 25.10
Number of obs: 304, groups: WWTP, 7
Fixed effects:
Estimate Std. Error t value
(Intercept) 33.3962451 12.3664073 2.701
Conductivity -0.0003857 0.0011058 -0.349
Correlation of Fixed Effects:
(Intr)
Conductivity -0.328

Confidence intervals:

2.5 % 97.5 %
.sig01 17.231088644 53.771498504
.sigma 23.171292177 27.220074862
(Intercept) 7.865829732 58.685060734
Conductivity -0.002606351 0.001757171

Significance codes: 0 '***' 0.001 '**' 0.01 '*' 0.05 '.' 0.1 ' ' 1

Table S22. Global linear mixed model between removal efficiency of total phosphorus (RE_TP) as a function of conductivity for each WWTP. WWTPRSS: Roses wastewater treatment plant. WWTPLLN: Llançà wastewater treatment plant. WWTPCES: Castelló d'Empúries wastewater treatment plant. WWTPRUS: Reus wastewater treatment plant. WWTPAMP: Amposta Wastewater Treatment Plant. WWTPALC: Les Cases d'Alcanar Wastewater Treatment Plant WWTPSCR: Sant Carles de la Ràpita Wastewater Treatment Plant

Models: Mixed_Model: RE_TP ~ Conductivity + (1 | WWTP) Null_Model: RE_TP ~ 1 + (1 | WWTP)	npar	AIC	BIC	logLik	deviance	Chisq	Df	Pr(>Chisq)
Null_Model	3	2641.5	2652.7	-1317.8	2635.5			
Mixed_Model:	4	2643.5	2658.4	-1317.8	2635.5	0.0033	1	0.9544

Linear mixed model fit by REML ['lmerMod']
Formula: RE_TP ~ Conductivity + (1 | WWTP)
Data: EDAR1
REML criterion at convergence: 2643.5
Scaled residuals:
Min 1Q Median 3Q Max
-4.3523 -0.5486 0.2820 0.6360 1.8371
Random effects:
Groups Name Variance Std.Dev.
WWTP (Intercept) 117.5 10.84
Residual 323.1 17.97
Number of obs: 304, groups: WWTP, 7
Fixed effects:
Estimate Std. Error t value
(Intercept) 7.075e+01 5.106e+00 13.858
Conductivity 6.913e-05 7.451e-04 0.093
Correlation of Fixed Effects: (Intr)
Conductivity -0.541

Confidence intervals:

2.5 % 97.5 %
.sig01 17.231088644 53.771498504
.sigma 23.171292177 27.220074862
(Intercept) 7.865829732 58.685060734
Conductivity -0.002606351 0.001757171

Significance codes: 0 '***' 0.001 '**' 0.01 '*' 0.05 '.' 0.1 ' ' 1

Table S23. Summary of Structural equation model showing the effects of electrical conductivity on the abundance and diversity protozoa indices and pollutant removal efficiencies in WWTPs. Conductivity: conductivity (μS cm^{-1}); RE_BOD: biochemical oxygen demand removal percentage; RE_COD: chemical oxygen demand removal percentage; RE_TKN: nitrogen total Kjeldahl removal percentage; RE_NO3: nitrate removal percentage; RE_TP: total phosphorus removal percentage; Richness: Taxa richness of protozoan and bacterial communities in the activated sludge process; Shannon: Shannon diversity of protozoan and bacterial communities in the activated sludge process. Margalef: Margalef richness of protozoan and bacterial communities in the activated sludge process.

Summary SEM model. Lavaan 0.6.17 ended normally after 55 iterations						
Estimator	ML					
Optimization method	NLMINB					
Number of model parameters	34					
Number of observations	304					
Model Test User Model:						
Test statistic	160.045					
Degrees of freedom	10					
P-value (Chi-square)	0.000					
Model Test Baseline Model:						
Test statistic	1351.440					
Degrees of freedom	36					
P-value	0.000					
User Model versus Baseline Model:						
Comparative Fit Index (CFI)	0.886					
Tucker-Lewis Index (TLI)	0.589					
Loglikelihood and Information Criteria:						
Loglikelihood user model (H0)	-2851.154					
Loglikelihood unrestricted model (H1)	-2771.132					
Akaike (AIC)	5770.309					
Bayesian (BIC)	5896.688					
Sample-size adjusted Bayesian (SABIC)	5788.857					
Root Mean Square Error of Approximation:						
RMSEA	0.222					
90 Percent confidence interval - lower	0.193					
90 Percent confidence interval - upper	0.253					
P-value H_0: RMSEA <= 0.050	0.000					
P-value H_0: RMSEA >= 0.080	1.000					
Standardized Root Mean Square Residual:						
SRMR	0.117					
Parameter Estimates:						
Standard errors	Standard					
Information	Expected					
Information saturated (h1) model	Structured					
Regressions:						
	Estimate	Std.Err	z-value	P(>|z|)	Std.lv	Std.all
Richness ~						
Conductivity	-0.262	0.059	-4.482	0.000	-0.262	-0.261

Summary SEM model. Lavaan 0.6.17 ended normally after 55 iterations						
Margalef ~						
Conductivity	-0.300	0.057	-5.290	0.000	-0.300	-0.300
Shannon ~						
Conductivity	-0.196	0.061	-3.201	0.001	-0.196	-0.195
Richness ~						
RE_COD	-0.084	0.054	-1.555	0.120	-0.084	-0.084
RE_BOD	0.116	0.058	2.010	0.044	0.116	0.115
RE_TKN	-0.071	0.054	-1.313	0.189	-0.071	-0.070
RE_NO3	-0.014	0.055	-0.263	0.793	-0.014	-0.014
RE_TP	0.161	0.054	2.993	0.003	0.161	0.160
Margalef ~						
RE_COD	-0.113	0.052	-2.161	0.031	-0.113	-0.113
RE_BOD	0.141	0.056	2.529	0.011	0.141	0.141
RE_TKN	0.006	0.052	0.118	0.906	0.006	0.006
RE_NO3	0.011	0.053	0.211	0.833	0.011	0.011
RE_TP	0.178	0.052	3.427	0.001	0.178	0.178
Shannon ~						
RE_COD	-0.015	0.056	-0.260	0.795	-0.015	-0.015
RE_BOD	-0.028	0.060	-0.461	0.645	-0.028	-0.028
RE_TKN	0.085	0.056	1.520	0.129	0.085	0.085
RE_NO3	-0.082	0.057	-1.438	0.151	-0.082	-0.082
RE_TP	0.059	0.056	1.059	0.290	0.059	0.059
RE_COD ~						
Conductivity	-0.101	0.057	-1.769	0.077	-0.101	-0.101
RE_BOD ~						
Conductivity	-0.358	0.054	-6.678	0.000	-0.358	-0.358
RE_TKN ~						
Conductivity	0.003	0.057	0.045	0.964	0.003	0.003
RE_NO3 ~						
Conductivity	-0.168	0.057	-2.973	0.003	-0.168	-0.168
RE_TP ~						
Conductivity	0.016	0.057	0.279	0.780	0.016	0.016
Covariances:						
	Estimate	Std.Err	z-value	P(>|z|)	Std.lv	Std.all
.Richness ~~						
.Margalef	0.831	0.068	12.207	0.000	0.831	0.981
.Shannon	0.258	0.054	4.742	0.000	0.258	0.283
.Margalef ~~						
.Shannon	0.275	0.053	5.178	0.000	0.275	0.311
Variances:						
	Estimate	Std.Err	z-value	P(>|z|)	Std.lv	Std.all
.Richness	0.875	0.071	12.329	0.000	0.875	0.868
.Margalef	0.821	0.067	12.329	0.000	0.821	0.824
.Shannon	0.953	0.077	12.329	0.000	0.953	0.953
.RE_COD	0.987	0.080	12.329	0.000	0.987	0.990
.RE_BOD	0.869	0.071	12.329	0.000	0.869	0.872
.RE_TKN	0.997	0.081	12.329	0.000	0.997	1.000
.RE_NO3	0.969	0.079	12.329	0.000	0.969	0.972
.RE_TP	0.996	0.081	12.329	0.000	0.996	1.000
R-Square:						
	Estimate					
Richness	0.132					
Margalef	0.176					

Summary SEM model. Lavaan 0.6.17 ended normally after 55 iterations	
Shannon	0.047
RE_COD	0.010
RE_BOD	0.128
RE_TKN	0.000
RE_NO3	0.028
RE_TP	0.000

Table S24. Summary of Structural equation model showing the effects of electrical conductivity peaks on protozoan community indices for ciliates and percent pollutant removal. Conductivity: conductivity (µS cm-1); RE_BOD: biochemical oxygen demand removal percentage; RE_COD: chemical oxygen demand removal percentage; RE_TKN: nitrogen total Kjeldahl removal percentage; RE_NO3: nitrate removal percentage; RE_TP: total phosphorus removal percentage; Richness: Taxa richness of ciliates in the activated sludge process; Shannon: Shannon diversity of ciliates in the activated sludge process. Margalef: Margalef richness of ciliates in the activated sludge process.

Summary SEM model. Lavaan 0.6.17 ended normally after 55 iterations	
Estimator	ML
Optimization method	NLMINB
Number of model parameters	34
Number of observations	41
Model Test User Model:	
Test statistic	23.880
Degrees of freedom	10
P-value (Chi-square)	0.008
Model Test Baseline Model:	
Test statistic	242.393
Degrees of freedom	36
P-value	0.000
User Model versus Baseline Model:	
Comparative Fit Index (CFI)	0.933
Tucker-Lewis Index (TLI)	0.758
Loglikelihood and Information Criteria:	
Loglikelihood user model (H0)	-352.106
Loglikelihood unrestricted model (H1)	-340.166
Akaike (AIC)	772.211
Bayesian (BIC)	830.473
Sample-size adjusted Bayesian (SABIC)	724.038
Root Mean Square Error of Approximation:	
RMSEA	0.184
90 Percent confidence interval - lower	0.089
90 Percent confidence interval - upper	0.280
P-value H_0: RMSEA <= 0.050	0.017
P-value H_0: RMSEA >= 0.080	0.962
Standardized Root Mean Square Residual:	

Summary SEM model. Lavaan 0.6.17 ended normally after 55 iterations						
SRMR	0.110					
Parameter Estimates:						
Standard errors	Standard					
Information	Expected					
Information saturated (h1) model	Structured					
Regressions:						
	Estimate	Std.Err	z-value	P(>|z|)	Std.lv	Std.all
Richness ~						
Conductivity	-0.912	0.173	-1.227	0.220	-0.212	-0.210
Margalef ~						
Conductivity	-0.810	0.174	-1.209	0.227	-0.210	-0.208
Shannon ~						
Conductivity	-0.241	0.167	-0.246	0.805	-0.041	-0.041
Richness ~						
RE_COD	0.006	0.152	0.038	0.970	0.006	0.006
RE_BOD	-0.597	0.169	-1.168	0.243	-0.197	-0.196
RE_TKN	0.028	0.151	0.187	0.851	0.028	0.028
RE_NO3	-0.217	0.152	-1.428	0.153	-0.217	-0.216
RE_TP	0.012	0.151	0.079	0.937	0.012	0.012
Margalef ~						
RE_COD	-0.036	0.153	-0.236	0.813	-0.036	-0.036
RE_BOD	-0.184	0.170	-1.085	0.278	-0.184	-0.182
RE_TKN	0.088	0.152	0.575	0.565	0.088	0.087
RE_NO3	-0.197	0.153	-1.285	0.199	-0.197	-0.194
RE_TP	0.027	0.152	0.176	0.861	0.027	0.026
Shannon ~						
RE_COD	-0.127	0.147	-0.866	0.387	-0.127	-0.127
RE_BOD	0.256	0.163	1.568	0.117	0.256	0.256
RE_TKN	0.027	0.146	0.185	0.853	0.027	0.027
RE_NO3	-0.137	0.147	-0.934	0.350	-0.137	-0.137
RE_TP	0.180	0.146	1.234	0.217	0.180	0.181
RE_COD ~						
Conductivity	-0.137	0.155	-0.889	0.374	-0.137	-0.137
RE_BOD ~						
Conductivity	-0.452	0.139	-3.245	0.001	-0.452	-0.452
RE_TKN ~						
Conductivity	0.101	0.155	0.647	0.517	0.101	0.101
RE_NO3 ~						
Conductivity	-0.142	0.155	-0.920	0.358	-0.142	-0.142
RE_TP ~						
Conductivity	0.103	0.155	0.660	0.509	0.103	0.103
Covariances:						
	Estimate	Std.Err	z-value	P(>|z|)	Std.lv	Std.all
.Richness ~~						
.Margalef	0.906	0.201	4.509	0.000	0.906	0.992
.Shannon	0.595	0.165	3.598	0.000	0.595	0.679
.Margalef ~~						
.Shannon	0.585	0.165	3.543	0.000	0.585	0.664
Variances:						
	Estimate	Std.Err	z-value	P(>|z|)	Std.lv	Std.all

Summary SEM model. Lavaan 0.6.17 ended normally after 55 iterations						
.Richness	0.908	0.200	4.528	0.000	0.908	0.915
.Margalef	0.919	0.203	4.528	0.000	0.919	0.920
.Shannon	0.845	0.187	4.528	0.000	0.845	0.871
.RE_COD	0.957	0.211	4.528	0.000	0.957	0.981
.RE_BOD	0.776	0.171	4.528	0.000	0.776	0.796
.RE_TKN	0.966	0.213	4.528	0.000	0.966	0.990
.RE_NO3	0.956	0.211	4.528	0.000	0.956	0.980
.RE_TP	0.965	0.213	4.528	0.000	0.965	0.989
R-Square:						
Estimate						
Richness	0.085					
Margalef	0.080					
Shannon	0.129					
RE_COD	0.019					
RE_BOD	0.204					
RE_TKN	0.010					
RE_NO3	0.020					
RE_TP	0.011					

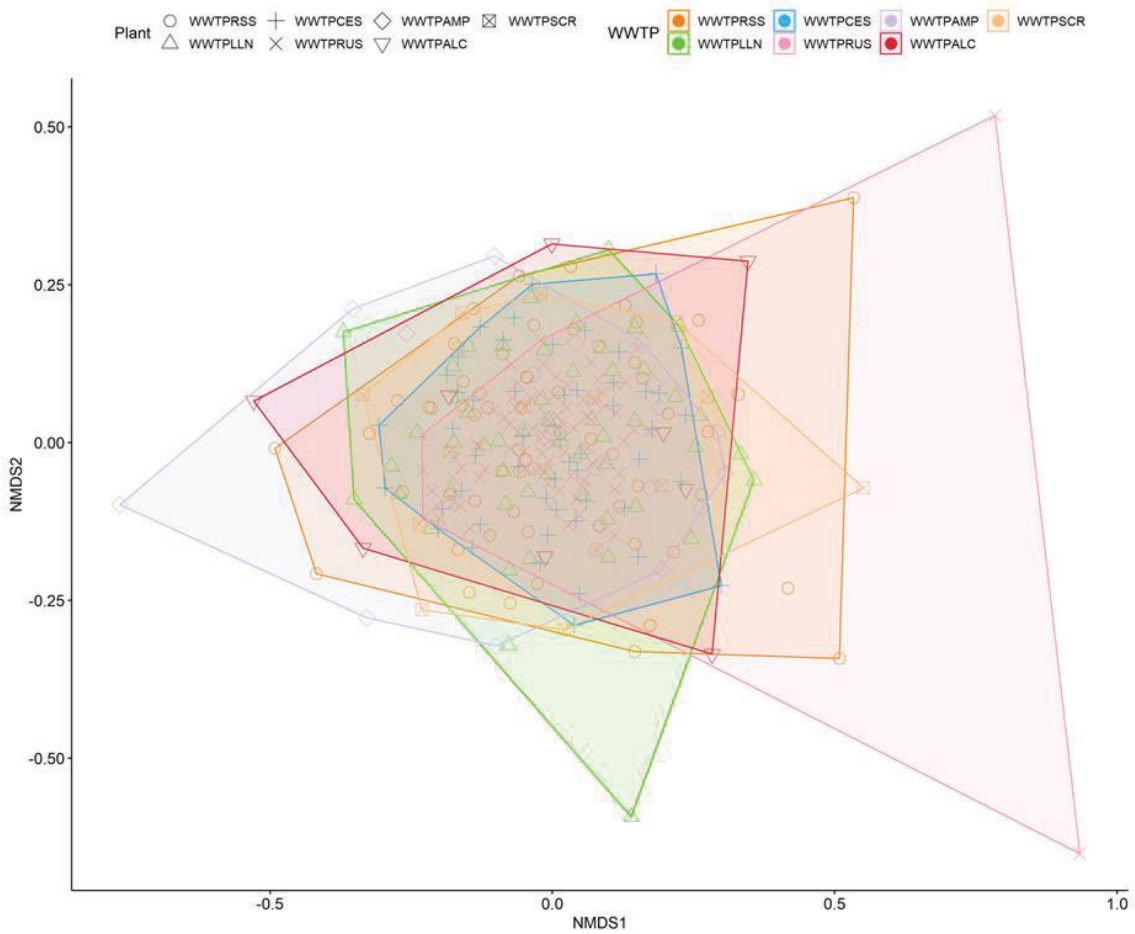


Figure S1. Results of NMDS for each WWTPs. WWTPRSS: Roses wastewater treatment plant. WWTPLLN: Llançà wastewater treatment plant. WWTPCES: Castelló d'Empúries wastewater treatment plant. WWTPRUS: Reus wastewater treatment plant. WWTPAMP: Amposta Wastewater Treatment Plant. WWTPALC: Les Cases d'Alcanar Wastewater Treatment Plant WWTPSCR: Sant Carles de la Ràpita Wastewater Treatment Plant

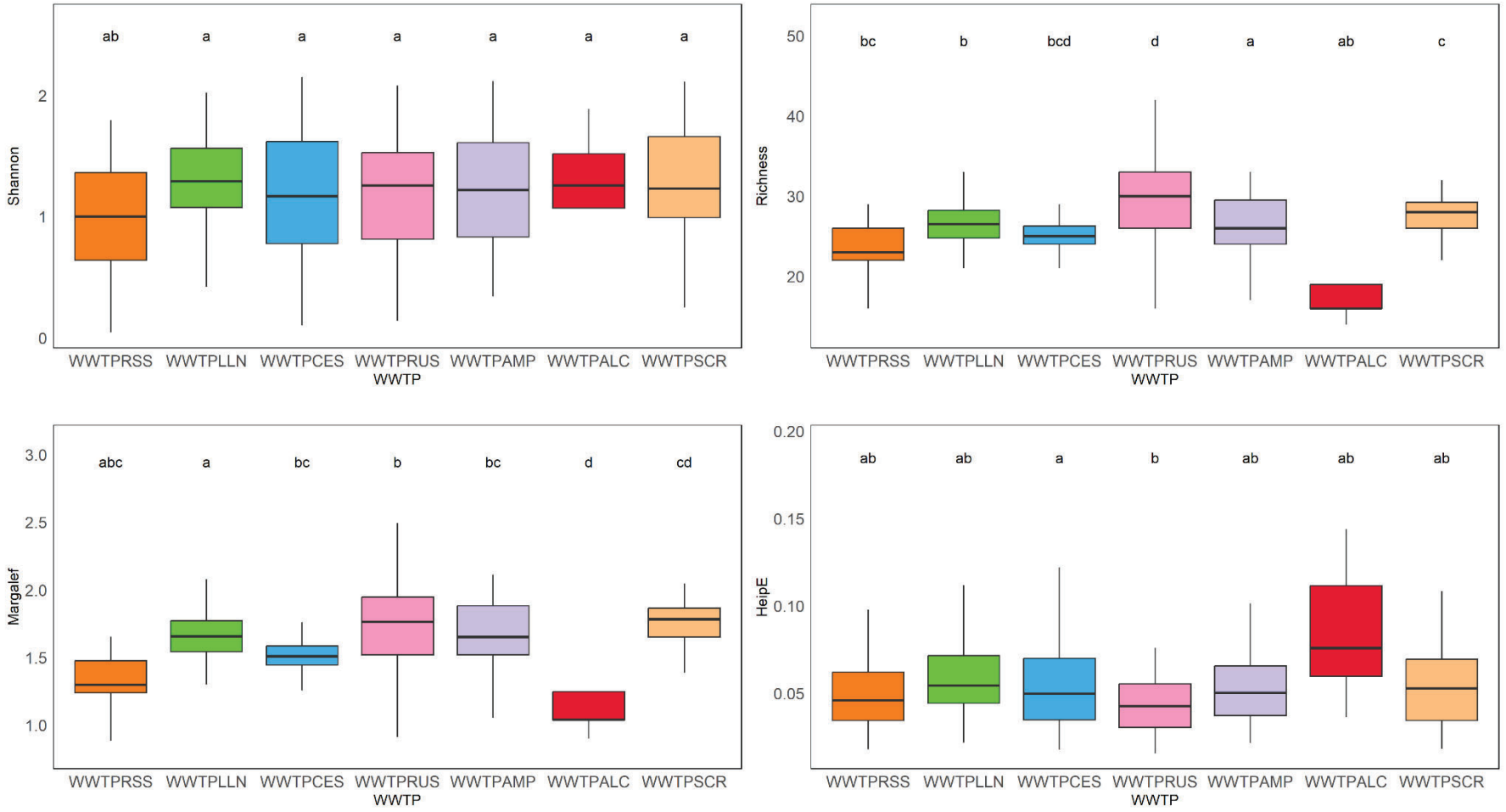


Figure S2. Boxplot of the microbial richness, Shannon, Margalef and HeipE indices for each WWTP: WWTPRSS: Roses wastewater treatment plant. WWTPLLN: Llançà wastewater treatment plant. WWTPCES: Castelló d'Empúries wastewater treatment plant. WWTPRUS: Reus wastewater treatment plant. WWTPAMP: Amposta Wastewater Treatment Plant. WWTPALC: Les Cases d'Alcanar Wastewater Treatment Plant WWTPSCR: Sant Carles de la Ràpita Wastewater Treatment Plant

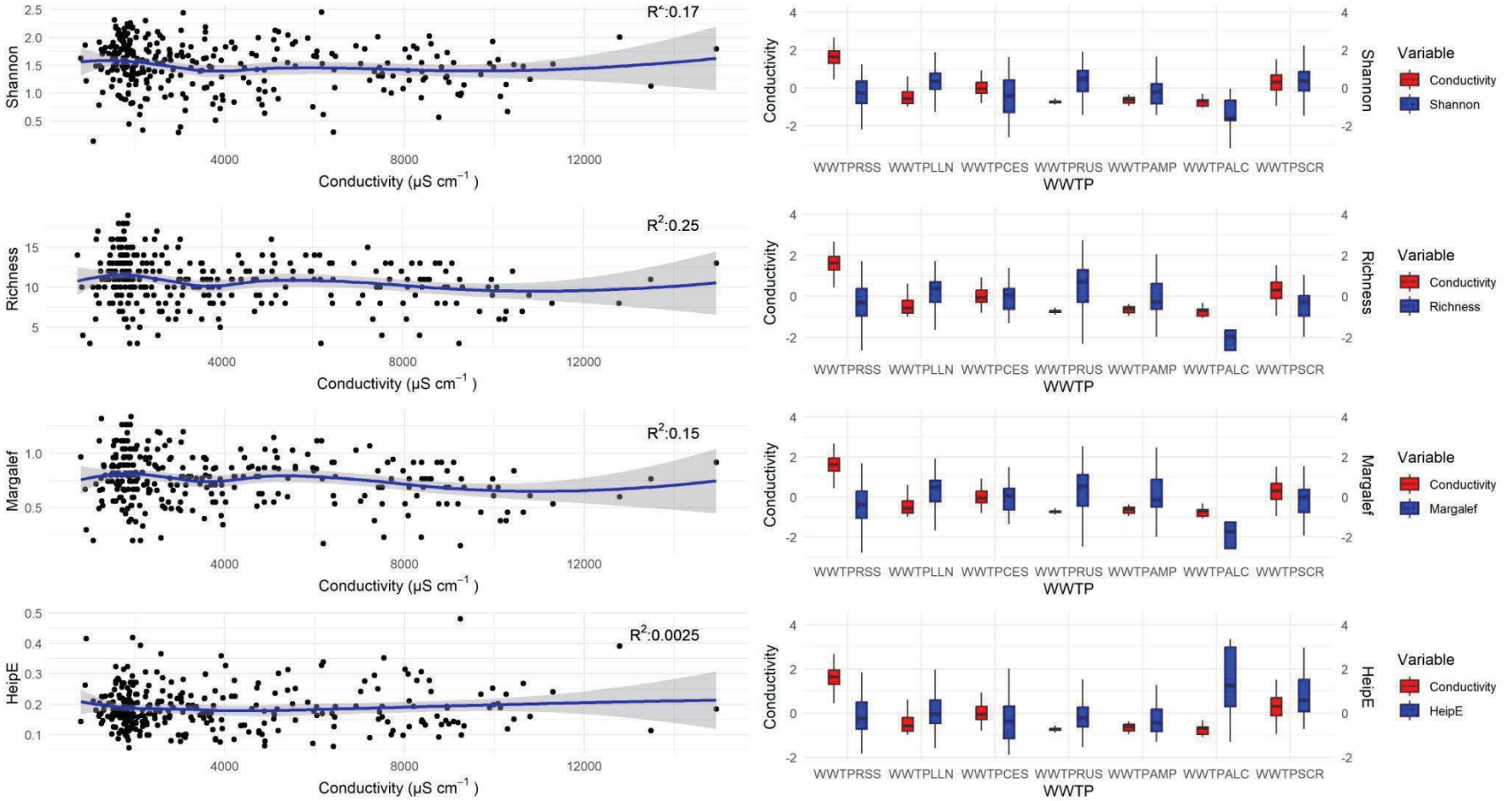


Figure S3. Linear mixed model between Shannon, Richness, Margalef and HeipE biodiversity indices of total microbial community as a function of conductivity for each WWTP. Box plot comparing conductivity and biodiversity indices for each WWTP. WWTPRSS: Roses wastewater treatment plant. WWTPLLN: Llançà wastewater treatment plant. WWTPCES: Castelló d'Empúries wastewater treatment plant. WWTPRUS: Reus wastewater treatment plant. WWTPAMP: Amposta Wastewater Treatment Plant. WWTPALC: Les Cases d'Alcanar Wastewater Treatment Plant WWTPSCR: Sant Carles de la Ràpita Wastewater Treatment Plant.

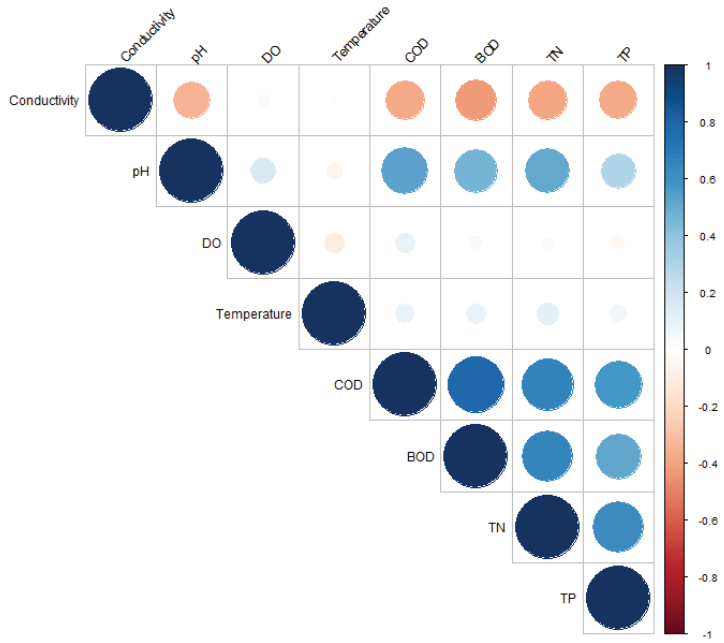


Figure S4. Spearman Correlation for environmental and water quality parameters in WWTP. The intensity of the color in the plot indicates the strength of the relationship between the variables. Blue signifies a positive correlation, while orange signifies a negative correlation. DO: Dissolved oxygen mg L^{-1}; BOD_5: Biochemical oxygen demand mg L^{-1}; COD: chemical oxygen demand mg L^{-1} ; TN: Total Nitrogen mg L^{-1} ; TP: Total phosphorus mg L^{-1}

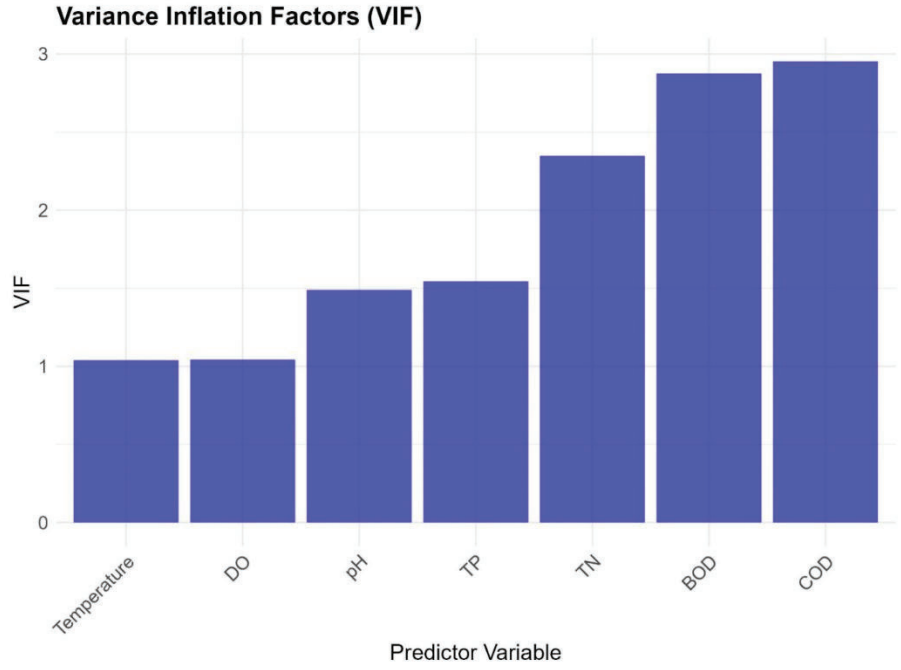


Figure S5. Bar chart showing the variance inflation factors (VIF) for conductivity and environmental and water quality variables in the activated sludge system at WWTPs.DO: Dissolved oxygen mg L^{-1}; BOD_5: Biochemical oxygen demand mg L^{-1}; COD: chemical oxygen demand mg L^{-1} ; TN: Total Nitrogen mg L^{-1} ; TP: Total phosphorus mg L^{-1} model <- lm(Conductivity ~ pH + DO + Temperature + COD+ BOD + TN + TP, data = data). vif_values <- vif(model).

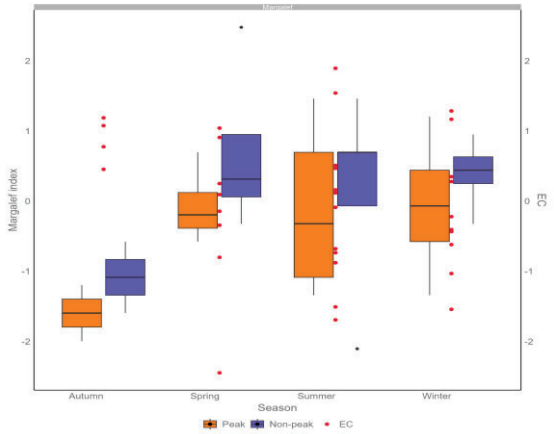


Figure S6. Margalef index associated with peaks and non-peaks of electrical conductivity by season for WWTPRSS: Roses wastewater treatment plant

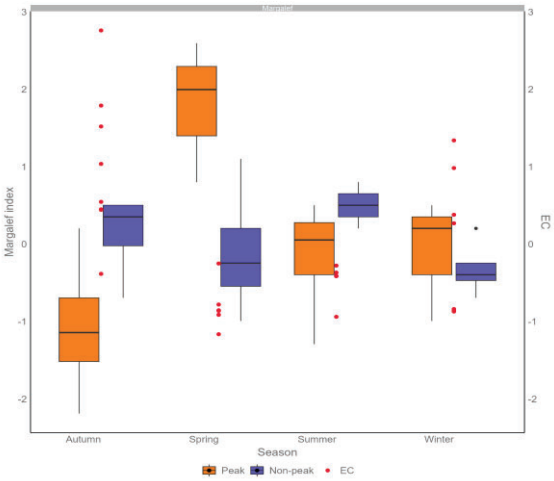


Figure S7. Margalef index associated with peaks and non-peaks of electrical conductivity by season for WWTPLLN: Llançà wastewater treatment plant.

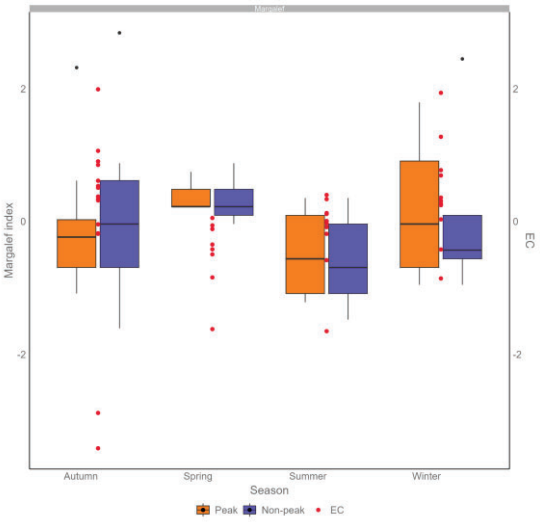


Figure S8. Margalef index associated with peaks and non-peaks of electrical conductivity by season for WWTPRUS: Reus wastewater treatment plant.

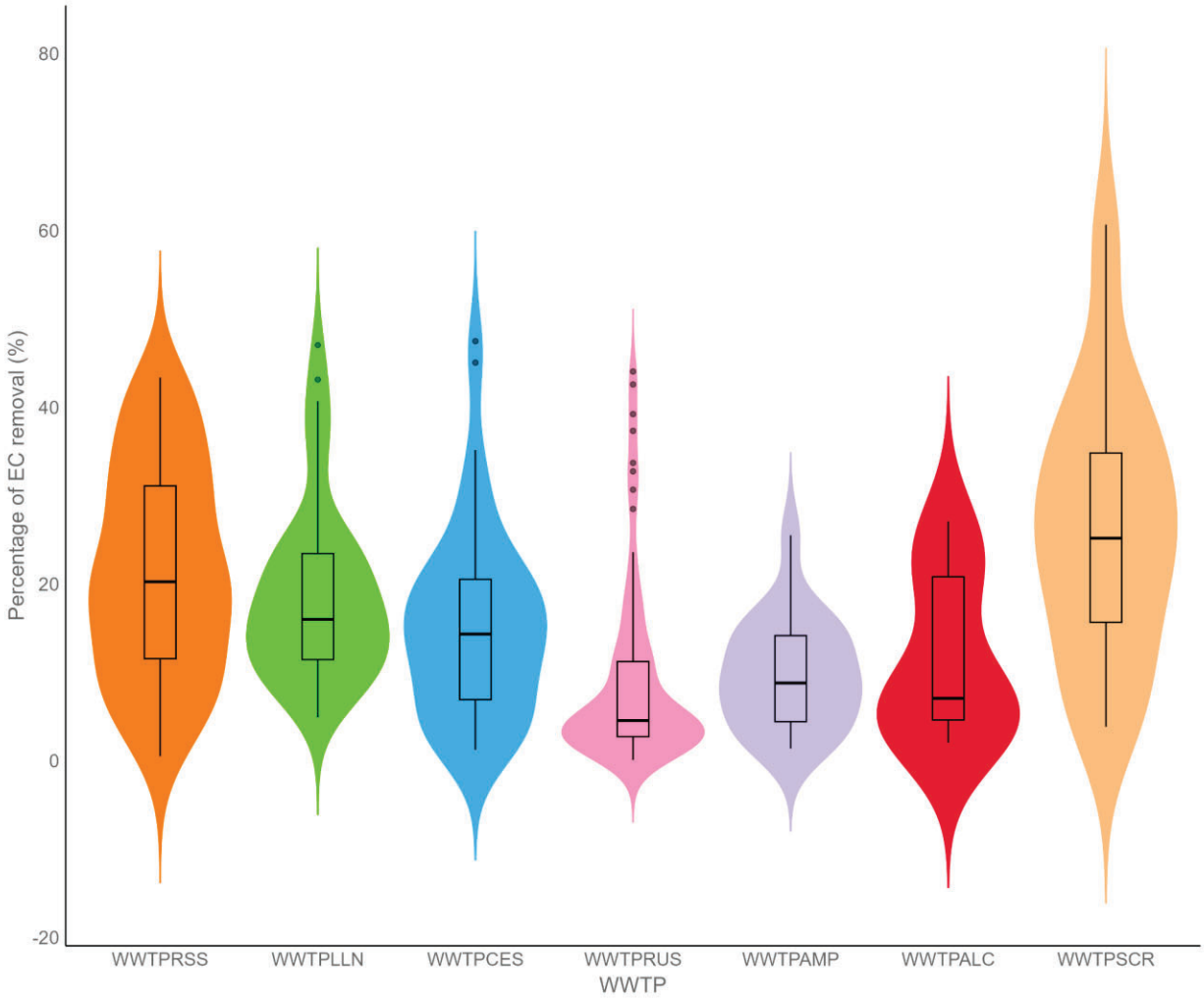


Figure S9. Electrical conductivity removal efficiency by WWTP. WWTPRSS: Roses wastewater treatment plant. WWTPLLN: Llançà wastewater treatment plant. WWTPCES: Castelló d'Empúries wastewater treatment plant. WWTPRUS: Reus wastewater treatment plant. WWTPAMP: Amposta Wastewater Treatment Plant. WWTPALC: Les Cases d'Alcanar Wastewater Treatment Plant WWTPSCR: Sant Carles de la Ràpita Wastewater Treatment Plant.

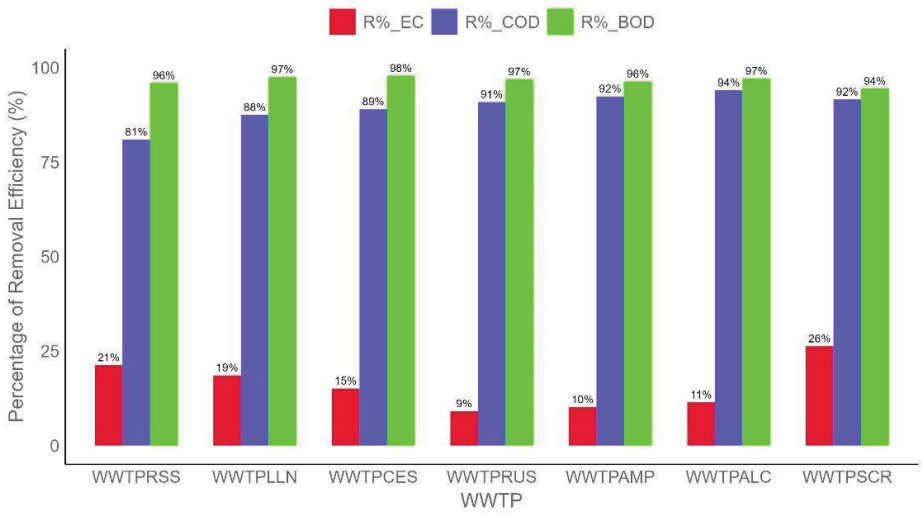


Figure S10. Bar graph showing total removal of electrical conductivity, chemical oxygen demand (COD) and biological oxygen demand (BOD) and their ratio by WWTP. WWTPRSS: Roses wastewater treatment plant. WWTPLLN: Llançà wastewater treatment plant. WWTPCES: Castelló d'Empúries wastewater treatment plant. WWTPRUS: Reus wastewater treatment plant. WWTPAMP: Amposta Wastewater Treatment Plant. WWTPALC: Les Cases d'Alcanar Wastewater Treatment Plant WWTPSCR: Sant Carles de la Ràpita Wastewater Treatment Plant

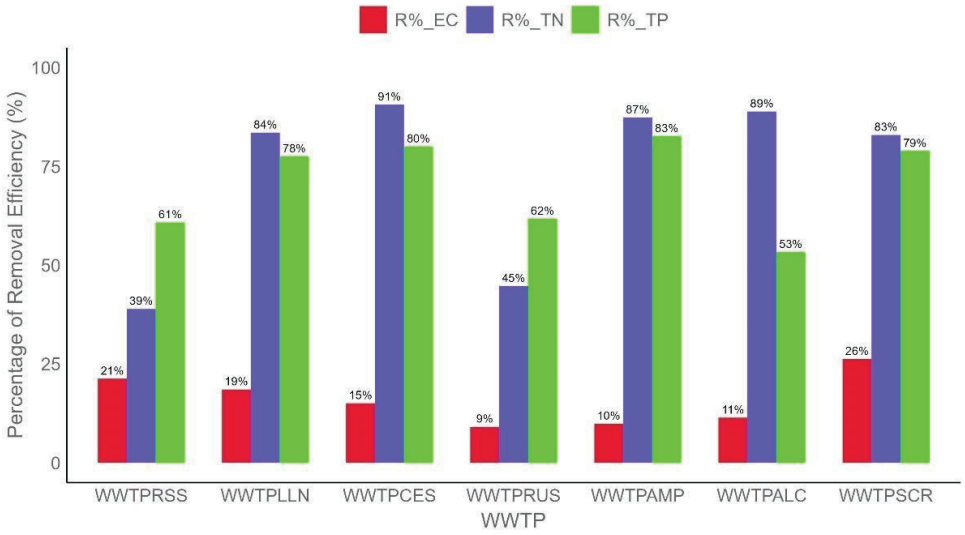


Figure S11. Bar graph showing total removal of electrical conductivity, total nitrogen (TN) and total phosphorus (TP) and their relationship by WWTP. WWTPRSS: Roses wastewater treatment plant. WWTPLLN: Llançà wastewater treatment plant. WWTPCES: Castelló d'Empúries wastewater treatment plant. WWTPRUS: Reus wastewater treatment plant. WWTPAMP: Amposta Wastewater Treatment Plant. WWTPALC: Les Cases d'Alcanar Wastewater Treatment Plant WWTPSCR: Sant Carles de la Ràpita Wastewater Treatment Plant

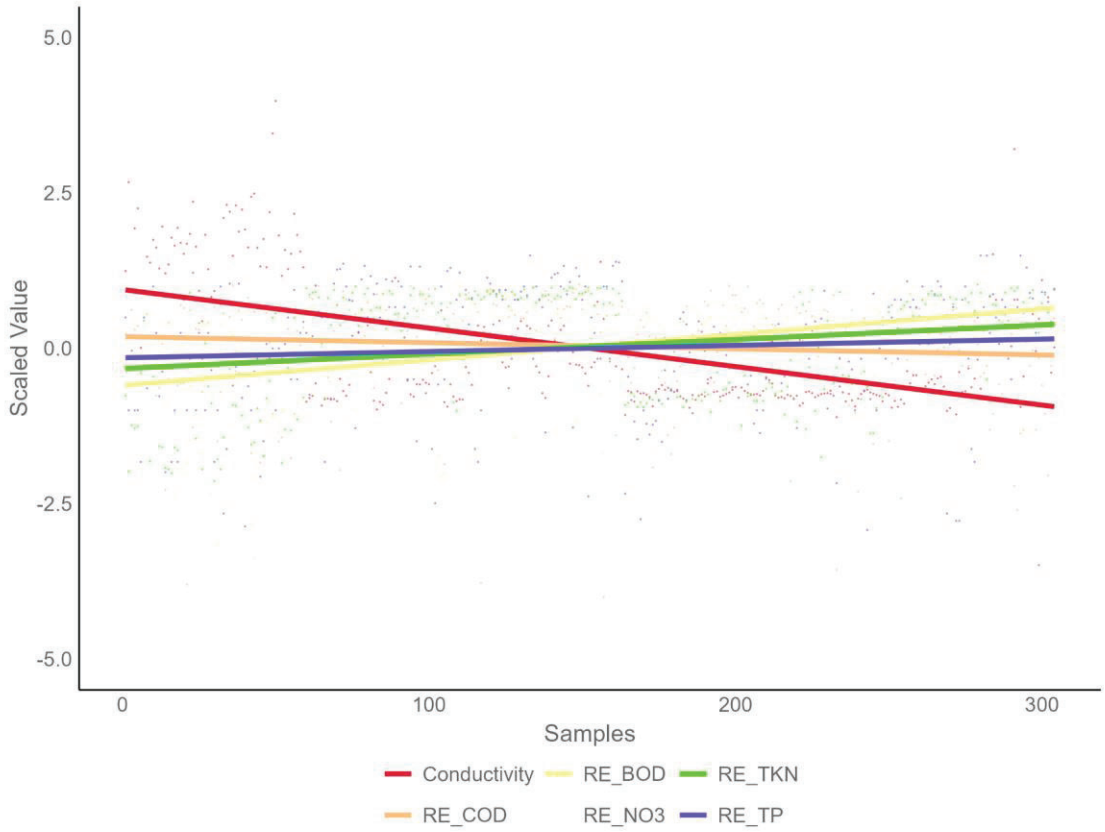
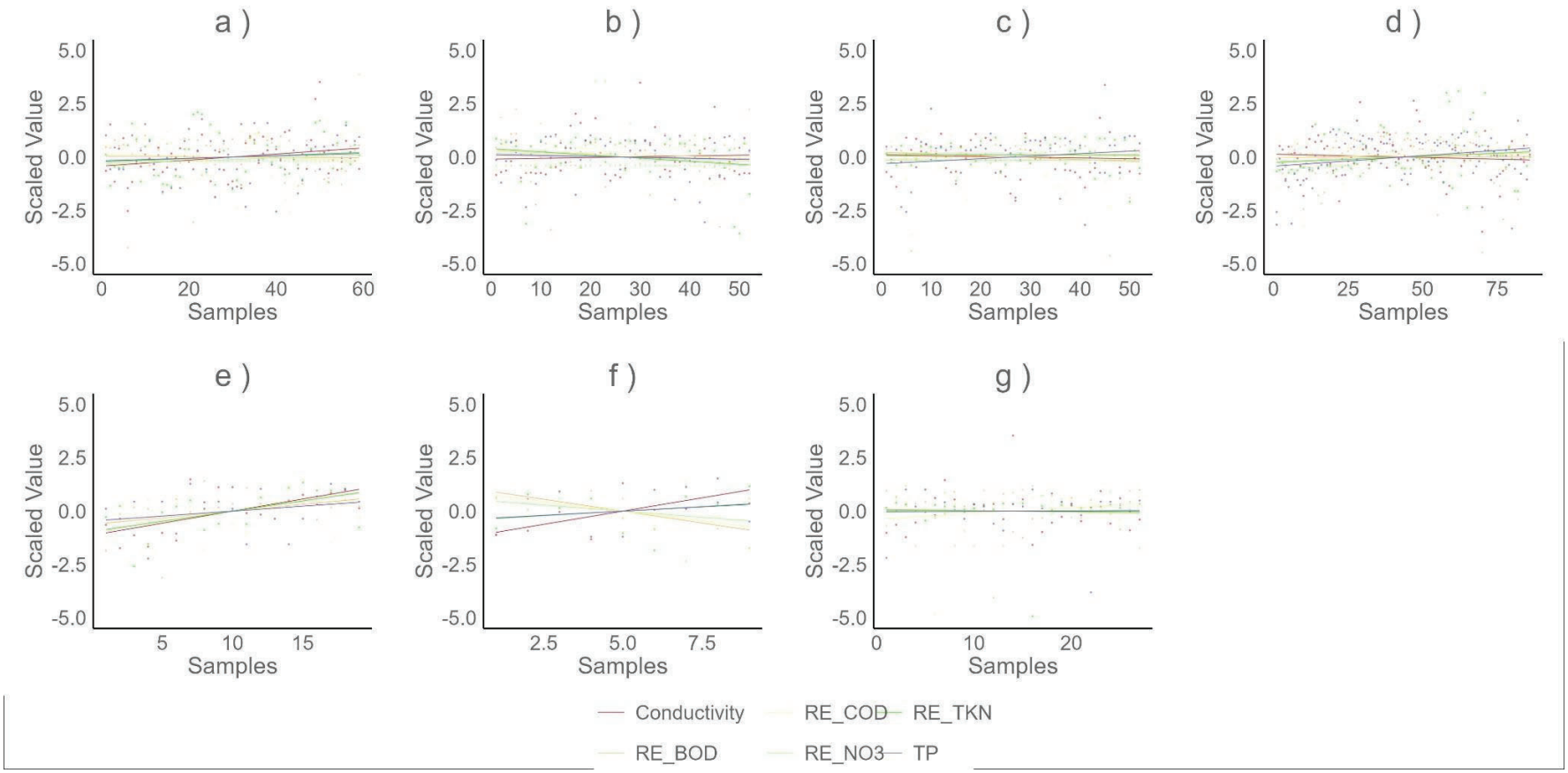


Figure S12. Plot of a global Linear Mixed Model Analysis illustrating the relationship between Conductivity and the Efficiency Removal of Richness, Margalef, and HeipE Biodiversity Indices, with conductivity considered as a function at each WWTP. Additionally, box plots are included, comparing conductivity and biodiversity indices across various WWTPs: WWTPRSS (Roses Wastewater Treatment Plant), WWTPLLN (Llançà Wastewater Treatment Plant), WWTPCES (Castelló d'Empúries Wastewater Treatment Plant), WWTPRUS (Reus Wastewater Treatment Plant), WWTPAMP (Amposta Wastewater Treatment Plant), WWTPALC (Les Cases d'Alcanar Wastewater Treatment Plant), and WWTPSCR (Sant Carles de la Ràpita Wastewater Treatment Plant).



Figures S13. Individual linear models between Electrical Conductivity (EC) and removal efficiencies of Chemical Oxygen Demand (RE_COD), Biological Oxygen Demand (RE_BOD), Nitrate (RE_NO3), Total Kjeldahl Nitrogen (TKN), and Total Phosphorus (TP) by WWTPs. The colors red, yellow, green, orange, light green, and purple represent EC, RE_COD, RE_BOD, RE_NO_3, TKN, and TP, respectively. a) WWTPRSS: Roses Wastewater Treatment Plant. b) WWTPLLN: Llançà Wastewater Treatment Plant. c) WWTPCES: Castelló d'Empúries Wastewater Treatment Plant. d) WWTPRUS: Reus Wastewater Treatment Plant. e) WWTPAMP: Amposta Wastewater Treatment Plant. f) WWTPALC: Les Cases d'Alcanar Wastewater Treatment Plant. g) WWTPSCR: Sant Carles de la Ràpita Wastewater Treatment Plant.

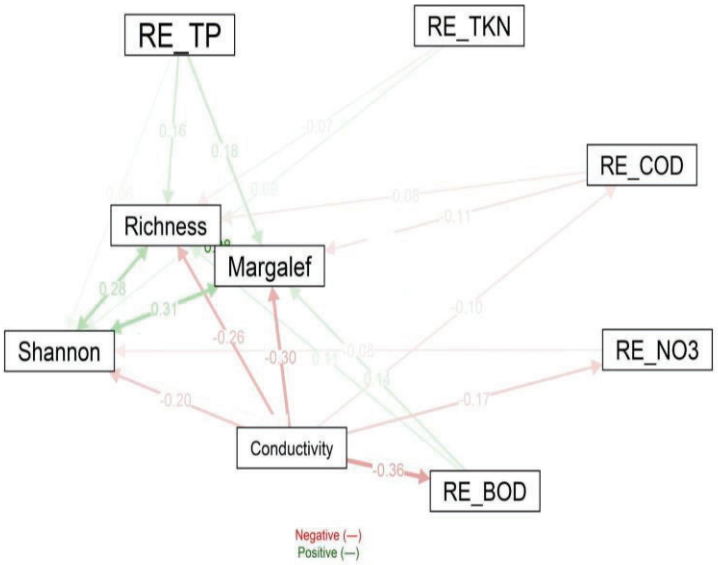


Figure. S14. Global structural equation model showing the effects of electrical conductivity on protozoan and bacterial community indices and percent pollutant removal. *

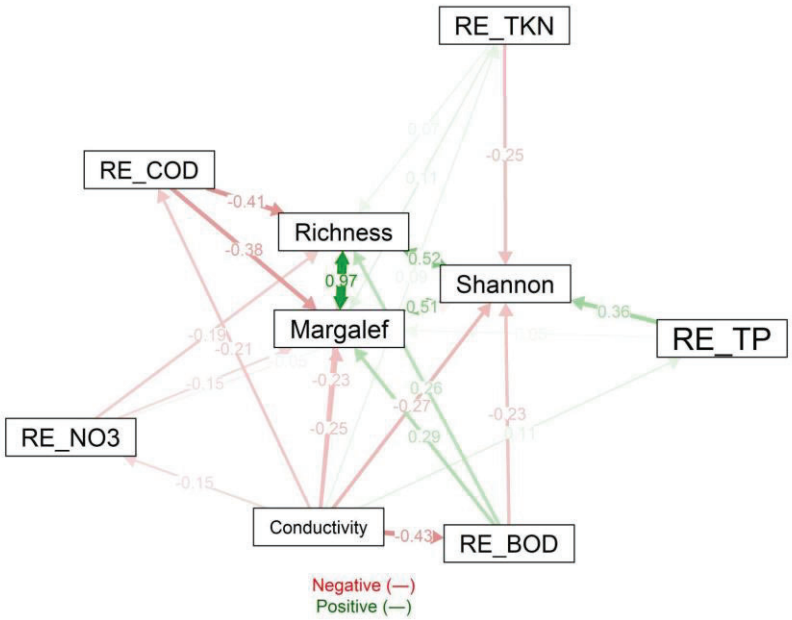


Figure S15. Structural equation model showing the effects of electrical conductivity on protozoan community indices for ciliates and percent pollutant removal. *Conductivity: conductivity (µS cm-1); RE_BOD: biochemical oxygen demand removal percentage; RE_COD: chemical oxygen demand removal percentage; RE_TKN: nitrogen total Kjeldahl removal percentage; RE_NO3: nitrate removal percentage; RE_TP: total phosphorus removal percentage; Richness: Taxa richness of protozoan and bacterial communities in the activated sludge process; Shannon: Shannon diversity of protozoan and bacterial communities in the activated sludge process. Margalef: Margalef richness of protozoan and bacterial communities in the activated sludge process. Red and green lines indicate negative and positive relationships, respectively. Model fit indices were set at CFI ≥ 0.90 and RMSEA ≤ 0.05.

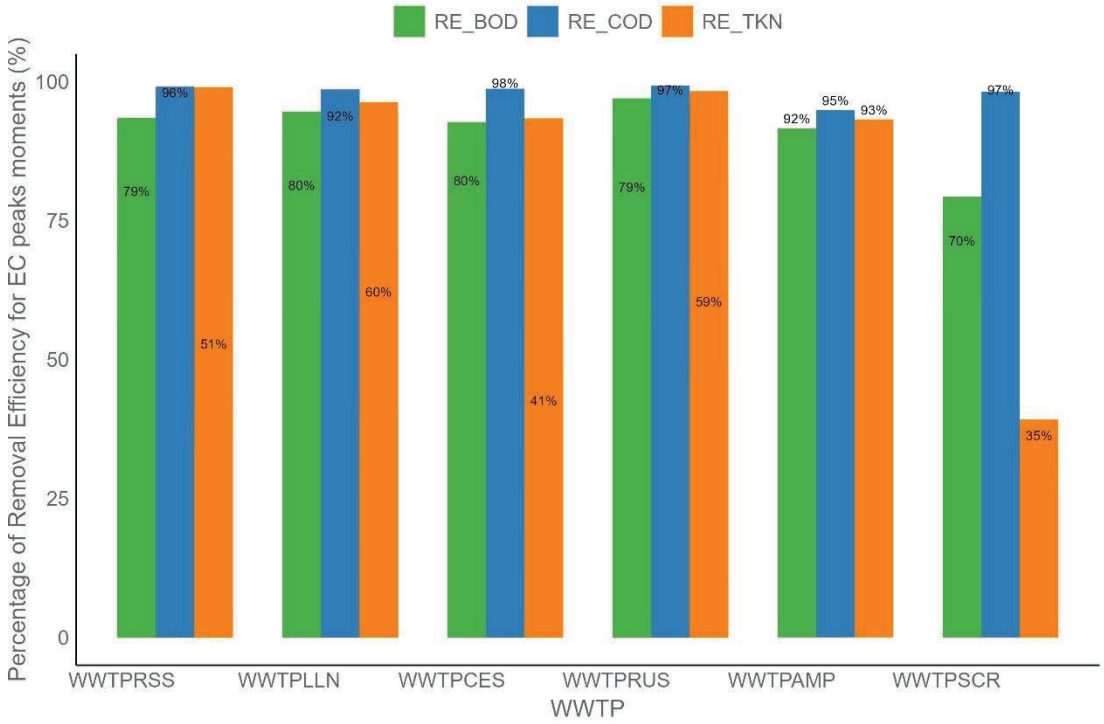


Figure S16. Bar graph showing total removal of chemical oxygen demand (COD), biological oxygen demand (BOD) and Total Kjeldahl Nitrogen (TKN) for electrical conductivity peaks moments by WWTP. WWTPRSS: Roses wastewater treatment plant. WWTPLLN: Llançà wastewater treatment plant. WWTPCES: Castelló d'Empúries wastewater treatment plant. WWTPRUS: Reus wastewater treatment plant. WWTPAMP: Amposta Wastewater Treatment Plant. WWTPALC: Les Cases d'Alcanar Wastewater Treatment Plant WWTPSCR: Sant Carles de la Ràpita Wastewater Treatment Plant.

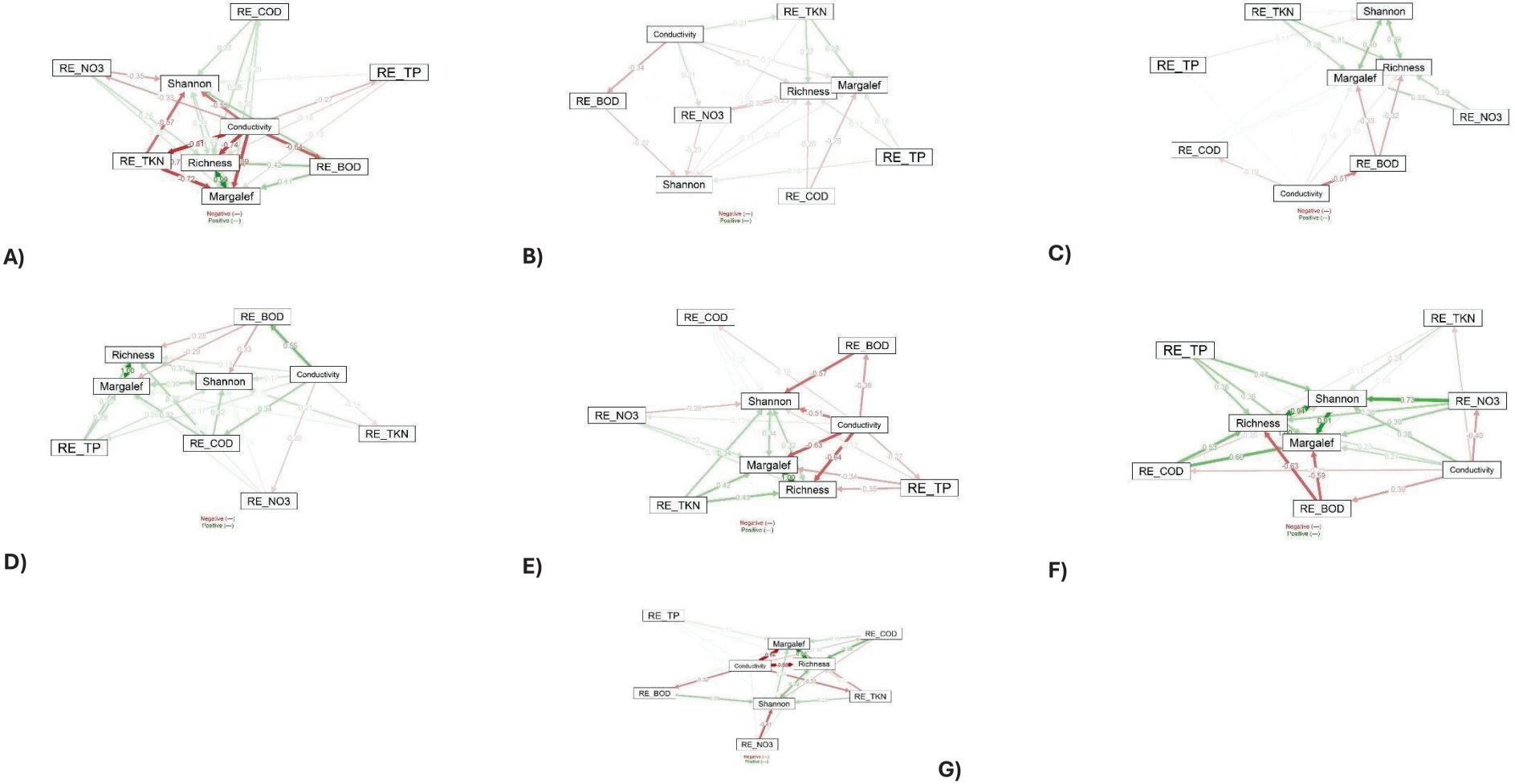


Figure S17. Structural equation model showing the effects of electrical conductivity on protozoan community indices for ciliates and percent pollutant removal. *Conductivity: conductivity (µS cm-1); RE_BOD: biochemical oxygen demand removal percentage; RE_COD: chemical oxygen demand removal percentage; RE_TKN: nitrogen total Kjeldahl removal percentage; RE_NO3: nitrate removal percentage; RE_TP: total phosphorus removal percentage; Richness: Taxa richness of ciliates in the activated sludge process; Shannon: Shannon diversity of ciliates in the activated sludge process. Margalef: Margalef richness of ciliates in the activated sludge process. Red and green lines indicate negative and positive relationships, respectively. Model fit indices were set at CFI ≥ 0.85 and RMSEA ≤ 0.05. A) WWTPRSS: Roses wastewater treatment plant. B) WWTPLLN: Llançà wastewater treatment plant. C) WWTPCES: Castelló d'Empúries wastewater treatment plant. D) WWTPRUS: Reus wastewater treatment plant. E) WWTPAMP: Amposta Wastewater Treatment Plant. F) WTPALC: Les Cases d'Alcanar Wastewater Treatment Plant. G) WWTPSCR: Sant Carles de la Ràpita Wastewater Treatment Plant